

Agronomy Research

Established in 2003 by the Faculty of Agronomy, Estonian Agricultural University

Aims and Scope:

Agronomy Research is a peer-reviewed international Journal intended for publication of broad-spectrum original articles, reviews and short communications on actual problems of modern biosystems engineering incl. crop and animal science, genetics, economics, farm- and production engineering, environmental aspects, agro-ecology, renewable energy and bioenergy etc. in the temperate regions of the world.

Copyright:

Copyright 2009 by Estonian University of Life Sciences, Latvia University of Life Sciences and Technologies, Aleksandras Stulginskis University, Lithuanian Research Centre for Agriculture and Forestry. No part of this publication may be reproduced or transmitted in any form, or by any means, electronic or mechanical, incl. photocopying, electronic recording, or otherwise without the prior written permission from the Estonian University of Life Sciences, Latvia University of Life Sciences and Technologies, Aleksandras Stulginskis University, Lithuanian Research Centre for Agriculture and Forestry.

***Agronomy Research* online:**

Agronomy Research is available online at: <http://agronomy.emu.ee/>

Acknowledgement to Referees:

The Editors of *Agronomy Research* would like to thank the many scientists who gave so generously of their time and expertise to referee papers submitted to the Journal.

Abstracted and indexed:

SCOPUS, EBSCO, CABI Full Paper and Thompson Scientific database: (Zoological Records, Biological Abstracts and Biosis Previews, AGRIS, ISPI, CAB Abstracts, AGRICOLA (NAL; USA), VINITI, INIST-PASCAL.)

Subscription information:

Institute of Technology, EULS
St. Kreutzwaldi 56, 51014 Tartu, ESTONIA
E-mail: timo.kikas@emu.ee

Journal Policies:

Estonian University of Life Sciences, Estonian Research Institute of Agriculture, Latvia University of Life Sciences and Technologies, Aleksandras Stulginskis University, Lithuanian Institute of Agriculture and Lithuanian Institute of Horticulture and Editors of *Agronomy Research* assume no responsibility for views, statements and opinions expressed by contributors. Any reference to a pesticide, fertiliser, cultivar or other commercial or proprietary product does not constitute a recommendation or an endorsement of its use by the author(s), their institution or any person connected with preparation, publication or distribution of this Journal.

ISSN 1406-894X

CONTENTS

A. Arshadi, E. Karami, A. Sartip, M. Zare and P. Rezaabakhsh Genotypes performance in relation to drought tolerance in barley using multi-environment trials.....	5
F. da Borso, C. Di Marzo, F. Zuliani, F. Danuso and M. Baldini Harvest time and ensilage suitability of giant reed and miscanthus for bio-methane production and characterization of digestate for agronomic use.....	22
V. Bulgakov, S. Nikolaenko, V. Adamchuk, Z. Ruzhylo and J. Olt Theory of retaining potato bodies during operation of spiral separator.....	41
V. Bulgakov, S. Nikolaenko, V. Adamchuk, Z. Ruzhylo and J. Olt Theory of impact interaction between potato bodies and rebounding conveyor.....	52
G. Cekstere, A. Osvalde, V. Nollendorfs, A. Karlsons, J. Pormale, P. Zalitis, G. Sņepsts, S. Minova, L. Jankevica and M. Laivins Effects of fertilization on <i>Picea abies</i> stands situated on drained peat soils	64
M. Gaworski, A. Leola, H. Kiiman, O. Sada, P. Kic and J. Priekulis Assessment of dairy cow herd indices associated with different milking systems	83
M.H. Jørgensen Agricultural field production in an ‘Industry 4.0’ concept	94
T.A. Kalinina, O.A. Vysokova, L.A. Khamidullina, A.A. Kochubei, O.E. Cherepanova and T.V. Glukhareva The effect of ethyl 5'-(4-methoxybenzoyl)-5',7'-dihydrospiro[cyclopentane-1,6'-[1,2,3]triazolo[5,1- <i>b</i>][1,3,4]thiadiazin]-3'-carboxylate on <i>Pinus sylvestris</i> L. seed germination	103
J. Katrevičs, B. Džeriņa, U. Neimane, I. Desaine, Z. Bigača and Ā. Jansons Production and profitability of low density Norway spruce (<i>Picea abies</i> (L.) Karst.) plantation at 50 years of age: case study from eastern Latvia.....	113

E. Kokin, M. Pennar, V. Palge and K. Jürjenson	
Strawberry leaf surface temperature dynamics measured by thermal camera in night frost conditions	122
I. Laktionov, O. Vovna, O. Cherevko and T. Kozlovskaya	
Mathematical model for monitoring carbon dioxide concentration in industrial greenhouses	134
A. Linina and A. Ruza	
The influence of cultivar, weather conditions and nitrogen fertilizer on winter wheat grain yield.....	147
J. Malat'ák, J. Bradna, J. Velebil, A. Gendek and T. Ivanova	
Evaluation of dried compost for energy use via co-combustion with wood	157
K. Meile, A. Zhurinsh, L. Briede and A. Viksna	
Investigation of the sugar content in wood hydrolysates with iodometric titration and UPLC-ELSD	167
K. Meiramkulova, A. Bayanov, T. Ivanova, B. Havrland, J. Kára and I. Hanzlíková	
Effect of different compositions on anaerobic co-digestion of cattle manure and agro-industrial by-products	176
M. Obergruber, V. Hönig, P. Procházka and P. Zeman	
Energy analysis of hydrogen as a fuel in the Czech Republic	188
K. Ouakli, M. Benidir, S. Ikhlef and H. Ikhlef,	
Typological analysis of the sustainability of dairy cattle farming in the Chelif valley (Algeria)	198
I. Plūduma-Pauniņa, Z. Gaile, B. Bankina and R. Balodis	
Field Bean (<i>Vicia faba</i> L.) Yield and Quality Depending on Some Agrotechnical Aspects	212
A. Rybka, P. Heřmánek and I. Honzík	
Analysis of Hop Drying in Chamber Dryer	221
E. Samadzadeh Ghale Joughi, E. Majidi Hervan, A.H. Shirani Rad and GH. Noormohamadi	
Fatty acid composition of oilseed rapeseed genotypes as affected by vermicompost application and different thermal regimes.....	230

A. Senberga, L. Dubova and I. Alsina	
Germination and growth of primary roots of inoculated bean (<i>Vicia faba</i>) seeds under different temperatures.....	243
S. Šēnhofa, M. Zeps, L. Ķēniņa, U. Neimane, R. Kāpostiņš, A. Kārklīņa and Ā. Jansons	
Intra–annual height growth of hybrid poplars in Latvia. Results from the year of establishment.....	254
U. Spulle, E. Buksans, J. Iejavs and R. Rozins	
Swelling Pressure and Form Stability of Cellular Wood Material.....	263
B. Tamelová, J. Malat’ák and J. Velebil	
Energy valorisation of citrus peel waste by torrefaction treatment.....	276
H.R. Tohidi Moghadam, T. W. Donath, F. Ghooshchi and M. Sohrabi	
Investigating the probable consequences of super absorbent polymer and mycorrhizal fungi to reduce detrimental effects of lead on wheat (<i>Triticum aestivum L.</i>).....	286
P. Vaculik, M. Prikryl, J. Bradna and L. Libich	
Energy consumption of milking pump controlled by frequency convertor during milking cycle	297

Genotypes performance in relation to drought tolerance in barley using multi-environment trials

A. Arshadi¹, E. Karami^{2,*}, A. Sartip¹, M. Zare³ and P. Rezabakhsh⁴

¹Department of Agronomy and Plant Breeding, Campus of Agriculture and Natural Resources, Razi University, Kermanshah, Iran

²Department of Agronomy and Plant Breeding, College of Agriculture and Natural Resources, Islamic Azad University, Sanandaj Branch, Sanandaj, Kurdistan, Iran

³Department of Agriculture, Firoozabad Branch, Islamic Azad University, Firoozabad, Iran

⁴Department of Agroecology, Islamic Azad University, Mahabad Branch, Mahabad, Iran

*Correspondence: Ezzatut81@yahoo.com

Abstract. The selection of stable and superior genotypes, with the aim of improving grain yield in breeding programs, requires the evaluation of genotypes under different environments. In this study, the yields of 10 barley genotypes were evaluated in eight different environments using a graphical method (GGE biplot). These experiments were conducted from 2011 to 2015. There were irrigated and rain-fed conditions, as a randomized complete block design (RCBD) with three replications. Results indicated that the two components of PC1 and PC2 explained 62.9% and 14.9% of the total variation observed in the yield, respectively. Genotypes with a positive value for PC1 (i.e., $PC1 > 0$) had the adaptable and the highest performance, whereas genotypes with a negative value for the first component (i.e., $PC1 < 0$) were non-adaptable and had the lowest performance. Likewise, among the genotypes, some had their second component scores near zero, and they exhibited the greatest stability compared to other genotypes. Specifically, genotype 3 had the highest grain yield and stability, while genotypes 2 and 8 showed relatively high yields.

Key words: *Hordeum vulgare*, drought intensity, drought tolerance index, genotype \times environment interaction index.

INTRODUCTION

Barley is a cereal crop with good adaptation to drought stress, and it can be considered as a genetic model plant to evaluate drought resistance mechanisms (Ceccarelli, 1987; Baum et al., 2007). However, most of these investigations are applied under simulated drought stress conditions to enhance experimental accuracy, but its relevance to real drought stress conditions is unreliable and questionable (Lakew et al., 2011). Among all environmental stresses, drought is responsible for the greatest amounts of damage to plant products on a global scale (Pennisi, 2008; Ceccarelli, 2010). A rise in the frequency of drought stress can be expected because of climate change (Ceccarelli, 2010).

The selection of drought tolerant genotypes by means of long-term breeding programs is a way to reduce the effect of drought stress on crop production. Tolerance to drought stress is influenced by poly-genetic heritability and the high level of environmental diversity. Tolerance may also depend on drought stress intensity and duration, along with its interaction with other environmental factors, which make breeding programs a valuable approach to the improvement of drought tolerance (Lakew et al., 2011). Environmental factors refer to a set of external conditions that affect plant growth and development. Soil texture, pH, soil depth, organic matter, fertility, diseases and insects can influence the environment (Roozeboom et al., 2008). The interaction of genotype and environment generate the type of response to a variety of environmental changes (Crossa et al., 1991). This interaction is a fundamental issue in plant breeding studies, and these can contribute to the improvement of genetic efficiency in plants. This is a continuous concern for plant breeders, especially when there are strong interactions or when the selection of varieties is a difficult task to perform (Roozeboom et al., 2008). The evaluation of adaptability and yield stability of varieties in different environmental conditions are subjects of frequent research in plant breeding programs. When considering the process of selection, it is better to estimate the environmental adaptability of plants, in addition to their grain yield stability, rather than to consider grain yield alone (Mohammadi & Amri, 2009).

When the interaction between genotype and environment is weak, there are two ways to develop varieties. First, there is the process of dividing an area under study into smaller and homogeneous areas where varieties with special adaptability are cultivated. Secondly, there is the possibility of creating cultivars with a wide range of adaptability which can be cultivated in different areas; Ideal varieties are those with high grain yield and proper adaptability to a wide range of environmental conditions (Yan et al., 2007; Yan, 2014). The evaluation of varieties in different environments is often performed to select the best varieties for an environment. This can be accompanied by determining the mega-environments if they are available (Yan et al., 2000). Evaluation of genotypes can involve the interaction between the genotype and environment, and then the selection of superior genotypes can occur when the final selection step is expected. This is essential under multiple environments (Kaya et al., 2006; Mitrović et al., 2012). One important point in the evaluation of genotypes in different environments is that in most cases the effect of environment is great but hard to document. Only the effect of genotype and the interaction between genotype and environment are important in selection of stable genotypes. Both genotype effect and the interaction of genotype and environment must be examined simultaneously (Yan & Kang, 2002).

The GGE biplot (genotype (G) main effect plus genotype by environment interaction ($G \times E$) method makes possible the study of genotype effect and the interaction between genotype and environment simultaneously, which can acquire a graphical form (Yan & Kang, 2002). The biplot technique is a very useful tool for visual assessment and interpretation of varieties, environments and their interaction responses. It is a graphical display and representation of simultaneous behavior of two variables which was proposed for the first time by Gabriel in 1971. The graphical method has been introduced by other authors as a suitable technique for analysis of a large number of observations (Crossa et al., 1991; Gauch, 2006). This technique was developed using spatial regression methods (SREG) by combining the main effect of genotype and interaction of genotype effect versus the environment (Jalata, 2011). The biplot method

is also used in order to interpret results of regression. In the process of this method, data pertaining to regional trials are obtained. The factors calculate by the graphical GGE biplot method, in which both genotypes and environments are shown visually (Yan et al., 2000; Yan, 2001). Using the GGE biplot method, a second order matrix can be displayed by using a biplot (Choukan, 2011). This method is superior to other methods because plant breeders can visualize the relationship between genotypes and environments and then determine which variety in any given environment or subgroup has a higher potential, based on the drawn graphical plot (Yan et al., 2000).

Mohammadi et al. (2012) recognized that the GGE biplot model is more accurate and efficient than other models (e.g. regression coefficient, sum of squared deviations from regression, stability variance and additive main effects and multiplicative interaction (AMMI). Farshadfar et al. (2012) used the GGE biplot model to evaluate the stability of 25 wheat genotypes. They introduced the most stable genotype suiting a given environment. Mortazavian et al. (2014) used the GGE biplot method to group environments with barley genotypes. Choukan (2011) studied the genotype, environment and interaction between genotype and environmental effects in 14 corn lines using the GGE biplot, leading to the recognition of stable genotypes. Ahmadi et al. (2012) evaluated the performance of 18 barley genotypes under rain-fed conditions in several stations. The results of the GGE biplot graphical analysis revealed two large environments and the superior genotypes. The GGE biplot model is generally a suitable method for multi-environmental data analysis, the evaluation of big environments and the determination of stable genotypes (XU et al., 2014; Luo et al., 2015; Yan, 2015).

In this research, we have evaluated different barley genotypes by considering the interaction between genotype and environments. The objective of this study was to determine the general and specific adaptability of selected genotypes by using the GGE biplot method, and to compare the performance of different genotypes.

MATERIALS AND METHODS

Plant material

In this study, 10 different genotypes of barley (Table 1) in four agricultural research stations were studied in (RCBD) with three replications, by rain-fed and irrigated conditions for a period of four years (Table 2 and Fig. 1). Planting was done by hand in early November.

Filed experiment

Each experimental plot consisted of six rows, each was two meters in length, having a distance of 25 cm in between the rows, and a planting density of 200 seeds per square meter. Planting was done under rain-fed conditions without irrigation and only relied on natural rainfall. For irrigating, 500 liters of water were applied to each experimental plot for irrigation. During the growing season, weed control was performed manually. The precipitation (i.e., amount and distribution of rainfall) during the experimental period was variable (Table 2). Irrigation occurred during tilling, elongation, flowering, and grain filling stages. After adjusting for margins at harvest, sampling was done from the middle of experimental units in order to measure grain yield of each variety using a digital scale. Then, the yield (kilograms per unit) was converted to tons per hectare.

Table 1. Description of the 10 genotypes of barley used in this study

Code	Cultivar	Spike type	Origin	Year of release	Classification by climate	Drought tolerant /susceptible	Reference
G1	Gorgan	2	Sweden	-	Moderate	Susceptible	(Arshadi et al., 2016)
G2	Rihane	6	ICARDA	1993	Moderate	Moderate	(Nazari & Pakniyat, 2010; Arshadi et al., 2016)
G3	Kavir	6	USA	1979	Moderate	Tolerant	(Nazari & Pakniyat, 2010; Arshadi et al., 2016)
G4	Nosrat	6	Iran	2008	Moderate	Tolerant	(Saeidi et al., 2013; Sadeghi-Shoae et al., 2014)
G5	Nimruz	2	CIMMYT	1997	Warm	Susceptible	(Zare, 2012)
G6	Valfajr	6	Egypt	1985	Moderate	Susceptible	(Nazari & Pakniyat, 2010)
G7	Makuyi	6	Italy	1990	Cold	Susceptible	(Nazari & Pakniyat, 2010)
G8	Zarjo	6	Iran	1949	Cold	Tolerant	(Sadeghi-Shoae et al., 2014)
G9	Gorgan 4	2	Sweden	1962	Moderate	Moderate	(Saeidi et al., 2013; Arshadi et al., 2016)
G10	Strin	2	-	-	-	Susceptible	(Arshadi et al., 2016)

ICARDA: International Center for Agricultural Research in the Dry Areas;

CIMMYT: International Maize and Wheat Improvement Center.

Table 2. Trial sites of the diverse barley for harvest during 2011–2015

Code	Year of cultivation	Site	Location	Latitude	Longitude	Altitude (m)	Precipitation (mm)
E1	2011–2012	Rain-fed	Shiraz	37°29'N	32°52'E	1,540	296
E2	2011–2012	Irrigated	Shiraz	37°29'N	32°52'E	1,540	296
E3	2012–2013	Rain-fed	Firoozabad	35°28'N	40°52'E	1,327	381
E4	2012–2013	Irrigated	Firoozabad	35°28'N	40°52'E	1,327	381
E5	2013–2014	Rain-fed	Sanandaj	35°16'N	47°1'E	1,380	254
E6	2013–2014	Irrigated	Sanandaj	35°16'N	47°1'E	1,380	254
E7	2014–2015	Rain-fed	Ghamloo	35°23'N	46°41'E	1,850	118
E8	2014–2015	Irrigated	Ghamloo	35°23'N	46°41'E	1,850	118

m: meter; mm: millimeter.

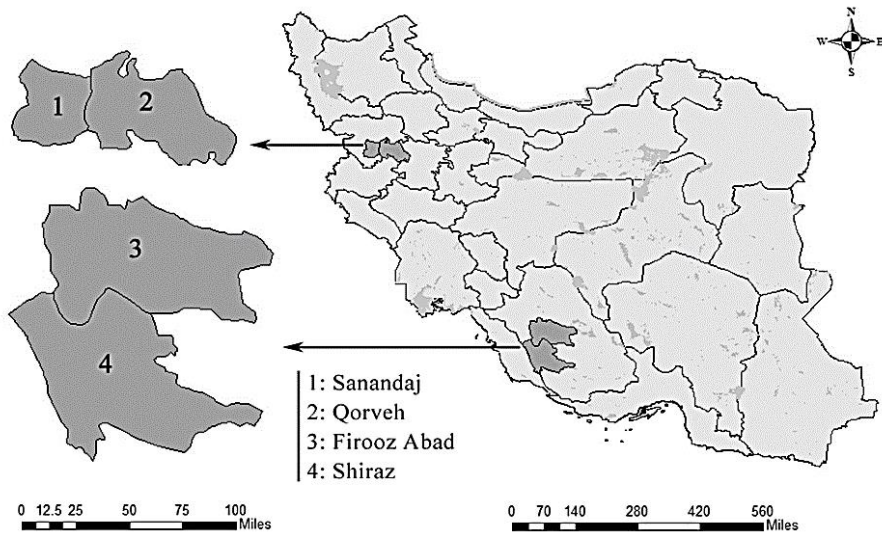


Figure 1. Location of experimental sites on the Iran's map.

Statistical analysis

The Normality Test was done using the SAS statistical software (v9.4). Eight conditions were evaluated, i.e. considering the two conditions of irrigated and rain-fed plants multiplied by the four years (2011–2015). Graphical studies on the interaction between genotype and environmental effects were done using the GGE biplot 6.3 software (Yan, 2001; Yan & Kang, 2002) according to the method proposed by Yan & Hunt (2001). In this study, the genotypes were evaluated according to grain yield in 8 different environments (Table 2). Drought sensitivity index (DSI) was calculated according to the suggested equation by Fischer & Maurer (1978):

$$DSI = \frac{1 - \frac{YD}{\bar{Y}P}}{DII} \quad (1)$$

where YD is the average grain yield under stress conditions and YP is the average grain yield under a normal condition. DII (%) is the Drought intensity index which is calculated by the following equation:

$$DII = 1 - \left(\frac{\bar{Y}D}{\bar{Y}P} \right) \quad (2)$$

The value of this intensity in this study was calculated as 0.50% (2011–2012), 0.51% (2012–2013), 0.46% (2013–2014) and 0.50% (2014–2015). Genotypes with the least DSI value were then considered as tolerant to drought stress.

RESULTS

The results of combined analysis of variance for yield are shown in Table 3. According to this analysis, grain yield showed a significant difference across environments and genotypes, and also their interaction was highly significant ($p \leq 0.01$). The significance of the interaction between genotype and environmental effects showed that the environments can be arranged in groups according to the effects of interaction.

Table 3. Combined analysis of variance for yield data of 10 barley genotypes evaluated across eight environments

Source of variation	df	SS	MS	F	P
Replication	2	0.224	0.112	0.15	0.865
Environment	7	1317.30	188.19	244.53	0.0001
Error 1	14	10.77	0.769	-	-
Genotype	9	398.644	44.29	103.71	0.0001
G × E	63	306.565	4.866	11.39	0.0001
Error 2	144	61.50	0.43	-	-
CV%	-	-	10.29	-	-

G × E: genotype by environment interaction.

The grain yields of genotypes were significantly different among the various environments. Genotype 3 had the highest yield in environments 1, 3, 4, 5, and 6, whereas genotypes 4, 9, and 8 had the highest yields in environments 2, 7, and 8, respectively. Generally, genotype 3 had the highest yield in all environments and genotype 10 had the lowest grain yield (Table 4). Among the tested environments, the highest average grain yield was obtained in environment 6.

In order to study and interpret the performance of the genotypes, environmental variations and their interaction effects, a graphical analysis was generated and used (Figs 2–6). These charts represent 77.80% of the total data variance (i.e., 62.90% and 14.90% of total variance for PC1 (principal component) and PC2, respectively). Also, the factors PC1 and PC2 indicate the effects of genotype and the interaction of genotype with the environment, respectively. According to the GGE biplot, genotypes with PC1 scores above zero are considered as efficient genotypes (with high grain yield) and genotypes with PC1 scores below zero are known as low yielding genotypes (with low grain yield). The factors PC1 and PC2 divide genotypes into two groups of stable and unstable genotypes based on their scores. Group 1 included stable genotypes of G3, G2 and G8 which had the highest grain yield and the least value of the second factor PC2 (close to zero). The second group included unstable genotypes, such as G4 which had the highest amount of grain yield and scores for PC2. In Fig. 2 the vector length of a tester represents its discriminating ability. The angle between a tester and the AEC abscissa (average environment coordination) axis represents the representativeness of the tester: the larger the angle, the less representative the tester. In this figure, four environments (E2, E3, E6, and E8) were highly correlated in their ranking of the genotypes, indicating that these environments produced similar information about the genotypes (Fig. 2). Correlation analysis of the 8 environments is given in Table 5. Most environments showed a positive correlation with each other except environments 1 and 7 ($r = -0.007$) (Table 5).

Table 4. Mean grain yield (t ha⁻¹) of 10 barley genotypes tested across eight environments

Genotype	2011–2012			2012–2013			2013–2014			2014–2015			mean yield (t ha ⁻¹)
	E1	E2	DSI	E3	E4	DSI	E5	E6	DSI	E7	E8	DSI	
G1	3.93	5.94	0.68	4.30	6.54	0.67	5.60	5.89	0.11	2.60	3.13	0.34	4.74 (9)
G2	3.83	8.09	1.06	5.47	10.50	0.93	6.38	11.10	0.92	4.31	7.57	0.86	7.16 (4)
G3	4.73	9.48	1.01	7.57	12.29	0.75	7.22	14.83	1.11	4.13	9.34	1.11	8.70 (1)
G4	3.31	9.90	1.34	5.34	12.06	1.08	4.94	11.47	1.23	3.84	7.98	1.03	7.36 (3)
G5	3.09	7.36	1.17	3.45	10.39	1.30	4.94	9.37	1.02	1.96	4.61	1.14	5.65 (8)
G6	3.25	7.18	1.10	4.08	8.52	1.01	3.93	12.70	1.49	3.12	7.03	1.11	6.23 (5)
G7	4.44	6.21	0.58	3.49	8.49	1.14	4.40	8.41	1.03	1.91	8.11	1.52	5.68 (7)
G8	3.95	8.43	1.07	5.39	10.32	0.93	6.49	11.53	0.94	3.83	10.54	1.27	7.56 (2)
G9	3.34	6.00	0.89	4.43	9.48	1.04	5.28	8.89	0.88	5.75	5.89	0.05	6.13 (6)
G10	3.42	5.35	0.73	3.08	7.42	1.14	3.91	4.60	0.32	2.41	3.86	0.75	4.26 (10)
Mean yield	3.73	7.39	-	4.66	9.60	-	5.31	9.88	-	3.39	6.81	-	6.35
LSD 0.05	1.005	0.816	-	0.518	1.261	-	1.345	1.702	-	0.697	1.15	-	-

E: environments; DSI: Drought sensitivity index.

Table 5. Correlation coefficients among tested environments

Year	Environment		E1	E2	E3	E4	E5	E6	E7	E8
2011–2012	E1	Stress	1.00							
	E2	Non-stress	0.197	1.00						
2012–2013	E3	Stress	0.551	0.788**	1.00					
	E4	Non-stress	0.135	0.901**	0.724*	1.00				
2013–2014	E5	Stress	0.582	0.567	0.856**	0.551	1.00			
	E6	Non-stress	0.258	0.828**	0.764*	0.793**	0.514	1.00		
2015–2016	E7	Stress	-0.007	0.322	0.580	0.454	0.498	0.424	1.00	
	E8	Non-stress	0.484	0.705*	0.650*	0.676*	0.498	0.783**	0.363	1.00

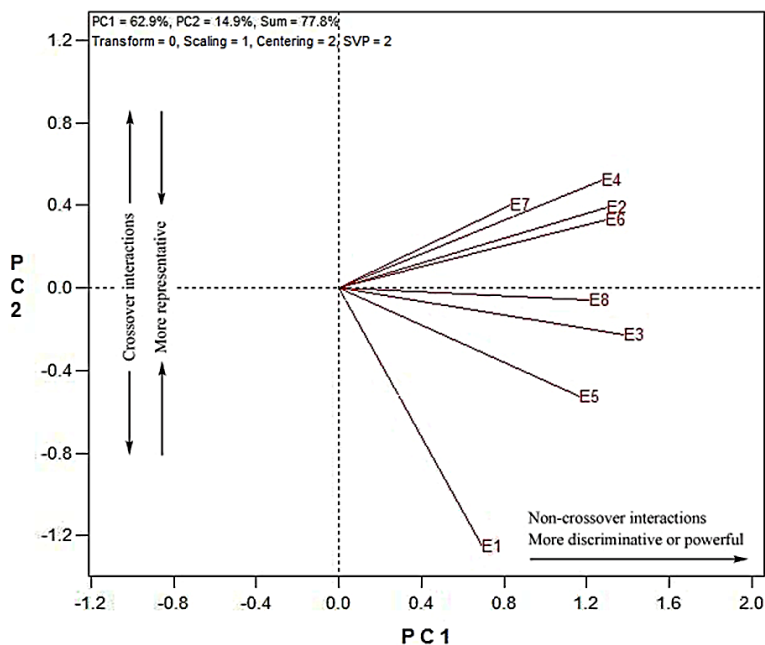


Figure 2. GGE biplot based on environment-focused scaling. PC and E stand for principal component and environment, respectively.

A multi-dimensional diagram is used in order to determine the best genotype for each location (Fig. 3). In this diagram, the varieties which are placed in a special section or environment can prove to have a good performance. Genotypes 2, 3 and 8 had the highest yield in all environments. Moreover, genotype 4 showed the highest yield in environments 2 and 4. The best genotype in each section is a genotype that is placed at the head of the multi-dimensional diagram. Therefore, genotype 3 was the best genotype in the most environments, with respect to its yield. According to the Fig. 4, the origin of the plot is connected to the average of the environments by a direct line (the point of the total average of environments has been determined by a small circle). Genotypes with higher positive values on this axis had the highest yield. Accordingly, genotypes were divided into two groups: group (1) consisting of the genotypes with high grain yield (G3, G8, G2 and G4) and group (2) consisting of genotypes with low grain yield (G9, G6, G7, G5, G1 and G10). An ideal genotype would have the highest performance and stability, which would set a benchmark for other genotypes to be compared and evaluated accordingly. In this study, the ranking of genotypes was shown based on the comparison with the ideal genotype (Fig. 5). For this purpose, the origin is connected to the average point of genotypes by a direct line and continues from two ends. The best genotype is a genotype that is inclined to the positive end of this axis and its vertical distance is shortest from this line. Genotypes with the shortest distance from the center are better. It is demonstrated that genotype 3 is located in the central circle and therefore possesses a high stability and performance. Accordingly, it was considered as the most ideal genotype. Also, genotypes 8 and 2, followed by genotype 4, were placed in the second and third circles, respectively, and were considered as genotypes with acceptable performance.

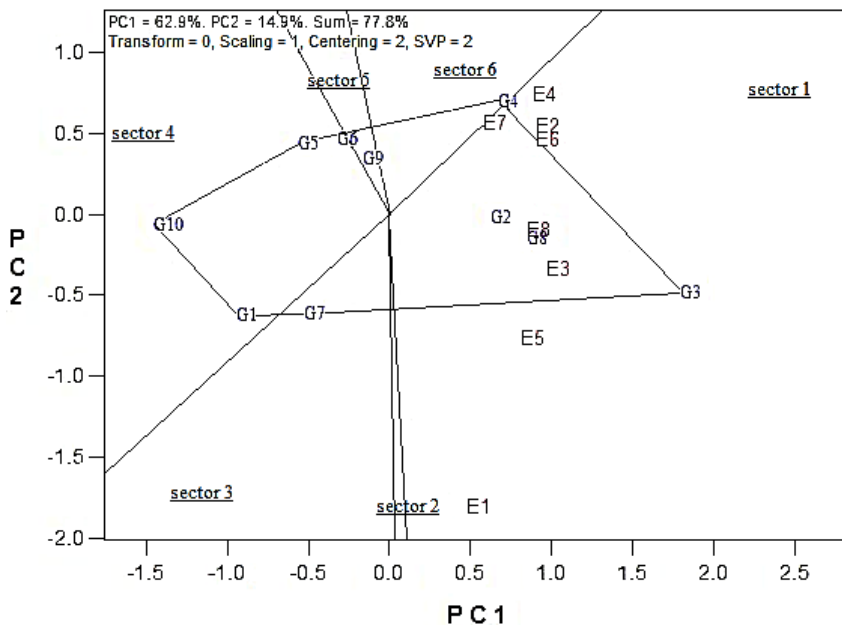


Figure 3. Polygon views of the GGE biplot based on symmetrical scaling for the which-won-where pattern for genotypes and environments. PC, G and E stand for principal component, genotype and environments, respectively.

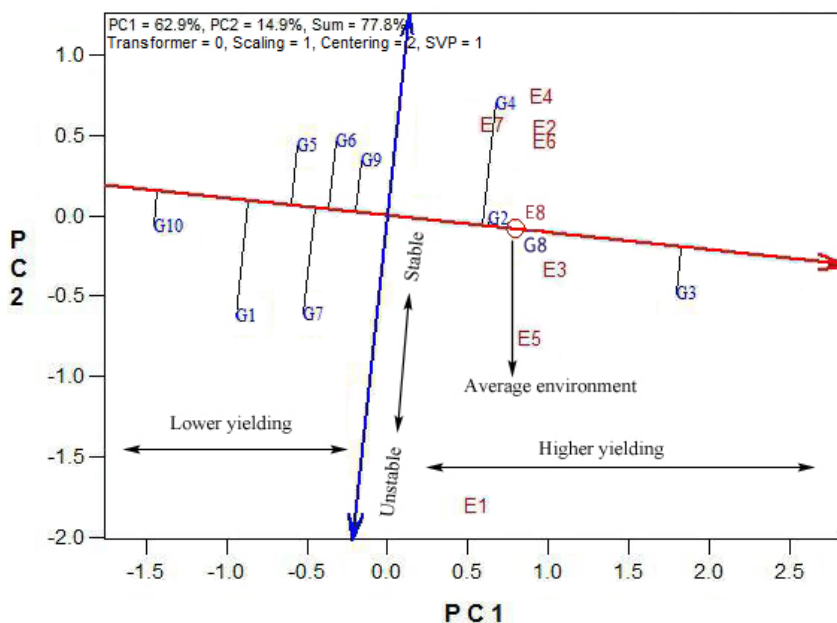


Figure 4. Average environment coordination (AEC) views of the GGE biplot based on environment-focused scaling for the means performance and stability of genotypes. PC, G and E stand for principal component, genotype and environments, respectively.

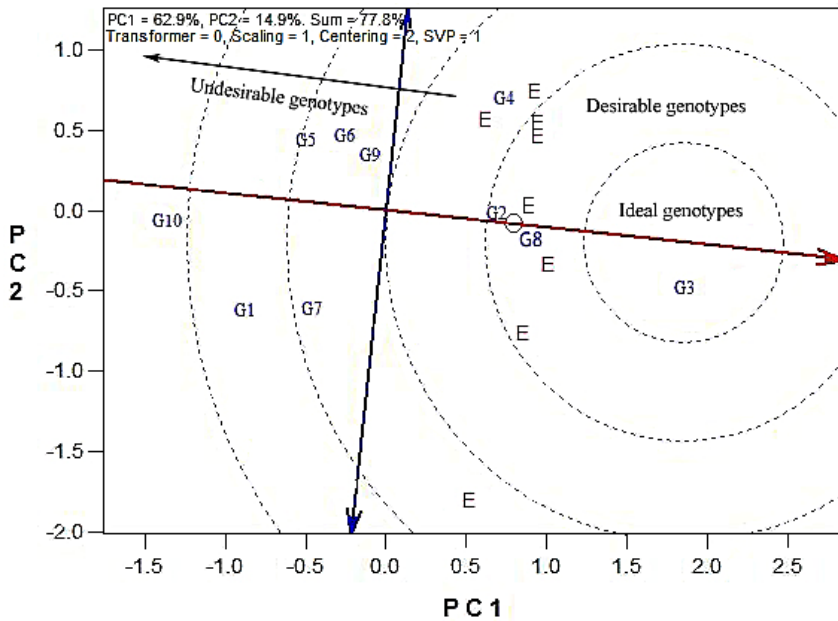


Figure 5. GGE biplot based on genotype-focused scaling for comparison the genotypes with the ideal genotype. PC, G and E stand for principal component, genotype and environments, respectively.

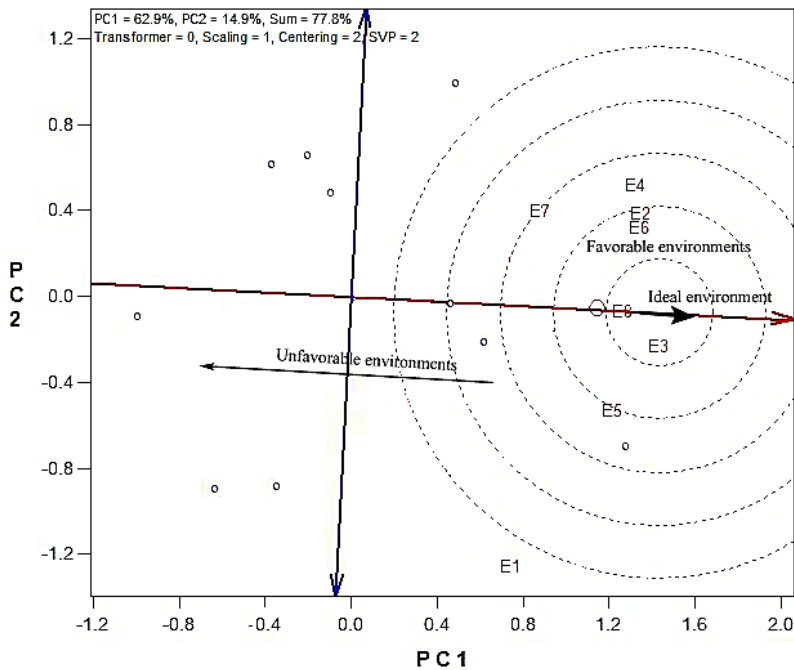


Figure 6. GGE biplot based on environment-focused scaling for comparison the environments with the ideal environment. PC, G and E stand for principal component, genotype and environments, respectively.

The ideal environment had the highest amount of first component (PC1) score and the lowest amount of second component (PC2) score. Fig. 6 shows the ranking of environments based on the ideal environment. The environment that is inclined towards the positive end of the axis and has the shortest vertical distance from it is considered as the best environment. According to Fig. 6, the best point is the center of concentric circles. Other environments are then grouped according to this point. The environments closest to the center are better. As a result, environments 3 and 8 were more ideal environments followed by environments 6, 2, 5, 4, 7 and 10, respectively (Fig. 6).

The drought sensitivity index (DSI) was calculated by assessment of the average yield under normal conditions (YP) and under drought stress conditions (YD) (Eq. (1)). According to Eq. (2), the stress intensity value was calculated in the first season (0.50%), second season (0.51%), third season (0.46%) and fourth season (0.50%). The range of the DSI index in this experiment varied from 0.05 (for genotype 9 in the fourth season) to 1.52 (for genotype 7 in the fourth season) (Table 4). Genotypes with the least drought sensitivity index were most tolerant to drought stress. Generally, this index indicates the type of behaviors exhibited by genotypes under the rain-fed condition. According to this index, genotype 1 had the lowest value of the DSI index, and it did not show a substantial reaction to drought stress. This genotype was more drought tolerant compared to other genotypes under rain-fed conditions and, consequently, showed less yield reduction. Nonetheless, it was not recognized as a desirable genotype because of its low yield potential. In contrast, genotypes 2 and 9 had the highest yield potential, but also had DSI values that were less when compared to other genotypes. Therefore, these genotypes were considered as suitable genotypes under drought stress conditions. Furthermore, genotypes 3 and 2 exhibited the highest stability and yield. On the other hand, genotypes 4, 5 and 6 exhibited DSI values more than one, compared to the other tested genotypes, implying their yields decreased most substantially under rain-fed conditions, and therefore were less tolerant to drought stress.

DISCUSSION

Combined analysis of variance (Table 3) indicated that the effects of environment and genotype versus the environment interaction were significant ($P \leq 0.01$). Also, there was a significant difference among genotypes ($P \leq 0.01$). The interaction effect between genotype and the environment was significant, and genotype performance was different across the environments.

The results indicated that the first and second main components, representing 77.8% of the total variation, related to genotype. The interaction between genotype and environment validated the graph of the biplot in order to explain G and $G \times E$ variations in this study. According to Yang et al. (2009), if this diagram can represent at least 60 percent of the total data variance, it can be used to extract positions of mega-environments. In a biplot diagram, the horizontal axis (PC1) represents the main effect of genotype, while the vertical axis (PC2) indicates the interaction between the genotype and the environment. Accordingly, these are considered as a measure of a genotype's instability (Yan, 2002).

When conducting experiments, similar environments can be detected and removed which could reduce the research costs. This can be done by determining the correlation between the environments, during the stability and compatibility tests of varieties which

are performed in several years and several places (Yan & Kang, 2002; Yan & Rajcan, 2002). Based on Fig. 2, a test environment may be classified into one of three types. Type 1 environments have short vectors and provide little or no information about the genotypes and, therefore, should not be used as test environments. Type 2 environments have long vectors and small angles with the AEC abscissa and are ideal for selecting superior genotypes. If budgetary constraints allow only a few test environments, Type 2 test environments are the first choice (Yan et al., 2007). Type 3 environments have long vectors and large angles with the AEC abscissa (e.g., E1); they cannot be used in selecting superior genotypes, but are useful in culling unstable genotypes. This AEC view is based on genotype-focused singular value partitioning (SVP), that is, the singular values are entirely partitioned into the genotype scores (GGE biplot option ‘SVP = 2’) (Yan, 2002). Gauch & Zobel (1997) reported that large environments have two characteristics: first, different superior genotypes are available in different large environments and, second, the variance among large environments is significantly more than the variance within each large environment.

Badu-Apraku et al. (2011) identified four mega environments by evaluating early maturing cultivars of corn in West Africa based on the GGE biplot analysis. A positive significant correlation among the environments indicates that a direct selection for grain yield can be practical among the tested environments that correlate with each other. For example, genotypes with a high and stable performance in environment 2 can also show a similar performance in environments 3, 4, 6 and 7. However, a direct selection in an environment may not be reliable in other environments.

A multi-dimensional diagram is very suitable to determine which variety performs best in the environments (Yan et al., 2000). In this study, genotypes 2, 3, 4 and 8 were placed in sector 1 (Fig. 3). Also, genotype 3 was located at the peak of the multi-dimensional diagram and showed a greater yield and stability among the other genotypes. Furthermore, genotypes that were located near to the origin do not interact much with environmental variations, and environments near the origin do not react to genotype variations. Therefore, genotypes 2, 7 and 8 showed more stability. In order to conduct a simultaneous investigation on a genotype’s yield and stability, an average environment coordinate graph was used (Yan & Kang, 2002). This graph was also called the average biplot against stability (Yan et al., 2007). Generally, genotypes near the origin have more stability and do not interact considerably with environmental variation (Abay & Bjørnstad, 2009). An ideal genotype must have a high yield and it must have greater stability. In other words, it must be near the positive end of the average environments axis, and its distance from the axis must be a minimum. Accordingly, genotypes 3 and 8 are the best genotypes (Fig. 4). These genotypes can be used as criteria for the evaluation of other cultivars. On the environment coordinate graph, the closer a genotype is located to the ideal genotype, the more successful and superior it would be in general terms. The ranking of genotypes by this method has been reported by other researchers on several crops (Yan & Kang, 2002; Fan et al., 2007; Baxevanos et al., 2008; Hamayoon et al., 2011; Al-Ubaidi et al., 2013; Roostaei et al., 2014). Yan (2001) stated that a genotype can generate a unique image on the average environment coordinate axis (AEC), giving a proper estimation of the genotype’s yield. It was also reported that when considering 33 different wheat genotypes in 8 environments, the correlation between the real yield and the relevant estimations by the biplot method equaled 0.98. The efficiency of genotype image on the average environment coordinate

axis has been confirmed in tomato (Kaya et al., 2006) bread wheat (Gedif & Yigzaw, 2014) and barley (Sarkar et al., 2014).

An ideal genotype is a hypothetical genotype which has the highest yield and stability and is located in the center of concentric circles of the biplot. This genotype can further be used to assess other genotypes (Yan, 2001; Mitrović et al., 2012; Mustapha et al., 2014). According to the results of this research, genotype 3 was recognized as an ideal genotype. Other tested genotypes were compared with the ideal genotype. It was indicated that genotypes 2 and 8 are the most similar to the ideal genotype (Fig. 5). Sharma et al. (2010) studied bread wheat genotypes during 5 years and then introduced superior genotypes with qualities close to the ideal genotype. In the current research, there was a sequence in the yield of genotypes in the average environment coordinate biplot (Fig. 4). According to Yan & Kang (2002), this will occur when the amplitude of the first component (PC1) is much more than the second component (PC2). The ideal environment is a hypothetical environment that has a maximum distinction capacity and is located in the middle of the concentric biplot circles (Yan & Kang, 2002). In this research, environments 3 and 8 were known as ideal environments because they were located in the middle of the concentric biplot circles. Since the desirability value of each environment is measured based on its distance from an ideal environment, the environments 6 and 2 were designated as desirable environments because of their closeness to the ideal environment and their environmental vector length (Fig. 6). Previous studies have confirmed that stressful environments create more heterozygosity in populations, when compared to normal conditions (Ceccarelli et al., 2007). This is probably due to the variability in frequency, duration and severity of climatic stresses, particularly when there are differences between the years (not only with respect to the quantity of precipitation, but also regarding rainfall distribution and the interaction between rainfall and temperature). Therefore, this would lead to difficulties in the progress of selecting grain yield within a single location that receives low and variable amounts of rainfall (Lakew et al., 2011).

There are a few advantages in the biplot method: (1) the graphical scheme increases the researchers' understanding and awareness about data (2) it facilitates the interpretation of comparisons between genotypes (3) and is a useful method for the visual discovery of superior genotypes, traits and grouping of genotypes compared to other complex statistical methods (Sabaghnia et al., 2011; Dehghani et al., 2012). Other researchers have also used this method on soybean (Yan & Rajcan, 2002), wheat (Ma et al., 2004), rapeseed (Dehghani et al., 2008), sunflower (Darvishzadeh et al., 2010), bread wheat (Dehghani et al., 2012; Mohamed, 2013; Temesgen et al., 2015) and barley (Solonechnyi et al., 2015; Kendal, 2016; Meng et al., 2016). Furthermore, it has been illustrated that there is a high efficiency in using the GGE biplot method for the evaluation and selection of superior genotypes and environments (Yan et al. (2007), Ding et al. (2007), Yan & Holland (2010) and Yan (2015). In our study, based on the GGE biplot analysis, genotypes 3, 2 and 8 are recognized as superior genotypes with respect to the tested environments. Therefore, these genotypes can be used in future breeding programs. However, these genotypes were also selected as suitable genotypes by Arshadi et al. (2016) when using other methods.

CONCLUSION

The results revealed that the performance of barley genotypes was influenced by different environments. In the current study, genotype 3 showed the best performance in the different environments, and can be suggested as an ideal genotype compared to other tested genotypes. Regarding the GGE biplot analysis, genotype 2 and 8 were recognized as relatively stable and high yielding genotypes because they were (1) close to the ideal genotype, (2) possessed a first component (PC1) value above zero and (3) possessed a second component (PC2) value close to zero. The results indicated that the GGE biplot analysis is a suitable model in order to evaluate the stability of barley genotypes in different environments, and to identify genotypes with respect to proper environments.

ACKNOWLEDGEMENTS. We thank Reza Amiri from Razi University, Kermanshah, for providing the GGE-biplot software. Also, we would like to thank Hossinali Ramshini and Edward D. Cobb for their helpful comments on the original manuscript. Mohsen Hamedpour-Darabi is thanked for editing the research language.

REFERENCES

- Abay, F. & Bjørnstad, A. 2009. Specific adaptation of barley varieties in different locations in Ethiopia. *Euphytica* **167**, 181–195.
- Ahmadi, J., Vaezi, B. & Hossein Fotokian, M. 2012. Graphical analysis of multi-environment trials for barley yield using AMMI and GGE-biplot under rain-fed conditions. *Journal of Plant Physiology & Breeding* **2**, 43–54.
- Al-Ubaidi, M.O., Al-kaisy, A.M., Al-issawi, M.H., Fadhel, F. & Fuller, M. 2013. Performance assessment of wheat cultivars under three locations using GGE-biplot. *Journal of Genetic and Environmental Resources Conservation* **1**, 262–270.
- Arshadi, A., Karami, E., Khateri, B. & Rezabakhsh, P. 2016. Drought stress effects on the grain yield among different barley cultivars. *Genetika* **48**, 1087–1100.
- Badu-Apraku, B., Oyekunle, M., Akinwale, R. & Lum, A.F. 2011. Combining ability of early-maturing white maize inbreds under stress and nonstress environments. *Agronomy journal* **103**, 544–557.
- Baum, M., Von Korff, M., Guo, P., Lakew, B., Hamwih, A., Lababidi, S., Udupa, S.M., Sayed, H., Choumane, W. & Grando, S. 2007. Molecular approaches and breeding strategies for drought tolerance in barley. Genomics-assisted crop improvement. *Springer*, 51–79.
- Baxevanos, D., Goulas, C., Tzortzios, S. & Mavromatis, A. 2008. Interrelationship among and repeatability of seven stability indices estimated from commercial cotton (*Gossypium hirsutum* L.) variety evaluation trials in three Mediterranean countries. *Euphytica* **161**, 371–382.
- Ceccarelli, S. 1987. Yield potential and drought tolerance of segregating populations of barley in contrasting environments. *Euphytica* **36**, 265–273.
- Ceccarelli, S. 2010. Drought and drought resistance. *Encyclopedia of Biotechnology in Agriculture and Food* **1**, 205–207.
- Ceccarelli, S., Grando, S. & Baum, M. 2007. Participatory plant breeding in water-limited environments. *Experimental Agriculture* **43**, 411.
- Choukan, R. 2011. Genotype, environment and genotype× environment interaction effects on the performance of maize (*Zea mays* L.) inbred lines. *Crop Breeding Journal* **1**, 97–103.
- Crossa, J., Fox, P., Pfeiffer, W., Rajaram, S. & Gauch, H. 1991. AMMI adjustment for statistical analysis of an international wheat yield trial. *Theoretical and Applied Genetics* **81**, 27–37.

- Darvishzadeh, R., Pirzad, A., Hatami-Maleki, H., Poormohammad-Kiani, S. & Sarrafi, A. 2010. Evaluation of the reaction of sunflower inbred lines and their F1 hybrids to drought conditions using various stress tolerance indices. *Spanish Journal of Agricultural Research* **8**, 1037–1046.
- Dehghani, H., Dvorak, J. & Sabaghnia, N. 2012. Biplot analysis of salinity related traits in beard wheat (*Triticum aestivum* L.). *Ann. Biol. Res.* **3**, 3723–3731.
- Dehghani, H., Omidi, H. & Sabaghnia, N. 2008. Graphic analysis of trait relations of rapeseed using the biplot method. *Agronomy Journal* **100**, 1443–1449.
- Ding, M., Tier, B. & Yan, W. 2007. Application of GGE biplot analysis to evaluate Genotype (G), Environment (E) and G×E interaction on *P. radiata*: a case study. 15p.
- Fan, X.-M., Kang, M.S., Chen, H., Zhang, Y., Tan, J. & Xu, C. 2007. Yield stability of maize hybrids evaluated in multi-environment trials in Yunnan, China. *Agronomy Journal* **99**, 220–228.
- Farshadfar, E., Mohammadi, R., Aghaee, M. & Vaisi, Z. 2012. GGE biplot analysis of genotype× environment interaction in wheat-barley disomic addition lines. *Australian Journal of Crop Science* **6**, 1074.
- Fischer, R. & Maurer, R. 1978. Drought resistance in spring wheat cultivars. I. Grain yield responses. *Crop and Pasture Science* **29**, 897–912.
- Gabriel, K.R. 1971. The biplot graphic display of matrices with application to principal component analysis. *Biometrika*, 453–467.
- Gauch, H. & Zobel, R.W. 1997. Identifying mega-environments and targeting genotypes. *Crop Science* **37**, 311–326.
- Gauch, H.G. 2006. Statistical analysis of yield trials by AMMI and GGE. *Crop science* **46**, 1488–1500.
- Gedif, M. & Yigzaw, D. 2014. Genotype by Environment Interaction Analysis for Tuber Yield of Potato (*Solanum tuberosum* L.) Using a GGE Biplot Method in Amhara Region, Ethiopia. *Agricultural Sciences* 2014.
- Hamayoon, R., Khan, H., Naz, L., Munir, I., Arif, M., Khalil, I.A. & Khan, A.Z. 2011. Performance of chickpea genotypes under two different environmental conditions. *African Journal of Biotechnology* **10**, 1534.
- Jalata, Z. 2011. GGE-biplot analysis of multi-environment yield trials of barley (*Hordeum vulgare* L.) genotypes in Southeastern Ethiopia highlands. *International Journal of Plant Breeding and Genetics* **5**, 59–75.
- Kaya, Y., Akçura, M. & Taner, S. 2006. GGE-biplot analysis of multi-environment yield trials in bread wheat. *Turkish Journal of Agriculture and Forestry* **30**, 325–337.
- Kendal, E. 2016. GGE biplot analysis of multi-environment yield trials in barley (*Hordeum vulgare* L.) cultivars. *Ekin Journal of Crop Breeding and Genetics* **2**, 90–99.
- Lakew, B., Eglinton, J., Henry, R.J., Baum, M., Grando, S. & Ceccarelli, S. 2011. The potential contribution of wild barley (*Hordeum vulgare* ssp. *spontaneum*) germplasm to drought tolerance of cultivated barley (*H. vulgare* ssp. *vulgare*). *Field Crops Research* **120**, 161–168.
- Luo, J., Pan, Y.-B., Que, Y., Zhang, H., Grisham, M.P. & Xu, L. 2015. Biplot evaluation of test environments and identification of mega-environment for sugarcane cultivars in China. *Scientific reports* **5**, 1–11.
- Ma, B., Yan, W., Dwyer, L., Fregeau-Reid, J., Voldeng, H., Dion, Y. & Nass, H. 2004. Graphic analysis of genotype, environment, nitrogen fertilizer, and their interactions on spring wheat yield. *Agronomy Journal* **96**, 169–180.
- Meng, Y., Ren, P., Ma, X., Li, B., Bao, Q., Zhang, H., Wang, J., Bai, J. & Wang, H. 2016. GGE Biplot-Based Evaluation of Yield Performance of Barley Genotypes across Different Environments in China. *Journal of Agricultural Science and Technology* **18**, 533–543.

- Mitrović, B., Stanislavljević, D., Treskić, S., Stojaković, M., Ivanović, M., Bekavac, G. & Rajković, M. 2012. Evaluation of experimental maize hybrids tested in multi-location trials using AMMI and GGE biplot analyses. *Turk. J. Field Crops* **17**, 35–40.
- Mohamed, N.E. 2013. Genotype by environment interactions for grain yield in bread wheat (*Triticum aestivum* L.). *Journal of Plant Breeding and Crop Science* **7**, 150–157.
- Mohammadi, R. & Amri, A. 2009. Analysis of genotype× environment interactions for grain yield in durum wheat. *Crop Science* **49**, 1177–1186.
- Mohammadi, R., Armion, M., Zadhasan, E., Ahmadi, M. & Ahari, D.S. 2012. Genotype× environment interaction for grain yield of rainfed durum wheat using the GGE bipot model. *Seed and Plant Improvement Journal* **28**, 503–518.
- Mortazavian, S., Nikkhah, H., Hassani, F., Sharif-al-Hosseini, M., Taheri, M. & Mahlooji, M. 2014. GGE biplot and AMMI analysis of yield performance of barley genotypes across different environments in Iran. *Journal of Agricultural Science and Technology* **16**, 609–622.
- Mustapha, M., Bakari, H. & Alkali, A. 2014. Statistical Evaluation of Grain Yield in Millet Trials Using Principal Component Analysis. *Curr. Trend. Tech. Sci* **3**, 422–428.
- Nazari, L. & Pakniyat, H. 2010. Assessment of drought tolerance in barley genotypes. *Journal of Applied Sciences* **10**, 151–156.
- Pennisi, E. 2008. The blue revolution, drop by drop, gene by gene. *Science* **320**, 171–173.
- Roostaei, M., Mohammadi, R. & Amri, A. 2014. Rank correlation among different statistical models in ranking of winter wheat genotypes. *The crop journal* **2**, 154–163.
- Roozeboom, K.L., Schapaugh, W.T., Tuinstra, M.R., Vanderlip, R.L. & Milliken, G.A. 2008. Testing wheat in variable environments: genotype, environment, interaction effects, and grouping test locations. *Crop Science* **48**, 317–330.
- Sabaghnia, N., Dehghani, H., Alizadeh, B. & Moghaddam, M. 2011. Yield analysis of rapeseed (*Brassica napus* L.) under water-stress conditions using GGE biplot methodology. *Journal of Crop Improvement* **25**, 26–45.
- Sadeghi-Shoae, M., Paknejad, F., Rika, Z.F., Nasri, R. & Tookaloo, M.R. 2014. Selection for drought tolerant barley (*Hordeum vulgare* L.) genotypes under climatic conditions of Karaj, Iran. *Research on Crops* **15**.
- Saeidi, M., Abdoli, M., Azhand, M. & Khas-Amiri, M. 2013. Evaluation of drought resistance of barley (*Hordeum vulgare* L.) cultivars using agronomic characteristics and drought tolerance indices. *Albanian Journal of Agricultural Sciences* **12**, 545.
- Sarkar, B., Sharma, R., Verma, R., Sarkar, A. & Sharma, I. 2014. Identifying superior feed barley genotypes using GGE biplot for diverse environments in India. *Indian J. Genet. Plant Breed* **74**, 26–33.
- Sharma, R.C., Morgounov, A.I., Braun, H.J., Akin, B., Keser, M., Bedoshvili, D., Bagci, A., Martius, C. & van Ginkel, M. 2010. Identifying high yielding stable winter wheat genotypes for irrigated environments in Central and West Asia. *Euphytica* **171**, 53–64.
- Solonechnyi, P., Vasko, N., Naumov, A., Solonechnaya, O., Vazhenina, O., Bondareva, O. & Logvinenko, Y. 2015. GGE biplot analysis of genotype by environment interaction of spring barley varieties. *Žemdirbystė (Agriculture)* **102**, 431–436.
- Temesgen, M., Almerew, S. & Eticha, F. 2015. GGE Biplot Analysis of Genotype by Environment Interaction and Grain Yield Stability of Bread Wheat Genotypes in South East Ethiopi. *World Journal of Agricultural Sciences* **11**, 183–190.
- XU, N.-y., Fok, M., Zhang, G.-W., Jian, L. & ZHOU, Z.-g. 2014. The application of GGE biplot analysis for evaluating test locations and mega-environment investigation of cotton regional trials. *Journal of Integrative Agriculture* **13**, 1921–1933.
- Yan, W. 2001. GGEbiplot—a Windows application for graphical analysis of multi-environment trial data and other types of two-way data. *Agronomy Journal* **93**, 1111–1118.
- Yan, W. 2002. Singular-value partitioning in biplot analysis of multi-environment trial data. *Agronomy Journal* **94**, 990–996.

- Yan, W. 2014. *Crop variety trials: Data management and analysis* John Wiley & Sons, 360 pp.
- Yan, W. 2015. Mega-environment analysis and test location evaluation based on unbalanced multiyear data. *Crop Science* **55**, 113–122.
- Yan, W. & Holland, J.B. 2010. A heritability-adjusted GGE biplot for test environment evaluation. *Euphytica* **171**, 355–369.
- Yan, W. & Hunt, L. 2001. Interpretation of genotype× environment interaction for winter wheat yield in Ontario. *Crop Science* **41**, 19–25.
- Yan, W., Hunt, L., Sheng, Q. & Szlavnic, Z. 2000. Cultivar evaluation and mega-environment investigation based on the GGE biplot. *Crop Science* **40**, 597–605.
- Yan, W. & Kang, M.S. 2002. GGE biplot analysis: A graphical tool for breeders, geneticists, and agronomists CRC press, 288 pp.
- Yan, W., Kang, M.S., Ma, B., Woods, S. & Cornelius, P.L. 2007. GGE biplot vs. AMMI analysis of genotype-by-environment data. *Crop science* **47**, 643–653.
- Yan, W. & Rajcan, I. 2002. Biplot analysis of test sites and trait relations of soybean in Ontario. *Crop Science* **42**, 11–20.
- Yang, R.-C., Crossa, J., Cornelius, P.L. & Burgueño, J. 2009. Biplot analysis of genotype× environment interaction: Proceed with caution. *Crop Science* **49**, 1564–1576.
- Zare, M. 2012. Evaluation of drought tolerance indices for the selection of Iranian barley (*Hordeum vulgare*) cultivars. *African Journal of Biotechnology* **11**, 15975–15981.

Harvest time and ensilage suitability of giant reed and miscanthus for bio-methane production and characterization of digestate for agronomic use

F. da Borso, C. Di Marzo, F. Zuliani, F. Danuso and M. Baldini*

Department of Agricultural, Food, Environmental and Animal Sciences, University of Udine, Via delle Scienze, 206, IT33100 Udine, Italy

*Correspondence: mario.baldini@uniud.it

Abstract. In many countries, biogas plants are mainly fed by livestock slurry and dedicated crops, including maize, which still represents one of the main energy crops utilized. Many concerns are now arising on environmental impact due to the high water consumption, chemical fertilizer and pesticide requirements and on adverse effect of maize as energy crop on the price of food and feed commodities. For these reasons two perennial crops, in particular miscanthus (*Miscanthus x giganteus*) and giant reed (*Arundo donax* L.), were cultivated at very low input and evaluated for their bio-methane yield at different harvest times and ensilage suitability, in a north-eastern area of Italy. Moreover, considering the agronomic use of the obtained digestate as fertilizer, this has been characterized by the content of heavy metals. Both multi-annual crops have proved highly productive in biomass especially with a harvest time in autumn, at which a satisfactory completion of the silage process without additives was observed. Conversely, bio-methane yield per hectare were not satisfactory with respect to the reference crops such as maize. The low BMP attained showed the main bottleneck of the methanisation of ensiled giant-reed and miscanthus, which is represented by fiber composition with high degree of lignification. The simulation use of digestate obtained as fertilizer in vulnerable areas, could lead to slightly exceed the levels allowed by the legislation of some European countries with regard of heavy metals as Cu, Zn and Cd.

Key words: multiannual crops, biomass, silage, energy, bio-methane, digestate.

INTRODUCTION

The agricultural sector must participate in the effort in promoting the conversion from a fossil fuel-based to a bio-based economy (Richardson, 2012), supplying biomass to be transformed into various forms of energy. Among them, biofuels including methane represent, an important strategy to reduce GHG, thus complying with the Kyoto Protocol and subsequent legislation. In Europe, maize is the most commonly used energy crop as biogas feedstock, especially in Germany (Weiland, 2006) and Italy (Carrosio, 2013), the two main biogas producing countries in the European Union. However, the cultivation in fertile agricultural land with high input crop-management techniques made the maize, as energy crop, responsible of elevated environmental impact, increment in food price volatility and in associated risks for food security (FAO, 2008). The use of multi-annual

species, in particular miscanthus (*Miscanthus x giganteus*) and giant reed (*Arundo donax*), resulted in clearly positive environmental loads and able to valorising marginal land (Hastings et al., 2008; Fazio & Monti, 2011; Cadoux et al., 2014), could overcome these drawbacks. Although both crops are subject of several recent anaerobic digestion (AD) experiments, especially in Mediterranean area (Lewandoski et al., 2003; Heaton et al., 2004; Angelini et al., 2005; Angelini et al., 2009; Mantineo et al., 2009; Massé et al., 2010; Ragolini et al., 2014), the amount and quality production and the specific species to adopt remains strictly affected by different climate conditions and management practices of the specific environment (Beale & Long, 1997; Heaton et al., 2009; Arundale et al., 2014). In particular, harvest time is a major factor determining biomass productivity (Beale & Long, 1997; Heaton et al., 2009; Hoagland et al., 2013), quality (Kludze et al., 2013; Baxter et al., 2014) and, consequently, the efficiency of the biochemical processes affected by fibre composition in microbial activity during fermentation (Klimiuk et al., 2010; Monlau et al., 2013). Although ensilage is today commonly performed in maize and other grasses to preserve biomass until use for AD in many farm biogas plants (Yahaya et al., 2001; Neureiter et al., 2005; Vervaeren, et al., 2010; Herrmann et al., 2011), studies on naturally occurring ensilage of giant reed and miscanthus, with subsequent silage utilization in an AD experiment for methane production, are still limited (Dragoni et al., 2015; Liu et al., 2015).

A complete study on the efficiency and environmental impact aspects on giant reed and miscanthus biogas chain cannot be limited to the cultivation aspect of both crops, but also the chemical characteristics of the main AD co-product, such as the digestate, generally used as fertilizer in agricultural practices, could be of great interest. The EU Nitrate Directive (Council Directive 91/676/EEC and followings) states that agricultural use of livestock manure must comply with the limit of 170 kg N ha⁻¹ and per year in vulnerable zones; consequently the knowledge of nitrogen content is essential to estimate the distributable volume of digestate containing animal originated nitrogen. Moreover, heavy metal content in digestate or manure sludge represents another important aspect in using digestate as fertilizer; however, Italian law does not set limits for such products. In effect, the digestate if not properly checked for these pollutants elements, could contaminate susceptible soils, with great difficulty to remedy.

For the above reasons, we addressed the effects of harvesting time (summer vs. autumn vs. winter) on quantitative and qualitative biomass productions, ensilage suitability and biochemical AD process for bio-methane yield of giant reed and miscanthus silages in a northeast Mediterranean area. Furthermore, despite the digestate characterization is normally performed in real scale anaerobic digesters, operating under stable and continuous load conditions, nowadays these kind of data are lacking for giant reed and miscanthus and first approaches to their determination are needed. Consequently, the digestate of the both multiannual crops at the end of AD was submitted to a chemical evaluation in order to monitoring its nitrogen and heavy metals content, as the same will be used as fertilizer to distribute in the soils.

MATERIALS AND METHODS

Field experiment and biomass samples preparation

The field experiment was conducted at the Experimental Farm of Udine University, Udine, Italy (46° 04' N, 13° 22' E, height 109 m a.s.l. and 0% slope). The experimental site is characterized by a shallow soil (about 50 cm) and by a continental climate with main traits reported in Table 1 and Fig. 1, respectively.

In 2014, five years giant reed and miscanthus crops were compared for biomass and bio-methane yield, ensilage suitability and digestate characteristics as fertilizer. Harvesting was done on August (summer), October (fall) and December (winter) for both multiannual crops, in order to assess the influence of growth stage and meteorological conditions on biomass characteristics and methane yield.

The crop management details adopted for the experiment were reported in Baldini et al. (2017).

The experiment was organized following a split plot design with four replication, in order to analyse species (giant reed and miscanthus) x harvest time (summer, fall and winter) effects, with 8 main plots of 60 m² each (species), subdivided in 24 sub-plots (harvest time) of 20 m² each.

At harvest time, fresh and dry biomass (moisture content was obtained maintaining representative samples of fresh biomass at 105 °C until constant weight) was determined by hand sampling 6 m² area within each plot, discarding the border rows. On a subsample of ten plants per plot, number of green and lost leaves per plant were also determined. Representative samples were air dried in greenhouse conditions (30–40 °C), and stored at -18 °C for subsequent chemical analyses.

Ensilage lab experiment

At each harvest time, four plants were randomly chosen in each replication, chopped and placed in 1,000 mL sealed waterproof vessels, for a laboratory ensilage experiment, following the methodology already described by (Baldini et al., 2017). Plants harvested at winter harvest time, due to high dry matter content, prevented air excluding and a suitable packing for being submitted to ensilage process. Therefore, water was added to increase the moisture level before silage. 28 plastic vessels were used for the experiment, which, at the end of about 40 days, were stored at -18 °C prior to chemical analysis.

Biochemical Methane Potential (BMP) assay

To determine Biochemical Methane Potential (BMP), the Automatic Methane Potential Test System (AMPTS I, Bioprocess ControlTM, Sweden) was used. Incubation bottles of 400 mL containing triplicated samples of giant reed, miscanthus and inoculum were incubated at a temperature of 37 ± 1 °C, with an inoculum to substrate VS ratio (I:S) of 2:1 (Baldini et al., 2017). BMP of substrates was calculated net of methane production from inoculum as the cumulative methane yield at the end of the test and the relative VS content (NmL CH₄ g⁻¹ VS). Methane yields per hectare (Nm³ CH₄ ha⁻¹ year⁻¹) were calculated by the product of the organic substance produced taking into account of the ensilage losses (kg VS ha⁻¹ year⁻¹) and the relative BMP obtained (calculated as Nm³ kg⁻¹ VS).

At the end of anaerobic digestion tests, which lasted 36 days, the representative samples of digestate from each bottle were taken and stored at -18 °C for subsequent chemical analyses.

Chemical analysis

Representative subsamples were dried at 100 °C for 16 h in a fan-assisted oven to estimate total solids content (TS). The rest of the samples were dried at 50 °C for 48 h before being milled in a rotor mill equipped with a 1 mm grid for further qualitative analysis.

On representative samples of biomass, silage and digestate after AD, the content of oxygen, nitrogen, hydrogen and carbon was determined using an Elemental Analyzer (vario Micro cube, Hanau, Germany) operating on the principle of catalytic combustion under oxygen supply and high temperatures. Crude protein content (Dumas method) was calculated as 6.25 (conversion factor) multiplied by the elemental nitrogen content detected. Ether extract (EE) was determined according to Soxhlet method. Volatile Solids (VS) concentration was subsequently determined ($VS = TS - \text{ash}$).

Starch was calculated following the amyloglucosidase- α -amylase method (McCleary et al., 1997).

Hemicellulose, cellulose, lignin and non-soluble ash contents were determined on these dried and finely powered samples in accordance with the methods of Goering & van Soest (1970). Neutral detergent fiber (NDF) was first determined as the material remaining after heating with neutral reagent. Next acid detergent fiber (ADF) was determined as the material remaining after heating with a 0.5 M H₂SO₄-reagent for 1 h. Acid lignin fiber (ALF) was then determined as the material remaining after treatment with 72% H₂SO₄ for 24 h. Lastly, the non-soluble ash content was determined as the material remaining after combustion at 525 °C for 3 h in a muffle furnace. Hemicellulose was calculated as the difference between NDF and ADF, cellulose as the difference between ADF and ALF and lignin as the difference between ALF and non-soluble ash.

Soluble carbohydrates (SC), volatile fatty acids (VFA) and ammonia nitrogen (TAN) were obtained following the methodologies already described in Baldini et al. (2017).

The mineral elements and heavy metals contents were detected on digestate, in order to consider its further utilization as fertilizer in the field. Samples of digestate were oven-dried (105 °C for 48 h) and digested in 10 mL of 65% (v/v) HNO₃ in Teflon cylinders for 10 min at 175 °C in a microwave (CEM MARS). After digestion, samples were diluted to 20 mL with milliQ water, filtered through 0.45 μm filters ptfе and diluted 1:10 prior analysis with an ICP-OES (Vista MPX, Varian Inc.). The accuracy of the analytical procedure was checked running standards every 20 samples and quality control was conducted using Y (Yttrium) as the internal standard, reagent blank samples, and triplicates reading for each sample (USEPA, 2007). The main elements detected were: nitrogen (N), aluminium (Al), calcium (Ca), cadmium (Cd), chromium (Cr), cobalt (Co), copper (Cu), iron (Fe), potassium (K), magnesium (Mg), sodium (Na), manganese (Mn), nickel (Ni), phosphorus (P), lead (Pb) and zinc (Zn).

Statistical analysis

All data were subjected to two-way analysis of variance (ANOVA). A fixed-model was adopted, with species and harvest times as independent variables. When ANOVA revealed significant differences between means, *Student–Newman–Keuls* test at $P \leq 0.05$ was adopted to separate means. The term ‘significant’ is only used where a statistical analysis of significance has been performed. Means values of energy yield and digestate mineral elements are given ± 1 SE.

RESULTS AND DISCUSSIONS

ANOVA results and biomass yield

Table 1. Main soil characteristics (0–0.5 m layer)

Parameter	Unit	Value	Method adopted
Sand ($> 0.05 < 2$ mm)	%	43	Ministero per le Politiche Agricole (1999)
Loam ($> 0.002 < 0.05$ mm)	%	40	Ministero per le Politiche Agricole (1999)
Clay (< 0.002 mm)	%	17	Ministero per le Politiche Agricole (1999)
pH	-	7.35	In water solution; Ministero per le Politiche Agricole (1999)
Total calcareous	%	5.5	Gas-volumetric; Ministero per le Politiche Agricole (1999)
Active calcium carbonate	%	0.2	Drouienau; Ministero per le Politiche Agricole (1999)
Organic matter	%	1.8	Walkley and Black; Ministero per le Politiche Agricole (1999)
Total nitrogen	g kg ⁻¹	1.85	Kjeldahl; Ministero per le Politiche Agricole (1999)
C/N	-	10	-
Phosphorus available	mg kg ⁻¹	34	Ferrari; (AOAC, 1990)
Potassium available	mg kg ⁻¹	164	Dirks and Scheffer; (AOAC, 1990)
Cationic exchange capacity	Meq 100 g ⁻¹	18.2	Barium chloride; Ministero per le Politiche Agricole (1999)

The growing season 2014 (April–December) was characterized by an average minimum and maximum daily air temperature of 11.4 and 21.9 °C, respectively; maximum air temperature never peaked above 30 °C and rainfall amounted to 1,346 mm. The climatic conditions (Fig. 1) were quite similar to these recorded in the last 30 years, with the exception of a significant warmer fall-winter period (October–December, +2.0 °C as average temperature) and a slightly more dry springtime (April–June period, -50 mm of rainfall) (ARPA FVG–OSMER, 2016).

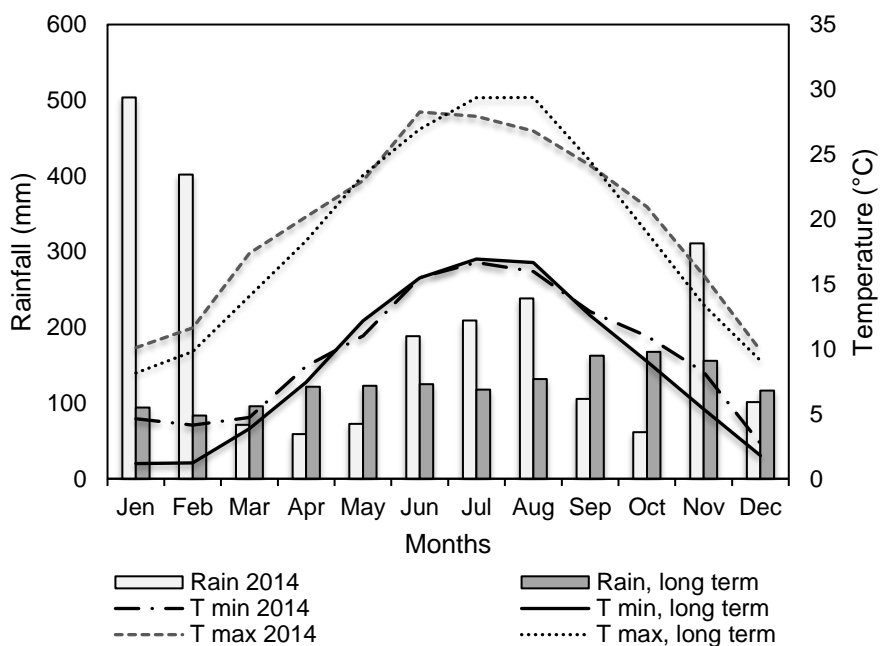


Figure 1. Monthly rainfall and average daily maximum and minimum air temperature patterns in the 2014 as compared to the long-term (20 years) average.

In Tables 2 and 3 are reported the ANOVA results of different traits.

Table 2. ANOVA results, biomass yield and qualitative traits of fresh biomass

Factors	biomass yield	dry matter	starch	sc	hem	cell	lign	prot
Harvest time	**	**	**	**	**	*	*	**
Species	**	**	**	**	n.s.	*	n.s.	*
Harvest time x species	x**	**	**	**	**	n.s.	n.s.	n.s.

*, ** – $P \leq 0.05$ and 0.01 , respectively; sc – soluble carbohydrates; hem – hemicellulose; cell – cellulose; lig – lignin; prot – crude protein.

Table 3. ANOVA results, qualitative traits of silage

Factors	starch	sc	hem	cell	lign	prot	lac	ac	pr	but	an
Harvest time	**	**	n.s.	n.s.	*	**	**	**	**	**	**
Species	n.s.	n.s.	n.s.	n.s.	n.s.	n.s.	n.s.	**	**	**	**
Harvest time x species	*	*	n.s.	n.s.	n.s.	n.s.	**	**	**	**	**

*, ** – $P \leq 0.05$ and 0.01 , respectively; lac – lactic acid; ac – acetic acid; pr – propionic acid; but – butyric + isobutyric acid; an – ammonia nitrogen.

A significant increase in biomass yield was registered between summer and fall harvest for both crops (increase of 21.5 and 33.5% for giant reed and miscanthus, respectively), due essentially to the increase in stem height and leaves number (data not shown), with a negligible leaf loss (Fig. 2).

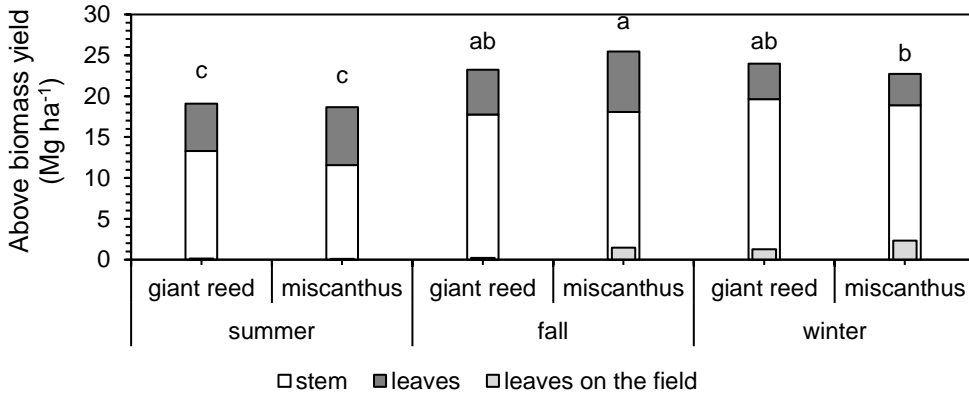


Figure 2. Partitioning of above biomass yield and lost production from fallen leaves on the field of giant reed and miscanthus at three harvest times (summer, fall and winter). For total above biomass yield, different letters indicate statistically different means (*SNK test*; $P \leq 0.05$).

The results obtained in the experiments, (Fig. 2), evidenced that the highest above dry biomass was obtained at fall harvest for miscanthus (25.4 Mg ha^{-1}) and at fall and winter harvest (23.3 and 24.0 Mg ha^{-1} , respectively) for giant reed. These results are in agreement with several experiments, showing that the highest productions are in autumn (Maughan et al., 2012; Mitchell, 2012; Larsen et al., 2014; O’Flynn et al., 2014) especially for miscanthus, which evidenced a significant decrease of biomass yield from fall to winter harvest, essentially due to the leaves loss, with an average of 7.2 leaves losses per plant, corresponding to about 2.31 Mg ha^{-1} of dry matter, confirming other results (Ragolini, et al., 2014).

Both the perennial crops evidenced a very good potential in terms of biomass yield per hectare. The miscanthus biomass yield recorded in this study is in agreement with (Lewandoski et al., 2003), who showed that potential production of miscanthus can reach up to 25 Mg ha^{-1} in central Europe, without irrigation and with data obtained by (Giovanardi et al., 2009) in the same environment. Similarly, giant reed biomass yield obtained, is in agreement with the performances of the crop in Europe (Lewandoski et al., 2003) and comparable to a recent experiment in central Italy (26.3 Mg ha^{-1}), but where was applied annual nitrogen fertilization (Barbanti et al., 2014).

Chemical characteristics

Although ensilage and anaerobic digestion are particularly suitable for high moisture content biomass, a low dry matter content (31.4 and 34.2% for giant reed and miscanthus, respectively, at summer harvesting), associated to a very low content of soluble sugars, could affect the ensilage process, causing risk of nutrients leakage, biomass losses and mould formation (Barontini et al., 2014). Biomass moisture content

changed very differently from fall to winter harvest: in giant reed remained about stable (~50%), whilst miscanthus reduced its moisture during wintertime from 53.5% to 41.8% (data not shown), with a similar trend obtained by Monti et al. (2015). This level of dry matter, prevented a suitable silage compression to exclude air and packing; therefore, a determinate water amount was added to increase the moisture level (till to 57% for both crops) before ensilage.

Crude protein (CP) was highest at summer harvest (54.7 and 40.1 g kg⁻¹ TS) and lowest at winter harvest (28.7 and 20.6 g kg⁻¹ TS) in giant reed and miscanthus biomass, respectively. Values and trend for silages were similar, with the exception of the winter harvest, in which proteins content resulted significantly decreased in both crops (data not shown).

The C/N ratio of the biomass and silage reflected the relative N variation, since the C contents were substantially very similar for all species and harvest times (data not shown). Consequently, the ratio increased in correspondence to fall harvest, with values around 100, in biomass and silages confirming results obtained by other experiments on giant reed (Ragaglini et al., 2014; Liu et al., 2015); on the contrary, the values of both crops reach values around 200 in the silages at winter harvest.

Both perennial species, despite the very limited level of starch accumulation, showed a significant increase from summer to fall harvest time and a significant decrease from fall and winter harvest (Fig. 3). The highest starch amount was obtained at fall harvest for giant reed, (50.3 g kg⁻¹ TS), on the contrary the lowest at winter harvest for miscanthus (4.1 g kg⁻¹ TS).

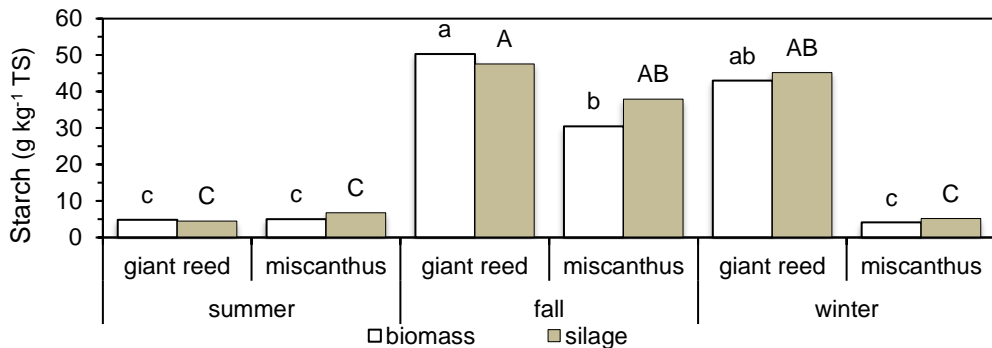


Figure 3. Starch content in fresh and post-ensilage biomass of giant reed and miscanthus at three harvest times (summer, fall and winter). Different letters, lowercase and capital letters for biomass and silage, respectively, indicate statistically different means (SNK test; $P \leq 0.05$).

Giant reed exhibited the lowest and highest SC biomass content at summer and fall harvest respectively (39.4 and 80.3 g kg⁻¹ TS) and an intermediate value at winter harvest (55.3 g kg⁻¹ TS). As temperate C3 grass, the main reserve carbohydrates are fructans (Pollock & Cairns, 1991) which are stored temporary in the stalk at the beginning of flowering (stage corresponding to fall harvest in our experiment), before uploading to the storage organs (as tubers or important rhizomes as in giant reed) at complete maturity (Majjer & Mathijssen, 1991). Conversely, miscanthus coming from another area of origin, with a different physiological functionality (C4 plant) and with

less important rhizomes with respect to giant reed, showed a SC content that increased at fall harvest ($56.1 \text{ g kg}^{-1} \text{ TS}$), remaining unchanged at winter harvest ($56.5 \text{ g kg}^{-1} \text{ TS}$) (Fig. 4).

Silages of both species showed a significant reduction (from 75 to 90%) in SC with respect to biomass content, especially in fall and winter harvest; in this last harvest the SC content showed very low values almost negligible in both species. (Fig. 4).

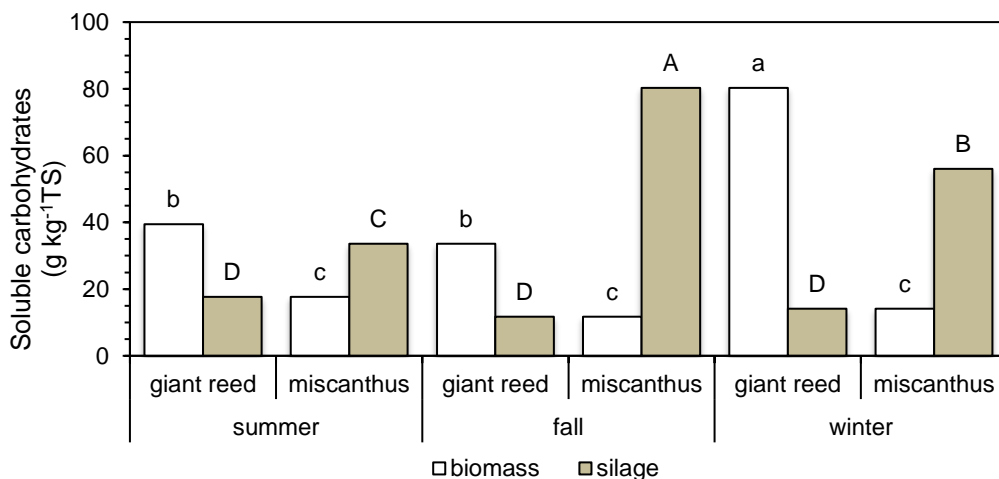


Figure 4. Water soluble carbohydrates (WSC) content in fresh and post-ensilage biomass of giant reed and miscanthus at three harvest times (summer, fall and winter). Different letters, lowercase and capital letters for biomass and silage respectively, indicate statistically different means (*SNK test*; $P \leq 0.05$).

Fiber components

According to ANOVA (Table 2), biomass composition clearly changed with harvesting time. Both crops showed a significant increase in lignin and cellulose content in biomass and a decrease in hemicellulose concentration in correspondence of winter harvest time, especially evident in miscanthus mainly due to a significant leaf loss when harvested in winter, confirming the results obtained by others authors (Hodgson et al., 2010; Hayes, 2013) (Table 2, Fig. 5). The increase of lignin, a widely recognized physical constrain for enzymatic hydrolysis (Pan et al., 2005), at winter harvest, could negatively affect the feedstock quality for anaerobic digestion for bio-methane production. This is confirmed by the substantial uniformity in fiber composition in silage, indicating a very limited hydrolytic activity of both crops during the ensilage process (Fig. 5). Conversely, maize seems to have a wide range of complex hydrolytic activities able to transform a part of hemicellulose in soluble sugars during ensilage (Dewar et al., 1963; Shepherd & Kung, 1996), confirming that hemicellulose is sensitive to low pH and partially hydrolysable under acidic conditions (Morrison, 1979; Jones et al., 1992; Rooke & Hatfield, 2003).

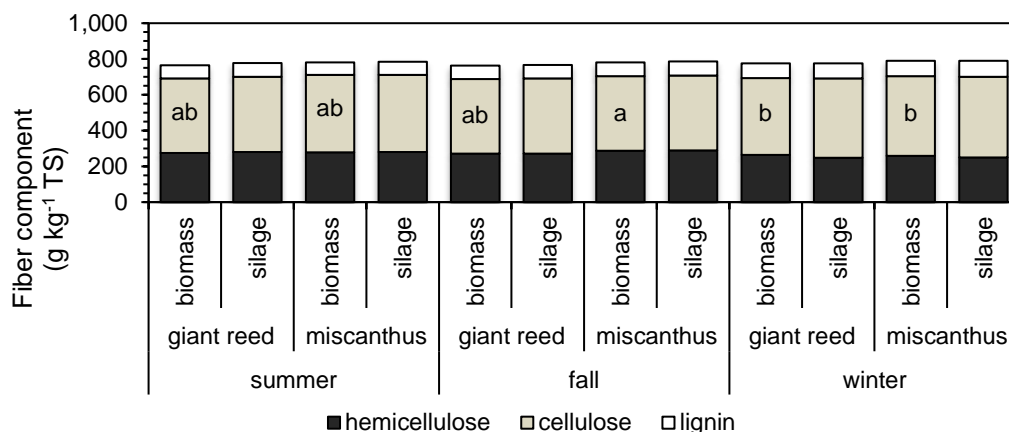


Figure 5. Fiber component in fresh and post-ensilage biomass of giant reed and miscanthus at three harvest times (summer, fall and winter). For hemicellulose in fresh biomass, different letters indicate statistically different means (*SNK test*; $P \leq 0.05$).

Silages fermentation quality

The highest levels of lactic acid were detected at fall harvest in giant reed and miscanthus (54.2 and 46.7 g kg^{-1} TS, respectively), conversely the same acid practically disappeared in both crops silages obtained with winter harvest (Fig. 6). On the contrary, the acetic acid levels resulted very high in correspondence of winter harvest, in particular in miscanthus with a concentration (28.3 g kg^{-1} TS) above the 20 g kg^{-1} TS, considered a maximum threshold of a silage fermented adequately (Ferreira, 2001) (Fig. 6). Butyric acid content, that in silages with proper fermentation must show values lower than 1 g kg^{-1} TS (Ferreira, 2001), in miscanthus ever resulted at very high concentration with values between 7.3 and 8.9 g kg^{-1} TS, and in winter harvest the same acid resulted increased significantly also in giant reed (8.4 g kg^{-1} TS).

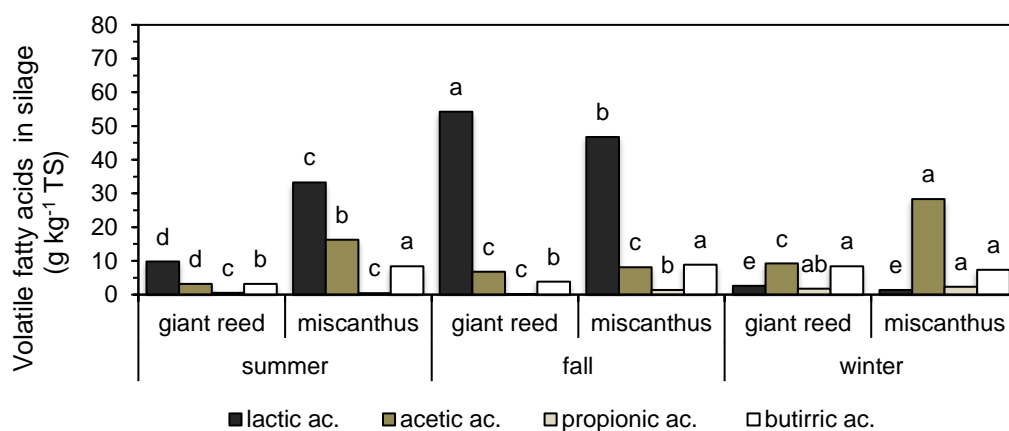


Figure 6. Volatile fatty acids (VFA) content in silage of giant reed and miscanthus at three harvest times (summer, fall and winter). For each VFA, different letters indicate statistically different means (*SNK test*; $P \leq 0.05$).

The production of ammonia nitrogen ($\text{NH}_3\text{-N}$) in silages of good quality has to be lower than 100 gN kg^{-1} of the total nitrogen (Ferreira, 2001) and values very close to the above limit were found in both crop silages harvested in fall. Conversely, the same ammonia nitrogen increased significantly in silages with summer harvest and especially with winter harvest, with values of 626.8 and $781.6 \text{ g N kg}^{-1}$ in giant reed and miscanthus, respectively (Fig. 7). Probably the miscanthus ensilages in the winter harvest was negatively affected by the very high dry matter content (581.7 g kg^{-1}) which determined also the highest silage pH value (5.9) of the trial (data not shown). On the contrary, both silages crops harvested at fall, reached final values of pH below 4, creating favorable conditions for development of lactic acid bacteria responsible for a successful ensilage process.

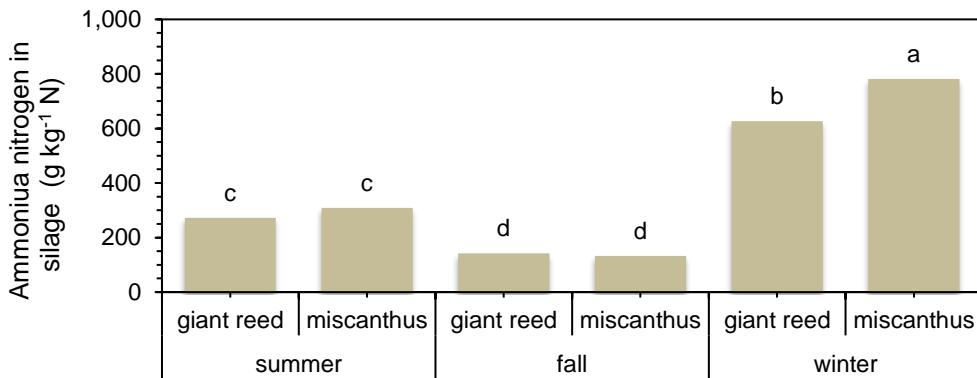


Figure 7. Ammonia nitrogen (N-NH_3) content in silage of giant reed and miscanthus at three harvest times (summer, fall and winter). Different letters indicate statistically different means (SNK test; $P \leq 0.05$).

Methane production (BMP and yield per hectare)

BMP tests were considered concluded when the cumulative biogas curve was addressed toward the plateau phase, precisely when daily methane production rate lowered below than $1.0 \text{ NmL CH}_4 \text{ g}^{-1} \text{ VS day}^{-1}$. This happened after 36 days of digestion for all the comparative thesis and cumulative methane productions (BMP) were calculated at that moment.

Giant reed showed the highest BMP when harvested at the fall harvest ($169.7 \text{ NmL CH}_4 \text{ g}^{-1} \text{ VS}$), conversely miscanthus at the first cut ($171.4 \text{ NmL CH}_4 \text{ g}^{-1} \text{ VS}$), and both results were significantly higher than those obtained from the other harvesting periods (Table 4). The significantly lower BMPs were found at the winter harvest, both for giant reed and miscanthus (116.6 and $113.6 \text{ mL CH}_4 \text{ g}^{-1} \text{ VS}$, respectively).

The effect on BMP of different harvesting period is largely discussed in literature. Giant reed harvested in five different periods in Mediterranean climate and submitted directly to anaerobic tests showed a BMP decrease from 332.9 to $258.3 \text{ NmL CH}_4 \text{ g}^{-1} \text{ VS}$ from June to September harvest time (Ragolini et al., 2014). Giant reed harvested in October period showed a BMP of $150.8 \text{ NmL CH}_4 \text{ g}^{-1} \text{ VS}$.

Table 4. Biochemical methane potential (BMP), methane and energy yield of perennial crops harvested at three different times. Results are means \pm *Standard Error*

Harvest time	Crop	BMP (mL CH ₄ g ⁻¹ VS)	Bio-methane yield (m ³ CH ₄ ha ⁻¹)
Summer	G	148.1 \pm 2.8	2,676.0 \pm 263.1
	M	171.4 \pm 4.0	3,083.4 \pm 526.7
Fall	G	169.7 \pm 3.9	3,795.8 \pm 473.7
	M	159.6 \pm 1.6	3,959.9 \pm 381.3
Winter	G	116.6 \pm 3.8	2,686.5 \pm 514.7
	M	120.5 \pm 5.5	2,645.5 \pm 189.1

G = giant reed; M = miscanthus.

Yang & Li (2014) found BMPs from giant reed similar to those obtained in this study (130–150 mL CH₄ g⁻¹ VS), however operating with fresh plants and adopting a I:S ratio (1:2) different to that adopted in this study (2:1).

Miscanthus harvested after the winter showed BMP as low as 84 NmL CH₄ g⁻¹ VS (Menardo et al., 2012); conversely BMP obtained by miscanthus harvested before the winter and ensiled, showed values higher than 200 NmL CH₄ g⁻¹ VS (Mayer et al., 2014), still slightly higher than that measured in this study (171.4 NmL CH₄ g⁻¹ VS). Even higher values of BMP (345–374 mL CH₄ g⁻¹ VS) can be reached when miscanthus is pre-treated before the anaerobic digestion with steam-explosion, as confirmed by (Menardo et al., 2012).

It is conceivable that the BMP decline with harvesting season (from summer to fall-winter) was determined by an higher content in slowly digestible or un-digestible fibre (lignin, in particular) and by major problems that could have occurred during the silage, especially in relation to changes in VFA composition. High concentration of propionic and butyric acid could have an effect in reducing methane potential of giant reed and miscanthus. As the characteristics of the ensiled substrates are concerned, the highest concentration of propionic acid was found in winter harvest, amounting to 1.8–2.3 g kg⁻¹, respectively for giant reed and miscanthus. Moreover, in this study at the same winter harvest time, butyric acid in ensiled substrates was considerably higher than propionic, resulting 8.4 and 7.3 mg kg⁻¹. These values could have contribute to reach in the system values at which the activity of acidogenic bacteria is repressed, resulting in VFA accumulation, methanogenic bacteria repression and, consequently, methane production reduction, until a complete cessation (Wang et al., 2009).

The accumulation of longer chain acids (mainly propionic and butyric acids) within the system could be related to a low I:S ratio of VS. The acetate produced in first steps of the digestion at lower I:S ratio could inhibit methanogens activity and consequently an increase of I:S ratio could improve the ultimate methane yield of substrate (Raposo et al., 2011; Dechruga et al., 2013).

The combination between biomass production per hectare and BMPs lead to the highest methane productions and energy yield at the second harvest (fall), both for giant reed and miscanthus (3795.8–3959.9 m³ CH₄ ha⁻¹, respectively). It is noticeable to observe that the highest methane production was reached by miscanthus at the fall harvest, despite the BMP lower than giant reed, confirming the relevance of biomass

yield; several authors (Amon et al., 2007; Kreuger et al., 2011; Ragaglini et al., 2014) previously described similar results. Moreover, very similar results were obtained for miscanthus to that observed by Wahid et al. (2015), who concluded that the optimal harvesting period for miscanthus was between September-October (3,824 m³ CH₄ ha⁻¹), corresponding to the fall harvest time of this study. Conversely, methane yields per hectare obtained by giant reed were slightly lower than those reported by other authors, who, however, used fresh or dried plants (Ragaglini et al., 2014; Yang & Li, 2014) or chemical-thermal pre-treated plants (Girolamo et al., 2013). However, the methane production per hectare obtained from giant reed and miscanthus, although of some interest, was about 70%, as mean, that of maize, as reported by Baldini et al. (2017) in a similar experiment carried out in the same location.

Digestate characterization for agricultural use

Digested effluents from lab-scale batch tests, in consequence of the higher I:S rate adopted, could have very similar characteristics to effluents produced during the starting phase of a real scale digester, when substrates are loaded with a low organic loading rate, and a characterization of such effluents could be useful for assessing possible critical factors for their use in agriculture.

Digestate obtained from giant reed had a lower TS content than that obtained from miscanthus, respectively ranging from 54.0 to 49.3 g kg⁻¹ and 62.9 to 56.8 g kg⁻¹ (Table 5). TS content was slightly higher in summer harvest than in other harvesting periods, both for giant reed and miscanthus (Table 5). An opposite tendency was observed for VS content of digestate, which was highest at summer harvest (780 g kg⁻¹ TS), and the lowest at winter harvest (630 g kg⁻¹ TS) in giant reed.

Table 5. Some parameters and heavy metals content of digestate of giant reed and miscanthus harvested at three different times (summer, fall, winter)

Traits	Unit	Giant summer	Misc. summer	Giant fall	Misc. fall	Giant winter	Misc. winter
TS	g kg ⁻¹	54.0	62.9	51.4	60.3	49.3	56.8
VS	g kg ⁻¹ TS	780.0	734.0	779.0	768.0	630.0	653.0
N	g kg ⁻¹ TS	21.4	20.6	28.4	25.4	30.9	22.6
C/N	-	16.0	16.0	12.6	15.2	13.1	16.9
Zn	mg kg ⁻¹ TS	664.3	546.7	752.0	704.9	886.7	607.4
Cu	mg kg ⁻¹ TS	194.6	171.3	222.4	235.5	356.2	223.5
Cr	mg kg ⁻¹ TS	22.5	19.5	24.5	25.0	30.7	22.7
Ni	mg kg ⁻¹ TS	16.8	13.6	16.1	16.2	22.6	17.4
Pb	mg kg ⁻¹ TS	1.9	1.7	1.6	2.4	3.8	1.9
Cd	mg kg ⁻¹ TS	0.8	0.6	0.9	0.8	1.0	0.7

The total N content of digestate was between 20.6 g kg⁻¹ TS (miscanthus at summer harvest) and 30.9 g kg⁻¹ TS (giant reed at winter harvest) (Table 5); in each harvesting time, giant reed digestate had an higher N content than miscanthus, with a general slight N increase from spring to winter harvesting. C/N ratio varied between 12.6 and 16.9 (for giant reed at summer and miscanthus at winter harvest, respectively), with a general trend lower in giant reed than in miscanthus digestate, due to the higher fiber content of this latter species, also. C/N ratio during anaerobic digestion is expected to decrease, due to the C volatilization as CO₂ and CH₄, and the final C/N ratio of digestate normally is

stabilized on values lower than 20 (Li et al., 2011; Zeshan et al., 2012), confirming our results.

Digestate consisted of crops and inoculum as feedstock contained different amounts of microelements and heavy metals, which are important elements for the plants but also potentially dangerous for the soil (Moller & Muller, 2012). The most represented elements in digestate were Zn, Cu, Cr, Ni, Pb and Cd (Table 5), the firsts (Zn and Cu) contained as hundreds, the seconds (Cr and Ni) as dozens and the lasts (Pb and Cd) contained from 0.6 to 3.8 mg kg⁻¹ TS.

As nitrogen contained in digestate is concerned, a number of different approaches are adopted in EU member states for the calculation of 170 kg ha⁻¹ year⁻¹ limit and for the efficiency values adopted for land application of digestate as fertilizer. In this study, accounting the whole N of digestate to comply with the maximum limit of nitrogen allowable in nitrate vulnerable zones (170 kg ha⁻¹ year⁻¹), the highest distributable volume of digestate was ranging between 111.0 m³ ha⁻¹ year⁻¹ (miscanthus at fall harvest) and 147.1 m³ ha⁻¹ year⁻¹ (giant reed at summer harvest) (Table 6). Thus, in relation of the digestate distributable volumes, the maximum annual input of heavy metals in soil was calculated (Table 6).

Table 6. Digestate volume and amount of heavy metals distributable in the soil, utilizing digestate after AD of giant reed and miscanthus silage, harvested at three different harvest times (summer, fall, winter)

Traits	Unit	Giant summer	Misc. summer	Giant fall	Misc. fall	Giant winter	Misc. winter
Volume	m ³ ha ⁻¹	147.1	131.2	116.5	111.0	111.6	132.4
Zn	kg ha ⁻¹	5.28	4.51	4.50	4.72	4.88	4.57
Cu	kg ha ⁻¹	1.55	1.41	1.33	1.58	1.96	1.68
Cr	kg ha ⁻¹	0.18	0.16	0.15	0.17	0.17	0.17
Ni	kg ha ⁻¹	0.13	0.11	0.09	0.11	0.12	0.13
Pb	kg ha ⁻¹	0.015	0.014	0.010	0.016	0.020	0.014
Cd	kg ha ⁻¹	0.006	0.005	0.005	0.005	0.006	0.005

Many European Countries, indeed, have specific rules and limits for heavy metals in digestate used as fertilizer (Al Saedi et al., 2013). Conversely, the only legal limits in force in Italy are those stated in the Legislative Decree (D.Lgs. 99/92), which accomplish to the European Directive on the use of sewage sludge in agriculture (86/278/EEC). From Table 7, it is possible to compare the heavy metals concentration calculated by this study to heavy metal limits of Italy and some European Countries. It was evident that heavy metals content were largely below the limits and the only cases of threshold overcoming was for Cu and Zn, if the most compelling rules of some Northern European Countries are considered (the Netherlands, Sweden and United Kingdom). The same Cu and Zn contents would have overcome the Austria limits, which are calculated in term of heavy metals distributed over a 2 years period; in this last case, the limit overcoming was calculated also for Cd.

Table 7. Several countries limits for heavy metals in digestate used as fertilizer

Countries	Unit	Zn	Cu	Cr	Ni	Pb	Cd
Austria	g ha ⁻¹ in two years	3,000	700	600	400	600	10
Denmark	mg kg ⁻¹ TS	4,000	1,000	100	30	120	0.8
France	mg kg ⁻¹ TS	3,000	1,000	3,000	200	800	20
Germany	mg kg ⁻¹ TS	2,500	1,000	900	200	900	10
Netherland	mg kg ⁻¹ TS	300	75	75	30	100	1.25
Sweden	mg kg ⁻¹ TS	800	600	100	50	100	1.0
United Kingdom	mg kg ⁻¹ TS	400	200	100	50	200	1.5
Italy ^a	mg kg ⁻¹ TS	2,500	1,000	Nd	300	750	20
From this study	mg kg ⁻¹ TS	886.7	356.2	30.7	22.6	3.8	1.0
(max values)	g ha ⁻¹ in two years	14,087.8	5,879.0	367.5	302.5	41.8	15.0

^a – values referred to the use of sewage sludge in agriculture (D.Lgs. 99/92).

CONCLUSIONS

Both giant reed and miscanthus have demonstrated an excellent biomass aboveground potential in the environment under study despite the low-input cultivation technique adopted, with respect to maize. In particular, autumnal harvesting seems to be the most appropriate as it combines the highest biomass, bio-methane and energy yield, also allowing a good performance of the silage process, which takes place naturally, without the need for additives, providing a good quality silage.

The low attained BMP showed the bottlenecks of the methanisation of ensiled giant-reed and miscanthus with respect to maize, mainly due a general recalcitrance of lignocellulosic biomass. In this case, a feasible solution could be a suitable biomass pre-treatment able to weaken the lignocellulosic bonds, to increase the amount of water-soluble carbohydrates and consequently to enhance methane production.

The digestate obtained in this experiment, comparable to that of starting phases of a real scale digester, exceeded the legal limits allowed of Cu, Zn and Cd content if the rules of some countries (i.e. The Netherland, United Kingdom and Austria) are considered. Therefore, in countries like Italy, which have not yet specific rules, it should be a good practice to establish precise limits to heavy metals – besides to N – for calculating the maximum amount of digestate disposable in the vulnerable areas.

ACKNOWLEDGEMENTS. The authors would like to thank Dr. Barbara Piani and Andrea Fabris for the laboratory analysis.

REFERENCES

- Al Saedi, T., Drogg, B., Fuchs, W., Rutz, D. & Janssen, R. 2013. Biogas digestate quality and utilization. In: Wellinger, A., Murphy, J.D. & Baxter, D. (ed.): *The Biogas Handbook: Science, Production and Applications*. WP Woodhead Publishing Limited, 267–298.
- Amon, T., Amon, B., Kryvoruchko, V., Machmuller, A., Hopfner-Sixt, K., Bodiroza, V., Hrbek, R., Friedel, J., Potsch, E., Wagentristl, H., Schreiner, M. & Zollitsch, W. 2007. Methane production through anaerobic digestion of various energy crops grown in sustainable crop rotations. *Bioresource Technol.* **98**, 3204–3212.

- Angelini, L.G., Ceccarini, L. & Bonari, E. 2005. Biomass yield and energy balance of giant reed (*Arundo donax* L.) cropped in central Italy as related to different management practices. *Eur. J. Agron.* **22**, 375–89.
- Angelini, L.G., Ceccarini, L., Nasso, N. & Bonari, E. 2009. Comparison of *Arundo donax* L. and *Miscanthus x giganteus* in a long-term field experiment in Central Italy: analysis of productive characteristics and energy balance. *Biomass Bioenerg.* **33**, 635–643.
- ARPA FVG–OSMER 2016. Schede climatiche del Friuli Venezia Giulia. 311. <http://www.clima.fvg.it>. Accessed 05 January 2017 (in Italian).
- Arundale, R., Dohleman, F., Heaton, E., Mcgrath, J., Voigt, T. & Long, S. 2014. Yields of *Miscanthus x giganteus* and *Panicum virgatum* decline with stand age in the Midwestern USA. *GCB Bioenergy* **6**(1), 1–13.
- Baldini, M., Da Borso, F., Ferfuaia, C., Zuliani, F. & Danuso, F. 2017. Ensilage suitability and bio-methane yield of *Arundo donax* and *Miscanthus x giganteus*. *Ind. Crop. Prod.* **95**, 264–275.
- Barbanti, L., Girolamo, G.D., Grigatti, M., Bertin, L. & Ciavatta, C. 2014. Anaerobic digestion of annual and multi-annual biomass crops. *Ind. Crop. Prod.* **56**, 137–144.
- Barontini, M., Crognale, S., Scarfone, A., Gallo, P., Gallucci, F., Petruccioli, M., Pesciaroli, L. & Pari, L. 2014. Airborne fungi in biofuel wood chip storage sites. *Int. Biodeter. Biodegr.* **90**, 17–22.
- Baxter, X.C., Darvell, L.I., Jones, J.M., Barraclough, T., Yates, N.E. & Shield, I. 2014. *Miscanthus* combustion properties and variations with *miscanthus* agronomy. *Fuel* **117**, 851–869.
- Beale, C.V. & Long, S.P. 1997. Seasonal dynamics of nutrient accumulation and partitioning in the perennial C4-grasses *Miscanthus x giganteus* and *Spartina cynosuroides*. *Biomass Bioenerg.* **12**(6), 419–428.
- Cadoux, S., Ferchaud, F., Demay, C., Zard, H.B., Machet, J.M., Fourdinier, E., Preudhomme, M., Chabbert, B., Gosse, G. & Mary, B. 2014. Implications of productivity and nutrient requirements on greenhouse gas balance of annual and perennial bioenergy crops. *GCB Bioenergy* **6**, 425–438.
- Carrosio, G. 2013. Energy production from biogas in the Italian countryside: policies and organizational models. *Energ. Policy* **63**, 3–9.
- Dechruga, S., Kantachote, D. & Chaiprapat, S. 2013. Effects of inoculum to substrate ratio, substrate mix ratio and inoculum source on batch co-digestion of grass and pig manure. *Bioresource Technol.* **146**, 101–108.
- Dewar, W., McDonald, P. & Whittenbury, R. 1963. The hydrolysis of grass hemicelluloses during ensilage. *J. Sci. Food Agr.* **14**, 411–417.
- Dragoni, F., Ragolini, G., Corneli, E., Nasso, N. o di Nasso, Tozzini, C., Cattani, S. & Bonari, E. 2015. Giant reed (*Arundo donax* L.) for biogas production: land use saving and nitrogen utilisation efficiency compared with arable crops. *Ital. J. Agron.* **10**, 664.
- FAO. 2008. The State of Food and Agriculture. BIOFUELS: prospects, risks and opportunities. FAO Agriculture Series No. **38**. Rome.
- Fazio, S. & Monti, A. 2011. Life cycle assessment of different bioenergy production systems including perennial and annual crops. *Biomass Bioenerg.* **35**, 4868–4878.
- Ferreira, J.J. 2001. Estágio de maturação ideal para ensilagem do milho e do sorgo. In Cruz, J.C., Pereira Filho, I.A., Rodrigues, J.A.S. et al. (ed.): *Produção e utilização de silagem de milho e sorgo*. Sete Lagoas: Embrapa Milho e Sorgo, pp. 405–428.
- Giovanardi, R., Castelluccio, M.D., Rosso, S., Tassan-Mazzocco, G. & Picco, D. 2009. La coltivazione del Miscanto in Friuli Venezia Giulia: aspetti agronomici, energetici e ambientali. *Notiziario ERSA* **3**, 42–48 (in Italian).
- Goering, H.K. & Van Soest, P.J. 1970. Forage Fiber Analysis (apparatus, reagents, procedures and some applications). *USDA Agricultural Handbook* No. **379**.

- Hastings, A., Clifton-Brown, J., Wattenbach, M., Stampfl, P., Mitchell, C. & Smith, P. 2008. Potential of Miscanthus grasses to provide energy and hence reduce greenhouse gas emissions. *Agron. Sustain. Dev.* **28**, 465–472.
- Hayes, D.J.M. 2013. Mass and compositional changes relevant to biorefining, in Miscanthus x giganteus plants over the harvest window. *Bioresource Technol.* **142**, 591–602.
- Heaton, E.A., Dohleman, F.G. & Long, S.P. 2009. Seasonal nitrogen dynamics of Miscanthus x giganteus and Panicum virgatum. *GCB Bioenergy* **1**, 297–307.
- Heaton, E.A., Long, S.P., Voigt, T.B., Jones, M.B. & Clifton-Brown, J. 2004. Miscanthus for renewable energy generation: European Union experience and projections for Illinois. *Mitig. Adapt. Strat. GL* **9**, 433–51.
- Herrmann, C., Heiermann, M. & Idler, C. 2011. Effects of ensiling, silage additives and storage period on methane formation of biogas crops. *Bioresource Technol.* **102**, 5153–5161.
- Hoagland, K.D., Ruark, M.D., Renz, M.J. & Jackson, R.D. 2013. Agricultural management of switchgrass for fuel quality and thermal energy yield on highly erodible land in the driftless area of southwest Wisconsin. *Bioenerg. Res.* **6**, 1012–1021.
- Hodgson, E.M., Lister, S.J., Bridgwater, A.V., Clifton-Brown, J. & Donnison, I.S. 2010. Genotypic and environmentally derived variation in the cell wall composition of Miscanthus in relation to its use as a biomass feedstock. *Biomass Bioenerg.* **34**, 652–660.
- Jones, B., Hatfield, R. & Muck, R. 1992. Effect of fermentation and bacterial inoculation on lucerne cell walls. *J. Sci. Food Agr.* **60**, 147–153.
- Klimiuk, E., Pokój, T., Budzyński, W. & Dubis, B. 2010. Theoretical and observed biogas production from plant biomass of different fiber contents. *Bioresource Technol.* **101**, 9527–9535.
- Kludze, H., Deen, B. & Dutta, A. 2013. Impact of agronomic treatments on fuel characteristics of herbaceous biomass for combustion. *Fuel Process. Technol.* **109**, 96–102.
- Kreuger, E., Prade, T., Escobar, F., Svensson, S., Englund, J. & Bjornsson, L. 2011. Anaerobic digestion of industrial hemp—Effect of harvest time on methane energy yield per hectare. *Biomass Bioenerg.* **35**, 893–900.
- Larsen, S.U., Jørgensen, U., Kjeldsen, J.B. & Lærke, P.E. 2014. Long-term Miscanthus yields influenced by location, genotype, row distance, fertilization and harvest season. *Bioenerg. Res.* **7**, 620–635.
- Lewandowski, I., Scurlock, J.M., Lindvall, E. & Christou, M. 2003. The development and current status of perennial rhizomatous grasses as energy crops in the US and Europe. *Biomass Bioenerg.* **25**, 335–361.
- Li, Y., Park, S.Y. & Zhu, J. 2011. Solid-state anaerobic digestion for methane production from organic waste. *Renew. Sust. Energ. Rev.* **15**, 821–826.
- Liu, S., Ge, X., Liew, L.N., Liu, Z. & Li, Y. 2015. Effect of urea addition on giant reed ensilage and subsequent methane production by anaerobic digestion. *Bioresource Technol.* **192**, 682–688.
- Maijer, W. & Mathijssen, E.W.J.M. 1991. The relation between flower initiation and sink strength of stems and tubers of Jerusalem artichoke. *Neth. J. Agr. Sci.* **39**, 123–135.
- Mantineo, M., D’Agosta, G.M., Copani, V., Patane, C. & Cosentino, S.L. 2009. Biomass yield and energy balance of three perennial crops for energy use in the semi-arid Mediterranean environment. *Field Crop. Res.* **114**, 204–213.
- Massé, D., Gilbert, Y., Savoie, P., Bélanger, G., Parent, G. & Babineau, D. 2010. Methane yield from switchgrass harvested at different stages of development in Eastern Canada. *Bioresour. Technol.* **101**, 9536–9541.
- Maughan, M., Bollero, G.N., Lee, D.K., Rarmody, R., Bonos, S., Cortese, L., Murphy, J., Gaussoin, R., Sousek, M., Williams, D., Williams, L., Miguez, F. & Voigt, T. 2012. Miscanthus × giganteus productivity: the effects of management in different environments. *GCB Bioenergy* **4**, 253–265.

- Mayer, F., Gerin, P.A., Noo, A., Lemaigre, S., Stilmant, D., Schmit, T., Leclech, N., Ruelle, L., Gennen, J. & Von Francken-Welz, H. 2014. Assessment of energy crop salter-native to maize for biogas production in the Greater Region. *Bioresource Technol.* **166**, 358–67.
- Menardo, S., Airolidi, G. & Balsari, P. 2012. The effect of particle size and thermal pre-treatment on the methane yield of four agricultural by-products. *Bioresource Technol.* **104**, 708–714.
- McCleary, B.V., Gibson, T.S., Mugford, D. C. 1997. Measurement of total starch in cereal products by amyloglucosidase - α -amylase method: Collaborative study. *J. AOAC Int.* **80**, 571–579.
- Mitchell, M.S.R. 2012. Switchgrass harvest and management. In Monti, A. (Ed.), *Switchgrass*, l. Springer-Verlag, London, UK, **1**, pp. 113–127.
- Moller, K. & Müller, T. 2012. Effects of anaerobic digestion on digestate nutrient availability and crop growth: A review. *Eng. Life Sci.* **12**(3), 242–257.
- Monlau, F., Barakat, A., Trably, E., Dumas, C., Steyer, J. & Carrere, H. 2013. Lignocellulosic materials into biohydrogen and biomethane: impact of structural features and pretreatment. *Crit. Rev. Env. Sci. Tec.* **43**, 260–322.
- Monti, A., Zanetti, F., Scordia, D., Testa, G. & Cosentino, S.L. 2015. What to harvest when? Autumn, winter, annual and biennial harvesting of giant reed, miscanthus and switchgrass in northern and southern Mediterranean area. *Ind. Crop. Prod.* **75**, 129–134 (Part B).
- Morrison, I. 1979. Changes in the cell wall components of laboratory silages and the effects of various additives on these changes. *J. Agr. Sci.* **93**, 581–586.
- Neureiter, M., Dos Santos, J., Lopez, C., Pichler, H., Kirchmayr, R. & Braun, R. 2005. Effect of silage preparation on methane yields from whole crop maize silages. *Proceedings of the 4th International Symposium on Anaerobic Digestion of Solid Waste*. Copenhagen, Denmark, **1**, pp. 109–115.
- O'Flynn, M.G., Finnan, J.M., Curley, E.M. & McDonnell, K.P. 2014. Reducing crop damage and yield loss in late harvests of *Miscanthus × giganteus*. *Soil Till. Res.* **140**, 8–19.
- Pan, X., Xie, D., Gilkes, N., Gregg, D.J. & Saddler, J.N. 2005. Strategies to enhance the enzymatic hydrolysis of pretreated softwood with high residual lignin content. *Appl. Biochem. Biotech.* **121**, 1069–1079.
- Pollock, C.J. & Cairns, A.J. 1991. Fructan metabolism in grasses and cereals. *Annu. Rev. Plant. Phys.* **42**, 77–101.
- Ragaglini, G., Dragoni, F., Simone, M. & Bonari, E. 2014. Suitability of giant reed (*Arundo donax* L.) for anaerobic digestion: effect of harvest time and frequency on the biomethane yield potential. *Bioresource Technol.* **152**, 107–115.
- Raposo, F., Fernández-Cegri, V., De la Rubia, M.A., Borja, R., Béline, F., Cavinato, C., Demirer, G., Fernández, B., Fernández-Polanco, M., Frigon, J., Ganesh, R., Kaparaju, P., Koubova, J., Méndez, R., Menin, G., Peene, A., Scherer, P., Torrijos, M., Uellendahl, H., Wierinck, I. & de Wilde, V. 2011. Biochemical methane potential (BMP) of solid organic substrates: evaluation of anaerobic biodegradability using data from an international interlaboratory study. *J. Chem. Technol. Biot.* **86**, 1088–1098.
- Richardson, B. 2012. From a fossil-fuel to a biobased economy: The politics of industrial biotechnology. *Environ. Plann. C* **30**, 282–296.
- Rooke, J.A. & Hatfield, R.D. 2003. Biochemistry of Ensiling. USDA-ARS/UNL Faculty, Paper 1399. <http://digitalcommons.unl.edu/usdaarsfacpub/1399>. Accessed 01.06.16.
- Sheperd, A. & Kung, L. 1996. Effects of an enzyme additive on composition of corn silage ensiled at various stages of maturity. *J. Dairy Sci.* **79**, 1767–1773.
- USEPA (U.S. Environmental Protection Agency). 2007. Nanotechnology white paper - external review draft. EPA 100/B-07/001.
Available from: <https://www.epa.gov/osa/nanotechnology-white-paper>

- Vervaeren, H., Hostyn, K., Ghekiere, G. & Willems, B. 2010. Biological ensilage additives as pretreatment for maize to increase the biogas production. *Renew. Energ.* **35**, 2089–2093.
- Wahid, R., Nielsen, S., Hernandez, V.M., Ward, A., Rene Gislum, R., Jørgensen, U. & Møller, H. 2015. Methane production potential from *Miscanthus* sp. Effect of harvesting time, genotypes and plant fractions. *Biosyst. Eng.* **133**, 71–80.
- Wang, Y., Zhang, Y., Wang, J. & Meng, L. 2009. Effects of volatile fatty acid concentrations on methane yield and methanogenic bacteria. *Biomass Bioenerg.* **33**, 848–853.
- Weiland, P. 2006. State of the art of solid-state digestion-recent developments. In Rohstoffe, F.N. (ed.): *Solid-State Digestion-State of the Art and Further R&D Requirements*. Gulzower Fachgespräche, **24**, pp. 22–38.
- Yahaya, M.S., Kimura, A., Harai, J., Nguyen, H.V., Kawai, M., Takahashi, J. & Matsuoka, S. 2001. Effect of length of ensiling on silo degradation and digestibility of structural carbohydrates of Lucerne and orchardgrass. *Anim. Feed Sci. Tech.* **92**, 141–148.
- Yang, L. & Li, Y. 2014. Anaerobic digestion of giant reed for methane production. *Bioresource Technol.* **171**, 233–239.
- Zeshan, Karthikeyan, O.P. & Visvanathan, C. 2012. Effect of C/N ratio and ammonia-N accumulation in a pilot-scale thermophilic dry anaerobic digester. *Bioresource Technol.* **113**, 294–302.

Theory of retaining potato bodies during operation of spiral separator

V. Bulgakov¹, S. Nikolaenko¹, V. Adamchuk², Z. Ruzhlyo¹ and J. Olt^{3,*}

¹National University of Life and Environmental Sciences of Ukraine, 15, Heroyiv Oborony street, UA03041Kyiv, Ukraine

²National Scientific Centre, Institute for Agricultural Engineering and Electrification, 11, Vokzalna street, Glevakha-1, Vasylkiv District, UA08631 Kiev Region, Ukraine

³Estonian University of Life Sciences, Institute of Technology, Kreutzwaldi 56, EE51014 Tartu, Estonia

*Correspondence: jyri.olt@emu.ee

Abstract. The increase of the efficiency and quality of performance of the work process of potato heap separation can be achieved by means of improving the design of the vibrational spiral separator and substantiating theoretically its rational parameters under the condition of eliminating damage to the potato tubers. An equivalent schematic model of the interaction between the potato tuber and the surface of the cantilever spiral springs has been devised. On the basis of the model, the kinematic characteristics of the tuber's flight and its impact contact with the elastic surface of the over mounted rebounding conveyor have been investigated. A new analytical mathematical model of the potato tuber's flight from the surface of the spiral separator and its subsequent encounter with the rebounding conveyor mounted above the spiral springs has been developed. New analytical dependences have been obtained for finding out the distance and height of the potato tuber's flight to the point of impact contact as well as the trajectory equation for the travel to the said contact, which makes it possible to obtain the kinematic constraints imposed on the allowed rate of travel under the condition of not damaging the tuber. On the basis of the obtained analytical dependences, the kinematic parameters of the improved design of the spiral potato harvester separator in its interaction with a potato tuber under the condition of not damaging the latter have been investigated.

Key words: potato, tuber, harvester, spiral separator, rebounding.

INTRODUCTION

Cultivation and harvesting of potatoes is one of the most power- and material-intensive production processes in agriculture. For example, regarding the power consumption, it features about 4–5 times greater specific energy costs as compared to the energy spent for the production of a unit of cereal crops (Petrov, 2004). Therefore, the issue of cutting down those parameters in the production of potatoes is urgent and, in the continued process of developing and improving the tools of potato harvesters and optimising their parameters, it is necessary not only to increase their quality indicators, but at the same time to provide for the reduction of their material and energy consumption rates.

The analysis of the process design and structural layout of a majority of potato harvesters and potato combines has shown that the largest share of their total weight is accounted for their separating tools, since the required level of cleanliness of the output product is achieved through the increase of the potato heap separation duration, which implies the respectively greater number and complexity of the tools. This is explained by the fact that the cleaning tools are effectively the main element in the process of ensuring the qualitative indicators of performance of the potato harvester as a whole.

For the purpose of improving the potato harvester's operation quality indicators through the intensification of the process of cleaning the potato tubers from soil impurities and plant debris, we have developed the new design of the spiral potato heap separator (UA43907).

The spiral separator comprises three driven cylindrical spirals mounted in parallel, which are made in the form of spiral springs cantilever-fitted on their drive hubs. During the operation of the spiral separator under consideration, the potato heap to be cleaned is fed to the upper work face created by the spiral springs, the rotation of which results in the entrainment and subsequent sifting downwards of significant masses of soil. At the same time, the potato tubers are moving along the axes of the springs' spiral windings, mostly in the troughs formed by the neighbouring springs, and, due to their violent contacts with the rotating and, at the same time, vibrating spiral springs, the stuck soil is efficiently separated from their side surfaces.

Thus, the main distinctive feature of the spiral potato heap separator under consideration is the presence of sizable gaps between the coils of the springs, in order to let the soil impurities and plant debris immediately pass through and fall down. Also, such a design provides for a significant increase of the effective cleaning area (i.e. the total area of the separating gaps) as compared to the total area of the separator's cleaning surface. This, in its turn, results in the rise of the throughput capacity of the separating surface, which contributes to the growth of the quality indicators of the process of cleaning the heap of tuberous roots from impurities. Moreover, the absence of driving shafts inside the cleaning spirals makes impossible for plant debris to wind on the shafts, while the free space inside each spiral is capable of transporting the soil impurities falling into it along the axis towards the unobstructed face end of the cantilevered spring, then further outside from the separator.

The obstruction of the separating gaps in the spiral separator by caked humid soil is eliminated, because the cleaning spirals are positioned with overlapping and the coils of each cleaning spiral partially enter the gaps between the coils of the neighbouring spiral. Such an arrangement facilitates self-cleaning of the spirals during the operation of the spiral separator.

The undertaken experimental laboratory and field studies of the spiral separator (Bulgakov et al., 2017) mounted on the test unit modelling a single-row potato-digger have shown the high efficiency of its operation.

However, the results of the experimental studies have also proved that some part of potato tubers and also firm soil lumps with the size and mass characteristics similar to those of the tubers overflies the separator's spirals, which results not only in the deterioration of tuber cleaning quality, but in some cases even in the loss of tubers. This happens not only at the initial stage, just as the potato heap is fed to the cleaning surface, but also during the later transfer of the potato bodies from one spiral to the other. Besides, the mentioned effect hinders the further improvement of the separator's performance,

because it imposes limitations on the angular velocities of the rotating spirals.

In order to eliminate the overflight of potato tubers across the spiral separator, an improved design of the latter has been proposed with the introduction of the rebounding plain belt conveyor mounted above the cleaning spirals at a certain angle to the line passing through the centres of axes of the separator spirals (Fig. 1).

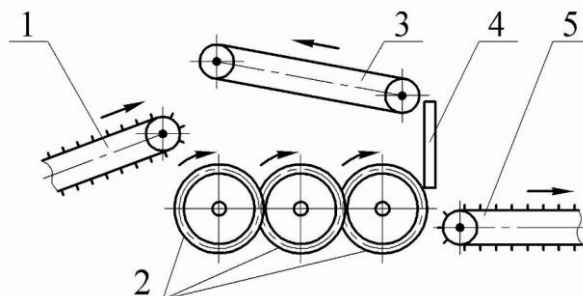


Figure 1. Potato heap separator of improved design (side view): 1 – feeding conveyor; 2 – cantilevered spiral springs of cleaning rolls; 3 – rebounding belt conveyor; 4 – protecting apron; 5 – discharge conveyor.

Due to such an arrangement, during the operation of the improved-design separator, when a potato tuber takes off from the surface of the cleaning spiral and flies up, it hits eventually the down side of the belt of the rebounding conveyor and returns again onto the separating spiral surface.

It has become evident from the analysis of a large number of scientific publications and patent studies that the potato heap separators must be capable of not only reliably performing the work process with good quality, but also continuously self-cleaning during the operation. It is common knowledge that the systems of separating tools used on conventional potato combine harvesters not always ensure the high level of soil impurities separation (Petrov, 2004; Wei et al., 2013). The most frequent cause of the shortcoming is the intensive blockage of the separating tool surfaces by the sticking humid soil.

The problem of developing high-efficiency and reliably operating potato heap separators for the harvesting process as well as cleaning systems for fixed-site potato dressing stations is covered in studies (Zaltzman & Schmilovitch, 1985; Feller et al., 1987; Misener & McLeod, 1989; Ichiki et al., 2013; Klindtworth, 2016; Feng et al., 2017). However, despite the great variety of potato heap cleaning work processes and studies on them, the papers on the optimisation of kinematic and design parameters specifically of spiral separators are relatively scarce.

The aim of this study was increasing the efficiency and quality of performance of the potato heap separation work process by means of providing for the retention of potato bodies in the improved design of the vibrational spiral separator and substantiating theoretically its rational parameters under the condition of eliminating potato damage.

MATERIALS AND METHODS

The theoretical study of the potato body retention by the improved potato heap separator has been carried out with the use of fundamental provisions of the mathematics, theoretical mechanics as well as the methods of composing programmes for numerical computation on the PC, plotting graphical dependences and their analysis.

The theoretical substantiation of the parameters of the improved spiral potato heap separator is based on the development of the mathematical model (France & Thornley, 1984) of behaviour of the potato tuber that is first ejected from the surface of the spiral separator, then performs flight upwards and finally interacts with the elastic surface of the rebounding belt conveyor mounted above.

For that purpose it is necessary, first of all, to form the equivalent schematic model of the ejection, subsequent flight and rebound of the potato tuber during the operation of the improved-design spiral separator (Fig. 2). The equivalent schematic model shows the structural elements of the improved spiral separator (two spiral springs mounted alongside each other and rebounding conveyor mounted above them) and designations of their kinematic and design parameters. It shows the potato tuber modelled as a material point, to which the forces acting after the tuber reached the surface of the spiral spring (winding) and started interacting with it are applied.

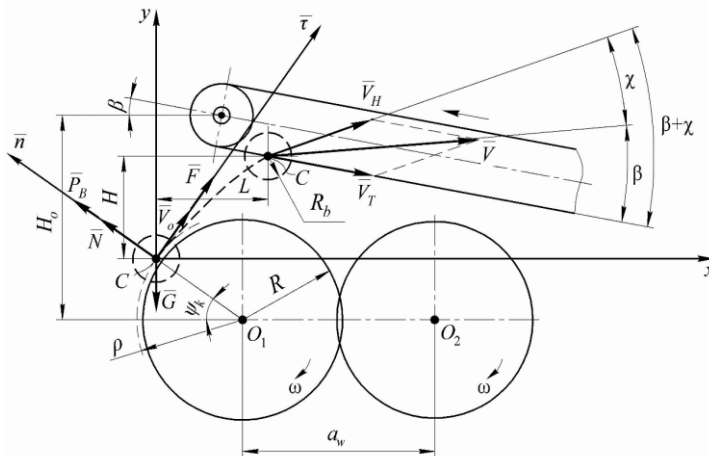


Figure 2. Equivalent schematic model of potato tuber's flight in spiral separator of improved design.

In this model, the potato tuber is analysed sequentially in its two positions: at the point of ejection from the spiral separator and at its impact contact with the surface of the rebounding belt conveyor. In order to simplify the analytical calculations, the potato tuber body is approximated by a full sphere.

RESULTS AND DISCUSSION

First, the motion of the potato tuber with a shape close to the sphere with a determined radius of R_b on the surface of the spiral separator with an outer radius of R , a winding pitch of S and a spiral wire diameter of d_n is examined. The separator's spirals

are installed in series with a center-to-center distance of a_w and some overlapping. The spirals rotate about their figure axes clockwise with equal angular velocities of ω . It is assumed that the separator's spiral at a first approximation is a plain cylindrical surface. The position of the potato tuber on the surface of the spiral is defined by certain radial parameter ρ and angular parameter ψ . The interaction between the potato tuber and the spiral's surface can take place in either of the following two ways (Bulgakov et al., 2017):

- tuber moving on the surface of the spiral coil with a one-point contact;
- tuber moving in the intercoil space of the spirals.

Therefore, the radial parameter ρ for these options is equal to, respectively:

- in case of motion in the intercoil space:

$$\rho = \left(R - \frac{d_n}{2} \right) + \frac{1}{2} \sqrt{(d_n - 2R_b)^2 - S^2}, \quad (1)$$

- in case of motion on the outer surface of the spiral:

$$\rho = R + R_b. \quad (2)$$

When a certain critical value $\psi = \psi_k$ of the angular parameter is reached, the potato tuber takes off from the spiral surface. This becomes possible, when the normal reaction of the spiral coil is $N = 0$. In order to consider that, the schematic diagram of the forces acting on the potato tuber with a specified mass of m and the centre in the point C during its motion on the surface of a spiral in the cleaning unit (Fig. 3) is to be examined. In this schematic diagram \vec{G} – force of gravity; \vec{N} – force of spiral's normal reaction vectored normally to the trajectory of relative motion of the tuber body on the spiral; \vec{F} – force of sliding friction of the tuber body on the surface of the spiral; \vec{P}_b – centrifugal force of inertia vectored normally to the trajectory of motion.

Let's investigate the relative motion of the potato tuber on the spiral's surface at the moment of its take-off from the said surface in the natural system of coordinates $\bar{\tau}C\bar{n}$ with the origin set at the point C – the centre of the potato tuber.

In accordance with the set up schematic diagram of forces, the equations of the relative motion in its projections on the axes $\bar{\tau}$ and \bar{n} of the mentioned natural system of coordinates can be written in the form of the following system of differential equations:

$$\left. \begin{aligned} ma_\tau &= F, \\ ma_n &= N + P_B - G \sin \psi_k. \end{aligned} \right\} \quad (3)$$

Since the potato tuber's motion takes place only along the tangential axis τ , then $a_n = 0$ and, consequently, the following is derived from the second equation of the system (3):

$$N + P_B - G \sin \psi_k = 0. \quad (4)$$

Hence, taking into account the condition that the potato tuber takes off from the spiral's surface ($N = 0$), the value of the angular parameter ψ_k , at which the potato tuber takes off from the spiral's surface, can be found. It is obtained as follows:

$$\sin \psi_k \geq \frac{P_B}{G}. \quad (5)$$

As

$$G = mg \quad (6)$$

and

$$P_B = m\omega^2 \rho_i, \quad (7)$$

then:

$$\psi_k \geq \arcsin \frac{\omega^2 \rho_i}{g}. \quad (8)$$

As regards the first equation in the system (3): at the moment, when the tuber takes off from the spiral's surface, the force \bar{F} goes to zero; accordingly, the tangential acceleration a_t also becomes equal to zero. Hence, when the potato tuber starts moving away from the separator's spiral, the initial velocity of its motion V_0 has a specific value. Having completed its flight in the space between the spiral and the rebounding conveyor, the potato tuber reaches the lower flight of the rebounding belt conveyor. It is possible to determine the point of (impact) contact between the potato tuber and the rebounding conveyor as well as the velocity attained by the tuber by that point. For that purpose, it is assumed that the potato tuber, taking off from the spiral's surface at an angular position of ψ_k , has the initial motion velocity V_0 of the following value:

$$V_0 = \omega \rho. \quad (9)$$

In accordance with the known relations (Petrov, 2004), the distance and height of the potato tuber's flight are determined on the basis of the following formulae:

$$L = V_0 t \cdot \cos \psi_k \quad (10)$$

and

$$H = V_0 t \cdot \sin \psi_k - \frac{gt^2}{2} \quad (11)$$

After the time parameter t is eliminated from the relations (10) and (11) and they are combined with each other, the expression describing the potato tuber centre's motion trajectory in the form of the relation between the height and the distance of its flight is obtained:

$$H(L) = L \tan \psi_k - \frac{gL^2}{2V_0^2 \cos^2 \psi_k}. \quad (12)$$

Whereby at the point situated at a height of H the potato tuber will have the following rate of travel:

$$\begin{aligned} V_H &= \sqrt{V_0^2 - 2gH} = \\ &= \sqrt{V_0^2 - 2g \left(L \tan \psi_k - \frac{gL^2}{2V_0^2 \cos^2 \psi_k} \right)}. \end{aligned} \quad (13)$$

If a fixed Cartesian coordinate system xCy with the horizontal axis x , the vertical axis y and the origin at the potato tuber's centre C at the moment, when the tuber takes off from the spiral's surface, is set and the parameters L and H in the expression (12) are replaced by the current coordinates x and y , respectively, then the law of the tuber's flight in this coordinate system will assume the following appearance:

$$y(x) = x \cdot \operatorname{tg} \psi_k - \frac{gx^2}{2V_0^2 \cos^2 \psi_k}. \quad (14)$$

In the design of the improved spiral potato heap separator, a rebounding belt conveyor is installed at a height of H_o relative to the centre of the first spiral at an angle of β to the horizon with a tilt towards the process mass conveyor. Its surface (the working lower flight) in the same coordinate system is described by the following equation:

$$y(x) = H_o - (\rho + R_b) \sin \psi_k - x \tan \beta \quad (15)$$

Obviously, the point C of the contact between the potato tuber and the rebounding conveyor is the point of intersection of the tuber's flight trajectory (14) and the conveyor's surface (described by the expression (15)). Therefore, the coordinates of the mentioned point of contact in the reference system xCy can be determined by solving the system of equations (14)–(15). Since the left-hand sides of the said equations are in this case equal to each other, then the right-hand sides of the equations can be equated and, after certain transformations, the following quadratic equation in the unknown coordinate x is obtained:

$$\begin{aligned} & \frac{gx^2}{2V_o^2 \cos^2 \psi_k} - (\tan \beta + \tan \psi_k) x + \\ & + [H_o - (\rho + R_b) \sin \psi_k] = 0. \end{aligned} \quad (16)$$

By solving the obtained equation, the value of the distance of the tuber's flight to the point of contact and interaction with the rebounding belt conveyor is found:

$$\begin{aligned} x = & \frac{V_o^2 \cos^2 \psi_k}{g} \cdot \left\{ \tan \left(\tan \beta + \tan \psi_k \right) + \right. \\ & \left. + \sqrt{\left(\tan \beta + \tan \psi_k \right)^2 - \frac{2g [H_o - (\rho + R_b) \sin \psi_k]}{V_o^2 \cos^2 \psi_k}} \right\}. \end{aligned} \quad (17)$$

The height of the potato tuber centre's flight and the velocity of its motion at the point of contact C is determined by means of substituting the solution (17) into the expressions (15) and (13), respectively.

The potato tuber's velocity V_H at the point of contact C is vectored at an angle of χ to the horizon; its tangent is determined as the derivative of the function (14) with respect to the argument x :

$$\tan \chi = \frac{dy}{dx} = \tan \psi_k - \frac{gx}{V_o^2 \cos^2 \psi_k}. \quad (18)$$

The resulting velocity \bar{V} of the potato tuber at the impact is equal to the vector sum of the tuber's velocity \bar{V}_H at the point of contact C and the linear velocity \bar{V}_T of the rebounding conveyor:

$$\bar{V} = \bar{V}_H + \bar{V}_T \quad (19)$$

or

$$V = \sqrt{V_H^2 + V_T^2 - 2V_H V_T \cos \left(\widehat{V_H, V_T} \right)}, \quad (20)$$

where $\cos \left(\widehat{V_H, V_T} \right)$ – direction cosine of the potato tuber's velocity vector \bar{V}_H at the moment of its contact with the rebounding conveyor's velocity vector V_T .

According to the schematic model (Fig. 2):

$$\cos\left(\widehat{V_H, V_T}\right) = -\cos(\beta + \chi). \quad (21)$$

Hence, the resulting velocity V of the potato tuber is equal to:

$$V = \sqrt{V_H^2 + V_T^2 + 2V_H V_T \cos(\beta + \chi)}. \quad (22)$$

In order to meet the condition of undamaged potato tubers at the output, it is necessary for their resulting velocity V after the impact not to exceed the maximum acceptable value, which, according to Petrov (2004), is assumed to be equal to 4–5 m s⁻¹. After the expression (13) is substituted in the expression (20) and the above-mentioned limitation on the potato tuber's velocity V after the impact is taken into account, the following kinematic condition, which ensures the tuber remaining undamaged during its impact on the rebounding conveyor's surface, is obtained:

$$\sqrt{\omega^2 \rho^2 - 2g \left[L \cdot \tan \psi_k - \frac{gL}{2\omega^2 \rho^2 \cos^2 \psi_k} \right] + V_T^2} + 2\sqrt{\omega^2 \rho^2 - 2g \left[L \cdot \tan \psi_k - \frac{gL}{2\omega^2 \rho^2 \cos^2 \psi_k} \right]} V_T \cos(\beta + \chi) \leq [V]. \quad (23)$$

The implementation of the obtained relation (23) with the use of application software for the PC has allowed to determine the parameters of the improved design of the spiral separator that would operate without damaging the potato tubers or losing them; that, in its turn, would result in the increase of the spiral separator's productivity.

Using the specially developed PC programme, numerical calculations have been performed in the Mathcad environment, which has enabled plotting the following curves (Fig. 3–5).

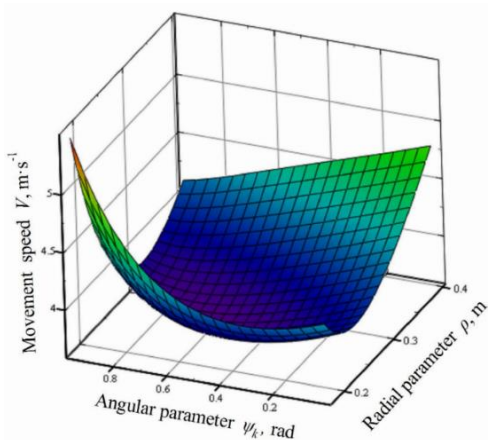


Figure 3. Relation between potato tuber's velocity and angular parameter ψ_k and radial parameter ρ .

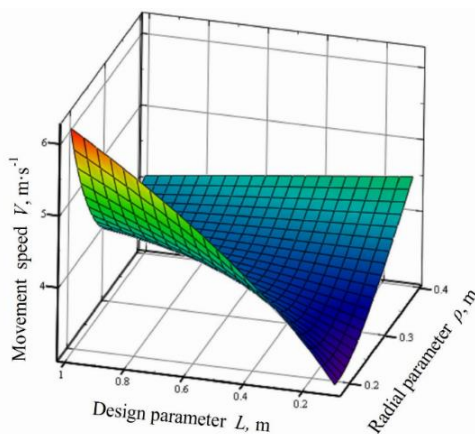


Figure 4. Relation between tuber's velocity and design parameter L and radial parameter ρ .

As may be inferred from the curves in Fig. 3, the angular parameter ψ_k can be selected on the basis of the values of the radial parameter within a range of $\rho = 0.24 \dots 0.27$ m, which corresponds to the values of the former within a range of $0.4 \dots 0.6$ rad. Any other values of ρ are undesirable, as they bring about the increase of the spiral separator's overall dimensions. The results presented in Fig. 4 prove that preference is to be given to lengths L within a range of $0.2 \dots 0.5$ m, based on the earlier accepted values of ρ . Also, on the assumption of the above-accepted design parameters of the spiral separator (ρ and L), the radial parameter ψ_k is to have the values indicated earlier, i.e. $\psi_k = 0.4 \dots 0.6$ rad, which becomes obvious from Fig. 5.

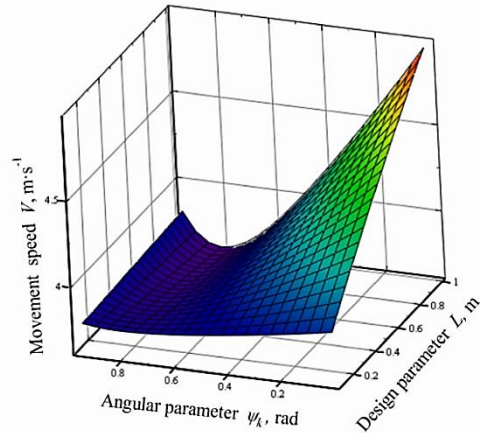


Figure 5. Relation between tuber's velocity and angular parameter ψ_k and design parameter L .

During the experimental studies, the quality characteristics of the cleaning of potato tubers from soil impurities and plant residues as well as their loss and damaging in relation to the spiral separator's design and kinematic parameters (Bulgakov et al., 2017) were assessed. The statistical analysis of the results of the experimental studies provided for obtaining the graphical dependences that show the potato tuber loss and damage rates as functions of the pilot unit's travel speed (Fig. 6).

The dependences between the potato tuber loss and damage rates and the linear velocity of the separator's spiral coils in the presence of the rebounding belt conveyor mounted above are shown in Fig. 7.

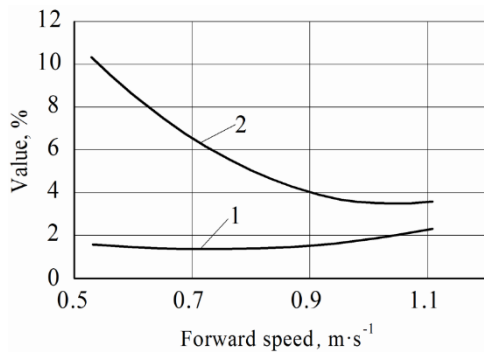


Figure 6. Relation between potato tuber loss (1) / damage (2) rates and field pilot unit travel speed (Bulgakov et al., 2017).

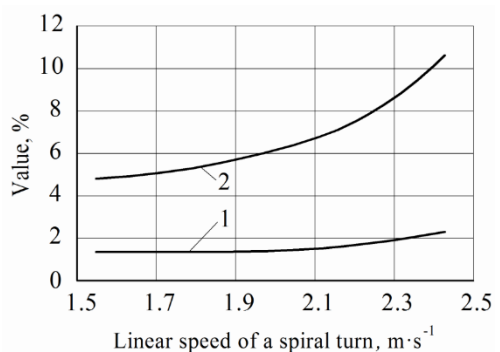


Figure 7. Relation between potato tuber loss (1) / damage (2) rates and linear (circumferential) velocity of spiral's outside surface.

As is seen from the curves in Fig. 7, the rebounding conveyor recovers virtually 100% of the departing potato tubers. Their loss rate stays below 2%. As regards the tuber damaging, its rate does not exceed 4...6% as long as the linear velocity of the spiral coils' working surfaces stays within a range of up to 2 m s⁻¹. Thus, the damage to tubers is caused mainly by the initial impacts of the fed potato tubers on the spirals and not by their "tossing" or their impacts on the belt of the rebounding conveyor.

The repulsion of potato tubers and their subsequent flying are most probable and possible only during the initial loading of the spiral separator or in case of the potato body transfer from one spiral to the next one, i.e. when it moves perpendicular to the axis. But, in the latter case the transfer of single potato tubers from one spiral to the other one takes place virtually without the tuber departing from the coil surface or hitting it (there is simply no cause for any other kind of movement, such as take-off and flight), the adjacent spirals rotate at equal angular velocities, the potato bodies in this scenario travel only for negligible distances and virtually in continuous contact with the surface. It has been established by experiments that the transfer from one spiral to the other one is possible only under the impact of the new inflow of the fed heap, which in effect propels the cleaned potato heap forward.

On the other hand, if the progression of the potato body along the spiral's axis has already started, the take-off and flight of the potato body towards the rebounding conveyor is impossible. In that event, the potato body captured by the coils of the two adjacent spirals will travel in continuous contact and without impacts along the spirals' axes towards their ends.

CONCLUSIONS

1. A new analytical mathematical model of the potato tuber's flight from the surface of the spiral separator with an improved design up to its impact on the above-mounted rebounding conveyor has been developed.

2. On the basis of the obtained analytical dependences, the kinematic parameters of the improved-design spiral potato harvester separator during its interaction with the potato tuber subject to a condition of not damaging the product have been theoretically investigated.

3. The following design parameters of the spiral separator are to be considered reasonable under the condition of not damaging the potato tubers: $\rho = 0.24...0.27$ m, $\psi_k = 0.4...0.6$ rad and $L \leq 0.5$ m.

REFERENCES

- Bulgakov, V., Ivanovs, S., Adamchuk, V. & Ihnatiev, Y. 2017. Investigation of the influence of the parameters of the experimental spiral potato heap separator on the quality of work. *Agronomy Research* **15**(1), 44–54.
- Feller, R., Margolin, E., Hetzroni, A. & Galili, N. 1987. Impingement angle and product interference effects on clod separation. *Transactions of the American Society of Agricultural Engineers* **30**(2), 357–360.
- Feng, B., Sun, W., Shi, L., Sun, B., Zhang, T. & Wu, J. 2017. Determination of restitution coefficient of potato tubers collision in harvest and analysis of its influence factors. *Nongye Gongcheng Xuebao/Transactions of the Chinese Society of Agricultural Engineering* **33**(13), 50–57.

- Thornley, J.H.M. & France, J. 2007. *Mathematical Models in Agriculture: Quantitative Methods for the Plant, Animal and Ecological Sciences*. CABI, 906 pp.
- Ichiki, H., Nguyen Van, N. & Yoshinaga, K. 2013. Stone-clod separation and its application to potato in Hokkaido. *Engineering in Agriculture Environment and Food* **6**(2), 77–85.
- Klindtworth, M. 2016. Potato Technology. In: Frerichs, L (Hrsg): *Jahrbuch Agritechnik 2015*. Braunschweig: Institut für mobile Maschinen und Nutzfahrzeuge, 1–12.
- Misener, G.C. & McLeod, C.D. 1989. Resource efficient approach to potato-stone-clod separation. *AMA, Agricultural Mechanization in Asia, Africa and Latin America* **20**(2), 33–36.
- Petrov, G. 2004. *Potato harvesting machines*. Mashinostroeniye, Moskow, 320 pp (in Russian).
- Zaltzman, A. & Schmilovitch, Z. 1985. Evolution of the potato fluidized bed medium separator. Summer meeting – American Society of Agricultural Engineers, *Engineering the Future – Harnessing Nature Through Technology*, 27 p.
- Wei, H., Wang, D., Lian, W., Shao, S., Yang, X. & Huang, X. 2013. Development of 4UFG-1400 type potato combine harvester. *Transactions o the Chinese Society of Agricultural Engineering* **29**(1), 11–17.

Theory of impact interaction between potato bodies and rebounding conveyor

V. Bulgakov¹, S. Nikolaenko¹, V. Adamchuk², Z. Ruzhlyo¹ and J. Olt^{3,*}

¹National University of Life and Environmental Sciences of Ukraine, 15, Heroyiv Oborony street, UA03041 Kyiv, Ukraine

²National Scientific Centre, Institute for Agricultural Engineering and Electrification, 11, Vokzalna street, Glevakha-1, Vasylkiv District, UA08631 Kiev Region, Ukraine

³Estonian University of Life Sciences, Institute of Technology, Kreutzwaldi 56, EE51014 Tartu, Estonia

*Correspondence: jyri.olt@emu.ee

Abstract. In order to increase substantially the quality of the potato heap separation, it is necessary to carry out the theoretical substantiation of the spiral separator's parameters with regard to the impact interaction between the product and the tools of the unit under the condition of not damaging the tubers. An equivalent schematic model of the impact interaction between a potato tuber and the surface of the rebounding conveyor has been devised. Taking into account the coefficient of restitution of the tuber's velocity in case of an impact, new analytical expressions have been obtained for determining the magnitude and direction of the potato tuber's velocity after the impact. They provided the basis for applying the principle of momentum at impact and obtaining the analytical expressions that allow determining the impact impulse and impact force at the impact of the tuber on the surface of the rebounding conveyor and, eventually, the dynamic constraints on the permitted velocity of the tuber prior to the impact interaction under the condition of not damaging it. A new analytical mathematical model of the impact interaction of the potato tuber during the potato heap separation has been developed. On the basis of the obtained theoretical results, studies have been carried out on the rational kinematical parameters of the high-quality performance of the above-mentioned work process under the condition of keeping the potato tubers undamaged.

Key words: potato, tuber, heap separation, impact interaction, impact impulse, rational parameters.

INTRODUCTION

As is known the potato growing is one of the agriculture sectors, where the energy consumption rates are rather high. Hence, in the development of new tools for potato harvesters and the improvement of the existing ones it is necessary to provide for the significant reduction of their energy consumption rates and the substantial increase of the output quality coupled with the minimal loss of product in the harvesting operations. One of the essential process operations in the harvesting of potatoes is the separation of the potato heap, which ensures the cleanliness of the delivered product. Thus, the cleaning tools play the principal role in securing the high performance quality indicators

of potato harvesters. With that objective in mind, a new design of the potato heap separator has been developed (patent UA43907).

The experimental studies have shown that some part of the potato tubers, as well as the ground impurities with the size and mass characteristics similar to those of the tubers, overflies the cleaning tools and falls either on the field surface or on the discharge conveyor (Bulgakov et al., 2017). That results, on the one hand, in yield losses and, on the other hand, in the contamination of the obtained product with ground impurities.

Therefore, in order to eliminate the overflight of tubers above the separator, it is proposed to install a rebounding plain rubber belt conveyor. With such an arrangement, the tuber that has taken off from the separating surface will hit the elastic surface of the rebounding conveyor and returns back to the separating surface. Though, the impact interaction between the tuber and the conveyor's surface can result in damage to the former and that can reduce the overall quality of the product. Thus, to provide for the potato tubers remaining intact after the impact interaction is a rather relevant task, which is impossible to solve without carrying out theoretical research, in particular, developing the necessary mathematical model of the impact interaction. That model will provide the basis for substantiating the rational kinematic parameters of the separator's operation under the condition that potato tubers remain undamaged during the harvesting operations.

The separating tools used in state-of-the-art potato harvesters must not only ensure the reliable, high-quality performance of the work process of cleaning potato tubers from ground impurities, plant residues and stuck ground, but also be capable of self-cleaning during operation, which would provide for the required performance rate. However, it is known that the majority of separating tool systems employed in conventional potato harvesters not always ensure the high level of separation of ground impurities (Petrov, 2004). Most often this happens because of the heavy clogging of the separating tools' cleaning surfaces with wet ground.

Quite a few scientists and designers have worked on the problem of developing efficient and reliable potato heap separators as well as various cleaning systems for the use in stationary potato cleaning facilities (Zaltzman & Schmilovitch, 1985; Feller et al., 1987; Ichiki et al., 2013; Wei et al., 2013; Feng et al., 2017). Spiral separators are considered to be the most promising and technologically appropriate for the performance of the potato tuber cleaning process during the extraction of the tubers from soil under various edaphic and climatic harvesting conditions. However, while there is quite a number of existing potato heap cleaning technologies, the studies on the optimisation of the kinematic and design parameters of spiral separators are relatively few. That is especially true as regards the issue of establishing the conditions for preventing damage to potato tubers during their interaction with spiral windings, rebounding from various surfaces and further impact contacts with other tools.

The aim of this study was improving the efficiency and quality of the potato heap separation through the theoretical substantiation of the separator's rational parameters subject to the condition that the tubers are not damaged during their impact interactions.

Therefore, the potato tuber rebounded from the translationally moving rubber belt of the rebounding conveyor will land now on the other spirals of the separator (the belt completely decelerates the tuber's flight): after the collision, the tuber will come down already at a small velocity (in effect tangentially) and, after travelling a very short distance, land now ahead, on the next spiral. But, this landing will not cause a significant impact effect, since almost the whole cleaning surface of the spiral separator will be completely covered with soil impurities and plant residues, hence, the 'return' of the potato tuber repulsed by the rebounding conveyor will be virtually shock-free. The tuber under consideration can sustain a repeated impact, if it hits another potato tuber. But that negative possibility can be eliminated by adjusting the inclination of the rebounding conveyor belt relative to the plane of the cleaning surface. Then the repeated impacts will certainly be oblique and have a small effect on the overall rate of damage sustained by the potato tuber bodies during their cleaning in the spiral separator.

Since the normal component of the impact impulse plays the decisive role in the process of the mentioned impact contact, it is reasonable, for the purpose of investigating the process of collision, to establish the natural system of coordinates $\bar{t}C\bar{n}$ with the origin set at the potato tuber's centre (point C), the axis \bar{t} directed parallel to the rebounding conveyor's lower flight, the axis \bar{n} – perpendicular to the said flight (i.e. along the line of action of the normal component of the impact impulse) (Fig. 1).

The following velocity vectors have to be shown in the equivalent schematic model:

\bar{V}_1 – potato tuber's velocity prior to collision;

\bar{V}_2 – velocity of rebounding conveyor's belt;

\bar{U}_1 – potato tuber's velocity after collision.

In this case, the velocity vector \bar{V}_1 is directed at an angle of χ to the horizon, the velocity vector \bar{V}_2 – at an angle of β to the horizon.

As a result, the angle between the vectors \bar{V}_1 and \bar{V}_2 is equal to $\beta + \chi$ (Fig. 1).

RESULTS AND DISCUSSION

On the basis of the aforesaid, the collision between a potato tuber with a mass of m and the rotating rebounding conveyor (its moving lower flight) with a mass of M , which moves with a velocity of \bar{V}_2 , will be analysed. In comparison with the potato tuber's mass, it can be assumed that the rebounding conveyor's mass $M \rightarrow \infty$. Also, it is assumed that the impact is oblique and partially elastic (coefficient of restitution during the impact interaction $k < 1$) (Wriggers, 2006).

The velocities of the potato tuber and the rebounding conveyor after the impact can be determined following the general technique described in Petrov (2004), which is applicable for the most general case of the collision between two bodies, which have different masses and velocities. In accordance with the mentioned technique, first, the projections of the velocities on the coordinate axes \bar{n} and \bar{t} are determined for the potato tuber and the rebounding conveyor prior to the impact. According to Fig. 1, they will be:

$$\begin{aligned} V_{1n} &= V_1 \sin(\beta + \chi), & (1) \\ V_{1t} &= V_1 \cos(\beta + \chi); \quad V_{2n} = 0; \quad V_{2t} = V_2. \end{aligned}$$

Further, in accordance with the same technique, the projection of the common velocity \bar{U} of both bodies on the axis \bar{n} at the end of the perfectly inelastic collision is determined. It will be:

$$U_n = \frac{mV_{1n} + MV_{2n}}{m + M} \quad (2)$$

Since $V_{2n} = 0$ and $M \rightarrow \infty$, the final result is $U_n = 0$.

Hence, the projections of the velocities of the potato tuber and the rebounding conveyor prior to the impact on the coordinate axes \bar{n} and $\bar{\tau}$ will be determined by the following expressions:

$$\begin{aligned} U_{1\tau} &= V_{1\tau}, \\ U_{2\tau} &= V_{2\tau}, \\ U_{1n} &= U_n(k+1) - kV_{1n}, \\ U_{2n} &= U_n(k+1) - kV_{2n}. \end{aligned} \quad (3)$$

After substituting the found values of the projections of the velocities prior to the impact (1) and the value $U_n = 0$ into (3), the following is obtained:

$$\begin{aligned} U_{1\tau} &= V_1 \cos(\beta + \chi), \\ U_{2\tau} &= V_2, \\ U_{1n} &= -kV_1 \sin(\beta + \chi), \\ U_{2n} &= 0. \end{aligned} \quad (4)$$

Meanwhile, the magnitudes of the velocities of the potato tuber and the rebounding conveyor after the impact are equal to, respectively:

$$\begin{aligned} U_1 &= \sqrt{U_{1\tau}^2 + U_{1n}^2} = V_1 \sqrt{\cos^2(\beta + \chi) + k^2 \sin^2(\beta + \chi)}, \\ U_2 &= \sqrt{U_{2\tau}^2 + U_{2n}^2} = V_2. \end{aligned} \quad (5)$$

The directions of the velocities of the bodies after the impact make angles with the normal line, their tangents being equal to:

$$\begin{aligned} \tan(\hat{\bar{n}}, \hat{\bar{U}}_1) &= \frac{U_{1\tau}}{U_{1n}} = -\frac{\text{ctg}(\beta + \chi)}{k}, \\ \tan(\hat{\bar{n}}, \hat{\bar{U}}_2) &= \frac{U_{2\tau}}{U_{2n}} = \infty. \end{aligned} \quad (6)$$

The next step is to find out the force of impact of the potato tuber on the moving flat surface of the rebounding conveyor.

In order to do that, the principle of momentum will be applied to the potato tuber during the collision; in the vector notation, it will appear as follows:

$$m(\bar{U}_1 - \bar{V}_1) = \bar{S}, \quad (7)$$

where m – mass of tuber; $M \rightarrow \infty$ – impact impulse.

The equation (7) of the tuber's impact on the moving flat surface of the rebounding conveyor can be broken down into its projections on the axes \bar{n} and $\bar{\tau}$. That will produce:

$$\left. \begin{aligned} m(U_{1n} - V_{1n}) &= S_n, \\ m(U_{1\tau} - V_{1\tau}) &= S_\tau. \end{aligned} \right\} \quad (8)$$

After substituting the values of the velocity projections $U_{1n}, V_{1n}, U_{1\tau}, V_{1\tau}$ that were obtained earlier into (8), the following values will be obtained for the projections of the impact impulse on the axes \bar{n} and $\bar{\tau}$:

$$\left. \begin{aligned} S_n &= -mV_1 \sin(\beta + \chi) \cdot (k + 1), \\ S_\tau &= 0. \end{aligned} \right\} \quad (9)$$

Taking into consideration the fact that the total impulse S is determined by the following expression:

$$S = \sqrt{S_\tau^2 + S_n^2}, \quad (10)$$

it follows that $S = S_n$, i.e.:

$$S = -m \cdot (k + 1) \cdot V_1 \sin(\beta + \chi). \quad (11)$$

After having found the impact impulse S , it becomes possible to determine at a certain approximation the force of impact F_{imp} of the potato tuber on the moving belt of the rebounding conveyor.

With that aim in view, the integral expression of the impact impulse in terms of the impact force (Dreizler & Lüdde, 2010) will be employed:

$$\bar{S} = \int_{t_0}^{t_0 + \Delta t} \bar{F}_{imp} dt, \quad (12)$$

where \bar{F}_{imp} – impact force; Δt – duration of impact.

Subsequently, in accordance with the mean-value theorem from the integral calculus, the following can be written down:

$$S = F_{imp.av.} \Delta t, \quad (13)$$

where $F_{imp.av.}$ – average impact force for the time of impact Δt .

It can be found from (13) that:

$$F_{imp.av.} = \frac{S}{\Delta t}. \quad (14)$$

According to (Dreizler & Lüdde, 2010), the maximum impact force F_{imp} will approximately be equal to:

$$F_{imp} = 2F_{imp.av.}, \quad (15)$$

or, taking into account (14),

$$F_{imp} = \frac{2S}{\Delta t}. \quad (16)$$

The substitution of the expression (11) into the expression (16) produces:

$$F_{imp} = -\frac{2m(k+1)V_1 \sin(\beta + \chi)}{\Delta t}. \quad (17)$$

The sign ‘-’ in the expressions (11) and (17) indicates that the direction of the vectors \vec{S} and \vec{F}_{imp} is opposite to the direction of the axis \vec{n} . Nevertheless, in this case the magnitudes of these values are of primary importance, therefore, the sign ‘-’ can be omitted in the following expressions.

Obviously, in order to prevent damage to the potato tuber, it is necessary to provide for the following condition being fulfilled:

$$F_{imp} \leq [F_{imp}], \quad (18)$$

where $[F_{imp}]$ – permissible force of impact of the potato tuber on the surface of the rebounding conveyor, at which the tuber remains intact.

Thus, taking into account the expression (17), the following inequation is arrived at:

$$\frac{2m(k+1)V_1 \sin(\beta + \chi)}{\Delta t} \leq [F_{imp}]. \quad (19)$$

It is possible to derive from the obtained inequation (19) the limit for the magnitude of the potato tuber’s velocity V_1 prior to its collision with the surface of the rebounding conveyor, set by the requirement to prevent damage to the tuber. The said velocity limit actually represents the condition for the potato tuber’s impact interaction without damaging it, and it will hold true in case of tubers colliding with any surface. The limit of the velocity magnitude is:

$$V_1 \leq \frac{[F_{imp}] \Delta t}{2m(k+1) \sin(\beta + \chi)}. \quad (20)$$

Thus, the dynamic condition has been obtained that ensures ruling out damage to the potato tuber during its collision with a moving or static surface, in this particular case – the surface of the rebounding belt conveyor.

Having calculated the permissible velocity V_1 of the potato tuber prior to the impact, it is possible to determine the design and kinematic parameters of the separating tool that will provide that velocity. At the same time, in the paper (Bulgakov et al., 2018) a formula was obtained for finding the potato tuber’s velocity prior to the impact in case of the spiral separator, i.e. the velocity of the tuber’s free flight:

$$V_1 = \sqrt{V_o^2 - 2gH}, \quad (21)$$

where H – height of trajectory of the potato tuber’s flight from the separating surface to the point of impact contact; V_o – potato tuber’s velocity at the moment of taking off from the separating surface.

Subsequently:

$$V_1^2 = V_o^2 - 2gH, \quad (22)$$

or

$$V_o^2 = V_1^2 + 2gH. \quad (23)$$

From the expression (23), it is possible to determine the value V_o , which will be equal to:

$$V_o = \sqrt{V_1^2 + 2gH}. \quad (24)$$

Since:

$$V_o = \omega \rho_i, \quad (25)$$

where ω – angular velocity of rotation of the cleaning spiral about its longitudinal axis, and

$$\rho = R + R_b, \quad (26)$$

where R – radius of the cleaning spiral; R_b – radius of the potato tuber, the following is obtained from the expression (24), taking into account the expressions (25) and (26):

$$\omega(R + R_b) = \sqrt{V_1^2 + 2gH}. \quad (27)$$

Finally, the permissible angular velocity of rotation ω of the cleaning spiral under the condition of not damaging the potato tuber will be:

$$\omega = \frac{\sqrt{V_1^2 + 2gH}}{R + R_b}. \quad (28)$$

Similarly, the radius R of the spiral at the specified angular velocity ω of its rotation will be:

$$R = \frac{\sqrt{V_1^2 + 2gH}}{\omega} - R_b. \quad (29)$$

Hence, the value of the potato tuber's flight velocity V_1 determined in accordance with the expression (20), i.e. the limit set for the potato tuber's flight velocity by the condition of having an impact contact without damaging the tuber, can be substituted into the obtained expressions (28) and (29), which are based on the kinematic constraint of the potato tuber's flight velocity prior to the impact.

As a result of the mentioned substitution, the final expressions for ω and R are obtained, which can be used for numerical calculations on the PC.

They are:

$$\omega = \frac{\sqrt{\frac{[F_{imp}]^2 \Delta t^2}{4m^2 (k+1)^2 \sin^2(\beta + \chi)} + 2gH}}{R + R_b}, \quad (30)$$

and

$$R = \frac{\sqrt{\frac{[F_{imp}]^2 \Delta t^2}{4m^2 (k+1)^2 \sin^2(\beta + \chi)} + 2gH}}{\omega} - R_b. \quad (31)$$

In order to perform numerical calculations on the PC, it is necessary to specify the constant values (design and force parameters) of the spiral potato heap separator. According to the results of the design efforts, intralaboratory and field laboratory experimental studies performed by us, the above-said parameters have the following values (Table 1).

Table 1. Design and force parameters of spiral potato heap separator

Item no.	Description and designation of parameter	Unit of measurement	Value
1.	Mass of average size potato tuber, m	kg	0.074...0.453
2.	Radius of potato tuber, R_b	m	0.03...0.055
3.	Coefficient of restitution, k	–	0.80
4.	Tilt and β obliquity angles: χ	deg	15...35 25...65
5.	Height of potato tuber's flight path from separating surface to point of impact contact, H	m	0.30
6.	Radius of spiral, R	m	0.065
7.	Duration of impact, Δt	s	0.06
8.	Maximum permissible impact force, $[F_{imp}]$	N	52

Following the results of the numerical calculations performed on the PC with the use of a specially developed software programme, the curves presented in Figs 2–5 have been plotted.

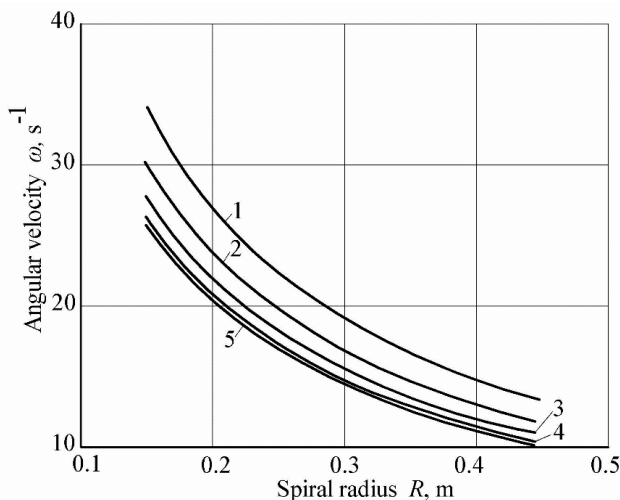


Figure 2. Relation between spiral's angular velocity ω and spiral's radius R at various values of angle χ : 1) $\chi = 25^\circ$; 2) $\chi = 35^\circ$; 3) $\chi = 45^\circ$; 4) $\chi = 55^\circ$; 5) $\chi = 65^\circ$.

The analysis of the relations plotted in Fig. 2 has shown that the increase of the separator spiral's radius R results in the decrease of the permissible angular velocity ω of spiral under the condition of not damaging the tubers, and the increase of the value of the angle χ also implies lower values of the permissible angular velocity ω . The relations presented in Fig. 3 prove that increasing the rebounding conveyor installation height H makes it possible to operate the spiral springs at higher values of the angular velocity ω , which in the end contributes to improving the performance of the spiral potato heap separator.

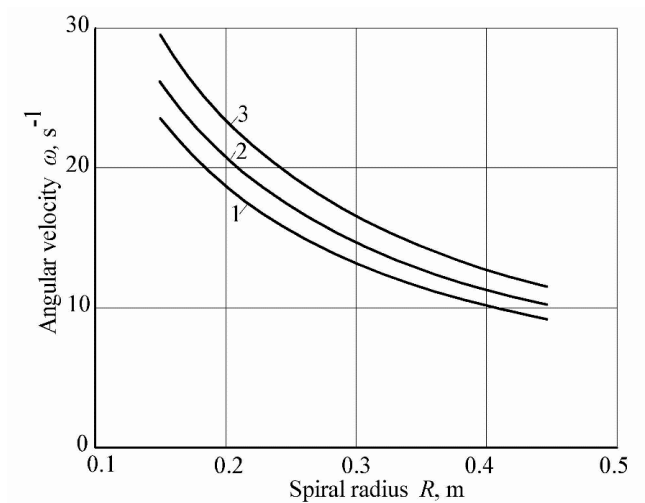


Figure 3. Relation between spiral's angular velocity ω and spiral's radius R at various values of tuber's flight height H : 1) $H = 0.1$ m; 2) $H = 0.35$ m; 3) $H = 0.7$ m.

The analysis of the relations represented by the curves in Fig. 4 has revealed the significant influence of the potato tuber's radius R_b and, accordingly, its mass m on the permissible angular velocity ω of the separator's spirals.

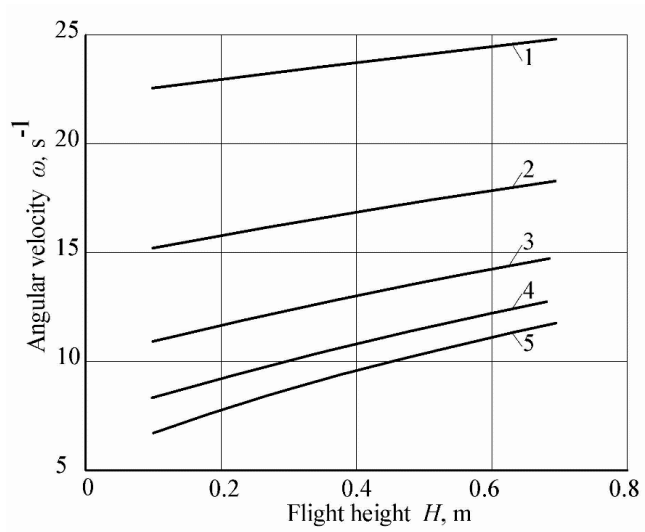


Figure 4. Relation between spiral's angular velocity ω and potato tuber's flight height H at various values of tuber's radius R_b : 1) $R_b = 0.035$ m; 2) $R_b = 0.040$ m; 3) $R_b = 0.045$ m; 4) $R_b = 0.050$ m; 5) $R_b = 0.055$ m.

The relations between the angular velocity ω and the rebounding conveyor's tilt angle β are presented in Fig. 5.

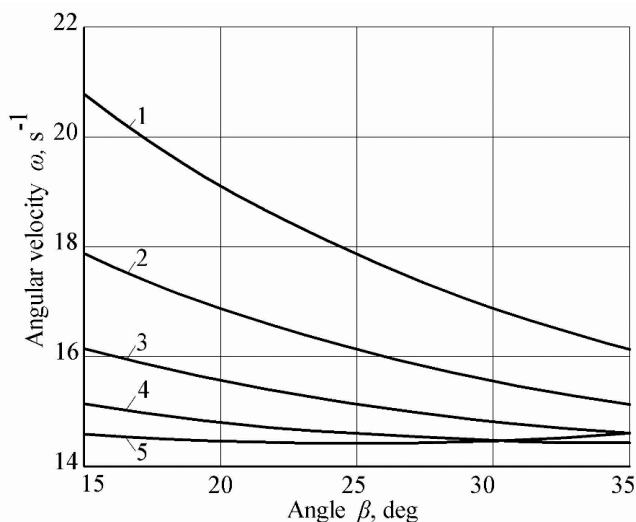


Figure 5. Relation between spiral's angular velocity ω and conveyor's tilt angle β at various values of angle χ : 1) $\chi = 25^\circ$; 2) $\chi = 35^\circ$; 3) $\chi = 45^\circ$; 4) $\chi = 55^\circ$; 5) $\chi = 65^\circ$.

As may be inferred from the presented curves, the mentioned relations are of significance only when the potato tuber's impact angle varies within a range of $\chi = 25\text{--}45^\circ$.

The undertaken experimental laboratory and field studies of the spiral separator (Bulgakov et al., 2017 and 2018) mounted on the test unit modelling a single-row potato-digger have shown the high efficiency of its operation.

CONCLUSIONS

1. A new analytical mathematical model of the impact interaction of the potato tuber during the potato heap separation has been developed.

2. Analytical expressions have been obtained, which allow calculating the impact impulse and impact force, in case of the tuber colliding with the elastic surface of the rebounding conveyor, as functions of the separator's kinematic parameters.

3. The dynamic constraints on the permissible velocity of the potato tuber prior to the impact interaction imposed by the condition of not damaging the tuber have been analytically determined.

4. The obtained relations and the results of the PC-assisted calculations provide for determining the rational parameters of the spiral potato heap separator as well as lead to the conclusion that the mounting height and tilt angle of the rebounding conveyor have to be adjusted depending on the average diameter of the potato tubers R_b . Thus, for an average tuber mass of $m = 0.2$ kg the rational parameters of the spiral separator are as follows: $\chi = 25\text{--}45^\circ$; tuber's flight height $H = 0.15\text{--}0.35$ m; rebounding conveyor tilt angle $\beta = 15\text{--}25^\circ$; angular velocity of the cleaning spirals $\omega = 15\text{--}20$ s⁻¹.

REFERENCES

- Bulgakov, V., Ivanovs, S., Adamchuk, V. & Ihnatiev, Y. 2017. Investigation of the influence of the parameters of the experimental spiral potato heap separator on the quality of work. *Agronomy Research* **15**(1), 44–54.
- Bulgakov, V., Nikolaenko, S., Adamchuk, V., Ruzhylo, Z., Olt, J. 2018. Theory of retaining potato bodies during operation of spiral separator. *Agronomy Research* **16**(1), 41–51.
- Dreizler, R.M. & Lüdde, C.S. 2010. *Theoretical Mechanics*. Springer, 402 pp.
- Feller, R., Margolin, E., Hetzroni, A. & Galili, N. 1987. Impingement angle and product interference effects on clod separation. *Transactions of the American Society of Agricultural Engineers* **30**(2), 357–360.
- Feng, B., Sun, W., Shi, L., Sun, B., Zhang, T. & Wu, J. 2017. Determination of restitution coefficient of potato tubers collision in harvest and analysis of its influence factors. *Nongye Gongcheng Xuebao/Transactions of the Chinese Society of Agricultural Engineering* **33**(13), 50–57.
- Ichiki, H., Nguyen Van, N. & Yoshinaga, K. 2013. Stone-clod separation and its application to potato in Hokkaido. *Engineering in Agriculture Environment and Food* **6**(2), 77–85.
- Misener, G.C. & McLeod, C.D. 1989. Resource efficient approach to potato-stone-clod separation. *AMA, Agricultural Mechanization in Asia, Africa and Latin America* **20**(2), 33–36.
- Petrov, G. 2004. *Potato harvesting machines*. Mashinostroeniye, Moskow, 320 pp (in Russian).
- Zaltzman, A. & Schmilovitch, Z. 1985. Evolution of the potato fluidized bed medium separator. Summer meeting – American Society of Agricultural Engineers, *Engineering the Future – Harnessing Nature Through Technology*, 27 p.
- Wei, H., Wang, D., Lian, W., Shao, S., Yang, X. & Huang, X. 2013. Development of 4UFG-1400 type potato combine harvester. *Transactions of the Chinese Society of Agricultural Engineering* **29**(1), 11–17.
- Wriggers, P. 2006. *Computational contact mechanics*. Springer Berlin Heidelberg. 518 pp. DOI: 10.1007/978-3-540-32609-0.

Effects of fertilization on *Picea abies* stands situated on drained peat soils

G. Cekstere^{1,*}, A. Osvalde¹, V. Nollendorfs¹, A. Karlsons¹, J. Pormale¹,
P. Zalitis², G. Sņepsts², S. Minova³, L. Jankevica³ and M. Laivins²

¹University of Latvia, Institute of Biology, Laboratory of Plant Mineral Nutrition, Miera street 3, LV-2169 Salaspils, Latvia

²Latvian State Forest Research Institute ‘Silava’, Riga street 111, LV-2169, Salaspils, Latvia

³University of Latvia, Institute of Biology, Laboratory of Experimental Entomology and Microbiology, Miera street 3, LV-2169 Salaspils, Latvia

*Correspondence: gunta.cekstere@lu.lv

Abstract. Norway spruce used for afforestation of drained peat soils frequently has low productivity and decay in a long-term, which could be related to soil chemical composition and nutrient status. The research aim was to elucidate the effect of PSM on new Norway spruce plantings (1st experiment) and 20-year-old spruce stands (2nd experiment) on drained peat soils by evaluating: (1) nutrient accumulation in soil-plant system, (2) soil microbiological activity, (3) health status of spruce individuals, (4) growth intensity and productivity of spruce, (5) changes in composition of vascular plant and moss species. The study was conducted at two forest (*Myrtillosa turf.mel.*) sites in Latvia, each consisting of two plots: control and treated with PMS (100 g m⁻² in September 2007, 50 g m⁻² in April 2008). During 2008–2016, regular analysis of soil, spruce needles, soil microbiology, assessment of tree crown vitality, stand productivity, inventory of vascular plant and moss species were done. The results showed that the fertilization with PMS resulted in a significantly improved K, Ca, Zn, and N status of trees, crown vitality and up to three times increased tree growth parameters at both experiments during the study period. The average count of bacteria and fungi in soil of fertilized plots, accompanied by a remarkable variability in the study years, was significantly higher only for the 1st experiment. Fungi: bacteria ratio for the fertilized and control plots differed significantly only for the 1st experiment. Significant increase of cover with nitrophilic plant (*Urtica dioica*, *Antriscus sylvestris*, *Rubus idaeus*) and moss (*Plagiomnium cuspidatum*, *P. ellipticum*) species at both fertilized sites were stated.

Key words: Norway spruce, productivity, mineral nutrition, vegetation, microbiology.

INTRODUCTION

A common practice worldwide is to do afforestation in the soils unlikely suitable for agriculture like peatlands. In many northern countries, peatlands have been extensively drained for forestry (He et al., 2016), e.g., about 4.6 million hectares or 52% of peatlands and wet mineral soil sites have been drained for forestry in Finland (Finnish Statistical Year Book of Forestry, 2014). One of the most suitable commercial forest

species used for afforestation of peatlands is Norway spruce (*Picea abies* (L.) Karst.). Norway spruce is also one of the dominant tree species in forests at the boreo-nemorale climate zone. Unfortunately, the afforestation is not always successful and sustainable. In Latvia, Norway spruce forests cover 18.2% of the total forest area, around 10% of them occurs on drained peat soils (VMD, 2016). Decay and low vitality have been observed mainly for 30–40-year-old pure spruce stands (Lībiete & Zālītis, 2007). During the last decades, spruce dieback has been observed also in various sites in Europe (Malek et al., 2012; Błońska et al., 2015). Low productivity and decay of spruce stands in a long-term frequently could be related to soil chemical composition (Zālītis, 1991; Berger et al., 2009; Moilanen et al., 2010; Błońska et al., 2015).

Important issue for forestry in boreal peatlands is sufficiency or deficiency of K (Finer, 1989; Tripler et al., 2006; Caisse et al., 2008; Moilanen et al., 2010; Sarkkola et al., 2016), B (Möttönen et al., 2005), and other nutrients. Sufficient supply with nutrients promotes not only intensity of tree growth, but also tolerance to diseases and stress conditions (Halmschlager & Katzensteiner, 2017). In this respect, the importance of potassium, copper, zinc, boron, calcium etc. has been specially emphasized (Mengel & Kirkby, 2001; Saarsalmi & Tamminen, 2005).

Soil fertilization is one of the effective forest management tools to increase forest vitality and tree growth (Saarsalmi & Mälkönen, 2001; Moilanen et al., 2015). It has been showed that the effects and success of fertilization varied depending on peat characteristics, nutrient status of stand, dose and kind of applied fertilizers and other factors (Finer, 1989; Zālītis, 1991; Saarsalmi & Tamminen, 2005; Moilanen et al., 2015; Klavina et al., 2016; Libiete et al., 2016; Okmanis et al., 2016; etc.). Nevertheless, there is a lack of information about complex impact of mineral K fertilizers like potassium magnesium sulfate (PMS) application on nutrient status of different age spruce stands, stand productivity, possible fertilization impact on soil microbiological activity and species composition in drained peat soil forests in the boreo-nemoral climate zone. PMS as K source is pH neutral, provides a readily available supply of K, Mg, and S to plants and is acceptable for use in organic crop production. The research aim was to elucidate the effect of PMS on different age Norway spruce stands on drained peat soils by evaluating: (1) nutrient accumulation in soil-plant system, (2) soil microbiological activity, (3) health status of spruce individuals, (4) growth intensity and productivity of spruce, (5) changes in composition of vascular plant and moss species. We hypothesized that fertilization with PMS might improve spruce supply not only with K, Mg and S, but also with other nutrients by significant changes in peat soil chemical composition, microbiological activity and species composition of herb layer plants, thereby facilitating tree growth.

MATERIALS AND METHODS

Site description and experimental design

The study, consisting of two experiments with fertilization, was conducted at two sites (Valka, 57°41'N, 26°09'E, and Kalsnava, 56°40'N, 25°50'E) in Latvia, situated in the boreo-nemoral climatic zone.

The first site 'Valka' is situated on Tālava Lowlands Seda Plain. The quarter sediment depth is 10–20 m. Glaciofluvial sand sediments are dominant, but peat deposits are dominant in relief depressions. The climate is moderately warm and humid: the

average annual amount of precipitations is 610 mm, the average temperature in January is -6.0 °C, in July +16.9 °C, but annual - +5.2 °C (Kļaviņš et al., 2008). The aim of the 1st experiment was to assess the impact of treatment with PMS on new spruce planting developed on drained peat soil. The experiment was set up in a forest glade (*Myrtillosa turf.mel.*, alluvial land), where spruce trees were planted 25 years ago and > 95% decayed during the up-coming 10 years. The peat layer was > 1 m thick, the degree of humification according to Post scale (von Post & Granlund, 1926) varied between H3 and H8 in the 0–0.05 and 0.05–0.20 m layers and between H4 and H8 in the 0.20–0.30 m layer. Before fertilization, all shrubs and trees were sawed down and removed from the research area in August 2007. One experimental plot with a size of 100 m² was used as a control and another with the same size was fertilized with PMS (24.9% K, 6% Mg, 17% S): 100 g m⁻² in September 2007 and 50 g m⁻² during seedling planting in April 2008. 30 one-year-old container seedlings (ca. 20 cm in height) from the local tree nursery ‘Strenci’ were planted in each experimental plot, design of seedling sites: 1.5×2.0 m.

The second site ‘Kalsnava’ is situated on East-Latvian Lowland, Arona Undulating Plain. The depth of quarter sediments is 10–50 m, consisting mainly of sand, gravel, as well as local clay deposits and peat deposits in relief depressions. The climate is also moderately warm and humid: the average annual amount of precipitations is 680 mm, the average temperature in January is -5.8 °C, in July +17.0 °C, but annual - +5.4 °C (Kļaviņš et al., 2008). The aim of the 2nd experiment was to assess the impact of treatment with PMS on 20-year-old spruce stand with low vitality (> 60% defoliation and discoloration of tree crown) growing on drained peat soil. Thus, in 2007, two experimental plots, each with a size of 100 m², were established in the spruce stand (*Myrtillosa turf.mel.*) planted at Kalsnava in 1989. The density of spruce trees was 5,000 trees ha⁻¹ in 1989, and 1,500 – in 2007. One experimental plot was used as a control and another was fertilized with PMS: 100 g m⁻² in September 2007 and 50 g m⁻² in April 2008.

Soil samples and plant tissue collection

Soil and plant material sampling for laboratory analysis was done according to Table 1.

Table 1. Sample collection for laboratory analysis

Material	Time							
	08.2007	04.2008	09.2008	09.2010	09.2012	09.2014	09.2016	10.2016
Soil, chemistry	x		x	x	x	x	x	
Soil, microbiology					x		x	
Needles	x	x*	x	x	x	x	x	
Wood cores**								x

* only for the new seedlings for the 1st experiment; ** only for the 2nd experiment.

To detect the nutrient status and select the fertilizer dose, soil and needle samples from the current year shoots of spruces were collected for chemical analysis from all experimental plots before the experiment establishment in August 2007. Subsequent regular collection of soil samples was done until 2016. Soil samples were separately taken at 0 to 20 cm depth of the perimeter area of five randomly distributed spruce trees at each plot. Each soil sample (2 L) consisted of thoroughly mixed five subsamples

collected by a soil probe was placed in a plastic bag and transported to the laboratory. Along with soil sampling, spruce needles from the current year shoots from previously selected five trees in each plot were collected for chemical analysis. For quantification of culturable microorganisms, four soil sub-samples from each plot were taken within 0–10 cm depth, placed in sterile plastic bags (*Nasco WHIRL-PAK*) and taken to the laboratory where stored at +4 °C until microbial analysis.

Tree measurements

At both experimental sites, trees were numbered. Measurements of total height were done for the trees of the 1st experiment in October 2008, 2012, 2016. The measurements of stem diameter at the stem basis and assessment of tree crown vitality according to the Forest monitoring guidelines (UN/ECE, 2006; Schomaker et al., 2007) to characterize the general physiological status of trees was done in autumn 2008 and 2016. This was based on the following bioindicators: visual evaluation of crown defoliation and needle discoloration (dechromation) in percent. Based on the results, tree condition was classified as following: healthy – 0–10%, slightly damaged – > 10–25%, medium damaged – > 25–60%, and seriously damaged – > 60% defoliation and discoloration. At the 2nd experimental site, the diameter of spruce trees at 1.3 m height and tree height were measured in October 2007, 2012, 2016. Tree-ring width samples (wood cores) were taken from all spruce trees with a Presler increment drill in 2016. Assessment of tree crown status was done similar to the 1st experiment.

Vegetation inventory

All tree (E₃), shrub (E₂), herb (E₁) and moss (E₀) layer species were recorded before the experiment establishment at both sites in August 2007, then in 2012, and 2016. The projective cover of each layer and the percentage of each plant and moss species were evaluated visually at each plot (Dierschke, 1994). To estimate the ecological growth conditions, Ellenberg indicator values (Ellenberg et al., 1992) were calculated for detected plant species.

Laboratory analysis

For chemical analyses, the collected soil samples were dried at room temperature and passed through a 2 mm sieve. The soil analyses were done using 1 M HCl extraction for all nutrients (N, P, K, Ca, Mg, S, Fe, Mn, Zn, Cu, Mo, B), where soil/extractant (v/v) mixture was 1:5. This extractant is universal and quite aggressive thereby characterizes not only the amount of nutrient currently available for the plant uptake from the soil, but also indicates the amount of reserves of the element for the remaining vegetation season (Osvalde, 2011). For P, S and Mo determination, 1 M HCl extract of soil was oxidized with HNO₃, H₂O₂ and HClO₄ on a hot plate, the obtained salts were dissolved in HCl and diluted with distilled water (Rinkis et al., 1987). The concentrations of Ca, Mg, Fe, Cu, Zn and Mn in plant samples were determined by atomic absorption spectrophotometer (*Perkin Elmer AAnalyst 700*), acetylene-air flame (Page et al., 1982; Anonymous, 2000). The contents of P, Mo, N, S and B were determined by colorimetry: P by ammonium molybdate in an acid-reduced medium, Mo by thiocyanate in reduced acid medium, B by hinalizarine in sulfuric acid medium, S by turbidimetric method by adding BaCl₂ with a spectrophotometer JENWAY 6300 (Barloworld Scientific Ltd., Gransmore Green Felstad, Dunmow, Essex, UK). N in soil extraction (mineral (NH₄+NO₃) and total) – by

Nesler's reagent in an alkaline medium with a spectrophotometer JENWAY 6300. K – with the flame photometer *JENWAY PFPJ* (Jenway Ltd, Gransmore Green, Felsted Dunmow, Essex, UK). Soil pH was measured in 1 M KCl extraction (soil-extractant mixture 1:2.5) using the pH-meter *Sartorius PB-20* (Sartorius AG, Goettingen, Germany), but EC – in distilled water extraction (soil-water mixture 1:5) with the conductometer *Hanna EC 215* (Hanna instruments, USA). The obtained results of chemical elements were expressed in mg L⁻¹, because plant roots growth in a certain volume and in peat soil this volume significantly differ from the weight of this volume. The average volume weight for the peat soil of the 1st experiment control plot was 0.53 ± 0.04 g cm⁻¹, fertilized plot - 0.61 ± 0.02 g cm⁻¹; for the 2nd experiment control plot – 0.44 ± 0.03 g cm⁻¹, fertilized plot – 0.43 ± 0.03 g cm⁻¹.

Spruce needles were quickly washed with distilled water, dried at +60 °C and ground. Plant samples were dry-ashed in concentrated HNO₃ vapors and re-dissolved in 3% HCl for K, P, Ca, Mg, Fe, Cu, Zn, Mn and Mo detection. Wet digestion for N was done in conc. H₂SO₄, for S – in HNO₃, for B – plant samples were dry-ashed in concentrated HNO₃ vapors. N in plants was determined by modified Kjeldal method. P, K, Ca, Mg, S, Fe, Mn, Zn, Cu, Mo, and B were analyzed similar to the procedures described for analysis of soil extracts.

Total soil moisture was determined for soil samples after drying in oven at +105 °C for 24 hours, analytical replication was three times. These results were further used to calculate coefficients to convert data of colony forming units (CFU) from 1 g soil (analysed) to 1 g dry soil. Number of culturable bacteria and fungi in soil was determined by plate count on nutrient agar ('Biolife', Italia) and bengal agar with chloramphenicol ('Laboratorios Conda', Spain), respectively. 10 g of analysed soil were added to 250 mL flask with 90 mL of sterile distilled water and shaken for 30 min. on automatic shaker (Alef, 1995). Decimal dilutions were prepared and inoculated on agar plates. Bacteria and fungi were incubated at temperature 20 ± 2 °C for 72 and 120 hours, respectively. After incubation, the numbers of CFU were counted and their abundance per one gram of soil was calculated.

Wood cores from the 2nd experimental site were processed using a LINTAB 4 measuring table and TSAPWIN software.

Statistical analysis

Statistical analysis (standard errors, *Student's t-test*, $p < 0.05$, etc.) were done using R-Studio. Linear mixed models using *SPSS for Windows 14.0* were calculated to evaluate the fertilization effect on soil and needle chemical composition and tree growth parameters. Gradients in plant species composition, stand productivity and habitat factors were determined and analysed using detrended correspondence analysis (DCA) and PCord-5 software (McCune & Grace, 2002). To determine differences for fungal, bacterial CFU in soil between research plots, data were log-transformed to achieve normality and submitted to one-way ANOVA, followed by Tukey's test ($p < 0.05$) using program R 2.14.1. The spruce stock volume was calculated according to Liepa (1996) equation, because height of trees was > 1.5 m and diameter - > 1.5 cm:

$$V = 2.3106 \cdot 10^{-4} \cdot H_g^{0.78193} \cdot D_g^{0.34175 \cdot \lg H_g + 1.18811} \cdot N \quad (1)$$

where V – stand stock volume, m³ ha⁻¹; H_g – average height of stand, m; D_g – average stem diameter for stand at 1.3 m height, cm; N – number of stand trees, ha⁻¹.

RESULTS AND DISCUSSION

Nutrient status of Norway spruce

The results did not reveal significant differences for the chemical composition of soil and needle samples between the selected plots before fertilization in August 2007 and were given in Table 2 as the average values for the site. The chemical composition of seedling needles before planting at the 1st experiment site in April 2008 are also given in Table 2.

Table 2. Mean nutrient concentrations at the Norway spruce experimental sites in Latvia before treatment with PMS (background status)

Element	Peat soil (August 2007)		Needles (August 2007)		Needles (seedlings before planting, April 2008)
	1 st exp.	2 nd exp.	1 st exp.	2 nd exp.	1 st exp.
	mg L ⁻¹ , 1 M HCl extraction				
N min ⁻¹	34.5 ± 1.5	31.0 ± 1.0	-	-	
N _{tot}	205.0 ± 5.0	190.50 ± 3.50	7.4 ± 0.4	8.1 ± 0.5	12.0
P	311.0 ± 38.0	105.5 ± 20.5	1.4 ± 0.2	1.2 ± 0.1	2.6
K	47.0 ± 3.0	47.5 ± 7.5	1.7 ± 0.2	1.6 ± 0.2	10.0
Ca	8,038.0 ± 125.0	3,225.5 ± 62.5	3.6 ± 0.3	5.2 ± 0.3	4.7
Mg	127.0 ± 5.0	188.5 ± 11.5	0.7 ± 0.1	0.9 ± 0.1	1.9
S	41.0 ± 10.0	28.0 ± 0.0	0.7 ± 0.1	0.5 ± 0.1	0.8
	mg L ⁻¹		mg kg ⁻¹		mg kg ⁻¹
Fe	15,141.0 ± 710.0	6,350.0 ± 900.0	24.0 ± 1.5	60.0 ± 5.2	220.0
Mn	412.50 ± 17.5	25.00 ± 9.00	580.0 ± 65.0	720.0 ± 134.5	134.0
Zn	16.25 ± 3.25	5.20 ± 0.30	24.00 ± 0.75	15.00 ± 1.05	36.00
Cu	1.33 ± 0.08	0.70 ± 0.15	2.60 ± 0.17	2.20 ± 0.12	5.00
Mo	0.05 ± 0.01	0.04 ± 0.00	0.10 ± 0.03	0.15 ± 0.01	1.20
B	0.50 ± 0.00	0.15 ± 0.05	11.00 ± 1.00	12.00 ± 0.09	23.00
pH _{KCl}	4.50 ± 0.04	4.39 ± 0.06	-	-	-
EC mS cm ⁻¹	0.33 ± 0.03	0.47 ± 0.02	-	-	-

Both visual observation (yellowing or discoloration of the 2nd year and older spruce needles) and chemical analyses of peat soil and spruce needles before experiment establishment (Table 2) confirmed the deficiency of K at the experimental sites, as well as low level or deficiency of N, Mg, S, Fe, Cu, and B in spruce needles according to several authors: optimal for K – 0.5–1.2%, N – 1.35–1.70%; Mg – 0.10–0.25%; Cu – 4–10 mg kg⁻¹; B – 15–50 mg kg⁻¹ (Bergmann, 1988); satisfactory for N – > 1.5%; K – > 0.7%; S – > 0.15%; Fe – > 50 mg kg⁻¹; B – > 20 mg kg⁻¹; Cu – > 4 mg kg⁻¹ (compiled by Renou-Wilson & Farrell, 2007); critical concentrations (close to a general optimum range): N – 1.40–1.75 %; K – 0.52–0.82%; Mg – 0.08–0.13% (Mellert & Göttlein, 2012). Although the results of soil analysis in general showed sufficient concentration of Ca and Mg for tree growth, probably the unfavorable high Ca : Mg ratio (17–63 : 1) can be additional factor affecting spruce vitality for damaged stands. For plant nutrition the most optimal Ca : Mg ratio in soils using 1 M HCl extraction is 5–8 : 1 (Rinkis & Nollendorf, 1982; Cekstere & Osvalde, 2013). Additionally, the study

indicated deficiency of N (in mineral form) and Cu in peat soil. In peat soils, N is mainly presented in organic form which is not directly available for plant uptake and can significantly limit tree growth (Moilanen et al., 2010). Our research showed that the N content in spruce needles was significantly below the optimal values, even in the range of extreme deficiency according to Mellert & Göttlein (2012). For high wood productivity sufficient N availability is one of the main prerequisite. Despite of overall foliar N deficiency, N : K ratio for damaged trees (5.43) were too high based on latest nutrient ratio thresholds for Norway spruce: N : K 1.7–3.3 (Mellert & Göttlein, 2012), pointing out severity of K deficiency. Therefore, N fertilization might be suggestable only after prevention of serious K starvation and should be based on the results of additional experimental studies. Thus, imbalanced conditions of mineral nutrition predisposed trees to discoloration and stunted growth frequently observed for middle-aged Norway spruce stands in Latvia.

In general, the pre-treatment nutrient status has been found to have a significant role as regards to the extent of the stand response after fertilization (Moilanen et al., 2015). Selection of PMS for our experiments underplayed on diagnosed nutritional disorders: overall K deficiency, Ca : Mg ratio unfavorable to Mg, as well as, in general, low level of S in current year needles. Regardless of spruce stand vitality the foliar S concentration found in the current year needles before the treatment were on the deficiency threshold according to Renou-Wilson & Farrell (2007). Additionally, PMS did not contribute to soil acidity or alkalinity. It is a relevant advantage of this fertilizer in the conditions of soil pH in general optimal for spruce growth.

A significant impact of fertilization on concentrations of several nutrients in the soil and spruce needles was stated according the results of LMM analysis (Tables 3, 4). Generally, a significantly higher K concentration in the soil showed a trend toward decrease from 2008 to 2016, while increase in N_{\min} was found for both fertilized plots from 2008 to 2016 (Fig. 1, a, b). The pronounced increase in S concentrations were mainly characteristics for the fertilized plots during 2008 (Fig. 1, c). The fertilization significantly affected the concentrations of plant available Mg and N_{tot} in soil for the 1st experiment (Fig. 1, d, Table 5) without strong impact for the 2nd experiment.

Table 3. Results of LMM analyzing nutrient content in soil under fertilization with PMS (only significant results for nutrients, $p < 0.01$, were included in the table)

Dependent variable	Source	1 st experiment			2 nd experiment		
		Num. df	Den. df	F	Num. df	Den. df	F
K	Intercept	1	16.99	12,527	1	8.70	8,332
	Fertilization	1	16.99	4,523	1	8.70	1,444
	Year	4	9.09	143	4	7.32	120
	Fert.*Year	4	9.09	211	4	7.32	164
N_{\min} .	Intercept	1	15.90	20,275	1	18.81	12,758
	Fertilization	1	15.90	1,314	1	18.81	78
	Year	4	7.57	1,041	4	8.25	42
	Fert.*Year	4	7.57	59	4	8.25	90
N_{tot} .	Intercept	1	17.85	45,482	-	-	-
	Fertilization	1	17.85	586	-	-	-
	Year	4	6.90	169	-	-	-
	Fert.*Year	4	6.90	113	-	-	-

Table 3 (continued)

S	Intercept	1	8.80	8,136	1	13.79	9,775
	Fertilization	1	8.80	718	1	13.79	884
	Year	4	8.10	308	4	9.16	85
	Fert.*Year	4	8.10	136	4	9.16	124
Mg	Intercept	1	5.98	5,318	1	18.39	11,681
	Fertilization	1	5.98	1,730	1	18.39	46
	Year	4	6.72	231	4	7.26	45
	Fert.*Year	4	6.72	273	4	7.26	10

Table 4. Results of LMM analyzing nutrient content in spruce needles under fertilization with PMS (only significant results for nutrients, $p < 0.01$, were included in the table)

Dependent variable	Source	1 st experiment			2 nd experiment		
		Num. df	Den. df	F	Num. df	Den. df	F
K	Intercept	1	15.78	13,133	1	18.90	13,545
	Fertilization	1	15.78	4,886	1	18.90	4738
	Year	3	7.95	16	4	8.15	50
	Fert.*Year	3	7.95	12	4	8.15	55
N	Intercept	1	15.78	58,011	1	18.98	19,485
	Fertilization	1	15.78	1,363	1	18.98	57
	Year	3	7.76	76	4	7.83	133
	Fert.*Year	3	7.75	133	4	7.82	12
Ca	Intercept	1	15.80	26,124	1	19.17	18,468
	Fertilization	1	15.80	360	1	19.17	403
	Year	3	7.90	27	4	7.155	36
	Fert.*Year	3	7.90	39	4	7.155	17
Fe	Intercept	1	15.39	14,807	1	10.52	15,639
	Fertilization	1	15.39	133	1	10.52	25
	Year	3	7.99	78	4	6.56	429
	Fert.*Year	3	7.99	30	4	6.56	104
Zn	Intercept	1	13.64	23,406	1	18.17	18,069
	Fertilization	1	13.64	1,605	1	18.17	602
	Year	3	8.96	334	4	7.75	72
	Fert.*Year	3	8.96	212	4	7.75	84
B	Intercept	1	15.01	8,684	-	-	-
	Fertilization	1	15.01	735	-	-	-
	Year	3	7.05	51	-	-	-
	Fert.*Year	3	7.05	10	-	-	-

Significantly higher concentrations of K in needles were found at the both experimental plots treated with PMS compared to the control plots till 2016 (Fig. 1, e), as well as Ca and Zn, generally (Table 5). The increase in the content of N (Fig. 1, f), a significantly higher Fe, lower B level (Table 5) in needles was stated only for trees from the fertilized plot of the 1st experiment. There was no significant difference for other nutrients (Table 6). It is notable that the level of Cu, B and Mo in spruce needles was low for all experimental plots. It was not surprising for Mo which is the only micronutrient with low availability in acid soils (Mengel & Kirkby, 2001). Our study showed that mean Mo concentration in spruce needles was below 0.50 mg kg⁻¹; proposed

as the sufficiency threshold for woody plants in acid growing medium (Karlsons & Osvalde, 2017).

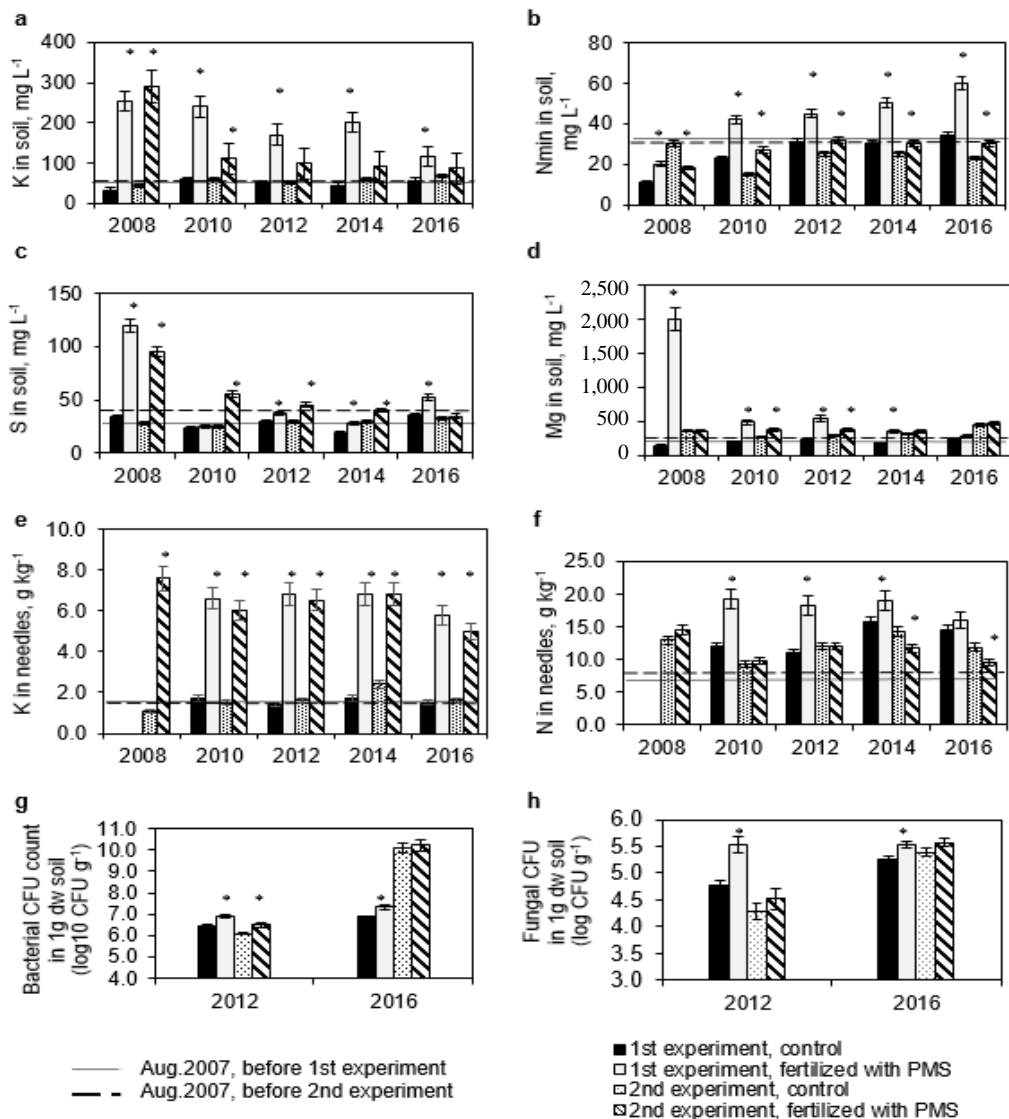


Figure 1. Changes in nutrient content in peat soil (1M HCl extraction) (a-d), needles (e, f) and bacterial (g) and fungal CFU count (h) in peat soils in the spruce experimental sites in Latvia. Date represent results of September 2008–2016. (Means ± SE, asterisk indicates significant difference (LMM, $p, 0.01$) for the experimental site between the control and fertilized plot).

During the research at 2008–2016, almost permanent 3–4 times higher concentration of K in spruce needles, significantly above the deficiency limits, was characteristic for all experimental plots with K application. Moreover, the fertilization treatment completely balanced foliar N : K ratio. Based on the previous research (Silverberg & Moilanen, 2008; Moilanen et al., 2015) it is expectable that the effect of

K fertilization could last for the coming 10–15 years. It is surprising that soil K response to the PMS treatment also continued to be significant until the end of the study period. PMS is totally water soluble, but dissolves slower than most of other common K fertilizers. Unforeseen, the fertilization with PMS did not increase the content of S and Mg in spruce needles, which was still low or at deficiency level. Probably, the reasons could be the dilution effect caused by increased biomass production of trees and involvement of these elements in intensive growth of herb-layer vegetation, as well as element antagonism (Ca : Mg, K : Mg). For improvement of Mg and S status additional fertilization with appropriate fertilizers is suggestable.

Table 5. Average nutrient concentrations in peat soils and current year needles from the Norway spruce experimental sites in Latvia over 2008–2016 (fertilized in 2007–2008 with PMS)

Element	1 st Experiment		2 nd Experiment	
	Control	Fertilized	Control	Fertilized
Soils (mg L ⁻¹ , 1M HCl extraction)				
	2008–2016		2008–2016	
N _{tot}	218.6 ± 4.4 a*	272.8 ± 47.6 b ↑	201.3 ± 16.8 a	214.3 ± 20.2 a
Needles				
	2010–2016		2008–2016	
Ca, g kg ⁻¹	3.5 ± 0.1 a	4.4 ± 0.3 b ↑	3.4 ± 0.3 a ↓	4.5 ± 0.2 b
Fe, mg kg ⁻¹	42.50 ± 1.50 a ↑	51.50 ± 5.32 b ↑	53.50 ± 14.08 a	49.40 ± 13.85 a
Zn, mg kg ⁻¹	17.55 ± 2.16 a ↓	30.00 ± 4.69 b	17.50 ± 0.29 a	25.12 ± 3.10 b ↑
B, mg kg ⁻¹	17.75 ± 1.38 b ↑	9.75 ± 0.85 a	13.75 ± 2.66 a	13.00 ± 0.71 a

* – means with different letters in a row were significantly different for the experiment (*t-Test*, $p < 0.05$, $b > a$). ↑↓ – significantly lower or higher compared to the pre-treatment status in 2007.

Table 6. Average chemical composition of peat soil and current year needles from the Norway spruce experimental plots over 2008–2016 (control+fertilized*) in Latvia

	1 st Experiment	2 nd Experiment
	2008–2016	2008–2016
Peat Soils (mg L ⁻¹ , 1M HCl extraction)		
P	234.31 ± 35.02	151.57 ± 24.36
Ca	5,316.05 ± 401.50 ↓	3,556.07 ± 362.04
Fe	14,739.25 ± 1,321.45	6,640.00 ± 630.08
Mn	233.33 ± 23.75 ↓	58.00 ± 19.92
Zn	11.32 ± 1.01	5.99 ± 1.81
Cu	0.89 ± 0.11	0.89 ± 0.13
Mo	0.04 ± 0.01	0.06 ± 0.01
B	0.76 ± 0.21	0.37 ± 0.06
pH _{KCl}	4.35 ± 0.10	4.24 ± 0.07
EC, mS cm ⁻¹	0.43 ± 0.08	0.47 ± 0.06
Needles		
	2010–2016	2008–2016
P, g kg ⁻¹	2.0 ± 0.1 ↑	1.7 ± 0.2 ↑
Mg, g kg ⁻¹	1.1 ± 0.2	0.9 ± 0.1
S, g kg ⁻¹	0.8 ± 0.1	0.7 ± 0.1
Mn, mg kg ⁻¹	614.00 ± 26.02	721.00 ± 157.18
Cu, mg kg ⁻¹	2.65 ± 0.57	2.50 ± 0.24
Mo, mg kg ⁻¹	0.20 ± 0.06	0.24 ± 0.08

* – no statistically significant ($p < 0.05$) differences were found, on average, between the control and fertilized plot of the experiment during 2008–2016. ↑↓ – significantly lower or higher compared to the pre-treatment status in 2007.

Assessment of soil microbiological activity

The average count of bacteria and fungi in soil of fertilized plot, accompanied by a remarkable variability in the study years, was significantly higher than in the control plot only for the 1st experiment (Fig. 1, g, h). As high abundance of bacteria was found for all soil samples analyzed, fungi : bacteria (F : B) ratio did not exceed 0.044. This highest value was obtained for the fertilized plot of the 1st experiment in 2012. The lowest values were characteristics for the 2nd experiment in 2016 (F : B 0.000019-0.000022). In general, F : B ratio in the fertilized and control plots differed significantly only for the 1st experiment. Different studies demonstrate that soil microbes and fungi are highly sensitive to environmental conditions; fungi often dominate in acid soil while bacteria in nutrient-rich soils, often with high pH (Schimel & Bennett, 2004; Shen et al., 2014). Our results revealed a high abundance of soil bacteria in both low pH study sites regardless of the fertilization. Although there was a tendency of the promotive impact of fertilization on the count of bacteria and fungi in soil, this increase was statistically significant only for the 1st experiment with young trees. Our results were also in a good agreement with findings by Klavina et al. (2016) on significantly higher microbial abundance in fertilized (wood ash, K₂SO₄) peat soil of young spruce. It is approved that F : B ratio depends on forest ecosystems of different vegetation types, forest fertility and N availability (Högberg et al., 2007). Our research revealed that F : B ratios could vary in response to changes in herb and moss layer vegetation caused by PMS fertilization (1st experiment, 2012), as well as due to local soil conditions, for example increased soil moisture for the 2nd experiment in 2016.

Spruce crown status and stand productivity

A significant impact of fertilization on spruce stand productivity of both experiments was stated (Table 7). Fertilization with PMS resulted in up to 3 times higher spruce height ($4.20 \pm 1.50 \text{ m} > 1.71 \pm 0.11 \text{ m}$, $p < 0.05$) and 2 times larger stem diameter ($7.23 \pm 0.24 \text{ cm} > 3.05 \pm 0.19 \text{ cm}$, $p < 0.05$) compared to the control at the end of 1st experiment in 2016. Simultaneously, significant differences in crown status were also stated between plots: the crown status was healthy for fertilized trees (defoliation: $14.8 \pm 0.9\%$, discoloration: $5.3 \pm 0.4\%$), but seriously damaged for the control (defoliation: $27.3 \pm 2.8\%$, discoloration: $85.4 \pm 0.7\%$).

Results of the 2nd experiment revealed a significant continuous improvement of tree crown vitality at the fertilized plot compared to the control already from 2008. Thereby in 2008 and 2016, the defoliation and dechromation level of tree crown was significant lower ($p < 0.05$) at the fertilized plot compared to the control (2008: defoliation $21.7 \pm 2.2\% < 30.7 \pm 2.5\%$; discoloration $5.2 \pm 0.6\% < 82.7 \pm 0.5\%$; 2016: defoliation $14.7 \pm 7.0\% < 29. \pm 3.1\%$, discoloration $5.2 \pm 0.4\% < 90.7 \pm 0.7\%$, respectively).

Table 7. Results of LMM analyzing responses of tree growth parameters under fertilization with PMS ($p < 0.01$)

Dependent Variable	Source	1 st Experiment			2 nd Experiment		
		Num. df	Den. df	F	Num. df	Den. df	F
Mean tree height	Intercept	1	66.01	2,304	1	70.49	5,374
	Fertilization	1	66.01	334	1	70.49	47
	Year	2	54.66	790	2	46.84	97
	Fert.*Year	2	54.66	189	2	46.84	18
Mean tree diameter	Intercept	1	50	1,150	1	71.760	2,503
	Fertilization	1	50	190	1	71.760	27
	Year	0	-	-	2	49.15	60
	Fert.*Year	0	-	-	2	49.15	9
Mean tree volume	Intercept	-	-	-	1	50.49	622
	Fertilization	-	-	-	1	50.49	57
	Year	-	-	-	2	40.25	100
	Fert.*Year	-	-	-	2	40.25	26

Abbreviations: Num. df – numerator degree of freedom; Den. df – denominator degree of freedom; Fert. – fertilization.

The rapid increase in the increment of tree rings (planting 1989, 2nd experiment) started on the 2nd year after fertilization (Fig. 2, a). Generally, the positive effect of fertilization significantly facilitated spruce growth: annual tree ring increment was up to 3.5 times higher compared to the control, tree height – 1.5 times, stem diameter 1.4 times larger at the end of 2016 (Table 8). As the result (Fig. 2, b), the stock volume for the fertilized plot was 3.5 times higher compared with the calculated prognostic (theoretical) stock volume without application of PMS and 2.8 times higher compared to the control.

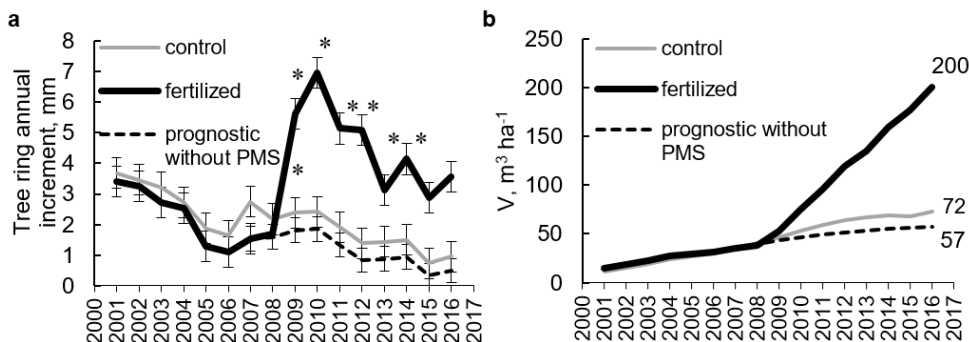


Figure 2. Annual increment of tree rings (a) and stock volume (b) for control and fertilized with PMS (2007, 2008) Norway spruce at the 2nd experimental site (planting 1989); a: \pm standard error, $n=15$; b: V – stand stock volume; prognostic without PMS – theoretical stock volume for the fertilized plot without fertilization. Asterisk indicates significant difference (t -Test, $p < 0.05$) for the experimental site between the control and fertilized plot.

Table 8. Results of estimated marginal means for spruce growth parameters at the 2nd experiment plots in Kalsnava (planting 1989)

Dependent Variable*Plot	Year	Mean	Std. Error	95% Confidence Interval		
				Lower Bound	Upper Bound	
Mean tree diameter, Fertilized cm	2007	8.67	0.41	7.82	9.51	
		13.79	0.57	12.63	14.95	
		16.66	0.67	15.27	18.04	
	Control	2007	8.66	0.41	7.82	9.51
		2012	10.86	0.57	9.69	12.02
		2016	12.23	0.75	10.70	13.77
Mean tree height, Fertilized m	2007	5.86	0.16	5.54	6.19	
		9.54	0.19	9.16	9.92	
		11.58	0.20	11.17	12.00	
	Control	2007	5.94	0.16	5.61	6.26
		2012	7.28	0.19	6.90	7.67
		2016	8.25	0.23	7.78	8.71
Stand stock volume, Fertilized m ³ ha ⁻¹	2007	34.89	3.46	27.83	41.95	
		119.17	7.93	102.97	135.36	
		200.22	12.08	175.43	225.01	
	Control	2007	36.24	3.46	29.18	43.29
		2012	64.21	7.93	48.01	80.40
		2016	72.50	10.89	50.15	94.85

* LMM showed a significant effect of ‘fertilization’, ‘time’ and ‘fertilization*time’ on the dependent variable (Table 6).

Thereby our study convincingly approved significant effect of fertilization with PMS on additional increment of stock volume by up to 3 times during the study period, as well as a higher growth response compared to the previous studies with other fertilizers (wood ash, KCl, K₂SO₄) for Norway spruce at drained peat soil in the boreo-nemoral climate zone (Zālītis, 1991; Okmanis et al., 2016). It was found that four years after fertilization with K in dose 62–65 kg ha⁻¹, applied by wood ash or potassium sulphate, the additional volume increment reached 9–19 m³ ha⁻¹ (Okmanis et al., 2016). Our results revealed 55 m³ ha⁻¹ of additional increment for 2009–2012, and 128 m³ ha⁻¹ in 2016. We suggested that higher growth response could be attributed to approximately five times higher K dose, complexity of PMS for simultaneously ameliorating nutrient (K, Mg, S) deficiency in growing medium, as well as possibility to use higher amount of fertilizer without detrimental increase in soil reaction and electrical conductivity. Several studies have demonstrated a distinct positive correlation between K, Ca and Zn nutrition and wood production of trees (Barrelet et al., 2006; From, 2010; Guerriero et al., 2014). Our study also revealed a higher Ca and Zn content in spruce needles from the fertilized plots of both experiments. It is notable that these foliar concentrations of Ca and Zn in needles completely met the standards for Norway spruce reported by Renou-Wilson & Farrell (2007).

Dynamics of stand vegetation

The vegetation observations revealed no significant differences for species cover and composition between the plots of the 1st experiment before the treatment with PMS in 2007. Generally, herb layer covered 72% of the total plot area, while moss

layer – 52%. 18 vascular plant species and 8 moss species were recorded. The most dominant plant species were *Festuca rubra* with projective cover of 30%, *Deschampsia cespitosa* – 11%, *Geum rivale* and *Galium album* – each 8%, and the dominant moss species were *Rhytidiadelphus squarrosus* – 21%, *Climacium dendroides* – 12%, and *Plagiomnium cuspidatum* – 5%. Although the amount of vascular plant (24) and moss (10) species had increased in 2016, the same dominant species were prevalent for the control also after 10 years. During the first years after treatment, the amount of nitrophilic tall herbaceous species, e. g., *Anthriscus sylvestris* (40%), *Urtica dioica* (10%), *Rubus idaeus* (8%), and *Chamerion angustifolium* (8%) has rapidly increased at the fertilized plot. With the increase of spruce role as edificator, the amount of previously mentioned nitrophilic species has decreased forward to 2016, nevertheless they were dominant at the herb layer also during 2016. The amount of *Plagiomnium* sp. (*P. cuspidatum* – 30%, *P. ellipticum* – 16%, *P. undulatum* – 10%) has rapidly increased at the moss layer after fertilization, reaching 56% of the total plot area in 2016.

At the 2nd experiment, no significant differences for species cover and composition between the plots of the 2nd experiment before the treatment were stated. Thus, in 2007, 33 vascular plant species and 12 moss species were recorded in total, covering 80% and 70% of each plot area, respectively. The dominant plant species were *Ranunculus repens* (12%), *Viola palustris* (12%), *Deschampsia cespitosa* (8%), but for the moss species – *Climacium dendroides* (25%), *Rhytidiadelphus squarrosus* (16%) and *Plagiomnium cuspidatum* (12%). These species with no significant changes were dominant at the control plot during all the study period. Whereas at the fertilized plot, a rapid increase of cover with *Urtica dioica* (12%) and *Anthriscus sylvestris* (21%) was stated in 2012 compared to 2007. In 2016, a significant increase of moss species *Plagiomnium cuspidatum* (30%) and *P. ellipticum* (10%) cover, as well as decrease of plant species cover (35%) and diversity (25 species) was recorded due to high level of shading formed by spruce crown cover (95%) at the fertilized plot. Thereby, the cover of *Ranunculus repens* was only 5%, *Urtica dioica* – 2%.

The DCA of the 1st experiment vegetation results revealed the highest positive values ('tau coefficient') for *Urtica dioica* (0.966), *Plagiomnium elatum* (0.828) and *Anthriscus sylvestris* (0.690), as well as soil reaction (0.467) and nitrogen (0.759) in ordination with the 1st axis. Similar results were stated also for the 2nd experiment: the highest positive correlations with the 1st axis were determined for plant species typical for neutral and nitrogen abundant sites (*Plagiomnium cuspidatum* (0.900), *Anthriscus sylvestris* (0.602) and soil reaction (0.501). Whereas the highest negative correlations with the 1st axis were stated for the background species of the control plot: *Veronica chamaedrys* (-0.828) and *Rhytidiadelphus squarrosus* (-0.867) in the 1st experiment, and *Climacium dendroides* (-0.966) and *Dechampsia cespitosa* (-0.867) at the 2nd experiment.

The content of N, P, and K in soils may affect not only plant growth but also plant community composition (Knecht & Göransson, 2004; Tripler et al., 2006). The results emphasized the fact that fertilization with PMS undeniable caused changes in drained peat soil chemical composition, microbiological activity and plant species composition. Significant increase of nitrophilic plant species indicated increase of biologically active N in soil surface and thus on activation of nutrient cycling, also reflected by environment gradient analysis by Ellenberg values, specially four years after fertilization (Fig. 3). During the study period, the increase in plant available N_{min} was stated for the fertilized

plots of both experimental sites established on peat soils. The contributing impact of fertilization on total N was found only for the new planting where, according to Ellenberg's values for N, the treated plot could be characterized as more fertile habitat. In peat soils, N is mainly presented in organic form which is not directly available for plant uptake and can significantly limited tree growth (Moilanen et al., 2010). However, several studies have shown that a range of plant species, including conifers, can take up N also from organic N sources (Öhlund & Näsholm, 2001). Consequently, foliar N status of trees from fertilized plot of 1st experiment was from latent deficiency to normal range, while for older trees (2nd experiment) – at the deficiency level.

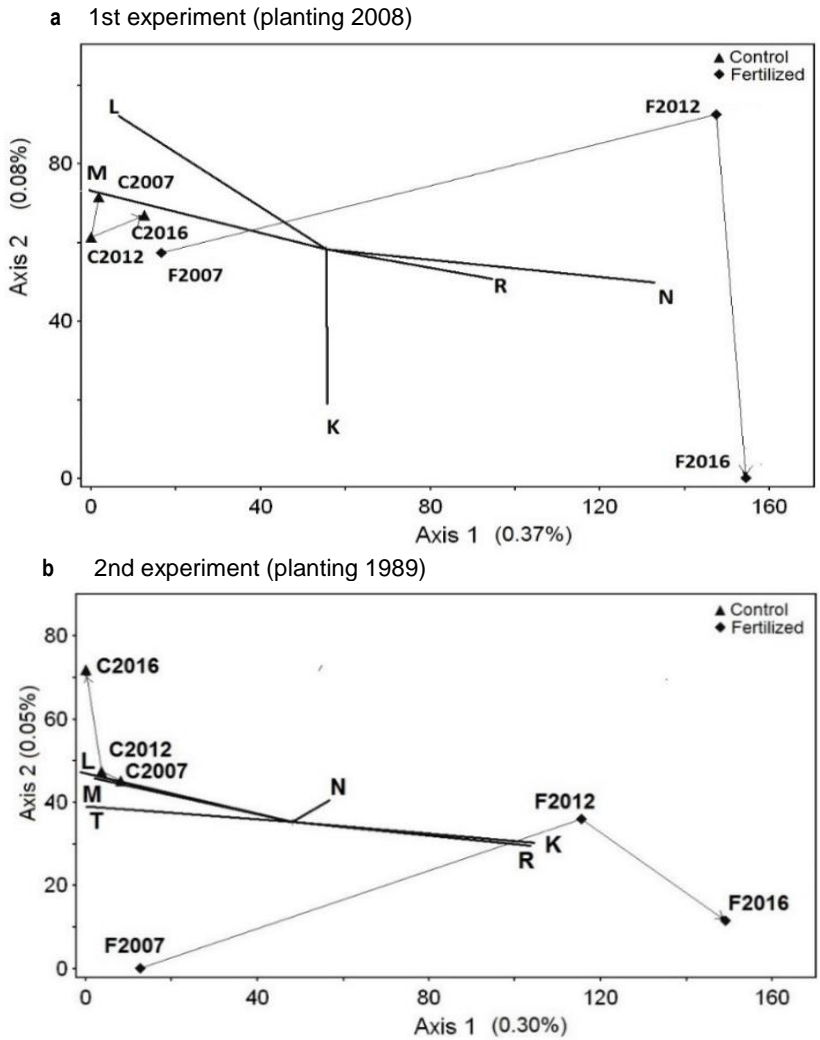


Figure 3. Detrended correspondence analysis of distribution of plant and moss species composition at the Norway spruce experimental plots and gradients of ecological factors. (Vectors: Ellenberg values for detected plant species: L – light; T – temperature; K – continentality; M – humidity; R – reaction; N – nitrogen).

Undeniable, the fertilization results might depend on various factors as stand age, initial nutrient status, kind and dose of fertilizer, tree density, microclimate, etc. Besides a significant aspect is also the fertilization impact on vegetation, changes in soil/peat chemical composition, nutrient cycling, mycorrhiza, etc. Thus further research and additional experiments with various PMS doses and study sites should be carried out in the future. In addition, our study revealed significant deficiency of N, Cu, Mo and B for spruce needles on drained peat soils. Thereby, studies on optimization of fertilization regimes in order to provide tree demands, to increase wood production, and to find a balance between economy and ecological aspects is very important task. Correct application of appropriate fertilizers in adequate doses is critical to avoid soil and groundwater pollution as well as imbalance with other nutrients.

CONCLUSIONS

The results revealed that fertilization with 150 g m⁻² of PMS resulted in a significantly better nutrient (K, Ca, Zn, and N) status of Norway spruce stands, improved crown vitality and tree growth at both experiments on drained peat soil. This effect lasted all the study period of 2008–2016. Nine years after the fertilization, up to three times higher spruce height, two times larger stem diameter for a new planting, and up to 3.5 times higher annual tree ring increment, 1.4 times – tree height, 1.3 times – stem diameter, and the additional stock volume – 128 m ha⁻¹ was found for older spruce stand (2nd experiment). The average count of bacteria and fungi in soil of fertilized plots, accompanied by a remarkable variability in the study years, was significantly higher only for the 1st experiment (new planting). F : B ratio did not exceed 0.044 for both experiments, with significant differences between fertilized and control plots only for the 1st experiment. Significant increase of cover with nitrophilic plant (*Urtica dioica*, *Antriscus sylvestris*, *Rubus idaeus*) and moss (*Plagiomnium cuspidatum*, *P. ellipticum*) species at both fertilized experimental sites indicated increase of biologically active N and activation on nutrient cycling.

ACKNOWLEDGEMENTS. The financial support partly provided by the Forest Development Fund in Latvia for project ‘*Degradation of Norway spruce stands in Latvia: reasons and measures for possible solutions*’ during 2007-2008, as well as the Basic Research Funding, University of Latvia, for project ‘*Biological diversity – impacts, functions and protection*’, N° AAP2016/B034, ZD2015/AZ81, during 2016-2017, are gratefully acknowledged. The authors thank two anonymous reviewers for their valuable scientific advises and comments.

REFERENCES

- Alef, K. 1995. Enrichment, isolation and counting of soil microorganisms. In: *Methods in Applied Soil Microbiology and Biochemistry*. Academic Press, London, pp. 123–191.
- Barrelet, T., Ulrich, A., Rennenberg, H. & Kraehenbühl, U. 2006. Seasonal profiles of sulphur, phosphorus, and potassium in Norway spruce wood. *Plant Biology* **8**, 462–469.
- Berger, T.W., Inselbacher, E., Mutsch, F. & Pfeffer, M. 2009. Nutrient cycling and soil leaching in eighteen pure and mixed stands of beech (*Fagus sylvatica*) and spruce (*Picea abies*). *Forest Ecology and Management* **258**, 2578–2592.

- Bergmann, W. 1988. *Disbalance in crop plant fertilization. Origin, visual and analytical diagnosis*. Gustav Fischer Verlag, Jena (in German).
- Błońska, E., Małek, S., Januszek, K., Barszcz, J. & Wanic, T. 2015. Changes in forest soil properties and spruce stands characteristics after dolomite, magnesite and serpentinite fertilization. *European Journal of Forest Research* **134**, 981–990.
- Caisse, G., Boudreau, S., Munson, A.D. & Rochefort, L. 2008. Fertiliser addition is important for tree growth on cut-over peatlands in eastern Canada. *Mires and Peat* **3**, 1–15.
- Cekstere, G. & Osvalde, A. 2013. A study of chemical characteristics of soil in relation to street trees status in Riga (Latvia). *Urban Forestry and Urban Greening* **12**(1), 69–78.
- Dierschke, H. 1994. *Plant sociology. Basic concepts and methods*. Stuttgart, Verlag Eugen Ulmer. 583 pp. (in German).
- Ellenberg, H., Weber, H.E., Düll, R., Wirth, V., Werner, W & Paulissen, D. 1992. *Indicator values of ecological conditions for Central Europe plant species. Scripta Geobotanica* **18**, 1–258 (in German).
- Finer, L. 1989. Biomass and nutrient cycle in fertilized and unfertilized pine, mixed birch and pine and spruce stands on a drained mire. *Acta Forestalia Fennica* **208**.
- Finnish Statistical Yearbook of Forestry*, 2014. Official Statistics of Finland: Agriculture, Forestry and Fishery, Summary, 417-426. http://www.metla.fi/metinfo/tilasto/julkaisut/vsk/2014/vsk14_summary.pdf. Accessed 28.02.2018
- Fromm, J. 2010. Wood formation of trees in relation to potassium and calcium nutrition. *Tree Physiology* **30**(9), 1140–1147.
- Guerriero, G., Sergeant, K. & Hausman, J.F. 2014. Wood biosynthesis and typologies: a molecular rhapsody. *Tree Physiology* **34**, 839–855.
- Halmschlager, E. & Katzensteiner, K. 2017. Vitality fertilization balanced tree nutrition and mitigated severity of Sirococcus shoot blight on mature Norway spruce. *Forest Ecology and Management* **389**, 96–104.
- He, H., Jansson, P.E., Svensson, M., Meyerc, A., Klemedtssona, L. & Kasimir, Å. 2016. Factors controlling Nitrous Oxide emission from a spruce forest ecosystem on drained organic soil, derived using the CoupModel. *Ecological Modelling* **321**, 46–63.
- Högberg, M.N., Högberg, P. & Myrold, D.D. 2007. Is microbial community composition in boreal forest soils determined by pH, C-to-N ratio, the tree, or all three? *Oecologia* **150**, 590–601.
- Karlsons, A. & Osvalde, A. 2017. Nutrient status of the American cranberry in Latvia (2005–2016). *Agronomy Research* **15**(1), 196–204.
- Klavina, D., Lazdiņš, A., Bārdule, A., Nikolajeva, V., Okmanis, M., Skranda, I., Gaitnieks, T. & Menkis, A. 2016. Fine root development and mycorrhization in Norway spruce stands one year after fertilization with potassium sulphate and wood ash. *Journal of Forest Science* **62**(1), 17–23.
- Kļaviņš, M., Blumberga, D., Bruņiniece, I., Briede, A., Grišule, G., Andrušaitis, A. & Ābolīņa, K. 2008. *Climate changes and global warming*. Rīga, LU Akadēmiskais apgāds, 174 pp. (in Latvian).
- Knecht, M.F. & Göransson, A. 2004. Terrestrial plants require nutrients in similar proportions. *Tree Physiology* **24**, 447–460.
- Liepa, I. 1996. *Increment Science*. Latvijas Lauksaimniecības Universitāte, Jelgava (in Latvian).
- Libiete, Z., Bardule, A. & Lupikis, A. 2016. Long-term effect of spruce bark ash fertilization on soil properties and tree biomass increment in a mixed scots pine-Norway spruce stand on drained organic soil. *Agronomy Research* **14**(2), 495–512.
- Lībiete, Z. & Zālītis, P. 2007. Determining the growth potential for even-aged stands of Norway spruce (*Picea abies* (L.) Karst). *Baltic Forestry* **13**, 2–9.

- Małek, S., Barszcz, J. & Majsterkiewicz, K. 2012. Changes in the threat of spruce stand disintegration in the Beskid Śląski and Żywiecki Mts. in the years 2007–2010. *Journal of Forest Science* **58**(12), 519–529.
- McCune, B. & Grace, J.B. 2002. *Analysis of ecological communities*. MjM Software Design, Glendon Beach, Oregon, 304 pp.
- Mellert, K.H. & Göttlein, A. 2012. Comparison of new foliar nutrient thresholds derived from van den Burg's literature compilation with established central European references. *European Journal of Forest Research* **131**, 1461–1472.
- Mengel, K. & Kirkby, E.A. 2001. *Principles of plant nutrition*. 5th edn. Kluwer Academic Publishers, Dordrecht, the Netherlands, 849 pp.
- Moilanen, M., Hytönen, J., Hökkä, H. & Ahtikoski, A. 2015. Fertilization increased growth of Scots pine and financial performance of forest management in a drained peatland in Finland. *Silva Fennica* **49**(3), article id 1301.
- Moilanen, M., Saarinen, M. & Silfverberg, K. 2010. Foliar nitrogen, phosphorus and potassium concentrations of Scots pine in drained mires in Finland. *Silva Fennica* **44**, 583–601, article id 129.
- Möttönen, M., Lehto, T., Rita, H. & Aphalo, P.J. 2005. Recovery of Norway spruce (*Picea abies*) seedlings from repeated drought as affected by boron nutrition. *Trees* **19**, 213–223.
- Öhlund, J. & Näsholm, T. 2001. Growth of conifer seedlings on organic and inorganic nitrogen sources. *Tree Physiology* **21**, 1319–1326.
- Okmanis, M., Skranda, I., Lazdiņš, A. & Lazdiņa, D. 2016. Impact of wood ash and potassium sulphate fertilization on growth of Norway spruce stand on organic soil. *Research for Rural Development* **2**, 62–68.
- Osvalde, A. 2011. Optimization of plant mineral nutrition revisited: the role of plant requirements, nutrient interactions, and soil properties in a fertilization management. *Environmental and Experimental Biology* **9**, 1–8.
- Page, A.L., Miller, R.H. & Keeney, D.R. 1982. *Methods of soil analysis. Part 2. Chemical and microbiological properties*. Wisconsin.
- Renou-Wilson, F. & Farelli, E.P. 2007. The use of foliage and soil information for managing the nutrition of Sitka and Norway spruce on cutaway peatlands. *Silva Fennica* **41**(3), 409–424.
- Rinkis, G. & Nollendorf, V. 1982. *Integrated plant nutrition with macro- and micronutrients*. Zinatne, Riga, 304 pp. (in Russian).
- Rinkis, G., Ramane, H. & Kunickaya, T. 1987. *Methods of soil and plant analysis*. Zinatne, Riga. (in Russian).
- Saarsalmi, A. & Mälkönen, E. 2001. Forest fertilization research in Finland: A literature review. *Scandinavian Journal of Forest Research* **16**(6), 514–535.
- Saarsalmi, A. & Tamminen, P. 2005. Boron, phosphorus and nitrogen fertilization in Norway spruce stands suffering from growth disturbances. *Silva Fennica* **39**(3), 351–364, article id 373.
- Sarkkola, S., Ukonmaanaho, L., Nieminen, T.M., Laiho, R., Laurén, A., Finér, L. & Nieminen, M. 2016. Should harvest residues be left on site in peatland forests to decrease the risk of potassium depletion? *Forest Ecology and Management* **374**, 136–145.
- Schimel, J.P. & Bennett, J. 2004. Nitrogen mineralization: challenges of a changing paradigm. *Ecology* **85**, 591–602.
- Schomaker, M.E., Zarnoch, S.J., Bechtold, W.A., Latelle, D.J., Burkman, W.G. & Cox, S.M. 2007. *Crown-condition classification: a guide to data collection and analysis*. General Technical Report SRS-102. Asheville NC, US Department of Agriculture. Forest service. Southern Research Station.:I+VIII.

- Shen, C., Liang, W., Shi, Y., Lin, X., Zhang, H., Wu, X., Xie, G., Chain, P., Grogan, P. & Chu, H. 2014. Contrasting elevational diversity patterns between eukaryotic soil microbes and plants. *Ecology* **95**, 3190–3202.
- Silfverberg, K. & Moilanen, M. 2008. Long-term nutrient status of PK fertilized Scots pine stands on drained peatlands in North-Central Finland. *Suo - Mires and Peat* **59**(3), 71–88.
- Tripler, C.E., Kaushal, S.S., Likens, G.E. & Walter, M.T. 2006. Patterns in potassium dynamics in forest ecosystems. *Ecology Letters* **9**, 451–466.
- UN/ECE 2006. *Manual on methods and criteria for harmonized sampling, assessment, monitoring and analysis of the effects of air pollution on forests. Part II Visual assessment of crown condition*. Hamburg and Prague, 69 pp.
- VMD 2016. *Forest statistics CD*. State Forest Service. <http://www.vmd.gov.lv/valsts-meza-dienests/statiskas-lapas/publikacijas-un-statistika/meza-statistikas-cd?nid=1809#jump>. Accessed 29.06.2017 (in Latvian).
- Von Post, L. & Granlund, E. 1926. Peat resources in southern Sweden I. Sveriges Geologiska Undersökning, Yearbook, Stockholm, C 335, **19**, 128 (in Swedish).
- Zālītis, P. 1991. Silvicultural development of potentially fertile, but poorly yielding drained eutrophic moors. *Jaunākais mežsaimniecībā* **33**, 54–60 (in Latvian).

Assessment of dairy cow herd indices associated with different milking systems

M. Gaworski^{1,*}, A. Leola², H. Kiiman², O. Sada², P. Kic³ and J. Priekulis⁴

¹Warsaw University of Life Sciences, Department of Production Management and Engineering, Nowoursynowska street 164, PL02-787 Warsaw, Poland

²Estonian University of Life Sciences, Institute of Technology, Fr.R. Kreutzwaldi 56, EE51014 Tartu, Estonia

³Czech University of Life Sciences Prague, Faculty of Engineering, Kamycka 129, CZ16521 Prague 6, Czech Republic

⁴Latvia University of Life Sciences and Technologies, Faculty of Engineering, Cakstes blvd. 5, LV-3001 Jelgava, Latvia

*Correspondence: marek_gaworski@sggw.pl

Abstract. The objective of the research was to find whether any differences exist between cattle herds operated by certain milking installations. The cattle herds were studied not only by herd size but also by certain data, like annual milk yield, age and number of lactations. Data collected on dairy farms that operate pipeline milking systems, milking parlours and automatic milking systems were analysed. These farms are situated in three Baltic States. The investigated Estonian dairy farms indicated a decreased tendency in the prevalence of disease cases for udder diseases with an increase in cow herd size. An index of cow production potential was proposed to compare different (including number of lactations) group of cows in dairy farms.

Key words: AMS, cow herd, dairy production, milking parlour, pipeline milking system.

INTRODUCTION

A dairy farm constitutes a complex system, in which many factors and relationships between the factors can be identified. Dairy cattle, technical equipment, biological material (e.g. forages and other necessary feed resources and water) as well as technological solutions, such as housing systems, determine the dairy production potential in particular farms. Each of these elements of the dairy farm production potential can encourage the development of detailed research.

Milking is one of the most important jobs on a dairy cattle farm, and it also can be the most tedious one, having to be done two or three times every day. Hence, many studies have been carried out with the intention to further increase milking efficiency in dairy farms. In practice technical parameters, functional facilities, productivity, labour intensity, energy consumption, the structure of some activities (e.g. milking, washing and idle time), cow herd management and others have been used as criteria to assess milking. Cooper & Parsons (1999) indicated the significance of economic aspects in a simulation model of automatic milking assessment. They concluded that dairy farmers,

who are to switch from conventional milking to automatic milking, they should decide how to deal with the increase in milk yield, e.g. by reducing their herd size. Nitzan et al. (2006) developed models for simulating different type of milking parlours to predict milking parlor performance including herd size, number of milking stalls, labour quality, and cow characteristics. It was found that for a parlour with up to 14 milking stalls, a side-opening design provided greater capacity than parallel or rotary parlours. Wirtz et al. (2002) presented the problem of comparing AMS to conventional milking parlour, while Gygax et al. (2007) indicated that it would be valuable to compare functional aspects in certain automatic milking systems and milking parlours. Rotz et al. (2003) considered possible relationships between milking, farm size and milk production. Some connections between producer satisfaction, efficiency, and investment cost factors of different milking systems were investigated by Wagner et al. (2001).

Milking systems differ considerably in particular countries based on the type of agriculture applied. In Estonia, similar to the USA, farms often hold large herds of dairy cows and the milking process is performed by specialised personnel. This type of production is economically profitable only for large herds. In Estonia, as well as in Western Europe, there are also small farms, where most work is performed by the farmer and his family members. Currently there is an increase in number of farms with an average annual milk yield exceeding 10,000 kg of milk per cow. According to data obtained from the Estonian Livestock Performance Recording Ltd., at the end of 2016 there were 24 dairy farms with an annual milk yield of more than 10,000 kg milk per cow and in five farms even more than 11,000 kg. On one dairy farm the milk yield per cow was 12,239 kg at a herd size of 534.

In order to facilitate increased milk yield considerations regarding milking aspects such as milking system and/or farm equipment and personnel have to be included and related to the given production settings.

The objective of the current study was to explore differences between cattle herds operated by pipeline milking systems, milking parlours and automatic milking systems situated in three Baltic States. It was expected to find associations between herd characteristics and different milking systems that could be used to analyse milking efficiency. Identification of herds were evaluated by means of herd size, annual milk yield, age, number of lactations and health problems.

MATERIALS AND METHODS

To carry out detailed analyses, proper data were monitored and collected in dairy farms in Estonia, Latvia and Poland. The sampling strategy of data depended on availability of particular data in the investigated dairy farms.

Estonian data were collected from eight dairy cattle farms. The main criterion to select the farms for investigation was the type of used milking system. When compiling data, the number of milking stalls was also included in farms equipped with both AMS and milking parlour (Table 1). The farms differed in cow herd size. All farms in Estonia raised the Estonian Holstein breed. The herds were housed indoors throughout the year in a free-stall barn on six enterprises and on two enterprises in tie-stall barn.

Estonian research data – apart from information given in Table 1 – included cow performance and health data. The health data, i.e. udder diseases, feet diseases, fertility problems, accidents, metabolic problems and low productivity problems were included

as outcome variables, while milking system and cow herd size there were explanatory variables in the statistical analysis to assess possible associations between cow health and herd size or milking system. Based on the numbers of each kind of health and productivity problems prevalence of disease cases of the given problems in individual dairy farms were calculated. The prevalence of disease cases was calculated as a relation of the number of health / productivity problems to average cow herd size, including observations for one year.

The two Latvian dairy farms differed as to milking systems. One farm was keeping a group of 145 cows and milking them with use of two AMS installations, while the second dairy farm was equipped with side by side milking parlour to handle 320 cows (Table 1).

Table 1. Data concerning dairy farms included in the investigation

Country	Milking system	Number of farms	Cow herd size	Description of milking system
Estonia	AMS	2	347, 380	6×1-stall AMS, 6×1-stall AMS
	Milking parlour	4	360, 505, 605, 617	2×7 hb, 2×10 p, 2×10 p, 2×10 p
	Pipeline	2	130, 170	
Latvia	AMS	1	145	2×1-stall AMS
	Milking parlour	1	320	2×10 sbs
Poland	AMS	1	140	2×1-stall AMS
	Pipeline	1	65	

Description: AMS – automatic milking system; hb – herringbone milking system; p – parallel milking system; sbs – side by side milking system.

The two Polish dairy farms were equipped with different milking systems, too. One of the farms was using two AMS to handle two independent groups of cows. The total herd size in the farm with automatic milking system was 140 cows. The second Polish farm was milking 65 cows using a pipeline milking system (Table 1). The farms raised Holstein Friesian breed. Apart from cow herd size, other data were compiled on Polish farms comprised by the study, i.e. milk yield, milk fat and protein content. These independent variables were used to calculate a proposed index of cow production potential for two farms. Cow production potential was only calculated for Polish farms. Since not all research data were accessible in each dairy farm and country, it was only possible to compare proper data and indices for dairy farms within each country, but not between the countries.

To calculate the index of cow production potential the following formula was proposed:

$$I_{cpp} = \frac{\sum_1^n Y_m \cdot P_f \cdot P_p}{100 \cdot n} \quad (1)$$

where I_{cpp} – index of cow production potential; Y_m – milk yield per day (kg day⁻¹); p_f – percentage of milkfat content (%); p_p – percentage of protein content (%); n – number of analysed months (periods).

To find the I_{cpp} value for each cow, the data collected during one year were taken into account. The data concerning milk yield per day, percentage of milkfat and protein were compiled at a frequency of one day per month, according to general rules provided in Poland by the national system of dairy cows recording.

The index of cow production potential (I_{cpp}) was used to assess cows in two Polish dairy farms equipped with AMS and pipeline milking system. With the use of the index we compared two cow herds. Cows in the herds represented different lactation numbers on farms. The calculated index values for each cow were taken to show distribution of the index for cows with different lactation number in two considered herds.

Statistical analysis only for collected Estonian data was performed using the Statistic v.13 software. The descriptive statistical indicators, i.e. mean and standard deviation were determined for the assessed cows and cow herds. The comparison of data obtained in the dairy farms with three different milking systems (automatic milking system, milking parlour and pipeline milking system) was conducted using the ANOVA test. The significance level was $\alpha = 0.05$. A multiple range test for comparing means in the analysis of variance, i.e. Duncan test was used; homogeneous groups were identified. The data were also analyzed by analysis of variance with herd as a random effect and the annual milk yield per cow, and the prevalence of health problems as fixed effects. Linear regression was used to show relationship between herd size and some factors concerning cows.

RESULTS AND DISCUSSION

An analysis of data concerning cow herd size and milk yield for Estonian dairy farms equipped with various milking systems showed that the highest and lowest value of standard deviation (SD) concern farms, in which automatic milking system (AMS) was used (Table 2). There were only two Estonian farms with AMS included in the survey. Farms were equipped with the same number of six stalls (Table 1), while the difference between cow herd size was about 10%. For such data the SD amounted to ± 23 cows. On the other hand the SD for annual milk yield per cow in farms with AMS amounted to $\pm 1,843$ kg cow⁻¹ year⁻¹. Such SD value was ten times higher as compared to the relevant SD value for dairy farms equipped with a milking parlour (Table 2). Annual milk yield per cow in both Estonian farms with AMS was as following: 11,637 and 9,030 kg cow⁻¹ year⁻¹. Such data suggest possible differences between dairy farms in terms of efficiency of AMS use and confirm other observations showing differences in efficiency of AMS use on the national level – between countries (Gaworski, 2016).

Considering milk fat content recorded in the investigated Estonian dairy farms the following data were found for farms with AMS, milking parlour and pipeline milking system (mean \pm SD): $3.99 \pm 0.08\%$, $3.91 \pm 0.21\%$ and $4.26 \pm 0.33\%$, respectively. The milk protein content for the mentioned milking systems amounted to (mean \pm SD): $3.35 \pm 0.04\%$, $3.32 \pm 0.04\%$ and $3.37 \pm 0.04\%$, respectively.

A comparison of data – according to results of analysis of variance (ANOVA) – obtained from Estonian dairy farms (Table 2) showed significant differences ($p < 0.05$) in herd size of dairy cows operated by distinguished milking systems. But results of the analysis of variance did not point to significant differences in mean values ($p > 0.05$) for annual milk yield per cow based on the different milking systems.

The significant differences in herd size of dairy cows kept in the farms comprised by the study confirm that general rules concerning selection of milking system to number of cows were fulfilled. Generally, an increase in cow herd size is associated by selection of milking system characterized by higher and higher capacity, i.e. amount of milk collected per hour. Proper milking systems in dairy farms can be a source of satisfaction, efficiency, and optimized investment costs that are beneficial for producer (Wagner et al., 2001). Thanks to criteria for optimization (Kic, 2015) it is possible to equip farms with milking installations that support effective dairy production systems.

Results of the variance analysis (Table 2) point to substantial differences in mean values ($p < 0.05$) for prevalence of udder diseases between the compared milking systems. Thus, the results of the present study emphasize the importance of the milking system for variables representing health of dairy cow herd. Examples of in-depth investigations (Rasmussen et al., 2001) show that the problem of mastitis and other diseases in dairy farms can be a field of individual assessment of each milking system, including AMS.

The problem of udder diseases is connected with milking (Svennersten-Sjauna et al., 2000). However, the data collected in Estonian dairy farms included also other health problems. The analysis of variance showed significant differences – concerning some other health problems, i.e. feet diseases, fertility and metabolic problems – between farms with considered milking systems (Table 2).

Table 2. Analysis of variance for cow and cow herds, including prevalence – mean \pm SD – for compared cow herds operated by different milking systems within recorded data for one year

Farms with milking system	Herd Size	Milk yield	Udder diseases	Feet diseases	Fertility problems	Accidents	Metabolic problems	Low product
	Heads	kg cow ⁻¹ year ⁻¹	%	%	%	%	%	%
AMS	364 ^{a,b}	10,334	6.05 ^a	4.25 ^a	6.22 ^a	1.80	2.74 ^{a,b}	1.79
	± 23	$\pm 1,843$	± 0.00	± 0.31	± 0.98	± 0.31	± 0.21	± 0.08
MP	522 ^b	10,598	4.61 ^a	3.15 ^a	3.92 ^a	2.00	1.88 ^a	0.77
	± 119	± 178	± 1.45	± 0.78	± 0.81	± 0.80	± 0.63	± 0.33
PPL	150 ^a	8,307	13.87 ^b	8.62 ^b	11.83 ^b	3.69	4.07 ^b	1.74
	± 28	± 284	± 2.14	± 3.04	± 1.76	± 0.22	± 0.77	± 0.80
<i>p-value</i>	0.0158	0.0609	0.0020	0.0216	0.0012	0.0513	0.0233	0.0620

AMS – automatic milking system; MP – milking parlour system; PPL – pipeline milking system; ^{a, b} – denoted homogenous groups; the different letters a and b refer to the significance of difference between the values in column at the level of at least 95%.

Analysis of variance with herd as a random effect showed significant difference ($p < 0.05$) in mean values for udder diseases, metabolic diseases, and fertility problems for Estonian dairy farms.

Data concerning annual milk yield per cow and health problems, i.e. prevalence of udder diseases in Estonian dairy farms, were correlated with cow herd size in these farms (Figs 1, 2). The annual milk yield per cow is characterised by increase trend, while prevalence of udder diseases is characterised by decrease trend when the farms with higher and higher cow herd size are considered. The results of the linear models show a high r value for the analysed relationship between prevalence of udder diseases and cow herd size ($r = 0.93$), while r value for the relationship between annual milk yield per cow

and cow herd size amounted to 0.65. The high (r) value indicates that the model for the prevalence of udder diseases well fit the data included in the analysis. On the other hand because of relatively small sample size extrapolation in general should be made with caution and it would be valuable to consider data comprising more cow herds to confirm observed relationship between the prevalence of udder diseases and cow herd size.

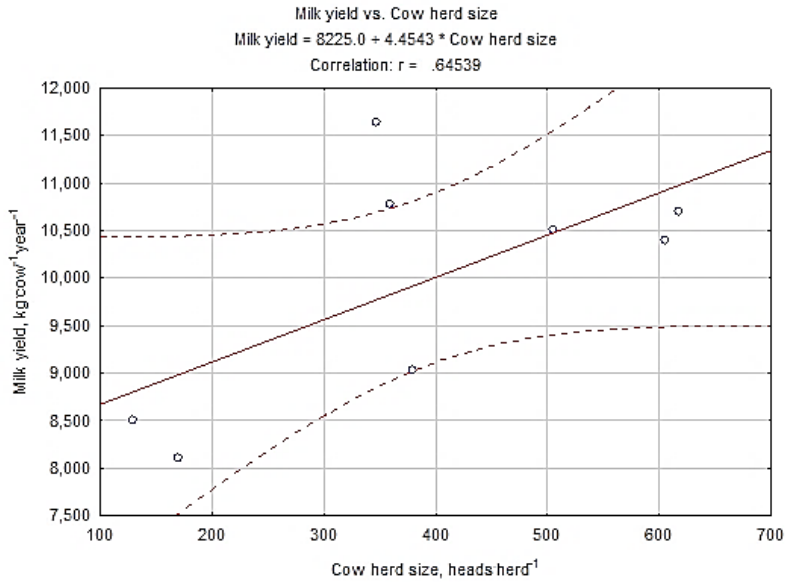


Figure 1. Relationship between cow herd size and annual milk yield per cow.

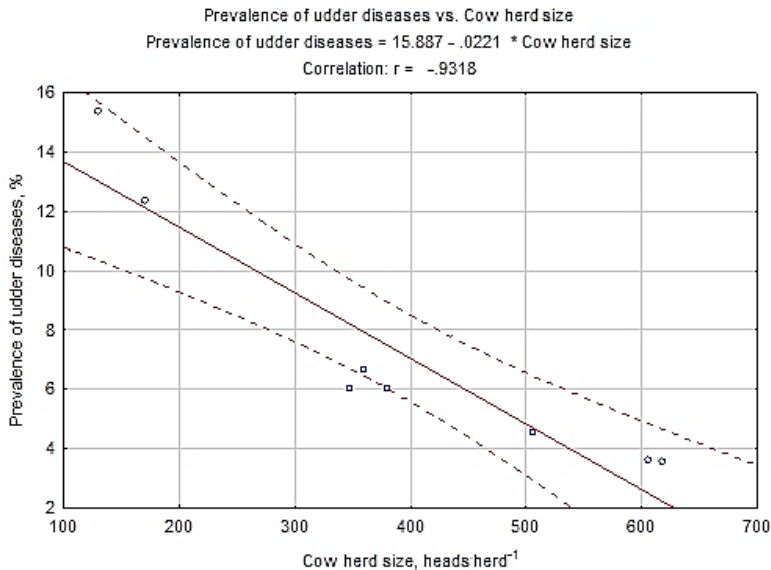


Figure 2. Relationship between cow herd size and prevalence of udder diseases.

The health problems included in the executed investigations constitute only a smaller part of health aspects considered in the specialist literature. Hillerton et al. (2004) emphasized the role of further elements in the cow health assessment, including such features as locomotion, body condition (including teat conditions), fertility, cell count and generally udder health. King et al. (2016) investigated lameness prevalence as well as herd-level housing and management to find any associations with productivity and cow behaviour in herds with automated milking systems. The prevalence of severe lameness was positively associated with stocking density, while doubling the prevalence of severe lameness (from 2.5 to 5%) was associated with decrease in milk production of 0.7 kg per cow per day. Cook & Nordlund (2009) investigated influence of the environment on claw health and herd lameness dynamics. The environment included different type of floor, bedding material and stall design in lying area as a main criteria to compare dairy farms. For such data there was possible to show effect of some factors representing direct contact with animals on health problems. In our research approach the health problems were considered for different cow herd size, which can be included as an indirect factor in the cow health analyses. Some aspects of cow health problems recognized in dairy herds with tiestall, freestall, and automated milking systems were investigated by Higginson Cutler et al. (2017). It was concluded that producers underestimate lameness prevalence, which highlights that lameness detection continues to be difficult in all housing systems, including especially herds with tiestall system.

The most interesting results were obtained by the comparison of the number of lactations in the two Latvian dairy farms. In the farm equipped with automatic milking system the number of lactations per cow was 4.19 ± 0.38 , while number of lactations per cow in the farm with side by side milking parlour amounted to 3.15 ± 0.20 . Such results can be inspiration to develop discussion on the problem of cow longevity. Improved longevity can show effect on an increased productivity of the herd, because replacement, reproduction and veterinary costs are lowered, while mean milk production of the herd is increased (Olechnowicz et al., 2017). Rushen & de Passillé (2013) indicated that elimination of the main causes of involuntary culling significantly improves cow longevity and increases profits of the farm.

Results of Latvian dairy farms comparison indicate differences between some data describing cows in the farms equipped with AMS and milking parlour. When compared AMS with typical milking parlour it is possible to notice that because cow do seek more milkings when they can do it voluntarily in the AMS systems so it might be expected, that farms with conventional milking systems could increase their number of daily milkings. Considering milking data of 34 single automatic milking system (AMS) units on 29 Galician dairy farms Castro et al. (2012) found that the daily milking throughput could be maximized at 2.4 to 2.6 milkings per cow. The same authors indicated that the efficiency of the AMS use can be recognized by percentage of milking time, i.e. the percentage of hours the AMS is actually milking per day. Milking capacity expressed by the number of cows that the automatic milking system is able to milk, can be determined by the individual performance of the cow and the settings of the system parameters (Komiya et al., 2002). To evaluate automatic milking system and milk yield Bach & Busto (2005) measured milking interval regularity and teat cup attachment failures; uneven frequency (weekly coefficient of variation of milking intervals $> 27\%$) decreased daily milk yield.

Another criteria to compare dairy farms with AMS and conventional milking parlour there is technical efficiency. Steeneveld et al. (2012) analysed actual farm accounting data for 400 Dutch dairy farms. They found that farms with AMS had significantly higher capital costs (12.71 euro per 100 kg of milk) than farms with conventional milking system (10.10 euro per 100 kg of milk). Another hand, total labour costs and net outputs were not significantly different between farms with AMS and conventional milking system.

An analysis of data compiled in two Polish dairy farms allowed the identification of the percentage of cows representing the different lactation numbers in the farms. A comparison of the farm equipped with pipeline milking system and a farm with AMS shows that a considerable part of the given herds include young animals, i.e. cows in first and second lactation in this case study example (Fig. 3). It can be interesting that total percentage of cows in first, second and third lactation is nearly the same (about 89%) in each of two farms. Results of the observation can inspire further analyses of more herds to confirm or negate these trends concerning the distribution of age groups by taking lactation numbers into account.

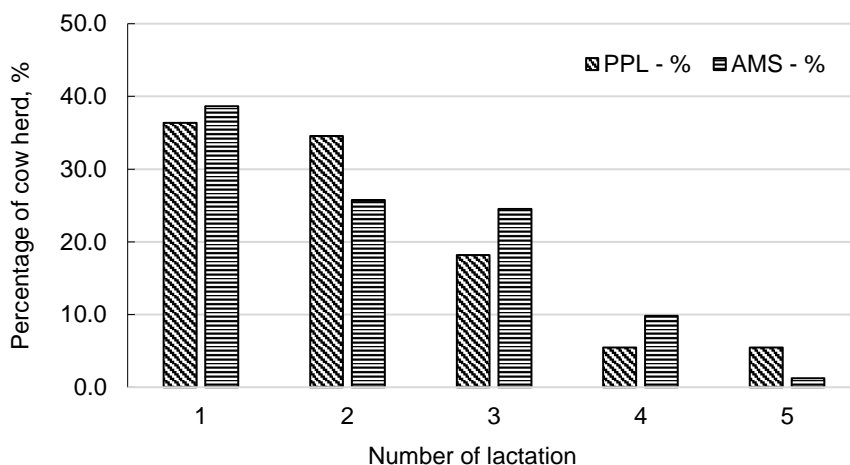


Figure 3. Percentage of cows in different lactation for two Polish farms, i.e. equipped with pipeline milking system (PPL) and automatic milking system (AMS).

Changes in the index of cow production potential were presented for an independent variable, i.e. the number of lactations, including cows handled by pipeline milking system (Fig. 4) and automatic milking system (Fig. 5).

Based on the shape of the two curves presenting changes of the index of cow production potential (I_{cpp}) for cows handled by pipeline milking system and automatic milking system, respectively, differences in the age distribution of cows are seen. The curve for the pipeline milking system herd shows an increasing tendency for successive lactation groups (Fig. 4), while the curve for the automatic milking system herd indicates maximum value of the I_{cpp} index for fourth lactation group (Fig. 5).

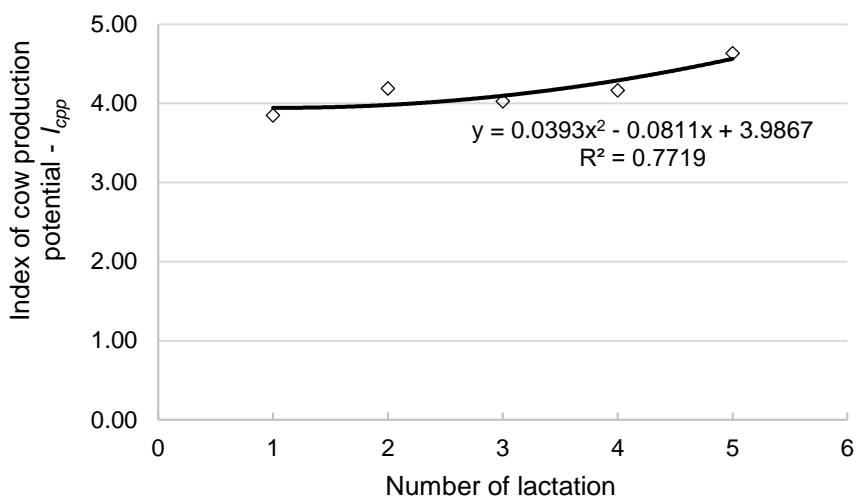


Figure 4. Changes in index of cow production potential (I_{cpp}) for cows in different lactation in farm equipped with pipeline milking system.

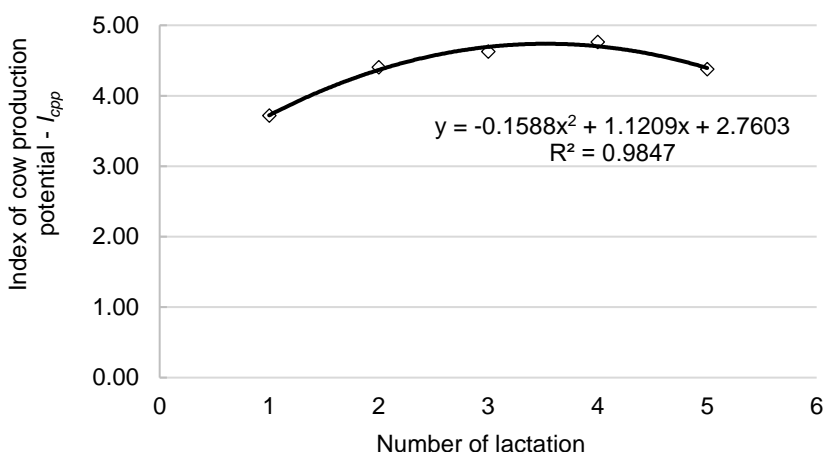


Figure 5. Changes in index of cow production potential (I_{cpp}) for cows in different lactation in farm equipped with automatic milking system.

Including data collected in the two Polish dairy farms and results of calculation suggests that that highest values of the index of cow production potential (Figs 4–5) are associated with the lowest values of the percentage of cows in the analysed herds, i.e. cows in fourth and fifth lactations (Fig. 3). Such observation for two investigated farms show that animals with most valuable production indices constitute the lowest percentage in the cow herds handled by pipeline and automatic milking systems.

Milking systems, cows and cow herds are subjects included in the process of dairy production improvement, where one of the most important aims is the achievement of higher and higher efficiency of dairy production. Dairy production efficiency can be expressed by different indices, e.g. concerning milking systems and details concerning milking performance (Davis & Reinemann, 2002; Bach & Busto, 2005) and quality

(Klungel et al., 2000; Rasmussen, 2002) to show changes in milk quality parameters before and after introduction of interventions in dairy farms like automatic milking systems. Factors that affect the capacity of the automatic milking system (Priekulis & Laurs, 2012), including different conditions of dairy production development and effective AMS use (Gaworski et al., 2013), constitute a key element in the execution of studies concerning relationships between technical and biological potential in dairy production (Gaworski & Leola, 2014).

CONCLUSIONS

Results of the undertaken study confirmed that general rules concerning selection of milking system to number of cows were fulfilled in the investigated Estonian dairy farms. Generally, the increase in cow herd size was associated with selection of milking system characterized by higher and higher annual milk yield per cow.

The cases investigated in the Estonian dairy farms showed a decreased tendency in prevalence of udder diseases with increase in cow herd size. Such results are limited to the present study and cannot be extrapolated to the dairy population. In the perspective approach it could prove to be valuable to continue analyses related to cow health problems arising from different milking systems.

The Latvian cases showed possible differences as to the number of lactations per cow in farms with AMS and milking parlour.

ACKNOWLEDGEMENTS. The authors would like to thank Dominik Jobda for his help in compilation of data concerning Polish dairy farms.

REFERENCES

- Bach, A. & Busto, I. 2005. Effects on milk yield of milking interval regularity and teat cup attachment failures with robotic milking systems. *Journal of Dairy Research*, **72**, 101–106.
- Castro, A., Pereira, J.M., Amiama, C. & Bueno, J. 2012. Estimating efficiency in automatic milking systems. *Journal of Dairy Science* **95**(2), 929–936.
- Cook, N.B. & K.V., Nordlund. 2009. The influence of the environment on dairy cow behavior, claw health and herd lameness dynamics. *The Veterinary Journal* **179**(3), 360–369.
- Cooper, K. & Parsons, D.J. 1999. An economic analysis of automatic milking using a simulation model. *Journal of Agricultural Engineering Research* **73**(3), 311–321.
- Davis, M.A. & Reinemann, D.J. 2002. Evaluation of milking performance of cows milked with a conventional parlor compared to an automatic milking system. *ASAE Annual International Meeting / CIGR XVth World Congress*. 8 p.
- Gaworski M. 2016. Assessment of dairy production development on the example of Polish conditions and comparisons with certain European countries. *Agraarteadus: Journal of Agricultural Science* No. **XXVII**(1), 12–18.
- Gaworski, M. & Leola, A. 2014. Effect of technical and biological potential on dairy production development. *Agronomy Research* **12**(1), 215–222.
- Gaworski, M., Leola, A. & Priekulis, J. 2013. Comparative analysis on effectiveness of AMS use on an example of three European countries. *Agronomy Research* **11**(1), 231–238.
- Gygax, L., Neuffer, I., Kaufmann, C., Hauser, R. & Wechsler, B. 2007. Comparison of functional aspects in two automatic milking systems and auto-tandem milking parlors. *Journal of Dairy Science* **90**(9), 4265–4274.

- Higginson Cutler, J.H., Rushen, J., de Passillé, A.M., Gibbons, J., Orsel, K., Pajor, E., Barkema, H.W., Solano, L., Pellerin, D., Haley, D. & Vasseur, E. 2017. Producer estimates of prevalence and perceived importance of lameness in dairy herds with tiestalls, freestalls, and automated milking systems. *Journal of Dairy Science* **100**(12), 9871–9880.
- Hillerton, J.E., Dearing, J., Dale, J., Poelarends, J.J., Neijenhuis, F., Sampimon, O.C., Mitenburg, J.D.H.M. & Fossing, C. 2004. Impact of automatic milking on animal health. In: Meijering, A., Hogeveen, H., de Koning C.J.A.M. (Eds.), *Automatic Milking: A Better Understanding*, Wageningen Academic Publishers, Wageningen, The Netherlands, p. 11.
- Kic, P. 2015. Criteria for optimization of milking parlour on dairy farm. In: *Proceedings of 14th International Scientific Conference on Engineering for Rural Development*. Latvia University of Agriculture, Jelgava, 106–111.
- King, M.T.M., Pajor, E.A., LeBlanc, S.J. & DeVries, T.J. 2016. Associations of herd-level housing, management, and lameness prevalence with productivity and cow behavior in herds with automated milking systems. *Journal of Dairy Science* **99**(11), 9069–9079.
- Klungel, G.H., Slaghuis, B.A. & Hogeveen, H. 2000. The effect of the introduction of automatic milking systems on milk quality. *Journal of Dairy Science*, **83**(9), 1998–2003.
- Komiya, M., Morita, S., Izumi, K. & Kawakami, K. 2002. Mathematical simulation of milking capacity in automatic milking system. In: *The First North American Conference on Robotic Milking*. Toronto, Canada, pp. III89–III92.
- Nitzan, R., Bruckental, I., Bar Shira, Z., Maltz, E. & Halachmi, I. 2006. Stochastic models for simulating parallel, rotary, and side-opening milking parlors. *Journal of Dairy Science* **89**(11), 4462–4472.
- Olechnowicz, J., Kneblewski, P., Jaśkowski, J.M. & Włodarek, J. 2017. Effect of selected factors on longevity in cattle: a review. *The Journal of Animal & Plant Sciences* **26**(6), 1533–1541.
- Priekulis, J. & Laurs, A. 2012. Research in automatic milking system capacity. In: *Proceedings 11th International Scientific Conference on Engineering for Rural Development*. Latvia University of Agriculture, Jelgava, pp. 47–51.
- Rasmussen, M.D. 2002. Defining acceptable milk quality at time of milking. *The First North American Conference on Robotic Milking*. Toronto, Canada, pp. 9–17.
- Rasmussen, M.D., Blom, J.Y., Nielsen, L.A.H. & Justesen, P. 2001. Udder health of cows milked automatically. *Livestock Production Science* **72**, 147–156.
- Rotz, C.A., Coiner, C.U. & Soder, K.J. 2003. Automatic milking system, farm size and milk production. *Journal of Dairy Science* **86**(12), 4167–4177.
- Rushen, J. & de Passillé, A.M. 2013. The importance of improving cow longevity. *Proceedings of the Conference on Cow longevity*, August 28th–29th 2013, Hamra Farm, Tumba, Sweden, 3–21.
- Steenefeld, W., Tauer, L.W., Hogeveen, H. & Oude Lansink, A.G.J.M. 2012. Comparing technical efficiency of farms with an automatic milking system and a conventional milking system. *Journal of Dairy Science* **95**(12), 7391–7398.
- Svennersten-Sjauna, K., Berglund, I. & Pettersson, G. 2000. The milking process in an automatic milking system, evaluation of milk yield, teat condition and udder health. In: *Hogeveen, H., Meijering, A. (Eds.), Proc. Int. Symp. Robotic Milking*. Lelystad, The Netherlands, Wageningen Pers., 277–288.
- Wagner, A., Palmer, R.W., Bewley, J. & Jackson-Smith, D.B. 2001. Producer satisfaction, efficiency, and investment cost factors of different milking systems. *Journal of Dairy Science* **84**(8), 1890–1898.
- Wirtz, N., Oechtering, K., Tholen, E. & Trappmann, W. 2002. Comparison of an automatic milking system to a conventional milking parlor. In: *The First North American Conference on Robotic Milking*. Toronto, Canada, **3**, 50–55.

Agricultural field production in an ‘Industry 4.0’ concept

M.H. Jørgensen

University of Southern Denmark, Maersk Mc-Kinney Moller Institute, Campusvej 55, DK5230 Odense M, Denmark

*Correspondence: MAHEJ@mmmi.sdu.dk

Abstract. Precision Agriculture is a well-established concept in agricultural field production. It has developed over the last three decades. As part of this concept, farmers are used to collect and handle data. Farmers are also used to create solutions for field operations based on their knowledge of diversity and local data.

When compared to classic industrial production, agricultural field operations interact with a biologically-active system. From a production management system point of view, industrial production takes place in close, well-defined environments in which performance data can, to a great extent, be measured by deterministic matters: mass (kg), volume/dimensions (m^3/m), time (sec), etc.

In agricultural operations such as work involving tillage, seeding, fertilising, and plant care, there are by nature a good many possible adjustments available in order to optimise the operation method, plus intensity and timing. The challenge here is to establish the levels of knowledge that are necessary to support the control of the individual and/or graduated, precision-based operations. Within this context, parameters such as, for example, the workability of the soil cannot be defined in terms of a few deterministic parameters. Neither can the operational impact upon the soil which is made by the tools being used. It is assumed that this challenge is part of the reason why the concept of precision agriculture still contains a great deal of unutilised potential. The hypothesis raised by this article is that analysis should be carried out in regard to whether inspiration for the concept of an ‘Industry 4.0’ can facilitate the establishment of operational solutions in the field of precision farming.

Key words: precision farming, Industry 4.0, precision tillage, spot spraying.

INTRODUCTION

Analysing the synergy between industrial and agricultural production is not new. Agricultural production has already adapted a good deal of inspiration from industrial tools and solutions that have been dedicated and implemented for agricultural systems, such as, for example: lean, digitalisation, ERP(Sap) systems for data management and production planning. Thanks to such steps that have already been taken, agricultural field production has already been prepared for making its ‘4.0’ next step.

One of the main elements in the concept of an ‘Industry 4.0’ (Creutzmacher et al., 2015; Zezulka et al., 2016) is to look at the system as a whole, not only empirically but also by ensuring that all data and measurements are stored and are visible for analysis in one coherent system. This creates the foundation for a robust, database-lead process of

prioritisation and decision-making. A central tool in extracting the valuable information from the data pool is the 'big data' approach (Sabarina & Priya, 2015) which can show itself to be potentially valuable in the development of the agricultural system. This implies that all elements in the production chain including production tools and products is assumed to be part of a 'cyber-physical system' (Lee et al., 2015), meaning that all data monitored is measured and communicated to a local cloud and/or the cloud in general. What makes the difference in the 4.0 concept is that the knowledge that is stored and hidden in this pool of data is actively used and analysed in the operational management of the production systems (Stock & Seliger, 2016).

In the development of 'precision farming', it has not been possible to establish the necessary decision support to allow work to be carried out, such as tillage operations, with a local, graduated approach at a commercial scale. This results in resistance to the further development of the concept of 'precision farming' (Pierpaoli et al., 2013). The hypothesis being put forward here that the 'Industry 4.0' and/or big data approach could be even more beneficial when used in this form of system. All of the required information is available via the cloud, which also includes quality measurements of the yield, not only in terms of volume but also including the main characteristics of the quality parameters.

Van Evert et al., 2017 describes how data models can be developed and trained for use in weed control and crop protection. Based on this it can be assumed that similar models can be developed for the potential improvement over the control of other operations in agricultural production. One example covering large-scale potential which deserves to be tested is the hypothesis that beneficial information can be extracted by analysing the links in-between such as, for example, the content of some minerals in the yield and root efficiency in the growing period, and then extracting any information which is suitable for describing the potential need for tillage. Similarly, if the occurrence of weeds and weed seeds are analysed during the harvesting process then a potential link may be discovered to previous herbicide application in the growing period and to the local need for herbicide composition and intensity in the coming year. Within this perspective the concept of 'Industry 4.0' can support the next step of development in precision farming.

Globally the industrialised part of the world has been looking for options in terms of systemising the optimisation of industrial production in order to create more value. The overall goal has been to enable the capability of handling more complexity as described by Walter et al. (2017), in order to be able to meet market trends in which a higher degree of customisation creates more value. This involves the feeling of value for the customer who is in a situation of use/consumption, but it also involves environmental impact and impact upon society in general. For production purposes this challenges the ability to produce the correct scaling, adapting variety, and making changes in design, and there is an even higher focus on quality and environmental/ social impact. This leads to a higher degree of adaptive technology in manufacturing systems, adding value in all chains by transparency and coordination and/or collaboration along the entire chain, horizontally and vertically. This involves a close connection with suppliers to the market and, internally, between the various departments and units, it involves design, testing, production preparation, general production, logistics, validation, and so on. As described by Van Evert et al. (2017), the concept of big data can be expected to form a strong tool

to link together isolated models and to extract information from individual sources and sensors.

Within the industry in general, the goal is to develop the production facility by adapting the newest technology and utilising it in an intelligent manner, such that production can be economically beneficial in a dynamic environment with a much greater degree of customisation, demanding scalability (production volume) and high complexity in design variations and design shifts.

In development work which has been controlled by German thinking, this has been defined within the framework of 'Industry 4.0' in a way which is similar to that of the American 'Industrial Internet of Things' and the Japanese 'Robot Revolution'.

In very short-term presentation, Berger et al. (2007) defines 'Industry 4.0' in three elements: Smart Data, Smart Manufacturing, and Smart Workforce. This means that all parameters which are part of the products and production system are digitalised, and data can be collected in one big coherent system which provides the visibility between different products and different production operations/processes. In the industrial context, information is stored, ideally, in the cloud in order to achieve full visibility, and this also allows a connection to be formed between suppliers and customers. The development of technical solutions is progressing at a high velocity, and many new, beneficial production systems are being introduced onto the market. This is a way in which the industry is able to meet the demands of customers for dedicated products and solutions. The task for the industry is to establish a framework so that it can, in a rational way, take the right decisions in a complex context. A summary entitled 'Smart Manufacturing' outlines the means of outputting high valuable products with the most efficient usage of new technology in an adaptive, optimised production system. Even when data can be systemised and structurally analysed there is a need for a 'Smart Workforce' so that an overview can be maintained, one which takes care of operational control and the prioritisation of the more long term decisions.

When looking more specifically into the challenge posed by and the potential offered for agriculture, the image differs a bit, but with substantial similarities (Pierpaoli et al., 2013). In agricultural production, sensors and data harvesting are already well implemented. The workforce is skilled in handling this together with modern advanced production equipment, especially in terms of tractors and implements in the latter case. Production equipment is already designed or prepared for 'site specific' control.

When looking a little deeper in the business models for agricultural field production, this can be divided in two (Busse et al., 2014). The first of these covers large-scale bulk production in which the focus is on value optimisation through high quality output, minimal environmental impact, and achieving cost reductions by planning and optimising operations due to timing, method, and intensity. Farmers running this type of production already cover the advanced equipment that is available on the market. The second business model focuses more on diversity and local sales. Here the distances from farm to customer are typically smaller. There is a higher focus on the diversity in the delivery, the value for the customer, and the environmental and social impact from production.

In this work the focus has been placed on the first business model, covering the bigger production units as the farmers here are the most prepared (Busse et al., 2014). Paustian & Theuvsen (2017) describes how farmers growing more than 100 ha adopt the concept of precision farming and digitalisation, whereas the same tendency is not seen

by smaller farmers. Kutter et al. (2011) describes the same tendency for countries like the Czech Republic, Denmark, and Greece. Although it has not yet been developed, it can be assumed that there is also similar potential for smaller enterprises. An argument for this can be the fact that smaller enterprises typically have a close connection with their the customers, and that they therefore have the potential to be able to develop customised products. Walter et al. (2017) describes how smart farming can be the key to handling diversity and the missing deterministic models in the development of sustainable agriculture. Walter et al. (2017) also describes how disruptive solutions can be expected to push development forwards. Busse et al. (2013) describes from a survey amongst German farmers how farmers play a positive role in the adoption of precision farming, but limited adoption is due to a lack of operative systems that can be shown to be valuable in practical use, thanks to significant limitations.

Looking a little deeper into the development stage of precision agriculture, precision agriculture took its first steps during the last few decades of the twentieth century (Pierpaoli et al., 2014), where the environmental impact from agriculture was put into focus. It was probably due to this that the first developments focused on fertilising and spraying. Fertilising had its focus on graduating the applied amount of fertiliser over the entire field, while aiming for the best possible plant uptake and yield. In terms of spraying, the challenge has been to reduce the amount of fertiliser being used. To this end, more appropriate technology has been developed (Malneršič et al., 2016). The concept of patch spraying has taken off thanks to this concept, where the pesticide is applied only in spots in which a specific weed specie/disease is represented (Gonzales-de-Soto et al., 2016). On a minor scale a good deal of effort is being put into the development of adaptive spraying, where the spray is placed precisely on the leaves of the specific weed plant (Tang et al., 2016). The principle behind precision agriculture is also available for tillage operations and seeding, although this is something that has not yet been introduced on a big scale.

The technology for precision agriculture is already to a great extent available on the market. Injection spraying is a system which injects the pesticide into the water in a pipeline to spray nozzles, or a more advanced version involves it being introduced directly for individual nozzles. Alternatively, systems have already been introduced with more pipelines and nozzles in which the individual pipeline can be activated when needed (Gonzalez-de-Soto et al., 2016; Malneršič et al., 2016).

A graduation of fertilising efforts is possible with almost all of the new spreading machines on the market. Here the spray levels are controlled the workings of the machinery, as the spreader normally does not have any subsections.

Implements for tillage operations have, to a broad extent, been developed in sections and with integrated adjustment options. Not much development is required to operate this precision-based method.

The big challenge is the input data for controlling operations. Ideally, this would involve information: how much fertiliser is available, which pesticide is needed, and in which doses - what is the need for tillage operations here, etc. This has been a central topic for research into precision farming. Due to the nature and complexity of the task no unique solutions have so far been found. The information required is not measurable by any unique sensors and neither can it be deterministically calculated.

Since the early twenty-first century, GPS positioning has been accessible for commercial agricultural use. Now it is close to being standard equipment on modern tractors. Through this, systems are available for monitoring positioning and for the storage of additional measurements or control data. From static measurements, information about the soil can be extracted. This can be extended by an online measurement of the soil temperature and humidity. The use of 'Leaf Index' measurements from IR and RGB measurements is well established and is used for measurements of crop density and growth.

Measurements of density and species of weed are still under development, but the available options have increased through the development of drones as sensor carriers (Walter et al., 2017).

At harvest time the yield measurement system has been operational for some years. In this area it could also be possible to measure selected quality parameters.

The overall data handling and production planning processes imply the use of SAP/ERP systems which fully reach industrial standards in terms of visibility and options for cross-linking data.

In developmental terms, until now progress has been controlled by adapting new technologies that can benefit agricultural production. Lindblom et al. (2016) describes how the available precision adaptable technology is utilised in practice, in connection with the available systems for precision-based control. Experience shows that the economical benefits are weak in the current setup. Lindblom et al. (2016) concludes that a stronger implementation of precision agriculture is required for development to be able to reach more sustainable levels of agriculture. It seems that there still is a great deal of potential in the improvements, both in regard to economical and environmental benefits. Turning this into something which can be made operational requires new thinking and dedicated development. This is where the concept of 'Industry 4.0' seems to open up some fresh possibilities. Sheng & Brindal (2012) describes how policy implications can also support development, with dedicated actions being taken by developed countries.

MATERIALS AND METHODS

When looking at agricultural production from a 4.0 perspective, the overall goal could be defined as follows:

The overall goal:

The right form of operation and application on the right spot at the right time. This means that individual operations have to be scheduled and executed at the right time. The planning for this is based on economy, yield, crop quality, and environmental impact in a broad sense.

As part of the basic concept of 4.0 all operations are planned as part of the full production system. The potential in possible developments in terms of the production system are evaluated in a '4.0 Check-Up' by analysing the available options and foreseen costs against the gains, based on the economy and environmental impact. In a broader view, elements such as customer, acceptance, and influence upon society in general could also be analysed, although these areas are not included in this work. From the 'Industry 4.0' perspective, the concept of the 'check-up' is designed to be used for individual companies or production units. In specific use, the check-up also involves 'readiness' for the actual farmer to take the step into utilising 'Industry 4.0'. Following

this paragraph are some guidelines and statements which concern agricultural plant production.

Decision support: there are a good many individual solutions, each being of a pretty good level of quality, but each missing the benefits of sharing data (which means using the cloud), and the big data approach. This is an area in which agriculture could learn from systems being used by industry figures. Unfortunately, only the structure and thinking could be transferred, as the agricultural production system involves a good many unknown and stochastically-determined parameters. There is a great deal of value in being able to handle this uncertainty, and in being able to introduce ‘big data’ thinking.

Data: agricultural operations are characterised by the fact that there are no unique or specific measures or definitions for the needs of individual operations such as tillage or seeding, etc. This is even more of a challenge within the perspective of site-specific operations.

Access to operational technology: the technology in this area is in fact very well developed, and is also very well understood, especially in terms of how to adjust to obtain a local impact in relation to the allocation of fertiliser, pesticide, or other materials.

Potential impacts: the impacts – including potential impact upon environmental and economic issues – have been pretty well analysed in literature.

The Table 1 below covers an example of a systematic description of potentials and the needs for different elements in the production chain in terms of agricultural field production.

Table 1. Potential and needs for different operations in the cropping system: ■ – commercially accessible; ■ – partly accessible/ to be developed; ■ – to be developed

	Tillage	Seeding	Fertilising	Plant care	Harvesting
Potential goal	Being able to carry out tillage operations while only applying the intensity needed locally	Being able to vary the seeding volume to suit the potential and challenges offered by the local soil conditions	Delivering the right amount at the right spot at the right time. Due to potential plant uptake and yield	To adjust the dosage to suit local requirements, and to optimise the timing	To set out the overall planning for harvesting in the any requirements and to ensure an on-time operation. To gather useful information about the yield and other indicators
Access to system for decision support	In principal system support is available when the available information is sufficient	Decision support is commercially available	Commercially accessible	Commercially accessible for dose control. Individual plant care or spot spraying in the design phase	Close to being available on a commercial basis

Table 1 (continued)

Access to data needed for decision	Access to data is the missing link	Data possibly accessible, but not on a commercial basis	State-of-the-art, to implement empirical knowledge in the application planning	Data accessible, but hard and expensive to gather	Yield measurements have been implemented for decades. Other sensors have to be defined
Access to operational technology	Technology is developed so that it can adapt to different soil types. But it is not yet equipped with sensors and control systems	Commercially accessible	Commercially accessible	With limitations, accessible for dose control	Commercially available
Potential impact on environmental effects	Important. Influences nitrogen uptake, and nitrogen leaks to recipients. Erosion. CO ₂ emissions and erosion can be reduced	Moderate. Saving on the need for pesticides	Moderate. Better usage. Moderate saving in nitrogen leaks to recipients	Important. Saving on the consumption of pesticides	Indirectly important
Potential economical impact	Important Fuel-saving	Moderate	Moderate	Important. The cost of pesticides	Indirectly important

RESULTS AND DISCUSSION

The analysis shows a fairly high degree of readiness by farmers. There are central missing elements which, together, means that the concept of precision farming has only shown a very small part of its possible potential. However, despite the missing elements, the framework for enabling precision farming is well established within existing professional systems. There is also a readiness to adapt to the thinking required for 4.0. By using state-of-the-art technology, farmers are able also to implement forthcoming features and solutions for other forms of operations.

Table 1 shows that there is a great deal of potentials both environmental and economic, when it comes to operational spraying and tillage. For both areas the operational technology is already available on the market, or is accessible with minor developmental investment being required. The task of spraying has been a topic for a good deal of the research effort. This is where it is possible to find ‘low hanging fruit’ solutions such as, for example, spot spraying for problems which show a high degree of stability from year to year (Tang et al., 2016). New research with drone-based scouting also shows promising results for this use. For tillage work there has not been the same level of research, although a substantial level of impact can be expected both economically and environmentally. The common strategy at the field level is to apply

the tilling method and intensity required to achieve good results even on the most challenging of spots. As texture and soil conditions often vary locally at the field level, the potential is to apply a more gentle implementation of design and to reduce the intensity levels for substantial parts of the area. As an effect of this, the environmental impact relies on reduced leakage levels of nitrogen which are caused by unnecessary tillage, and a reduction of fuel consumption and CO₂ emissions (Sarauskis et al., 2014; Sarauskis et al., 2017). In the soil, reduced levels of tillage also provided a positive influence when it came to microbiology and the overall fertility of the soil with reduced CO₂ emissions and N-leak. As the cost of fuel is a large element in overall plant production, the introduction of precision tillage would also result in a large economic gain.

As explained, the problem is in the planning, for which the big data approach is proposed as one option when it comes to establishing useful data. For an accelerated start it could be worth analysing the possibility of and potential in utilising the benefits gained from a systematic mapping of soil conditions which is dedicated to the use of tillage planning. Successfully making such a system operational demands operators who are well skilled and who already have experience with the actual soil areas.

Even though the arguments included in this paper are based on overall arguments, it seems to be clear that there is substantial unused potential which could be made operational for wider development and the use of ‘precision farming’ in field production. It also seems to be clear that there are substantial potentials in applying the principles from ‘Industry 4.0’ in the further planning and development of this.

It is important to realise that ‘Industry 4.0’ is more than just a standard for digitalisation, data storage, and data interaction. Equally important is the fact that the concept also implies guidelines for planning and decision-making in a complex and context with a high degree of stochastic parameters. The concept of ‘Industry 4.0’ can in this way also be a tool which brings the source of any decision back to the farm and the local economy and conditions there. When looking at technology which has been developed for precision agriculture up until now, it can be seen that it has been controlled by the research community, which has much of its focus on the environmental aspects, and by the bigger companies such as the tractor manufacturers who support the use of GPS, field computer systems, etc. Implements for tillage work are to a great extent provided by medium-sized manufacturers who do not have the resources for carrying out development work on the scale of tractor manufacturers.

CONCLUSIONS

From the results and discussion it appears that the concept of ‘Industry 4.0’ involves a range of positive potentials as the framework for the further development of ‘precision farming’ for agricultural plant production. The analysis shows, especially in terms of spraying and tillage operations, that there is a great deal of potential which could lead to an improved production economy and to a reduced environmental impact. For both operations the technology is already ready or is close to being ready for use in the precision farming concept in a coarse resolution application. Development activities also have to be dedicated to enhancing the operability of the system and to improving precision/resolution, and thereby the potential offered by the system.

REFERENCES

- Berger, U., Thiebus, S., Vargas, A. & Algebra, V. 2007. MATURITY AND EXPERIENCE MANAGEMENT FOR RAMP-UP OF AUTOMATED MANUFACTURING SYSTEMS. In: *IFAC Papers-OnLine*.
- Busse, M., Doernberg, A., Siebert, R., Kuntosch, A., Schwerdtner, W., König, B. & Bokelmann, W. 2014. Innovation mechanisms in German precision farming. *Precision Agric.* **15**, 403–436.
- Creutzmacher, T., Berger, U., Lepratti, R. & Lamparter, S. 2016, The transformable factory: adapting automotive production capacities. In: *48th CIRP Conference on MANUFACTURING SYSTEMS – CIRP CMS 2015, Procedia CIRP 41*, pp. 171–176.
- Gonzalez-de-Soto, M., Emmi, L., Perez-Ruiz, M., Aguera, J. & Gonzalez-de-Santos, P. 2016. Autonomous systems for precise spraying – Evaluation of a robotised patch sprayer. In: *Journal of Biosystems Engineering* **146**, 165–182.
- Kutter, T., Tiemann, S., Siebert, R. & Fountas, S. 2011. The role of Communication and co-operation in the adoption of precision farming. *Precision Agric.* **12**, 2–17.
- Lee, J., Bagheri, B. & Kao, H.-A. 2015. A Cyber-Physical Systems architecture for Industry 4.0-based manufacturing systems. *Manufacturing Letters* **3**, 18–23.
- Lindholm, J., Lundström, C., Ljung, M. & Jonsson, A. 2017. Promoting sustainable intensification in precision agriculture: review of decision support systems development and strategies. *Precision Agric.* **18**, 309–331.
- Malneršič, A., Dular, M., Širok, B., Oberti, R. & Hočevar, M. 2016. Close-range air-assisted precision spot-spraying for robotic applications: Aerodynamics and spray, coverage analysis. *Journal of Biosystems Engineering* **146**, 216–226.
- Paustian, M. & Theuvsen, L. 2017. Adoption of precision agriculture technologies by German crop farmers. *Precision Agric.* **18**, 701–716.
- Pierpaoli, E., Carli, G., Pignatti, E. & Canavari, M. 2013. Drivers of Precision Agriculture Technologies Adoption: A Literature Review. *Procedia Technology* **8**, 61–69.
- Sabarina, K., Priya, N. 2015. Lowering Data Dimensionality in Big Data For The Benefit of Precision Agriculture. *Procedia Computer Science* **48**, 548–554.
- Sarauskis, E., Buragien, S., Masilionyt, L., Romaneckas, K., Avizienyt, D. & Sakalauskas, A. 2014. Energy balance, costs and CO₂ analysis of tillage technologies in maize Cultivation. *Energy* **69**, 227–235.
- Sarauskis, E., Vaitauskien, K., Romaneckas, K., Jasinskas, A., Butkus, V. & Kriauciunien, Z. 2017. Fuel consumption and CO₂ emission analysis in different strip tillage scenarios. *Elsvier Energy* **118**, 957–968.
- Sheng Tey, Y. & Brindal, M. 2012. Factors influencing the adoption of precision agricultural technologies: a review for policy implications. *Precision Agric.* **13**, 713–730.
- Stock, T. & Seliger, G. 2016. Opportunities of Sustainable Manufacturing in Industry 4. In: *13th Global Conference on Sustainable Manufacturing - Decoupling Growth from Resource Use, Procedia CIRP 40*, pp. 536–541.
- Tang, J.-L., Chen, X.-Q., Miao, R.-H. & Wang, D. 2016. Weed detection using image processing under different illumination for site-specific areas. *Computers and Electronics in Agriculture* **122**, 103–111.
- Van Evert, F.K., Fountas, S., Jakovetic, D. Crnojevic, V., Travlos, I. & Kempenaar, C. 2017. Big Data for weed control and crop protection. *Weed Research* **57**, 218–233.
- Walter, A., Finger, R., Huber, R. & Buchmann, N. 2017. Smart farming is key to developing sustainable agriculture. In: *PNAS 6148–6150, vol. 114, no. 24*. pp. 250–257.
- Zezulka, F., Marcon, P., Vesely, I., Sajdl, O. 2016. Industry 4.0 – An Introduction in the phenomenon. In: *IFAC-PapersOnLine* 49–25, pp. 008–012.

The effect of ethyl 5'-(4-methoxybenzoyl)-5',7'-dihydrospiro[cyclopentane-1,6'-[1,2,3]triazolo[5,1-b][1,3,4]thiadiazin]-3'-carboxylate on *Pinus sylvestris* L. seed germination

T.A. Kalinina¹, O.A. Vysokova¹, L.A. Khamidullina^{1,2}, A.A. Kochubei³,
O.E. Cherepanova³ and T.V. Glukhareva^{1,*}

¹Ural Federal University named after the first President of Russia B.N. Yeltsin, Mira street 19, RU620002 Ekaterinburg, Russia

²Postovsky Institute of Organic Synthesis UB RAS, Sofia Kovalevskaya street 22, RU620990 Ekaterinburg, Russia

³Botanical Garden UB RAS, 8 Marta street 202a, RU620144 Ekaterinburg, Russia

*Correspondence: taniagluhareva@yandex.ru

Abstract. Plant growth stimulators are capable of enhancing both agricultural output and the rate of plant maturation, consequently improving the total crop yield and increasing their resistance to disease and adverse environmental conditions. This is why such compounds are used in the cultivation of both agricultural and ornamental plants. The aim of this work was to study the effect of ethyl 5'-(4-methoxybenzoyl)-5',7'-dihydrospiro[cyclopentane-1,6'-[1,2,3]triazolo[5,1-b][1,3,4]thiadiazin]-3'-carboxylate on *Pinus sylvestris* L. seed germination. The article describes the synthesis of ethyl 5'-(4-methoxybenzoyl)-5',7'-dihydrospiro[cyclopentane-1,6'-[1,2,3]triazolo[5,1-b][1,3,4]thiadiazin]-3'-carboxylate and the data from spectral and X-ray crystal analysis. The results of the experimental stimulation of *Pinus sylvestris* L. seed germination using spiro-1,2,3-triazolo[5,1-b]1,3,4-thiadiazine are given compared to the commercially available phytohormones thidiazuron and 6-benzylaminopurine. The estimation of germination, vitality, healthy seed ratio and cotyledon length indicated that the tested compound at a concentration of 0.5 mg L⁻¹ had an effect similar to 6-benzylaminopurine: indeed, the speed of germination and fungal invasion rate exceeded the effect of 6-benzylaminopurine.

Key words: *Pinus sylvestris* L., seed germination, phytohormones, plant growth regulators, 6-benzylaminopurine, thidiazuron, 1,2,3-triazoles.

INTRODUCTION

Seed germination is one of the main stages of plant ontogenesis. The dormancy and germination of seeds might be controlled by affecting various exogenous factors, namely temperature (Giolo et al., 2017), electromagnetic and electrostatic fields (Palov et al., 2012), treatment with natural and synthetic growth regulators (Miransari & Smith, 2014) and others.

Recently, the application of phytohormones and their synthetic analogues has become widespread in agriculture and horticulture (Miransari & Smith, 2014; Shu et al., 2016; Zwanenburg et al., 2016), which is conditioned by the reduction of acreage, poorly predicted climate changes, the reduction of resource bases in separate regions of the Earth and increased food resource consumption (Anderson et al., 2010). For the aforementioned reasons, the search for new plant growth regulators is of great interest.

Using seeds is convenient for testing the plant hormone activity of new compounds. During seedling formation, the plant quickly goes through several steps, from mass cell division and the beginning of photosynthesis to the appearance of the first true organs (first leaf). In view of this, several parameters can be evaluated during treatment (germinating force, germinating capacity, seedling length, radicle length, development of cotyledons and first true leaves) regardless of the external factors (temperature, humidity, illumination, climatic seasonality etc.) (Kumar et al., 2014; Han et al., 2015; Takeuchi et al., 2015).

Previously (Kalinina et al., 2015) we demonstrated the effect of 5'H,7'H-spiro[1,2,3]triazolo[5,1-b][1,3,4]thiadiazines on the proliferative activity of animal cells; the compounds which could selectively stimulate or suppress their growth were determined. The influence of these compounds upon plant cells was not studied.

A comprehensive study of the effect of a new compound on plant cells should be conducted using the seeds of those species for which the processes of germination, growth and consequent first true seedling formation are well known. *Pinus sylvestris* L. is one such species (Ivanov et al., 2011). The comprehensive collected data regarding the physiology of seed germination and consequent seedling formation allows us to use the seeds of the aforementioned species as a model for evaluating both the positive and negative influence of new synthetic compounds.

The aim of the work was the synthesis of 1,2,3-triazolo[5,1-b]1,3,4-thiadiazine and an investigation of its growth-regulating activity on the seeds of *Pinus sylvestris* L. has compared to 6-BAP and TDZ. It was expected that the compound would affect the growth and development of plants, since its influence on animal cells has previously been detected.

MATERIALS AND METHODS

¹H and ¹³C NMR spectra were acquired on a Bruker Avance II spectrometer (400 and 100 MHz, respectively) in DMSO-*d*₆ with TMS as the internal standard. Mass spectra were recorded on a GCMS-QP2010 Plus gas chromat-mass spectrometer (EI ionization at 70 eV). Elemental analysis was performed on a Perkin Elmer PE 2400 CHNS-analyser. Melting points were determined on a Stuart SMP3 apparatus.

The tested compound (STT) was produced according to the previously described method (Kalinina et al., 2017). The spectroscopic characteristics of the compound are in accordance with the previously reported data (Kalinina et al., 2017).

Ethyl ester 5'-(4-methoxybenzoyl)-5',7'-dihydrospiro[cyclopentane-1,6'-[1,2,3]triazolo[5,1-b][1,3,4]thiadiazin]-3'-carboxylic acid (STT). Reaction yield is 82%, light-lilac powder, melting temperature 192–193 °C. Found, %: C 56.53; H 5.60; N 13.78. C₁₉H₂₂N₄O₄S. Calculated, %: C 56.70; H 5.51; N 13.92.

X-ray crystal analysis of the compound (STT). Single crystals (colourless plates) suitable for X-ray diffraction studies were obtained by slow evaporation of a dimethyl sulfoxide solution of the title compound at room temperature. Single-crystal X-ray diffraction was performed on an Oxford Diffraction Xcalibur-3 diffractometer with Mo K α radiation, $\lambda = 0.7107 \text{ \AA}$. Absorption correction was not applied. The structure was calculated and corrected using the Olex2 software (Dolomanov et al., 2009). The structure was solved by direct methods using the program SHELXS97 and refined on F^2 by full-matrix least-squares procedures using the program SHELXL97 (Sheldrick et al., 2008). The non-hydrogen atoms were refined in the anisotropic approximation: hydrogen atoms were included in the refinement isotropically in the riding model.

Crystallographic data (excluding structure factors) for the structure in this paper have been deposited with the Cambridge Crystallographic Data Center as the supplementary publication No. CCDC 1576559. Copies of the data can be obtained, free of charge, on application to CCDC, 12 Union Road, Cambridge CB21EZ, UK (deposited@ccdc.cam.ac.uk).

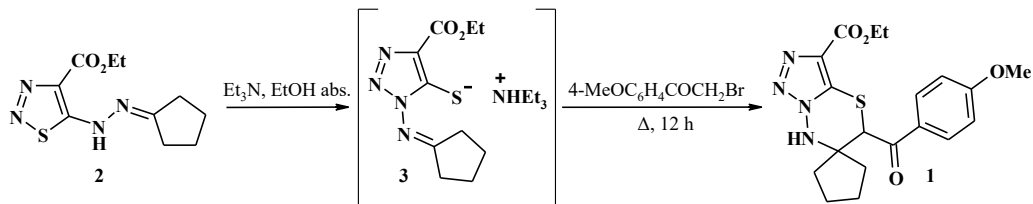
Biological study

The experimental research on compound impact was conducted in the Binder growth chamber in order to create temperature, humidity and illumination levels close to the natural conditions for seed germination (20 °C, humidity level 55–60%, 8 daylight hours) and to regulate them throughout the entire experiment. It allowed us to eliminate the influence of extraneous factors on the formation of pine seedlings. The seeds with a laboratory germination of 98%, taken from a pine forest in the II productivity class (the sowing quality of seeds corresponded to GOST 14161-86), were used to estimate the effect of the compound upon the germination process. The seeds were couched in lots of 100 pieces (GOST 13056.6-97) in sterile Petri dishes covered with two layers of filter paper, previously disinfected by ultraviolet germicidal irradiation. The experimental material included 3,000 seeds (three repetitions for each concentration) in total. Three milliliters of aqueous solutions of compounds were added into the Petri dishes at the beginning of the experiment. Furthermore, the dishes were weighed each alternate day to ensure the preset humidity level. The experiment lasted 21 days; the main parameters (vitality and germinating force) were evaluated on the 7th and 15th day according to GOST 12038-84. The major results were obtained on the 21st day of the experiment.

Two well-known phytohormones (6-BAP and TDZ) and one synthetic compound (STT) at three concentrations (0.5, 1 and 5 mg L⁻¹) were chosen as the objects of the study. Each line was provided a control tube with distilled water. The seedling quality was evaluated based on the following parameters: total seedling length, cotyledon length and thickness of the stem at the bottom of the cotyledons (because it is precisely these parameters that indicate the seedling vitality and quality of formed palisade apparatus). The experimental results were processed using the Statistica 6.0 software (ANOVA). All the attributes used in statistical analysis are normally distributed. Levene's test was used to check that variances are equal for all the samples.

RESULTS AND DISCUSSION

The spiro-1,2,3-triazolo-1,3,4-thiadiazine STT (see Scheme 1), which turned out to be one of the most active compounds during the tests conducted with animal cells, was chosen to study the effect of the compounds on *Pinus sylvestris* L. seed germination. The STT was obtained following the previously developed method (Kalinina et al., 2017): through the Dimroth rearrangement of starting 1,2,3-thiadiazolylhydrazone **2** under the effect of triethylamine and interaction of formed 1,2,3-triazolylthiolat **3** with α -bromo-4-methoxyacetophenone (Scheme 1).



Scheme 1. Synthesis of STT.

The structure and purity of the obtained compound were confirmed using NMR spectroscopy data ^1H and ^{13}C , mass spectrometry and elemental analysis. Single-crystal X-ray diffraction analysis of the compound was performed for the first time (Fig. 1). The main parameters of structural experiments for the STT are given in Table 1.

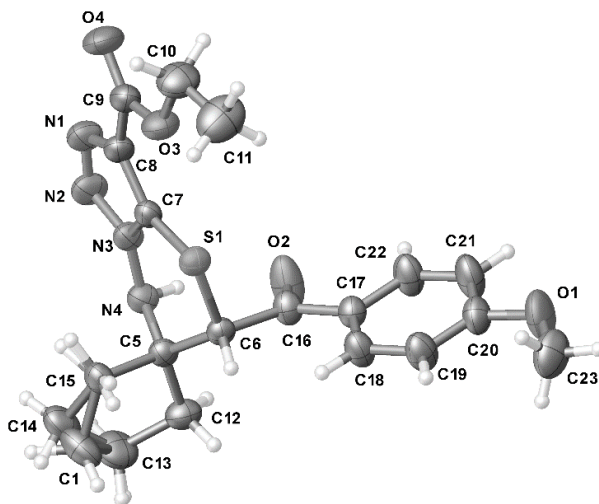
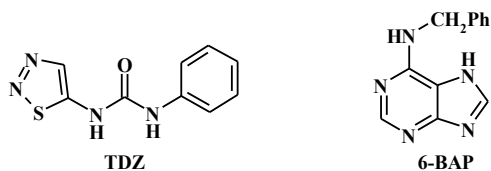


Figure 1. ORTEP view of the molecular conformation of the STT with the atom-labelling scheme. The displacement ellipsoids are drawn at the 50% probability level.

Table 1. Crystal data and structure refinement for the STT

Molecular formula	C ₁₉ H ₂₂ N ₄ O ₄ S
Molecular weight, gmole ⁻¹	402.47
Temperature, K	295
Crystal system	Triclinic
Space group	P ₁
a, Å	9.1304 (5)
b, Å	9.9986 (6)
c, Å	11.8551 (6)
α, degree	107.458 (5)
β, degree	99.719 (4)
γ, degree	99.414 (5)
V, Å ³	990.84 (9)
Z	2
D _{calc.} , gm ⁻³	1.349
μ, mm ⁻¹	0.20
F(000)	424
Crystal size, mm	0.3 × 0.25 × 0.2
Range θ for data collection, degree	2.6 ≤ θ ≤ 30.7
Subscript ranges	-12 ≤ h ≤ 12 -12 ≤ k ≤ 14 -16 ≤ l ≤ 16
Measured / independent reflections	9553/5400
Reflections with c I > 2σ(I)	4047
Corrected parameters	272
R-factor based on F ² > σ(F ²)	0.047
wR ₂ for all reflections	0.156
Residual electron density (min/max), eÅ ⁻³	-0.21/0.34

Commercially available synthetic heterocyclic phytohormones (applied for plant growth regulation and development), thidiazuron (TDZ) and 6-benzylaminopurine (6-BAP) (Victor et al., 1999; Abad et al., 2004; Kong et al., 2016; Zhang et al., 2016) were used as positive controls (Scheme 2) during the investigation of the effect of STT on *Pinus sylvestris* L. seed germination.



Scheme 2. The structure of phytohormones thidiazuron (TDZ) and 6-benzylaminopurine (6-BAP).

The seed germinating force was estimated on the 7th day of the experiment and varied from 21.6% to 54.3% in the studied lines. *Pinus sylvestris* L. seeds treated with STT (54.33 ± 3.48%) with concentration 0.5 mg L⁻¹ had the maximum germinating force, while seeds treated with TDZ (21.60 ± 2.73%; 5 mg L⁻¹) had the minimum germinating force. The germinating force of the control lot was 43.30 ± 10.49%. In the case of the STT line with concentration 5 mg L⁻¹, we noticed almost a decrease in the germinating force almost double to that of the control lot – 21.60 ± 2.70%. The 6-BAP line with concentrations 0.5 and 1 mg L⁻¹ had the same seed germinating force as the control lot; in the line with concentration 5 mg L⁻¹, the force was close to the maximum (51.00 ± 1.52%).

The linear parameters of the pine seedlings were estimated on the 14th day. The compound STT with concentration 0.5 mg L⁻¹ demonstrated the best results in growth stimulation (Table 2). This line had the maximum total seedling length (5.91 ± 0.25 cm) and cotyledon length (1.21 ± 0.08 cm) increase compared to the control lot. The lines treated with the same concentration showed the minimum seedling stem thickness (0.63 ± 0.02 mm), which is probably connected with fast cell growth by stretching (see Table 2). Lines treated with TDZ demonstrated the slowest seedling growth, especially with concentration 5 mg L⁻¹.

Table 2. The morphological parameters of *Pinus sylvestris* L. seedlings on the 15th and 21st experimental day

Concentration, mg L ⁻¹	15 th day (M ± m)*			21 st day (M ± m)*		
	Total length, cm	Cotyledons length, cm	Stem thickness, mm	Total length, cm	Cotyledons length, cm	Stem thickness, mm
STT						
0.5	5.91 ± 0.25	1.21 ± 0.08	0.63 ± 0.02	6.40 ± 0.11	1.76 ± 0.04	0.74 ± 0.01
1	4.94 ± 0.22	1.20 ± 0.27	0.67 ± 0.02	5.68 ± 0.12	1.36 ± 0.03	0.72 ± 0.01
5	5.80 ± 0.18	1.08 ± 0.07	0.68 ± 0.02	6.33 ± 0.11	1.52 ± 0.04	0.70 ± 0.01
TDZ						
0.5	4.20 ± 0.21	0.97 ± 0.07	0.71 ± 0.02	5.35 ± 0.11	1.51 ± 0.04	0.67 ± 0.01
1	3.85 ± 0.14	0.95 ± 0.06	0.66 ± 0.02	4.83 ± 0.11	1.33 ± 0.05	0.72 ± 0.02
5	3.11 ± 0.19	0.71 ± 0.07	0.78 ± 0.03	3.13 ± 0.12	0.65 ± 0.03	0.99 ± 0.03
6-BAP						
0.5	5.19 ± 0.36	1.01 ± 0.08	0.83 ± 0.02	4.55 ± 0.26	1.23 ± 0.06	0.48 ± 0.03
1	5.36 ± 0.28	1.10 ± 0.10	0.83 ± 0.01	6.29 ± 0.11	1.59 ± 0.04	0.62 ± 0.02
5	4.73 ± 0.24	1.08 ± 0.07	0.86 ± 0.02	3.82 ± 0.13	1.08 ± 0.05	0.43 ± 0.02
Control lot						
–	5.31 ± 0.23	1.07 ± 0.08	0.84 ± 0.02	5.72 ± 0.33	1.35 ± 0.13	0.81 ± 0.02

* M – mean value; m – standard deviation.

The growth tendencies on the 21st day were the same. Following the overall estimation of all parameters, the compound STT ensured the best growth stimulation on the 21st day. The seeds treated with this compound in minimal (0.5 mg L⁻¹) and maximal (5 mg L⁻¹) concentrations had the best parameters or were close to them compared to the results shown by the other experimental compounds (see Table 2). In the case of a medium concentration (1 mg L⁻¹), the total seedling length and cotyledon length parameters were slightly less than that of the seedlings treated with 6-BAP with concentration 1 mg L⁻¹, but they were better than in the other lines.

The total quantity of seedlings in the TDZ line with concentration 0.5 mg L⁻¹ on the 21st day was maximal – 93.3 ± 0.6%; the quantity of healthy seedlings in this line was 1.16 times higher (51.1 ± 0.6%) than in the control lot (44.0 ± 0.5%) (Table 3). The STT lines with all concentrations were characterised with the total minimal quantity of germinated seeds compared to the control lot: 0.5 mg L⁻¹ – 83.6 ± 0.2%, 1 mg L⁻¹ – 86.1 ± 0.6%, 5 mg L⁻¹ – 81.3 ± 0.3%. The aforementioned STT line with concentration 0.5 mg L⁻¹ had the maximum quantity of healthy seedlings – 52.3 ± 0.2%. The 6-BAP lines with all concentrations had a stable high total quantity of seedlings (90%), but the

percentage of fungal-affected seedlings in these lines was higher than in all the other lines and the control one.

Table 3. The quantity of healthy, suppressed and underdeveloped *Pinus sylvestris* L. seedlings on the 21st day

Concentration, mg L ⁻¹	Healthy, %	Suppressed, %	Underdeveloped, %
STT (M ± m)*			
0.5	52.34 ± 0.22	26.63 ± 0.84	8.63 ± 1.46
1	22.36 ± 0.64	57.95 ± 0.87	5.69 ± 0.68
5	49.35 ± 0.31	6.91 ± 0.71	25.04 ± 0.49
TDZ (M ± m)*			
0.5	51.11 ± 0.61	20.37 ± 7.12	21.82 ± 0.58
1	37.41 ± 0.5	17.04 ± 0.4	39.56 ± 1.07
5	14.35 ± 0.32	19.31 ± 0.21	60.34 ± 0.63
6-BAP (M ± m)*			
0.5	19.26 ± 0.68	42.22 ± 4.79	28.52 ± 4.28
1	29.63 ± 0.49	47.41 ± 1.56	12.96 ± 1.25
5	35.56 ± 0.4	45.18 ± 1.27	9.26 ± 0.55
Control lot (M ± m)*			
–	44.00 ± 0.5	38.89 ± 0.8	16.11 ± 0.56

* M – mean value; m – standard deviation.

The obtained linear parameters, germination data, percentage of fungal-affected and healthy seedlings were collected in an overall data matrix with two time points (15th and 21st day) and processed with the help of software package Statistica 6.0 (ANOVA) (Fig. 2). According to the analysis results on the 15th and 21st days, the TDZ lines with concentration 5 mg L⁻¹ significantly differed from the STT line (5 mg L⁻¹) – 0.000025 (21st day), 6-BAP line (5 mg L⁻¹) – 0.000017 (21st day) and control lot 0.000017 (21st day). In turn, the 6-BAP lines and STT lines did not show significant differences either with respect to each other or to the control, which evidenced for normal pine seedling growth in these lines throughout the experiment.

The TDZ line was characterised by a strong growth suppression with the increasing levels of concentration (see Table 2). With maximal concentration, the cotyledons did not develop at all or were very small (compared to the control lot and other lines); the root system was also underdeveloped. Petri dishes treated with this compound were less fungal-affected, which probably demonstrates some retardation of the floccus in the presence of the aforementioned compound. The average linear parameters in TDZ line with all concentrations were much lower than in the control lot. These peculiarities of TDZ influence on *Pinus sylvestris* L. seed germination have been reported before (Kalinina et al., 2016). The STT line with a concentration of 0.5 mg L⁻¹ had the best parameters of total seedling length and cotyledon length and exceeded the control lot parameters. The seedling thickness was minimal compared to the control lot and all the studied compounds with 0.5 mg L⁻¹ concentration. The sharp decrease of stem thickness can be attributed to the cell growth stimulation by stretching (Gonzalez et al., 2012; Tsukaya et al., 2006). The percentage of fungal-affected seeds was minimal in concentrations of 0.5 mg L⁻¹ and 1 mg L⁻¹. This parameter was best for all the studied compounds and control lot. In case of 0.5 mg L⁻¹ concentration, the percentage of healthy

seedlings was maximal (about 60%) compared to all the studied compounds and control lot.

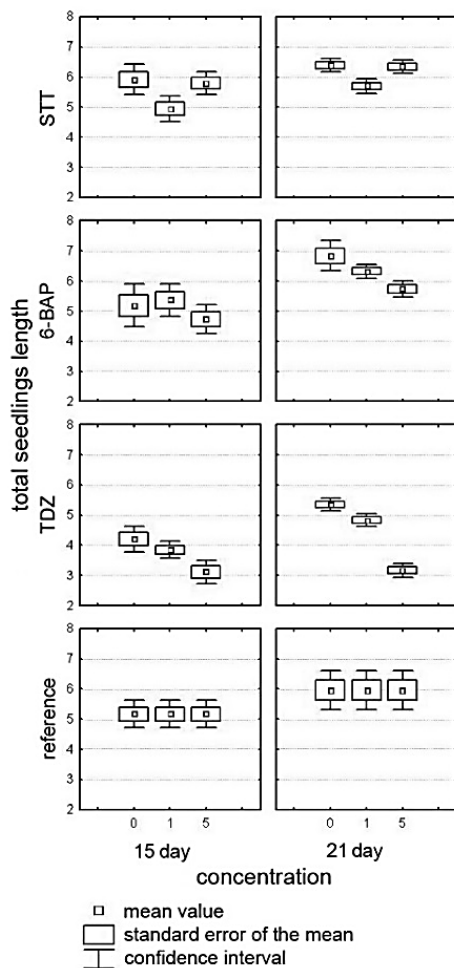


Figure 2. Total seedling length in the studied lines on the 15th and 21st days of the experiment.

CONCLUSIONS

Following the obtained experimental results, we can conclude that the growth regulating properties of the compound STT are close to that of 6-BAP and their impact is similar but for some parameters, such as cotyledon length and healthy seed percentage, STT exceeds the 6-BAP. No adverse effect of the synthesized compound on a seed germination of *Pinus sylvestris* which have good natural germination, was observed. The seedlings obtained by day 21 were found to have increased viability, longer cotyledon length and less fungal invasion with respect to the 6-BAP and TDZ lines. Consequently, it is advisable to check the effect of this compound on another plant species that has difficulties in germination and the formation of healthy, viable seedlings. The practical application of the compounds with the aforementioned properties lies in the stimulation

of root formation and sprout formation in case of micropropagation and *in vitro* propagation. Thus, the study of the effect of 1,2,3-triazolo[5,1-*b*]-1,3,4-thiadiazines on plants is of current interest as they can be applied in agriculture and plant biotechnology.

ACKNOWLEDGEMENTS. This research was supported by the Russian Science Foundation (grant № 16-16-04022).

REFERENCES

- Abad, A., Agullo, C., Cuñat, A.C., Jiménez, R. & Vilanova, C. 2004. Preparation and promotion of fruit growth in kiwifruit of fluorinated N-phenyl-N'-1,2,3-thiadiazol-5-yl ureas. *Journal of Agricultural and Food Chemistry* **52**, 4675–4683.
- Anderson, K. 2010. Globalization's effects on world agricultural trade, 1960–2050. *Philosophical Transactions of the Royal Society B* **365**, 3007–3021.
- Dolomanov, O.V., Bourhis, L.J., Gildea R.J., Howard, J.A.K. & Puschmann, H. 2009. OLEX2: a complete structure solution, refinement and analysis program. *Journal of Applied Crystallography* **42**, 339–341.
- Giolo, M., Dalla Montà, A., Barolo, E., Ferrari, F., Masin, R. & Macolino, S. 2017. High-temperature effects on seed germination of fourteen Kentucky bluegrass (*Poa pratensis* L.) cultivars. *Agronomy Research* **15**, 123–132.
- Gonzalez, N., Vanhaeren, H. & Inze, D. 2012. Leaf size control: complex coordination of cell division and expansion. *Trends in Plant Science* **17**, 332–340.
- Han, X., Wan, C., Li, X., Li, H., Yang, D., Du, S., Xiao, Yu. & Qin, Z. 2015. Synthesis and bioactivity of 2',3'-benzoabscisic acid analogs. *Bioorganic & Medicinal Chemistry Letters* **25**, 2438–2441.
- Ivanov, Yu.V., Savochkin, Yu.V. & Kuznetsov, V.V. 2011. Scots pine as a model plant for studying the mechanisms of conifers adaptation to heavy metal action: 1. Effects of continuous zinc presence on morphometric and physiological characteristics of developing pine seedlings. *Russian Journal of Plant Physiology* **58**, 871–878.
- Kalinina, T.A., Bystrykh, O.A., Pozdina, V.A., Glukhareva, T.V., Ulitko, M.V. & Morzherin, Y.Y. 2015. Synthesis of spiro derivatives of 1,2,3-triazolo[5,1-*b*][1,3,4]thiadiazines and biological activity thereof. *Chemistry of Heterocyclic Compounds* **51**, 589–592.
- Kalinina, T.A., Bystrykh, O.A., Glukhareva, T.V. & Morzherin, Y.Y. 2017. Transformation of 1,2,3-thiadiazolyl hydrazones as method for preparation of 1,2,3-triazolo[5,1-*b*][1,3,4]thiadiazines. *Journal of Heterocyclic Chemistry* **54**, 137–146.
- Kalinina, T.A., Khamidullina, L.A., Shakhmina, Yu.S., Glukhareva, T.V., Kochubei, A.A., Cherepanova, O.E., Fan, Zh., Zhu, Yu. & Morzherin, Yu.Yu. 2016. Synthesis of (1,2,3-thiadiazolyl)imidazolidine-2,4-diones by microwave irradiation and characterization of their biological activity. *Chemistry of Heterocyclic Compounds* **52**, 910–917.
- Kong, L., von Aderkas, P. & Zaharia, L.I. 2016. Effects of exogenously applied gibberellins and thidiazuron on phytohormone profiles of long-shoot buds and cone gender determination in lodgepole pine. *Journal of Plant Growth Regulation* **35**, 172–182.
- Kumar, M., Agnihotri, R.K., Vamil, R. & Sharma, R. 2014. Effect of phytohormones on seed germination and seedling growth of *Coriandrum sativum* L. *Pakistan Journal of Biological Sciences* **17**, 594–596.
- Miransari, M. & Smith, D.L. 2014. Plant hormones and seed germination. *Environmental and Experimental Botany* **99**, 110–121.
- Palov, Iv., Kuzmanov, E., Sirakov, K., Stefanov, St. & Neykov, Y. 2012. Results from a preliminary research on the pre-sowing electromagnetic treatment of rape seeds. *Agronomy Research* **10**, 335–340.

- Sheldrick, G.M. 2008. A short history of SHELX. *Acta Crystallographica Section A: Foundations of Crystallography* **64**, 112–122.
- Shu, K., Liu, X., Xie, Q. & He, Z. 2016. Two faces of one seed: hormonal regulation of dormancy and germination. *Molecular Plant* **9**, 34–45.
- Takeuchi, J., Ohnishi, T., Okamoto, M. & Todoroki, Y. 2015. Conformationally restricted 3'-modified ABA analogs for controlling ABA receptors. *Organic and Biomolecular Chemistry* **13**, 4278–4288.
- Tsukaya, H. & Beemster, G.T.S. 2006. Genetics, cell cycle and cell expansion in organogenesis in plants. *Journal of Plant Research* **119**, 1–4.
- Victor, J.M.R., Murch, S.J., Krishna Raj, S. & Saxena, P.K. 1999. Somatic embryogenesis and organogenesis in peanut: The role of thidiazuron and N⁶-benzylaminopurine in the induction of plant morphogenesis. *Plant Growth Regulation* **28**, 9–15.
- Zhang, S., Huang, L., Yan, A., Liu, Y., Liu, B., Yu, C., Zhang, A., Schiefelbein, J. & Gan, Y. 2016. Multiple phytohormones promote root hair elongation by regulating a similar set of genes in the root epidermis in Arabidopsis. *Journal of Experimental Botany* **67**, 6363–6372.
- Zwanenburg, B., Pospíšil, T. & Zeljković, S.C. 2016. Strigolactones: new plant hormones in action. *Planta* **243**, 1311–1326.

Production and profitability of low density Norway spruce (*Picea abies* (L.) Karst.) plantation at 50 years of age: case study from eastern Latvia

J. Katrevičs, B. Džeriņa, U. Neimane, I. Desaine, Z. Bigača and Ā. Jansons*

Latvian State Forest Research Institute ‘Silava’, Rigas street 111, LV–2169 Salaspils, Latvia

*Correspondence: aris.jansons@silava.lv

Abstract. Norway spruce (*Picea abies* (L.) Karst.) is one of the most important commercial tree species, for which wider spacing are being advocated to reduce management costs and improve radial growth. Nevertheless, little is known about tree and stand parameters at the larger age in stands of extremely low density. The aim of our study was to assess growth and economic profitability of 50 years old low density Norway spruce plantation in Latvia. Allometric parameters for all trees of Norway spruce clonal plantation planted in 1964 with two spacings (1×3 m and 5×5 m) were measured and profitability were estimated. Norway spruce plantation with wider (5×5 m) spacing ensured significantly larger tree diameter and height (35 cm and 25 m, respectively) than trees from higher density trial. However, mean net present value (3% interest rates) was non-significantly ($P = 0.12$) different between 5×5 m and 1×3 m spacings, $2,571.9 \pm 355.6$ and $3,085.8 \pm 452.9$ € ha⁻¹, respectively. Values observed in low density (5×5 m) plantation fitted well in the-observation of impact of density and stand parameters drawn based on National inventory data, showing a considerable potential to use plantations with low density in practice.

Key words: initial spacing, target diameter, clonal plantation, net present value.

INTRODUCTION

In northern Europe, Norway spruce (*Picea abies* (L.) Karst.) is one of the most important commercial tree species, used for board as well as pulp and paper production (Gerendiain et al., 2008; Neimane et al., 2015). Due to the economic importance of coniferous trees, intensive tree breeding has been applied (Jansons et al., 2015) and substantial amounts of studies has addressed the silvicultural treatments required to ensure their vitality and growth under a changing climate (Bergh et al., 2005; Hébert et al., 2016; Matisons et al., 2017). Studies have reported larger radial increment and higher resistance against different biotic and abiotic factors, e.g. windstorms, root-rot, and dendrophagous insects, in stands and plantations with lower density at young age (McClain et al., 1994; Gardiner & Quine, 2000; Hébert et al., 2016). Due to this, as well as decreased intraspecific competition between trees, low density plantations usually are characterized by lower mortality (Peltola et al., 2000; Slodicak & Novak, 2006; Akers et al., 2013); except in sites with severe browsing pressure, where higher density might

reduce the browsing damage occurrence and increase the number of surviving trees (Edenius et al., 2002; Díaz-Yáñez et al., 2017). Drawbacks of low density stands often are smaller yield (standing volume) per hectare, presumably higher risk of stem cracks in drought-prone sites, and lower stem quality due to larger branch diameters and consequently also slower natural pruning (Mäkinen & Hein, 2006; Pfister et al., 2007; Zeltiņš et al., 2016; Baders et al., 2017). From an economic point of view this might be compensated by reduced costs of establishment and pre-commercial thinning as well as length of rotation period (cutting by target diameter, if possible) (Willcocks & Bell, 1994; Zhang et al., 2002; Hynynen et al., 2010). However, economic profitability (net present value (NPV)) of timber production and total investments of forest stands with different planting density are seldom analysed (Coordes, 2013).

In eastern Europe initial spacing in Norway spruce stands was kept rather high (4,000–6,000 trees ha⁻¹) in the second half of the 20th century and reduced to around 2,000 trees ha⁻¹ in most of countries from the beginning of this century (Mangalis, 2004; Gizachew et al., 2012). Current trends are toward wider initial spacing (often in combination with improved soil preparation, planting and/or fertilization) in order to boost the profitability of management of Norway spruce stands (Gizachew et al., 2012; Dzerina et al., 2016; Jansons et al., 2016). However, little is known about tree and stand parameters at the age with maximized volume production in stands of extremely high spacing (Hein et al., 2007; Gil, 2014; Hébert et al., 2016). Such information would be of a practical value, when setting the lower limit for the planting density as well as for elaboration of legal requirements for pre-commercial thinning. Therefore, the aim of our study was to assess growth and economic profitability of 50 years old low density Norway spruce plantation. For this purpose, tree and stand parameters (e.g., tree diameter at breast height, mean annual increment), as well as NPV were assessed.

MATERIALS AND METHODS

The study was carried out in a Norway spruce clonal plantation, located on fertile mineral soil with normal moisture regime, suitable for this tree species, *Oxalidos* forest type (Bušs, 1976) in eastern Latvia (56°42'N, 25°53'E). The site index for spruce at the experimental site (the dominant height at 100 years; Matuzānis, 1983) was 36.0 m. According to data from the Latvia Environmental, Geology and Meteorology Centre, mean annual temperature at study area is around + 6 °C with annual mean precipitation of 640 mm. Plantation was established in 1964 using vegetatively propagated planting material from 20 plus-trees. Two trials at spacing of 1×3 m (3,330 trees ha⁻¹) and 5×5 m (400 trees ha⁻¹) in 15 and 21 rows (100 m long), respectively, were established beside each other in two adjacent replications. Weed control was carried out in planting year and first year after planting; no thinning was conducted prior the sampling. No measurements in the trials before age of 50 years were carried out.

The plantation of Norway spruce was sampled in August 2016. All trees in plantation were measured at mature age, i.e., age of 50 years. Some allometric parameters such as diameter at breast height (DBH) (± 0.05 cm), height (H) (± 0.1 m), height to its first living and dry branch (± 0.1 m) were measured for all trees. Dried and damaged trees were recorded and, if possible, the cause of damage (e.g., ungulates, stem deformations) was indicated.

Slenderness (H/D ratio) and basal area were calculated for all trees. The crown ratio was calculated by dividing total tree H by crown length. The individual tree standing volume has been calculated according to the formula by Liepa (1996):

$$v = \psi H^\alpha DBH^\beta l^{\gamma L + \varphi} \quad (1)$$

where v – stem volume with bark, m³; H – tree height, m; DBH – stem diameter at breast height, cm; ψ , α , β , φ – coefficients depending on tree species (for Norway spruce 2.3106 10⁻⁴, 0.78193, 0.34175, 1.18811, respectively).

Total volume and basal area of each trial were computed as the sum of the individual trees. Site index was calculated based on dominant tree height at age 50 according to Matuzānis (1983). Survival of trees in trials was expressed in percentage relation of live trees in the year of measurements to the number of trees in the year of establishment.

Mean annual increment (MAI) (standing volume divided by stand age) and mean tree diameter of each spacing were compared with data from 10 National forest inventory (NFI) sample plots at the age from 45 to 52 years, located on comparable forest types with a site index of 30 to 36 m in the same region of Latvia. Only sample plots with lowest current density (360–1,280 trees ha⁻¹) available from NFI data were selected for the comparison, though, it was not known what factors and when caused the reduction of number of trees per ha to such a low level in these stands.

To compare the net present value (NPV) between both spacings, the volume of stemwood assortments of individual trees was calculated according to Ozoliņš (2002). According to the joint-stock company ‘Latvia’s State Forest’ Quality requirements of round timber (2016), five classes by length and diameter of segments for Norway spruce stems were set (Table 1).

Table 1. Characteristics of Norway spruce timber assortments

	Large	Middle	Small I	Small II	Pulpwood
Top-diameter, cm	28	18	14	10	6
Length, m	3.6	3.6	3.6	3.0	3.0

Monetary value of each sampled tree was calculated based on average assortment prices. Net present value of final felling (50 years) was calculated with the 1%, 3%, 5%, and 10% interest rates. In calculations, the costs of regeneration (soil preparation, planting, planting material), two weed controls, as well as logging (wood preparation, delivery, transportation) costs were taking into account. All the costs of treatments were equal for both spacings, since the contracts were done per ha basis, except the costs of planting material. Average assortment prices and all included forest management costs for the years 2006–2016 were obtained from Central Statistical Bureau (CSB, 2016).

Analysis of variance (ANOVA) was used to analyse the existence of significant differences among the spacings for tree quantitative parameters (DBH, H, H/D ratio etc.) and NPV. When the differences were significant according to ANOVA, the multiple post hoc comparison test (Tukey’s Honest Significant Difference (HSD) test) was performed. Proportion of damaged trees as well as survival of trees were evaluated using the generalized linear model (GLM) applying binomial residual distribution (‘logit’). Additional, mean values ± 95% of confidence interval (CI) were calculated. The obtained data were statistically analysed using R v.3.3.1 (R Core Team, 2016).

RESULTS AND DISCUSSION

At age of 50 years, spacing significantly ($P < 0.001$) affected the survival of trees. Higher survival was observed in wider spacing (5×5 m) – 69.5%, lower – in narrower spacing – 30.3%. It is in accordance with other studies, suggesting a notable impact of intraspecific competition (Amateis et al., 1997; Akers et al., 2013) and thus increase of survival of trees from narrowest (1×3 m) to widest (5×5 m) spacing. However, such studies typically do not include the extremely wide spacing as in our trial. Higher survival of trees with increased spacing has also been found in younger stands in other studies for *Pinus* sp. (e.g., Baldwin Jr. et al., 2000; Hébert et al., 2016). Survival can be linked to natural selection, i.e., gradual reduction of proportion of slower-growing (less fit) genotypes (Gerendiain et al., 2008).

Damages – mainly bark striping by cervids (96–100% from observations) – in trial with 5×5 m spacing was significantly ($P < 0.001$) less frequent than in trial with 1×3 m spacing, reaching 9% and 75%, respectively. This might indicate that greater branchiness decreased the level of damaged trees in 5×5 m spacing (Vospernik, 2006; Månsson & Jarnemo, 2013; Baders et al., 2017). Statistically significant differences of H or DBH between groups of damaged and un-damaged trees were not observed, but it does not exclude the negative impact of it on stem quality due to fungal infections (Arhipova et al., 2015; Burneviča et al., 2016).

Mean DBH and H of the trees were significantly ($P < 0.001$) different between spacings (Table 2): widest spacing 5×5 m had larger DBH and H, likely due to the light, nutrient resources and moisture availability (Vospernik et al., 2010). This trend has been also observed in other studies, including spacings from 2×2 m to 4×5 m at the age of 24 to 33 (Deans & Milne, 1999; Pfister et al., 2007). The widest 5×5 m spacing produced significantly ($P < 0.001$) greater stem volume per individual tree (59%) than the denser 1×3 m spacing (Table 2).

Table 2. Spacing effect on measured Norway spruce tree parameters and mean stand characteristics

Tree parameters	1×3 m	5×5 m	<i>F</i> value (DF = 1, 1,261)	<i>P</i> value
Tree DBH ± CI, cm	24.29 ± 0.61	36.52 ± 0.66	694.7	< 0.001
Tree height ± CI, m	21.5 ± 0.3	25.1 ± 0.3	261.0	< 0.001
H/D ratio	0.92 ± 0.17	0.70 ± 0.01	401.9	< 0.001
Crown ratio	0.52 ± 0.01	0.75 ± 0.01	607.2	< 0.001
Height of first living branch ± CI, m	10.2 ± 0.3	6.3 ± 0.3	329.7	< 0.001
Height of first dry branch ± CI, m	0.6 ± 0.04	0.5 ± 0.02	34.3	< 0.01
Tree stem volume, m ³	0.54 ± 0.03	1.31 ± 0.06	676.5	< 0.001
Stand characteristics	1×3 m	5×5 m		
Basal area, m ² ha ⁻¹	42.5	27.1	×	×
Standing volume, m ³ ha ⁻¹	453.5	301.8	×	×
Site index, m	24.8	27.4	×	×
Number of measured trees	736	521	×	×

DBH – diameter at breast height; CI – confidence interval; DF = degree of freedom.

Impact of spacing on tree H observed in our study, in contrast to impact only on tree DBH and stem volume (reported by Tong & Zhang, 2005; Mäkinen & Hein, 2006; Hébert et al., 2016) could be explained by highly variable densities, revealing differences in light accessibility and competition (Oker–Blom & Kellomäki, 1982; Hébert et al., 2016).

Between trials the observed differences of mean H/D ratio was significantly ($P < 0.001$) influenced by spacing, increasing from 0.70 to 0.92 in lowest and highest spacing, respectively (Table 2). Significantly ($P < 0.001$) larger H/D ratio in 1×3 m spacing, being in accordance to results of other studies (Mäkinen & Isomäki, 2004). The H/D ratio was highly variable in 1×3 m spacing, ranging from 0.55 to 1.59, likely due to notable suppression as competition between individual trees increase (Cremer et al., 1982; Fahlvik et al., 2005) and uneven distribution of remaining trees. Spacing 5×5 m overall had lower H/D ratio (ranging from 0.51 to 0.92) due to faster DBH increase (Slodiacak & Novak, 2006), suggesting higher tree stability against environmental stresses (Valinger & Petterson, 1996; Karlsson et al., 2000; Peltola et al., 2000).

Spacing had a significant effect on the tree crown parameters (Table 2). Height to the first living branch, as well as crown ratio were significantly different between both spacings, showing better natural pruning as well as shorter tree crowns in narrower spacing (Bachofer & Zingg, 2001; Pfister et al., 2007). Although, spacing had a significant effect on height to first dry branch, observed differences were small, underlying slow overall natural pruning of Norway spruce (Mäkinen & Hein, 2006). These differences were not considered in the calculations of assortment structure in our study, thus providing an actual upper limit for the net present value (NPV) in all assessed densities of plantations.

In the low density Norway spruce stands with un-known management history (National forest inventory (NFI) data), the mean standing volume \pm CI was $276.7 \pm 56.7 \text{ m}^3 \text{ ha}^{-1}$, ranged from 194 to $422 \text{ m}^3 \text{ ha}^{-1}$. The mean tree diameter of NFI stands significantly correlated ($r = -0.74$) with stand density, as found also by McClain et al. (1994) and Deans & Milne (1999) (Fig. 1A). However, stand density in the assessed range (NFI data; 360 to 1,280 trees ha^{-1}) had only slight link with its mean annual increment (MAI) (Fig. 1B).

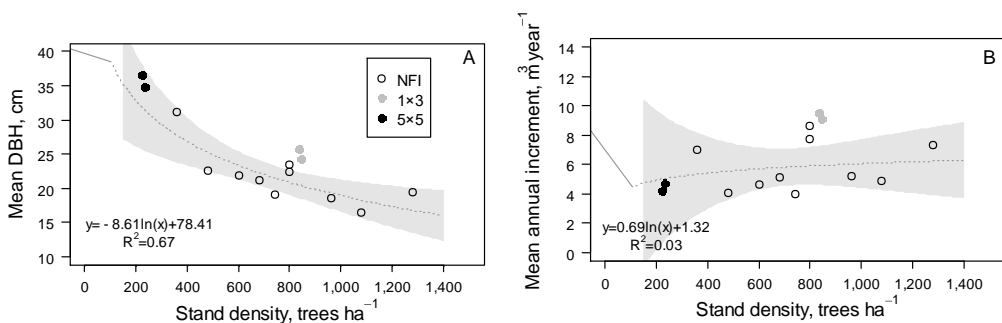


Figure 1. The mean tree diameter at breast height (DBH) (A) and mean annual increment (B) \pm 95% confidence interval (grey area) in trials (filled circles) and forest stands (National forest inventory – NFI data) with different density.

Nevertheless, values of both DBH and MAV observed in the widest 5×5 m spacing mostly occurred within the CI of the observations from NFI data. Although, mean DBH was notably higher, the MAV in widest 5×5 m spacing appeared to be lower; indicating that over reduced density may not provide similar NPV as in denser stands (Fig. 1).

For the comparison of economic profitability between both spacings, NPV over the 10 years period with different wood prices and interest rates were calculated (Table 3).

Table 3. Comparison of net present value (NPV), € ha⁻¹ in both 1×3 m and 5×5 m spacings with different interest rates (i) (1%, 3%, 5%, 10%) for the years 2006 to 2016

Year	i =1%		i =3%		i = 5%		i = 10%	
	1×3 m	5×5 m	1×3 m	5×5 m	1×3 m	5×5 m	1×3 m	5×5 m
2006	8,655.9	7,031.0	2,836.4	2,409.9	678.2	696.1	-527.0	-260.9
2007	13,068.3	10,154.6	4,487.0	3,577.0	1,304.5	1,137.6	-472.7	-224.6
2008	8,749.8	6,914.0	2,721.4	2,270.7	485.7	548.7	-762.8	-413.0
2009	6,094.9	4,829.8	1,961.3	1,559.9	428.2	347.2	-427.9	-330.0
2010	8,308.5	6,696.0	2,617.8	2,232.6	507.3	577.2	-671.2	-347.2
2011	8,778.2	7,097.3	2,739.4	2,346.8	499.8	585.0	-750.9	-398.9
2012	8,820.6	7,221.3	2,727.9	2,384.2	468.3	590.3	-793.5	-411.5
2013	10,872.1	8,835.8	3,517.0	2,991.1	789.2	823.5	-734.0	-387.0
2014	11,503.3	9,020.2	3,676.6	3,038.0	774.0	819.4	-846.9	-419.5
2015	10,528.2	8,165.2	3,326.5	2,733.0	655.6	718.3	-835.8	-406.7
2016	10,425.1	8,185.1	3,332.2	2,748.2	701.8	731.9	-767.2	-394.1
Mean	9,618.6 ±	7,650.0 ±	3,085.8 ±	2,571.9±	663.0 ±	688.7 ±	-690.0 ±	-363.0 ±
NPV	1,268.6	959.2	452.9	355.7	166.9	135.8	98.8	44.4

Variation of NPV in both trails was linked to fluctuations in timber prices, reaching the highest level before Global economic crisis in 2007 and dramatically declining right after it (Campello et al., 2010). Higher NPV (with 1, 3 and 5% interest rates) were in trial with narrower spacing (1×3 m) than in trial with wider (5 x 5 m) by 20, 17, and 4%, respectively, despite the additional costs of planting material. Differences in NPV between 1×3 m and 5×5 m spacings with the interest rates 3% and 5% were non-significant ($P = 0.12$ and 0.79 , respectively).

Wider spacing may become a cost saving alternative for the forest owners setting higher interest rate for their investment, however, the financial return is very much affected by the fluctuations of round wood prices. Although, it should be remembered that our calculations did not include the branch or wood quality parameters, likely reducing the value of timber in plantation with wider spacing. Furthermore, the positive effect of establishment costs and valuable timber assortments in low density plantations may be applied only ensuring high survival of tree in young age (Zhang et al., 2002; Hynynen et al. 2010).

CONCLUSIONS

Low initial density (400 trees ha⁻¹) ensured significantly larger diameter and height (35 cm and 25 m, respectively) of Norway spruce at the age of 50 years than higher initial density (3,333 trees ha⁻¹). Notably (34%) lower yield at the point of final harvest still ensured similar income for the forest owner from the investment in establishment of

the plantation with the interest rate 5%, but the actual profitability (NPV) was much dependent on the market prices of roundwood assortments.

ACKNOWLEDGEMENTS. Study was carried out in National Research Programme of Latvia No. 2014.10-4/VPP-6/6 'Forest and Subsoil Exploration, Sustainable Use – New Products and Technologies (ResProd)'.

REFERENCES

- Akers, M.K., Kane, M., Zhao, D., Teskey, R.O. & Daniels, R.F. 2013. Effects of planting density and cultural intensity on stand and crown attributes of mid-rotation loblolly pine plantations. *For. Ecol. Manage* **310**, 468–475.
- Amateis, R., Burkhart, H.E. & Lui, J. 1997. Modelling survival in juvenile and mature loblolly pine plantations. *For. Ecol. Manage* **90**, 51–58.
- Arhipova, N., Jansons, A., Zaluma, A., Gaitnieks, T. & Vasaitis, R. 2015. Bark stripping of *Pinus contorta* caused by moose and deer: wounding patterns, discoloration of wood, and associated fungi. *Can. J. For. Res.* **45**(10), 1434–1438.
- Bachofen, H. & Zingg, A. 2001. Effectiveness of structure improvement thinning on stand structure in subalpine Norway spruce (*Picea abies* (L.) Karst.) stands. *For. Ecol. Manage* **145**, 137–149.
- Baders, E., Donis, J., Snepsts, G., Adamovics, A. & Jansons, A. 2017. Pruning effect on Norway spruce (*Picea abies* (L.) Karst.) growth and quality. *Forestry Studies* **66**, 33–48.
- Baldwin Jr., V.C., Peterson, K.D., Clark III, A., Ferguson, R.B., Strub, M.R. & Bower, D.R. 2000. The effects of spacing and thinning on stand and tree characteristics of 38-year-old Loblolly Pine. *For. Ecol. Manage* **137**, 91–102.
- Bergh, J., Linder, S. & Bergström, J. 2005. Potential production of Norway spruce in Sweden. *For. Ecol. Manage* **204**, 1–10.
- Burneviča, N., Jansons, Ā., Zaļuma, A., Kļaviņa, D., Jansons, J. & Gaitnieks, T. 2016. Fungi inhabiting bark stripping wounds made by large game on stems of *Picea abies* (L.) Karst. in Latvia. *Baltic Forestry* **22**(1), 2–7.
- Bušs, K. 1976. *Basis of Forest Classification in SSR of Latvia*. LRZTIPI, Rīga, Latvia, 24 pp. (in Latvian).
- Campello, M., Graham, J.R. & Harvey, C.R. 2010. The real effects of financial constraints: Evidence from financial crisis. *J. Financial Econ.* **97**(3), 470–487.
- Central Statistical Bureau 2016.
http://data.csb.gov.lv/pxweb/en/lauks/lauks__ikgad__mezsaimn/?tablelist=true&rxid=cdb978c-22b0-416a-aacc-aa650d3e2ce0. Accessed 25.9.2017.
- Coordes, R. 2013. Influence of planting density and rotation age on the profitability of timber production for Norway spruce in Central Europe. *Eur. J. For. Res.* **132**(2), 297–311.
- Cremer, K.W., Borough, C.J., McKinnell, F.H. & Carter, P.R. 1982. Effects of stocking and thinning on wind damage in plantations. *New Zeal. J. For. Sci.* **12**(2), 244–268.
- Deans, J.D. & Milne, R. 1999. Effects of respacing on young Sitka spruce crops. *Forestry* **72**(1), 47–57.
- Díaz-Yáñez, O., Mola-Yodogo, B. & González-Olabarria, J.R. 2017. What variables make a forest stand vulnerable to browsing damage occurrence? *Silva Fenn.* **51**(2), id1693, doi:10.14214/sf.1693.
- Dzerina, B., Girdziusas, S., Lazdina, D., Lazdins, A., Jansons, J., Neimane, U. & Jansons, Ā. 2016. Influence of spot mounding on height growth and tending of Norway spruce: case study in Latvia. *Forestry Studies* **65**, 24–33.
- Edenius, L., Bergman, M., Ericsson, G. & Danell, K. 2002. The role of moose as a disturbance factor in managed boreal forests. *Silva Fenn.* **36**(1), 57–67.

- Fahlvik, N., Agestam, E., Nilsson, U. & Nyström, K. 2005. Simulating the influence of initial stand structure on the development of young mixtures of Norway spruce and birch. *For. Ecol. Manage* **213**, 297–311.
- Gardiner, B.A. & Quine, C.P. 2000. Management of forests to reduce the risk of abiotic damage – a review with particular reference to the effect of strong winds. *For. Ecol. Manage* **135**, 261–277.
- Gerendiain, Z., Peltola, H., Pukkinen, P., Ikonen, V.P. & Jaatinen, R. 2008. Differences in growth and wood properties between narrow and normal crowned types of Norway spruce grown at narrow spacing in southern Finland. *Silva Fenn.* **42**(3), 423–437.
- Gil, W. 2014. The influence of initial spacing on growth and survival of Scots pine in 40 years period of cultivation in varied habitat conditions. *Forest Research Papers* **75**(2), 117–125.
- Gizachew, B., Brunner, A. & Øyen, B.H. 2012. Stand responses to initial spacing in Norway spruce plantations in Norway. *Scand. J. For. Res.* **27**, 637–648.
- Hein, S., Mäkinen, H., Yue, C. & Kohnle, U. 2007. Modelling branch characteristics of Norway spruce from wide spacings in Germany. *For. Ecol. Manage* **242**, 155–164.
- Hébert, F., Krause, C., Plourde, P.Y., Achim, A., Prigent, G. & Ménétrier, J. 2016. Effect of trees spacing on tree level volume growth, morphology, and wood properties in a 25-years-old *Pinus banksiana* plantation in the boreal forest of Quebec. *Forests* **7**, id 276, doi:10.3390/f7110276.
- Hynynen, J., Niemistö, P., Viherä-Aarnio, A., Brunner, A., Hein, S. & Velling, P. 2010. Silviculture of birch (*Betula pendula* Roth and *Betula pubescens* Ehrh.) in northern Europe. *Forestry* **83**(1), doi: 10.1093/forestry/cpp035.
- Jansons, Ā., Matisons, R., Krišāns, O., Džeriņa, B. & Zeps, M. 2016. Effect of initial fertilization on 34-year increment and wood properties of Norway spruce in Latvia. *Silva Fenn.* **50**(1), id1346, doi:doi.org/10.14214/sf.1346.
- Jansons, A., Donis, J., Danusevičius, D. & Baumanis, I. 2015. Differential analysis for next breeding cycle for Norway spruce in Latvia. *Baltic Forestry* **21**(2), 285–297.
- Karlsson, K. 2000. Stem form and taper changes after thinning and nitrogen fertilization in *Picea abies* and *Pinus sylvestris* stands. *Scand. J. For. Res.* **15**, 621–632.
- Latvia's State Forest Quality requirements of round timber 2016.
https://www.lvm.lv/images/lvm/Profesionaliem/Me%C5%BEizstr%C4%81de/Pielikumi/AKKP_21.10.2015.pdf. Accessed 2.10.2017. (in Latvian).
- Liepa, I. 1996. *Theory of Increment*. LLU, Jelgava, 123 pp. (in Latvian).
- Mangalis, I. 2004. *Forest regeneration and afforestation*. Et Cetera, Rīga, 455 pp. (in Latvian).
- Matisons, R., Bardulis, A., Kanberga-Silina, K., Krisans, O. & Jansons, A. 2017. Sap flow in xylem of mature Norway spruce—a case study in northwestern Latvia during the season of 2014–2015. *Baltic Forestry* **23**(2), 477–481.
- Matuzānis, J. 1983. *Stand growth and yield models*. LatZTIZPLI, Rīga, 32 pp. (in Latvian).
- Mäkinen, H. & Hein, S. 2006. Effect of wide spacing on increment and branch properties of young Norway spruce. *Eur. J. Forest Res.* **125**, 239–248.
- Mäkinen, H. & Isomäki, A. 2004. Thinning intensity and log-term changes in increment and stem form of Norway spruce trees. *For. Ecol. Manage* **201**, 295–309.
- Månsson, J. & Jarnemo, A. 2013. Bark-stripping on Norway spruce by red deer in Sweden: level of damage and relation to tree characteristics. *Scand. J. For. Res.* **28**, 117–125.
- McClain, K.M., Morris, D.M., Hills, S.C. & Buss, L.J. 1994. The effect of initial spacing on growth and crown development for planted northern conifers. *For. Chronicle* **70**, 174–182.
- Neimane, U., Zadina, M., Sisenis, L., Dzerina, B. & Pobiarsens, A. 2015. Influence of lammas shoots on productivity of Norway spruce in Latvia. *Agronomy Research* **13**(2), 354–360.
- Oker-Blom, P. & Kellomäki, S. 1982. Theoretical computations on the role of crown shape in the absorption of light by forest trees. *Math. Biosci.* **59**(2), 291–311.

- Ozoliņš, R. 2002. Forest stand assortment structure analysis using mathematical modelling. *Forestry Studies* **7**, 33–42.
- Peltola, H., Kellomäki, S., Hassinen, A. & Granander, M. 2000. Mechanical stability of Scots pine, Norway spruce and birch: an analysis of tree-pulling experiment in Finland. *For. Ecol. Manage* **135**, 143–153.
- Pfister, O., Wallentin, C., Nilsson, U. & Ekö, P.M. 2007. Effects of wide spacing and thinning strategies on wood quality in Norway spruce (*Picea abies*) stands in southern Sweden. *Scand. J. For. Res.* **22**, 333–343.
- R Core Team 2016. R: A language and environment for statistical computing. R Foundation for Statistical Computing, Vienna, Austria. <https://www.R-project.org/>.
- Slodicak, M. & Novak, J. 2006. Silvicultural measures to increase the mechanical stability of pure secondary Norway spruce stands before conversion. *For. Ecol. Manage* **224**, 252–257.
- Tong, Q.J. & Zhang, S.Y. 2005. Impact of initial spacing and precommercial thinning on jack pine tree growth and stem quality. *Forest Chron.* **81**(3), 418–428.
- Valinger, E. & Petterson, N. 1996. Wind and snow damage in a thinning and fertilization experiment in *Picea abies* in southern Sweden. *Forestry* **69**, 25–33.
- Vospertnik, S., Monserud, R.A. & Sterba, H. 2010. Do individual-tree growth models correctly represent height:diameter ratios of Norway spruce and Scots pine? *For. Ecol. Manage* **260**, 1735–1753.
- Willcocks, A.J. & Bell, F.W. 1994. *Effect of stand density on the growth and timing of harvest and establishment costs of coniferous stands*. Ont. Min.Nat. Resour., South Porcupine, ON. 12 pp.
- Zeltiņš, P., Katrevičs, J., Gailis, A., Maaten, T., Jansons, J. & Jansons, Ā. 2016. Stem cracks of Norway spruce (*Picea abies* (L.) Karst.) provenances in Western Latvia. *Forestry Studies* **65**, 57–63.
- Zhang, S.Y., Chauret, G., Ren, H.Q. & Desjardins, R. 2002. Impact of initial spacing on plantation black spruce lumber grade yield bending properties, and MSR yield. *Wood Fiber Sci.* **34**(3), 460–475.

Strawberry leaf surface temperature dynamics measured by thermal camera in night frost conditions

E. Kokin^{*}, M. Pennar, V. Palge and K. Jürjenson

Estonian University of Life Sciences, Institute of Technology, Chair of Energy Application Engineering, Kreutzwaldi 56, EE51014 Tartu, Estonia

^{*}Correspondence: eugen.kokin@emu.ee

Abstract. The aim of the study was to define the strawberry leaf surface and ambient air temperature differences in night frost conditions. The study was carried out at the commercial strawberry field in late autumn at a specific natural climatic situation, corresponding to night frost conditions. Thermal camera FLIR P660 was used for obtaining thermal images and corresponding visual colour images of the strawberry leaves. The images were taken at ten-minute interval. The ambient air temperature, relative humidity, dew point, solar radiation and wind speed data were obtained by Davis Vantage Pro2 weather station. It was estimated that the surface temperature of the specific leaf is comparatively similar at different parts of the specimen and changes noticeably with the variation of solar radiation intensity. The speed of temperature changes was also analysed. During all the measurement period, the considerable difference between the temperature of the leaf and the ambient air temperature was established, especially in absence of solar radiation. The difference of the leaf surface and ambient air temperature reached 8 °C. The study showed that in night frost conditions the plants might be endangered by low temperatures even at the air temperatures above 0 °C due to intensive energy loss by long wave radiation to the sky. It is suggested that the thermal imaging or infrared radiation measurement should be used simultaneously with air temperature measurements for more exact timing of night frost prevention measures at strawberry cultivation.

Key words: thermal imaging, strawberry leaf, surface temperature, night frost conditions, precision agriculture.

INTRODUCTION

The last three decades of twentieth century were productive concerning the research works that aimed to find the suitable model for describing the balancing energy flow in radiative night frost conditions. The discussion was evolving around the plants' heat balance components (Businger, 1965; Hamer, 1986; Perry, 1986 and others). Though the models could differ significantly by their outcomes, the modelling gave in practice good results in plants survival rate at low temperatures and because of that, new, improved theories were not developed. Today it seems that for the most effective and widely used sprinkler-protection frost prevention methods there were mainly analyses of their application rates suggested but the subject of exact timing of these measures was not studied thoroughly. As a result, mostly the air temperatures were monitored and used

as an alert criteria but not the temperatures of plant surfaces, that may differ from the air temperatures (Perry, 1994).

The advancements in development of infrared (IR) measurement instruments and technique made it possible to apply IR thermometers and cameras for thermographic measurements of plants. These were mainly the laboratory instruments, which were used for physiological processes analysis in different plants (Jones et al., 2003; Maes et al., 2012 and Costa et al., 2013). Later, these methods were applied also in open-air conditions. The results of thermal radiation measurements made in natural environment by Aubrecht et al. (2016) showed that at high positive temperatures of air in daytime the surface temperature of plant might be higher than air temperature. Though already Perry (1994) suggested that the surface temperature of plants in radiative night frost conditions might be lower than the air temperature by 1.6 to 2.7 °C, the dynamics of plants' temperature dependences on radiative heat exchange were not analysed.

The main objective of our research is to find more exact surface temperature variations in case of strawberry leaf in field experiment at radiative frost conditions using the measurement possibilities of IR thermography.

Theoretical aspects

All heat energy calculations for night frost conditions, where the intensity of additional heat flux needed for description of heat flows of plant parts is sought, are presented by heat balance equations of different forms (Businger, 1965; Hamer, 1986; Perry, 1986 and others).

In this work here, we described the heat balance of strawberry leaf as

$$m_l \cdot c_l \cdot \frac{dT_l}{d\tau} = E_n - C - H, \quad (1)$$

where m_l is leaf mass, kg; c_l – specific heat capacity of leaf material, J kg⁻¹ K⁻¹; dT_l – leaf temperature change within the time step, K; $d\tau$ – time step, s; E_n – net radiant flux of leaf surface, W; C – sensible heat flow of the leaf, W and H – latent heat flow of the leaf, W (Jones et al., 2011).

The components of Eq. 1 were defined as

$$\begin{aligned} E_n &= E_{\uparrow l} + E_{\downarrow sky} + E_{\downarrow l} + E_{\uparrow ground} = \\ &= 2 \cdot F_l \cdot \varepsilon_l \cdot \sigma \cdot T_l^4 + F_l \cdot \varepsilon_{sky} \cdot \sigma \cdot T_{sky}^4 + F_l \cdot \varepsilon_{soil} \cdot \sigma \cdot T_{soil}^4, \end{aligned} \quad (2)$$

$$C = 2 \cdot F_l \cdot k_l \cdot (T_l - T_a), \quad (3)$$

$$H = \frac{2 \cdot F_l \cdot L \cdot \beta}{R_w \cdot T_l} \cdot (e_l - e_a). \quad (4)$$

Here $E_{\uparrow l}$, $E_{\downarrow sky}$, $E_{\downarrow l}$, $E_{\uparrow ground}$ are total radiant fluxes emitted from the leaf to sky, sky to leaf, leaf to ground and ground to leaf; σ – Stefan-Boltzmann constant; ε_l , ε_{sky} , ε_{soil} – emissivity of strawberry leaf, sky and soil; T_l , T_{sky} , T_{soil} – absolute temperatures of leaf, sky and surface of soil; F_l – leaf surface area; k_l – heat transfer coefficient between leaf and surrounding air; T_a – air temperature; L – latent heat of vaporization; R_w – specific gas constant for water vapour; β – coefficient of mass transfer; e_l – vapour pressure at leaf surface; e_a – vapour pressure of the surrounding air. For simplification, the radiation angle factors were not included.

Inserting Eq. 2, Eq. 3 and Eq. 4 into Eq. 1, we got the heat balance equation for the leaf in a form that is more complex:

$$m_l \cdot c_l \cdot \frac{dT_l}{d\tau} = 2 \cdot F_l \cdot \varepsilon_l \cdot \sigma \cdot T_l^4 + F_l \cdot \varepsilon_{sky} \cdot \sigma \cdot T_{sky}^4 + F_l \cdot \varepsilon_{soil} \cdot \sigma \cdot T_{soil}^4 + 2 \cdot F_l \cdot k_l \cdot (T_l - T_a) + \frac{2 \cdot F_l \cdot L \cdot \beta}{R_w \cdot T_l} \cdot (e_l - e_a). \quad (5)$$

The purpose of this work was to monitor T_l changes in time. From Eq. 5, it is possible to derive T_l and find the changes of its value analytically. In practice, this method is not very reliable, as the sky and soil temperatures are defined in a different way by different authors and therefore might be the cause for errors. It is more convenient to measure each component of the heat balance separately and to define the leaf temperature from measurement results.

Thermal camera visualizes the temperature of measurement object based on the radiant flux (in comparatively narrow long wave spectrum region that corresponds to infrared radiation) and in that case, we do not need the whole heat balance equation (Eq. 1) but only one of its components $E_{\uparrow l}$ from Eq. 2. to establish the temperature of the leaf (T_l).

Infrared thermography

The IR camera work principle can be described by the heat balance of the camera IR sensor (Usamentiaga et al., 2014), as

$$E_{n\,sensor} = E_l + E_{refl} + E_{atm}, \quad (6)$$

$$E_l = \varepsilon_l \cdot \tau_{atm} \cdot \sigma \cdot T_l^4, \quad (7)$$

where $E_{n\,sensor}$ is the net radiant flux to camera sensor; E_l – radiant flux from the leaf to the sensor depending on the leaf surface temperature; E_{refl} – radiant flux reflected to the sensor from the leaf surface; E_{atm} – radiant flux emitted to the sensor by the atmosphere and τ_{atm} – the atmosphere transmissivity between the leaf and the camera. We can write out these components as

$$E_{refl} = (1 - \varepsilon_l) \cdot \tau_{atm} \cdot \sigma \cdot T_{refl}^4, \quad (8)$$

$$E_{atm} = (1 - \tau_{atm}) \cdot \sigma \cdot T_{atm}^4, \quad (9)$$

where T_{refl} is temperature corresponding to reflected radiant flux and ε_l is leaf surface emissivity.

In our experiments, the distance between camera and leaf is about 0.5 m, so we can choose the transmissivity of the atmosphere $\tau_{atm} = 1$. That means that $E_{atm} = 0$ and the variables influencing the net radiant flux to camera sensor and thus measured temperature value are only T_l , T_{refl} and ε_l . The leaf surface emissivity is suggested to be $\varepsilon_l = 0.95$ (Aubrecht et al., 2016).

The objectives of our work are:

1. To find whether the thermographic measurements by IR camera are applicable for monitoring the temperature of strawberry leaf surface in radiative night frost conditions.
2. To measure the strawberry leaf surface and surrounding air temperatures, to define and analyse their variation in time and to compare their levels.
3. To find out if the air and dew point temperature measurements are sufficient for leaf temperature estimation, and to assess the significance of camera measurement error in IR thermogram analysis.
4. To assess the suitability of the thermography temperature measurement method to be used for the more exact estimation of night frost alerts moments and prevention measures application timing.

MATERIALS AND METHODS

The current study of strawberry leaves' surface temperature was carried out using thermal camera (FLIR P660) with thermal sensitivity 30 mK and accuracy ± 1 K for obtaining thermal images of leaves and ground surface (soil surface without vegetation on the same image with the leaves) with corresponding visual colour images. The sensing system of the camera is based on 640×480-pixel Focal Plane Array uncooled microbolometer perceiving thermal radiation with wavelength 7.5–13 μm (IR) and allowing to measure temperature at more than 40,000 points on the leaf surface. The camera calibrated temperature range of -40.0 °C up to $+120.0$ °C was used. The images were taken at ten-minute interval from 0.5 m distance and analysed with FLIR ResearchIR Max software (version 4.30.3.76). The ambient air temperature (°C), relative humidity (%), dew point (°C), solar radiation (W m^{-2}) and wind speed (m s^{-1}) data were obtained by weather station (Davis Vantage Pro2) at 2 m above the ground. During calibration of the camera and preliminary measurements, the mean emissivity of strawberry leaves was found to be 0.96. The temperature units, used in the results presentation, are (°C) for temperature values and (K) for speed of change of temperature.

Temperature correction was applied, using ambient air temperature, relative humidity and reflected temperature based on the measured infrared radiant flux reflected to the camera from the surface of the target (Standard test methods for measuring and compensating for reflected temperature using infrared imaging radiometers, 1998; FLIR, 2011).

For achievement of broached objectives, the measurements were carried out on three successive days in late autumn (19.10.2016 to 21.10.2017) at the commercial field of *Fragaria*×*Ananassa* 'Sonata' on the three leaves of the same plant planted in May, 2016. The specific natural climatic situation corresponded to night frost conditions. The days and nights were cloudless, the air temperature at the experimental area was around $+7$ °C in daytime and down to -5.0 °C at night. The wind speed was 0.0 to 2 m s^{-1} . To minimize the effect of additional radiation sources and to prevent the IR radiation shading, the camera was controlled remotely. Thermal images were taken with the camera fixed on a tripod approximately from distance of 50 cm and at an angle of 30 degrees from the leaf surface normal.

From the point of view of the resulting influence of plant leaf radiative balance on the leaf temperature, based on preliminary measurements, the time of the day during the sunset and immediately after it is most informative. At that time, the solar radiation diminishes quickly and the leaf temperature may become lower than ambient air temperature due to exposure to the cloudless sky with temperatures (T_{sky}) below $-50.0\text{ }^{\circ}\text{C}$ (outside of calibrated temperature range of camera).

Fig. 1 shows the strawberry plant thermal image with three leaves. The thermogram is supplied with the temperature scale in $^{\circ}\text{C}$ and three ellipse-shaped and one polygon ROI with corresponding names. The temperature distribution histogram of the selected ROI is also shown.

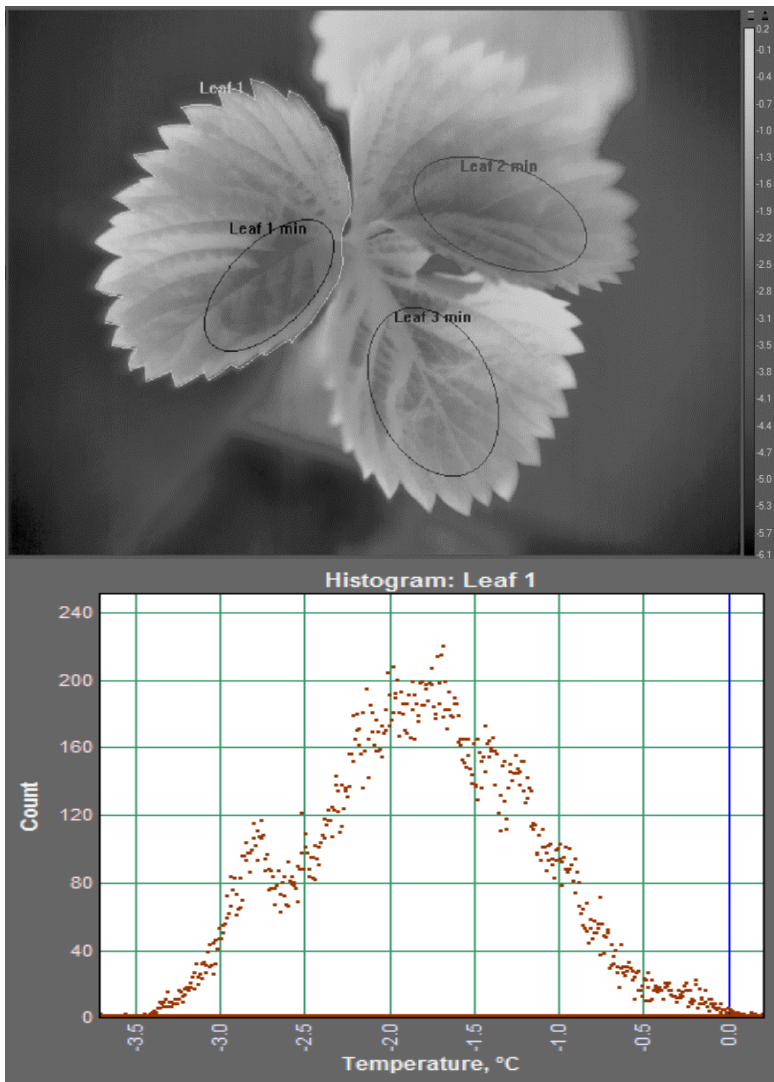


Figure 1. Strawberry leaves' thermal image and selected area (ROI *Leaf 1*) temperature distribution histogram.

Strawberry leaf is complex. It consists of a base, petiole and three leaves. The leaf surface is not uniform – it is divided by veins into angular lamina regions of different size with individual inclination angles to the horizontal plane. The leaf itself is divided into halves by midrib, which is lower than adjoining regions. The result of such surface unevenness is IR radiant flux variation to and from the surface of the leaf and consequently, different leaf surface temperature (T_l) at different parts. For the analysis of T_l the regions of interest (ROI) on the surface of the leaf were selected on thermal images and contoured by the coloured lines, to define the areas with lowest temperatures as most endangered in case of night frost. The number of pixels in these areas were 8,140 to 12,539 – three to four times less than the whole leaf ROI area with 41,150 pixels (Table 1). The ground surface ROI included 1,824 measurement points. The temperature inside the selected ROIs was more uniform and its difference with the whole leaf ROI stayed nearly constant. In all images the area, shape and position of the ROIs were constant (Table 1).

Table 1. Statistical analysis results of thermal image as presented by FLIR ResearchIR Max software for selected areas: *Leaf 1* – the ROI of whole Leaf 1 and *Leaf 1 min*, *Leaf 2 min* and *Leaf 3 min* – ROIs of minimum temperature areas on Leaf 1, 2 and 3 correspondingly

Statistic	ROI <i>Leaf 1</i>	ROI <i>Leaf 1 min</i>	ROI <i>Leaf 2 min</i>	ROI <i>Leaf 3 min</i>	ROI <i>Ground</i>
Mean, °C	-1.5	-2.4	-2.1	-1.7	-5.9
Std. Dev., °C	0.6	0.2	0.2	0.5	0.2
Centre, °C	-1.3	-2.4	-2.5	-1.7	-5.9
Maximum, °C	0.4	-1.6	-1.3	-0.8	-5.4
Minimum, °C	-3.4	-3.2	-2.9	-2.7	-6.4
Number of Pix	41,150	8,140	10,733	12,539	1,824
Emissivity	0.96	0.96	0.96	0.96	0.96
Distance, m	0.5	0.5	0.5	0.5	0.5

The FLIR ResearchIR Max software enables to apply the temperature correction procedures and performs the statistical analysis of the thermal images based on selected ROIs data. The resulting information includes the temperature distribution histograms and numerical values for minimum, maximum and mean temperatures and standard deviation for the temperature inside the ROI.

In Table 1 the numerical values of statistical analysis results of thermal image pixel temperatures for four selected areas of the leaves as presented as given by FLIR ResearchIR Max software. Three of these areas with minimal surface temperatures were selected as most endangered. For the final analysis, the ROI with minimum temperatures (*Leaf 1 min*) was used. The correlation analysis was performed using MS Office Excel software.

RESULTS AND DISCUSSION

Perry (1994) suggested that the surface temperature of plants in radiative night frost conditions might be lower than the air temperature by 1.6 to 2.7 °C. Some later research works describe possibilities of determining the leaf emissivity by IR thermometry (Chiachung Chen, 2015), changes of IR spectra of plants caused by stress (Maria F. Buitrago et al., 2016) and early detection of it by IR techniques (Laury Chaerle et al.,

2000). But no results of temperature dynamics in night frost conditions were yet published.

Our measurement series gives the possibility to see the strawberry leaf surface temperature and other measured parameters change starting from 15:10, 19.10.2016 and up to 24:00, 19.10.2016. In Table 2, the numerical results of statistical analysis of thermograms describe the most essential period from 17:00 to 20:20 for ROI *Leaf1*, with 8,140 pixels. The ground surface mean temperature is also included. This measurement period corresponds to T_{leaf} rapid diminishing to 0 °C at the sunset while the air temperature reaches 0 °C only three hours later.

Table 2. Thermal images statistical analysis results for ROI *Leaf1* and ground surface temperatures from 17:00 to 20:20, 18.10.2016

Time	Ground surface mean temperature, °C	Leaf surface temperatures, °C				
		minimum	maximum	mean	ROI central point	standard deviation
17:00	-1.3	0.6	2.9	1.5	1.4	0.5
17:10	-2.1	-0.9	1.0	0.0	0.0	0.4
17:20	-3.4	-2.9	-0.9	-2.1	-2.0	0.4
17:30	-5.6	-3.8	-2.0	-3.0	-2.9	0.4
17:40	-6.4	-3.9	-1.9	-3.1	-3.0	0.3
17:50	-6.8	-4.3	-2.7	-3.5	-3.4	0.3
18:00	-7.2	-4.5	-3.2	-3.9	-3.8	0.2
18:10	-8.1	-5.1	-3.6	-4.3	-4.5	0.3
18:20	-7.3	-4.5	-3.3	-3.8	-3.8	0.2
18:30	-8.6	-5.8	-4.5	-5.2	-5.4	0.2
18:40	-8.6	-5.9	-4.7	-5.3	-5.5	0.2
18:50	-9.6	-7.1	-6.0	-6.6	-6.7	0.2
19:00	-9.9	-7.1	-5.7	-6.5	-6.5	0.2
19:10	-10.3	-8.0	-6.9	-7.5	-7.6	0.2
19:20	-10.3	-5.4	-4.4	-4.9	-5.0	0.2
19:30	-10.9	-7.3	-6.3	-6.9	-7.0	0.2
19:40	-11.3	-7.6	-6.8	-7.2	-7.3	0.1
19:50	-11.5	-7.9	-6.9	-7.4	-7.4	0.1
20:00	-11.9	-8.4	-7.3	-7.7	-7.9	0.1
20:10	-12.3	-8.4	-7.6	-7.9	-8.0	0.1
20:20	-12.2	-8.5	-7.6	-8.0	-8.0	0.1

The analysis results of measurement series of leaf's surface temperatures along with the weather station data are presented on Fig. 2. The weather station data is shown for the period of 24 hours while T_l measurements start at 15:10 and end at midnight. The minimum, maximum and mean temperature variations of one ROI is shown along with variations of ground surface and ambient air temperatures, air relative humidity, dew point temperature and solar radiation.

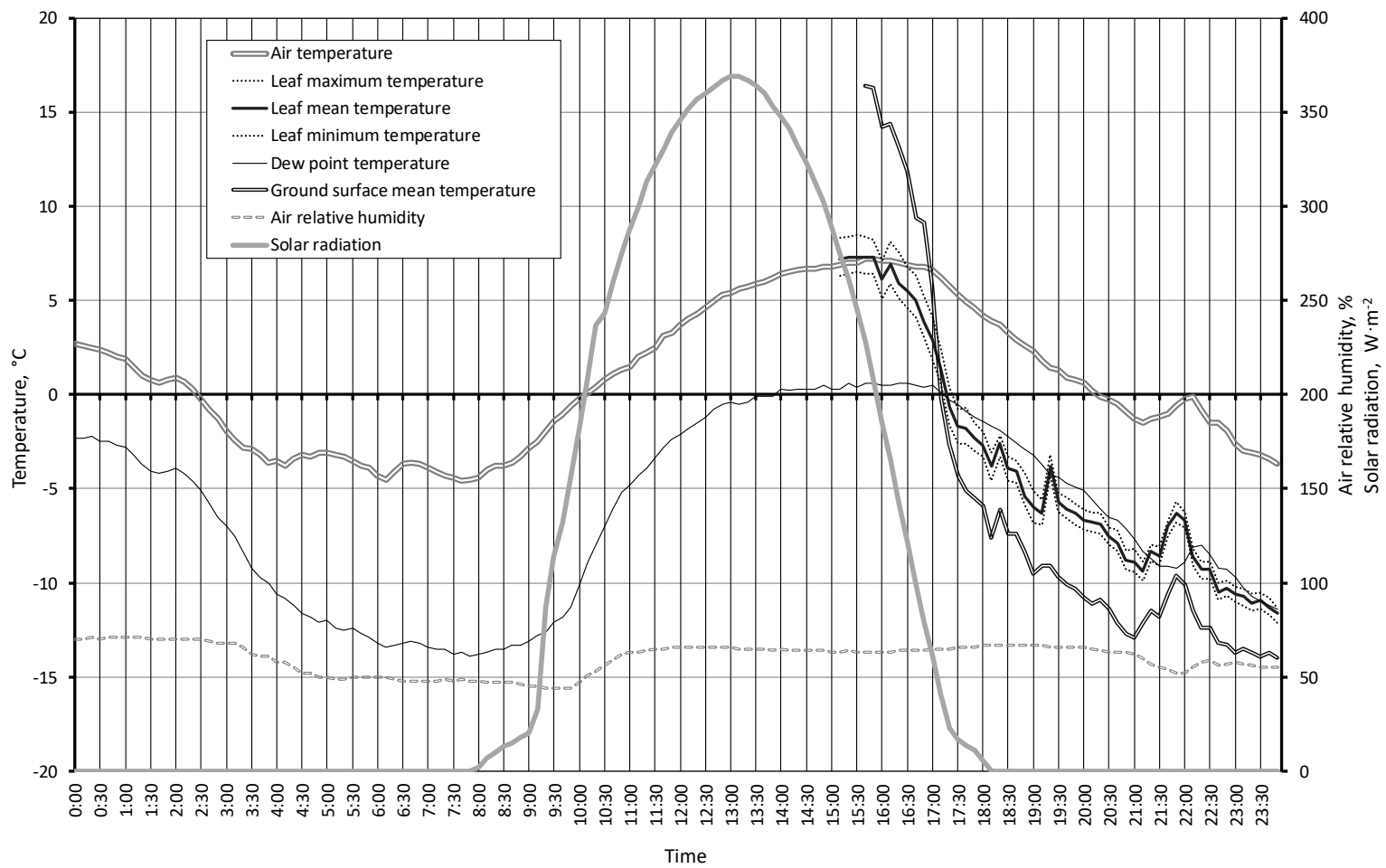


Figure 2. Strawberry leaf's surface temperature variations in night frost conditions.

We can see that the mean value of leaf surface temperature ($T_{l\ mean}$) being close to the air temperature up to 16:20 starts to decrease quickly with the diminishing of solar radiation and reaches 0 °C at 17:10 to 17:20. The air temperature at that moment is still +6.8...+6.0 °C and stays positive up to 20:20. After reaching 0 °C at 17:20, $T_{l\ mean}$ continues to diminish and at 20:20 is already -7.6 to -8.5 °C. We also see that starting from 17:20, $T_{l\ mean}$ is considerably lower than the dew point temperatures. The leaf temperature quick lessening is a result of the radiative heat flow to the cloudless sky, while the radiative heating by the sun is rapidly diminishing. The positive air temperature is not high enough to compensate by convection the radiant heat loss to the sky.

At 16:30 and later, the leaf temperature changes correlates with the solar radiation intensity, and after it diminishes to zero, the $T_{l\ mean}$ correlates to the air temperature, but stays considerably lower both at air positive and negative temperatures. Short-time variations of $T_{l\ mean}$ during measurements may be caused by changes of IR radiant flux to the sky depending on atmosphere transmission. There are also some additional factors, such as the freezing process of dew, condensed on the leaf surface.

Example of that intensive freezing we probably see as horizontal line on the graph at 17:30. We may also suppose, that at some lower temperatures the process of supercooling in plants may cause short-time rise of leaf surface temperature. We see suitable peak at 19:10 when $T_{l\ mean}$ is -7.5 °C. Corresponding temperature peak of ground surface is absent on the graph. That may mean that there are some other causes for rise of leaf surface temperature than IR radiation variation. Though we registered similar peaks on other days also, this hypothesis needs further investigation.

After 17:30, the change of plant temperature is highly correlated to air ($r = 0.959$) and ground surface ($r = 0.988$) temperatures. We may notice that on the graph, the changes of $T_{l\ mean}$ and ground surface temperature at 21:50 slightly precede the rise of air temperature. As the air was practically still, we can suggest that the variations of air temperature after sunset were caused mainly by cooling of the surface of the ground because of IR radiation.

The difference of temperatures between leaf and ground surfaces are explainable by the convective heat-exchange between the leaf and surrounding air. The stem of the plant is about 10 cm high and air can freely move around the leaf and thanks to its small mass warm it to some extent.

The temperature differences between the air and strawberry leaf and between the air and ground surface and their variations are shown on Fig. 3. The difference increase nearly linearly until 17:30 and then becomes more stable, changing only with fluctuation of IR radiant flux, with slight rising trend. One of the possible causes for that may be the forming of ice crystals on the surfaces that prevent further temperature difference rapid increase.

In Fig. 4, the speed of leaf temperature changes during the test is shown. The highest speeds coincide with the temperature peaks and reach 0.25 °C min^{-1} (15 °C h^{-1}).

The test results show, that the surface temperature of strawberry leaf in night frost conditions is much lower than air temperature and this difference reaches 8 to 9 °C at air positive temperatures. It means, that the plant temperature is below 0 °C already immediately before the sunset and after it. While it is not so dangerous for the strawberry leaves that can withstand lower temperatures without serious damage it may be fatal for the flowers of the plant if such conditions occur in springtime.

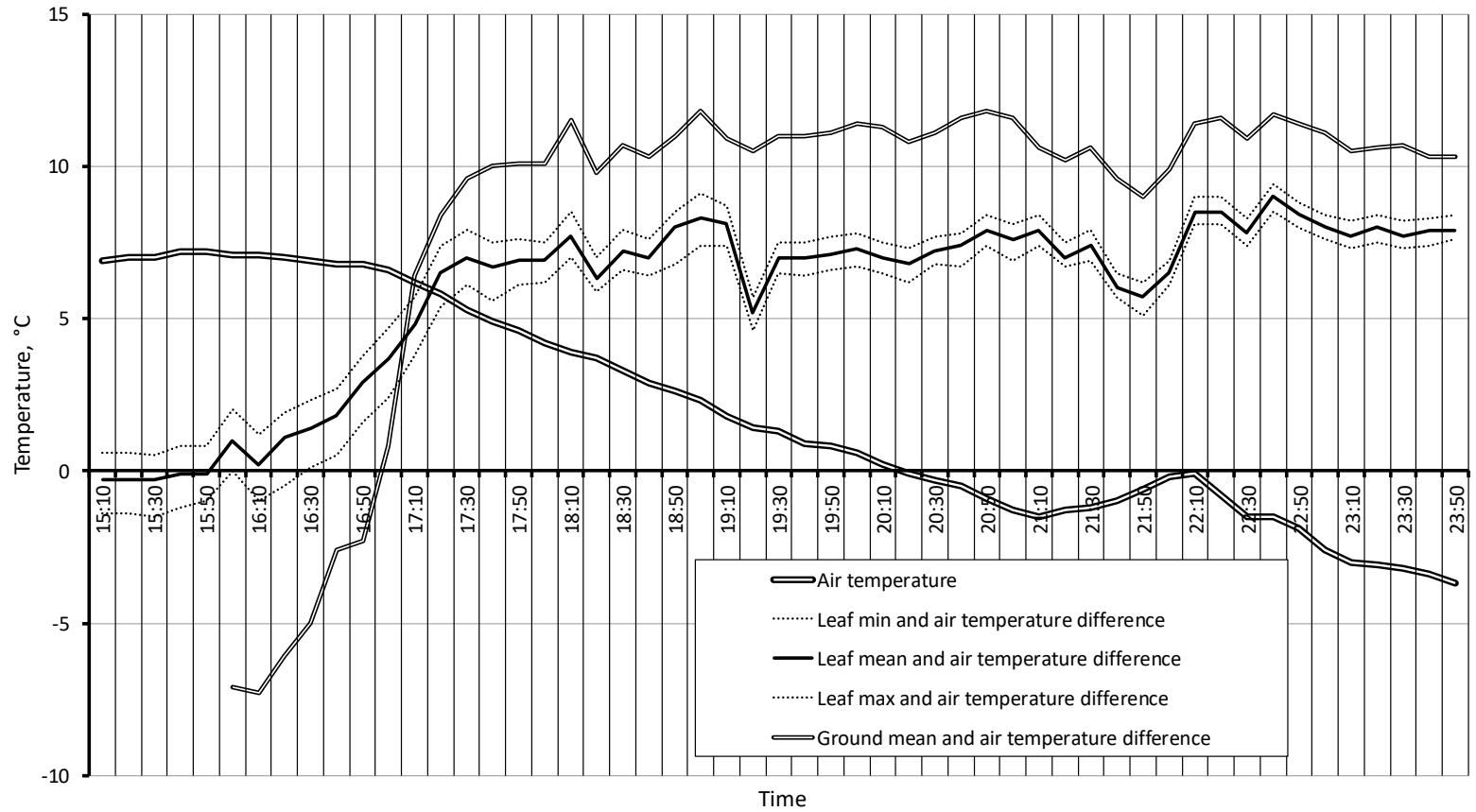


Figure 3. Temperature differences between the air, plant leaf and ground surface.

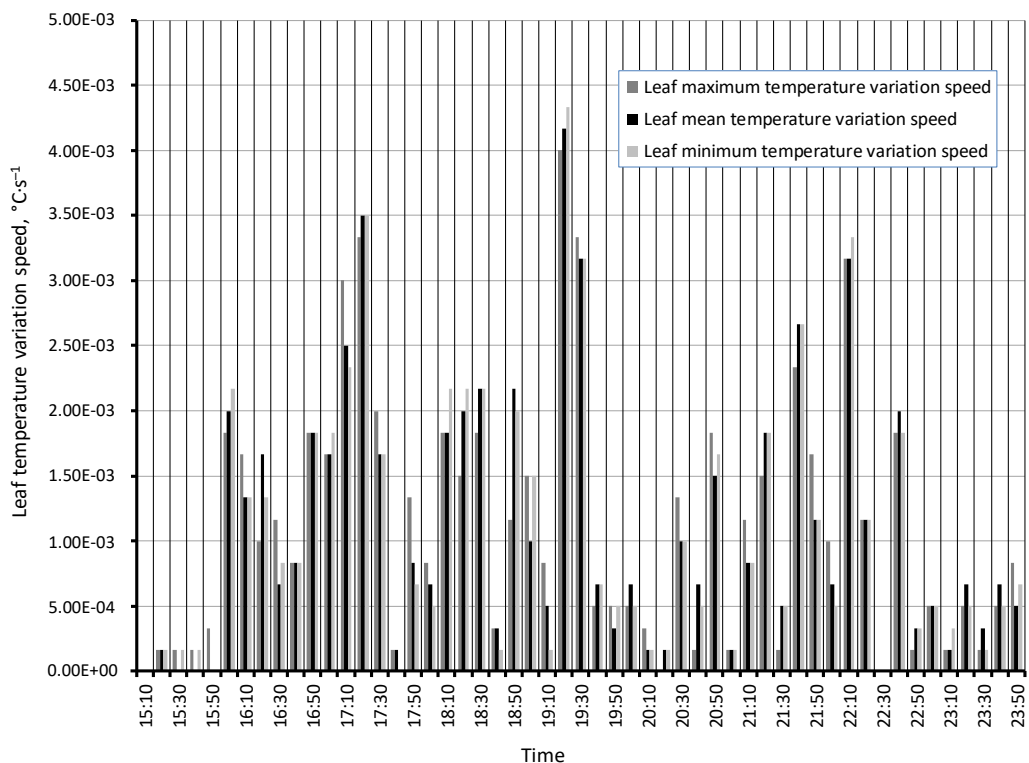


Figure 4. The speed of change of strawberry leaf temperatures.

We propose that the thermal imaging or infrared radiation measurement should be used simultaneously with air temperature measurements for more exact timing of night frost prevention measures at strawberry cultivation.

CONCLUSIONS

Our test affirms that IR thermography, as a method that is based on non-invasive, simply handled tools with specific analysing software is applicable for strawberry plant surface temperature dynamics measurements *in situ* in negative radiative balance conditions. The IR camera applied in our experiment is suitable for these purposes.

We found that in night frost climatic conditions the temperature of strawberry leaf surface is considerably (up to 9 K) lower than the air temperature. That confirms the need to apply the thermal radiation measurement equipment and to include radiative heat-balance theory for establishing plants' surface temperatures and investigation of plants' behaviour.

The thermal imaging or infrared radiation measurement should be used simultaneously with air temperature measurements for more exact timing of night frost prevention measures for plants, especially at strawberry cultivation.

The results of test show, that solely dew point and air temperatures measurements are not sufficient to produce frost alerts.

The difference of air and leaf surface temperatures is considerably higher than the possible maximum measurement error in case of thermal camera. To produce the

correctly timed frost alerts, comparatively cheap widely used commercial IR equipment is suitable.

For more deep investigation of leaves' temperature dynamics and behaviour of plants, additional night frost radiative balance research is needed.

ACKNOWLEDGEMENTS. The authors would like to thank the participating farmers for their support during farm visits. This research did not receive any specific grant from funding agencies in the public, commercial, or not-for-profit sectors.

REFERENCES

- Aubrecht, D., Helliker, B., Goulden, M., Roberts, D., Still, C. & Richardson, A. 2016. Continuous, long-term, high-frequency thermal imaging of vegetation: Uncertainties and recommended best practices. *Agricultural and forest Meteorology* **228–229**, 315–326.
- Barfield, B., Walton, L. & Lacey, R. 1981. Prediction of sprinkler rates for night-time radiation frost. *Agricultural and forest meteorology* **2**(4), 1–9.
- Businger, J. 1964. Frost protection with irrigation. *Meteorological Monographs* **6**(28) 74–80.
- Costa, M., Grant, O & Chaves, M. 2013. Thermography to explore plant – environment interactions. *Journal of Experimental Botany* **13**(64), 3937–3949.
- Chiachung Chen. 2015. Determining the Leaf Emissivity of Three Crops by Infrared Thermometry. *Sensors* **15**, 11387–11401.
- FLIR. User's manual. 2011. Publ. No. 1558550, Rev. a557. *Flir Systems, Inc.*, 308 p.
- Gerber, J. & Harrison, D. 1964. Sprinkler irrigation for cold protection of Citrus. *Transactions of the ASAE*, 464–468 pp.
- Hamer, P. 1986. The heat balance of apple buds and blossom. Part III. The water requirements for evaporative cooling by overhead sprinkler irrigation. *Agricultural and Forest Meteorology* **37**, 175–188.
- Jones, H., Archer, N., Rotenberg, E. & Casa, R. 2003. Radiation measurement for plant ecophysiology. *Journal of Experimental Botany* **384**(54), 879–889.
- Jones, H. & Rotenberg, E. 2011. Energy, radiation and temperature regulation in plants. In: eLS. John Wiley & Sons Ltd.
- Laury Chaerle, Dominique Van Der Straeten. 2000. Imaging Techniques and the Early Detection of Plant Stress. *Trends in Plant Science* **5**(11), 495–501.
- Maes, W. & Steppe, K. 2012. Estimating evapotranspiration and drought stress with ground-based thermal remote sensing in agriculture: a review. *Journal of Experimental Botany* **13**(63), 4671–4712.
- Maria, F. Buitrago, Thomas A. Groen, Christoph A. Hecker, Andrew K. Skidmore. 2016. Changes in Thermal Infrared Spectra of Plants Caused by Temperature and Water Stress. *ISPRS Journal of Photogrammetry and Remote Sensing* **111**, 22–31.
- Perry, K. 1986. FROSTPRO, a model of overhead irrigation rates for frost/freeze protection of apple orchards. *HortScience* **21**(4), 1060–1061.
- Perry, K. 1994. Frost/freeze protection for horticultural crops. Horticulture Information Leaflets. North Carolina A&T State University, 9.
- Standard test methods for measuring and compensating for reflected temperature using infrared imaging radiometers. 1998. *An American National Standard*. ASTM, USA, 3.
- Usamentiaga, R., Venegas, P., Guerediaga, J., Vega, L. & Molleda, J. 2014. Infrared thermography for temperature measurement and non-destructive testing. *Sensors* **14**(7), 12305–12348.

Mathematical model for monitoring carbon dioxide concentration in industrial greenhouses

I. Laktionov^{1,*}, O. Vovna¹, O. Cherevko² and T. Kozlovskaya³

¹State Higher Educational Institution 'Donetsk National Technical University', Ministry of Education and Science of Ukraine, Department of Electronic Engineering, Shibankova sq., 2, UA85300 Pokrovsk, Ukraine

²State Higher Educational Institution 'Priazovsky State Technical University', Ministry of Education and Science of Ukraine, Department of Automation and Computer Technologies, University street 7, UA87500 Mariupol, Ukraine

³Kremenchuk Mykhailo Ostrohradskyi National University, Department of biotechnologies and bioengineering, Pershotravneva street 20, UA39600, Kremenchuk, Ukraine

*Correspondence: ivan.laktionov@donntu.edu.ua

Abstract. Processes of monitoring and control the industrial greenhouses microclimate play a decisive role in growing crops under protected cultivation. Providing optimal climatic conditions in the production process of greenhouse agricultural products requires solving the scientific and applied problem of developing and researching a mathematical model for monitoring carbon dioxide concentration in industrial greenhouses. The proposed model takes into account the processes of diffusion and absorption of carbon dioxide, the geometric parameters of greenhouses, as well as the types and vegetation periods of crops grown under protected cultivation. Time characteristics of the carbon dioxide dynamics process under greenhouse conditions are estimated. Quantitative estimates of the diffusion transfer duration and carbon dioxide absorption are made for indeterminate varieties of tomatoes during planting and fruiting periods. Recommendations are given on the development of an adaptive methodology for the functioning and structural and algorithmic organization of computerized monitoring and management system for carbon dioxide top-dressing modes for greenhouse crops. The necessity of improving the proposed mathematical model and confirming the adequacy of its implementation efficiency on yield indicators of greenhouse crops is substantiated.

Key words: modeling, mass transfer, photosynthesis, dynamics.

INTRODUCTION

The key to the state social and economic development is a high level of food security. The need to ensure the production of a sufficient amount of environmentally friendly products, as well as the climatic and structural and sectoral features of the state development, raise attention to the production of crop products under protected cultivation. A promising area for increasing the efficiency of agro-industrial complex facilities is the modernization of industrial greenhouses through the development and

implementation of modern computerized infocommunication monitoring and management tools for growing the greenhouse flora.

Having analyzed the greenhouse parameters as objects of control and monitoring, it is established that the development of climate controllers operation algorithms is a science-intensive and non-standard procedure. For optimal control of the greenhouse crops growing processes, mathematical physics equations are used. They describe the dynamic processes of mass and energy balance taking into account the processes of diffusion and convection.

One of the main physico-chemical parameters of the industrial greenhouses microclimate, which affects the rates of growth and production of growing crops, is the concentration of carbon dioxide (CO₂) (Katsoulas & Kittas, 2008; Santosh et al., 2017).

In the process of analysis of research results in the field of vegetable growing under protected cultivation (Theoretical substantiation of methods for increasing the cucumber yield in greenhouses, 1995) established fact of the correlation dependence between the productivity of growing cucumbers and the current concentration of carbon dioxide in greenhouses. It was found that a change in the concentration from 0.03% to 0.2% leads to a proportional increase in productiveness. The optimal concentration of CO₂ depending on the types of plants grown and the periods of their vegetation varies from 0.05 to 0.2% (Departmental rules of the technological engineering NTP 10-95, 1996; Departmental rules of the technological engineering VNTP APK-19-07, 2007). This fact confirms the relevance of the research for different types of crops and the periods of their vegetation.

The technological characteristics of the existing control and monitoring systems for the carbon dioxide concentration in industrial greenhouses claimed by the manufacturers (OX-AN, 2017; TechGrow CO₂-controllers, 2017) do not allow us to assess adequately the possibility of adapting these systems for different types of crops and greenhouse structures. This drawback is due to the lack of open access to the description of the principles of the industrial climate controllers operation for greenhouses.

The analysis of existing software products of the type (Greentrees Hydroponics CO₂ Calculator, 2017) for calculating the CO₂ concentration required for greenhouse plants top-dressing has made it possible to establish their notable drawback. It lies in the absence of a description of the algorithms for their functioning, which makes it difficult to objectively analyze the results.

This limits the possibility of using this type of software for adaptive calculating the optimum concentration of carbon dioxide, taking into account the geometric parameters of the greenhouses and the types of crops grown.

Thus, there arises the need to solve the scientific and applied problem of developing a mathematical model for the process of the dynamics of the carbon dioxide concentration in conditions of growing crops under protected cultivation, considering the geometric characteristics of greenhouses, as well as the types and periods of plants vegetation. This will make it possible to create an adaptive system for monitoring and controlling the microclimate of greenhouses and give recommendations on increasing the yield of industrial greenhouse complexes.

The subject of the article is the mathematical model and the corresponding adaptive technique for increasing the efficiency of the functioning of computerized monitoring and control systems for the carbon dioxide top-dressing of greenhouse flora.

The aim of the research is to develop and study the mathematical model of the process of carbon dioxide dynamics under greenhouse conditions to develop scientific and theoretical positions and to carry out practical research on the structural and algorithmic organization of computerized systems for monitoring and controlling the concentration of carbon dioxide. This will increase the efficiency of agro-industrial vegetable crop complexes functioning under protected cultivation.

MATERIALS AND METHODS

In the course of the research, the authors have developed the model for monitoring the carbon dioxide concentration in industrial greenhouses by applying physical and mathematical modeling methods and modern software packages NI LabView and Mathcad. Wireless information exchange is implemented by using the RemoteXY service. Principles of functioning of this service correspond to the concept of Internet of Things and described in detail in the literature source (RemoteXY, 2017). Values of the coefficients in the CO₂ dynamics equation under conditions of industrial greenhouses have been obtained by analyzing scientific sources (Koshkin & Shirkevich, 1976; Carbon Dioxide In Greenhouses, 2017; Gas exchange in greenhouses, 2017), as well as by laboratory testing of the developed hardware and software of the automated greenhouse physical model (Vovna et al., 2016; Laktionov et al., 2017b) (see Fig. 1, a, b), which takes into account the condition of geometric similarity to real industrial greenhouses (ratio of height (h): length of base (a): width of base (b) is 1: 1: 0.6), followed by regression analysis of empirical data. The dimensions of the implemented physical model of the greenhouse are the following: h = 1.5 m, a = 1.5 m, b = 0.9 m.

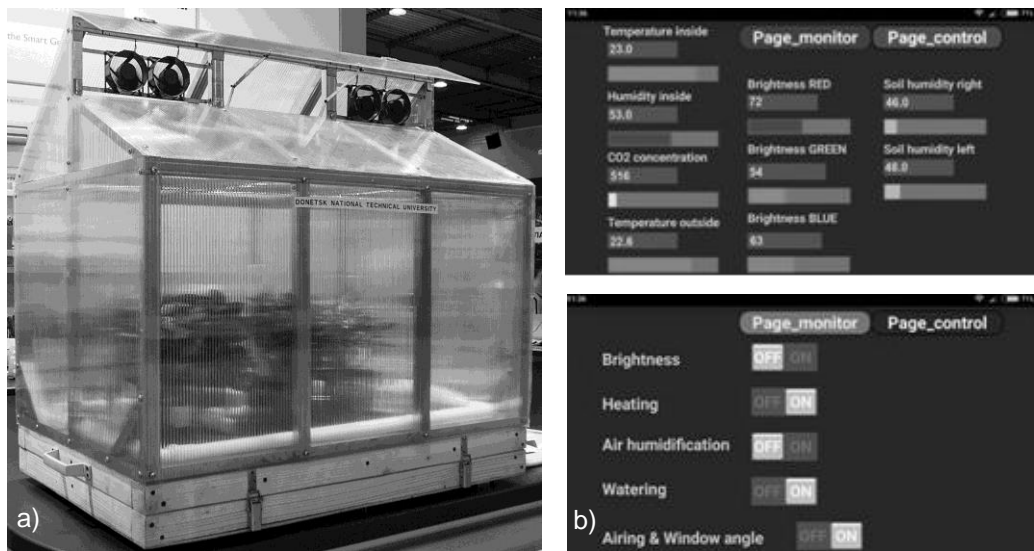


Figure 1. Hardware-software implementation of the automated physical model of a greenhouse: a) external view of the physical model of an automated greenhouse; b) interface of the software component of the monitoring and control system.

The measuring channel for the carbon dioxide concentration is a structural component of the system for monitoring and controlling the parameters of the industrial greenhouses microclimate (Laktionov et al., 2017a). It is based on the MG-811 sensor which is compatible with the Arduino Mega microprocessor platform characterized by the basic relative error of $\pm 0.3\%$ with a dynamic measuring range of 350 to 10,000 ppm.

Simulation of the process of carbon dioxide dynamics for industrial greenhouses was carried out under the following conditions, which are shown in Table 1.

Table 1. Modeling conditions

Condition type	Accepted restriction
The concentration of carbon dioxide in the source area at the initial moment of time	$C_{CO_2}(0,0) = 0.3\%$
The concentration of carbon dioxide at the base of the greenhouse at the initial moment of time	$C_{CO_2}(H,0) = 0.15\%$
The optimal level of carbon dioxide concentration for top-dressing, which is measured in the greenhouse at the initial time	$C_{max} = 0.2\%$
Coefficient of carbon dioxide molecular diffusion	$D_{CO_2} = 0.14 \cdot 10^{-4} \text{ m}^2 \text{ s}^{-1}$
Type of greenhouse	Vegetable, year-round use, hangar
Greenhouse material	Honeycomb polycarbonate
Height of the greenhouse	$H = 4 \text{ m}$
Study period	$T = 1 \text{ hour}$
Coordinates of the carbon dioxide dynamics Z (distance from the gas source to the location of the cultivated crops)	$Z_1 = 3.7$ (height of the tomato shrub in the planting period $h = 0.3 \text{ m}$); $Z_2 = 2.8$ (the height of the tomato shrub in the fruiting period $h = 1.2 \text{ m}$)
Imposed constraints	Isothermal process; convective mass transfer of CO_2 is absent
Types of plants grown	Indeterminate varieties of tomatoes

As a basic technology for carbon dioxide top-dressing of greenhouse plants, a system of supplying pure (liquefied) carbon dioxide using small diameter pipes was used to construct a mathematical model for monitoring the CO_2 concentration in industrial greenhouses (see Fig. 2). This technology was chosen on the basis of a comparative analysis of technical characteristics of existing engineering solutions for agronomic tasks of top-dressing greenhouse plants with carbon dioxide (Lotonov & Iuferev, 2012; Consideration of the main factors in modeling vegetable production in the greenhouse, 2017).

This technology allows performing accurate and economical automatic dosing of carbon dioxide taking into account the daily dynamics of the photosynthetic process, regulating the distance from the CO_2 source to plants, and evenly distributing the gas in the greenhouse volume. However, the claimed type of systems has a number of technological imperfections associated with the limited research results on the regularities of the optimal CO_2 flow depending on the types of plants grown and the

periods of their vegetation, which leads to the lack of algorithms for adaptive management of the process of top-dressing plants with carbon dioxide.

Thus, to justify adaptive algorithms for the operation of automatic carbon dioxide top-dressing systems for plants on the basis of climate controllers in industrial greenhouses, the scientific and technical task of developing a mathematical model for the process of monitoring the carbon dioxide concentration arises.

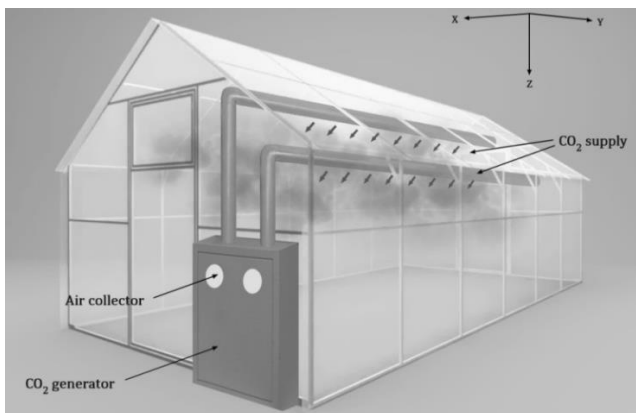


Figure 2. Technological scheme of top-dressing plants with CO₂ using small diameter pipes.

The results of the research were obtained during the implementation of the research in the State Higher Educational Establishment 'Donetsk National Technical University': 'Development of methods and means for increasing the efficiency of computerized information and measuring systems of technological processes' and 'Development of intelligent measuring modules for electronic systems for monitoring physical parameters of physical media'. The results were also piloted at the XXI International Exhibition elcomUkraine (Kiev, Ukraine, 2017).

RESULTS AND DISCUSSION

The mathematical model of the process of monitoring carbon dioxide concentration in industrial greenhouses is based on the balance equation of mass (Hashimoto & Day, 1991):

$$\varphi_{\text{CO}_2}^{\text{sour}} - \varphi_{\text{CO}_2}^{\text{vent}} - \varphi_{\text{CO}_2}^{\text{phot}} = 0 \quad (1)$$

where $\varphi_{\text{CO}_2}^{\text{sour}}$ is the amount of carbon dioxide entering the greenhouse; $\varphi_{\text{CO}_2}^{\text{vent}}$ is the amount of carbon dioxide removed from the greenhouse by means of ventilation; $\varphi_{\text{CO}_2}^{\text{phot}}$ is the amount of carbon dioxide consumed by plants as a result of the photosynthesis process.

The distribution of carbon dioxide in the greenhouse volume takes place under the influence of two processes, one of which is molecular diffusion, that is, the movement of CO₂ molecules in the direction opposite to the concentration gradient. The other is the molecules transport as a result of the air currents motion (convection). As a rule, these processes occur simultaneously.

Thus, considering the Eq. (1) for the isothermal case, the equation of carbon dioxide convective diffusion (Shervud et al., 1982; Kashirskaya et al., 2008; Parfenteva et al., 2013) under the conditions of industrial greenhouses for the Cartesian coordinate system is as follows:

$$\frac{\partial C_{\text{CO}_2}}{\partial t} = D_{\text{CO}_2} \left(\frac{\partial^2 C_{\text{CO}_2}}{\partial x^2} + \frac{\partial^2 C_{\text{CO}_2}}{\partial y^2} + \frac{\partial^2 C_{\text{CO}_2}}{\partial z^2} \right) - \underbrace{\left(\overline{V}_x \frac{\partial C_{\text{CO}_2}}{\partial x} + \overline{V}_y \frac{\partial C_{\text{CO}_2}}{\partial y} + \overline{V}_z \frac{\partial C_{\text{CO}_2}}{\partial z} \right)}_{\varphi_{\text{CO}_2}^{\text{vent}}} + \varphi_{\text{CO}_2}^{\text{sour}}(x, y, z, t) - \varphi_{\text{CO}_2}^{\text{phot}}(x, y, z, t), \quad (2)$$

where C_{CO_2} is carbon dioxide concentration; D_{CO_2} is the coefficient of carbon dioxide molecular diffusion; \overline{V}_x , \overline{V}_y , \overline{V}_z is the air currents velocity along the corresponding coordinates; $\varphi_{\text{CO}_2}^{\text{sour}}$ is the amount of carbon dioxide entering the greenhouse from the source; $\varphi_{\text{CO}_2}^{\text{phot}}$ is the amount of carbon dioxide consumed by plants as a result of photosynthesis.

Having analyzed the technological scheme for top dressing of greenhouse plants with carbon dioxide, shown in Fig. 2, as well as the physicochemical properties of carbon dioxide, it is assumed that the intensity of the change in the carbon dioxide concentration in the coordinate (z) is much greater in comparison with the coordinates x and y , since CO_2 is heavier than air. This leads to its settling in the direction of the (z) coordinate (see Fig. 2). The technological scheme of top-dressing plants with CO_2 is constructed in such a way that the concentration gradient in the (x) and (y) direction can be zero, taking into account the assumption regarding the absence of convective gas transfer ($\frac{\partial^2 C_{\text{CO}_2}}{\partial x^2} = 0$, $\frac{\partial^2 C_{\text{CO}_2}}{\partial y^2} = 0$).

The solution of the problem of constructing and analyzing the mathematical model of the process of carbon dioxide dynamics under industrial greenhouse conditions, which in general is described by the Eq. (2), can be obtained by using the source method (Source method (impulse method), 2017). The physical meaning of this method is to generate a concentration field of the diffusing substance, in this case CO_2 , which is formed by diffusant point sources distributed in space and time (Mors & Feshbakh, 1960).

When compiling a differential equation that describes the processes of carbon dioxide emission and absorption under greenhouse conditions, the restriction on the process of convective gas transfer is introduced. This process is caused by the ventilation of the greenhouses. In this case, we will consider the greenhouse to be a closed system, and there is no convective component of carbon dioxide mass transfer, because in scientific sources there is no up-to-date information on the quantitative characteristics of its effect on the dynamics of carbon dioxide. To take into account the process of convective carbon dioxide transport, additional experimental studies are required.

Thus, the problem in question can be formulated as follows: the greenhouse is a closed system in which the processes of carbon dioxide emission by point sources take place, with the initial distribution of the $C_{\text{CO}_2}(0)$ concentration and the boundary conditions $C_{\text{CO}_2}(0, t) = C_1$ and $C_{\text{CO}_2}(H, t) = C_2$; at the initial time in the greenhouse the

required level of carbon dioxide concentration $C_{CO_2}(0) = C_{max}$, is reached, and the sources of the diffusant are switched off ($\varphi_{CO_2}^{sour}(x, y, z, t) = 0$); convective mass transfer of carbon dioxide is absent ($\varphi_{CO_2}^{vent}(x, y, z, t) = 0$); when analyzing the dynamics of CO_2 in the greenhouse, gas is absorbed by plants with uniform density; the estimated value of the intensity of CO_2 absorption by plants (Carbon Dioxide In Greenhouses, 2017; Gas exchange in greenhouses, 2017) remains constant in space and time, but depends only on the types of crops grown. Current results of researches in the field of quantitative estimates of an indicator intensity of CO_2 absorption of various types of plants are rather limited. Possible ranges of intensity change of photosynthesis depending on the area of leaves of the grown-up cultures are specified in literature sources (BiologyGuide, 2017; Vegetables growing in hydroponic greenhouses, 2017). This parameter can be determined by authors' algorithm which is presented in the flow-chart form in Fig. 3 as a result of researches. The value for early ripening indeterminate varieties of tomatoes is equal: $\varphi_{CO_2}^{phot} = 27 \text{ mg dm}^{-3} \text{ h}^{-1}$.

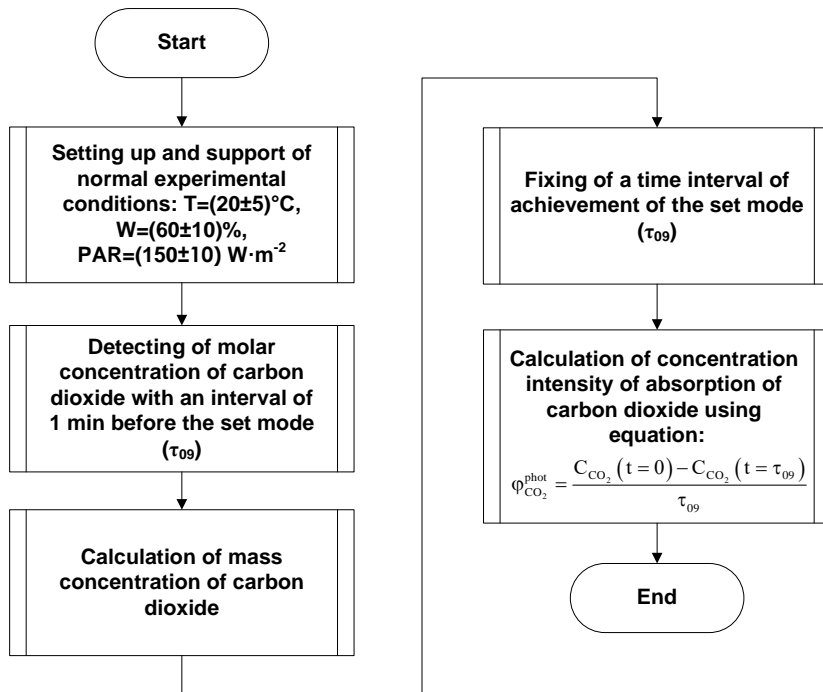


Figure 3. Flow-chart form of algorithm of calculation of CO_2 absorption intensity (T – temperature of the air; W – humidity of the air; E – efficient lighting of crop growing area in the visible light range; τ_{09} – the time to reach steady-state process).

Based on the analysis of the above processes of carbon dioxide dynamics in industrial greenhouses, the differential equation for the problem under consideration is as follows:

$$\frac{\partial C_{CO_2}}{\partial t} = D_{CO_2} \frac{\partial^2 C_{CO_2}}{\partial z^2} - \varphi_{CO_2}^{phot} \quad (3)$$

The differential Eq. (3) while using the Green's function method (Mikhailova & Domanova, 2012; Source method (impulse method), 2017) in general form can be solved through the following expression:

$$C_{CO_2}(z, t) = f_1(z) + f_2(z, t) - f_3(z, t), \quad (4)$$

where $f_1(z)$ is the function taking into account the initial distribution of CO_2 concentrations in the greenhouse under zero boundary conditions and the absence of gas consumption; $f_2(z, t)$ is the function taking into account the boundary conditions for the distribution of CO_2 in the greenhouse under zero initial conditions and the absence of gas consumption; $f_3(z, t)$ is the function taking into account gas consumption by plants in the process of photosynthesis with zero initial and boundary conditions.

Thus, the function $f_1(z)$ in Eq. (4) is a solution for the stationary state of carbon dioxide diffusion in greenhouse conditions, i. e. solution to the equation of the form $\frac{\partial^2 C_{CO_2}}{\partial z^2} = 0$ under boundary conditions $f_1''(z) = 0$, $f_1(0) = C_1$, $f_1(H) = C_2$:

$$f_1(z) = C_1 + \frac{z}{H}(C_2 - C_1), \quad (5)$$

where C_1 and C_2 are the boundary concentrations of carbon dioxide at the gas source points and in the plant area, respectively; H is the distance from the source of gas to the plant beds; z is the integration variable (coordinate).

Function $f_2(z, t)$ is the solution for the non-stationary case:

$$\frac{\partial f_2}{\partial t} = D_{CO_2} \cdot \frac{\partial^2 f_2}{\partial z^2}, \quad (6)$$

under simple boundary conditions $f_2(z, 0) = C_{max} - f_1(z)$.

Based on the analysis of literature sources (Lykov, 1967; Carbon Dioxide In Greenhouses, 2017; Source method (impulse method), 2017) concerning non-stationary differential equations of mathematical physics, the differential Eq. (6) is solved:

$$f_2(z, t) = \frac{2}{\pi} \sum_{n=1}^{\infty} \left[\left(\frac{C_2 \cdot \cos(n\pi) - C_1}{n\pi} \right) \cdot \sin\left(\frac{n\pi z}{H}\right) \cdot e^{-\frac{n^2 \pi^2 D_{CO_2} t}{H^2}} \right] + \frac{4}{\pi} C_{max} \sum_{k=0}^{\infty} \frac{1}{2k+1} \cdot \sin\left(\frac{(2k+1)\pi z}{H}\right) \cdot e^{-\frac{(2k+1)^2 \pi^2 D_{CO_2} t}{H^2}}, \quad (7)$$

where C_1 and C_2 are the boundary concentrations of carbon dioxide at the gas source points and in the plant area, respectively; n, k are the serial numbers of the pulse obtained as a result of multiple reflections of CO_2 molecules from the walls of the greenhouse; H is the distance from the source of gas to the plant beds (approximately equal to the height of the greenhouse); C_{max} is the required carbon dioxide concentration level diagnosed in the greenhouse at the initial time; D_{CO_2} is the required carbon dioxide concentration, which is diagnosed in the greenhouse at the initial time; z, t are the integration variables, respectively, coordinate and time.

The function $f_3(z,t)$ in the Eq. (4) takes into account the gas consumed by plants in the process of photosynthesis under zero initial and boundary conditions. It is considered that the value of the CO_2 absorption by plants does not depend on the coordinate (z) and time (t). The function was obtained by analyzing general form of the equations of mathematical physics, given in specialized sources (Lykov, 1967; Source method (impulse method), 2017) and has the following form:

$$f_3(z, t) = \frac{4H^2 \varphi_{\text{CO}_2}^{\text{phot}}}{\pi^3 D_{\text{CO}_2}} \sum_{n=0}^{\infty} \left(\frac{1}{(2k+1)^3} \cdot \sin\left(\frac{2k+1}{H} \cdot z\right) \cdot \left(1 - e^{-\frac{(2k+1)^2 n^2 D_{\text{CO}_2} t}{H^2}}\right) \right), \quad (8)$$

where H is the distance from the source of gas to the plants beds; $\varphi_{\text{CO}_2}^{\text{phot}}$ is the intensity of CO_2 absorption by plants; D_{CO_2} is the coefficient of carbon dioxide molecular diffusion; n, k are the serial numbers of the pulse obtained as a result of multiple reflections of CO_2 molecules from the walls of the greenhouse (in this case, the main impulse is considered $k = 1$); z, t are the integration variables, respectively, coordinate and time.

Thus, by substituting the solutions (5), (7) and (8) into the Eq. (4), the mathematical model describing the processes of carbon dioxide dynamics under the technological conditions of growing crops on sheltered grounds is obtained:

$$C_{\text{CO}_2}(z, t) = \underbrace{\left\{ C_1 + \frac{z}{H}(C_2 - C_1) \right\}}_{f_1(z)} + \underbrace{\left\{ \frac{2}{\pi} \sum_{n=1}^{\infty} \left[\left(\frac{C_2 \cdot \cos(n\pi) - C_1}{n\pi} \right) \cdot \sin\left(\frac{n\pi z}{H}\right) \cdot e^{-\frac{n^2 \pi^2 D_{\text{CO}_2} t}{H^2}} \right] + \frac{4}{\pi} C_{\text{max}} \sum_{k=0}^{\infty} \frac{1}{2k+1} \cdot \sin\left(\frac{(2k+1)\pi z}{H}\right) \cdot e^{-\frac{(2k+1)^2 \pi^2 D_{\text{CO}_2} t}{H^2}} \right\}}_{f_2(z,t)} + \underbrace{\left\{ -\frac{4H^2 \varphi_{\text{CO}_2}^{\text{phot}}}{\pi^3 D_{\text{CO}_2}} \sum_{n=0}^{\infty} \left(\frac{1}{(2k+1)^3} \cdot \sin\left(\frac{2k+1}{H} \cdot z\right) \cdot \left(1 - e^{-\frac{(2k+1)^2 n^2 D_{\text{CO}_2} t}{H^2}}\right) \right) \right\}}_{f_3(z,t)}, \quad (9)$$

Based on the developed mathematical model of the carbon dioxide monitoring process under industrial greenhouse conditions (9), taking into account the required CO_2 concentration for efficient photosynthesis for the varieties of tomatoes in question and its gradient in a closed volume, the normalized characteristics of the CO_2 dynamics were obtained (Carbon Dioxide In Greenhouses, 2017; Increasing the productivity of greenhouse farms by using the emissions of contact water heaters, 2017) (see Fig. 4) under the conditions described above.

The qualitative analysis of the parameters in Fig. 4 can be used to construct adaptive algorithms for the functioning of phytocontrollers. The essence of the proposed methodology is to adapt the operating modes of monitoring and control systems for

fertilizing plants with carbon dioxide as measured by the current CO₂ concentration in real time, depending on the parameters z – plant height (indirectly takes into account the vegetation period) and $\varphi_{\text{CO}_2}^{\text{phot}}$ – CO₂ absorption intensity (indirectly takes into account the type of crops).

The quantitative analysis of the results of modeling the process of carbon dioxide dynamics in industrial greenhouses, which are shown in Fig. 4, reveals that within an hour, the concentration of CO₂ decreases from the initially established level by 6% for indeterminate varieties of tomatoes during the fruiting period and by 2% during the planting period. It has also been established that the process of CO₂ dynamics in greenhouses can be divided into three characteristic stages: 1 – sharp decline in the parameter (no more than 1–2 min) is due to a significant predominance of the photosynthetic process over the CO₂ diffusion at the initial moment of time at the height of plants; 2 – linear decline in the parameter (approximately 25 min – for crops during the period of planting, 55 min – for crops in the period of fruiting) is due to the predominance of the process of photosynthesis over CO₂ diffusion; 3 – the steady process (starting from 25 minutes – for crops during the period of planting, from 55 minutes – during the fruiting period) is due to the balancing of competing processes of diffusion and CO₂ absorption by plants.

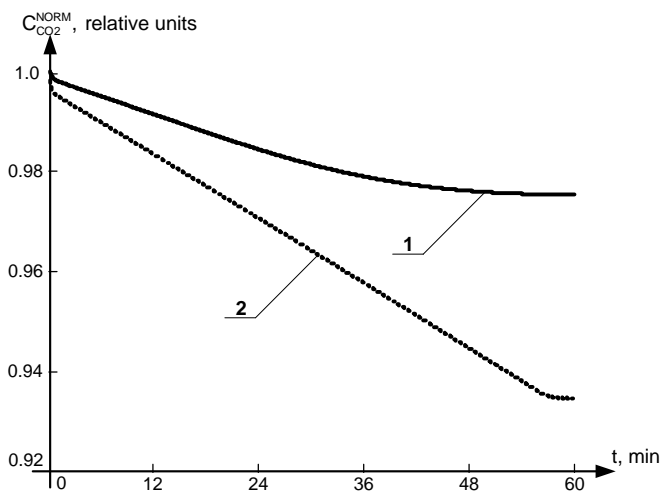


Figure 4. Results of modeling the carbon dioxide dynamics in industrial greenhouses (1 – for indeterminate varieties of tomatoes in the period of planting, $h = 0.3$ m; 2 – for indeterminate varieties of tomatoes during fruiting, $h = 1.2$ m).

Thus, the developed mathematical model of the process of carbon dioxide dynamics under greenhouse conditions has allowed developing scientific and theoretical provisions on the structural and algorithmic organization of computerized systems for monitoring and controlling the concentration of carbon dioxide. In future this will improve the efficiency of the agro-industrial objects for growing vegetable crops on sheltered grounds. To improve the proposed mathematical model and confirm the adequacy of its implementation in the yield indicators of greenhouse crops, it is necessary to conduct comprehensive studies on establishing the regularities in the

influence of CO₂ convective mass transfer on the process of crops photosynthesis under real conditions of industrial greenhouses.

A structural diagram of the system for automatic regulation of carbon dioxide concentration for industrial greenhouses based on the developed mathematical model is shown in Fig. 5.

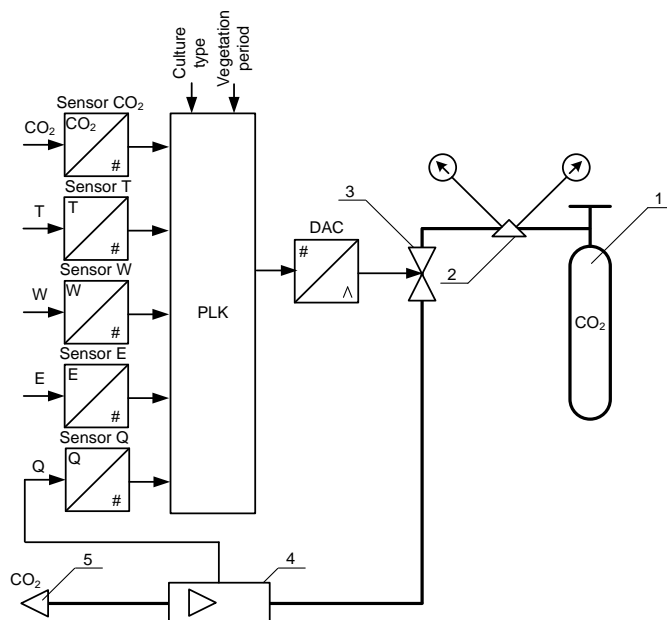


Figure 5. Structural diagram of the automatic regulation system of CO₂ concentration for industrial greenhouses (1 – cylinders with carbon dioxide; 2 – reducer; 3 – regulation valve with solenoid flap; 4 – rotameter; 5 – carbon dioxide collection in the ventilation system of industrial greenhouses).

The digital sensors placed in the industrial greenhouse carry out measurements of carbon dioxide concentration in crop growing area (sensor CO₂), temperature of the air (sensor T), humidity of the air (sensor W) and efficient lighting of crop growing area in the visible light range with due regard to circadian dynamics of the natural light (sensor E). Information from the sensors outputs comes to the controller (PLK) where the necessary volume of carbon dioxide for feeding up the grown-up cultures calculates using developed algorithms taking into account their types and current vegetation periods.

Carbon dioxide from cylinders (see Fig. 5) arrives through a reducer on the regulation valve. Smooth regulation by the electromagnetic flap of the valve of supply of carbon dioxide from cylinders carried out from PLK via the digital-to-analog converter (DAC). Carbon dioxide arrives on the rotameter which defines its volume expense after the regulation valve. In the developed system of automatic control injected the feedback on a volume flow for decreasing of an overshoot error. Information about this parameter entered into PLK using a digital flow-rate sensor (sensor Q). Carbon dioxide dumped into the ventilation system of the industrial greenhouse after the rotameter.

The developed diagram realizes the offered mathematical model. It will allow confirming efficiency development introduction on indicators of productivity of greenhouse cultures when carrying out complex researches on establishment of influence's regularities of a convective carbon dioxide mass transfer on process of cultures photosynthesis in actual operating conditions.

CONCLUSIONS

The article studies the development of scientific, theoretical and practical foundations for increasing the productivity of industrial greenhouse complexes by justifying the mathematical model for monitoring the carbon dioxide concentration in industrial greenhouses. The developed mathematical model is an analytical solution of the differential equation of the carbon dioxide mass balance, which takes into account the diffusion and absorption of carbon dioxide, the geometric parameters of the greenhouses, and the types and periods of vegetation of crops grown under protected cultivation.

The main stages and time characteristics of the process of carbon dioxide dynamics under greenhouse conditions are defined. Quantitative estimates of the duration of diffusion transfer and carbon dioxide absorption periods are established for indeterminate varieties of tomatoes during the period of planting and fruiting.

Based on the analysis of modeling results, recommendations are given on the development of an adaptive methodology for the functioning, as well as structural and algorithmic organization of the computerized monitoring and management system for the top-dressing of greenhouse crops with carbon dioxide.

The necessity to improve the proposed mathematical model and confirm the adequacy of its implementation effectiveness on the yield indicators of greenhouse crops is substantiated by carrying out complex studies on establishing the regularities of the influence of carbon dioxide convective mass transfer on the process of crops photosynthesis under real conditions of industrial greenhouses.

REFERENCES

- BiologyGuide. 2017. <http://www.biologyguide.ru/gbids-178-6.html>. Accessed 06.11.2017. (in Russian).
- Carbon Dioxide In Greenhouses. 2017. <http://www.omafra.gov.on.ca/english/crops/facts/00-077.htm>. Accessed 05.08.2017.
- Consideration of the main factors in modeling vegetable production in the greenhouse. 2017. goo.gl/iLCPr8. Accessed 06.07.2017 (in Russian).
- Departmental rules of the technological engineering NTP 10-95. 1996. *Norms of technological designing greenhouses and greenhouse combines for growing vegetables and sprouts*. Giproniselprom, Moscow, 87 pp. (in Russian).
- Departmental rules of the technological engineering VNTP APK-19-07. 2007. *Greenhouse and greenhouse businesses. Structures protected ground for farming (rural) farm*. HIK, Kiev, 140 pp. (in Ukrainian).
- Gas exchange in greenhouses. 2017. <http://www.activestudy.info/gazoobmen-v-teplicax/>. Accessed 05.08.2017 (in Russian).
- Greentrees Hydroponics CO₂ Calculator. 2017. https://www.hydroponics.net/learn/co2_calculator.php. Accessed 03.08.2017.

- Hashimoto, Y. & Day, W. 1991. *Mathematical and control applications in agriculture and horticulture*. Pergamon press, Oxford, 449 pp.
- Increasing the productivity of greenhouse farms by using the emissions of contact water heaters. 2017. goo.gl/yMhqgQ. Accessed 12.08.2017 (in Russian).
- Kashirskaya, O., Lotkhov, V. & Dil'man, V. 2008. A new method for measurement of diffusion coefficients in gas mixtures. In Lotkhov, V. & Dil'man, V.: *Summaries of the 18th Int. Congress of Chemical and Process Engineering*. Prague, Czech Republic, pp. 1018–1019.
- Katsoulas, N. & Kittas, C. 2008. Impact of greenhouse microclimate on plant growth and development with special reference to solanaceae. *The European Journal of Plant Science and Biotechnology* **S1**, 31–44.
- Koshkin, N.N. & Shirkevich, M.G. 1976. *Handbook of elementary physics*. Science, Moscow, 256 pp. (in Russian).
- Laktionov, I., Vovna, O. & Zori, A. 2017a. Concept of low cost computerized measuring system for microclimate parameters of greenhouses. *Bulgarian Journal of Agricultural Science* **23**(4), 668–673.
- Laktionov, I.S., Vovna, O.V. & Zori, A.A. 2017b. Realization of computerized system for remote monitoring and control of the parameters of industrial greenhouses microclimate. *Scientific papers of DonNTU 'Informatics, Cybernetics and Computing Technology'* **1**(24), 85–90 (in Ukrainian).
- Lotonov, A.V. & Iuferev, L.Iu. 2012. System for monitoring and automatic regulation of CO₂ content under protected cultivation. *Innovations in agriculture* **1**, 24–30. (in Russian).
- Lykov, A.V. 1967. *Theory of heat conductivity*. High School, Moscow, 600 pp. (in Russian).
- Mikhailova, T.Iu. & Domanova, E.D. 2012. *Methods for solving ordinary differential equations. Boundary problems. Green's function*. Novosibirsk State University, Novosibirsk, 57 pp. (in Russian).
- Mors, F.M. & Feshbakh, G. 1960. *Methods of theoretical physics*. Publishing House of Foreign Literature, Moscow, 898 pp. (in Russian).
- OX-AN® Carbon Dioxide Monitoring Systems. 2017. http://www.ox-an.com/carbon_dioxide_monitoring_systems.asp. Accessed 03.08.2017.
- Parfenteva, N.A., Trukhanov, N.A. & Kashintseva, V.L. 2013. Integral method for solving the convective diffusion problem. *Bulletin of MSTU. Named after N.E. Bauman. 'Natural Sciences'* **3**, 97–105 (in Russian).
- RemoteXY. 2017. <http://remotexy.com/en>. Accessed 06.11.2017.
- Santosh, D.T., Tiwari, K.N., Singh, V.K. & Raja Gopala Reddy, A. 2017. Micro Climate Control in Greenhouse. *International Journal of Current Microbiology and Applied Sciences* **6**(3), 1730–1742.
- Shervud, T., Pigford, R. & Uilki, Ch. 1982. *Mass transfer*. Chemistry, Moscow, 696 pp. (in Russian).
- Source method (impulse method). 2017. <http://profbeckman.narod.ru/MDL7.pdf>. Accessed 02.08.2017 (in Russian).
- TechGrow CO₂-controllers. 2017. <https://www.techgrow.nl/co2-controllers-en/>. Accessed 03.08.2017.
- Theoretical substantiation of methods for increasing the cucumber yield in greenhouses. 1995. <http://earthpapers.net/preview/471381/a?#?page=14>. Accessed 06.11.2017. (in Russian).
- Vegetables growing in hydroponic greenhouses. 2017. <http://www.bibliotekar.ru/7-gidroponika/24.htm>. Accessed 06.11.2017 (in Russian).
- Vovna, O.V. Laktionov, I.S. & Akhmedov, R.N. 2016. Hardware and software realization of the computerized carbon concentration meter for agrarian and coal mining enterprises. Laktionov, I.S. & Akhmedov, R.N.: *Proceedings of the III International Scientific and Practical Conference 'Science and Education – Our Future'*. Ajman, UAE, pp. 10–15 (in Ukrainian).

The influence of cultivar, weather conditions and nitrogen fertilizer on winter wheat grain yield

A. Linina* and A. Ruza

Latvia University of Life Sciences and Technologies, Faculty of Agriculture, Institute of Agrobiotechnology, Liela iela 2, LV3001 Jelgava, Latvia

*Correspondence: anda.linina@llu.lv

Abstract. Winter wheat (*Triticum aestivum* L.) is one of the most productive and significant cereal species in Latvia used for food grain production. The aim of the research was to evaluate winter wheat grain yield depending on nitrogen fertilizer rate, crop-year (meteorological conditions) and cultivar and determine the impact and interaction of research factors on grain yield. Field experiments with winter wheat cultivars ‘Bussard’ and ‘Zentos’ were conducted at the Latvia University of Agriculture, Study and Research farm Peterlauki during a three year period (2009/2010, 2010/2011 and 2011/2012). Nitrogen (N) was applied (N60, N90, N120, N150 kg ha⁻¹) in spring after resumption of vegetative growth. Assessment of both winter wheat cultivars showed that crop-year, cultivar, nitrogen fertilizer, crop-year × cultivar had a significant ($p < 0.05$) impact on grain yield. Nitrogen fertilizer did significantly ($p < 0.05$) affect the grain yield of winter wheat, treatment with N90 showed of yield increase, compared to N60, while further use of increasing amounts of N fertilizer did not increase grain yields significantly. Results suggest, that winter wheat grain yield by 34% depended on cultivar, by 33% on crop-year (weather conditions), and by 13% on crop-year × cultivar. Influence of the nitrogen fertilizer effect was small – 3%. Medium strong positive correlation was found between HTC in the vegetation period from winter wheat heading to grain ripening.

Key words: grain yield, nitrogen fertilizer, hydrothermic coefficient.

INTRODUCTION

Winter wheat (*Triticum aestivum* L.) is the main cereal crop used for human consumption in many areas worldwide. In 2014, according to FAO data (FAOSTAT, 2017) 221 million ha were the total sown area by wheat in the world, while the harvested yield exceeded 730 million tonnes of grain, but the average yield of wheat was 3.3 t ha⁻¹. The total amount of grain in different parts of the world varies annually, mainly due to changing climatic conditions owing to drought or excessive moisture.

In Latvia, winter wheat (*Triticum aestivum* L.) is the most widely grown crop. The sown area, grain yield per ha and the total harvested yield tends to increase. According to statistical data, 256 thousand ha were under winter wheat in 2008, whereas in 2011 it occupied 200 thousand ha, but in 2012 the sown area reached 258 thousand ha. In 2015, the area sown to wheat occupied 448 thousand ha including 291 thousand ha devoted to winter wheat, which was 43% of the total sown area planted with cereals. Winter wheat

is the most productive cereal in Latvia, high yield was achieved in 2008 – 4.35 t ha⁻¹, in 2011 the average yield was lower – 3.1 t ha⁻¹, but in 2012 – 4.7 t ha⁻¹ were obtained, while the highest winter wheat yield was achieved in 2015 – 5.5 t ha⁻¹ as influenced by favourable meteorological conditions during vegetation period (Graudu statistikas dati, 2015).

Wheat yield is influenced by the interaction of a number of factors including cultivar, soil, climate, and cropping practices (Shejbalova et al., 2014; Jonczuk & Stalenga, 2016). Wheat grain yield depends on weather conditions in the investigation years (Skudra & Linina, 2011; Fetere & Strazdina, 2014; Famēra et al., 2015, Karklins & Ruza, 2015; Alijošius et al., 2016). Wheat is sensitive to the prevailing weather conditions, such as precipitation. In Hungary Márton, L. (2008) found significant correlation between winter wheat yield and precipitation in vegetative period. He concludes that optimum yields develop in response to rainfall in the 450–500 mm range. Above or below this rainfall yields reduce. While results in Poland (Bujak et al., 2013) suggest that no correlation has been found between the yields and the total precipitation. The soil type proved to be the environmental factor of particular importance in determining winter wheat yields.

The lowest grain yield was harvested, when wintering of wheat was problematic, in rather dry weather conditions prevailing during filling of grain, and when the temperature in July (in grain ripening period) was higher than the long-term average (Jansone & Gaile, 2013). The influence of the crop-year on grain yield was observed best with seven winter wheat cultivars investigated in 2002–2004 at the State Stende Plant Breeding station in Latvia (Malecka, Bremanis & Miglane, 2005), and 13 winter wheat cultivars investigated across four locations and two years in Lithuania (Tarakanovas & Ruzgas, 2006). During ripening wheat plants require moderate moisture and warm weather conditions. These conditions secure biological maturity and acceptable technological properties of grain (Linina & Ruza, 2012; Fetere & Strazdina, 2014; Famēra et al., 2015; Rozbicki et al., 2015).

Winter wheat yield is related to nitrogen supply levels. Under temperate climate, nitrogen is a limiting factor of winter wheat growth and yield (Povilaitis & Lazauskas, 2010). Positive correlation between grain yield and nitrogen fertilizer was found by several researchers in Croatia (Svečnjak et al., 2013), in Czech Republic (Šip et al., 2000), in USA (Farrer et al., 2006) and also in Australia (Savin, Sadras & Slafer, 2006).

Grain yield significantly varied depending on the cultivars as previously observed (Márton, 2008; Skudra & Linina, 2011; Jansone & Gaile, 2013; Kaya & Akcura, 2014; Alijošius et al., 2016).

The aim of the research was to evaluate winter wheat grain yield depending on nitrogen fertilizer rate, crop-year (meteorological conditions) and cultivar and determine the impact and interaction of research factors on grain yield.

MATERIALS AND METHODS

Field experiments. A field trial was carried out in Study and Research farm Peterlauki (56° 30.658' N and 23° 41.580' E) of the Latvia University of Agriculture (LLU) during a three-year period: 2009/2010, 2010/2011 and 2011/2012. Soil at the site was Endocalcaric Abruptic Luvisol (by World Reference Base for Soil Resources) silt

loam. Soil agro-chemical parameters were different on a year (Table 1). Such conditions were suitable for winter wheat growing.

Table 1. Soil parameters at trial site depending on year

Parameter	Year		
	2010	2011	2012
Soil pH KCL	6.9	6.6	7.0
Available P mg kg ⁻¹ (by Egner – Riehm method)	182	118	121
Available K mg kg ⁻¹ (by Egner – Riehm method)	171	191	153
Organic matter, g kg ⁻¹ of soil (by Tyurin’s method)	27	31	27

In trial traditional soil treatment was used, which involves soil ploughing. Winter wheat was sown (13 September in 2009, 25 September in 2010 and 12 September in 2011) using a sowing machine Junkkari Simulta 2500 T. In the Study and Research farm Peterlauki have eight field crop sequence and winter wheat always sown after black fallow. The trial included two winter wheat cultivars ‘Bussard’ and ‘Zentos’ (released in Germany), because these cultivars from 2008 to 2012 was the most popular in Latvian farms.

Both wheat cultivars are of high bread-making quality (Elite cultivars), differing in their high molecular weight (HMW) glutenin composition. Wheat ‘Bussard’ possesses subunit 1 at Glu – A1 locus α allele, and ‘Zentos’ possesses subunit 0, respectively. Both cultivars have the same patterns 7 + 9 at Glu – B1 c and 5 + 10 at Glu – D1 locus d alleles (Mašauskienė et al., 2002).

These cultivars were grown in four replications with a plot size of 36 m², at the rate of 450 germinating seeds per m². Treatments were arranged in a randomized block design. The fertilizer background was P₂O₅ – 70 kg ha⁻¹ and K₂O – 90 kg ha⁻¹. Nitrogen was applied in spring after resumption of vegetative growth. Nitrogen (N) top-dressing rates were as follows: N60, N90, N120 and N150. All the necessary plant protection measures (herbicides, plant growth regulators and fungicides) were performed. Wheat grain was harvested at full ripening (GS 90 – 92) with harvester Sampo Rosenlew-130 on 4 August in 2010, on 5 August in 2011 and on 3 August in 2012. The yield of winter wheat grain was recalculated in t ha⁻¹ at 14% moisture and 100% purity.

Weather conditions. During three investigation years weather conditions were different. Winter wheat in all three years overwintered successfully. The duration of winter wheat growth from spring after the resumption of vegetative growth to harvesting was different in the trial years: in 2010 and 2011 – 126 and 121 days, respectively; in 2012 – 111 days (because that year, the vegetation period began later – on April 15) (Table 2). Precipitation in grain filling period in July, which is most decisive for grain quality formation, was 298, 179, and 197 mm in 2010, 2011, and 2012, respectively, which significantly exceeded the long-term average (81.7 mm). The sum of active temperatures (above +5 °C) in the winter wheat vegetation period in 2010 and 2011 was 1,777 and 1,769 °C, respectively, while the year 2012 was cooler with a lower active temperature – 1,561 °C.

To evaluate the conditions of dampness of the area, the Seljanin’s hydrothermal coefficient (HTC) was used, which shows the relationship between the amount of

precipitation and the air temperature (above +10 °C) in the vegetation period. It is given by the following relation:

$$HTC = \frac{\sum N}{\sum t} \times 10$$

where $\sum N$ – is the sum of precipitation (mm) during period; $\sum t$ – the sum of average daily temperatures (°C) during the same period; 10 – coefficient.

In the vegetation period of 2010 and 2012, excessive moisture was observed, and HTC was 2.79 and 2.65, respectively. In 2011, HTC was 1.92, which indicates a sufficient amount of moisture.

Table 2. Duration of winter wheat growth stages and description of weather conditions in 2010–2012

Traits	Year	Zadoks growth stages (GS)*			
		24–91	24–30	31–0	51–91
Duration of the period, days	2010	126	45	29	52
	2011	121	42	20	61
	2012	111	31	19	61
Sum of active temperatures (+ 5 °C)	2010	1,777	360	424	994
	2011	1,769	363	296	1,111
	2012	1,561	310	236	1,016
Mean daily temperature, °C	2010	14.1	8.0	14.6	19.1
	2011	14.5	8.9	14.8	18.2
	2012	14.7	10.0	12.4	16.7
Sum of precipitation, mm	2010	495	107	52	337
	2011	339	71	13	255
	2012	414	89	35	289
Hydrothermic coefficient (HTC)	2010	2.79	2.96	1.23	3.24
	2011	1.92	1.96	0.43	2.26
	2012	2.65	2.88	1.50	2.75

* Zadoks growth stages (GS); 24–91 (from tillering (main shoot and 4 tillers) to ripening); 24–30 (from main shoot and 4 tillers to stem elongation); 31–50 (from stem elongation (1st node detectable) to heading); 51–91 (from heading to ripening) (Zadoks, Chang & Konzak, 1974).

Statistical analysis. Experimental data evaluation was done using three – factor (SPSS) analysis of variance by Fisher’s criterion ($p < 0.05$) and least significant difference ($LSD_{0.05}$). Influence (η , %) of each factor (crop-year, nitrogen fertilizer, cultivar and interaction of them) was calculated of three – factor analysis of variance for winter wheat grain yield. It was expressed as percentage to the total variance. Correlation (r) and determination coefficient (R^2), regression equation between grain yield and hydrothermic coefficient were also carried out.

RESULTS AND DISCUSSION

Influence of weather conditions on grain yield. In total, obtained grain yields of both investigated winter wheat cultivars, averaged over three years, were $6.22 \pm 0.11 \text{ t ha}^{-1}$ (within the range (min-max) of 5.13 to 6.92 t ha^{-1}) with a coefficient of variation (V , %) 8%.

According to Fisher's criterion, the influence of weather conditions (2010–2012 crop-years) on winter wheat grain yield was significant ($p < 0.05$). According to the results of our research, significantly ($p < 0.05$) lower grain yield was obtained in 2011 (5.84 t ha^{-1}) (Fig. 1), when the average amount of precipitation in the vegetation period was lower (339 mm, HTC 1.92) (Table 1). There was a significant disturbance in plant nutrition (HTC 0.43) in GS 31–51, also the relatively high average temperatures in June ($17.2 \text{ }^\circ\text{C}$) and July ($19.5 \text{ }^\circ\text{C}$) negatively affected the ripening process and grain yield of winter wheat.

The higher grain yield was obtained in 2010 crop-year – 6.60 t ha^{-1} . The vegetation period in 2010 was rainy and HTC was the highest – 2.3, compared with others trial years (Table 2). The period from stem elongation to heading (GS 31–51) in this year was 29 days, which was by 5 and 15 days longer compared to the years 2011 and 2012 respectively, but HTK was 1.2, indicating that wheat plants had enough moisture and warmth, which positively influenced the growth and development of wheat plants. Increased rainfall greatly influenced the process of grain formation having a positive effect on grain yield, but negative effect on the quality of grain.

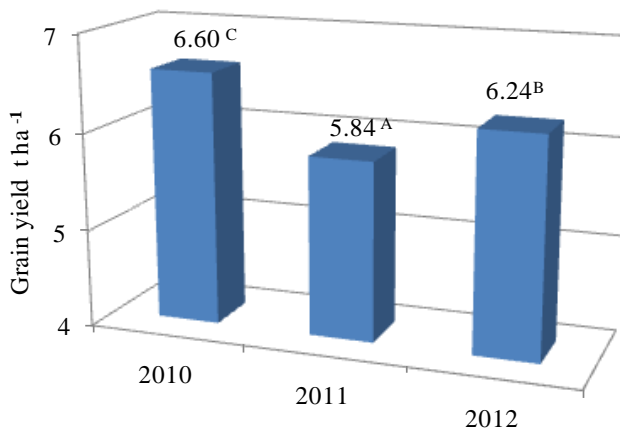


Figure 1. Influence of weather conditions on winter wheat grain yield (t ha^{-1}), 2010–2012 on average; ^{ABC} columns marked with different letter did differ significantly ($p < 0.05$).

Winter wheat yield significantly varied depending on the differences among cultivars (Cesevičienė et al., 2012; Kaya & Akcura, 2014). Investigation results in Lithuania (2000–2007) show that the average grain yield of the cultivar ‘Zentos’ was 6.6 t ha^{-1} (Liatukas et al., 2012) which is consistent with our results. The research data from other scientists show that winter wheat yield in favourable years was $8 - 10 \text{ t ha}^{-1}$ (Tarakanovas & Ruzgas, 2006; Jansone & Gaile, 2011; Jansone & Gaile, 2013; Fetere & Strazdina, 2014; Alijošius et al., 2016; Gaile et al., 2017), while in adverse year $3 - 5 \text{ t ha}^{-1}$ (Ivanova & Tsenov, 2012; Jablonskytė-Raščė, et al., 2013; Skudra & Ruza, 2016). Wheat productivity largely depends on climatic conditions, in particular on the total precipitation and temperature in the trial year (Bujak et al., 2013; Faměra et al., 2015; Karklins & Ruza, 2015). Similar results were obtained in our research. When the growing conditions are dry and warmer, compared with the long-term mean, wheat grain yield is poorest (Teesalu & Leedu, 2001; Cesevičienė, Leistrumaitė & Paplauskienė,

2009; Kozlovsky et al., 2009) while the grain quality is improving (Cesevičienė et al., 2012). In our investigation it was determined, that in 2010 and 2011 crop-years there were lower winter wheat grain yields but better grain quality, compared to 2012 crop-year, as described in our previous paper (Liniņa & Ruža, 2012; Linina & Ruza, 2015).

Interaction of hydrothermic coefficient (HTC) and wheat grain yield. HTC is one of the interpretations of humidity on plant development used in wheat and other crops. Statistically medium strong positive correlation was found between HTC in the vegetation period from winter wheat heading to grain ripening (GS 51–91) and grain yield $r = 0.577$ (significant at 99%) ($n = 24$, $\alpha_{0.01} = 0.515$) $R^2 = 0.37$, $p = 0.026$. As shown, the increase in HTC in 37% cases resulted also in grain yield increase (Fig. 2).

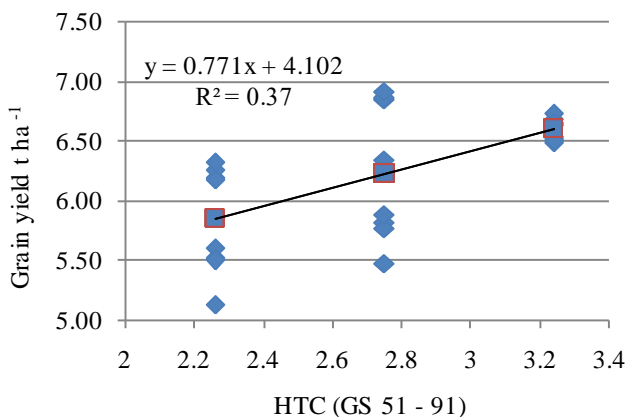


Figure 3. Influence of nitrogen fertilizer norm on winter wheat grain yield (t ha⁻¹), 2010–2012 on average, ^{ABC} columns marked with different letter did differ significantly (p < 0.05).

Grain yield significantly varied depending on the nitrogen fertilizer as previously observed (Cesevičienė et al., 2012; Jablonskitė-Raščė et al., 2012; Márton, 2008, Shejbalova et al., 2014; Skudra & Ruza, 2016). The nitrogen fertilizer is an important factor that stabilises the grain yield of winter wheat. However, the nitrogen effect is small compared to crop-year and cultivar influences (Teesalu & Leedu, 2001) and it is in agreement with our investigation. The effect of fertilizer depends on weather conditions during investigation year.

Influence of cultivar, crop-year and nitrogen fertilizer on grain yield. Influence (η , %) of each factor (crop-year, nitrogen fertilizer, cultivar and interaction of them) was calculated of three – factor analysis of variance for winter wheat grain yield. It was expressed as percentage to the total variance. Results suggest, that winter wheat grain yield by 34% depended on cultivar, by 33% on crop-year (weather conditions), and by 13% on crop-year \times cultivar. Influence of the nitrogen fertilizer effect was small – 3% (Table 3).

Table 3. Analyses of variance of winter wheat grain yield for two cultivars grown in three crop-years (2010–2012)

Source	DF	SS	MS	η , %
Total	95	28.21	–	–
Crop-year (A)	2	9.18	4.59*	33
N fertilizer (B)	3	0.74	0.25*	3
Cultivar (C)	1	9.63	9.63*	34
A \times C	2	3.66	1.83*	13
B \times C	3	0.03	0.01	0 (ns)
A \times B	6	1.00	0.17	4 (ns)
A \times B \times C	6	0.25	0.04	1 (ns)
Error	72	3.72	0.05	–

* – significant at the 0.05 probability level; DF – degree of freedom; SS – sum of squares; MS – mean square; ns – not significant at the 0.05 probability level.

There are not significant effect cultivar \times nitrogen fertilizer, crop-year \times nitrogen fertilizer and cultivar \times nitrogen fertilizer \times crop-year on winter wheat grain yield. Grain yield was affected most by the weather conditions during experimental year, but the genotype of the cultivar had some impact on the variation as well (Tarakanovas & Ruzgas, 2006) as it confirmed in the present trial.

Several authors have determined the effect of the cultivar, crop-year and interaction on the winter wheat grain yield (Rozbicki et al., 2015). The influence of the crop-year on grain yield was most important also in research results reported from Lithuania (Tarakanovas & Ruzgas, 2006; Cesevičienė et al., 2012). Only a few authors have studied nitrogen fertilizer, crop-year, and cultivar effects (impact factor – η , %) on winter wheat grain yield. Results (2002–2004) at the State Stende Plant Breeding station in Latvia suggest, that winter wheat grain yield by 23% depended on crop-years (weather conditions), by 16% on nitrogen fertilizer, by 29% on nitrogen fertilizer \times cultivar and by 3% on cultivar (Malecka, Bremanis & Miglane, 2005), while in the current research the nitrogen effect was smaller (Table 3).

CONCLUSION

1. The grain yield of winter wheat was affected mainly by cultivar and crop-year, less effect was to nitrogen fertilizer and interaction between these factors.
2. Insufficient precipitation and higher daily temperature from the stem elongation to heading of wheat resulted in lower grain yield.
3. Medium strong positive correlation was found between HTC in the vegetation period from winter wheat heading to grain ripening.

ACKNOWLEDGEMENTS. The research was supported by the national research program 'Agricultural resources for sustainable production of qualitative and healthy foods in Latvia' (AgroBioRes), project No. 1 'Sustainable use of soil resources and abatement of fertilisation risks (SOIL)'.

REFERENCES

- Alijošius, S., Švirmickas, J., Bliznikas, S., Gružasuskas, R., Šašytė, V., Racevičiūtė-Stupelienė, A., ... & Daukšienė, A. 2016. Grain chemical composition of different varieties of winter cereals. *Zemdirbyste-Agriculture* **103**(3), 273–280. DOI:10.13080/z-a.2016.103.035.
- Bujak, H., Trawal, G. Weber, R. & Kaczmarek, J., 2013. An analysis of spatial similarity in the variability of yields of winter wheat (*Triticum aestivum* L.) cultivars in Western Poland. *Zemdirbyste-Agriculture* **100**(3), 311–316.
- Cesevičienė, J., Leistrumaitė, A. & Paplauskienė, V. 2009. Grain yield and quality of winter wheat varieties in organic agriculture. *Agronomy Research* **7**(1), 217–223.
- Cesevičienė, J., Šlepetienė, A., Leistrumaitė, A., Ruzgas, V. & Šlepetys, J. 2012. Effects of organic and conventional production systems and cultivars on winter wheat technological properties. *Journal of the Science of Food and Agriculture* **92**(14), 2811–2818.
- Faměra, O., Mayerova, M., Burešová, I., Kouřimská, L. & Prášilová, M. 2015. Influence of selected factors on the content and properties of starch in the grain of non-food wheat. *Plant Soil Environment* **61**(6), 241–246. DOI:10.17221/13/2015-PSE.
- Farrer, D.C., Weisz, R., Heiniger, R., Murphu, J.P. & White, J.G. 2006. Minimizing protein variability in soft red winter wheat: impact of nitrogen application timing and rate. *Agronomy Journal* **98**, 1137–1145.
- FAOSTAT. 2017. Food and Agricultural Organization of the United Nations (FAO). Data base: Crops Resurss. Retrieved April 25, 2017, from <http://www.fao.org/faostat/en/#data/QC>
- Fetere, V. & Strazdina, V. 2014. Ziemas kviešu šķirņu novērtējums Valsts Stendes graudaugu selekcijas institūtā, 2011.–2013. gadā (Evaluation of winter wheat varieties at the State Stende cereal breeding institute, 2011–2013). In *Līdzsvarota lauksaimniecība, Zinātniski praktiskās konferences raksti*, (2014. g. 20–21. febr.). Jelgava, LLU, 65–68 pp. (in Latvian).
- Gaile, Z., Ruza, A., Kreita, D. & Paura, L. 2017. Yield components and quality parameters of winter wheat depending on tillering coefficient. *Agronomy Research* **15**(1), 79–93.
- Graudu statistikas dati. 2015. (Grain statistical data). Retrieved January 04, 2017, from <http://www.csb.gov.lv/dati/statistikas-datubazes-28270.html> (in Latvian).
- Ivanova, A. & Tsenov, N. 2012. Winter wheat productivity under favourable and drought environments. II Effect of previous crop. *Bulgarian Journal of Agricultural Science* **18**(1), 29–35.
- Jablonskitė-Raščė, D., Maikštenienė, S. & Mankevičienė, A. 2012. Evaluation of productivity and quality of common wheat (*Triticum aestivum* L.) and spelt (*Triticum spelta* L.) in relation to nutrition conditions. *Zemdirbyste-Agriculture* **100**(1), 45–56.

- Jansone, I. & Gaile, Z. 2011. Production of bio-ethanol from winter cereals. In Research for Rural Development 2011, Annual 17th International Scientific Conference Proceedings, 18–20 May 2011. 1 (pp. 29–34). Jelgava, Latvia: LLU.
- Jansone, I. & Gaile, Z. 2013. Production of bioethanol from starch based agriculture raw material. In Research for Rural Development, Annual 19th International Scientific Conference Proceedings, 15–17 May 2013. 1, (pp. 35–41). Jelgava, Latvia: LLU.
- Jonczuk, K. & Stalenga, J. 2016. Yielding of new Quality varieties of winter wheat cultivated in organic farming. *Journal of Research and Application in Agriculture Engineering* **61**(3), 200–205.
- Karklins, A. & Ruza, A. 2015. Nitrogen apparent recovery can be used as the indicator of soil nitrogen supply. *Zemdirbyste-Agriculture* **102**(2), 133–140. DOI:10.13080/z-a.2015.102.017.
- Kaya, Y. & Akcura, M. 2014. Effects of genotype and environment on grain yield and quality traits in bread wheat (*T. aestivum* L.). *Food Science and Technology Campinas* **34**(2), 386–393. DOI:http://doi.org/10.1590/fs2014.0041.
- Kozlovsky, O., Balik, J., Černý, J., Kulhanek, M., Kos, M. & Prašilova, M. 2009. Influence of nitrogen fertilizer injection (CULTAN) on yield, yield components formation and quality of winter wheat grain. *Plant Soil Environment* **55**(12), 536–543.
- Liatukas, Ž., Ruzgas, V., Razbadauskienė, K., Brazauskas, G. & Koppel, R. 2012. Winter wheat cultivars ‘Kovas DS’, ‘Zunda DS’, ‘Vikaras DS’, ‘Kaskada DS’ for high input farming: development and characterization. *Zemdirbyste-Agriculture* **99**(3), 225–264.
- Linīņa, A. & Ruža, A. 2012. Cultivar and nitrogen fertilizer effects on fresh and stored winter wheat grain quality indices. In *Proceedings of the Latvian Academy of Sciences, Section B: Natural, Exact and Applied science*. Vol. **66**(4/5), pp. 177–184.
- Linina, A. & Ruza, A. 2015. Weather conditions effect on fresh and stored winter wheat grain gluten quantity and quality. In *Proceedings of the 25 th congress (NJF) "Nordic View to sustainable Rural Development"*, Riga, Latvia, June 16–18, 2015, p. 148–153.
- Malecka, S., Bremanis, G. & Miglane, V. 2005. Effect of increase nitrogen fertilizer rates on yield and grain quality of winter wheat varieties. *Latvian Journal of Agronomy* **8**, 47–52.
- Márton, L. 2008. Long term study of precipitation and fertilization interaction on winter wheat (*Triticum aestivum* L.) yield in the Nyrlugos field trial in Hungary between 1973 and 1990. *Cereal Research Communications* **36**, 511–522. DOI: 10.1556/CRS.36.2008.3.15.
- Mašauskienė, A., Paplauskienė, V. & Cesevičienė, J. 2002. Evaluation of protein composition and interdiversity of indirect bread-making parameters of Lithuania – grown winter wheat cultivars. *Zemdirbyste-Agriculture* **78**(2), 42–48.
- Povilaitis, V. & Lazauskas, S. 2010. Winter wheat productivity in relation to water availability and growing intensity. *Zemdirbyste-Agriculture* **97**(3), 59–68.
- Rozbicki, J., Ceglinska, A., Gozdowski, D., Jakubczak, M., Cacak – Pietrzak, G., Magry, W., ... & Drzazga, T. 2015. Influence of the cultivar, environment and management on the grain yield and bread- making quality in winter wheat. *Journal of Cereal Science* **61**, 126–132.
- Savin, R., Sandras, V.O. & Slafer, G.A. 2006. Do Mediterranean environments set up upper limit in wheat nitrogen use efficiency? *Bibliotheca Fragmenta Agronomica* **11**(I), 339–340.
- Shejbalova, S., Cerny, J., Mitura, K., Lipinska, K.J., Kovarik, J. & Balik, J. 2014. The influence of nitrogen fertilization on quality of winter wheat grain. *Mendel Net* 105–109.
- Šip, V., Škorpik, M., Chrpova, J., Šottnikova, V. & Bartova, S. 2000. Effect of cultivar and cultural practices on grain yield and bread - making quality of winter wheat. *Rostlinna Vyroba* **46**(4), 159–167.
- Skudra, I. & Linina, A. 2011. The influence of meteorological conditions and nitrogen fertilizer on wheat grain yield and quality. In Innovations for food science and production” Foodbalt–2011: *Proceedings of the 6th Baltic Conference on Food Science and Technology*, May 5 – 6 2011, pp. 23–26. Jelgava, Latvia, LLU.

- Skudra, I. & Ruža, A. 2016. Winter wheat grain baking quality depending on environmental conditions and fertilizer. *Agronomy Research* **14** (S2), 1460–1465.
- Svecnjak, Z., Jenel, M., Bujan, M., Vitali, D. & Dragojevic, I.V. 2013. Trace element concentrations in the grain of wheat cultivars as affected by nitrogen fertilization. *Agricultural and Food Science* **22**, 445–451.
- Tarakanovas, P. & Ruzgas, V. 2006. Additive main effect and multiplicative interaction analysis of grain yields of wheat varieties in Lithuania. *Agronomy Research* **4**(1), 91–98.
- Teesalu, T. & Leedu, E. 2001. Effect of weather condition and use of fertilizers on crop and soil mineral nitrogen content in years 1999–2000 during field experiment IOSDV/Tartu. In *Research for Rural development, International Scientific Conference Proceeding*, 23–25 May 2001. (pp. 53–56). Jelgava, Latvia: LLU.
- Zadoks, J.C., Chang, T.T. & Konzak, C.F. 1974. A decimal code for the growth stages of cereals. *Weed Research* Vol. **14**, p. 415–421. Retrieved January 08, 2009. from http://old.ibpdev.net/sites/default/files/zadoks_scale_1974.pdf

Evaluation of dried compost for energy use via co-combustion with wood

J. Malat'ák^{1,*}, J. Bradna¹, J. Velebil¹, A. Gendek² and T. Ivanova³

¹Czech University of Life Sciences Prague, Faculty of Engineering, Department of Technological Equipment of Buildings, Kamýcká 129, CZ165 21 Prague, Czech Republic

²Warsaw University of Life Sciences, Department of Agricultural and Forest Machinery, Faculty of Production Engineering, Nowoursynowska 166, PL02-787 Warsaw, Poland

³Czech University of Life Sciences, Faculty of Tropical AgriSciences, Department of Sustainable Technologies, Kamýcká 129, CZ165 21 Prague, Czech Republic

*Correspondence: malatak@tf.czu.cz

Abstract. There is still a question of utilization of compost of unsatisfactory quality. This article deals with energy utilization of untreated compost. The energy utilization of raw compost as a fuel is not directly possible without further processing. Separation might be necessary due to large amount of mineral content (soils and other inert substances).

This article is focused on the analysis of the basic fuel characteristics of compost. Proximate and elemental analyses were performed and stoichiometric combustion was calculated. Finally, the sample was co-burned with wood biomass in a fixed grate combustion device and the gaseous emissions were determined in dependence on the amount of combustion air supplied. The emissions were expressed in graphs against excess air coefficient and flue gas temperature.

Elemental analysis of the compost sample shows high percentage of ash up to 61.70% wt. on dry basis causing low average calorific value of 8.51 MJ kg⁻¹ on dry basis. For combustion tests, the heating value was increased by addition of wood chips to reach an average calorific value of the mixture to 13.4 MJ kg⁻¹. The determined stoichiometric parameters can help in optimization of diffusion controlled combustion of composts or similar materials. In combustion of the mixture of compost and wood biomass an optimum of emission parameters was found not exceeding the emission limits. Measured emission concentrations show the possibility of optimizing the combustion processes and temperatures while lowering CO emissions via the regulation of combustion air.

Key words: combustion, emissions, elemental analysis, calorimetry.

INTRODUCTION

The current research of the energy resources is directed primarily at the search for and the use of new renewable resources (Tran & Smith, 2017). Traditional fossil resources have limited reserves (Shafiee & Topal, 2009). Therefore, one of the challenges for the energy sector is the expansion of the use of renewable energy sources (Hussain et al., 2017). As traditional renewable source of energy is mainly considered plant biomass (Jevič et al., 2007). The current potential of plant biomass is limited by the utilized agricultural area (Valdez et al., 2017). Therefore, new sources of biomass

are sought, one of possible sources being biodegradable municipal waste (Ball et al., 2017). In the field of waste management, one of the general objectives of law is reducing the amount of biodegradable waste disposal on landfills and increasing energy and material utilization. Within the European Union this necessity started mainly with the European Council directive on the landfill of waste. This has resulted in the conception of new biodegradable waste treatment facilities. In the Czech Republic, it has been mainly the establishment of biogas stations and industrial composting facilities (Kára et al., 2010; Herout et al., 2011).

Composting is one of the ways to recycle biodegradable municipal waste (Özbay, 2016). The primary use of composts is to increase soil fertility mainly by increasing soil humus content (Macias-Corral et al., 2017). In addition to composting solely for production of fertilizer, there are recently developed technologies for energy recovery from compost. Since biomass undergoes partial aerobic decomposition in the process it is possible to utilize the heat that is produced during the composting process (Smith & Aber, 2018). During composting, part of the organic matter i.e. combustible substance is decomposed and along with change in water content this changes the fuel characteristics (Marron, 2015; Vandecasteele et al., 2016). This means a reduction in the total energy content of the material with the detrimental effect of increasing especially the content of ash (Komilis et al., 2014). However, the compost still retains the majority of combustible matter so there is the option of producing energetic composts that are intended for direct combustion, gasification or pyrolysis (Finney et al., 2009). In terms of energy use, compost can be seen as a potential biomass fuel (Macias-Corral et al. 2017). In case that compost does not meet product standards and is not suitable for land use it becomes off-specification compost waste on the European waste list. In that case or in case of energetic composts, composts are still eligible for subsidies for energy production from biomass according to Czech Decree No. 477/2012 Coll. In case of composts with high incombustible content, i.e. water and ash, these would have to be incinerated as waste in an expressly permitted waste incineration plant which have to meet specific maximum emission levels given by the Decree No. 415/2012 Coll.

During combusting of products from energy composts, carbon oxides in the flue gas are the first indicators of the quality of the combustion process (Skanderová et al., 2015; Malat'ák et al., 2016). Another indicator of the combustion process is the excess of air (Johansson et al., 2004). In (Díaz-Ramírez et al., 2014) the effect is confirmed that increasing amount of fuel nitrogen as well as combustion air leads to increasing NO_x emission levels.

In (Skanderová et al., 2015; Malat'ák et al., 2016) analyses of energy compost were made, which were solid fuels made from dried and briquetted compost. These can also be designated as biologically dried biomass (Vassilev et al., 2010). The interest in the production of these biofuels usually comes from municipalities or entrepreneurs who already have built heating plants for biomass combustion or operate devices with grate furnaces for coal. Fuel production by biological drying process is an interesting alternative for composting plants with low sales of compost substrates (Vandecasteele et al., 2016). In theory, compost which does not meet quality standards for any land application could be also utilised as biofuel.

Unfortunately, especially for urban composting plants, composting does not always assure the recycling of biodegradable wastes as fertilizers or substrates. Often, the

compost created does not sell very well or is of very poor quality. This paper deals with the energy utilization of unmodified compost.

A sample of compost was analysed for basic fuel characteristics, such as elemental analysis and stoichiometric calculation. Thereafter, the samples were combusted in a combustion device with grate fireplace and the emissions were measured and plotted depending on the supplied amount of combustion air into the combustion chamber.

MATERIALS AND METHODS

The compost was obtained from the company Kompostárna Jarošovice, s.r.o. (GPS: 49°14'34.545"N, 14°26'49.672"E). This company produces compost by passive heap technology. Compost is made mainly from the following material inputs: straw, cattle manure, hay, leaves, wood chips, sludge from waste water treatment plant, sawdust, spoiled fruits and vegetables. The maturing of this compost takes approximately one year. Wood biomass for co-combustion were spruce chips.

The fuel properties of the examined samples are characterized by proximate analysis, elemental analysis and energy content. As part of proximate analysis water, ash and combustible content were determined.

In analysis of the compost it was firstly air dried and inorganic portion above 3 mm was removed. The sample was gently crushed to disintegrate clumps. Then the sample was divided on 1 mm sieve. The undersize and oversize fraction were then analysed separately. The sieved samples were milled to assure homogeneity in accordance with (Vaculík et al., 2013). All three parts were used to calculate the properties of the original and air-dried compost sample.

Non-combustible components, such as ash and water content, were determined using a thermogravimetric method on the thermogravimetric analyser LECO TGA-701. The temperature program first dried samples at 105 °C to constant weight to measure moisture. Subsequently, the samples were ignited in oxygen at 550 °C to constant weight to determine the ash content.

The elements carbon (C), hydrogen (H), nitrogen (N) and sulphur (S) were determined by combustion method. The analyses were repeated six times and on a elemental analyser LECO CHN628 + S. The detection method is non-dispersive infrared absorption for carbon, hydrogen, and sulphur. Nitrogen is determined by a thermal conductivity cell. Oxygen was calculated as difference from 100% of the sum of ash and analysed elements, all on dry basis.

The gross calorific value of the analysed fuel samples was determined by combustion in an isoperibol calorimeter LECO AC-600 according to ISO 1928:2010. The net calorific value is calculated by using the results of elemental analysis of individual samples (Hnilička et al., 2015).

Stoichiometric combustion calculation was used for approximate determination of combustion characteristics of samples. The results of the stoichiometric analysis also served for presetting the sample characteristics in a flue gas analyser and for determination of the heat output of the combustion device. Stoichiometric calculations are converted to normal conditions (temperature $t = 0$ °C and pressure $p = 101.325$ kPa). The stoichiometric amount of oxygen for complete combustion O_{\min} ($\text{m}^3 \text{kg}^{-1}$) is given by the equation:

$$O_{\min} = \frac{22.39}{12.01} \cdot C + \frac{22.39}{4.032} \cdot H + \frac{22.39}{32.06} \cdot S - \frac{22.39}{31.99} \cdot O \quad (1)$$

where C , H , S , and O are contents of carbon, hydrogen, sulphur and oxygen in the fuel sample (% wt.).

The stoichiometric amount of dry air L ($\text{m}^3 \text{kg}^{-1}$) is determined from the equation:

$$L = O_{\min} \cdot \frac{100}{20.95} \quad (2)$$

The stoichiometric amount of dry flue gas ($\text{m}^3 \text{kg}^{-1}$) is given by:

$$v_{sp,\min}^s = \frac{22.27}{12.01} \cdot C + \frac{21.89}{32.06} \cdot S + \frac{22.40}{28.013} \cdot N + 0.7805 \cdot L \quad (3)$$

The stoichiometric emission concentrations of CO_2 ($\text{m}^3 \text{kg}^{-1}$) is given by:

$$CO_{2,\max} = \frac{\frac{22.27}{12.01} \cdot C}{v_{sp,\min}^s} \cdot 100 \quad (4)$$

The emission measurements are carried out on a hot-air stove CALOR CZ with grate fireplace and manual fuel feed directly into the combustion chamber. The parameters of the combustion device are nominal power 12 kW with efficiency of 80% and standard wood fuel consumption of 3.6 kg h^{-1} . Due to the low net calorific value of the industrial compost sample, this material is combusted in mixture with spruce chips in 1:1 ratio. The corresponding mass flow rate (kg s^{-1}) of our sample mixture is 4.26 kg h^{-1} according to the equation:

$$dm_{pv} / dt = \frac{P_k \cdot 100}{q_n \cdot \eta} \quad (5)$$

where P_k the nominal heat output of the combustion device (W); q_n the net calorific value of the fuel (J kg^{-1} , J m^{-3}) and η the efficiency of the combustion device (%).

During combustion measurement, the primary combustion air income is regulated manually by monitoring of the amount of oxygen in the flue gases using a flue gas analyser MADUR GA-60. This value of excess air coefficient is derived from the equation:

$$n = 1 + \left(\frac{CO_{2,\max}}{CO_2} - 1 \right) \cdot \frac{V_{sp,\min}}{L_{\min}} \quad (6)$$

where $CO_{2,\max}$ – volumetric concentration of carbon dioxide in dry flue gas during stoichiometric combustion (%); CO_2 – volumetric concentration of carbon dioxide in dry flue gases (%); $V_{sp,\min}$ – stoichiometric amount of dry flue gas ($\text{m}^3 \text{kg}^{-1}$); L_{\min} – stoichiometric amount of air for complete combustion ($\text{m}^3 \text{kg}^{-1}$).

The quantities measured by the flue gas analyser Madur GA-60 were ambient temperature, flue gas temperature and concentrations of O_2 , CO , NO , NO_2 . The signal of the sensors is proportional to the volumetric concentrations of the measured component in ppm. Data are sampled in one-minute intervals during which the values are averaged. Before each combustion test, calibration of the instrument is performed. The data points were collected during stable operation of the combustion device. Emission concentrations of dry flue gas were converted from ppm concentrations to

normal conditions and to $\text{mg}\cdot\text{m}^{-3}$ at the reference oxygen content of 13% in the flue gas. The emission measurement results are processed by regression analysis to express dependencies of emissions of carbon monoxide, oxides of nitrogen, flue gas temperature and excess air coefficient. Second order polynomial functions were chosen and fitted using the least squares method. All calculations and graphs were made in the software Microsoft Excel.

RESULTS AND DISCUSSION

The elemental analysis shows a high proportion of non-flammable substances resulting in low calorific value (see in Table 1). Comparable results were obtained in (Komilis et al., 2014). The compost was air dried to moisture content of 4.26% by weight before combusting. The net calorific value of the samples thus dried increased to 7.61 MJ kg^{-1} , which corresponds to the results of Raclavska et al. (2011). The analysis of compost fractions above and below 1 mm are listed in the Table 1.

Table 1. Proximate, elemental and calorimetric analyses (OS – original sample, DM – dry matter)

Sample	Water Content (% wt.)	Ash. (% wt.)	Carbon C (% wt.)	Hydrogen H (% wt.)	Nitrogen N (% wt.)	Sulphur S (% wt.)	Oxygen O (% wt.)	Gross Calorific Value(MJ kg^{-1})	Net Calorific Value(MJ kg^{-1})
	<i>W</i>	<i>A</i>	<i>C</i>	<i>H</i>	<i>N</i>	<i>S</i>	<i>O</i>	Q_g	Q_i
Compost, OS	38.00	40.29	11.45	1.24	1.07	0.24	7.71	5.10	3.93
Compost: air-dried	4.26	59.07	18.28	2.46	1.70	0.39	13.84	8.15	7.61
Compost, DM	-	61.69	19.10	2.57	1.78	0.41	14.45	8.51	7.95
Compost fraction under 1 mm, DM	-	61.88	19.66	2.68	1.90	0.42	13.46	8.09	7.51
Compost fraction above 1 mm, DM	-	50.43	22.64	2.95	1.89	0.47	21.62	12.21	11.69
Wood chips, OS	8.45	0.35	47.53	4.23	0.30	0.03	39.11	18.96	17.83
Wood chips, DM	-	0.38	51.92	4.62	0.33	0.03	42.72	20.70	19.70

In the mixture for combustion test both the air-dried compost and the wood chips represent 50% by weight. Therefore, the composition, calorific value and combustion characteristics are influenced equally by both components. Table 2 shows the basic calculations in stoichiometric combustion of the examined samples. Notably, the large amount of ash in the compost sample results in low theoretical consumption of combustion air and flue gas production. This is significant in comparison with the sample of wood chips. In general, combustion air consumption and the amount of produced flue gas will affect the optimal setting of a combustion device (Watanabe & Torii, 2016). The stoichiometric values were used in Eq. (6) to determine the values of excess air coefficient.

Table 2. Consumptions of air for stoichiometric combustion and corresponding concentrations of CO₂

Sample	Stoichiometric amount of air ⁽³⁾		Stoichiometric amount of dry flue gases ⁽⁴⁾		Concentration of carbon dioxide in dry flue gas after stoichiometric combustion ⁽⁵⁾	
	kg kg ⁻¹	m ³ kg ⁻¹	kg kg ⁻¹	m ³ kg ⁻¹	% wt.	% vol.
Compost: original sample	1.42	1.10	3.51	1.08	11.97	19.70
Compost: air-dried	2.36	1.83	4.48	1.78	14.96	19.05
Compost fraction above 1 mm	2.57	1.98	4.75	1.96	16.59	20.32
Wood chips: original sample	5.24	4.04	7.70	4.03	22.64	21.85
Mixture of compost and wood chips in equal ratios	3.77	2.91	6.06	2.88	19.80	21.03

The average emission values are shown in Table 3. In (Malat'ák et al., 2016) compost derived fuel briquettes were combusted under comparable conditions. Average NO_x emission concentrations were higher compared to present fuel mixture by a factor of 2.2 which is mostly explained by overall higher nitrogen content by a factor 1.75. Emission concentrations of CO of present fuel were higher (879 mg m⁻³ vs. 827 mg m⁻³) and rose more steeply with higher excess air conditions mainly because the mixture was not briquetted. The difference between the dried compost briquettes and the mixture of compost and wood biomass studied herein is mainly in the combustion gas temperatures, which were lower by about 100 °C during combustion of present compost and wood chips mixture due to lower net calorific value.

Table 3. Average values of flue gas temperature and the concentrations of components in dry flue gas in combustion test of compost and wood chips mixture in the flue gas

	Flue gas temp.	O ₂	CO ₂	CO	CO	CO (O _{2r} = 13%)	NO _x	NO _x	NO _x (O _{2r} = 13%)
	°C	% vol.	% vol.	ppm	mg m ⁻³	mg m ⁻³	ppm	mg m ⁻³	mg m ⁻³
Average	306.41	12.88	3.61	842.75	1,053.8	878.74	96.47	198.06	268.92
Standard deviation	10.77	0.73	1.05	812.20	1,015.6	703.46	31.67	65.02	56.41
Max.	325.92	14.78	5.00	2961.0	3,702.6	3,340.0	165.0	338.76	431.00
Min.	284.00	12.19	1.31	77.00	96.28	290.14	31.00	63.65	207.00

The dependence of carbon monoxide and oxides of nitrogen emissions on the excess air coefficient are shown in Fig. 1. With increasing coefficient of excess air, the CO and NO_x emission levels increased in the range of the excess air ratio $n = 2.4 - 3.4$. Similar trends were found in (Skanderová et al., 2015; Malat'ák et al., 2016). The dependences of CO and NO_x emission levels on flue gas temperature are shown in Fig. 2. During combustion tests CO and NO_x emissions decreased with increasing flue gas temperature from 284 °C to approximately 300 °C and increased above 300 °C up to 326 °C which was the highest temperature reached.

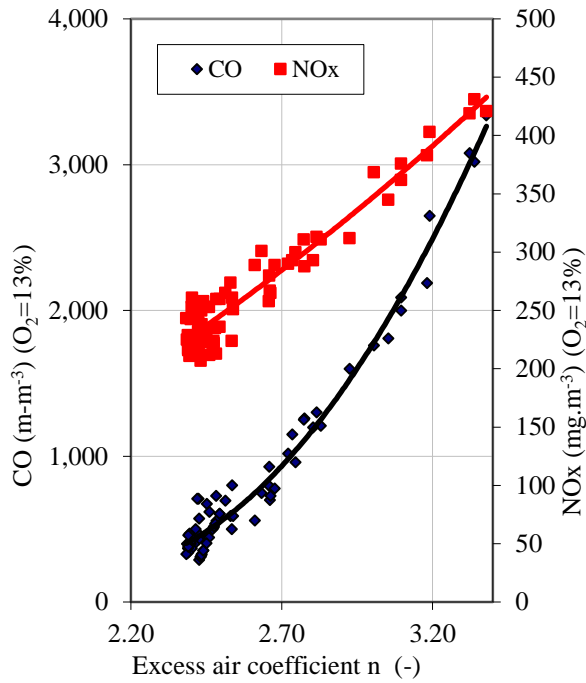


Figure 1. CO and NOx concentrations in flue gas against excess air coefficient.

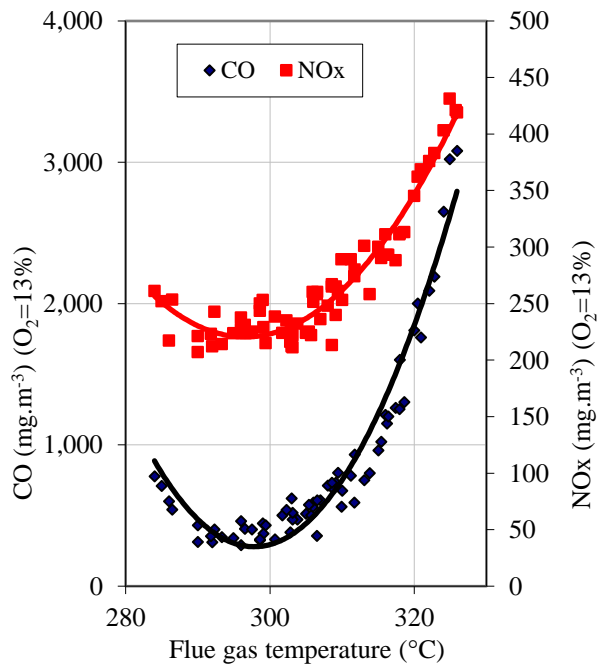


Figure 2. CO and NOx concentrations in flue gas against flue gas temperature.

The regression equations and the coefficient of determination for the emission concentrations are given in Table 4.

Table 4. Regression analysis of nitrogen oxides and carbon monoxide concentrations (mg m^{-3}) depending on excess air coefficient n and flue gas temperature T

	Regression equation	Coefficient of determination
Nitrogen oxides concentration in flue gas (for $n = 2.4 - 3.4$)	$NO_x = 30.612n^2 + 32.457n - 26.31$	$R^2 = 0.926$
Carbon monoxide concentration in flue gas (for $n = 2.4 - 3.4$)	$CO = 1764.6n^2 - 7293.8n + 7761.2$	$R^2 = 0.976$
Nitrogen oxides concentration in flue gas (for $T = 284 - 326$ °C)	$NO_x = 0.2294T^2 - 136.05T + 20394$	$R^2 = 0.923$
Carbon monoxide concentration in flue gas (for $T = 284 - 326$ °C)	$CO = 3.1838T^2 - 1896.3T + 282652$	$R^2 = 0.941$

CONCLUSION

The substrate from the compost cannot be directly combusted without a pre-treatment to lower the incombustible content, i.e. water and incombustible dry matter, which is around 60%. For combustion, the compost and wood chips were mixed in equal ratios. Only then could this mixture be considered as energy compost – biomass intended for direct combustion or for thermochemical conversion (pyrolysis). Direct combustion is technologically suitable for grate or fluid combustion devices, since the net calorific value is achieved by the mixture 13.4 MJ kg^{-1} .

Based on the results, it is possible to use combustion devices for biomass but also for coal where both low emission concentrations and low flue gas temperatures are achieved. The emission concentrations were mainly influenced by the amount of combustion air. Combustion temperature, which is linked, to the flue gas temperature also has a substantial effect on the emissions. The type of fuel mixture studied herein can be recommended for use in medium and large combustion devices. In small combustion devices, this mixture cannot be used in accordance with applicable regulations.

ACKNOWLEDGEMENTS. The article was financially supported by the Internal Grant Agency of the Czech University of Life Sciences Prague, Czech Republic, Grant No. 20183001.

REFERENCES

- Ball, A.S., Shahsavari, E., Aburto-Medina, A., Kadali, K.K., Shaiban, A.A.J. & Stewart, R.J. 2017. Biostabilization of municipal solid waste fractions from an Advanced Waste Treatment plant. *Journal of King Saud University – Science* **29**, pp. 145–150.
- Bradna, J. & Malat'ák, J. 2016. Flue gases thermal emission concentration during waste biomass combustion in small combustion device with manual fuel supply. *Research in Agricultural Engineering* **62**, 1–7.

- Decree No. 477/2012 Coll. on specifying types and parameters of supported renewable sources for production of electricity, heat or biomethane, and on the establishment and storage of documents, Czech Republic (in Czech).
- Decree No. 477/2012 Coll. on the permissible level of pollution and its detection and implementation of some other provisions of the Act on Air Protection, Czech Republic (in Czech).
- Díaz-Ramírez, M., Sebastián, F., Royo, J. & Rezeau, A. 2014. Influencing factors on NOX emission level during grate conversion of three pelletized energy crops. *Applied Energy* **115**, 360–373.
- Finney, K.N., Ryu, C., Sharifi, V.N. & Swithenbank, J. 2009. The reuse of spent mushroom compost and coal tailings for energy recovery: Comparison of thermal treatment technologies. *Bioresource Technology* **100**, 310–315.
- Herout, M., Malat'ák, J., Kučera, L. & Dlabaja, T. 2011. Biogas composition depending on the type of plant biomass used. *Research in Agricultural Engineering* **57**(4), 137–143.
- Hnilička, F., Hniličková, H. & Hejnák, V. 2015. Use of combustion methods for calorimetry in the applied physiology of plants. *Journal of Thermal Analysis and Calorimetry* **120**(1), 411–417.
- Hussain, A., Arif, S.M. & Aslam, M. 2017. Emerging renewable and sustainable energy technologies: State of the art. *Renewable and Sustainable Energy Reviews* **71**, 12–28.
- Jevič, P., Hutla, P., Malat'ák, J. & Šedivá, Z. 2007. Efficiency and gases emissions with incineration of composite and one-component biofuel briquettes in room heater. *Research in Agricultural Engineering* **53**(3), 94–102.
- Johansson, L.S., Leckner, B., Gustavsson, L., Cooper, D., Tullin, C. & Potter, A. 2004. Emission characteristics of modern and old-type residential boilers fired with wood logs and wood pellets. *Atmospheric Environment* **38**(25), 4183–4195.
- Kára, J., Janča, E. & Herák, D. 2010. Exploitation of anaerobic fermentation of bio-degradable wastes. *Research in Agricultural Engineering* **56**(1), 8–17.
- Komilis, D., Kissas, K. & Symeonidis, A. 2014. Effect of organic matter and moisture on the calorific value of solid wastes: An update of the Tanner diagram. *Waste Management* **34**(2), 249–255.
- Macias-Corral, M.A., Samani, Z.A., Hanson, A.T. & Funk, P.A. 2017. Co-digestion of agricultural and municipal waste to produce energy and soil amendment. *Waste Management and Research* **35**(9), 991–996.
- Malat'ák, J., Bradna, J. & Velebil, J. 2016. Combustion of briquettes from oversize fraction of compost from wood waste and other biomass residues. *Agronomy Research* **14**(2), 525–532.
- Marron, N. 2015. Agronomic and environmental effects of land application of residues in short-rotation tree plantations: A literature review. *Biomass and Bioenergy* **81**, 378–400.
- Özbay, I. 2016. Evaluation of municipal solid waste management practices for an industrialized city. *Polish Journal of Environmental Studies* **24**(2), 637–644.
- Raclavska, H., Juchelkova, D., Skrobankova, H., Wiltowski, T. & Campen, A., 2011. Conditions for energy generation as an alternative approach to compost utilization. *Environmental Technology* **32**(4), 407–417.
- Shafiee, S. & Topal, E. 2009. When will fossil fuel reserves be diminished? *Energy Policy* **37**(1), 181–189.
- Skanderová, K., Malat'ák, J. & Bradna, J. 2015. Energy use of compost pellets for small combustion plants. *Agronomy Research* **13**(2), 413–419.

- Smith, M.M. & Aber, J.D. 2018. Energy recovery from commercial-scale composting as a novel waste management strategy. *Applied Energy* **211**, 194–199.
- Tran, T.T.D. & Smith, A.D. 2017. Evaluation of renewable energy technologies and their potential for technical integration and cost-effective use within the U.S. energy sector. *Renewable and Sustainable Energy Reviews* **80**, 1372–1388.
- Vaculík, P., Maloun, J., Chládek, L. & Prikryl, M. 2013. Disintegration process in disc crushers. *Research in Agricultural Engineering* **59**(3), 98–104.
- Valdez, Z.P., Hockaday, W.C., Masiello, C.A., Gallagher, M.E. & Philip Robertson, G. 2017. Soil Carbon and Nitrogen Responses to Nitrogen Fertilizer and Harvesting Rates in Switchgrass Cropping Systems. *Bioenergy Research* **10**(2), 456–464.
- Vandecasteele, B., Boogaerts, C. & Vandaele, E. 2016. Combining woody biomass for combustion with green waste composting: Effect of removal of woody biomass on compost quality. *Waste Management* **58**, 169–180.
- Vassilev, S.V., Baxter, D., Andersen, L.K. & Vassileva, C.G. 2010. An overview of the chemical composition of biomass. *Fuel* **89**(5), 913–933.
- Watanabe, S. & Torii, S. 2016. Experimental study on combustion characteristics of compost using New-type combustor. *International Journal of Energy Research* **40**(6), 739–742.

Investigation of the sugar content in wood hydrolysates with iodometric titration and UPLC-ELSD

K. Meile^{1,2,*}, A. Zhurinsh¹, L. Briede¹ and A. Viksna²

¹Latvian State Institute of Wood Chemistry, Dzerbenes 27, LV-1006 Riga, Latvia

²University of Latvia, Faculty of Chemistry, Department of Analytical Chemistry, Jelgavas 1, LV-1004 Riga, Latvia

*Correspondence: kristine.meile@inbox.lv

Abstract. Autohydrolysis of birch wood is a mild pretreatment process, which gives a notable yield of sugars – monosaccharides and oligosaccharides – in the aqueous hydrolysate, while a solid lignocellulose fraction can be further processed into other valuable products within a biorefinery concept. In this work two analytical methods – iodometric titration and ultra-high performance liquid chromatography with evaporative light scattering detection (UPLC-ELSD) – have been optimized and compared for the determination of the sugar content in series of birch wood hydrolysates. The results of both methods were consistent and showed that the highest yield of sugars, mostly xylose, was obtained by hydrolysis at 180 °C after 75 min.

Key words: sugar analysis, birch wood hydrolysis, pentoses, hexoses, xylose, oligosaccharides.

INTRODUCTION

A biorefinery producing a combination of value-added products is at the core of a bio-based economy, which employs renewables instead of fossil resources (Star-COLIBRI, 2011). The biorefinery concept involves sequential processes for transforming biomass, such as wood. Hydrolysis is often the first stage in a biorefinery concept, during which wood is pretreated yielding a sugar-rich aqueous fraction (hydrolysate) and a solid lignocellulose fraction, which can be further subjected to other processes, such as pyrolysis (de Wild et al., 2011).

Hot water treatment is a pretreatment method which is obtaining popularity by its green and sustainable approach and moderate temperatures, and the hydrolysate mostly contains the destruction products of hemicelluloses. Hemicelluloses are a group of polysaccharides in wood or other plant-based biomass, and the qualitative and quantitative composition (e.g. the ratio of pentosans and hexosans) of hemicelluloses differs depending on the species of the material, but the composition of the hydrolysates is also influenced by the processing conditions – time, temperature, the presence or absence of a catalyst (Borrega & Sixta, 2015; Nitsos et al., 2016; Chen et al., 2017). Autohydrolysis is a comparatively mild process without the addition of a catalyst (Silva-Fernandes et al., 2015). However, acetic acid produced from hemicelluloses themselves acts as a catalyst. The products of autohydrolysis of wood are mostly C₅

monosaccharides and lower oligosaccharides, which can be used for the production of bioethanol (Luque et al., 2014) or 5-hydroxymethylfurfural.

The most popular sugar analysis methods are classical chemical methods, such as titration using Fehling's reagent (Porreta et al., 1992), spectrophotometry (Timmel et al., 1956), or liquid chromatography (Tihomirova et al., 2016). In this work two different methods are used – iodometric titration and ultra-high performance liquid chromatography with evaporative light scattering detection (UPLC-ELSD).

Iodometric titration of sugars is based on the oxidation of α -diols by sodium periodate. Unlike most of other titrimetric sugar determination methods, this method does not determine all reducing agents, but only α -diols, so it is more specific (Meile et al., 2014). While the titrimetric method is suitable for determining all sugars present in the samples as a chemical class, liquid chromatography is used to determine individual compounds. HILIC or ion exchange type liquid chromatography columns are used to analyse sugars (Oliver et al., 2013), but the separation of the many saccharides can still be a challenge, especially the separation of isomers (Wang et al., 2012; Nagy & Pohl, 2015). There are also limitations to the choice of detectors for sugar analysis, because due to the lack of chromophores the most widely used UV spectrophotometric detector is not applicable, but refraction index detectors, which are inexpensive and easy to operate, are not compatible with gradient elution and are also not very sensitive. A more recent alternative for sugar detection is the evaporative light scattering detector (Schuster, 2011).

The purpose of this work is to evaluate the applicability of iodometric titration and UPLC-ELSD analysis methods to determine the sugar content in wood or other industrial biomass hydrolysis products. Therefore, we present an overview of the method optimization, as well as results obtained for a series of birch (*Betula pendula*) wood hydrolysates.

MATERIALS AND METHODS

Materials

All chemicals were of analytical grade – purchased from Sigma Aldrich, and used without further purification.

Birch Wood Hydrolysis

300 g oven dry birch wood with particle size 0.2–0.63 mm was hydrothermally treated in a Parr 4554 high pressure reactor with 7.5 L volume. The treatment media was demineralized water at temperatures 150–200 °C. The ratio of water and wood was 15:1. Two hours after the necessary temperature had been reached, the reaction mixture was rapidly cooled, then it was filtered and washed, obtaining a solid lignocellulose residue 61–75 w% of the dry feedstock. The liquid samples for analysis were taken when temperature was reached (~90 min after heating started) after 0, 15, 30, 45, 60, 75, 90, 120 min.

Iodometric Titration

Kinetic curves for sugar oxidation with sodium periodate were obtained as follows. Aqueous solutions of hexoses (D-(+)-glucose, D-(+)-galactose and D-(+)-mannose) and pentoses (L-(+)-arabinose and D-(+)-xylose) were prepared with 4 mg mL⁻¹

concentration. A birch wood hydrolysate was diluted from 8 to 50 mL with deionized water. 0.1 mL 15% H₂SO₄ and 1 mL 0.2 M NaIO₄ was added to a series of 2 mL of each of the solutions and they were placed in a thermostat at 40 °C. After certain time (5, 60, 120, 180, 240 and 300 min) 10% ammonium molybdate was added to the oxidated solutions. After 15 min 1 mL acetic acid and 1 mL 10% KI was added and after another 15 min the solutions were titrated with 0.1 M sodium thiosulfate with starch as an indicator. Sample analysis was done by the same method with oxidation at 40 °C for 240 min. All analysis were performed in triplicate.

UPLC-ELSD

The UPLC experiments were performed on Waters ACQUITY UPLC equipment with a Waters ACQUITY UPLC BEH Amide column (1.7 µm, 2.1×100 mm) and a Waters ACQUITY UPLC ELS detector. The optimal ELS detector drift tube temperature was 50 °C, the nebulizing gas was nitrogen with 45 psi pressure, gain was set for 50. The gradient program was set for phase A – 80:20 acetonitrile/water with 0.1% ammonium hydroxide; phase B – 30:70 acetonitrile/water with 0.1% ammonium hydroxide. The results were acquired, integrated and processed using Waters Empower 3 software.

For the optimisation of separation conditions standard solutions of different sugars – 1,6-anhydro-β-D-glucose, D-(+)-xylose, L-(+)-arabinose, D-(+)-mannose, D-(+)-glucose, D-(+)-galactose, D-(+)-sucrose, D-(+)-cellobiose and D-(+)-raffinose were prepared in 50:50 acetonitrile/water. For quantitative analysis standard solutions of xylose were prepared with 0.02-0.24 µg mL⁻¹ concentrations. A linear (R² = 0.998) calibration curve was used with equation $y = (4.35 \times 10^6)x - 1 \times 10^6$. Hydrolysate samples were diluted from 10 to 25 mL with 50:50 water/acetonitrile. Solutions were filtered with KX Syringe filters (pore size 0.22 µm). The injection volume was 1 µL. All analysis were performed in triplicate.

Determination of by-products

Furfural and 5-HMF were determined by UPLC-PDA, using the same equipment as described before with a Waters ACQUITY UPLC BEH C18 column (1.7 µm, 2.1×50 mm). The gradient program was set for phase A – water with 0.1% formic acid; phase B – acetonitrile. For detection a Waters ACQUITY UPLC PDA detector was used with wave length 275 nm.

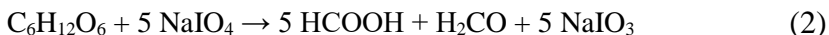
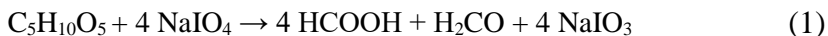
Acetic acid was determined by potentiometric titration with 0.1 M KOH (standardised with potassium hydrogen phthalate), using Radiometer Analytical SAS titrator TitraLab980.

RESULTS AND DISCUSSION

Iodometric Titration

Oxidation curves (Fig. 1) of solutions of several wood based sugars showed that the reaction rate was faster for pentoses than hexoses, however, all monosaccharides were completely oxidized at 120 min. Therefore, oxidation of samples for a time period at least 120 min would give accurate results for pentosan or hexosan hydrolysis products. There are differences in the formulas used for calculating the amount of pentoses and hexoses, because the periodate oxidation equations are different. Eqs 1 and 2 show that 1 mol pentoses reacts with 4 mol NaIO₄, but 1 mol hexoses – with 5 mol NaIO₄. On the

other hand, this stoichiometric difference is not significant, because taking into account the ratio of the stoichiometric coefficients and molecular masses, the final coefficients in the calculations are almost the same: 180 by 5 giving 36.0 for hexoses, and 150 by 4 giving 37.5 for pentoses. So, even if the sample contained a mixture of hexoses and pentoses, the accuracy of the results would still fall within 5%.



The oxidation curve of the birch wood hydrolysate sample was significantly different, as the reaction did not stop after 120 min. There are two likely reasons for the continuous increase of the reduced sodium periodate. Firstly, oligosaccharides are known to take longer to oxidize completely (Meile et al., 2014), so the presence of di-, tri- and higher saccharides or other sugar derivatives could be responsible for the rising oxidation curve after 120 min. Secondly, phenols produced from lignin or extractives could react with periodate unstoichiometrically (Pennington & Ritter, 1947; Antolovich et al., 2004; Gosselink et al., 2011) and increase the amount of the reduced periodate.

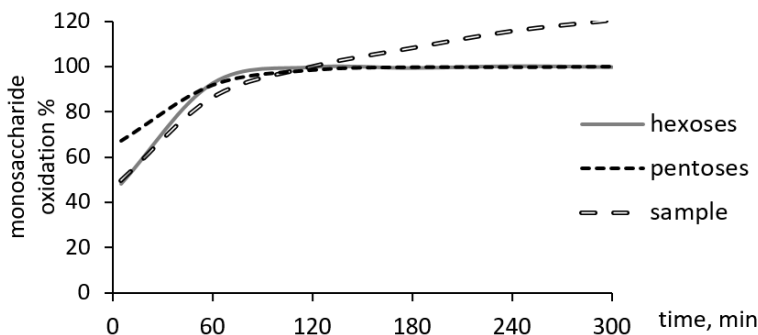


Figure 1. Oxidation curves of hexoses (mixture of glucose, galactose and mannose), pentoses (mixture of arabinose and xylose) and a sample of birch wood hydrolysate.

Even though the oxidation curves showed, that some extra periodate was reduced by the hydrolysis products, the iodometric titration method could be applied to characterize the content of sugars in hydrolysates, if a certain time of oxidation was maintained. The results might have a tendency to be increased by up to 20%, but this method could be a simple way of process monitoring by comparing the relative content of sugars in large series of wood hydrolysis product samples. It must also be noted that many samples can be prepared and oxidized simultaneously, thus decreasing the analysis time per sample. For example, if a series of 10 samples is analysed in triplicate, the oxidation time per sample is only 4 min (120 min by 30 titrations).

UPLC-ELSD

For the tested biomass related sugars the elution order from the amide-functionalized column was according to the molecular size and number of hydroxyl groups, as follows: levoglucosan, xylose, arabinose, mannose, glucose,

galactose, sucrose, cellobiose, raffinose. Fig. 2 shows the effect the column temperature had on the retention time and peak width. As described in literature (McCabe & Hudalla, 2010), because of mutarotation monosaccharides had broad and even split peaks at moderate column temperatures. This proved to be also true for the disaccharide cellobiose, which contained a reducing sugar moiety, unlike the nonreducing disaccharide sucrose and trisaccharide raffinose. Levoglucosan with its anhydrogroup between C1 and C6 also had a narrow peak regardless of the column temperature. With increasing the column temperature from 30 to 70 °C, the peak width for nonreducing sugars decreased by < 10% due to mass transfer processes, but the peak width of the reducing sugars decreased by up to 50%.

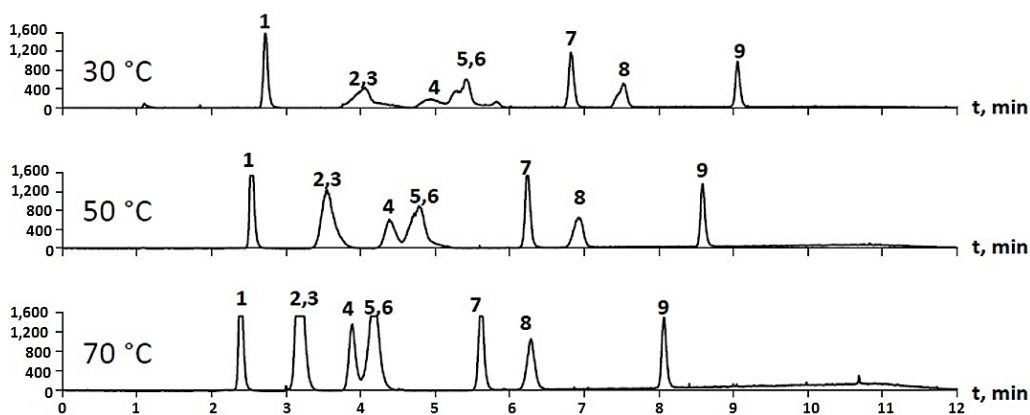


Figure 2. UPLC-ELSD chromatograms of several biomass related sugars with column temperature 30, 50 and 70 °C: 1 – levoglucosan; 2 – xylose; 3 – arabinose; 4 – mannose; 5 – glucose; 6 – galactose; 7 – sucrose; 8 – cellobiose; 9 – raffinose.

Despite our experiments with the composition of the mobile phase (varying proportions of water and acetonitrile with the addition of ammonium hydroxide or triethylamine), the peak pairs of xylose/arabinose and glucose/galactose remained overlapping, making it impossible to determine xylose in the presence of arabinose, just like glucose in the presence of galactose and vice versa. For the purpose of enzymatic processing of the sugars separation of C₅ and C₆ sugars as groups is sufficient, because many microorganisms that process the sugars into alcohol are pentose or hexose specific, instead of being specific for individual sugars (Azhar et al., 2017). However, there are some liquid chromatography columns which can separate xylose and arabinose, for example by ion chromatography (Zhang et al., 2017) or ligand exchange chromatography (Tiihonen et al., 2002). Neither of these methods are supported by UPLC columns, but the biggest disadvantage is that mobile phases containing sodium hydroxide (for ion chromatography), sulphuric acid or non-volatile salts (for ligand exchange chromatography) are not compatible with ELS detection or mass spectrometry. Since ELSD is a semi-universal detector, giving similar signals for analytes with similar volatilities, xylose and arabinose can be determined together as pentoses using the calibration curve of xylose, because in birch wood hydrolysates xylose is typically more abundant than other monosaccharides (Goldmann et al., 2017).

Analysis of Birch Wood Hydrolysates

Both sugar determination methods – titration and UPLC-ELSD – were applied to analyse series of birch wood hydrolysates. Fig. 3 shows a chromatogram of a sample of the hydrolysis products with complete separation of pentoses at 3.1 min and hexoses at 4.0 min. The precision for the methods was described as the relative standard deviation of the parallel measurements, which was $< 4\%$ and $< 2\%$ in all cases for titration and UPLC-ELSD, respectively. Results of recovery in spiked samples were $91 \pm 2\%$ and $92 \pm 1\%$, respectively.

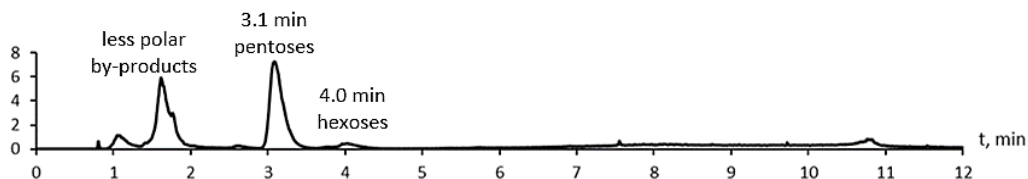


Figure 3. UPLC-ELSD chromatogram of birch wood hydrolysis products: pentoses eluted at 3.1 min, hexoses eluted at 4.0 min and less polar by-products co-eluted from 1 to 2 min.

Hydrolysis of birch wood was performed at six temperatures from 150° to 200° $^{\circ}\text{C}$ for up to 120 min. Fig. 4 illustrates the sugar content in the recovered hydrolysis liquids, depending on the treatment temperature and time. The results obtained by iodometric titration (total sugars) and UPLC-ELSD (pentoses, mostly xylose) were compared, showing a good agreement between the trends determined by the two methods. Both methods confirmed that the yield of sugars grew with the increase of the process temperature up to 180° $^{\circ}\text{C}$. The highest yield of sugars was obtained at 180° $^{\circ}\text{C}$ after 75 min. Similar hydrolysis conditions have been proposed for optimal wheat straw pretreatment (Sidiras et al., 2011). After 75 min as well as with higher temperatures the yield of sugars significantly decreased.

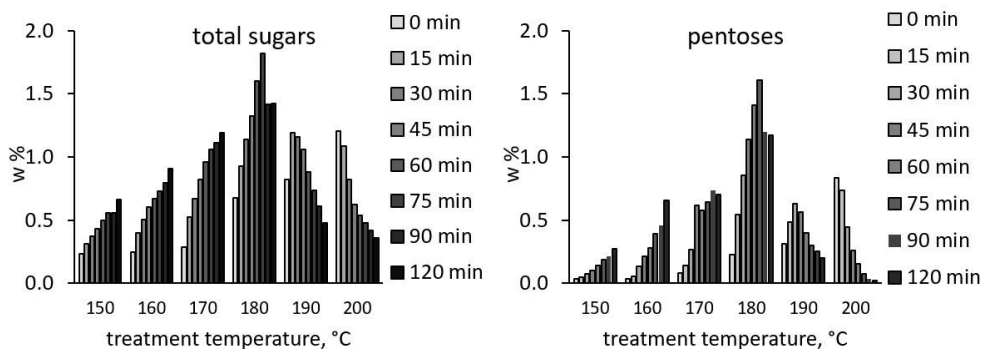


Figure 4. Sugar content in birch wood hydrolysates depending on the hydrolysis temperature: a comparison of the iodimetric titration (total sugars) and UPLC-ELSD (pentoses) results.

Fig. 5 shows the results of sugar analysis in the hydrolysates obtained at 180° $^{\circ}\text{C}$. As mentioned before, the highest yield of sugars was obtained after 75 min, namely, the sugar concentration in the hydrolysate was 1.8%, which corresponds to 27% yield from the feedstock. UPLC-ELSD showed that the yield of hexoses was considerably lower

than that of pentoses, but the sum of the UPLC-ELSD sugar results (pentoses + hexoses in Fig. 5) were mostly in line with the titration results of total sugars, except for the hydrolysates which were treated for 30 min or less. This divergence of the two methods can be explained by the presence of oligosaccharides in the hydrolysates at the beginning of the treatment. Since the titration results included oligosaccharides, the total sugar concentration was about two times higher than the monosaccharide results obtained by UPLC-ELSD. After 30 min treatment the oligosaccharides were broken down to monomers, so the results obtained by both methods corresponded. The total sugars determined by iodometry had an increased result at 120 min, most likely because of a higher concentration of some lignin origin phenols, which could also react with sodium periodate.

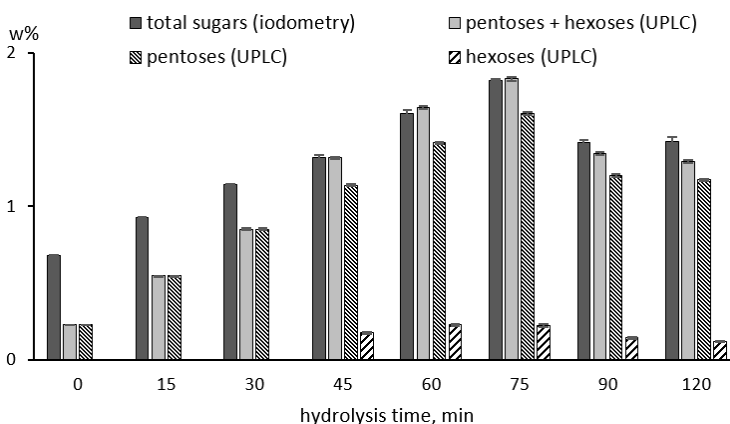


Figure 5. Sugar content in birch wood hydrolysates depending on treatment time at 180 °C, determined by titration as total sugars or UPLC-ELSD as pentoses and hexoses separately.

For a deeper understanding of the hydrolysis process acetic acid and aldehydes – furfural and 5-hydroxymethylfurfural (5-HMF) were determined. The concentration of acetic acid in the hydrolysates increased almost lineary up to 6% with treatment time, acting as a catalyst and increasing the yield of the other products. The concentration of furfural and 5-HMF, which are known as the dehydration products of pentoses and hexoses (Rasmussen, 2014), increased up to 0.2% and 0.03% in the hydrolysates, respectively. The formation of the aldehydes was responsible for the decrease of the sugar content after 75 min treatment time.

CONCLUSIONS

Consistent quantitative results of sugar determination in birch wood hydrolysates were obtained by two methods – iodometric titration and UPLC-ELSD, showing that the highest yield of sugars (27% of oven dry feedstock) was obtained by hydrolysis at 180 °C for 75 min. Both analytical methods showed acceptable precision with relative standard deviation < 5% and xylose recovery from a spiked sample about 90%, and could be used to monitor the yield of sugars in the wood pretreatment process. The advantages of UPLC-ELSD are the speed of analysis and superior selectivity, which allows not only to quantify pentoses and hexoses separately, but also to avoid possible interferences of

other non-sugar components in the samples. However, the iodometric method is a simple, inexpensive method for determining the total content of sugars, including oligosaccharides. Besides, more than ten samples can be oxidised for iodometry simultaneously to decrease the necessary time of analysis per sample.

ACKNOWLEDGEMENTS. The work was supported by the National Research Programme ‘Forest and earth entrails resources research and sustainable utilization – new products and technologies’ (ResProd) Project Nr.3 ‘Biomaterials and products from forest resources with versatile applicability’.

REFERENCES

- Antolovich, M., Bedgood, Jr., D.R., Bishop, A.G., Jardine, D., Prenzler, P.D. & Robards, K. 2004. LC-MS investigation of oxidation products of phenolic antioxidants. *Journal of Agricultural and Food Chemistry* **52**(4), 962–971.
- Azhar, S.H.M., Abdulla, R., Jambo, S.A., Marbawi, H., Gansau, J.A., Faik, A.A.M. & Rodrigues, K.F. 2017. Yeasts in sustainable bioethanol production: A review. *Biochemistry and Biophysics Reports* **10**, 52–61.
- Borrega, M. & Sixta, H. 2015. Water Prehydrolysis of Birch Wood Chips and Meal in Batch and Flow-through Systems: A Comparative Evaluation. *Industrial and Engineering Chemistry Research* **54**(23), 6075–6084.
- Chen, B.Y., Zhao, B.C., Li, M.F., Liu, Q.Y. & Sun, R.C. 2017. Fractionation of rapeseed straw by hydrothermal/dilute acid pretreatment combined with alkali post-treatment for improving its enzymatic hydrolysis. *Bioresource Technology* **225**, 127–133.
- De Wild, P., Reith, H. & Heeres, E. 2011. Biomass pyrolysis for chemicals. *Biofuels* **2**(2), 185–208.
- Goldmann, W.M., Ahola, J., Mikola, M. & Tanskanen, J. 2017. Formic acid aided hot water extraction of hemicellulose from European silver birch (*Betula pendula*) sawdust. *Bioresource Technology* **232**, 176–182.
- Gosselink, R.J.A., Van Dam, J.E.G., De Jong, E., Gellerstedt, G., Scott, E.L. & Sanders, J.P.M. 2011. Effect of periodate on lignin for wood adhesive application. *Holzforschung* **65**(2), 155–162.
- Luque, L., Westerhof, R., Van Rossum, G., Oudenhoven, S., Kersten, S., Berruti, F. & Rehm, L. 2014. Pyrolysis based bio-refinery for the production of bioethanol from demineralized ligno-cellulosic biomass. *Bioresource Technology* **161**, 20–28.
- McCabe, D. & Hudalla, C. 2010. Overcoming Challenges in Carbohydrate Separations. *Separation Science* **2**, 2–7.
- Meile, K., Zhurinsk, A. & Spince, B. 2014. Aspects of periodate oxidation of carbohydrates for the analysis of pyrolysis liquids. *Journal of Carbohydrate Chemistry* **33**(3), 105–116.
- Nagy, G. & Pohl, N.L.B. 2015. Complete Hexose isomer identification with mass spectrometry. *Journal of the American Society for Mass Spectrometry* **26**(4), 677–685.
- Nitsos, C.K., Choli-Papadopoulou, T., Matis, K.A. & Triantafyllidis, K.S. 2016. Optimization of hydrothermal pretreatment of hardwood and softwood lignocellulosic residues for selective hemicellulose recovery and improved cellulose enzymatic hydrolysis. *ACS Sustainable Chemistry and Engineering* **4**(9), 4529–4544.
- Oliver, J.D., Gaborieau, M., Hilder, E.F. & Castignolles, P. 2013. Simple and robust determination of monosaccharides in plant fibers in complex mixtures by capillary electrophoresis and high performance liquid chromatography. *Journal of Chromatography A* **1291**, 179–186.

- Pennington, D.E. & Ritter, D.M. 1947. Periodate oxidation of phenols. *Journal of American Chemical Society* **69**(1), 187–188.
- Porretta, S., Sandei, L., Crucitti, P.M., Poli, G. & Attolini, M.G. 1992. Comparison of the main analytical methods used in quality control of tomato paste. *International Journal of Food Science & Technology* **27**(2), 145–152.
- Rasmussen, H., Sørensen, H.R. & Meyer, A.S. 2014. Formation of degradation compounds from lignocellulosic biomass in the biorefinery: sugar reaction mechanisms. *Carbohydrate Research* **385**, 45–57.
- Schuster-Wolff-Bühling, R., Michel, R. & Hinrichs, J. 2011. A new liquid chromatography method for the simultaneous and sensitive quantification of lactose and lactulose in milk. *Dairy Science and Technology* **91**(1), 27–37.
- Sidiras, D., Batzias, F., Ranjan, R. & Tsapatsis, M. 2011. Simulation and optimization of batch autohydrolysis of wheat straw to monosaccharides and oligosaccharides. *Bioresource Technology* **102**(22), 10486–10492.
- Silva-Fernandes, T., Duarte, L.C., Carvalheiro, F., Loureiro-Dias, M.C., Fonseca, C. & Girio, F. 2015. Hydrothermal pretreatment of several lignocellulosic mixtures containing wheat straw and two hardwood residues available in Southern Europe. *Bioresource Technology* **183**, 213–220.
- Star-COLIBRI, Joint European Biorefinery Vision for 2030. 2011.
- Tihomirova, K., Dalecka, B. & Mezule, L. 2016. Application of conventional HPLC RI technique for sugar analysis in hydrolysed hay. *Agronomy Research* **14**(5), 1713–1719.
- Tiihonen, J., Markkanen, I. & Paatero, E. 2002. Complex stability of sugars and sugar alcohols with Na⁺, Ca²⁺, and La³⁺ in chromatographic separations using poly(styrene-co-divinylbenzene) resins and aqueous organic eluents. *Chemical Engineering Communications* **189**(7), 995–1008
- Timell, T.E., Glaudemans, C.P.J. & Currie, A.L. 1956. Spectrophotometric Methods for Determination of Sugars. *Analytical Chemistry* **28**(12), 1916–1920.
- Wang, Y.H., Avula, B., Fu, X., Wang, M. & Khan, I.A. 2012. Simultaneous determination of the absolute configuration of twelve monosaccharide enantiomers from natural products in a single injection by a UPLC-UV/MS method. *Planta Medica* **78**(8), 834–837.
- Zhang, Y., Wu, J., Ni, Q. & Dong, H. 2017. Multicomponent quantification of Astragalus residue fermentation liquor using ion chromatography-integrated pulsed amperometric detection. *Experimental and Therapeutic Medicine* **14**(2), 1526–1530.

Effect of different compositions on anaerobic co-digestion of cattle manure and agro-industrial by-products

K. Meiramkulova¹, A. Bayanov¹, T. Ivanova^{2,*}, B. Havrland², J. Kára³ and I. Hanzlíková³

¹L.N. Gumilyov Eurasian National University, Department of Management and Engineering in the Field of Environmental Protection, Satpayev street, KZ010008 Astana, Kazakhstan

²Czech University of Life Sciences, Faculty of Tropical AgriSciences, Department of Sustainable Technologies, Kamýcká 129, CZ16500 Prague, Czech Republic

³Research Institute of Agricultural Engineering, Drnovská 507, CZ16101 Prague, Czech Republic

*Correspondence: ivanova@ftz.czu.cz

Abstract. The present research is dedicated to the study of anaerobic co-digestion process of different biomass materials. Anaerobic co-digestion of digested sludge, grass silage, haylage and cattle manure was evaluated in mesophilic tank reactors in the lab-scale experiment. Twelve laboratory scale tank reactors (1.5 L) were used during the incubation period of 45 days. First triplet of reactors was fed with pure digested sludge and the other three with different mixtures having the volumetric ratios of 30/35/25/10, 40/30/20/10 and 50/25/15/10 for digested sludge/corn silage/grass haylage/cattle manure. Methane production was analyzed for all lab-scale reactors individually. The resulting specific methane production of above-mentioned batches was 336.34, 238.1 and 233.23 L_{STP}[CH₄] kg⁻¹[TVS], respectively. Other results such as cumulative biogas and methane yield, volumetric biogas and methane yield, volumetric biogas and methane yield per day were also assessed. These results had the highest meaning when complex substrate had no more than 30% of inoculum.

Key words: batch reactor experiments, cattle manure, co-digestion, crop residues, volumetric ratios.

INTRODUCTION

The need for energy to meet the social and economic needs of mankind is increasing. All societies need energy to meet basic human needs such a cooking, lighting, space comfort, mobility, communication, etc. (IPCC, 2012). Global energy demand raised ~2.7-fold from 5,000 Mtoe (million tonnes of oil equivalent) in 1971 to 13,276.3 Mtoe in 2016 (BP, 2017). At the present time, fossil fuels satisfy 80% of global energy consumption. Even if the current policy commitments adopted by countries on climate change and other energy-related issues are implemented, global energy demand is projected to grow by 40% in 2035, and the share of fossil fuels will still be 75%. (IEA, 2013). World proven coal reserves will be enough just over the next 153 years for use,

and oil and gas over ~52.5 (BP, 2017). These terms do not look promising indeed, and, thus, the need for alternative energy sources development becomes topical for mankind.

Recently, the use of RES (renewable energy sources), non-fossil energy resources in particular, has become an essential component of sustainable global energy strategy (Song et al., 2014). Renewable energy accounted for 19.3% of the global final energy consumption, and growth continued in 2016. In 2016 the renewable energy sector employed 9,8 million people. Renewable power generating sector showed its biggest growth in 2016, with an estimated 161 GW (gigawatts) of capacity added. ~ 9% of global total heat demand is supplied by renewable energy sector. In 2016, liquid biofuels provided around 4% of world road transport fuels. The use of biogas for the needs of the transport sector has increased significantly in the USA and continued to share in the fuel mix in European Union (REN21, 2017).

In 2015, world TPES (Total Primary Energy Supply) was 13,647 Mtoe, of which 13.4%, or 1,823 Mtoe (up from 1,784 Mtoe in 2014), was from RES. The share of solid biomass/fuelwood/charcoal is a biggest among RES, it provides 63.7% of global renewables supply. The hydro power is the second one, which represents 18.3% of renewable energy supply or 2.5% of world TPES. Biogases, liquid biofuels, solar, wind, geothermal, and tide constitute the rest of the renewables energy supply. Since 1990, RES have grown at an average annual rate of 2%, which is slightly higher than the growth rate of world TPES, 1.8%. Biogases had the third highest growth rate at 12.8%, followed by solar thermal (11.4%) and liquid biofuels (10.1%) (IEA, 2017).

Biomass energy is an encouraging resource for meeting upcoming needs for energy consumption. Sustainable bioenergy represents a huge potential for making a significant contribution to rural and economic development, enhancing energy security and reducing environmental impact. From biomass, modern energy carriers can be obtained that are clean, easy to use and have little or no connection with GHG (greenhouse gas) emissions. At present, various biomass conversion technologies are available or under development (Turkenburg et al., 2012). Carbonization, pyrolysis, gasification and AD (anaerobic digestion) are the main technologies by means of which biomass can be converted to useful renewable energy carriers such as biodiesel, ethanol, butanols, biomethane, hydrogen, DME (dimethyl ether) and other fuels and fuels additives. (Li et al., 2016). Pathways of biomass conversion as a transesterification or hydrogenation, fermentation or microbial processing, bio-photochemical and other biological and chemical routes also exist or under development (REN21, 2015). Among above-mentioned pathways AD (anaerobic digestion) technology is quite promising option, resulting in a useful energy carrier – methane. In short, AD is a microbial and biochemical process that results in the formation of a mixture of gases – biogas, mainly consisting of CH₄ and CO₂. AD process consists of four steps; hydrolysis, acidogenesis, acetogenesis and methanogenesis (Hassan et al., 2017a). AD is divided into three categories of wet ($\leq 10\%$), semi-dry (10–20%) and dry ($\geq 20\%$) in accordance with feedstock total solid (TS) content. Dry AD is more favorable than wet AD, due to the smaller volume of the reactor and lower energy requirements for heating (Elsamadony & Tawfik, 2015). Feedstock for biogas production vary depending on the country. In Europe, biogas is produced from manure, agricultural waste and energy crops (accounting for 5.1 GW of power production capacity), landfill gas (1.4 GW), and smaller amounts of sewage sludge and other sources. In the Czech Republic growth of biogas manufacturers was particularly strong (+15%) in 2015 (REN21, 2015).

Animal manure as a substrate for AD is an easily available resource worldwide. However, sometimes the capital costs for industrial biogas plants are not justified because of low biogas yield from manure as a single substrate (Cavinato et al., 2010). Usually, manure has a low total solids (TS) concentration: approximately 7–9 % for cattle manure and 5–7 % TS for pig manure. Lignocellulose high content fraction contained in manure represents an extremely resistant to degradation fraction – fiber. A high fraction of fibers with high water content result in poor methane production of animal manure and it usually ranges from 10 to 20 m³ CH₄ t⁻¹ [fresh weight]. Animal manure is considered to be the one of the most convenient substrate for initiating the fermentation reaction because it includes all the necessary microorganisms (Cavinato et al., 2010).

Co-fermentation of various substrates showed a better effect than mono-fermentation. Typically, each organic substrate rich in nutrients is required for anaerobic and aerobic bacteria growth. Nevertheless, the nutrient level differences are correlated with material age, species and growth conditions (Divya et al., 2015).

Co-digestion offers benefits such as: dilution of toxic compounds, increased biogas yield odor and pathogen reduction, enhanced nutrients balance, synergistic effect of microorganisms and increased weight of biodegradable organic substance (Sosnowski et al., 2008). Progressive studies of the C/N ratio (carbon to nitrogen ratio) optimization cases during co-fermentation conducted by Hassan et al. (2016), where co-digestion had enhanced the methane production from 31.49% to 85.11%. Rahman et al. (2017) showed that the best quality and a greater quantity of biogas can be produced as a result of the optimal selection of the C/N ratio of the complex substrate. Organic agricultural wastes have a large content of carbon and animal manure has a high content of nitrogen. Proper co-digestion of these two components increases biogas yield and improves the methane content (Bagudo et al., 2011; Rahman et al., 2017).

AcoD of different substrates with animal manure can increase the biogas production from 25 to 400% (Shah et al., 2015) and also offers benefits for the management of animal manure and organic wastes (Li et al., 2013). The concept of AcoD of different substrates is not a new idea since it has been investigated for a number of combinations of organic waste. At present, many studies were reported about AcoD of animal manure and agriculture biomass that it is considered as the most substantial topic within research of AD. Hassan et al. (2017b) conducted AcoD by using goose manure with alkali solubilized wheat straw in order to optimize C/N ratio and organic loading rate regression. A significant enhancement of biogas yield was achieved by Wu et al. (2010) during co-digesting of swine manure with an external source of carbon – crop residues (corn stalks, oat and wheat straw). Another studies were carried out on AcoD of nitrogen rich substrate – chicken manure and corn stover (Li et al., 2014a) and organic fraction of municipal solid waste (Matheri et al., 2017). All the above-mentioned researches stated significant biogas production improvement as a result of AcoD. CM (cattle manure) is the most widespread substrate for AD which has been assessed over the last 3–4 decades and is described as an excellent ‘carrier’ substrate that used by industrial biogas plants as a base substrate for AcoD (Andriamanohiarisoamanana et al., 2016). Recent researchers reported significant biogas production enhancement when CM was digested with another co-substrate such a domestic food waste (Zhang et al., 2012), cheese whey (Comino et al., 2012), maize (Amon et al., 2007) and crop residues (Li et al., 2014b). But, despite the fact that AcoD has several advantages, this technology is

still a challenging biomass treatment process, and even two-stage reactor technologies cannot solve the optimization and stability problems (Hagos et al., 2017). The methodology of this study – BMP (biomethane potential) test is the same to above-mentioned studies and novelty lies in the screening of different composition of complex substrate and types of co-substrates.

There is a close link between the biogas development intensification and agriculture industrialization and modernization (Mao et al., 2015). In order to make AD technologies more attractive and profitable for agricultural sector, co-digestion of manure with come-at-able agricultural byproducts can increase methane yield. The objective of this study was to evaluate the methane production during batch-experiments of screening trials with the determination of the best complex substrate of compositions 30/35/25/10, 40/30/20/10 and 50/25/15/10 for digested sludge/corn silage/grass haylage/cattle manure, accordingly.

MATERIALS AND METHODS

Feedstock sources

Three types of substrates were used in this study: corn silage (CS), grass haylage (GH), and cattle manure. CS and GH were the raw materials obtained from the crop rotation of the given farm situated in Mořina city, Czech Republic.

The digested sludge (DS) as an active inoculum used for starting up the fermentation was brought from large-scale BPP (biogas power plant) situated in Mořina city (Czech Republic), which operates at mesophilic mode and has 526 kW installed electric power. This BPS treats primarily cattle manure with some agricultural byproducts. The BPS operates at 41 °C. The effluent was transported in 20-liter plastic vessels. The temperature was always kept above the freezing point. In order to readapt the inoculum to 41 °C, ensure removing dissolved CH₄, the inoculum was stored under anaerobic condition for 5 days in the incubator at the 41 °C.

Experimental batch-up

Wet anaerobic co-digestion investigation under mesophilic conditions for biogas production and biochemical methane potential (BMP) from CS, GH, CM and DS were carried out. The research was batchtled up using 12 single-stage lab-scale reactors (1,500 mL plastic vessels). The reactors were positioned into the reservoir with water thermostat (Fig. 1).

Subsequently, numerous volumetric ratios (batches) of substrates (DS/CS/GH/CM) were dosed into the reactors and closed tightly. Each batch had three replications. All the reactors were run at the same time under the temperature of 41 °C. The batches were blown out with nitrogen to remove air, which contains oxygen. The pH inside the digesters was not controlled during the experiment. The amount of evolved biogas was measured every day during the incubation period 45 days. The biogas was collected by the downward displacement method which is based on the water displacement principle (Fig. 2). Gradated transparent glass jar of 3 L were placed into distilled water basin. The bubbles of biogas produced pass through the water layer and push the water level down in the vessel (Wang et al., 2014).

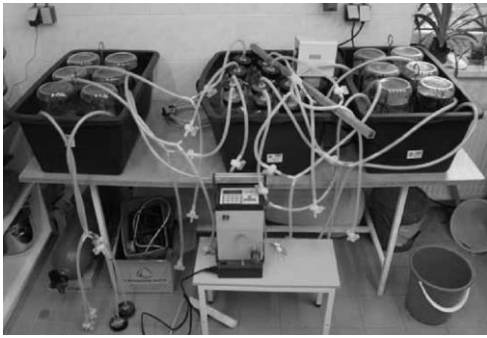


Figure 1. Lab-scale reactors for biogas production inside reservoir with accurate water thermostat.

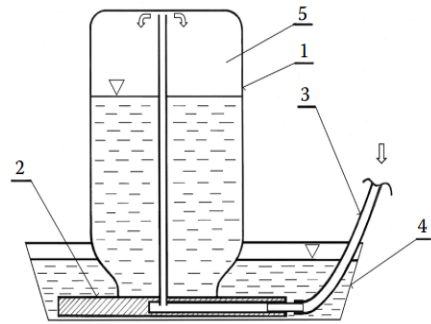


Figure 2. Equipment for measuring biogas volume based on water-column measuring system: 1 – glass jar; 2 – basic plate; 3 – biogas input; 4 – water basin; 5 – biogas produced.

Morina biogas plant at that time had problems with the production of biogas (high pH level about 8 and high concentration of ammonia nitrogen more than 7 g L^{-1}). In order to stabilize the anaerobic digestion process in a lab-scale experiment different mixtures of DS, CS, GH and CM were used. Mixtures of DS, CS, GH and CM were poured into the reactors on a wet weight basis for attainment suitable total solid (TS) content of 8 & for each mixture except of single substrate blank (see Table 1). Three reactors were fed only with an (effluent) inoculum, i.e. used as blank. The biogas yield from the blanks was subtracted from other batches when calculated.

Table 1. Batch assay parameters

Trial	Incubation period, days	Batch digester volume, mL	Blend weight, g	Initial blend TS content, %	DS, %	CS, %	GH %	CM, %
1	45	1,500	1,000	8.0	30	35	25	10
	45	1,500	1,000	8.0	30	35	25	10
	45	1,500	1,000	8.0	30	35	25	10
2	45	1,500	1,000	8.0	40	30	20	10
	45	1,500	1,000	8.0	40	30	20	10
	45	1,500	1,000	8.0	40	30	20	10
3	45	1,500	1,000	8.0	50	25	15	10
	45	1,500	1,000	8.0	50	25	15	10
	45	1,500	1,000	8.0	50	25	15	10
4	45	1,500	1,000	7.6	100	0	0	0
	45	1,500	1,000	7.6	100	0	0	0
	45	1,500	1,000	7.6	100	0	0	0

TS: Total solid; DS: Digested sludge; CS: Corn silage; GH: grass haylage; CM: Cattle manure.

Analytical methods

Characteristics of substrates were quantified using common procedures described by Standard methods for the examination of water and wastewater (APHA, 2005). In brief, TS was analyzed by filtering a well-mixed sample through a weighed standard glass-fiber filter and the residue retained on the filter was dried to a constant weight at $104 \text{ }^\circ\text{C}$ for 40 minutes (total time to reach a constant mass of the sample). The residue

from first method was ignited to constant weight at 550 °C for 30 minutes. The remaining solids represent the fixed total, dissolved, or suspended solids while the weight lost on ignition is the total volatile solids (TVS). Characteristics of the influent substrates are shown in the Table 2.

Table 2. Characteristics of influent substrates

	Units	DS	CS	GH	CM
pH		7.90	3.80	4.73	7.00
TS (initial)	%, FM basis	7.60	27.40	26.50	5.50
TVS (initial)	%, TS basis	5.74	26.25	23.85	3.93
Ash	%, FM basis	1.68	1.47	1.19	1.15

TS: Total solids. TVS: Total volatile solids; FM: Fresh matter. DS: Digested sludge; CS: Corn silage; GH: grass haylage; CM: Cattle manure.

Methane and carbon dioxide content of the evolved biogas was analyzed by Aseko Gas Analyzer AIR LF which measures the composition of biogas with linear NDIR technology (nondispersive infrared sensor). This measuring method by absorption of infrared radiation is highly resistant and provides stable measured data. Measured components are: CH₄, CO₂, O₂, H₂S, H₂, and NH₃; gas flow – 0.5–0.7 L min⁻¹; repeatability – ± 2–3% f.s. (full scale); response time – 90–20 s.

RESULTS AND DISCUSSION

Production and composition of biogas

The results of this experiment are presented in the Table 3. According to displayed data all 3 batches had expressively increased overall methane yields compared with previously reported data when cattle manure was fermented alone. Particularly, Ashraf et al. (2016) have reported average methane yield from CM about 90–100 L[CH₄] kg⁻¹[TVS]. Also, Angelidaki & Ellegard (2003) and Zhang et al. (2013) published that average methane yield from CM is approximately 150–200 L[CH₄] kg⁻¹[TVS]. These values are less than the results obtained by this study twice in terms of methane produced per kg of TVS.

Both, the highest specific biogas production per kg of TVS (674.38 ± 126.54 L_{STP}[CH₄] kg⁻¹[TVS]) and the highest specific methane production per kg of TVS (336.34 ± 110.18 L_{STP}[CH₄] kg⁻¹[TVS]) were obtained when complex substrate had the ratio 30/35/25/10 for DS, CS, GH and CM, respectively. This is very similar to a previous study (Westerholm et al., 2012) when methane potential had been enhanced through co-digestion batch experiments of cattle manure with whole stillage – 460 L[CH₄] kg⁻¹[TVS] after 60 days of fermentation. However, biochemical methane potential exceeded some other reported co-digestion investigations as of Cagri et al. (2016) when cow manure and barley were digested at different ratio and from the best one (1/1) specific methane yield – 230 L[CH₄] kg⁻¹[TVS] was obtained.

Other results in terms of biogas yield and composition such as: cumulative biogas yield (Fig. 3) and cumulative methane yield (Fig. 4); volumetric biogas and methane yield (L_{STP}[biogas] L⁻¹[wet weight]); volumetric biogas and methane yield per day (mL[methane] L⁻¹[wet weight] d⁻¹) also had the highest meaning when complex substrate

had no more than 30% of DS (see Table 3). Thus, increasing the volume of DS above 30% has not resulted in advanced methane yield.

Table 3. Chemical composition of the batches, biogas and methane yields obtained during incubation period – 45 days (mean ± standard deviation of 3 determinations)

	DS/CS/GH/CM ratios			
	30/35/25/10	40/30/20/10	50/25/15/10	100% DS
Initial TS (% , FM basis)	8.00 ± 0.1	8.00 ± 0.1	8.00 ± 0.1	7.6 ± 0.1
Final TS (% , FM basis)	4.85 ± 0.4	5.08 ± 0.5	5.47 ± 0.4	6.55 ± 0.2
Initial TVS (% , FM basis)	6.87 ± 0.2	6.73 ± 0.2	6.59 ± 0.2	5.74 ± 0.2
Final TVS (% , FM basis)	3.68 ± 0.5	3.53 ± 0.6	4.06 ± 0.3	4.89 ± 0.1
Ash (% , FM basis)	1.87 ± 0.2	1.58 ± 0.1	1.23 ± 0.2	1.39 ± 0.2
Initial pH	6.79 ± 0.9	6.68 ± 0.2	6.94 ± 0.2	7.97 ± 0.0
Final pH	7.48 ± 0.1	7.47 ± 0.1	7.43 ± 0.1	7.55 ± 0.1
Cumulative biogas yield (L)	46.33 ± 7.7	32.18 ± 4.6	28.33 ± 1.5	16.18 ± 2.8
Volumetric biogas yield (L _{STP} [biogas] L ⁻¹ [wet weight])	46.33 ± 7.7	32.18 ± 4.6	28.33 ± 1.5	16.18 ± 2.8
Volumetric biogas yield (mL[biogas] L ⁻¹ [wet weight] d ⁻¹)	1,029.56 ± 170.7	715.11 ± 101.8	629.56 ± 32.5	359.56 ± 62.0
Specific biogas yield (L _{STP} [biogas] kg ⁻¹ [TVS])	674.38 ± 126.5	478.16 ± 78.4	429.89 ± 31.9	281.88 ± 55.8
Cumulative methane yield (L)	26.91 ± 8.82	19.06 ± 6.54	18.66 ± 1.64	7.59 ± 2.49
Volumetric methane yield (L _{STP} [methane] L ⁻¹ [wet weight])	26.91 ± 8.82	19.06 ± 6.54	18.66 ± 1.64	7.59 ± 2.49
Volumetric methane yield (mL[methane] L ⁻¹ [wet weight] d ⁻¹)	598 ± 196.0	423.55 ± 145.3	414.67 ± 36.4	186.67 ± 55.3
Specific methane yield (L _{STP} [CH ₄] kg ⁻¹ [TVS])	336.34 ± 110.18	238.1 ± 81	233.23 ± 20.5	99.8 ± 32.49

TS: Total solid; TVS: Total volatile solids; FM: Fresh matter; DS: Digested sludge; CS: Corn silage; GH: grass haylage; CM: Cattle manure.

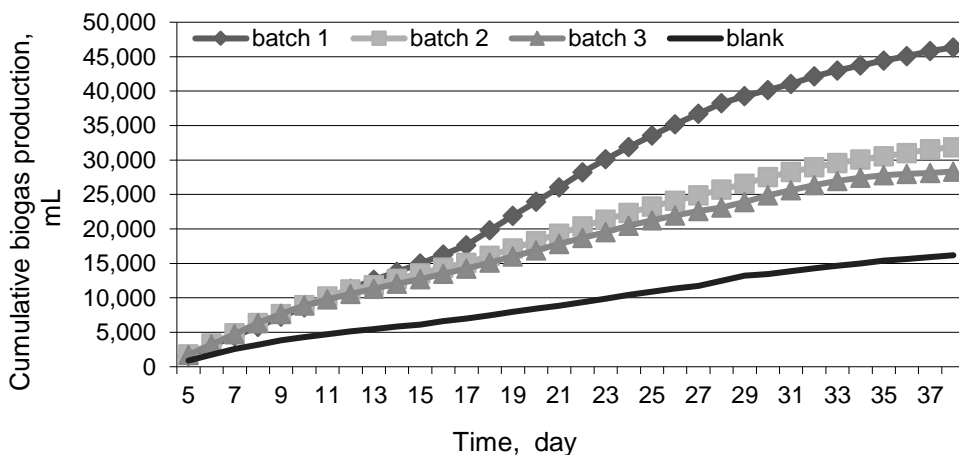


Figure 3. Cumulative biogas production of experimental batches.

Batch 1: 30% digested sludge (DS) + 35% corn silage (CS) + 25% grass haylage (GH) + 10% cattle manure (CM); Batch 2: 40% DS + 30% CS + 20% GH + 10% CM; Batch 3: 50% DS + 25% CS + 15% GH + 10% CM; Batch 4: 100% DS. DS: Digested sludge; CS: Corn silage; GH: grass haylage; CM: Cattle manure.

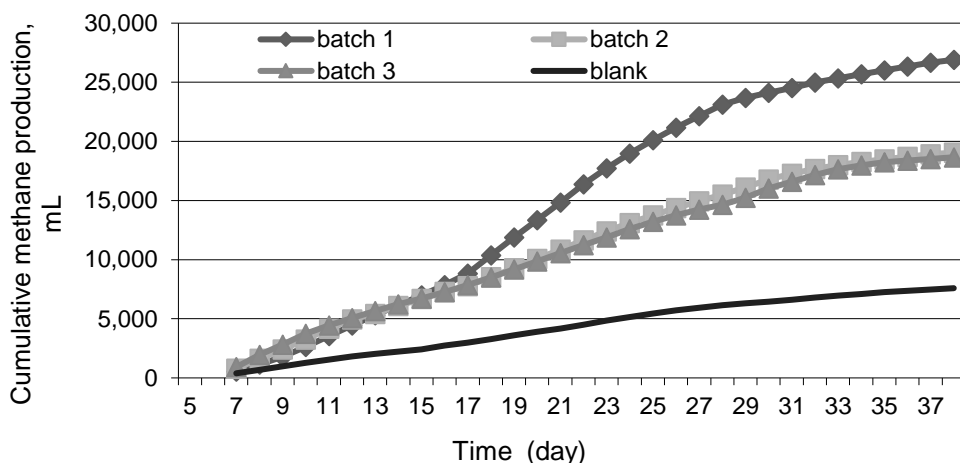


Figure 4. Cumulative methane production of experimental batches.

Batch 1: 30% digested sludge (DS) + 35% corn silage (CS) + 25% grass haylage (GH) + 10% cattle manure CM; Batch 2: 40% DS + 30% CS + 20% GH + 10% CM; Batch 3: 50% DS + 25% CS + 15% GH + 10% CM; Batch 4: 100% DS; DS: Digested sludge; CS: Corn silage; GH: grass haylage; CM: Cattle manure.

Table 4. Biogas and methane yields obtained from the batches with distracted results of control sample portion in mixture (mean \pm standard deviation of 3 determinations)

	DS/CS/GH/CM ratios		
	0/35/25/10	40/30/20/10	50/25/15/10
Cumulative biogas yield (l)	9.25 \pm 12.2	42.84 \pm 9.5	40.48 \pm 5.7
Volumetric biogas yield ($L_{STP}[\text{biogas}] L^{-1}[\text{wet weight}]$)	9.25 \pm 12.2	42.84 \pm 9.5	40.48 \pm 5.7
Specific biogas yield ($L_{STP}[\text{biogas}] \text{kg}^{-1}[\text{TVS}]$)	42.594 \pm 204.7	609.01 \pm 167.9	577.9 \pm 119.7
Cumulative methane yield (l)	2.7 \pm 12.23	23.65 \pm 9.3	24.2 \pm 3.73
Volumetric methane yield ($L_{STP}[\text{methane}] L^{-1}[\text{wet weight}]$)	2.7 \pm 12.23	23.65 \pm 9.3	24.2 \pm 3.73
Specific methane yield ($L_{STP}[\text{CH}_4] \text{kg}^{-1}[\text{TVS}]$)	07.32 \pm 153.04	293.42 \pm 126.4	300.04 \pm 47.22

TVS: Total volatile solids; DS: Digested sludge; CS: Corn silage; GH: grass haylage; CM: Cattle manure.

Agricultural by-products, including those used in this study, cannot be digested by itself, thus extra methane-producing bacteria are needed to start the digestive process. (Yu et al., 2014). Inoculum is usually dosed/added in weight concentrations 10–20% of dry matter (i.e. 10% from 8% of dry matter). In the present experiment the concentrations of 30, 40 and 50% were applied due to the fact that previous attempts from the same biogas plant didn't succeed in batch anaerobic laboratory process properly going. The reason could be an application of antibiotics in cattle stables (10% of the experimental mixture are cattle manure). However, the objective of this research was to determine whether the mixture composition is appropriate for the AD in given biogas plant and the reduction of gas production is not caused by the substrate composition. The control sample – DS from biogas plant's reactor (batch 4) was subjected to laboratory fermentation in three repetitions as well. The results of the biogas production/yield of

this sample were then used to read out adequate biogas yield produced by inoculum from the mixed sample. Summarizing Table 4 presents average yields of biogas and methane of the mixed samples minus adequate production of inoculum, which reduces the overall production of the sample.

From the obtained research data is visible that the best results had shown batch 1, wherein 30% of inoculum dry matter may be still considered as a standard. Biogas yield of mixed sample with inoculum ($674.38 \pm 126.54 \text{ L}_{\text{STP}}[\text{CH}_4] \text{ kg}^{-1}[\text{TVS}]$) and without inoculum ($842.594 \pm 204.69 \text{ L}_{\text{STP}}[\text{CH}_4] \text{ kg}^{-1}[\text{TVS}]$) was very high. Batches 2 and 3 only proved that the fermentation of substrate with the stated composition of green matter, i.e. corn silage and grass haylage in the ratio 1.4 to 1.6 with an addition of cattle manure is selected properly and is suitable for usage at the biogas plant.

Substrates and effluents characteristics

Table 2 shows that at the beginning of experiment higher TS and TVS contents were detected in CS and GH than in the DS and CM. But DS and CM both presented a greater ash content comparing to the other two co-substrates. Similar analysis results of that matters and analogous investigation in terms of AcoD can be found in the articles of Cavinato et al. (2010), Kalamaras & Kotsopoulos (2014) and Pokoj et al. (2015).

Cattle manure presents an insignificant C:N ratio (less than 15) (Cestonaro et al., 2015). Crop materials can improve the C:N ratio evading inhibition of ammonia (Xavier et al., 2015). It can be considered that addition of corn silage and grass haylage developed C:N ratio which afterwards enhanced final biogas production.

The final pH levels were upper up to 10% in all batches except of the blank sample where pH level was less than 5.7%. From the Fig. 5 it is possible to assess the degradation of TVS in various variants (batches). The best results again showed batch 1, which presented more advanced TVS degradation than other samples. It confirms the results of the Table 3 and 4.

The control sample of DS after processing produced a limited amount of biogas and it is evidenced by a small percentage of organic matter degraded (Fig. 5).

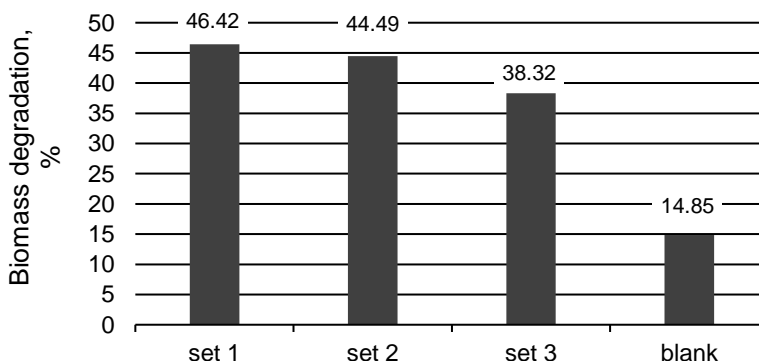


Figure 5. Degraded organic matter in the experimental batches in %.

Batch 1: 30% digested sludge (DS) + 35% corn silage (CS) + 25% grass haylage (GH) + 10% cattle manure CM; Batch 2: 40% DS + 30% CS + 20% GH + 10% CM; Batch 3: 50% DS + 25% CS + 15% GH + 10% CM; Batch 4 (blank): 100% DS; DS: Digested sludge; CS: Corn silage; GH: grass haylage; CM: Cattle manure.

CONCLUSIONS

Corn silage, grass haylage as co-substrates for anaerobic co-digestion of cattle manure improved total solids and total volatile solid content of the working mixture. This improvement in terms of substrate composition significantly increased volumetric and specific biogas production as well as methane yield. The best results showed batch 1 (30/35/25/10 for digested sludge/corn silage/grass haylage/cattle manure), wherein 30% of the inoculum dry matter can be still considered as a standard. Summarizing the results which were obtained from batch 2 (40/30/20/10 for digested sludge/corn silage/grass haylage/cattle manure) and batch 3 (50/25/15/10 for digested sludge/corn silage/grass haylage/cattle manure) it is concluded that the composition proportions of materials, i.e. vegetable biomass to animal manure were selected correct, thus, they can be used in biogas plants as working substrate mixtures to produce biogas.

ACKNOWLEDGEMENTS. The study was supported by Internal Grant Agency of the Faculty of Tropical AgriSciences, Czech University of Life Sciences Prague in the framework of research grant number 20165012 and 20175011, and by Internal project in the framework of Institutional support for a long-term conception development of Research Institute of Agricultural Engineering, number R00614.

REFERENCES

- Amon, T., Amon, B., Kryvoruchko, V., Zollitsch, W., Mayer, K. & Gruber, L. Biogas production from maize and dairy cattle manure – influence of biomass composition on the methane yield. *Agricult Ecosyst Environ* **118**, 173–82.
- Andriamanohiarisoamanana, F.J., Yamashiro, T., Ihara, I., Iwasaki, M., Nishida, T. & Umetsu, K. 2016. Farm-scale thermophilic co-digestion of dairy manure with a biodiesel byproduct in cold regions. *Energ. Conver. Manage* **128**, 273–80.
- APHA. 2005. *Standard methods for the examination of water and wastewater*. 21st ed. American Public Health Association, Washington, 1200 pp.
- Angelidaki, I. & Ellegaard, L. 2003. Co-digestion of Manure and Organic Wastes in Centralized Biogas Plants: Status and Future Trends. *Applied Biochemistry and Biotechnology* **109**, 95–105.
- Ashraf, M.T., Fang, C., Bochenski, T. & Cybulska, I. 2016. Estimation of bioenergy potential for local biomass in the United Arab Emirates. *Emir. J. Food Agric.* **28**(2), 99–106.
- Bagudo, B.U., Garba, B., Dangoggo, S.M. & Hassan, L.G. 2011. The qualitative evaluation of biogas samples generated from selected organic wastes. *Arch Appl. Sci. Res.* **3**(5), 549–555.
- BP. 2017. *Statistical Review of World Energy*. British Petroleum, Pureprint group, London, 49 pp.
- Cavinato, C., Fatone, F., Bolzonella, D. & Pavan, P. 2010. Thermophilic anaerobic co-digestion of cattle manure with agro-wastes and energy crops: Comparison of pilot and full scale experiences. *Bioresour. Technol.* **101**(2), 545–550.
- Cagri, A., Ozbayram, E.G., Ince, O., Kleinstueber, S. & Bahar, I. 2016. Anaerobic co-digestion of cow manure and barley: Effect of cow manure to barley ratio on methane production and digestion stability. *Environmental Progress & Sustainable Energy* **35**, 589–595.
- Comino, E., Riggio, VA & Rosso, M. 2012. Biogas production by anaerobic co-digestion of cattle slurry and cheese whey. *Bioresour. Technol.* **114**, 46–53.
- Divya, D., Gopinath, L.R. & Merlin Christy, P. 2015. A review on current aspects and diverse prospects for enhancing biogas production in sustainable means. *Renewable Sustainable Energy Rev.* **42**, 690–699.

- Elsamadony, M. & Tawfik, A. 2015. Dry anaerobic co-digestion of organic fraction of municipal waste with paperboard mill sludge and gelatin solid waste for enhancement of hydrogen production. *Bioresour. Technol.* **191**, 157–165.
- Hagos, K., Zong, JP, Li, DX, Liu, C. & Lu, XH. 2017. Anaerobic co-digestion process for biogas production: Progress, challenges and perspectives. *Renewable and Sustainable Energy Reviews* **76**, 1485–1496.
- Hassan, M., Ding, W., Umar, M., Hei, K., Bi, J. & Shi, Zh. 2017a. Methane enhancement and asynchronism minimization through codigestion of goose manure and NaOH solubilized corn stover with waste activated sludge. *Energy* **118**, 1256–1263.
- Hassan, M., Ding, WM., Umar, M. & Rasool, G. 2017b. Batch and semi-continuous anaerobic co-digestion of goose manure with alkali solubilized wheat straw: A case of carbon to nitrogen ratio and organic loading rate regression optimization. *Bioresour. Technol.* **230**, 24–32.
- Hassan, M., Ding, WM, Shi, ZD & Zhao, SQ. 2016. Methane enhancement through co-digestion of chicken manure and thermo-oxidative cleaved wheat straw with waste activated sludge: A C/N optimization case. *Bioresour. Technol.* **211**, 534–541.
- IEA. 2013. *Resources to Reserves. Oil, Gas and Coal Technologies for the Energy Markets of the Future.* 2nd Edition. International Energy Agency Publications, Paris, 268 pp.
- IEA. 2017. *Renewables information: Overview.* International Energy Agency Publications, Paris, 11 pp.
- IPCC. 2012. *Special Report on Renewable Energy Sources and Climate Change Mitigation.* Intergovernmental Panel on Climate Change, 230 pp.
- Kalamaras, S.D. & Kotsopoulos, T.A. 2014. Anaerobic co-digestion of cattle manure and alternative crops for the substitution of corn in South Europe. *Bioresour. Technol.* **172**, 68–75.
- Li, K., Liu, R. & Sun, C. 2016. A review of methane production from agricultural residues in China. *Renewable Sustainable Energy Rev.* **54**, 857–865.
- Li, YQ., Zhang, RH., He, YF., Zhang, CY., Liu, XY., Chen, C. & Liu, GQ. 2014a. Anaerobic co-digestion of chicken manure and corn stover in batch and continuously stirred tank reactor (CSTR). *Bioresour. Technol.* **156**, 342–347.
- Li, J., Wei, L., Duan, Q., Hu, G. & Zhang, G. 2014b. Semi-continuous anaerobic co-digestion of dairy manure with three crop residues for biogas production. *Bioresour. Technol.* **156**, 307–13.
- Li, YQ., Zhang, RH., Chen, C., Liu, G., He, YF. & Liu, XY. 2013. Biogas production from co-digestion of corn stover and chicken manure under anaerobic wet, hemi-solid, and solid state conditions. *Bioresour. Technol.* **149**, 406–412.
- Mao, CL., Feng, YZ., Wang, XJ. & Ren, GX. 2015. Review on research achievements of biogas from anaerobic digestion. *Renewable and Sustainable Energy Reviews* **45**, 540–555.
- Matheri, A.N., Ndiweni, S.N., Belaid, M., Muzenda, E. & Hubert, R. 2017. Optimising biogas production from anaerobic co-digestion of chicken manure and organic fraction of municipal solid waste. *Renewable and Sustainable Energy Review* **80**, 756–764.
- Pokoj, T., Bulkowska, K., Gusiatin, Z.M., Klimiuk, E. & Jankowski, K.J. 2015. Semi-continuous anaerobic digestion of different silage crops: VFAs formation, methane yield from fiber and non-fiber components and digestate composition. *Bioresour. Technol.* **190**, 201–210.
- Rahman, M.A., Moller, H.B., Saha, C.K., Alam, M.M., Wahid, R. & Feng, L. 2017. Optimal ratio for anaerobic co-digestion of poultry droppings and lignocellulosic-rich substrates for enhanced biogas production. *Energy for Sustainable Development* **39**, 59–66.
- REN21. 2015. *Renewables 2015 Global Status Report.* REN21 Secretariat, Paris, 250 pp.
- REN21. 2017. *Renewables 2017 Global Status Report.* REN21 Secretariat, Paris, 301 pp.

- Sosnowski, P., Klepacz-Smolka, A., Kaczorek, K. & Ledakowicz, S. 2008. Kinetic investigations of methane co-fermentation of sewage sludge and organic fraction of municipal solid wastes. *Bioresour. Technol.* **99**(13), 5731–5737.
- Shah, F.A., Mahmood, Q., Rashid, N., Pervez, A., Raja, I.A. & Shah, M.M. 2015. Co-digestion, pretreatment and digester design for enhanced methanogenesis. *Renewable Sustainable Energy Rev.* **42**, 627–642.
- Song, Z., Zhang, C., Yang, G., Feng, Y., Ren, G. & Han, X. 2014. Comparison of biogas development from households and medium and large-scale biogas plants in rural China. *Renewable Sustainable Energy Rev.* **33**, 204–213.
- Turkenburg, W.C., Arent, D.J., Bertani, R., Faaij, A., Hand, M., Krewitt, W., Larson, E.D., Lund, J., Mehos, M., Merrigan, T., Mitchell, C., Moreira, J.R., Sinke, W., Sonntag-O'Brien, V., Thresher, B., van Sark, W. & Usher, E. 2012. *Global Energy Assessment - Toward a Sustainable Future*. Chapter 11 - Renewable Energy. Cambridge University Press, Cambridge, New York, International Institute for Applied Systems Analysis, Laxenburg, pp. 761–900.
- Wang, B., Nges, I.A. & Nistor, M. 2014. Determination of methane yield of cellulose using different experimental batchups. *Water Science & Technology* **70**(4), 598–604.
- Westerholm, M., Hansson, M. & Schnürer, A. 2012. Improved biogas production from whole stillage by co-digestion with cattle manure. *Bioresour. Technol.* **114**, 314–319.
- Wu, X., Yao, W., Zhu, J. & Miller, C. 2010. Biogas and CH₄ productivity by co-digesting swine manure with three crop residues as an external carbon source. *Bioresour. Technol.* **101**, 4042–7.
- Xavier, C.A.N., Mobatch, V., Wahid, R. & Moller, H.B. 2015. The efficiency of shredded and briquetted wheat straw in anaerobic co-digestion with dairy cattle manure. *Biosyst. Eng.* **139**, 16–24.
- Yu, G., Xiaohua, C., Zhanguang, L., Xuefei, Z. & Yalei, Z. 2014. Effect of inoculum sources on the anaerobic digestion of rice straw. *Bioresour. Technol.* **158**, 149–155.
- Zhang, Y, Banks, CJ and Heaven, S. 2012. Co-digestion of source segregated domestic food waste to improve process stability. *Bioresour. Technol.* **114**, 168–78.
- Zhang, C., Gang, X., Liyu, P., Haijia, S. & Tianwei, T. 2013. The anaerobic co-digestion of food waste and cattle manure. *Bioresour. Technol.* **129**, 170–176.

Energy analysis of hydrogen as a fuel in the Czech Republic

M. Obergruber¹, V. Hönig^{2,*}, P. Procházka³ and P. Zeman¹

¹Czech University of Life Sciences Prague, Faculty of Agrobiological Sciences, Department of Chemistry, Kamýcká 129, CZ16521 Prague 6, Czech Republic

²University of Economics, Faculty of Business Administration, Department of Strategy, W. Churchill Sq., CZ130 67 Prague 3, Czech Republic

³Czech University of Life Sciences Prague, Faculty of Economics and Management, Department of Economics, Kamýcká 129, CZ16521 Prague 6, Czech Republic

*Correspondence: vladimir.honig@vse.cz

Abstract. The concept of ‘hydrogen economy’ dates back to the 1970s. It was first introduced as a response to the first oil crisis. In the context of the hydrogen economy, it is important to calculate how much hydrogen would be needed to power all motor vehicles in the Czech Republic. This is the main topic of this paper. To calculate the amount of hydrogen, we used two different methods. One is based on thermodynamic laws and the other on normal operating conditions. Both approaches yielded comparable results. It was found out that even with the use of all the electricity produced in the Czech Republic in 2016, we would not be able to cover the amount of energy that is required for production. It would cover only 75% resp. 76% depending on the calculation method used. Eventually, the Czech Republic could buy necessary amount of hydrogen and it would cost between 11 and 29 billion euros which is between 6% and 16% of GDP of the Czech Republic. In the calculations, authors found out that most fuel is burnt in the passenger cars. Therefore, we made a sensitivity analysis to find out how much our results would differ if fuel consumption changed. It turns out that with an increase in consumption of 11 per 100 km, hydrogen production coverage will decrease by about 4% (again with the use of all electricity produced in the Czech Republic).

Key words: Hydrogen, Alternative fuel, Hydrogen economy, Steam reforming.

INTRODUCTION

Currently, research and development is focused on wider use of alternative fuels to reduce dependence on lowering oil reserves. Conducted research focuses, for example, on fuels made from plant but also on long-known hydrogen (Hönig et al., 2014). It has been considered as a substitute of fossil fuel since the 1970s in response to the first oil crisis (Moliner et al., 2016). Hydrogen as a fuel has minimal impact on the environment, because no CO₂ is produced during combustion. Air and the resulting NO_x emissions can be well controlled through the amount of air supplied to the engine (Cassidy, 1977; Duana et al., 2017).

Its disadvantage is poor storage, inefficient and uneconomical production and the fact that hydrogen compared to fossil fuels is not the primary source of energy. This

means that energy needs to be converted first (e.g. in nuclear power plant) and then used for hydrogen production (Vojtěch, 2009).

There is a wide range of processes for producing hydrogen. Briefly, the following methods can be described: electrolysis (decomposition of water into hydrogen and oxygen); thermal decomposition of sulphate; gasification of coal; biochemical processes; steam reforming; partial coal oxidation; biomass pyrolysis; or use of thermolysis. Currently around 48% of hydrogen is produced from natural gas by steam reforming, 30% by oil and 18% by gasification (Abánades, 2012). There are also many new and innovative ways of producing hydrogen. Mainly hydro, geothermal and solar show a unique potential to support these innovative hydrogen production systems (Dincer et al., 2017).

Since steam reforming is the most common form of hydrogen production, the following calculations will account for this form of production. Also, according Ministry of Industry and Trade this method is the most suitable way how to produce hydrogen in Czech Republic (MIT, 2017). Main reactions of steam reforming go according to Eqs (1) and (2).



Hydrogen can be used as a fuel in two ways: Hydrogen internal combustion engines and fuel cells. Hydrogen burns very quickly, and its flame is stable due to its high calorific value even in the case of a very poor mixture, which can be used to reduce the emissions of nitrogen oxides. The disadvantage of hydrogen combustion is the low volume calorific value of the mixture, given by the low hydrogen density (Doucek et al., 2011; Shivaprasad et al., 2014).

A fuel cell is a device which, in an electrochemical reaction, converts the chemical energy of the continuously fed fuel with the oxidizing agent to the electrical energy. The fuel cell consists essentially of two electrodes and a membrane placed between the electrodes. While there is a reaction between the fuel and the oxidant, electrical charge and heat are formed. Compared to heat engine¹ (Borgnakke et al., 2012) with an electric energy generator, fuel cells produce with 35–50% efficiency, depending on the load and type of fuel cell. The high efficiency is mainly since the energy conversion is direct, not through the intermediate (thermal and mechanical), as in the case of combustion engines (Doucek et al., 2011; Yilmaz et al., 2015; Choongsik et al., 2017).

In the automotive industry, many studies have been undertaken to develop alternative fuel powered vehicles in the last three decades. Advatage of using hydrogen is that it doesn't produce any carbon dioxide during combustion and it gives significant advantages such as high heating value, short cooling distance, high spreading rate and high flame speed (Gurz et al., 2017).

As of now, there are many mass-produced cars of various brands, such as Toyota Mirai, Hyundai Tucson ix35 Fuel Cell or Honda Clarity. However, other automakers such as Audi, BMW, Toyota or Mercedes also think about the concepts of hydrogen cars. The Strategic Plan for the Use of Hydrogen Technologies KOM (2010) 2020 (Europe 2020: A strategy for smart, sustainable and inclusive growth) has been agreed

¹ Device that operates in a thermodynamic cycle. Convert part of heat into work (Borgnakke et al., 2012).

within the European Union, which helps to define more specific transport and economic development objectives (Soukup, 2017).

Moreover, Czech Hydrogen Technology Platform (HYTEP) opened new period of hydrogen technologies in the Czech Republic. It was established under auspice of the Ministry of Industry and Trade of the Czech Republic. HYTEP has organizes an international conference named Hydrogen Days. The Czech Republic has successfully finalized a series of projects: Tri-HyBus (fuel cell bus prototype), Hydrogen filling station Neratovice, Solid oxide steam electrolyzer (SOSE), Autarkic system. Platinum free novel electrocatalyst, etc., and participated successfully in several European projects (Iordache, 2016).

While there are already many initiatives, it is necessary to focus on the practical aspects of the hydrogen economy. Specifically, the question of how much hydrogen would need to be produced to power all motor vehicles in the Czech Republic needs to be answered.

MATERIALS AND METHODS

There are approximately 7.5 million vehicles on the Czech roads (Sda-cia, 2017). These vehicles were further divided into six groups:

1. Motorcycles – L1;
2. Buses – M3;
3. Passenger cars – M1;
4. Utility vehicles – N1;
5. Trucks – N2, N3;
6. Tractors – T.

From these groups, vehicles with the largest representation in the Czech Republic were selected. These have the greatest impact on the fuel consumption. Since only representatives of a given group are listed, their representation logically does not give 100%.

For this reason, the *Relative Representation* variable – Eq. (1) – was introduced, which recalculates the selected set of vehicles and its sum gives 100%. Other calculations are derived from this value.

$$v_r = \frac{v_i}{\sum_i v_i} \quad (1)$$

where v_r is the relative representation and v_i is the representation of one type of vehicle.

Typical representatives are listed in the tables 1–6 with their average consumption, representation and impact on consumption.

Analyzed motor vehicles

The first group are the motorcycles, which are analyzed in Table 1. On the Czech roads there are 1,108,362 (Sda-cia, 2017). One motorcycle runs for about 15,000 km in a year (CZSO, 2017).

Table 1. Consumption of motorcycles

Type	Consumption L 100 km ⁻¹	Representation	Total consumption of fuel L year ⁻¹
Jawa	5.00	41.2%	5.5·10 ⁸
ČZ	5.00	7.5%	1·10 ⁸
Honda	6.00	7.1%	1.1·10 ⁸
Yamaha	7.00	6%	1.1·10 ⁸

The second group are the buses (Table 2). On the Czech roads there are 20,645 (Sda-cia, 2017). One bus runs for about 200,000 km a year (CZSO, 2017).

Table 2. Consumption of buses

Type	Consumption L 100 km ⁻¹	Representation	Total consumption of fuel L year ⁻¹
Karosa	32.00	24.5%	1.3·10 ⁸
SOR	16.00	21.8%	5.8·10 ⁷
Irisbus	31.00	13.2%	6.8·10 ⁷
Mercedes-Benz	38.70	8.4%	5.4·10 ⁷

Another group are passenger cars (Table 3). On the Czech roads there are 5,491,868 (Sda-cia, 2017). One passenger car runs for about 15,000 km a year (CZSO, 2017).

Table 3. Consumption of passenger cars

Type	Consumption L 100 km ⁻¹	Representation	Total consumption of fuel L year ⁻¹
Škoda	7.00	33.7%	3.5·10 ⁹
Ford	6.00	8.8%	7.8·10 ⁸
Volkswagen	7.00	7.4%	7.7·10 ⁸
Renault	8.00	5.8%	6.9·10 ⁸

Another group are utility cars (Table 4). On the Czech roads there are 554,546 cars (Sda-cia, 2017). One commercial vehicle runs for about 50,000 km in a year (CZSO, 2017).

Table 4. Consumption of utility cars

Type	Consumption L 100 km ⁻¹	Representation	Total consumption of fuel L year ⁻¹
Ford	8.60	14%	7.1·10 ⁸
Škoda	8.20	12.8%	6.2·10 ⁸
Volkswagen	8.00	11.8%	5.6·10 ⁸
Renault	7.80	8.4%	3.9·10 ⁸

Next group are trucks (Table 5). On the Czech roads there are 189,402 (Sda-cia, 2017). Number of kilometers per year is different for each representative and is therefore listed separately (CZSO, 2017).

Table 5. Consumption of trucks

Type	Consumption L 100 km ⁻¹	Representation	km year ⁻¹	Total consumption of fuel L year ⁻¹
Avia	16.00	14.2%	50,000	5.4 · 10 ⁸
Tatra	42.00	8.7%	3,600	6.3 · 10 ⁷
MAN	36.00	8.5%	125,000	1.8 · 10 ⁹
Mercedes-Benz	27.00	8.4%	125,000	1.4 · 10 ⁹

The last group are tractors (Table 6). On Czech roads there are 174,848 (Sda-cia, 2017). Only one representative is listed, as it has a predominant representation over others. One tractor runs for 3,600 km per year (CZSO, 2017).

Table 6. Tractor consumption

Type	Consumption L 100 km ⁻¹	Representation	Total consumption of fuel L year ⁻¹
Zetor	17.50	77.70 %	1 · 10 ⁸

In addition, it is necessary to distinguish between gasoline and diesel vehicles because these fuels have different energy density – see Table 7 (Andrews et al., 2013; Lukeš et al., 2015).

Table 7. Energy density of individual fuels

Fuel	Energy density MJ L ⁻¹
Gasoline	32.18
Diesel	35.86
Hydrogen (6.9 · 10 ⁸ Pa, 388K)	4.50

For this paper, it has been selected that cars and motorcycles will be powered by gasoline and buses, utility vehicles, trucks and tractors will be powered by diesel. With this assumption, the required volume of fuel from tables 1–6 and calculate the amount of energy ε obtained from the fuels through the energy density can be calculated

$$\varepsilon_i = v_r \cdot N \cdot s \cdot C \cdot \rho \quad (2)$$

where ε_i is required energy for propulsion of vehicles i ; N is the number of vehicles i ; s is number of kilometers per year per vehicle, C is the consumption and ρ is the energy density.

Then, volume of hydrogen was calculated from energy density of hydrogen and the mass was calculated using the Peng-Robinson's equation (Eqs (3–7) (Peng et al., 1976; Orbey et al., 1998):

$$p = \frac{RT}{V_m - b} - \frac{a}{V_m^2 + 2bV_m - b^2} \quad (3)$$

$$a = 0.45724 \alpha \frac{R^2 T_c^2}{p_c} \quad (4)$$

$$b = 0.077796 \frac{RT_c}{p_c} \quad (5)$$

$$\alpha = \left[1 + \kappa \left(1 - \sqrt{\frac{T}{T_c}} \right) \right]^2 \quad (6)$$

$$\kappa = 0.37464 + 4.54226 \omega - 0.26992 \omega^2 \quad (7)$$

where p is the pressure; $R = 8.314$ is the universal gas constant; T is the thermodynamic temperature; V_m is the molar volume; T_c is the critical temperature; p_c is the critical pressure and ω is the acentric factor.

Equation parameters for hydrogen are in Table 8 (Orbey et al., 1998).

For the final comparison of the required amount of energy for hydrogen production, the amount of net electricity produced in the Czech Republic in 2016 was used: $E_{CZ} = 278,695,080$ GJ (ERO, 2017).

Table 8. Parameters of Peng-Robinson state equations

Parameter	Value
Critical temperature	33.3 K
Critical pressure	$12.97 \cdot 10^6$ Pa
Acentric factor	-0.215

The comparison was made in two different ways – empirical and theoretical.

The empirical calculation is based on the amount of energy required to produce hydrogen under normal process conditions: $\Delta H_{r,proc} = 2.25$ kWh Nm⁻³ (T-Raissi et al., 2004).

The theoretical calculation is based on the application of thermodynamic laws. By computing the reaction enthalpy in the standard state $T_1 = 20$ °C and subsequent use of Kirchhoff's law, the required reaction enthalpy in the temperature conditions of the steam reforming $T_2 = 800$ °C – Eq. (8) was calculated. Using the reaction enthalpy, the result with the efficiency of the process 90% was estimated.

$$\Delta H_r(T_2) = \Delta H_r(T_1) + \int_{T_1}^{T_2} C_p(T) dT \quad (8)$$

Both calculations will be based on reactions which occur during the steam reforming mentioned in the introduction.

For comparison itself a variable of quantity ‘coverage’ was introduced. This quantity represents ratio between calculated energy by these two ways and amount of net electricity produced in the Czech Republic. Equation for coverage ratio of empirical calculation is in Eq. (9), equation for coverage ratio of theoretical calculation is in Eq. (10).

$$\Phi_{emp} = \frac{\Delta H_{r,proc} \cdot E_{CZ}}{E_{H_2}} \quad (9)$$

$$\Phi_{theor} = \frac{0.9 \cdot \Delta H_r(T_2) \cdot E_{CZ}}{E_{H_2}} \quad (10)$$

It is also necessary to calculate, what the cost of hydrogen fuel is for the Czech Republic. The price for hydrogen differs according to the methodologies used in other papers. It is not primarily about choosing the right methodology. Rather it is important to cover the potential price range. Prices are found to be in range of (EUR per kg): 2.73

(Demir et al., 2017); 2.84 (Gregorini et al., 2010); 5.04 (Jorgensen et al., 2008); and 7.10 (Gim et al., 2012).

RESULTS AND DISCUSSION

The amount of energy required for propulsion ε_i and the sum of energies, which gives total energy ε are in Table 9. The results show that the biggest amount of energy is consumed in passenger cars and trucks.

Table 9. Energy required to propulsion vehicles

Vehicle	Consumption, L year ⁻¹	Energy ε_i , MJ year ⁻¹	Contribution to consumption
Motorcycles	$8.83 \cdot 10^8$	$2.84 \cdot 10^{10}$	6.39%
Buses	$3.12 \cdot 10^8$	$1.12 \cdot 10^{10}$	2.52%
Passenger cars	$5.72 \cdot 10^9$	$1.84 \cdot 10^{11}$	41.43%
Utility cars	$2.27 \cdot 10^9$	$8.15 \cdot 10^{10}$	18.34%
Trucks	$3.77 \cdot 10^9$	$1.35 \cdot 10^{11}$	30.43%
Tractors	$1.10 \cdot 10^8$	$3.95 \cdot 10^9$	0.89%
Sum	$1.31 \cdot 10^{10}$	$4.45 \cdot 10^{11}$	100.0%

From the total amount of energy, the required volume and the mass of hydrogen are calculated. The results are $4.09 \cdot 10^9$ kg or $9.88 \cdot 10^7$ m³ ($6.9 \cdot 10^8$ Pa, 388K).

To compare these enormous figures, a comparison was made with the electricity produced in the Czech Republic. The energy required for hydrogen production was obtained by two different calculations, empirical and theoretical.

Empirical calculation gives $3.07 \cdot 10^9$ kg of hydrogen, which would cover $\Phi = 75\%$. Theoretical calculation gives $3.13 \cdot 10^9$ kg, which would cover $\Phi = 76\%$.

Values are qualitatively the same from both calculations. This is because different procedures are used in the calculations. It can be assumed that the solution approximates closely introduced peculiarities. It is clear from the results that even with the use of all electricity produced in the Czech Republic, it would not be enough to cover all the necessary energy for hydrogen production.

The second way of comparing results is by using the amount of financial funds that would be required to pay for the necessary hydrogen. For the calculations, the minimum, average and maximum prices are used. These numbers are based on aforementioned papers. They are EUR 11.2 billion per year for the minimum price, EUR 18.1 per year for the average price and EUR 29.0 billion per year for the highest price respectively.

In order to compare these calculated numbers with economic peculiarities of the Czech Republic, total Czech GDP is selected. GDP in the Czech Republic in 2016 was 186 billion EUR (Eurostat, 2017). Ratio of required financial funds to GDP are 6%, 9.7% and 15.6% respectively for the lowest, average and highest prices.

It is also necessary to identify main source of these potential costs. Table 9 shows that the biggest energy consumption comes from passenger cars. Therefore, a sensitivity analysis was performed that provides information on how much the coverage would vary when consumption is changed.

The analysis is based on increasing and decreasing fuel consumption (Difference of consumption) of individual vehicles and monitoring of the change of coverage. The result is in Fig. 1.

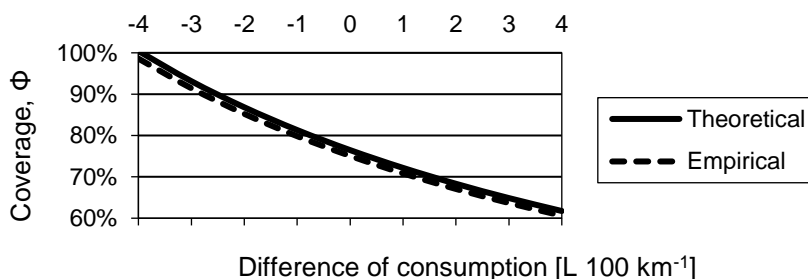


Figure 1. Sensitivity analysis of energy coverage in relation to consumption of passenger cars.

We can see from the Fig. 1 that when the consumption is changed by 1 liter per 100 km, the coverage drops by about 4% in both calculations. Specific numbers are provided in Table 10.

Table 10. Change in coverage depending on the change in consumption of passenger cars

Difference of consumption L 100 km ⁻¹	Coverage Φ		Difference of coverage	
	Theoretical	Empirical	Theoretical	Empirical
-3	93%	91%	17%	16%
-2	87%	85%	11%	10%
-1	81%	80%	5%	5%
0	76%	75%	0%	0%
1	72%	71%	-4%	-4%
2	68%	67%	-8%	-8%
3	65%	64%	-11%	-11%

This topic is widely discussed in research papers. For example, Moliner et al., 2016 evaluate the strategy of introducing the hydrogen economy. Their conclusion is that the use of hydrogen should be as a complementary energy source, rather than a competitive one. They propose synergy effects when hydrogen is used in the energy mix (Moliner et al., 2016). Other research groups (Iordache et al., 2013; Stygar et al., 2013; Pudukudy et al., 2014) deal with the introduction of the hydrogen economy in individual countries. The main problems identified are the development of energy infrastructure, the petrochemical and agrochemical industries, and the entire production and storage issues. Moreover, the slowing effect of the current geopolitical and economic situation, including the attitude of politicians towards investment in alternative energy sources, has been highlighted.

Besides these scientific papers, there are relatively few articles dealing with the issue of this article – marginally e.g. Liu et al., 2012.

CONCLUSIONS

This paper provides answer to the question how much hydrogen would be needed to power all motor vehicles in the Czech Republic? It is clear from the calculations above that this quantity is currently dramatically higher than the production capacity of the Czech Republic.

Results suggest that using all electricity produced in the Czech Republic wouldn't cover amount of required hydrogen needed. Alternatively, the Czech Republic could buy all hydrogen and it would cost up to 15.6% of GDP of the Czech Republic.

It was also found out that most of the energy is consumed in passenger cars. A sensitivity analysis was provided in the paper. Analysis shows that the increase of consumption by 1 liter per 100 km would increase the amount required hydrogen by about 4%.

REFERENCES

- Abánades, A. 2012. The challenge of Hydrogen production for the transition to a CO₂-free economy. *Agronomy Research Special Issue* **1**, 11–16.
- Andrews, J., Jelley, N. & Jelley, N.A. 2013. Energy Science: Principles, Technologies, and Impacts. *OUP Oxford*. pp. 435.
- Borgnakke, C. & Sonntag, R.E. 2012. Fundamentals of Thermodynamics, 8th Edition. *Wiley Global Education*, pp. 85, 195.
- Cassidy, J.F. 1977. Emissions and Total Energy Consumption of a Multicylinder Piston Engine Running on Gasoline and a Hydrogen-gasoline Mixture, *NASA*.
- Choongsik, B. & Jaehyun, K. 2017. Alternative fuels for internal combustion engines, *Proceedings of the Combustion Institute* **36**(3), pp. 3389–3413.
- CZSO – Czech Statistical Office. 2017. Transportation, Information and Communication, [online]. Available at czso.cz:
https://www.czso.cz/csu/czso/transport_and_communications_ekon Accessed: 2.11.2017 (in Czech)
- Demir, M.E. & Dincer, I. 2017. Cost assessment and evaluation of various hydrogen delivery scenarios. *International Journal of Hydrogen Energy*, in Press.
- Dincer, I. & Acar, C. 2017. Innovation in hydrogen production. *International Journal of Hydrogen Energy* **42**(22), 14843–14864.
- Doucek, A., Janík, L. & Tenkrát, D. 2011. Use of hydrogen to regulate the performance of renewable energy sources, [online]. Available at [Biom.cz](http://biom.cz): <http://biom.cz/cz/odborne-clanky/vyuziti-vodiku-k-regulaci-vykonu-obnovitelnych-zdroju-energie> Accessed: 15.11.2017 (in Czech).
- Duana, J., Liu, F., Yanga, Z., Sunb, B., Chena, W. & Wang, L. 2017. Study on the NO_x emissions mechanism of an HICE under high load. *International Journal of Hydrogen Energy* **42**(34), 22027–22035.
- ERO – Energy Regulatory Office. 2017. Annual Report on Operation of the Czech Republic. [online]. Available at [Eru.cz](http://eru.cz):
https://www.eru.cz/documents/10540/462820/Rocni_zprava_provoz_ES_2016.pdf/800e5a09-a58a-4a73-913f-abc30cda42a5. Accessed: 9.9.2017 (in Czech).
- Eurostat. 2017. National accounts and GDP. [online]. Available at [Europa.eu](http://ec.europa.eu/eurostat/statistics-explained/index.php/National_accounts_and_GDP):
http://ec.europa.eu/eurostat/statistics-explained/index.php/National_accounts_and_GDP. Accessed: 9.9.2017 (in Czech).
- Gim, B. & Yoon, W.L. 2012. Analysis of the economy of scale and estimation of the future hydrogen production costs at on-site hydrogen refueling stations in Korea. *International Journal of Hydrogen Energy* **37**(24), 19138–19145.
- Gregorini, V.A., Pasquevich, D. & Laborde, M. 2010. Price determination for hydrogen produced from bio-ethanol in Argentina. *International Journal of Hydrogen Energy* **35**(11), 5844–5848.
- Gurz, M., Baltacioglu, E., Hames, Y. & Kaya, K. 2017. The meeting of hydrogen and automotive: A review. *International Journal of Hydrogen Energy* **42**(36), 23334–23346.

- Hönig, V., Kotek, M. & Marik, J. 2014. Use of butanol as a fuel for internal combustion engines. *Agronomy Research* **12**(2), 333–340.
- Iordache, I. 2016. Hydrogen in an International Context: Vulnerabilities of Hydrogen Energy in Emerging Markets. *River Publishers*. pp. xvi–xvii.
- Iordache, I., Gheorghe, A.V. & Iordache, M. 2013. Towards a hydrogen economy in Romania: Statistics, technical and scientific general aspects. *International Journal of Hydrogen Energy* **38**(28), 12231–12240.
- Jorgensen, C. & Ropenus, S. 2008. Production price of hydrogen from grid connected electrolysis in a power market with high wind penetration. *International Journal of Hydrogen Energy* **33**(20), pp. 5335–5344.
- Liu, H., Almansoori, A., Fowler, M. & Elkamel, A. 2012. Analysis of Ontario's hydrogen economy demands from hydrogen fuel cell vehicles. *International Journal of Hydrogen Energy* **37**(11), 8905–8916.
- Lukeš, M., Kotek, M. & Růžicka, M. 2015. The energy consumption of public transit under rural and suburban conditions. *Agronomy Research* **13**(2), 585–595.
- MIT – Ministry of Industry and Trade. 2017. [online]. Available at mpo.cz: <https://www.mpo.cz/cz/energetika/statni-energeticka-politika/>. Accessed: 3.11.2017 (in Czech)
- Moliner, R., Lázaro, M.J. & Suelves, I. 2016. Analysis of the strategies for bridging the gap towards the Hydrogen Economy. *International Journal of Hydrogen Energy* **41**(43), 19500–19508.
- Orbey, H. & Sandler, S.I. 1998. Modeling Vapor-Liquid Equilibria: Cubic Equations of State and Their Mixing Rules. *Cambridge Series in Chemical Engineering*. New York: Cambridge University Press. pp. 19–20.
- Peng, D.-Y. & Robinson, D.B. 1976. A New Two-Constant Equation of State. *Industrial & Engineering Chemistry Fundamentals* **15**(1), 59–64.
- Pudukudy, M., Yaakob, Z., Mohammad, M., Narayanan, B. & Sopian, K. 2014. Renewable hydrogen economy in Asia – Opportunities and challenges: An overview. *Renewable and Sustainable Energy Reviews* **30**, 743–757.
- Sda-cia. 2017. Přehled stavu vozového parku. [online]. Available at Sda-cia.cz: <http://portal.sdacia.cz/stat.php?v#rok=2017&mesic=6&kat=&vyb=&upr=&obd=m&jine=false&lang=CZ&str=vpp>. Accessed: 9.12.2017 (in Czech).
- Shivaprasad, K.V., Raviteja, S., Chitragar, P. & Kumar, G.N. 2014. Experimental Investigation of the Effect of Hydrogen Addition on Combustion Performance and Emissions Characteristics of a Spark Ignition High Speed Gasoline Engine. *Procedia Technology* **14**, 141–148.
- Soukup, J. 2017. Sources and perspectives of European economies (Zdroje a perspektivy evropských ekonomik). *Management Press*. (in Czech), pp. 74–77.
- Stygar, M. & Brylewski, T. 2013. Towards a hydrogen economy in Poland. *International Journal of Hydrogen Energy* **38**(1), 1–9.
- T-Raissi, A. & Block, D.L. 2004. Hydrogen: automotive fuel of the future. *IEEE Power and Energy Magazine* **2**(6), 40–45.
- Vojtěch, D. 2009. Prospects of Hydrogen-Fuelled Cars. *Chemické listy* **103**, 484–486. (in Czech)
- Yilmaz, A.E. & Ispirli, M.M., 2015. An Investigation on the Parameters that Affect the Performance of Hydrogen Fuel Cell. *Procedia - Social and Behavioral Sciences* **195**, 2363–2369.

Typological analysis of the sustainability of dairy cattle farming in the Chelif valley (Algeria)

K. Ouakli^{1,2}, M. Benidir^{3,*}, S. Ikhlef¹ and H. Ikhlef¹,

¹Higher National School of Agronomy, El Harrach, DZ16200 Algiers, Algeria

²Saad Dahlab University, Department of Agronomy, DZ9000 Blida, Algeria

³Algeria's National Institute for Agricultural Research (INRAA), Setif DZ19000, Algeria

*Corresponding author: moh19ina@yahoo.fr

Abstract. To identify production systems that could increase local milk production in a sustainable manner, a study was conducted on 135 dairy farms in the three main plains of the Chelif Valley, Algeria. These have been evaluated for environmental, social and economic sustainability based on the IDEA (Farm Sustainability Indicators) method.

The Principal Component Analysis identified 4 different types dairy production systems, namely Type 1: Medium-size dairy farms with cereal crop production; Type 2: Small-size dairy farms; Type 3: Medium-size dairy farms diversified crop production, and Type 4: Large-size dairy farms with diversified crop production.

Comparative analysis of ecological sustainability showed better results for medium-size dairy farms with cereal crop production ($52.3 \pm 10.17 / 100$ points) and for large-size dairy farms with diversified crop production ($51.6 \pm 10.38 / 100$ points), while the economic sustainability was better for medium-size dairy farms with diversified crop production ($51.6 \pm 19.20 / 100$ points). On the other hand, social security was the weak point for all farm types.

On the regional level, it appeared that agri-environmental scores were better in Middle and Low Chelif valley while the best economic performances were recorded in High Chelif valley. On the regional level, it appears that the scores of agri-environmental scales are better in the middle and low Chelif while the economic performances are comparable between the three localities.

Key words: Algeria, dairy farming, IDEA, sustainability, typology.

INTRODUCTION

In the Chelif valley, located in the center of the country between the two major economic centers west of Algiers and east of Oran, three main plains are extended from the plain of Upper Chelif to the East, to that of Lower Chelif in the West, passing through the plain of Middle Chelif in the center. The entire river valley which covers an area of 44,630 km², does not lack assets. This area irrigated by the Chelif valley, it has most of the arable land where modern agriculture is developing and where there are important dairy production regions with a total of 123,017 heads of cows owned by 9,238 breeders and representing 7% of the national herd (MADR, 2013). Like other regions of the country, since the 1970s the valley has seen a series of dairy development plans that aimed to intensify production, to fight against underemployment and to develop rural areas (Adair, 1982; Bessaoud, 2006). However, the expected results have not been met.

The causes are linked to the absence of a global vision on the production systems and the lack of knowledge on the actual conditions of the farms due to lack of data on their structure and operation (Baouche, 2014). As of today, Algerian dairy farms face many uncertainties. The trend towards intensification of dairy operations is also increasingly questioned because of its impact on the environment and animal welfare (Fraser, 2006). The importance of a transition to more sustainable systems is, therefore, at the center of the current debate (Ozier-Lafontaine et al., 2011). Indeed, in the context of agriculture, sustainable development is a long-term, comprehensive, on-farm approach that maximizes the economic, environmental, and economic stability, equity, and health of the farm and family.

The major scientific task is therefore to identify how these dairy farms could evolve to respond to the above-mentioned challenges.

This article focuses on two essential points, namely the identification of the types of dairy cattle farms in the Chelif valley and the evaluation of the sustainability of these farms on the basis of the IDEA method (Vilain, 2003) which carries out a multidimensional diagnosis of the sustainability of the farm by the combination of three groups of indicators that measure agro-ecological, socio-territorial and economic sustainability. The IDEA method makes it possible to point out the strengths and weaknesses of a farm to show possible ways of improvement. The objectives of the agro-ecological scale refer to the agronomic principles of integrated agriculture. They must allow good economic efficiency for an ecological cost as low as possible. Those on the socio-territorial sustainability scale refer more to ethics and human development, which are essential features of sustainable farming systems. Finally, the objectives of the economic sustainability scale take into account the entrepreneurial function of the farm.

MATERIALS AND METHODS

The study was conducted between 2014 and 2015 on 135 dairy farms spread over the plains of the *Chelif valley*. It involved 64 farmers from *High Chelif* (*Wilaya of Ain Defla*), 50 from *Middle Chelif* (*Wilaya of Chlef*) and 21 from *Low Chelif* (*Wilaya of Relizane*). The choice of these farmers is based on their vocation (dairy cattle farming), the possession of the farming license and the adhesion to the milk collection network. A questionnaire was established as a survey guide with 190 questions relating to the operation of the dairy farm. It also made it possible to provide information on sustainability indicators using the IDEA method (Vilain, 2003), which includes three scales: agro-ecological, socio-territorial and economic. All scales have the same weight and range from 0 to 100 points.

1- The agro-ecological scale structured in three components of equal importance (capped at 33 and 34 points): domestic diversity (4 indicators), organization of space (7 indicators) and farming practices (7 indicators). The diversity component is introduced in the analysis to take into account the fact that an economical, autonomous and non-polluting agriculture relies on a high level of diversity of productions in order to take into account the complementarities and the natural regulation processes that work in the different types of cultivated ecosystems. Indicators associated with the organization of space component concern the organization of the plots, the management of non-productive environments and the valorization of spaces. The farming practices component analyzes the intensity of environmental pressure according to the farmer's

choices and technical itineraries (level of fertilization, intensity of phytosanitary treatments, consumption of fossil energy, etc.).

2- The socio-territorial scale refers to ethics and human development, it characterizes the insertion of exploitation in its territory and in society. It assesses the quality of life of the farmer and the weight of the market or non-market services he provides to the territory and society. The three components of socio-territorial sustainability (product quality, employment and services, ethics and human development) have the same weight and are capped at 33 on a scale of up to 100. In practice, this scale combines and weight practices and quantifiable behaviours with more qualitative elements (such as the architectural quality of the buildings, the landscape quality of the surroundings). Some indicator values such as likely sustainability, work intensity, quality of life and feeling of isolation are self-declaring and estimated by the farmer.

3- The economic sustainability scale analyzes the economic results beyond the short term and the cyclical uncertainties. Structured in 4 components and 6 indicators, the analysis goes beyond taking economic performance into account in terms of short-term economic or financial profitability, but also analyzes the degree of economic independence, the transferability capacity of the farm and efficiency of its productive process. On a scale of up to 100, each of these four components is capped at between 20 and 25 units.

Each scale groups together several indicators, totaling 37. The score of a farm for each of the three sustainability scales is the cumulative number of points obtained for the various indicators of the scale considered. The higher the score the more the farm is sustainable for the scale considered. The choice of this method is motivated by the fact that it is relatively simple and easy to implement.

The data thus collected were the subject of a series of analyzes and statistical treatments. ANOVA was performed using the Statgraphics Centurion XVI version 16.1.1.18 software, multiple correspondence analysis (MCA) followed were performed to describe the types of farms present. Principal Component Analysis (PCA) was conducted to identify sustainability classes by components and sustainability scales. These analyzes were performed using the SPAD software version 6.5 (Coheris-SPAD, France).

RESULTS

Farm characteristics

The farms surveyed share a remarkable productive potential (Table 1). It consists of a land base of 4,134 ha (30.62 ± 44.64 ha per farm) for a total cattle population of 3,819 head of which 51.37% were dairy cows, with an average of 14.64 ± 12.82 dairy cow per farm.

Cereal cropping was practiced on all farms ($N = 135$) while arboriculture ($N = 45$) was more widespread in High and Medium Chelif. Vegetable crops ($N = 40$) were mainly farmed in Middle Chelif. Irrigation was practiced on 71.85% of the farms, whereby 47.41% used sprinkler irrigation and 10% drip irrigation, the latter mainly reserved for arboriculture and vegetable crops. The availability of labour on the farms was quite variable, averaging 6.13 ± 7.62 LbU (Labour Unit) /farm. This means that 1 LbU on average had to take care of 2.38 dairy cows and 5 ha of UAA (Useable

Agricultural Area). Cultivated fodder, which is the guarantor of economic milk production, occupied an area of 1,572.13 ha cultivated with by oats (N = 135), with a predominance in High and Middle Chelif. Clover (N = 60) and sorghum (N = 76) were homogeneously distributed between the three localities and alfalfa was of low importance (N = 10). A common practice to overcome shortage in cultivated fodder is the use of spontaneous fodder (N = 53), most often coupled with the distribution of excessive amounts of concentrated feed ranging from 4 to 10 kg cow per day (N = 135) but without real benefits from it in terms of milk production (on average 14 L cow per day). Pasture use was rare (N = 25) and mainly found on High Chelif farms (8%). The fodder autonomy in these farms (N = 135) is low since the recorded stocking rate is on average 11.29 ± 3.95 LU per ha of forage area.

Table 1. Mean values (and standard deviation) of major characteristics of four types of dairy farming systems in the Chelif valley

TYPE	1	2	3	4	TOTAL
N	69	11	31	24	135
Age of farmer (years)	46.5 a (15.51)	43.7 a (13.61)	48.4 a (15.09)	43.4 a (12.12)	46.2 (14.67)
LbU (N)	4.0 b (2.04)	3.0 b (1.68)	9.1 a (11.94)	9.8 a (9.80)	6.1 (7.63)
Cattle (N)	21.5 b (8.11)	24.6 b (11.15)	57.5 a (37.54)	56.3 a (79.09)	36.2 (40.32)
Dairy cows (N)	8.3 c (3.85)	11.4 bc (6.07)	21.8 ab (12.32)	24.9 a (32.81)	14.6 (16.77)
UAA (ha)	17.4 b (9.64)	2.7 c (2.97)	27.8 b (19.30)	94.9 a (82.89)	30.6 (44.65)
FA (ha)	9.6 b (6.54)	1.0 c (1.45)	10.3 b (5.39)	52.0 a (50.07)	16.6 (27.12)
LU/ha FA	2.6 c (2.42)	9.1 a (10.72)	5.3 b (6.47)	1.0 c (0.90)	11.3 (39.47)

Values with common letters are not significantly different; LbU: Labour Unit; UAA: useful agricultural area; FA: forage area; LU: livestock unit.

Typology of farms

The first two axes of the multiple correspondence analysis (MCA) explain more than 30% of the total variation of the sample; the approach allowed to identify 4 types of farms (Fig. 1).

Type 1: Medium-size dairy farms with cereal crop production

This Type represented of 51.11% of the farms and comprises medium-sized farms with a low level of diversification in plant production; 78.26% of these farms are evenly distributed between the High and Middle Chelif. The farm land of about 17 ha per farm, is mainly used for cereals (barley and durum wheat). There is very little market vegetable gardening and very little arboriculture. The fodder on these farms covers an area of 9 ha, mainly oats, used green and as hay for a 20-head cattle herd and an 8-head dairy cow herd per farm. In 56% of the cases sheep are also farmed. The stocking rate is average with 2.62 LU per ha forage area. The labour availability on these farms is partly family-based and averages about 4 LbU.

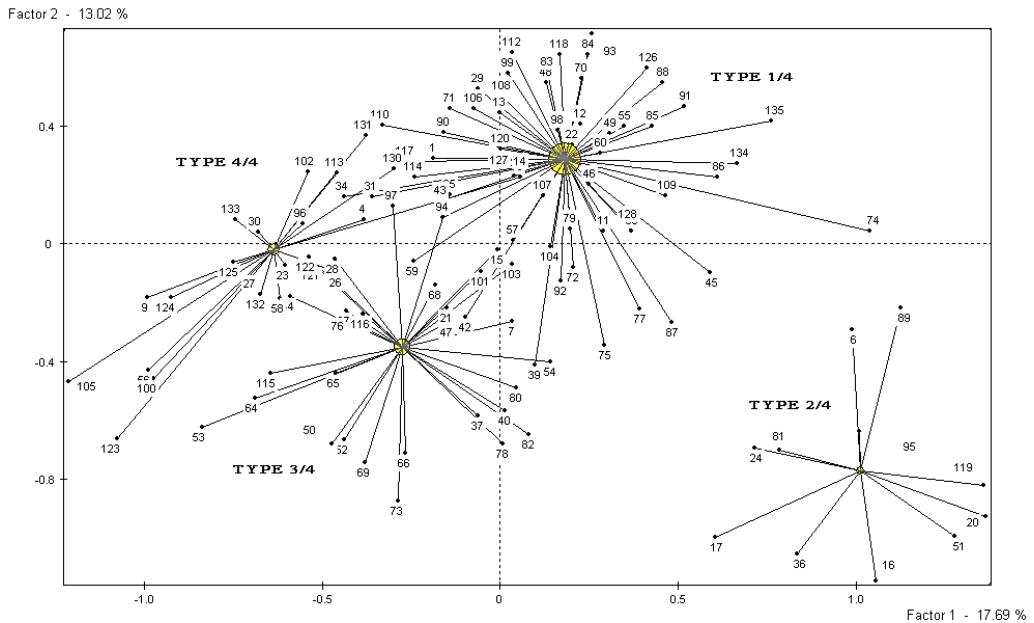


Figure 1. Representation on the first two axes of multiple correspondence analysis (MCA) deploying 190 variables that allowed identifying four distinct types of dairy farms.

Type 2: Small-size dairy farms

This type, which accounts for 8.14% of the farms with practically no land base, is spread over the entire study area with a slight concentration at High Chelif (63.63%). The number of dairy cows is small (11 cows per farm) and stocking rate is highest (9 LU per ha FA). In addition, all labour (3.54 LbU) mobilized on these farms belongs to the family.

Type 3: Medium-size dairy farms with diversified crop production

This Type includes 22.96% of the farms of which 45.16% are located in Middle Chelif. The farms are of medium size and focus on mixed crop-livestock farming. Average cattle population per farm is 57 heads with 22 dairy cows. The farm land of about 28 ha is cropped with fodder (10 ha), cereals, arboriculture and vegetables. The stocking rate is high (5 LU per ha FA), and the farms are moderately equipped with mechanical equipment and buildings. The frequent use of hired workers during labour peaks results in the presence of an important workforce (9 LbU).

Type 4: Large-size dairy farms with diversified crop production

This Type includes 17.78% of the farms and is spread over the three localities with a slight concentration in Low Chelif (45.83%). The large-size farms are characterized by a large land area (95 ha) devoted to cereals, arboriculture and market gardening, all irrigated, and a significant presence of fallow. The livestock unit is dominated by dairy cattle with 25 dairy cows on average. The forage area occupies an important place in the crop rotation, with an average of 52 ha per farm. The stocking rate recorded in this group is lowest with 1.1 LU per ha FA. The mixed management system mowing / grazing, a practice that avoids the depletion of certain plots. These farms are generally well equipped with agricultural equipment and buildings and the employment of hired labour is important (10 LbU on average).

Sustainability of farms: overall and regional characteristics

The agro-ecological scale had the highest score, i.e. 49.6 ± 10.86 out of 100 points with individual values ranging from 20 to 76 points (Table 2). It was followed by the economic scale with a score of 45.3 ± 20.56 points (ranging from 3 to 84 points) and finally by the socio-territorial scale with a mean score of 37.0 ± 6.26 points (ranging from 19 to 51 points) (Table 2). Overall sustainability estimated by the average of the lower scale for each farm was relatively low, i.e. 31.2 ± 7.83 points (ranging from 3 to 47 points). For 48.89% of the farms, minimum point values were attributed to the socio-territorial scale, whereas minimum values were attributed to the economic and agro-environmental scales for respectively 40.0% and 11.11% of the farms. The sum of the three sustainability scales yielded a score of 132.9 ± 23.86 out of 300 points (ranging from 73 to 178 points). The overall sustainability scores were similar between the three locations. However, the scores of the agri-environmental scales were better in Middle and Low Chelif while the best scores of the economic scale were recorded in High Chelif.

Table 2. Mean values (and standard deviation) of sustainability scales scores attributed to farm types and sustainability classes

Category	N	AGRO	SOCIO	ECO	SUM	SUS
CLASS 1	38	55.9 a (7.82)	36.4 b (5.28)	63.5 a (9.69)	155.9 a (12.44)	36.4 a (5.28)
CLASS 2	27	38.6 b (7.10)	42.5 a (4.66)	66.0 a (11.20)	147.2 b (13.74)	37.0 a (5.54)
CLASS 3	18	39.9 b (10.35)	29.7 c (6.53)	26.8 b (7.07)	96.2 d (11.28)	23.3 c (4.92)
CLASS 4	52	54.2 a (7.51)	37.3 b (4.73)	27.8 b (7.17)	119.3 c (9.05)	27.1 b (6.05)
TOTAL	135	49.6 (10.86)	37.1 (6.26)	45.4 (20.56)	132.1 (23.86)	30.5 (7.88)
TYPE 1	69	52.3 a (10.17)	36.7 b (6.19)	44.5 ab (21.13)	133.5 a (22.92)	30.8bc (7.94)
TYPE 2	11	36.6 c (11.79)	36.4 b (7.32)	33.5 b (16.34)	106.5 b (22.39)	25.7 c (6.53)
TYPE 3	31	46.8 b (8.62)	37.8 b (6.53)	51.6 a (19.20)	136.3 a (23.12)	34.6 a (7.35)
TYPE 4	24	51.6 ab (10.38)	37.8 a (5.84)	45.2 ab (20.59)	138.9 a (22.38)	31.5ab (7.29)
High Chelif	56	46.3 b (11.48)	37.6 a (7.47)	48.5 a (21.69)	138.9 a (27.21)	31.6 a (8.17)
Middle Chelif	48	51.7 a (10.42)	36.7 a (5.37)	43.9 a (20.78)	137.5 a (22.53)	30.9 a (8.54)
Low Chelif	31	52.5 a (8.88)	36.8 a (5.17)	42.0 a (17.77)	136.6 a (19.30)	31.0 a (6.07)

Values with common letters are not significantly different; N: Number; AGRO: agro-ecological; SOCIO: socio-territorial; ECO: economic; each yielding a maximum of 100 points; SUM: sum of score points (maximum 300) SUS: Overall sustainability (calculated by the average of the lower scale for each farm).

Classification of farms according to sustainability scores

The principal component analysis identified four axes, the first two of which accounted for 81.34% of the variability. The hierarchical classification helped to identify four sustainability classes (Fig. 2).

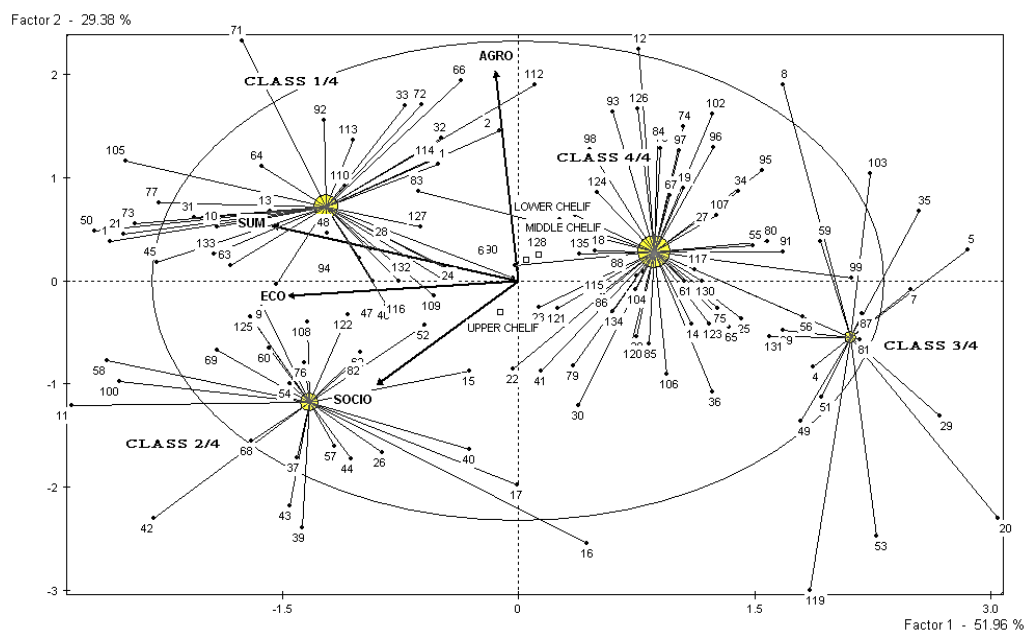


Figure 2. Distribution of dairy farms (numbers) across four sustainability classes as displayed by the first two axes of the hierarchical classification (principal component analysis).

Class 1: High sustainability limited by socio-territorial scale

This class comprised 28.15% of the surveyed farms; these were distributed between the High, Middle and Low Chelif with respectively 44.7%, 31.6%, and 23.7%. These farms yielded the highest sustainability score ($155.9 \pm 12.44 / 300$ points) and were characterized by good agro-environmental ($58.0 \pm 7.38 / 100$ points) and economic performance ($63.5 \pm 9.69 / 100$ points) but poor performance on the socio-territorial scale ($36.5 \pm 5.28 / 100$ points).

Class 2: Average sustainability limited by agro-ecological scale

This class consisted of 20% of the farms of which 55.56% were concentrated in High Chelif. It displayed the best scores for the economic and socio-territorial scales with respectively 66.1 ± 11.20 and $42.5 \pm 4.66 / 100$ points. However, it displayed average sustainability ($147.2 \pm 13.74 / 300$ points) because it was limited by the score of the agro-ecological scale ($38.4 \pm 7.10 / 100$ points).

Class 3: Low overall sustainability

This class comprised 13.33% of the farms of which 61.11% were located in High Chelif. It grouped the farms with the lowest sustainability score ($96.22 \pm 11.28 / 300$ points) with 39.9 ± 10.35 , 29.7 ± 6.53 and 26.7 ± 7.07 points / 100, respectively, for the agro-ecological, the socio-territorial and the economic scale.

Class 4: Moderate sustainability limited by economic scale

This class was represented by 38.52% of the farms that were distributed between the High, Middle and Low Chelif with respectively 25.0%, 46.2%, and 28.9%. Similar to class 1, they displayed good agro-ecological performance ($54.2 \pm 7.51 / 100$ points) but on the other hand low scores on the socio-territorial scale ($37.3 \pm 4.73 / 100$ points) and the economic scale ($27.8 \pm 7.17 / 100$ points).

Distribution of farm types across sustainability classes

Type 1: Medium-size dairy farms with cereal crop production

Of Type 1 farms, 79.7% were divided between class 1 (high sustainability limited by socio-territorial scale; 31.88%) and class 4 (moderate sustainability limited by economic scale; 47.82%). This Type obtained the highest score on the agro-ecological scale with $52.8 \pm 10.17 / 100$ points because of the diversity component which recorded a score of $20.0 \pm 5.78 / 33$ points. This is explained by the high animal diversity and the annual crop component. The organization of space ($16.97 \pm 4.41 / 34$ points) and the farming practices ($15.3 \pm 6.30 / 33$ points) contributed moderately through the complex rotations encountered, the small dimensions of the fields cultivated as well as the restricted use of pesticides. The low score of the social scale ($36.7 \pm 6.19 / 100$ points) resulted from the low scores recorded by the quality and employment components with respectively 8.9 ± 2.35 and 7.8 ± 3.82 points of a total of 33. The ethics component score was good ($20.8 \pm 3.25 / 34$ points) due to the lack of use of imported food and the average quality of life, estimated by the farmers of this Type and this, despite a slight feeling of isolation. The average score obtained for the economic scale ($44.5 \pm 21.13 / 100$ points) was mainly due to a considerable financial autonomy and a certain independence vis-à-vis public aid (Table 3).

Table 3. Mean points (and standard deviation) achieved by four different types of dairy farms for major sustainability components

TYPE	1	2	3	4	MEAN
Diversity	20.0 b (5.78)	14.8 c (5.60)	22.5 ab (5.41)	23.2 a (6.84)	20.7 (6.23)
Organisation of space	16.9 a (4.41)	8.7 c (7.96)	13.2 b (4.50)	13.2 b (3.74)	14.8 (5.30)
Farming practices	15.3 a (6.30)	16.3 ab (7.07)	11.2 b (3.57)	15.2 a (4.84)	18.70 (6.47)
Quality of products	8.1 b (2.35)	8.8 ab (2.27)	9.7 a (2.70)	9.2 ab (2.21)	8.8 (2.49)
Employment and services	7.8 a (3.82)	8.9 a (4.16)	6.3 a (3.84)	6.4 a (3.63)	7.31 (3.87)
Ethics and human development	20.8 ab (3.25)	18.6 b (4.39)	21.7 a (4.04)	22.1 a (2.89)	21.0 (3.56)
Economic viability	10.8 b (9.17)	5.4 b (7.22)	15.5 a (9.73)	10.5 b (9.64)	11.4 (9.53)
Independence	21.6 a (5.98)	22.6 a (53.73)	22.9 a (4.23)	22.9 a (5.43)	22.2 (5.49)
Transferability	2.9 ab (5.45)	1.1 ab (3.62)	0.3 b (1.44)	1.9 ab (4.66)	1.9 (4.63)
Efficiency	9.2 ab (9.67)	4.4 b (7.51)	12.9 a (10.35)	9.8 ab (10.84)	9.8 (10.03)

Values with common letters are not significantly different.

Type 2: Small-size dairy farms

Of this farm type, 45.45% reached the lowest scoring grade on the three sustainability scales (class 3; low overall sustainability). The rest was distributed homogeneously across the other sustainability classes. The low animal and crop diversity, the absence of annual crops, the simplified rotation, the high stocking rate and the energy dependency strongly penalized the biodiversity component ($14.3 \pm 5.6 / 33$ points) and the organization of space ($8.7 \pm 7.96 / 34$ points) resulting in a low score on the agro-environmental scale ($36.6 \pm 11.79 / 100$ points). Farmers' negative feelings about quality of life and isolation affected the socio-territorial scale ($36.4 \pm 11.79 / 100$ points). Furthermore, low income per family worker, Higher economic specialization and low efficiency of production system due to high use of inputs yielded low economic scores ($33.6 \pm 16.34 / 100$ points).

Type 3: Medium-size dairy farms with diversified crop production

Of this farm Type 51.6% are equitably divided between class 1 and class 4, while 38.70% belong to class 2 (class with medium sustainability limited by the agro-ecological scale). These farms recorded average scores for the agro-environmental scale ($46.8 \pm 8.62 / 100$ points), due to good animal and plant diversity, but reached low scores for the organization of space ($13.2 \pm 4.5 / 34$ points) due to high stocking rates and lack of pasture. If these farms tend towards zero pesticides, irrigation and the use of fertilizers as well as the absence of effluent treatment devices are negative aspects of farming practices ($11.2 \pm 3.57 / 33$ points). They have a good ethical score ($21.7 \pm 4.04 / 33$ points) since they positively value their quality of life and do not feel isolation. Yet, the low contribution to employment on these farms and the lack of multiple activities and / or collective work generated low scores on the socio-territorial scale ($37.8 \pm 6.53 / 100$ points). However, they recorded the highest economic score ($51.6 \pm 19.20 / 100$ points) due to high viability, which is mainly explained by high income per family worker, financial autonomy (government aid is less than 20% in these farms) and good economic efficiency because of the good proportion of inputs thus privileging their own resources, which guarantees their long-term sustainability.

Type 4: Large-size dairy farms with diversified crop production

Farms of this Type 4 to 41.66% belong to sustainability class 4, with $51.6 \pm 10.38 / 100$ points for agro-ecological sustainability due to the good score of the diversity component ($23.2 \pm 6.84 / 33$ points) despite the absence of local breeds in these farms. Although grazing is poorly practiced on these farms, the complex rotations encountered, the presence of intercropping, the partition of plots of modest size and the relative forage autonomy illustrated by the low stocking rate favor the space organization component of these farms ($13.21 \pm 3.74 / 34$ points). The score of the agricultural practices component ($15.21 \pm 4.89 / 33$ points) is directly related to the respect of animal welfare and the restricted use of pesticides and fertilizers. However, the practice of irrigation and the lack of soil protection and effluent treatment devices are negative aspects. The score obtained by the ethics component ($22.08 \pm 2.89 / 33$ points) is linked to the good quality of life of the farmers and the moderate work load. In addition, their relative financial autonomy and their independence from government aid explains their respectable economic performance ($45.21 \pm 20.59 / 100$ points).

DISCUSSION

A mixed farming system: Agriculture-livestock farming

Dairy cattle husbandry in the Chelif valley is practiced in a mixed crop-livestock system in farms of very variable size (30.6 ± 44.64 ha), but generally larger the average national estimated farm size of 8.3 ha (General Census of Agriculture, 2001). Most of the agricultural area is allocated to cereals, mainly barley and wheat, which often rotate with market gardening or fallow. Although Cereals practiced as rainfed system in spite of the irrigation capacities, according to Hartani et al. (2007) Cereals contributes to food security for humans and provides an essential feed for livestock. Despite the livestock number is important and as reported by Suttie (2004), the share of fodder crops, mainly oats, used as green feed and as hay in the rotation, is constrained by the competition with food crops. This great disparity in the distribution of land and the low diversification of the fodder area was also observed by Ghozlane et al. (2006) on dairy cattle farms in the Tizi-Ouzou region where the fodder area was only cultivated with vetch-oats and to a lesser extent with alfalfa. Irrigation is usually reserved for perennial crops described as heritage to be passed on to future generations (Djebbara, 2004) and to market gardening described as a high-value crop (Si-Tayeb, 2015). Fodder is often cultivated rainfed, while pastures, which are still the oldest and most natural way of using grassland and annual forages (Huyghe & Delaby, 2013), are of small size despite very low implementation cost (Le Gall et al., 2001). The farmers overcome fodder shortage by a large amount of concentrate in the ration of animals without really taking into account their needs. This practice was also observed by Srairi (2009) for dairy cattle farms in Morocco. Finally, the amount of labour used depends on the size of the farm; it is mostly family-based in small farms and, according to Bourenane et al. (1991), is geared at minimized spending and to cushion the unemployment shock amongst family members of working age. Unemployment is more pronounced in rural areas where agriculture provides the bulk of employment for the population.

Diversity of farms defined by regional potential

The Dairy Basin in the Chelif valley hosts completely differentiated dairy farms, which, like farms in other regions of the country, produce according to the ecological and climatic conditions (Benniou & Aubry, 2009; Boukkedid, 2014). Indeed, the results of the typology showed four types of dairy cattle farms marked by a regional diversity: the High Chelif plain is dominated by cereal farms of average size (39.13% of the Type 1) and farms of small size with reduced livestock numbers (63.63% of Type 2). According to Belhadia (2016), this region is characterized by a cereal-fallow association. The same author also indicated that cereal crops annually occupy more than 45% of the Useable Agricultural Area (UAA). Medium-size cereal farms are also widespread in Middle Chelif (39.13% of Type 1), but more important are medium-size farms with diversified crop production (45.16% of Type 3). Crop diversification in this region was also reported by El Mahi (2005). The Low Chelif is characterized by large farms with medium livestock numbers and diversified crop production (45.83% of Type 4). As reported by Douaoui et al. (2008), it appears that agriculture in Low Chelif mainly comprises orchards of citrus and olive trees, irrigated vegetable crops (melon, watermelon, artichoke, onion) and rainfed cereal crops.

Contribution of the agriculture-livestock farming association to the sustainability of farms

Sustainability in the Chellif Valley is in favor of large farms that practice mixed cropping: although the overall sustainability scores are comparable between the different types encountered (with the exception of indoor farms of Type A2), the overall sustainability is better in large diversified farms, (Type A3 and A4). Livestock-Mixed farming is a virtuous production system, both environmentally and economically (Veysset 2014, Sneeseens 2014).

Ecological sustainability is the strong point of these farms as it reaches 49.6% of the theoretical maximum. However, this value remains lower than those obtained in other regions of the country, particularly in the semi-arid region of Setif, evaluated at 67% by Yakhlef et al. (2008) and in the Mitidja Plain valued at 71.5 and 73% respectively by Bekhouche (2004) and Benatallah (2007). In addition, the comparative analysis of ecological sustainability shows better results for Type 1 and Type 4 farms, but limits the sustainability of 31.88% of Type 3 farms because of the large size of plots which promotes erosion phenomena (Villain et al., 2000), and the excessive use of fertilizers.

The economic sustainability that reaches 45.38% of the theoretical maximum is lower than that recorded by Ghozlane et al. (2010) in a similar study in the region of Tizi Ouzou (Algeria), 54.7%. Although this sustainability is the strong point of Type 3 farms, it remains the weak point for 47.82% of Type 1 farms and 46.66% of Type 4 farms because of a low efficiency of the production system. This weakness of the economic scale is noted by M'hamedi et al. (2009) in a similar study conducted in Tunisia on 30 dairy farms. In this regard, they suggest that technical innovations to stabilize yields must be adapted to the low financial capacities of producers.

On the other hand, social sustainability is the weak point for all identified groups; it reaches only 37% of the theoretical maximum. This weakness of the social ladder is also observed by Benatalah et al. (2013) for the dairy cattle farms of the Mitidja and Bir plain (2015) for farms in the semi-arid region of Sétif (North-East of the country). The socio-territorial sustainability scale does not depend on production systems but depends more on the lifestyle of the farmer (M'hamedi et al., 2009).

At the regional level, it appears that the scores of the agri-environmental scales are better in the middle and low Cheliff respectively 51.7 ± 10.42 and 52.5 ± 8.88 on 100 points, while the economic and social performances are comparable between the three localities.

CONCLUSIONS

Taking into account the diversity of agricultural situations is a fundamental condition for the success of interventions in rural areas. Livestock is an essential component of the production systems in the Chelif valley, despite its limited income potential compared to cash crop cultivation. The crop-livestock association is essential for the sustainability of these farms. Indeed, very good results for overall sustainability were observed in more than 28% of the surveyed farms. Ecological sustainability is the strong point of Type 1 and Type 4 farms, reaching 49% of the theoretical maximum across the whole sample. Economic sustainability, which reached 45% of the theoretical

maximum, was best on Type 3 farms. Social sustainability, on the other hand, was the weak point for all farms, reaching only 37% of the theoretical maximum.

Aggregating component scores allows multiple combinations to achieve a better sustainability outcome. The simple active involvement with associations and the collective work are likely to improve the scores for 32% of type1 farms whose sustainability is limited by the social scale. The valorization of the products of these farms by short chain would encourage the putting in relation of proximity farmers and consumers on the one hand and would improve the sustainability for 48% of these farms which is limited by the economic scale (in the same way as 42% of Type 4 farms). The low economic scale is often due to a low efficiency of the production system.

In fact, a better valuation of the farm's own resources would contribute to improving their perennality and thus ensuring their sustainability. Limiting the size of the plots and encouraging the establishment of mixed cropping would be a lever of action capable of improving the scores for 39% of Type 3 farms whose sustainability is limited by the agroecological scale. Similarly, the significant introduction of legumes into rotations allows better use of complementarities among cultivated species will also participate. The lowest scores of the three sustainability scales are recorded mainly in 45.45% of Type 2 farms, which are practically family farms (mainly indoor farms), they remain very dependent on the inputs market and their sustainability is questioned.

REFERENCES

- Adair, P. 1982. Myths and realities of agrarian reform in Algeria. Review of a decade. *Études Rurales* **85**(1), 49–66 (in french).
- Baouche, F. 2014. The evolution of agricultural land in Algeria through the reforms. [online]. Thèse Droit rural. Poitiers : Université de Poitiers. 2014, 306 pp. (in french).
- Bekhouche, N. 2004. Sustainability indicators for dairy farms in Algeria: Case of Mitidja. Thèse de Magister. INA El Harrach (Alger), 135 pp. (in french).
- Belhadia, M. 2016. Dairy farmers strategy and redeployment of the milk sector in the plains of Higher Chelif: formalizing the informal sector. Thèse de Doctorat en Sciences Agronomiques. ENSA. Alger, 198 pp. (in french).
- Benatallah, A., Yakhlef, H., Ghozlane, F. & Marie, M. 2013. Assessment of the sustainability of dairy cattle farms in the Birtouta area. Mitidja (Algeria) using the IDEA method. *Rencontres Recherches Ruminants*, 20 (in french).
- Benatallah, A. 2007. Assessment of the sustainability of the dairy cattle farms of the Mitidja. Thèse de Magister, INA. El Harrah (Alger), 187 pp. (in french).
- Benniou, R. & Aubry, C. 2009. Place and role of livestock in farming production systems in semi-arid regions of eastern Algeria. *Fourrages* **198**, 239–251 (in french).
- Bessaoud, O. 2006. La stratégie de développement rural en Algérie. *Options Méditerranéennes* **71**, 79–89 (in french).
- Bir, A. 2015. Analysis of the sustainability of dairy cattle breeding systems and their sensitivity to climatic hazards in difficult areas: the case of the Wilaya de Sétif. ENSA. Alger, 174 pp. (in french).
- Boukkedid, C. 2014. The use of productive resources in Algerian agriculture: Evolution and prospects. Thèse de magister en sciences économiques Université Constantine 2 Faculté des Sciences Economiques et des Sciences Commerciales et de Gestion, 323 pp. (in french).
- Bourenane, N., Campagne, P., Carvalho, A. & Elloumi, M. 1991. The question of pluriactivity in Algeria, France, Portugal and Tunisia. *Options Méditerranéennes* **5**, 23–50 (in french).

- Djebbara, M. 2004. The main constraints of the development of irrigated agriculture classified in large hydraulic in Algeria. Actes du Séminaire Modernisation de l'Agriculture Irriguée. Rabat du 19 au 23 avril 2004. IAV Hassan II, 13 pp. (in french).
- Douaoui, A., Hartani, T. & Lakehal, M. 2008. Salinization in the plain of Lower Chelif: achievements and perspectives, Water saving in Irrigated Systems in the Maghreb. Deuxième atelier régional du projet Sirma. 2006. Marrakech, Maroc (in french).
- El Mahi, T. 2005. Irrigation management in the perimeter of Middle Chelif. INA Département d'Economie Rurale, 98 pp. (in french).
- Fraser, D. 2006. Animal welfare and the intensification of animal production. Another interpretation. Document de la FAO sur l'éthique. 32 pp. (in french).
- General Census of Agriculture 2001. General report of the final results. Direction des Statistiques Agricoles et des Systèmes d'Information, Ministère de l'Agriculture et du Développement Rural, Alger, Algérie. 123 pp. (in french).
- Ghozlane, F., Belkheir, B. & Yakhlef, H. 2010. Impact of the National Fund for Agricultural Regulation and Development on the sustainability of dairy cattle in the Wilaya of Tizi-Ouzou (Algeria). *Mediterranean Journal of Economics, Agriculture and Environment* **9**, 22–27. (in french).
- Ghozlane, F., Yakhlef, H., Allane, M. & Bouzida, S. 2006. Assessment of the sustainability of dairy cattle farms in the Tizi-Ouzou Wilaya (Algeria). *Mediterranean Journal of Economics, Agriculture and Environment* **4**, 48–52 (in french).
- Hartani, T., Douaoui, A., Kuper, M. & Hassani, F. 2007. Strategies for individual management of salinity in the irrigated area of Lower Chelif: case of the Ouarizane perimeter. Troisième atelier régional du projet Sirma. Jun 2007. Nabeul Tunisie. CIRAD, 16 pp. (in french).
- Huyghe, C. & Delaby, L. 2013. Strategies for individual management of salinity in the irrigated area of Lower Chelif: case of the Ouarizane perimeter. 2^{ème} édition France agricole. Collection Agri Production, Paris, France, 529 pp. (in french).
- Le Gall, A., Faverdin, P., Thomet, P. & Verité, R., 2001. Grazing in New Zealand: Ideas for the watered regions of Europe. *Fourrages* **166**, 137–163 (in french).
- MADR 2013. Statistique agricoles série B. Ministère de l'Agriculture et du Développement Rural, Alger, Algérie, 64 pp. (in french).
- Evaluation of the sustainability of Tunisian dairy farms using IDEA method. *Biotechnologie, Agronomie, Société et Environnement* **13**(2), 221–228 (in french).
- Ozier-Lafontaine, H., Boval, M., Alexandre, G., Chave, M. & Grandisson, M. 2011. Towards the emergence of new sustainable farming systems for the satisfaction of food needs in the French West Indies. *Innovations Agronomiques* **16**(2011), 135–152. (in french).
- Si-Tayeb, H. 2015. *The transformations of Algerian agriculture in the perspective of accession to the WTO*. Thèse de Doctorat en Sciences Agronomiques. Université Mouloud Mammeri, Tizi-Ouzou, Algérie, 253 pp. (in french).
- Sneessens, I. 2014. *Does the complementarity between crops and livestock make it possible to improve the sustainability of farming production systems?* Université Blaise Pascal, Clermont-Ferrand. INRA Clermont Theix, France, 149 pp. (in french).
- Sraïri, MT. 2009. Typology of dairy cattle husbandry systems in Morocco for an analysis of their performance. Thèse de doctorat. FSA Gembloux, Belgique, 213 pp.
- Suttie, J. 2004. Hay and straw conservation: for small farmers and pastoralists. Collection FAO, Production végétale et protection des plante N°29, Rome, Italie, 24 pp. (in french).
- Veysset, P., Lherm, M., Bébin, D. & Roulenc, M. 2014 Mixed cropping-beef cattle farming: a sustainable beef production system? Farm Results, Questions and Perspectives. *Innovations Agronomiques* **39**, 83–97 (in french).
- Vilain, L. 2003. The IDEA method: farm sustainability indicators, User guide, second edition enriched and extended to arboriculture, gardening and horticulture. Educagri Editions, Dijon, France, 151 pp. (in french).

Yakhlef, H., Far, Z., Ghozlane, F., Madani, T. & Marie, M. 2008. Assessment of the sustainability of bovine agro-pastoral systems in the context of the semi-arid zone of Sétif (Algeria). *Mediterranean Journal of Economics, Agriculture and Environment* 4, 36–39. (in french).

Annexes:

Scale A --- agro-ecological				
Components	18 indicators		Maximum scores	
Domestic diversity	A1	Diversity of annual crops	14	Total capped at 33
	A2	Diversity of perennial crops	14	
	A3	Animal diversity	14	
	A4	Enhancement of genetic resources	6	
Space organization	A5	Cropping pattern	8	Total capped at 33
	A6	Plot size	6	
	A7	Organic matter management	5	
	A8	Ecological Buffer area	12	
	A9	Contribution to environmental issues	4	
	A10	Enhancement of space	5	
	A11	Forage area management	3	
Farming practices	A12	Nitrogen balance	8	Total capped at 34
	A13	Effluents processing	3	
	A14	Pesticides	13	
	A15	Veterinary treatments	3	
	A16	Soil resource protection	5	
	A17	Water resources management	4	
	A18	Energy dependence	10	
	Scale B --- Socio-territorial			
Components	18 indicators		Maximum scores	
Quality of products and territory	B1	Quality approach	10	Total capped at 33
	B2	Enhancement of buildings and landscape heritage	8	
	B3	Processing of non-organic waste	5	
	B4	Accessibility of space	5	
	B5	Social involvement	6	
Employment and services	B6	Short trade	7	Total capped at 33
	B7	Autonomy	10	
	B8	Services, multiactivities	5	
	B9	Contribution to employment	6	
	B10	Collective work	5	
	B11	Probable sustainability	3	
Ethics and human developmen	B12	Contribution to world food balance	10	Total capped at 334
	B13	Animal welfare	3	
	B14	Training	6	
	B15	Labor intensity	7	
	B16	Quality of life	6	
	B17	Isolotaion	3	
	B18	Reception, hygiene, and safety	4	
Scale C --- Économic				
Components	6 indicators		Maximum scores	
Economic Viability	C1	Economic Viability	20	30
Independence	C2	Economic specialization rate	10	25
	C3	Financial autonomy	15	
Transferability	C4	Sensitivity to aids	10	20
	C5	Capital transferability	20	
Efficiency	C6	Efficiency of production process	25	25

Field Bean (*Vicia faba* L.) Yield and Quality Depending on Some Agrotechnical Aspects

I. Plūduma-Pauniņa^{1,3,*}, Z. Gaile¹, B. Bankina² and R. Balodis¹

¹Latvia University of Life Sciences and Technologies, Faculty of Agriculture, Institute of Agrobiotechnology, Liela street 2, LV-3001, Jelgava, Latvia

²Latvia University of Life Sciences and Technologies, Faculty of Agriculture, Institute of Soil and Plant Science, Liela street 2, LV-3001, Jelgava, Latvia

³Latvia University of Life Sciences and Technologies, Faculty of Agriculture, Research and Study Farm "Pēterlauki", Platone parish, LV-3021, Latvia

*Correspondence: ievapluduma@inbox.lv

Abstract. Despite growing interest about field beans (*Vicia faba* L.), only few researches have been carried out in Baltic countries on the possibility to increase field beans' yield and quality depending on different agrotechnical measures. Field trial was carried out in 2015, 2016 and 2017. Researched factors during all years were: A – variety ('Laura', 'Boxer', 'Isabell'), B – seeding rate (30, 40 and 50 germinate able seeds m⁻²), C – treatment with fungicide (with and without application of fungicide). Beans' yield (t ha⁻¹) and yield quality characteristics were detected in the trial. Temperature and moisture conditions were mostly suitable for high yield formation of field beans in all three trial years. In all three trial years, field bean yield has been significantly affected by all factors. The highest yield ($p = 0.001$) was provided by variety 'Boxer' in all years (6.10–7.74 t ha⁻¹). Thousand seed weight (TSW) was significantly affected by variety and fungicide application. From agronomical point of view, crude protein level was not importantly affected by seeding rate changes or fungicide application. Volume weight was affected significantly by increased seeding rate only in 2016. Fungicide application also did not affect volume weight significantly during the whole trial period. Field bean yield increased by each year, but the main tendencies in all years were the same: higher yield and TSW was provided by variety 'Boxer', but higher protein content and volume weight – by 'Isabell'. Seeding rate increase gave positive impact on yield. Fungicide application affected field bean yield, but did not affect its quality significantly.

Key words: field beans, agrotechnology, fungicide application, seeding rate, variety.

INTRODUCTION

Field beans (*Vicia faba* L.), also known as faba or broad beans, is a plant which is widely used all around the world. It is the third most important leguminous plant after soybeans (*Glycine max* L.) and peas (*Pisum sativum* L.) (Singh et al., 2013). According to FAO-stat data, the biggest field bean producing countries depending on production quantity in 2016 were China, Ethiopia and Australia².

² FAO-stat data base. <http://www.fao.org/faostat/en/#data/QC>. Accessed 18.01.2018.

Field beans are mainly grown for seed production, which are used not only for animal feed but also for food. It is also grown for green forage because it has high nutritional value and crude protein content, but it is not the main reason for field beans growing. In addition, field beans are very suitable for crop rotation, because they improve soil fertility and leave good effect on after-crops (Sahile et al., 2008).

Due to the growing demand for crop products including crude protein sources and increasing pressure on economic and environmental requirements in agro-ecosystems, legumes (also field beans) could play a major role in the crop production system (Stagnari et al., 2017).

During the last decades there have not been a lot of studies about field beans in Baltic countries or even in Northern Europe. As field bean cultivation is becoming more and more relevant, various studies are started on the effect of variety and seeding rate on the yield of field beans. So far, few studies have been conducted in Latvia about the incidence and severity of diseases, but additional studies are necessary to evaluate the effects of disease control on the yield and quality of field beans. The four-factor research about field beans described in this article is the first so extensive study in Latvia in the 21st century. The aim of this study was to evaluate the effect of seeding rate, variety, fungicide application and conditions of a year on the yield and quality of field beans.

MATERIALS AND METHODS

Field trial was carried out at the Research and Study Farm 'Pēterlauki', (56°32'31.2"N 23°42'57.6"E), Latvia. Trial was operated for three years – 2015, 2016 and 2017. Every year the effect of three research factors (variety (three varieties – 'Laura', 'Boxer', 'Isabell'), seeding rate (three seeding rates – 30, 40 and 50 germinate able seeds m⁻²) and fungicide application (without fungicide and with fungicide Signum (boscalid, 267.0 g kg⁻¹, pyraclostrobin, 67.0 g kg⁻¹) application) was estimated. In total, 18 variants in four replications were sown each trial year. Varieties 'Laura' and 'Boxer' are the most popular among growers, but variety 'Isabell' was chosen because of its high protein content.

The soil at the site was a well-cultivated Endocalcaric Abruptic Luvisol (Cutanic, Hypereutric, Raptic, Siltic, Protostagnic, Epiprotovertic) (World Reference Base, 2014), silt loam which is suitable for field bean cultivation. Traditional soil tillage (ploughing in the previous autumn and soil cultivation before sowing) was used. Sowing date depended on meteorological conditions of the year and soil readiness for sowing: 26 March 2015, 05 April 2016, and 04 April 2017).

Fertilizing and spraying of plant protection products was carried out as necessary. Before sowing the fertilizer NPK 15-15-15+S (220–230 kg ha⁻¹) was incorporated into the soil, but foliar fertilizer (Yara Vita Bortrac and Yara Vita Brassitrel) was given at the same time as some of plant protection products. During the trial, herbicides Stomp CS (pendimethalin, 330.0 g L⁻¹) (all years, GS 07), Basagran 480 (bendioxide, 480.0 g L⁻¹) (2016; 2017, GS 14), Targa Super (quizalofop-P-etil, 50 g L⁻¹) (2016, GS 50) and Focus Ultra (cycloxydim, 100 g L⁻¹) (2017, GS 50) were used. Insecticides Fastac 50 (alpha-cypermethrin, 50.0 g L⁻¹) (GS 50) and Proteus OD (thiacloprid, 100 g L⁻¹, deltamethrin, 10 g L⁻¹) (GS 61–65) were used during all three trial years. Fungicide Signum was sprayed at the start of flowering (GS 61–65, depending on the trial year) based on trial scheme.

During vegetation, recordings of phenological observations were performed. Severity (0–9 point scale) of diseases on the leaves was assessed every week after emerging of the first symptoms (not analysed in this paper in detail).

Yield was directly harvested from each plot and recalculated to standard moisture level (14%) and 100% purity. Quality characteristics were detected from the harvested yield. Crude protein content (%) was detected using Infratec Analyzer 1241 (FOSS), thousand seed weight (TSW) (g) was detected according to the standard method LVS EN ISO 520, and volume weight (g L^{-1}) – according to the standard method LVS 273.

In 2015, temperature during germination of field beans was low, hence crop germination took longer time, but later the vegetation season was characterized as warm and sufficiently secured by humidity. At the second part of the season, temperatures increased significantly and drought was observed. In the second trial year (2016), the season began with warm weather and sufficient moisture provision. In the middle and end of field beans' vegetation season the amount of moisture exceeded significantly the long-term observations. Meteorological conditions were warm but overly wet to harvest beans on time. Vegetation season of the last trial year (2017) started with a bit cold weather, therefore field bean emergence was longer than in previous two years. Vegetation season was characterized as cool and with a high amount of precipitation, which delayed the harvest time for almost a month. Overall, despite the mentioned extremes, the meteorological conditions favoured high yield formation of field beans in all years.

For data mathematical processing three- and four-factor analysis of variance and correlation analysis was employed. Bonferroni test was used for comparison of factors' means. Variants are considered significantly different when $p \leq 0.05$. Data processing was performed using SPSS 15 and MS Excel software.

RESULTS AND DISCUSSION

Yield. Yield is the most important indicator, by which growers choose exact variety and the most suitable seeding rate, or the application of other agrotechnical measures. Experimental results of the three year trials allowed to reason about importance of the researched factors (variety, seeding rate and fungicide application) and meteorological conditions on field beans yield (Table 1) and quality (Table 2; Figs 1, 2).

High average yield ($5.89\text{--}7.38 \text{ t ha}^{-1}$, Table 1) of the field beans was obtained during all three trial years, however, yield differed significantly among them. In 2017, yield was the highest ($p < 0.001$) that can be explained by regular precipitation and comparatively moderate temperature. The lowest yield in 2015 can be explained by the drought at pod filling stage.

Variety 'Boxer' showed significantly ($p < 0.001$) higher average yield during all three trial years when compared with other two varieties. Nevertheless, the average yield of variety 'Laura' was higher if compared to 'Isabell'. In 2015, the yield of varieties 'Boxer' and 'Laura' did not differ significantly ($p = 0.386$), while variety 'Isabell' yielded significantly less. During the second year of the trial, significant differences ($p < 0.001$) of yield between all three varieties were observed, but still 'Boxer' provided the highest seed yield. The same was observed in the third trial year (2017) – 'Boxer' showed significantly higher yield ($p < 0.01$), but no significant differences were

observed between yields of varieties ‘Laura’ and ‘Isabell’ ($p = 1$). The highest yield of variety ‘Boxer’ could be explained with the highest value of one of the yield components, namely 1,000 seed weight. We found medium strong positive correlation between yield and 1,000 seed weight ($r = 0.697$; $n = 54$; $p = 0.01$).

Table 1. Yield (t ha⁻¹) depending on researched factors

Factors	Year			Average
	2015	2016	2017	
Variety ($p = 0.001$)				
‘Laura’	5.99 ^a	6.26 ^b	7.25 ^b	6.50 ^B
‘Boxer’	6.10 ^a	6.72 ^a	7.74 ^a	6.85 ^A
‘Isabell’	5.57 ^b	5.78 ^c	7.15 ^b	6.17 ^C
Seeding rate (germinate able seeds m ⁻²) ($p = 0.001$)				
30	5.52 ^b	5.85 ^c	7.18 ^b	6.18 ^B
40	6.01 ^a	6.18 ^b	7.36 ^{a,b}	6.51 ^{A,B}
50	6.13 ^a	6.73 ^a	7.60 ^a	6.82 ^A
Fungicide application ($p = 0.001$)				
F0	5.80 ^b	5.96 ^b	6.90 ^b	6.22 ^B
F1	5.97 ^a	6.54 ^a	7.85 ^a	6.79 ^A
Average	5.89 ^C	6.25 ^B	7.38 ^A	×

F0 – without fungicide application; F1 – with fungicide application; Significantly different means are labelled with different letters in superscript: ^{A, B, C} – significant difference for average yields of three trial years and means of factors’ gradations; ^{a, b, c} – significant difference in a specific trial year.

Significant influence of trial site, year, and variety on field beans’ yield was also shown by other researches in Latvia. Thus, in the Priekuļi Field Crops Breeding Institute (currently Institute of Agricultural Resources and Economics, Priekuļi Research Centre) in 2013, two of varieties used in the current experiment were compared. Average yield of variety ‘Laura’ (3.56 t ha⁻¹) was significantly higher than that of ‘Isabell’ (2.28 t ha⁻¹), but in 2014, the yield of ‘Laura’ was higher than the yield of variety ‘Boxer’ (Zute et al., 2014). The same varieties were compared also elsewhere in Latvia – at the Stende Cereals Breeding Institute (currently Institute of Agricultural Resources and Economics, Stende Research Centre) during the same years. This time contrary to the previously mentioned results yield of variety ‘Isabell’ was higher (average 5.77 t ha⁻¹) than that of variety ‘Laura’ (5.61 t ha⁻¹), but the difference was small (Zute, 2014). In another experiment, operated in Priekuļi Field Crops Breeding Institute, while cultivating field beans conventionally in 2013, the highest yield among three varieties was provided by ‘Isabell’, but yield was not significantly higher than that of ‘Laura’ and ‘Boxer’ (Zute et al., 2014).

The biggest seeding rate (50 germinate able seeds m⁻²) ensured the highest seed yield in all three experimental years. In 2015, significantly ($p < 0.001$) smaller yield was obtained using only 30 germinate able seeds m⁻². In the second year (2016), significant difference ($p < 0.05$; Table 1) was observed between yields obtained sowing all three seeding rates. In the third trial year, again significant difference was observed only between yield obtained sowing the smallest and the biggest seeding rate (30 and 50 germinate able seeds m⁻² respectively) ($p = 0.007$). At the same time, yields did not differ significantly in plots where 30 and 40 germinate able seeds per m² were sown. The same tendency as in 2017 was observed on average per all three years ($p < 0.001$) (Table 1).

In Latvia, a study by Holms (1967) carried out decades ago, showed that sowing of 33 germinate able seeds m⁻² gave a bit smaller yield than using 41 germinate able seed m⁻². The same tendency is visible in our experiment – by increasing the seeding rate also the yield increases, and our result conforms with the results of Holms (1967) that the highest yield is provided by 50 germinate able seeds m⁻² despite the use of varieties bred with 50 year difference in age.

Works by other authors (Lopez-Bellido et al., 2005) confirm the effect of different seeding rate depending on varieties, climatic conditions, vegetation duration and sowing time. It has been observed that at a certain level the seeding rate increase no longer gives an increase in yield. Even the opposite effect is observed – the yield begins to decrease, which can be explained by intra-species plant competition and self-regulation of plant density (Kikuzawa, 1999; Yucel, 2013). Field beans’ seeding rates used in our study were selected within the limits, where yield loss due to increased plant density was not observed.

Spectrum of diseases and their severity varied depending on the year. Chocolate spot (caused by *Botrytis* spp.) and leaf blotch caused by *Alternaria/Stemphylium* complex were observed every year. Faba bean rust (caused by *Uromyces viciae-fabae*) was also observed, but its severity was low, therefore, it did not affect the growth and development of field beans (Bankina et al., 2016). Downy mildew (caused by *Peronospora viciae*) was the most important disease in 2017. In all three trial years (2015–2017), fungicide application gave significant yield increase (respectively 2015 – $p < 0.01$; 2016 and 2017 – $p < 0.001$). In 2015, yield increase in variant with fungicide application was mathematically significant, but small in reality – 0.17 t ha⁻¹ (Table 1). It can be mostly explained with low disease pressure in 2015. As field bean growing area in Latvia increased and meteorological conditions in addition were favourable for diseases development, incidence of diseases also increased during 2016 and 2017, and fungicide application provided higher yield increase (0.58 and 0.95 t ha⁻¹ respectively).

Thousand seed weight (TSW) is a stable indicator that is closely related to the variety characteristics. It is an important indicator for the quality of the crop, which is at the same time also a yield component.

TSW was significantly affected by all researched factors. Variety, fungicide application and trial year provided the most significant influence ($p < 0.001$) on TSW (Table 2).

Table 2. TSW (g) depending on researched factors

Factors	Year			Average
	2015	2016	2017	
Variety ($p = 0.001$)				
‘Laura’	553 ^b	518 ^c	568 ^b	546 ^B
‘Boxer’	593 ^a	576 ^a	598 ^a	589 ^A
‘Isabell’	532 ^c	536 ^b	570 ^b	546 ^B
Fungicide application ($p = 0.001$)				
F0	553 ^b	527 ^b	557 ^b	546 ^B
F1	565 ^a	560 ^a	600 ^a	575 ^A
Average	559 ^B	544 ^C	579 ^A	×

F0 – without fungicide application; F1 – with fungicide application; Significantly different means are labelled with different letters in superscript: ^{A, B, C} – significant difference for average TSW of three trial years and means of factors’ gradations; ^{a, b, c} – significant difference in a specific trial year.

TSW of variety 'Boxer' was significantly higher in all trial years if compared with other two varieties ($p < 0.001$). Between TSW of varieties 'Laura' and 'Isabell' significant differences were observed in 2015 ($p < 0.001$) and 2016 ($p < 0.01$), but significant differences between their TSW were not observed on average per all three trial years.

Fungicide application affected TSW significantly as well ($p < 0.001$): TSW of field beans increased in variant where fungicide was applied. Especially in 2016 and 2017, when higher disease severity was observed, fungicide application provided more distinct effect on TSW increase. It can be mostly explained with a prolongation of leaf green area functioning, and plants can fill seeds in pods for a longer period. Similar results on fungicide influence on TSW were observed in Spain, where several fungicides were compared. Some of the fungicides used cause a mathematically significant increase of TSW, although it was not economically significant (Emeran et al., 2011).

Average TSW was significantly different ($p < 0.001$) depending on conditions in trial years. Significantly highest TSW, just like the highest yield, was observed in 2017 when moisture provision was even and air temperature – moderate.

TSW was also affected by seeding rate ($p < 0.01$). In the first trial year (2015), highest TSW was observed in variants where 50 germinate able seeds m^{-2} were sown, but it did not significantly differ from TSW in variant where 40 germinate able seeds m^{-2} were sown. Plants formed less pods and seeds in plots where 50 germinate able seeds m^{-2} were sown in 2015. As drought was observed during pod and seed fill, plants could ensure higher 1,000 seed weight, when less seeds per plant had to be fulfilled. In 2016, significant difference between any of seeding rate's variants was not observed. In 2017, highest TSW was observed in variant where 40 germinate able seeds m^{-2} (582 g) were sown, which significantly differed from TSW in variant where 50 germinate able seeds m^{-2} (574 g) ($p = 0.028$) were sown. On average, the tendency remained that by increasing seeding rate TSW increased. A similar trend has been observed by Holms (1967) in some years, although he indicated that mainly TSW is higher in thinner stands.

Crude protein (CP) content. The most important field bean seed quality parameter is the CP content in seeds. In this trial all factors affected CP content significantly, and the greatest influence was provided by variety and trial year (Fig. 1).

In 2015, the highest CP content was provided by the variety 'Boxer', but it did not significantly differ from that of other two varieties ($p = 1$). During 2016 and 2017, and on average per three years, the significantly highest CP content in seeds was provided by variety 'Isabell' ($p < 0.001$). CP content in field beans' seeds depends on the genetic characteristics of the variety, and on the genotype response to the meteorological conditions of the particular year. In Germany it is noted that varieties with yields rising above 5 t ha^{-1} have a tendency to exhibit lower crude protein content than lower yielding varieties. This could be explained by the *Rhizobium* bacteria ability to provide appropriate amount of nitrogen. The plant may not be able to assimilate the needed amount of nitrogen to achieve high crude protein content in high yields (Witten et al., 2015). This is established also in our experiment – variety 'Isabell' was the lowest yielding, but showed the highest CP content in seeds.

Seeding rate had a significant effect on CP content in seeds ($p = 0.045$). In all three years, CP content tended to be higher in variants when higher seeding rate was used. The same tendency was observed in trials in Egypt, where increase of seeding rate significantly increased the CP content in seeds (Bakry et al., 2011).

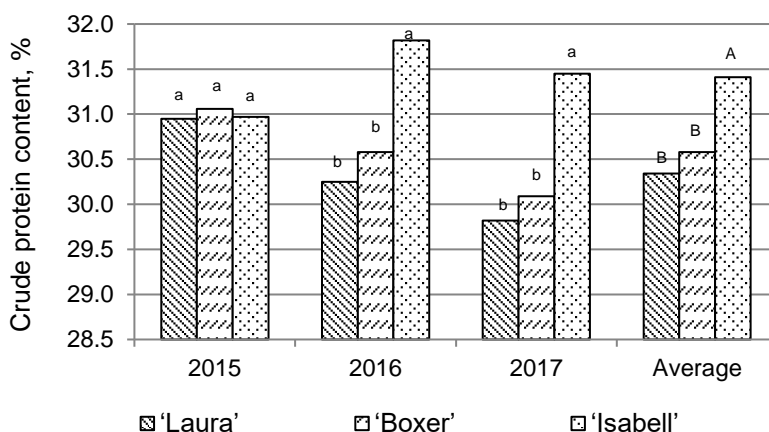


Figure 1. Crude protein content (%) in field beans' seeds depending on variety and trial year. A, B, C – significant difference on average per three trial years; ^{a,b,c} – significant difference between varieties in specific year.

In 2015, fungicide application raised CP content significantly ($p = 0.005$). Looking at the overall results of all three research years, the same tendency can be observed – application of fungicide increased the CP content in seeds significantly ($p = 0.046$). However, no significant effect of fungicide application on CP increase was observed in 2016 and 2017 ($p = 0.396$, $p = 0.789$ respectively). Positive effect of fungicide application on CP content is highlighted by a study in Poland (Micek et al., 2015). But a significant reduction of CP content in seeds is observed if seeds are treated with fungicide prior sowing (Ahmed & Elsheikh, 2010).

Overall obtained crude protein content in this trial is characterized as high and characteristic for varieties.

Volume weight. Volume weight is also a criterion used to determine quality of seeds and to measure the seed bulk density. Volume weight is significantly affected by variety and trial year ($p < 0.001$) (Fig. 2). The highest ($p < 0.001$) volume weight in all three years was provided by variety 'Isabell', (on average 807 g L^{-1}). In 2015 and 2016, volume weight of varieties 'Laura' and 'Boxer' was significantly different ($p < 0.05$), but in 2017, no significant difference ($p = 0.808$) between volume weights of these two varieties was observed. Average three year values of volume weight were significantly different between all three varieties ($p < 0.01$). The lowest volume weight was provided by variety 'Boxer' (on average 797 g L^{-1}). Between TSW and volume weight a close, negative correlation was detected. It means that with the TSW increase, the volume weight decreases. That is why variety 'Isabell' characterised with the lowest TSW provided the highest volume weight, but variety 'Boxer' provided lowest volume weight, while its TSW was the highest.

In 2015, the highest average field beans seed volume weight between three trial years (average 821 g L^{-1} ; $p < 0.001$) was observed. No significant difference ($p = 0.080$) was observed between the volume weights in 2016 and 2017 (791 and 792 g L^{-1} , respectively). It could be explained by weather conditions at the end of each year's vegetation period. In 2015, weather conditions at the pod filling stage were hot and dry, seeds were smaller, could better mature, thus the volume weight was higher. In other

two years (2016, 2017) sufficient moisture was provided not only during the pod filling, but during the whole vegetation period, and volume weight was lower.

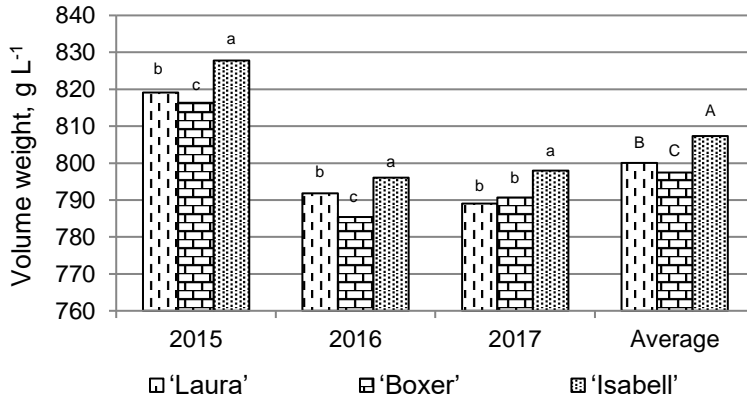


Figure 2. Volume weight (g L⁻¹) of field bean seeds depending on variety and trial year. A, B, C – significant difference on average per three trial years; ^{a,b,c} – significant difference between varieties in specific year.

Volume weight was not significantly affected by the used seeding rate ($p = 0.470$) and fungicide application ($p = 0.829$).

CONCLUSIONS

Field bean yield, thousand seed weight and crude protein content were affected by all researched factors – variety, seeding rate, fungicide application and conditions of the year. Variety ‘Boxer’ provided the highest yield and thousand seed weight; however, the highest crude protein content and volume weight was provided by variety ‘Isabell’.

The increase of the seeding rate up to 50 germinate able seeds m⁻² gave significantly positive impact on yield, TSW and crude protein content in seeds. Thus, it is advisable to use the highest seeding rate from investigated for field bean sowing.

Application of fungicide increased field beans’ seed yield and 1,000 seed weight significantly, especially in 2016 and 2017, when higher disease severity was observed. Average crude protein content in seeds was also increased by fungicide application; however, the results of separate trial years were contradictory.

Although high yield and seed quality was obtained in all three trial years, the significant influence of meteorological conditions on all evaluated parameters was observed. Especially yield and 1,000 seed weight was affected by drought in pod filling stage in 2015.

ACKNOWLEDGEMENTS. Research was carried out by the financial support of RSF “Pēterlauki” of LLU.

REFERENCES

- Ahmed, T.H.M. & Elsheikh, E.A.E. 2010. Effects of fungicide treatment and rhizobium inoculation on chemical composition of faba bean, *Vicia faba* L. seeds. *Journal of Soil Sciences and Agricultural Engineering* **1**(4), 219–228.
- Bakry, B.A., Elewa, T.A., El-Karamany, M.F., Zeidan, M.S. & Tawfik, M.M. 2011. Effect of row spacing on yield and its components of some faba bean varieties under newly reclaimed sandy soil condition. *World Journal of Agricultural Sciences* **7**(1), 68–72.
- Bankina, B., Bimšteine, G., Roga, A., Fridmanis, D. 2016. Leaf diseases – an emerging problem in the sowings of faba bean in Latvia. In *ESA 14 – Growing Landscapes – Cultivating Innovative Agricultural Systems: Conference*, Edinburgh, pp. 15–16.
- Emeran, A.A., Sillero J.C., Fernandez – Aparicio M. & Rubiales D. 2011. Chemical control of faba bean rust (*Uromyces viciae – fabae*). *Crop Protection* **30**, 907–912.
- Holms, I. 1967. Research on Field Beans Agrotechnology in Latvia SSR: Theses for Earning the Degree of Candidate of Agriculture Sciences. Latvia Academy of Agriculture, Faculty of Agronomy. 269 pp. (in Latvian).
- Kikuzawa, K. 1999. Theoretical relationships between mean plant size, size distribution and self-thinning under one-sided competition. *Annals of Botany* **83**, 11–18.
- Lopez-Bellido, F.J., Lopez-Bellido, L. & Lopez-Bellido, R.J. 2005. Competition, growth and yield of faba bean (*Vicia faba* L.). *Europ. J. Agronomy* **23**, 359–378.
- Micek, P., Kowalski, Z.M., Kulig, B., Kanski, J. & Slota, K. 2015. Effect of variety and plant protection method on chemical composition and In vitro digestibility of faba bean (*Vicia faba*) seeds. *Ann. Anim. Sci.* **15**(1), 143–154.
- Sahile, S., Fininsa, C., Sakhuja, P.K. & Ahmed, S. 2008. Effect of mixed cropping and fungicides on chocolate spot (*Botrytis fabae*) of faba bean (*Vicia faba*) in Ethiopia. *Crop Protection* **27**, 275–282.
- Singh, A.K., Bharati, R.C., Manibhushan, N.C. & Pedpati, A. 2013. An assesment of faba bean (*Vicia faba* L.) current status and future prospect. *African Journal of Agricultural Research* **8**(55), 6634– 6641.
- Stagnari, F., Maggio, A., Galieni, A. & Pisante, M. 2017. Multiple benefits of legumes for agriculture sustainability: an overview. *Chemical and Biological Technologies in Agriculture* **4**, 1–13.
- Witten, S., Bohm, H., Aulrich, K. 2015. Effect of variety and environment on the contents of crude nutrients, lysine, methionine and cysteine in organically produced field peas (*Pisum sativum* L.) and field beans (*Vicia faba* L.). *Landbauforsch – Appl Agric Forestry Res.* **65**, 205–216.
- Yucel, D.O. 2013. Impact of plant density on yield and yield components of pea (*Pisum sativum* ssp. *sativum* L.) cultivars. *ARPJ Journal of Agricultural and Biological Science* **8**(2), 169–174.
- Zute, S. 2014. Field beans – challenges and opportunities for forage producers. In *Demonstrations in Crop and Animal Production 2014*, Latvian Rural Advisory Centre, Ozolnieki, pp. 58–60 (in Latvian).
- Zute, S., Aplociņa, E. & Zariņa, L. 2014. Pulses – alternative for production of protein-rich fodder without use of soybean: agro-technical and economical substantiation in Latvia: Scientific Project financed by Ministry of Agriculture of Republic of Latvia (In Latvian). https://www.zm.gov.lv/public/ck/files/ZM/lauku_attistiba/zinatne/P%C4%81k%C5%A1au gi%20ZM%20512_2014.pdf. Accessed: 24.01.2018.

Analysis of Hop Drying in Chamber Dryer

A. Rybka*, P. Heřmánek and I. Honzík

Czech University of Life Sciences Prague, Faculty of Engineering, Department of Agricultural Machines, Kamýcká 129, CZ165 00 Praha 6 – Suchbát, Czech Republic

*Correspondence: rybka@tf.czu.cz

Abstract. This article is aimed at the analysis of the hop drying process that has been carried out in the chamber dryer of Rakochmel Co. Ltd. in Kolečovice with the Saaz hop variety. The values measured by means of dataloggers as well as fixed sensors show an identical trend. When the hops fall over from one slat box onto another, the drying air temperature declines and the relative humidity rises. A sharp increase in the relative humidity gradually decreases starting with the first slat box and finishing with the emptying conveyor, which points to a gradual levelling of the relative humidity and hop moisture. The hop moisture content, determined from laboratory samples, logically decreases depending on the measurement time. In comparison to belt dryers, chamber dryers clearly ensure continuous and more gentle drying during which the hops are not overdried and a moisture content of 10% is achieved practically only at the outlet of the dryer prior to conditioning.

Key words: hop cones; dryer monitoring; quality of hops.

INTRODUCTION

The vast majority of growers uses belt dryers for hop drying, most of them date back to the 60s of the last century and are technically outdated. Parallel to these also some older types of chamber dryers are partially used. Based on foreign experience, their principle of drying has the potential for further usage (Doe & Menary, 1979; Kořen et al. 2008).

During the process of drying the moisture content in hop cones is reduced from the initial approx. 75–85% to 5–7% which is a significant excessive drying due to required drying of the cone strig. Inside the dryer the hops are exposed to a drying temperature of 55–60% for 6–8 hours. Afterwards, the hop cones need to be conditioned to their final moisture of 10–12% (Rybka et al., 2017). However, for some heat-labile substances the drying temperatures mainly in the final stage of drying are too high, besides the long period of drying. This procedure leads to irreversible transformations and losses. Such substances are for instance hop essential oils that are contained in the amount of 0.5–3.5%, depending on hop variety (Hofmann et al., 2013; Kumhála et al., 2013). The pilot studies showed that under current conditions there is a decrease of 15 to 25% of the overall content of essential oils present in the hops prior to drying (Kieninger & Forster, 1973; Kirchmeier et al., 2005).

One possible solution to the above-mentioned state is developing a new concept for low-temperature drying of some special hop varieties in a chamber dryer (Heřmánek et al., 2017). In case of low-temperature drying at a drying temperature of approx. 40% no energy savings can be expected, but the main economic benefit will lie in the improvement of the product quality and the growers will be able to sell this product for higher prices (Podsedník, 2001; Hanousek et al., 2008). The new method of drying must enable to diversify temperatures and optimise drying parameters primarily for special hop varieties for which it is desirable to preserve, to the extent possible, their original composition (Rybáček et al., 1980; Srivastava et al., 2006; Kumhála et al., 2016). The heat-labile substances will be able to be used in processing in the sector of medicines and food supplements.

The study objective is therefore an analysis of the current state of hop drying in chamber dryer which needs to precede in content the innovation in the entire process of hop drying (Aboltins & Palabinskis, 2016; Aboltins & Palabinskis, 2017).

MATERIALS AND METHODS

The measurement was carried out in 4KSCH chamber dryer of Rakochmel Co. Ltd. Kolečovice with the Saaz hop variety. The given variety has a long tradition in the Czech Republic and is grown on approx. 87% of hop acreage. The Rakochmel company grows only this variety on an area covering 152 ha. The company is equipped with a chamber dryer suitable for the given experiments. The chamber dryer has four drying chambers located in twos in separate shafts with independent heating aggregates. The measurement each time involved one chamber in each shaft (the first and third chamber).

Inside the dryer temperature and air-conditioning parameters of the drying medium as well as qualitative parameters of dried hops (temperature, moisture, HSI – Hop Storage Index, alpha and beta bitter acids, drying time) were measured. The measured data were subsequently assessed.

The parameters were identified in three different ways:

- by measuring the air temperature and humidity using fixed sensors installed on the dryer wall,
- by measuring the air temperature and humidity using inserted dataloggers,
- by means of a laboratory analysis of the samples.

Each of these methods had different conditions for measuring and different measurement accuracy (Vitázek & Havelka, 2014).

Apart from monitoring the dryer, another objective was to assess the methods applied and to compare them between themselves.

On the dryer walls, there were installed nine fixed sensors. In the first and third chamber one sensor was placed by each slat and emptying conveyor (i.e. 8 altogether) and the ninth sensor was placed at the conditioning outlet. DL1 datalogger was placed in the first chamber and DL2 datalogger in the third chamber. The samples for the purposes of laboratory analyses were taken at filling and then successively from each of the three slat boxes immediately prior to the hops being poured down, from the emptying conveyor and at the end of conditioning (Fig. 1).

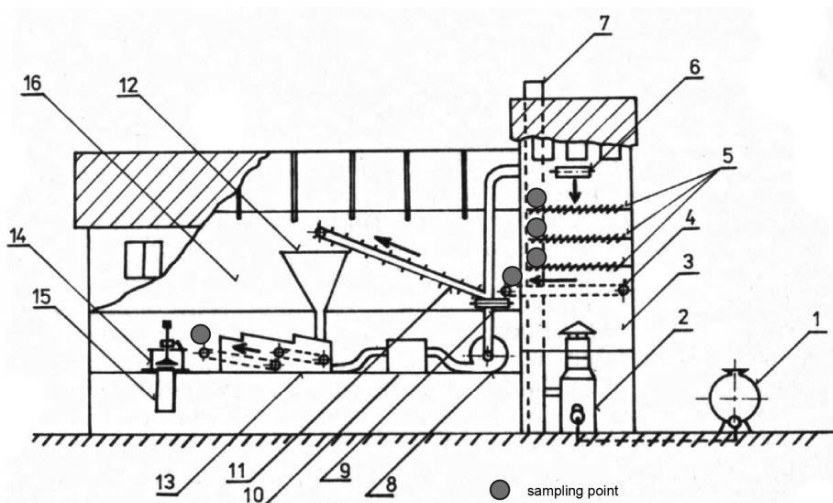


Figure 1. Scheme of the chamber dryer with marked points where samples are collected for laboratory tests: 1 – fuel tank; 2 hot-air aggregate; 3 – drying chamber; 4 – emptying conveyor; 5 – slat system; 6 – filling conveyor; 7 – chimney stack; 8 – draught fan; 9 – transverse takeaway conveyor; 10 – air filter; 11 – elevator conveyor; 12 – container; 13 – conditioning; 14 – press; 15 – prism; 16 – storage area.

Measuring by means of sensors installed on the dryer walls

On the dryer walls the assembly of Comet T3419 temperature and relative humidity fixed sensors was completed. They were always 8 sensors in a row connected to a Comet MS6D multi-channel datalogger. On the dryer 9 sensors and two multi-channel dataloggers had to be installed. All data from the multi-channel dataloggers were automatically stored in the computer on its hard disc.

Comet T3419 sensors had been installed by each of the three slat boxes and the emptying conveyor of the first and third chamber and one more at the outlet of the conditioning. The frequency of reading the values was set to 5 min. Immediate measured values could be read on the connected two-line display, which at the same time showed the actual temperature in °C and relative humidity in %. Together with the data reflecting temperature and relative humidity the exact time of measurement was also stored by means of which the data collected from all the different ways of measuring could be matched up.

Measuring by means of dataloggers

For continuous measurement of the air temperature and relative humidity in a layer of hops being dried VOLTcraft DL-121-TH dataloggers were used which enabled to programme the frequency of data storage (Jech et al., 2011; Jokiniemi et al., 2015).

In our case the frequency of data storage was set to 5 min, similarly to the fixed sensors. A datalogger is integrated together with a sensor in a plastic case and its power is supplied by an inserted battery. The plastic case is fitted with a USB connector at its one end via which the stored data are imported into the computer.

To protect the dataloggers against mechanical damage while carried throughout the dryer as well as against dirt we fixed the dataloggers rigidly in polyurethane foam and inserted them between two stainless sieves half-spherical in form. This was the best guarantee of protection and at the same time the sieves did not impede the air permeability (Fig. 2).

The advantage of the dataloggers compared to the rigidly fixed sensors in the dryer was that the dataloggers were carried together with hops through the dryer, continuously sensing the entire drying process.

In both chambers the dataloggers were placed one by one in filling. They were removed after having passed through the dryer and conditioning.



Figure 2. Placing a datalogger into a protective sieve.

Laboratory analyses of the samples

The laboratory analyses monitored the moisture content of all hop samples, which was subsequently compared with the drying medium relative humidity measured by means of dataloggers and fixed sensors in the dryer. At the same time the values of HSI and content of alpha and beta bitter acids in hop cones were determined (Claus et al., 1978; Green & Osborne, 1993).

Determination of moisture content in hops.

The moisture content of hops was determined gravimetrically as the weight loss of a defined amount of water during drying at a temperature of 105 °C for 60 min (Henderson & Miller, 1972; Henderson, 1973).

Determination of HSI in hop cones.

Hop storage index (HSI) is a dimensionless parameter that characterizes the level of hop ageing during storage and processing after harvest. Its numeric value is obtained as absorbance ratio of toluene hop extract in alkaline methanol solution at wavelengths of 275 and 325 nm. In green hops the value of this index is 0.20–0.25, immediately after drying ranges between 0.25 and 0.30. Its value continues rising constantly and irreversibly during further storage. In old hops the HIS values can be measured within an interval of 1.0–2.0.

Determination of alpha and beta bitter acid content and of DMX in hop cones.

Alpha and beta bitter acids as well as DMX are determined by liquid chromatography following the EBC 7.7 conventional method (Ono et al., 1984; Krofta, 2008).

RESULTS AND DISCUSSION

When entering the dryer, harvested hops are checked for their technical ripeness. The cone colour was bright yellow-green with natural gloss, the aroma was distinct and typical for that variety. The presence of biological impurities (leaves, parts of hop vines, stems) was proportionate, non-biological impurities there were none.

The results from the dataloggers as well as from the measurements by means of fixed sensors and the results of laboratory analyses are in Table 1 and graphical compared in Figs 3–6.

Table 1. Parameters of drying process

Measurement date:		Site:		Hop variety:										
24. 8. 2016		Rakochmel Co. Ltd. Kolečovice, CHAMBER DRYER 4KSCH							Saaz					
Dryer chamber		1					3							
Sampling point		Filling		1st slats prior to pouring down	2nd slats prior to pouring down	3rd slats prior to pouring down	Emptying conveyor		Filling		1st slats prior to pouring down	2nd slats prior to pouring down	3rd slats prior to pouring down	Emptying conveyor
Sampling time (in hh:mm format)		10:40		12:21	14:21	16:21	8:21		11:43		13:25	15:21	7:21	19:29
Measurement time		min	0	101	221	341	461		0	102	218	338	466	
Sensors		Temperature	°C	31.8	37.9	54.6	56.5	54.9	28.4	33.1	51.8	54.9	55.4	
		Rel. humidity	%	74.8	55.4	14.0	11.0	10.5	91.9	80.3	18.4	10.0	9.5	
DL1 datalogger		Temperature	°C	30.2	46.2	54.3	56.5	56.8						
		Rel. humidity	%	72.7	23.7	14.5	13.7	13.1						
DL2 datalogger		Temperature	°C						29.3	36.9	40.6	52.2	53.2	
		Rel. humidity	%						81.4	60.9	31.6	14.8	18.4	
Laboratory analyses of hops		Temperature	%	73.6	56.0	39.8	13.4	10.6	81.8	64.4	52.0	29.4	13.8	
		HSI		0.239	0.249	0.253	0.252	0.255	0.240	0.241	0.242	0.248	0.250	
		Alpha	%	4.49	4.31	4.23	4.18	3.38	4.60	5.03	4.98	4.20	4.26	
		Beta	%	7.49	6.47	6.82	6.15	5.25	6.61	7.09	6.71	6.19	6.21	

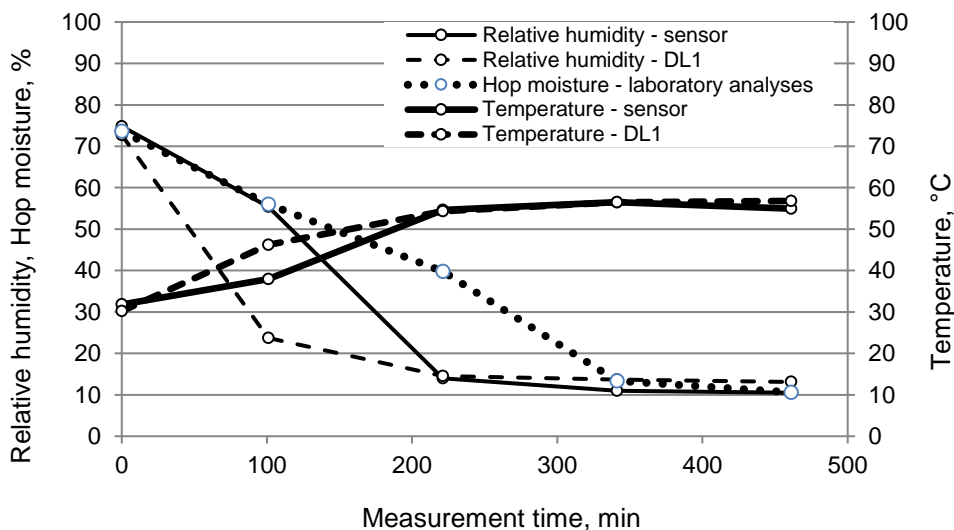


Figure 3. First chamber – datalogger (DL1), fixed sensors and laboratory analyses – dependence of temperature, relative humidity and hop moisture on measurement time.

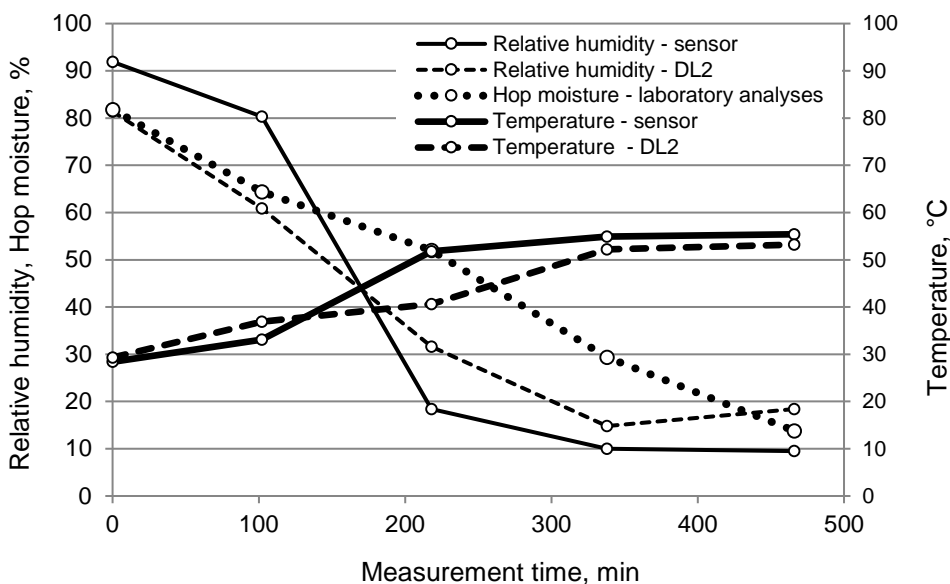


Figure 4. Third chamber – datalogger (DL2), fixed sensors and laboratory analyses –dependence of temperature, relative humidity and hop moisture on measurement time.

Discussion on each measurement

Uniformity in drying in individual chambers

The graphs in Figs 3–4 compare changes in the air temperature and relative humidity in the first and third chamber measured by those dataloggers that passed through the entire drying process in the drying chamber with the values obtained from the fixed sensors and with the values of hop moisture. Drying air temperature measured by dataloggers or fixed sensors is almost identical in both chambers. The relative humidity in both chambers is different with the first two slats, but logically this downward trend in the relative humidity corresponds to the declining hop moisture content. The relative humidity is being gradually equalized with the hop moisture. Contrary to belt dryers, the drying process is clearly continuous and gentle, and the hop moisture content of about 10% is achieved practically only at the outlet of the dryer prior to conditioning.

Laboratory analyses – hop moisture, HSI, alpha and beta bitter acids during the drying process.

The graphs in Figs 5–6 show results of the laboratory analyses of hop moisture, HSI, alpha and beta bitter acids during the process of drying in the first and third drying chamber. Based on the graphical patterns we can assess the changes in values of the moisture, HSI, alpha and beta bitter acids while the hops were passing through the dryer. The HSI values should increase minimally and the values of alpha and beta bitter acids should decrease minimally. The HSI values, according to the growers' long-standing experience with hop drying, subsequent processing and distribution, should not exceed 0.3 at the end of drying. With the first chamber (Table 1) the HSI value rose from 0.239 (filling) to 0.255 (emptying conveyor), which is an increase by 6.69% and it does not exceed the limit value. With the other chamber the HSI value rose from 0.240 (filling)

to 0.250 (emptying conveyor), which is an increase by a mere 4.17%. The values of alpha and beta bitter acids were relatively high at the inlet of both chambers, and the decline after passing through the dryer was only within the range of 0.34–2.24%. On the basis of an overall assessment it can be concluded that the process of drying in a chamber dryer has a minimal effect on the principal assessment parameters.

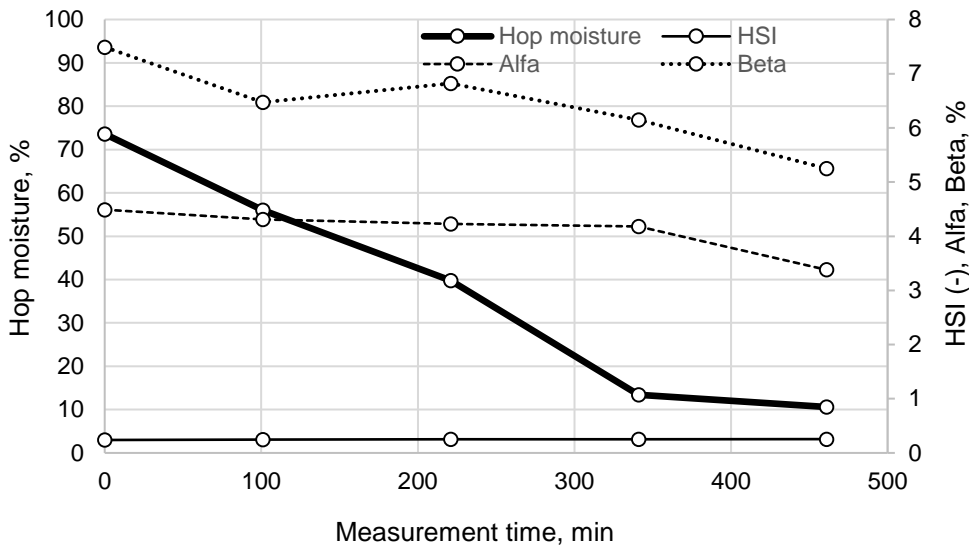


Figure 5. First chamber – laboratory analyses – hop moisture, HSI, alpha and beta bitter acids during the drying process.

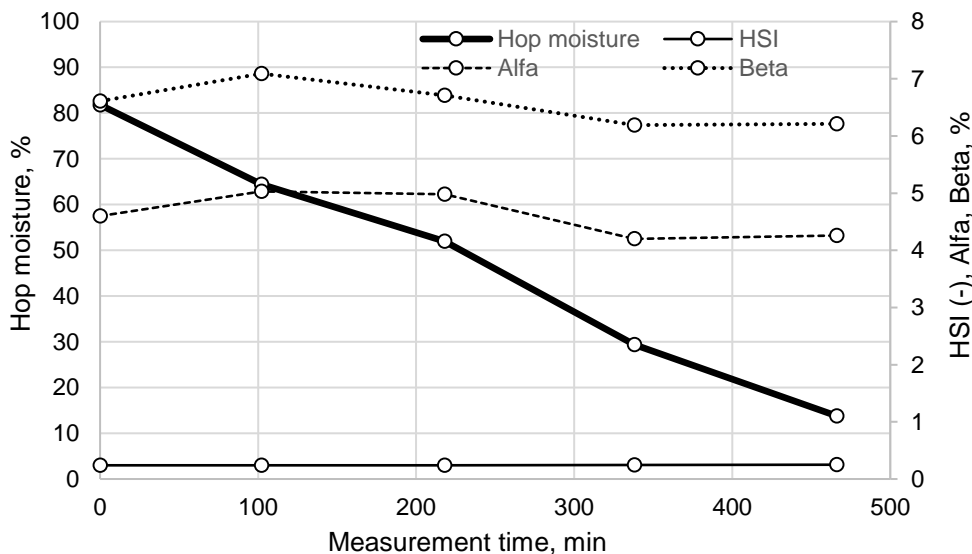


Figure 6. Third chamber – laboratory analyses – hop moisture, HSI, alpha and beta bitter acids during the drying process.

Finally, it has to be noted that by examining both domestic and foreign literature a large amount of information has been obtained about parameters of the drying medium and dried hops of different varieties mostly regarding drying in belt dryers, but these show a large variability affected by varietal, soil and climatic conditions and it is not possible to find any correlative links among them. The measurements summarized in this paper constitute the primary continuous monitoring of changes in air-conditioning and qualitative parameters (temperature, moisture, HSI, alpha and beta bitter acids, drying time) during the process of drying in a chamber dryer. There is a presumption that in the following years similar measurements will be repeated so that the changes in measured data could be gradually analysed more and the drying process could be prepared for so called gentle drying at a temperature of the drying air of up to 40 °C.

ACKNOWLEDGEMENTS. This paper was created with the contribution of the Czech Ministry of Agriculture as a part of NAZV No QJ1510004 research project. In the project solution, besides CULS Prague, are involved: Hop Research Institute Co., Ltd., Žatec; Chmelařství, cooperative Žatec; Rakochmel Co., Ltd., Kolečovice and Agrosopol Velká Bystrice Co., Ltd.

REFERENCES

- Aboltins, A. & Palabinskis, J. 2016. Fruit Drying Process Investigation in Infrared Film Dryer. *Agronomy Research* **14**(1), 5–13.
- Aboltins, A. & Palabinskis, J. 2017 Studies of vegetable drying process in infrared film dryer. *Agronomy Research* **15**(S2), 1259–1266.
- Claus, H., Van Dyck, J. & Verzele, M. 1978. Photometric constants of hop bitter acids. *J. Institute of Brewing* **84**, 218–220.
- Doe, P.E. & Menary, R.C. 1979. Optimization of the Hop Drying Process with Respect to Alpha Acid Content. *J. Agric. Engng Res.* **24**, 233–248.
- Green, C.P. & Osborne, P. 1993. Effects of solvent quality on the analysis of hops. *J. Institute of Brewing* **99**, 223–225.
- Hanousek, B., Rybka, A. & Bernásek, K. 2008. Evaluation of hop picker line PT 30/15 and hop drying in belt and kiln dryers in 2007. In: P. Svoboda (eds): *Economic-technological seminar about hop production problems*. Hop Research Institute Co. Ltd., Žatec, 43–61. (in Czech).
- Henderson, S.M. 1973. Equilibrium Moisture Content of Hops. *J. Agric. Engng Res.* **1**, 55–58.
- Henderson, S.M. & Miller, G.E. 1972. Hop Drying-Unique Problems and Some Solutions. *J. Agric. Engng Res.* **17**, 281–287.
- Heřmánek, P., Rybka, A. & Honzík, I. 2017. Experimental chamber dryer for drying hops at low temperatures. *Agronomy Research* **15**(3), 713–719.
- Hofmann, R., Weber, S. & Rettberg, S. 2013. Optimization of the Hop Kilning Process to Improve Energy Agric. Efficiency and Recover Hop Oils. *Brewing Science*, March/April **66**, 23–30.
- Jech, J., Artim, J., Angelovič, M., Angelovičová, M., Bernásek, K., Honzík, I., Krčálová, E., Kvíz, Z., Mareček, J., Polák, P., Poničan, J., Ružbarský, J., Rybka, A., Svoboda, A., Sosnowski, S., Sypula, M. & Žitňák, M. 2011. *Machines for Crop Production 3-Machinery and equipment for post-harvesting and treatment of plant material*. Profi Press s.r.o., Prague, 368 pp. (in Czech and Slovak).
- Jokiniemi, T., Oksanen, T. & Ahokas, J. 2015. Continuous airflow rate control in a recirculating batch grain dryer. *Agronomy Research* **13**(1), 89–94.

- Kieninger, H. & Forster, A. 1973. *Brauwiss* **26**, 214–217.
- Kirchmeier, H., Rodel, G. & Demmel, M. 2005. Verfahren zur Abtrennung von Drahtstücken bei der Hopfenernte. *Landtechnik* **60**(3), 148–149 (in German).
- Kořen, J., Ciniburk, V., Podsedník, J., Rybka, A. & Veselý, F. 2008. *Hop drying in chamber dryers*. Hop Research Institute Co. Ltd., Žatec, 31 pp. (in Czech).
- Krofta, K. 2008. *Evaluation of hop quality*. Hop Research Institute Co. Ltd., Žatec, 55 pp. (in Czech).
- Kumhála, F., Kavka, M. & Prošek, V. 2013. Capacitive throughput unit applied to hop picking machine. *Agric. Computers and Electronics in Agric.* **95**(7), 92–97.
- Kumhála, F., Lev, J., Kavka, M. & Prošek, V. 2016. Hop-picking machine control based on capacitance throughput sensor. *Applied Engng in Agric.* **32**(1), 19–26.
- Ono, M., Kakudo, Y. & Yamamoto, Y. 1984. Quantitative Analysis of Hop Bittering Components, its Application to Hop Evaluation. *J. American Soc. of Brewing Chemists* **42**, 167–172.
- Podsedník, J. 2001. Hop harvesting technology in the Czech Republic 1996-2000. *Proceedings of the Technical Commission I.H.G.C. of the XLVIIIth International Hop Growers Congress*. Canterbury-England.
- Rybáček, V., Fric, V., Havel, J., Libich, V., Kříž, J., Makovec, K., Petrлік, Z., Sachl, J., Srp, A., Šnobl, J. & Vančura, M. 1980. *Hop production*. SZN Prague, 426 pp. (in Czech).
- Rybka, A., Heřmánek, P. & Honzík, I. 2017. Theoretical Analysis of the Technological Process of Hop Drying. *Agronomy Research* **15**(3), 859–865.
- Srivastava, A.K., Goering, C.E., Rohrbach, R.P. & Buckmaster, D.R. 2006. *Engineering Principles of Agricultural Machines*. ASABE, 2nd Edition, Michigan, 569 pp.
- Vitázek, I. & Havelka, J. 2014. Sorption isotherms of aricultural products. *Res. in Agric. Engng.* **60**(special issue), 52–56.

Fatty acid composition of oilseed rapeseed genotypes as affected by vermicompost application and different thermal regimes

E. Samadzadeh Ghale Joughi¹, E. Majidi Hervan^{1,*}, A.H. Shirani Rad² and GH. Noormohamadi¹

¹Department of Agronomy, Science and Research Branch, Islamic Azad University, Tehran, Iran

²Department of Agronomy, Seed and Plant Improvement Institute, AREEO, Karaj, Iran

*Correspondence: majidi_e@yahoo.com

Abstract. Vegetable oils with a high relative amount of unsaturated fatty acids are of great significance for human health. Hence, in a 2-year factorial split plot experiment, the effects of different sowing date (optimum (October 17) and late (October 27)), vermicompost (0 and 20 ton ha⁻¹) and genotypes (BAL104, DIE710.08, BAL102, FJL330, FJL290 and Okapi) on the fatty acid composition of rapeseed were evaluated. Rapeseed genotypes and the combination of sowing date and vermicompost application were randomized to sub and main-plots, respectively. The present results revealed that yield, oil percentage and fatty acids composition is affected by sowing dates along with genotypes. However, the unsaturated fatty acid, eicosanoic acid was not affected by interaction sowing date and genotype. Vermicomposting increased the yield, oil percentage, oleic, linoleic and linolenic acids and decrease erucic unsaturated fatty acid. The FJL290 and BAL102 genotypes produced the highest values of grain yield (5,853 and 5,763 kg ha⁻¹, respectively), oil percentage (43.98% and 43.85%, respectively), linoleic % acid (20.51 and 20.37% respectively), oleic % acid (65.23 and 64.93% respectively) and linolenic % acid (7.20 and 7.09% respectively) in comparison to the other genotypes, when they were sown at the optimum sowing date. The FJL290 and BAL102 also accelerated their growth period at the late sowing date. Consequently, oleic, linoleic and linolenic acids had the highest direct and indirect effect influence on grain oil percentage indicating their importance as selection criteria to improve yield and oil quality of rapeseed. Concluding the combination of sowing date, vermicompost and FJL290 and BAL102 lines may be the most favourable cropping strategy for rapeseed production in Iran.

Key words: Fatty acids, Oil percentage, Rapeseed, Sowing date, Vermicompost.

INTRODUCTION

Oil crops have great deal of importance for world agriculture and associated industries. Rapeseed (*Brassica napus* L.) belongs to (Brassicaceae) family which becomes one of the most important sources of the vegetable oil in the world (Baghdadi et al., 2013). It is a valuable oil-seed attracting the attention of many people during the recent years. The production and usage of brassica seed oils has a making it rank third among the oilseed crops after soybean and oil palm in production of vegetable oils, while fifth in the production of oilseed proteins (Armin & Golparvar, 2013).

Canola is a specific type of rapeseed associated with high quality oil and meal. It has less than 2% erucic acid and its meal has less than 30 μg of glucosinolates (El-Nakhlawy & Bakhashwain, 2009). Moreover it contains 40–45% oil and 39% protein, and rapeseed oil contains a desirable profile of saturated fatty acids (~7%) and high level of unsaturated fatty oleic acids about 61% and medium level of linoleic 21% and 11% linoleic acids (Molazem et al., 2013); therefore it represents a healthy edible oil. Over 13.2% of the world's edible oil supply now comes from the oil seed Brassica (Eskandari & Kazemi, 2012). On the other hand, oil obtained from conventional rapeseed is not considered as regular cooking oil because of its low quality due to the presence of high erucic acid (more than 40%) and glucosinolates (more than 100 $\mu\text{m g}^{-1}$ of dry meal) and low level of oleic and linoleic acid (Abdul Sattar et al., 2013). That is the reason for using rapeseed oil potentially in the bio-diesel market (El-Nakhlawy & Bakhashwain, 2009). Romanian investigation with 50 rapeseed cultivars showed significant differences in the grain yields (Gheorghe et al., 2013). Fink et al. (2006) stated that sowing time is one of the most important production decisions. Appropriate sowing date of rapeseed has proven as a key point to maximize yield potential. With the delay in sowing date, all the investigated traits declined (Baghdadi et al., 2013). Winter-type rapeseed cultivars respond to temperature in different mechanisms. Therefore, sowing date in temperate and cold regions should be considered. Seedling growth and establishment are enhanced on optimum sowing dates compared with those on late sowing dates (Pasban Eslam, 2008). Rafiei et al. (2011) observed that yield and yield compounds decrease. Oil yield decreases on late sowing dates because of an increase in the risk of late season heat and drought stress, which decrease the photosynthetic rate and increase the respiratory rate in seed setting or seed filling stages (Daneshian et al., 2008).

Bio-fertilizers as a highly potent alternative are the increase of oleic acid and linoleic acid, and the reduction of linolenic acid content to chemical fertilizers because of important environmental issues. In this regard, composting as a waste management technique is used to treat various organic wastes for organic fertilizers. Vermicompost is a product of composting in which earthworms are used to create a heterogeneous mixture of decomposing organic wastes. Thus, it Increase fertility and quality of soil, improve its water retention capacity and enhance plant growth and development. Previous studies showed the influence of vermicompost and inorganic fertilizers on yield and protein of crops (Manivannan et al., 2009). Applications of vermicompost alone or in combination with other fertilizers have been proved to be effective to enhance growth and yield of various plants (Javed & Panwar, 2013). Kumar & Sood (2011) reported that rapeseed vegetative growth and oil yield and components are increased by vermicompost compared with cattle manure or other bio-fertilizers. Therefore the aim of this study was to evaluate the oil content and fatty acid composition of rapeseed from different genotypes. Moreover due to the significance of rapeseed as a crop with high nutritional values, it is very important to suggest the most suitable sowing date and vermicompost fertilizer level for canola production, with regard to the climatic conditions.

MATERIALS AND METHODS

The experiment were carried out at the Seed and Plant Improvement Institute, Karaj, Iran (35° 49' N, 51° 06' E, 1,321 m asl) in 2015 and 2016 growing seasons. A factorial split plot experiment was performed on the basis of the randomized complete block design with three replications. The factorial combination of two sowing dates (October 17 and 27 as optimum and late sowing dates, respectively) and two vermicompost amounts (0 and 20 ton ha⁻¹) were allocated to the main plots, and six rapeseed genotypes (BAL104, DIE710.08, BAL102, FJL330, FJL290, and Okapi; Table 1) were randomized in sub-plots.

Table 1. Growth type and origin of studied rapeseed genotypes

Name	Origin	Growth type	Hybrids	Cultivars	Lines	Lines pedigree
BAL1104	Iran	Winter			*	RNX-3621 Selfing
DIE710.08	Germany	Winter	*			-
BAL102	Iran	Winter			*	Bristol Selfing
FJL330	Iran	Winter			*	Sunday× Geronimo
FJL290	Iran	Winter			*	Sunday× Geronimo
Okapi	France	Winter		*		-

The 6 rows in each sub plot were 6 m long, with 60 cm interspacing. The plots were 3 m apart and seeds planted at a 5 cm distance on the rows (70,000 plants ha⁻¹). Weeds were controlled using Galant Super and Lontrel (1 L ha⁻¹) from 4-leaf stage to 8-leaf stage.

Table 2. Climate data experimental from Karaj between in 2015–2016 years

Month	October		November		December		January		February	
Year	2014	2015	2014	2015	2014	2015	2015	2016	2015	2016
Rainfall (mm)	13.4	3.5	13.7	77.4	31.6	28.6	6	15.6	47.8	8.7
Average	18.1	19.4	18.2	10.5	6.3	4.6	5.2	5.1	7.3	4.9
Temp (°C)										
Month	March		April		May		June		July	
Year	2015	2016	2015	2016	2015	2016	2015	2016	2015	2016
Rainfall (mm)	21.3	17.8	45.4	75.5	2.2	13	6.6	-	-	-
Average	6.7	11.8	13.8	11.7	20	19.9	26.4	24.2	30.9	28.9
Temp (°C)										

Climate data, including temperature and precipitation for the whole year are presented in Table 2. The results of soil analysis samples were obtained at depths of 0–30 cm before sowing presented in Table 3. Fertilization was performed according to the soil testing analyses. A total of 150 kg ha⁻¹ ammonium phosphate and 150 kg ha⁻¹ potassium sulphate were applied to the soil before grain sowing. In addition, 350 kg ha⁻¹ urea was applied at three separate times: 100 kg ha⁻¹ in the sowing time, 150 kg ha⁻¹ in the stem elongation, and 100 kg ha⁻¹ in the flowering stage. Then before seed was sown, vermicompost (20 ton ha⁻¹) was spread onto the soil surface and incorporated into the soil at a depth of 30 cm. Vermicompost fertilizer characteristics are presented in Table 4.

Table 3. Result of chemical and physical analysis of experimental soil

Year	Depth, cm	Ec, ds m ⁻¹	pH	Organic matter, %	Nitrogen, kg ha ⁻¹	Posphorus P ₂ O ₅ , kg ha ⁻¹	Potassium K ₂ SO ₄ , kg ha ⁻¹	Soil Texture
2014–15	0–30	1.45	7.9	0.91	0.09	14.7	197	Clay loam
2015–16	0–30	1.33	7.8	0.83	0.08	14.2	165	Clay loam

Table 4. Vermicompost nutritional parameters

Sample	N-total, %	P, %	K, %	C/N	OC, %	EC, ds m ⁻¹	pH
Vermicompost	1.5	0.81	0.75	19.2	15.2	7.2	6.5–8.5

Plants were harvested, when 40–50% of the seeds in the main pods and primary branches turned brown. After harvesting, the oil content and the fatty acid composition were determined. Oil content was determined by NMR (Mq20, Bruker, Germany) at the Seed and Plant Improvement Institute (ISO 10565, 1988). Fatty acid composition, including saturated (sum of palmitic (C16:0), stearic acid (C18:0) and arachidic acid (C20:0)) and unsaturated (sum of oleic (C18:1), linoleic (C18:2) and linolenic (C18:3), palmitoleic (C16:1), ecosanoic (C20:1) and erucic acid (C22:1)) acids, was analysed using gas chromatography of methyl esters (Metcalf et al., 1966; Lee et al., 1988) by the following procedure.

Fifty milligram of extracted oil was saponified with 5 mL of methanolic NaOH (2%) solution by refluxing for 10 min at 90 °C. After addition of 2.2 mL BF₃-methanolic, the sample was boiled for 5 min. The FAMES were extracted from a salt-saturated mixture with hexane. The FAMES were then analyzed using a gas chromatograph (UNICAM model 4600, UK) coupled with a FID detector. The column used for fatty acid separation was a fused silica BPX70 column, 30 m×0.22 mm i.d.×25 µm film thickness (from SGE, UK). The oven temperature was held at 180 °C during separation; the injector and detector temperatures were 240 and 280 °C, respectively. The carrier gas (helium) flow ratio was 1 mL min⁻¹. One microliter of methyl esters of free fatty acids was injected into the split injector. The split ratio was adjusted to 1:10. The compounds were identified by comparison of their retention times with authentic compounds. The internal standard C15:1 was used in the quantitative analysis of the separated fatty acid. Each fatty acid was expressed as a percent of the total fatty acids. Also, glucosinolate content was identified through HPLC (Thies, 1974).

Statistical analysis

Bartlett test was performed to evaluate homoscedasticity at a significance level of 0.05. In the presence of homoscedasticity in all of the traits except harvest index, combined ANOVA was conducted at a significance level of 0.05 on both sides and at a significance level of 0.01. LSD test was carried out to compare the means within ANOVA at a significance level of 0.05. Data were analyzed in SAS 9.0.

RESULT AND DISCUSSION

The monthly rainfall and average temperature data for 2015 and 2016 presented in Table 2. The average rainfall for 2016 (240.1 mm) was higher than observed (188 mm) in 2015.

According to The Tables 5, 6, 7 and 8, the growth season, sowing date, vermicompost, genotype and interaction effect of sowing date and genotype significantly affected the amount of saturated and unsaturated fatty acids. However, the unsaturated fatty acid, eicosanoic acid was not affected by interaction sowing date and genotype. In addition to the interaction effects of sowing date, vermicompost and genotype on the amount of palmitoleic unsaturated fatty acid was significant.

The highest values of grain yield (4,515 kg ha⁻¹), oil yield (1,929 kg ha⁻¹), oil percentage (42.31%), oleic, linolenic and linoleic acids (64.55, 5.89 and 19.05%) were obtained during the second growing season (Table 5 and 7). These enhancement at the second growth season may be due to improvement of the agronomic practices and particularly favourable weather conditions.

The highest values of grain yield (5,853 and 5,763 kg ha⁻¹), oil yield (2,576 and 2,528 kg ha⁻¹) and oil percentage (43.98 and 43.85%) were obtained by FJL290 and BAL102 lines sown at the optimum sowing date, while the lowest values were recorded from DIE710.08 hybrid sown at the late sowing date (Table 6), and the same trend was found by Siadat & Hemayati (2009) that explained the optimum sowing produced higher grain yield and this may be due to the variation in temperature, or attributed to more light, water and mineral absorption by plant canopies thus, increasing photosynthetic capacity. These results are in agreement with Shamsi (2012), reporting that sowing time had significant effect on oil content, the reduction in oil content with delayed after 15th Oct may be due to the increase of temperature during the grain filling stage. An increase in temperature above 16 °C after flowering stage causes (1.2–1.5) decrease in oil content for each 1 °C increase in temperature (Pritchard et al., 1999). This finding was in conformity with Soleymani & Shahrajabian (2013) that stated that oil yield is significantly affected by the interaction between sowing date and genotype.

The highest values of grain yield (4,394 kg ha⁻¹), oil yield (1,879 kg ha⁻¹) and oil percentage (42.35%) were obtained when vermicompost was applied (Table 5). Application of vermicompost is a sustainable technology capable that improve plants growth and yield of them (Castillo et al., 2010). Vermicompost is effective as organic fertilizer and bio-control agents that have organic nutrition role and increase plant growth (Arancon, 2005; Simsek, 2011). Oil yield and content can be increased by 10 ton ha⁻¹ vermicompost (Mohammadi et al., 2012). Karimi et al. (2011) reported that application of vermicompost significantly increased corn yield compared with control treatment. Furthermore, Amin Ghafari et al. (2010) demonstrated that castor bean grain yield is more effectively increased by vermicompost than by other organic fertilizers. Sesame oil yield also increases because of vermicomposting (Sajadi Nik et al., 2011).

Table 5. Analysis of variance and means of some quality traits of rapeseed genotypes under various sowing dates and vermicompost treatments

Parameters	Mean Squares ¹ and Mean Values					
	Grain yield, kg ha ⁻¹	Grain oil yield, kg ha ⁻¹	Oil percentage, %	Glucosinolate content, mg gr ⁻¹ dw	C18:1, %	C18:2, %
Growth season (df=1)	17,768,332**	3,532,520**	6.11**	10.01*	243.12**	86.95**
First	3,812b	1,616b	41.90b	1,292a	61.95b	17.50b
Second	4,515a	1,929a	42.31a	1,239b	64.55a	19.05a
<i>LSD</i> 0.05	138.25	58.55	0.10	0.21	0.18	0.19
Sowing date (Sd) (df=1)	223,868,925**	48,476,406**	254.16**	1,526.39**	293.12**	400.20**
Optimum sowing date	5,410a	2,352a	43.43b	9.41b	64.68a	19.94a
Late sowing date	2,916 b	1,192b	40.78a	15.92a	61.83b	16.61b
<i>LSD</i> 0.05	192.65	85.87	0.13	0.39	0.40	0.39
Vermicompost (V) (df=1)	7,660,440**	1,658,514**	8.73**	25.07**	28.72**	5.55**
Non application	3,933b	1,665b	41.86b	13.08a	62.81b	18.08b
Application	4,394a	1,879a	42.35a	12.25b	63.70a	18.47a
<i>LSD</i> 0.05	192.65	85.87	0.13	0.39	0.40	0.39
Genotype (G) (df=5)	18,206,990**	404,103**	2.70**	11.44**	2.55**	2.69**
BAL104	3,980bc	1,689bc	41.87c	13.08a	63.05cd	18.07cd
DIE710.08	3,886c	1,645c	41.76c	13.30a	62.87d	17.95d
BAL102	4,446a	1,907a	42.42a	11.95c	63.50ab	18.61ab
FJL330	4,201b	1,781b	42.17b	12.65b	63.35bc	18.30bc
FJL290	4,531a	1,949a	42.57a	11.70c	63.73a	18.74a
Okapi	3,935c	1,664c	41.84c	13.28a	63.03d	17.99cd
<i>LSD</i> 0.05	239.46	101.41	0.81	0.37	0.31	0.34
Gs×Sd (df=1)	225,662	68,994	0.33	5.34**	14.49**	29.62**
Gs×V (df=1)	283,112	57,760	0.05	0.12	0.27	0.21
Sd×V (df=1)	23,180	336	0.06	0.24	0.08	0.07
Gs×Sd×V (df=1)	60,639	11,990	0.15	0.07	0.03	0.01
Error (df=12)	281,457	55,916	0.13	1.16	1.24	1.16
Gs×G (df=5)	722	349	0.01	0.07	0.09	0.11
Sd×G (df=5)	993,630**	214,860**	1.25**	6.41**	1**	1.45**
Gs×Sd×G (df=5)	7294	1270	0.02	0.16	0.08	0.07
V×G (df=5)	88,583	15,135	0.01	0.09	0.23	0.01
Gs×V×G (df=5)	43,651	7,191	0.02	0.03	0.07	0.007
Sd×V×G (df=5)	48,274	9,647	0.01	0.31	0.26	0.05
Gs×Sd×V×G (df=5)	27,939	5,392	0.06	0.01	0.16	0.009
Error (df=80)	173,743	31,163	0.10	0.41	0.30	0.35
C.V (%)	10.01	9.95	0.75	5.07	0.86	3.23

* $P < 0.05$ and ** $P < 0.01$; ¹: Bold values across the main parameters in the table indicate mean squares; ²: Mean values with the similar letter in each column are not significantly different. ns: non- significant.

Increase in glucosinolate reduces canola food quality and nutritional value (Salisbury et al., 1987). The highest value of glucosinolate content was recorded by DIE710.08 hybrid (16.79 mg g⁻¹ dw) and BAL104 line (16.63 mg g⁻¹ dw) sown on the late sowing date. By contrast, the lowest value was detected in FJL290 and BAL102 lines sown on the optimum sowing date (Table 6). Glucosinolate content depends on genetic and environmental factors (Fieldsend et al., 1991). Genetic variations in glucosinolate content exist across canola genotypes (Burton, 2004). Generally, under optimum growth conditions nitrogen increases the glucosinolate concentration of seeds

(Bilborrow et al., 1993). The highest value glucosinolate (13.08 mg g⁻¹ dw) was obtained when vermicompost was non-applied (Table 5). Vermicomposting could reduce the glucosinolat content by 6.35%. Mostafavi Rad et al. (2013) observed that grain yield and glucosinolate content significantly differ among canola genotypes. Application of vermicompost increased plant production and total glucosinolate in plant tissue (Pant et al., 2011).

Table 6. Interaction effect of sowing date and genotype on assessed traits

Sowing date	Genotypes	Grain yield, kg ha ⁻¹	Oil yield, kg ha ⁻¹	Oil percentage, %	Glucosinolate content, mg gr ⁻¹ dw	C18:1, %	C18:2, %
17 October	BAL104	5,352b	2,322b	43.34b	9.52c	64.65bc	19.89bc
	DIE710.08	5,280b	2,285bc	43.24bc	9.81bc	64.41c	19.77c
	BAL102	5,762a	2,528a	43.85a	8.41d	64.93ab	20.37ab
	FJL330	5,049b	2,176c	43.05c	10.41d	64.37c	19.48c
	FJL290	5,853a	2,576a	43.98a	8.19d	65.23a	20.51a
	Okapi	5,163b	2,229bc	43.15bc	10.08ab	64.48c	19.63c
LSD (5%)		324.98	141.45	0.25	0.44	0.41	0.52
27 October	BAL104	2,608b	1,055b	40.40cd	16.63a	61.44b	16.26b
	DIE710.08	2,492b	1,007b	40.28d	16.79a	61.34b	16.12b
	BAL102	3,130a	1,285a	40.99b	15.49b	62.06a	16.84a
	FJL330	3,353a	1,386a	41.29a	14.88c	62.32a	17.12a
	FJL290	3,209a	1,322a	41.16ab	15.22bc	62.22a	16.97a
	Okapi	2,706b	1,099b	40.54c	16.48a	61.57b	16.34b
LSD (5%)		294.38	120.31	0.24	0.52	0.43	0.35

Means with similar letters in each column are not significantly different.

The kind and amount of fatty acids in oilseed reflect the quality of oil. Rapeseed is a good source of oleic or monounsaturated fatty acid and linoleic and linolenic acid or polyunsaturated fatty acids (Dmytryshyn et al., 2004; Carvalho et al., 2006). The desaturated change the saturated fatty acid into unsaturated ones, which is of great significance for the production of vegetable oils. The interaction sowing time and genotype affected significantly oleic, linoleic and linoleic acids percentage. The highest values oleic (65.23 and 64.93%), linoleic (20.51 and 20.37%) and linolenic (7.20 and 7.09%) acids were obtained by FJL290 and BAL102 lines sown on the optimum sowing date (Tables 6 and 8, respectively). Suggesting that more work is needed to improve oil quality among canola genotypes. Reducing long chain and saturated fatty acids in canola genotypes is one of the main objectives in canola breeding. On the other hand, sowing time is known as an important factor that not only affect grain yield, but also affect grain oil quality through changing fatty acids composition. It has been reported that reduction in seed germination speed, due to late sowing, increases fatty acid content (May et al., 1994) which is in disagree with the current results. These results agree with the findings of Turhan et al. (2011) that revealed the influence of sowing time and different genotypes on fatty acid synthesis of rapeseed (linoleic, linolenic and oleic acids).

Comparison of means revealed that the highest values linoleic acid, linolenic and oleic acid were obtained when vermicompost was applied (Tables 5 and 7, respectively). Mohammadi et al. (2011) reported that the vermicompost application in comparison with chemical fertilizers significantly increased the linoleic and oleic acids in rapeseed.

Mohammadi et al. (2011) reported that the vermicompost application in comparison with chemical fertilizers significantly increased the linoleic and oleic acids in rapeseed. Monir & Malik (2007) reported that the increase in the content of linoleic acid in comparison to the control is less pronounced, as in the variant with 40 t/decare of vermicompost it reaches 76.70%.

Table 7. Analysis of variance and means of some quality traits of rapeseed genotypes under various sowing dates and vermicompost treatments

Parameters	Mean squares ¹ and mean values					
	C18:3, %	C18:0, %	C16:0, %	C20:0, %	C20:1, %	C22:1, %
Growth season (Gs)	6.05**	2.18**	5.10**	0.007**	0.0008	0.02**
First	5.48b	2.97a	4.82b	0.57a	1.43a	0.30b
Second	5.89a	2.73b	5.20a	0.55b	1.43a	0.32a
<i>LSD</i> _{0.05}	0.07	0.05	0.09	0.01	0.08	0.009
Sowing date (Sd)	185.41**	56.25**	70.39**	6.72**	14.50**	2.30**
Optimum sowing date	6.82b	2.22b	4.31b	0.34b	1.11b	0.18b
Late sowing date	4.55a	3.47a	5.71a	0.78a	1.74a	0.44a
<i>LSD</i> _{0.05}	0.08	0.11	0.14	0.02	0.18	0.01
Vermicompost (V)	3.19**	3.37**	8.43**	0.14**	0.54	0.04**
Non application	5.54a	3a	5.25a	0.59a	1.49a	0.33a
Application	5.83b	2.70b	4.77b	0.53b	1.37a	0.29b
<i>LSD</i> _{0.05}	0.08	0.11	0.14	0.02	0.18	0.01
Genotype (G)	1.64**	0.35**	0.59**	0.06**	0.17*	0.02**
BAL104	5.85a	2.94a	4.89b	0.58b	1.46a	0.33a
DIE710.08	5.95a	2.97a	4.84b	0.61a	1.50a	0.34a
BAL102	5.43c	2.73bc	5.15a	0.50c	1.36ab	0.28c
FJL330	5.67b	2.80b	5.10a	0.58b	1.48a	0.31b
FJL290	5.31c	2.69c	5.20a	0.48c	1.29a	0.27c
Okapi	5.90a	2.95a	4.89b	0.60a	1.50a	0.34a
<i>LSD</i> _{0.05}	0.13	0.08	0.15	0.01	0.15	0.01
Gs×Sd	0.54**	0.62**	0.29	0.004*	0.40*	0.004*
Gs×V	0.002	0.009	0.01	0.0005	0.01	0.0001
Sd×V	0.002	0.28	0.008	0.01	0.10	0.0001
Gs×Sd×V	0.0001	0.05	0.08	0.002	0.09	0.0003
Error	0.04	0.09	0.16	0.003	0.26	0.001
Gs×G	0.009	0.001	0.03	0.0005	0.02	0.0002
Sd×G	0.83**	0.15**	0.36**	0.04**	0.12	0.01**
Gs×Sd×G	0.006	0.001	0.06	0.0005	0.01	0.0003
V×G	0.01	0.005	0.02	0.0004	0.01	0.0007
Gs×V×G	0.0007	0.004	0.02	0.0001	0.01	0.0004
Sd×V×G	0.01	0.006	0.01	0.0001	0.01	0.0005
Gs×Sd×V×G	0.001	0.01	0.04	0.0004	0.02	0.0002
Error	0.05	0.02	0.07	0.001	0.06	0.0008
C.V (%)	4.15	5.47	5.49	5.80	18.21	9.35

* $P < 0.05$ and ** $P < 0.01$;

¹: Bold values across the main parameters in the table indicate mean squares;

²: Means with similar letter in each column are not significantly different. ns: non-significant.

Table 8. Interaction effect of sowing date and genotype on assessed traits

Sowing date	Genotypes	C18:3, %	C18:0, %	C16:0, %	C20:0, %	C20:1, %	C22:1, %
17 October	BAL104	6.65b	2.26a	4.47cd	0.36d	1.11abc	0.20c
	DIE710.08	6.52bc	2.29a	4.54d	0.38dc	1.16ab	0.20bc
	BAL102	7.09a	2.11b	4.09b	0.25e	1.01bc	0.15d
	FJL330	6.44c	2.34a	4.62a	0.44a	1.29a	0.23a
	FJL290	7.20a	2.07b	4.01ab	0.23f	0.90c	0.13d
	Okapi	7.01a	2.31a	4.16c	0.42b	1.20ab	0.22ab
LSD (5%)		0.19	0.10	0.11	0.01	0.22	0.01
27 October	BAL104	4.21d	3.64a	5.83bc	0.82ab	1.81ab	0.47a
	DIE710.08	4.11d	3.66a	5.87c	0.83a	1.84a	0.48a
	BAL102	4.69b	3.37b	5.80ab	0.75c	1.71ab	0.42b
	FJL330	4.90a	3.28b	5.58c	0.73c	1.66b	0.39c
	FJL290	4.60c	3.32b	5.79a	0.74c	1.69ab	0.41bc
	Okapi	4.79ab	3.60a	5.63c	0.80b	1.79ab	0.47a
LSD (5%)		0.15	0.13	0.15	0.03	0.16	0.02

Means with the similar letters in each column are not significantly different.

Erucic acid is one of the most important fatty acids within Brassica genus. This 22-carbon fatty acid is harmful to the human health (Cazzato et al., 2014). The highest value of erucic acid (0.48%) was recorded from the interaction between (late sowing date and DIE710.08 hybrids), while the lowest value (0.13 and 0.15%) was recorded from (optimum sowing date and FJL290 and BAL102) (Table 8). The lowest value erucic acid was obtained when vermicompost was applied (Table 7). So, the results showed that application of vermicompost reduced this harmful fatty acid. Grain and oil yield and fatty acid composition are function of genotype, climate conditions, morphology and physiology as well as crop management (Arsalan, 2007). The highest values of palmitic (5.87 and 5.83%), stearic (3.66 and 3.63%) ecosanoic (1.84 and 1.81%) and arachidic (0.83 and 0.81%) acids were recorded from interaction between (late sowing date, DIE710.08 hybrid and BAL104 line). Also the highest values of palmitic (5.25%), stearic (3%), arachidic (0.59%), and ecosanoic (1.49%) acids were also determined when vermicompost were non-applied. According to the present results, vermicompost reduced of stearic, arachidic and ecosanoic saturated fatty acids. The highest value of palmitoleic acid (0.59%) was recorded from the interaction between late sowing date, non-application vermicompost and DIE710.08 hybrids, while the lowest value (0.13%) was recorded from optimum sowing date, vermicompost application and FJL290 line. (Fig. 1). Kumar, (1994) reported that the addition of vermicompost can increase the fatty acid content of the seeds. Angelova et al. (2015) the addition of vermicompost and compost leads to an increase in the content of palmitic acid and linoleic acid, and a decrease in the stearic and oleic acids compared with the control. A significant increase in the quantity of saturated acids was observed in the variants with 20 t per decare of compost and 20 t per decare of vermicompost (9.1 and 8.9% relative to the control).

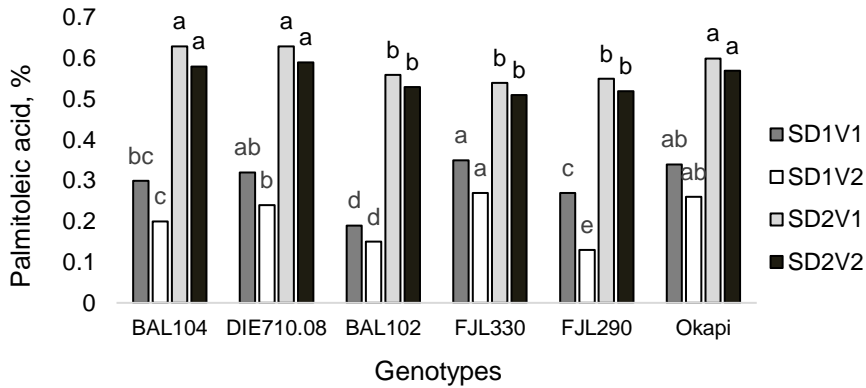


Figure 1. The interaction effects of sowing dates, vermicompost and genotypes on the palmitoleic acid content.

Notes: SD₁V₁: optimum sowing date and non-application vermicompost; SD₁V₂: optimum sowing date and vermicompost application; SD₂V₁: late sowing date and non-application vermicompost; SD₂V₂: late sowing date and vermicompost application.

CONCLUSIONS

In conclusion the sowing dates, genotypes and vermicompost fertilizer treatments substantially influenced fatty acid composition of rapeseed oil. The highest grain yield, oil percentage, fatty acid composition linoleic, linolenic and oleic was obtained in FJL290 and BAL102 lines under optimum sowing date. Application of vermicompost reduced harmful fatty acid (erucic acid) and increase useful fatty acids such as oleic, linoleic and linolenic acids. Considering the low organic matter of agricultural lands of Iran (less than 0.5%) application of vermicompost is recommended.

ACKNOWLEDGEMENTS. The authors would like to thank Seed and Plant Improvement Institute, Agricultural Research, Education and Extension Organization for providing the means and facilities to conduct this research.

REFERENCES

- Abdul Sattar, C., Wahid, M., Saleem, M.M., Ghaffari, M., Hussain, Sh. & Arshad, M. 2013. Effect of sowing time on seed yield and oil contents of Canola varieties. *J. Glob. Innov. Agric. Soc. Sci.* **1**(1), 1–4.
- Amin Gafouri, A., Rezvani Moghddam, P. & Nasiri Mehallati, M. 2010. Effect of organic manure on yield and yield components of *Ricinus sativus*. *First National Congress of Sustainable Agriculture and Development and Safe Crop Production. Isfahan.* (in persian).
- Angelova, V., Vanja, I., Akova, S.V., Krasimir, I. & Vanov, I. 2015. Potential of sunflower (*arthusus tinctorius L.*) for phytoremediation of soils contaminated with heavy metals. *International Journal of Biological, Biomolecular, Agricultural, Food and Biotechnological Engineering* **9**(6), 531–538.
- Arancon, N.Q., Edward, C.A., Bierman, P., Metzger, J.D. & Lucht, C. 2005. Effects of vermicomposts produced from cattle manure, food waste and paper waste on the growth and yield of peppers in the field. *Pedobiologia* **49**, 297–306.

- Armin, A. & Golparvar, A. 2013. Effect of planting dates on seed and oil yield of Canola (*Brassica napus L.*) cultivars. *International Journal of Modern Agriculture* **2**(2). 81–84.
- Arsalan, B. 2007. The Determination of oil and fatty acid compositions of domestic and exotic safflower (*Carthamus tinctorius L.*) genotypes and their interactions. *Journal of Agronomy* **6**(3), 415–420.
- Baghdadi, H., Taspinar, S., Yousefi, M. & Hosseinpour, A. 2013. Influence of different sowing dates on grain yield of Canola (*Brassica napus L.*) cultivars Inqazvin area. *International Journal of Agriculture: Research and Review* **2**(S). 1092–1096.
- Bilborrow, P.E., Evans, J. & Zhao, F. 1993. The influence of spring nitrogen on yield, yield components and glucosinolate concentration of autumn-sown oilseed rape (*Brassica napus*). *Journal of Agricultural Sciences* **120**, 219–224.
- Burton, W.A., Ripley, V.L., Potts, D.L. & Salisbury, P.A. 2004. 'Assessment of genetic diversity in selected breeding lines and cultivars of canola quality *Brassica juncea* and their implications for canola breeding,' *Euphytica* **136**, 181–192.
- Carvalho, I.S., Miranda, I. & Pereira, H. 2006. Evaluation of oil composition of some crop suitable for human nutrition. *Ind. Crop. Prod.* **24**, 75–78.
- Castillo, J.M., Nogales, R. & Romero, E. 2010. Vermicomposts from agro industrial wastes and pesticides effects on soil microbial activity. *Environmental and sanitary aspects of manure and organic residues utilization* **6**, 1–4.
- Cazzato, E., Laudadio, V., Ceci, E. & Tufarelli, V. 2014. Effect of sulphur fertilization on fatty acid composition of faba bean (*Vicia faba L.*), white lupin (*Lupinus albus L.*) and pea (*Pisum sativum L.*) grains. *Journal of Food, Agriculture and Environment* **12**, 136–138.
- Daneshian, A.M., Ahmadzadeh, A.R., Shahriar, H.A. & Khanizadeh, A.R. 2008. Effect of sowing dates on grain and biological yield, oil and meal protein percentage in three cultivars of rape (*Brassica napus L.*). *Res. J. Biol. Sci.* **3**, 729–732.
- Dmytryshyn, S.L., Dalai, A.K., Chaudhari, S.T., Mishra, H.K. & Reaney, M.J. 2004. Synthesis and characterization of vegetable oil derived esters evaluation for their diesel additive properties. *Biol. Technol.* **92**, 55–64.
- El-Nakhlawy, S. & Bakhshwain, A. 2009. Performance of Canola (*Brassica napus L.*) seed yield, yield components and seed quality under the effects of four genotypes and nitrogen fertilizer rates. *JKAU: Met., Env. & Arid Land Agric. Sci.* **20**(2). 33–47.
- Eskandari, H. & Kazemi, K. 2012. Changes in germination properties of (*Brassica napus L.*) as affected by hydro priming of seeds. *Journal of Basic and Applied Scientific Research* **2**, 3285–3288.
- Fieldsend, J.K., Murray, F.E., Bilborrow, P.E., Milford, G.F.L. & Evans, E.J. 1991. Glucosinolate accumulation during seed development in winter sown oilseed rape (*B. napus*). In: McGregor, D.I. (edn.). *Proceedings of 8th International Rapeseed Congress*. Canada Saskatoon, 686–694. Flanigen.
- Fink, N., Conley, S. & Christmas, E. 2006. *An Evaluation of the effects of planting date and seeding rate on the yield of winter Canola grown at three different geographic areas*. The ASA-CSSASSA, International Annual Meetings.
- Gheorghe, C., Raus, L., Coroi, I., Gales, D. & Jitareanu, G. 2013. Effect of tillage and cultivar on winter Oilseed Rape (*Brassica napus L.*) yield and economic efficiency in Suceava Plateau. *Pro-Environment* **6**, 130–135.
- Institute S.A.S. Inc., SAS/STAT users guide. Version 6, fourth ed., Statistical Analysis Institute Inc., North Carolina. 1988.
- International Standard Organization. 1988. Simultaneous determination of oil & water contents method using pulsed nuclear magnetic resonance spectrometry. ISO: 10565.
- Javed, S. & Panwar, A. 2013. Effect of bio-fertilizer, vermicompost and chemical fertilizer on different biochemical parameters of Glycine max and Vigna mungo. *Recent Research in Science and Technology* **5**(1), 40–44.

- Karimi H, Mazaheri, D., Peyghambari, S.A. & Mirabzadeh Ardakani, M. 2011. Effect of application of organic and mineral fertilizers on yield and yield components of maize single cross 704. *Iranian Journal of Crop Sciences* **2**, 611–626.
- Kumar, V. 1994. Nitrogen economy in Indian mustard through use of *Azotobacter chroococcum*, *Crop Research*, vol. **8**, 449–452.
- Kumar, V. & Sood, M. 2011. Effect of transplanting time, spacing and fertilizers on herbage and oil yield of *Mentha piperita*. *International Journal of Farm Sciences* **1**, 68–74.
- Lee, D., Noh, B., Bae, S. & Kim, K. 1988. Characterization of fatty acids composition in vegetable oils by gas chromatography and chemometrics. *Anal. Chim. Acta.* **358**, 163–175.
- Manivannan, S., Balamurugan, M. Parthasarathi, K. Gunasekaran, G. & Ranganathan, L.S. 2009. Effect of vermicompost on soil fertility and crop productivity beans (*Phaseolus vulgaris*). *J. Environ. Biol.* **30**(2), 275–281.
- May, W.E., Hume, D.J. & Hale, B.A. 1994. Effect of Agronomic Practices on Free Fatty Acid Levels in the Oil of Ontario Grown Spring Canola. *Canadian Journal of Plant Science* **74**(2), 267–274.
- Metcalfe, L.D., Schmitz, A.A., Pelka, J.R. 1966. Rapid preparation of fatty acid esters from lipids for gas chromatographic analysis, *Anal. Chem.* **38**, 514.
- Mohammadi, K.H., Pasari, B. Rokhzadi, A., Ghalavand, A., Aghaalikhani, M. & Eskandari, M. 2011. Response of grain yield and canola quality to different resources of farmyard manure, vermicompost and bio-fertilizers in Kurdistan region. *Elec. J. Crop Prod.* **4**(2), 81–102.
- Mohammadi, K.H., Pasary, B., Rakhzady, A., Ghalavand, A., Alikhani, M.A. & Eskandari, M. 2012. Response of rapeseed yield and quality of manure, compost and fertilizer in Kurdistan. *Electronic Journal of Crop Production* **4**(2), 101–81.
- Molazem, D., Azimi, J. & Dideban, T. 2013. Measuring the yield and its components, in the Canola in different planting date and plant density of the west Guilan. *International Journal of Agriculture and Crop Sciences* **6**(12), 869–872.
- Monir, M.A., Malik, M.A. & Saleem, M.F. 2007. 'Impact of integration of crop manuring and nitrogen application on growth, yield and quality of spring planted sunflower (*Helianthus annuus* L.)', *Pak. J. Bot.*, vol. **39**, 441–449.
- Mostafavi Rad, AM., Tahmasebi Sarvestani, A.M., Moddaress sanavi, V. & Ghalavand, A. 2011. Fatty acids and micronutrient elements in seed of high-quality canola cultivars under the influence of different amounts of sulfur. *Crops* **4**(1), 43–60.
- Pant, A., Radovich, T.J.K., Hue, N.V. & Arancon, N.Q. 2011. Effect of vermicompost tea (Aquedus Extract) on pak choi yield, Quality and on soil biological properties. *Compost science utilization. J. Agri. Sci.* 2014, 2383–2389.
- Pasban Eslam, B. 2008. Evaluation of yield and its components of superior winter oilseed rape genotypes under normal and late planting dates. *J. Agric. Sci.* **18**(2), 37–47.
- Prichard, F.M., Norton, R.M., Eagles, H.A., Salisbury, P.A. & Nicolas, M. 1999. The effect of environment on Victorian canola quality. In CD Proceedings of the International Rapeseed Congress, 26-29 Sept 1999, Canberra, Australia.
- Rafiei, S., Delkhosh, B., Shirani Rad, A.H. & Zandi, P. 2011. Effect of sowing dates and irrigation regimes on agronomic traits of Indian mustard in semi-arid area of Takestan. *Journal of American Science* **7**(10), 721–728.
- Sajadi Nik, R., Yadavi, A.R., Balouchi, H.R. & Farajee, H. 2011. Effect of chemical (Urea), organic (vermicompost) and biological (nitroxin) fertilizers on quantity and quality yield of Sesame (*Sesamum indicum* L.). *J. Agric. Sci. Sustain. Prod.* **21**(2), 87–101.
- Shamsi, M. 2012. Study of the effects of planting date on the phenological and morphological features, the seed yield, and the components of the yield of Oilseed Rape. *International Journal of Biology* **4**(1), 49–56.
- Siadat, S. & Hemayati, S. 2009. Effect of sowing date on yield and yield components of three oil seed rape varieties. *Plant Ecophysiology* **1**, 31–35.

- Simsek-Ersahin, Y. 2011. The Use of vermicompost Products to Control Plant Diseases and Pests. In: Karaca A (ed) *Biology of Earthworms, Soil Biology* Springer-Verlag Berlin Heidelberg.
- Soleymani, A. & Shahrajabian, M. 2013. Study the effects of relay cropping on yield and yield components, growth length, light interception and solar radiation depreciation of different species of Brassica. *International Journal of Farming and Allied Sciences* **2**(12), 329–333.
- Sulisbury, P., Sang, J. & Cawood, R. 1987. ‘Genetic and environmental factors influencing glucosinolate content in rapeseed in southern Australia,’ In: Proceedings of the 7th International rapeseed congress, Poland. *The plant breeding and acclimatization institute, Poznan*, 516–520.
- Thies, W. 1974. “New methods for the analysis of rapeseed constituents,” Proceedings of the 4th Rapeseed Congress. GCIRC Giessen, 275–282.
- Turhan, H., Gul, M., Egesel, C. & Kahrman, F. 2011. Effect of sowing time on grain yield, oil content, and fatty acids in Rapeseed. *Turk. J. Agric.* **35**, 225–234.

Germination and growth of primary roots of inoculated bean (*Vicia faba*) seeds under different temperatures

A. Senberga*, L. Dubova and I. Alsina

Latvia University of Agriculture, Institute of Soil and Plant Sciences, Liela street 1, LV-3001 Jelgava, Latvia

*Correspondence: alise.senberga@llu.lv

Abstract. Temperature stress strongly affects legumes, rhizobia, and the efficiency of legume-rhizobia interaction. An experiment in 2016 was developed to test the seed germination in Petri dishes using different microorganism inoculation under several temperature treatments (4, 8, 12 and 20 °C). The goal of this study was to test the effect of rhizobium inoculation under low root zone temperature, and to examine whether the addition of mycorrhiza fungi could enhance rhizobia resistance to abiotic stress and improve faba bean (*Vicia faba*) germination. Four faba bean cultivars were selected for the experiment (‘Lielplatone’, ‘Fuego’, ‘Bartek’ and ‘Karmazyn’). Four different seed inoculation variants were included in this experiment – 1) with rhizobium inoculation; 2) with a commercial preparation containing mycorrhiza fungi; 3) inoculation with both rhizobium and the mycorrhiza fungi preparation; 4) control variant. The number of germinated seeds, the length of the primary root and the primary root weight ratio were determined. The effect of inoculation was found out to be dependent not only on the temperature treatment, but it also significantly varied between the bean cultivars. Variants where seeds were inoculated with both mycorrhiza and rhizobia resulted in the highest results (length and weight ratio of primary roots), comparing with other inoculation variants, regardless of temperature. Variants where seeds were treated only with rhizobia mostly showed the lowest results – both length and weight ratio of primary roots, especially under treatment of 4 °C. Faba bean inoculation with only rhizobia might not be efficient, when sowing seeds under a low temperature stress. Inoculation with both rhizobia and mycorrhiza fungi could be a potential solution, when the root zone temperature is still below the optimal temperature.

Key words: rhizobia, mycorrhiza, abiotic stress, low root zone temperature, legumes, *Vicia faba*.

INTRODUCTION

Legume growers often use the bacteria from the genus *Rhizobia* (further – rhizobia) for seed inoculation, as rhizobia helps to supply legumes with the necessary amount of nitrogen. Legume inoculation with rhizobia results in an increased yield quantity and/or quality (Dash & Gupta, 2011; Ahemad & Kibret, 2014; Pawar et al., 2014; Voisin et al., 2014). Optimal growth conditions for both legumes and rhizobia are of great importance to achieve the optimal yield quality and quantity that can be achieved by this symbiosis. Root zone temperature (RZT) affects this symbiotic relationship even before nodule formation, including rhizobia survival in soil, competitiveness, legume root infection and subsequent nodule development, and nitrogen fixing ability (Paulucci et al., 2011;

Alexandre & Oliveira, 2013). An optimal temperature that fits most rhizobia has been suggested to be between 25–30 °C (Zhang et al., 1995). Nevertheless, there is no general temperature that can fit to all legume–rhizobia symbioses (Alexandre & Oliveira, 2013).

Farmers in Latvia tend to sow faba bean seeds early in the spring – starting from the end of March until the end of April (Balodis et al., 2016) to avoid the insufficient moisture necessary for bean seed germination in the soil. The average air temperature in March is -1 °C, in April the average air temperature is 5 °C (data obtained from the database of ‘Latvian Environment, Geology and Meteorology Centre’; <https://www.meteo.lv/>); therefore, faba beans are initially exposed to low RZT.

Extensive research on the effect of temperature on the symbiosis between leguminous plants and rhizobia bacteria has been done in southern regions, where the problem mostly is high temperature and insufficient soil moisture, which disturbs rhizobia and legume symbiosis. Fewer studies have looked at the low root zone temperature’s impact on legume-rhizobia symbiosis and legume growth (Zahran, 1999; Drouin et al., 2000). Several studies suggest that low RZT (2–15 °C), common in early spring in Northern Europe, can have a negative effect on legume nodule development and nitrogen fixation, leading to a subsequent reduced growth of legumes (Lynch & Smith, 1994; Zhang & Smith, 1994; Zhang et al., 1995; Ahlawat et al., 1998; Воробьев, 1998; Lira Junior et al., 2005). In the case of soybeans, nitrogen fixation can be reduced up to 40% if exposed to low RZT (Lynch & Smith, 1994). Faba bean seeds, germinated using Petri dishes, had normal seed germination at 15 °C, with significantly lower results at 4 °C and 10 °C (Rowland & Gusta, 1977). Slightly decreased RZT (10–12 °C) resulted in nodule formation up to 13 days later than normal temperature (18–22 °C), RZT of 5–7 °C delayed nodule formation up to 28 days compared to control; strong delay of nodule formation (up to 34 days compared to normal RZT) was caused by the RZT of 4–5 °C (Воробьев, 1998). In addition to delayed and reduced nodulation, low root zone temperature can also completely inhibit legume nodule formation (Graham, 1992; Lira Junior et al., 2005). In-depth knowledge about the low RZT induced stress affecting legumes is still required to provide the market with the most suitable legume seed inoculum. Moreover, compared to soybean, there is not enough research done on the effect of low RZT on faba bean early development.

To ensure optimal early development and growth of legumes, as well as to improve currently inhibited nodulation under suboptimal root zone temperatures, there is a need for new solutions that could be used by farmers. For this purpose, we tested the potential of a commercial rhizobia preparation that would also contain additional mycorrhiza fungi. In addition to rhizobia, mycorrhiza fungi are also used when growing legumes, as they both have been suggested to have a positive effect on the quality and quantity of legume yield (Kantar et al., 2003). Arbuscular mycorrhiza fungi formation on roots improves water and nutrient supply (i.e., P, Zn, and Cu) for plants, thus providing a healthier and denser root system and promoting growth of the whole plant, which is particularly important when growing in poor soil conditions (Ruotsalainen & Kytöviita, 2004; Dash & Gupta 2011; Grover et al., 2011). A consortium of rhizobia and mycorrhiza as a bioinoculant, instead of single inoculation, has been previously recommended, as these microorganisms have shown to complement each other. This consortium has been suggested to improve rhizobia induced nodulation, nitrogen fixation, mycorrhizal colonization, and the growth of the whole plant (Dash & Gupta, 2011). A higher faba bean yield was obtained, when seeds were treated with both rhizobia and mycorrhiza

before sowing, compared to single rhizobia inoculation (El-Wakeil & El-Sebai, 2007). However, mycorrhiza fungi activity, like rhizobia, can be adversely affected by low RZT. For instance, mycorrhization of pine seedlings was reduced at low RZT (5 °C) and it was reported that longer pine seedling exposure to lower soil temperature (starting only from week 6 and further) results in reduced mycorrhization (Domisch et al., 2002).

It is important to develop a recommendation for legume seed inoculation with microorganisms and germination for farmers, as cold stress is a widespread problem, which can significantly reduce the yield of important agricultural legume crops (Grover et al., 2011). Knowledge of the temperature impact on efficient microorganism activity would help farmers to choose more efficient sowing time, as well as to consider the appropriate microorganism preparation inoculation. Until now no previous study has been carried out testing Latvian rhizobia activity and the nodulation ability of legume roots under the temperature stress. In addition, no recent study has researched the effect of low root zone temperature on the efficiency of rhizobia and mycorrhiza double inoculation. The goal of this study is to determine which is the most suitable microorganism inoculum for faba bean seed treatment, that would improve the resistance to low RZT and ensure normal seed germination. An experiment was developed to test seed germination using different microorganism inoculation treatments under several temperature treatments.

MATERIALS AND METHODS

Experimental setup

Experiments were carried out using glass Petri dishes. Four bean (*Vicia faba*) cultivars were used: two *V. faba* var. *minor* Beck – ‘Lielplatone’ (obtained from State Priekuli Plant Breeding Institute, Latvia) and ‘Fuego’ (obtained from Norddeutsche Pflanzenzucht Hans–Georg Lembke KG, Germany), and two *V. faba* var. *major* Harz – ‘Bartek’ and ‘Karmazyn’ (obtained from Torseed®, Poland) For *V. faba* var. *minor*– 10 seeds per Petri dish; for *V. faba* var. *major* – 5 seeds per Petri dish were placed. Seeds were not surface sterilized, and no growth media was used in the Petri plates. Four variants of seed treatment were used in experiments: 1) *Rhizobium* sp. (‘Rh’), 2) mycorrhiza fungi containing preparation (‘M’), 3) rhizobia and mycorrhiza fungi preparation (‘Rh + M’) and 4) control without any symbiont (‘control’). Experiment was done in three replicates with each Petri dish as a replicate.

Seed treatment

A *Rhizobium leguminosarum* strain (RV407), isolated from beans (*Vicia faba*), was used for ‘Rh’ variant. This strain was isolated in Latvia and is included in the ‘Rhizobium Collection’ of the Institute of Soil and Plant Sciences, Latvia University of Agriculture. Rhizobia suspension was prepared by washing off *Rhizobium* bacterium pure culture, grown on Yeast Mannitol Agar media, with 20 mL of distilled water (not sterilized). The final concentration of inoculation suspension contained 10⁶ bacteria cells per millilitre. This rhizobium strain was chosen as it is the most commonly used strain in various experimental trials and has proven itself to be the most efficient when growing faba beans.

Commercial granulated mycorrhiza fungi preparation, used for ‘M’ and ‘Rh+M’ variants, was obtained from Symbiom® (Czech Republic). According to the mycorrhiza

fungi preparation producer, mycorrhiza inoculum contains a mixture of tree AMF (arbuscular mycorrhizal fungi) strains: *Glomus claroideum*, *G. intradices* and *G. mosseae*. For 'M' variant, one gram of mycorrhiza fungi preparation was added to 20 mL of distilled water in the Petri dish. For 'Rh+M' variant, one gram of the commercial granulated mycorrhiza fungi preparation was added in 20 mL of rhizobia bacteria suspension. In the case of control variant, 20 mL of distilled water was poured in the Petri dish.

Seed germination

Seed germination was done in dark conditions. Four different temperature treatments were tested under controlled conditions: 4, 8, 12 and 20 °C. Three days after seed inoculation, the number of germinated seeds was counted, the exudate was removed for further biochemical measurements (not discussed in this article) and additional 10 mL of distilled water was added. This step (removal of the exudate and addition of 10 mL distilled water) was repeated twice a week until the end of the experiment. The length of the experiment varied between the temperature treatments, as the germination in higher temperatures was much faster than in lower ones. Seeds under 20 °C treatment were germinated for 6 days; under 12 °C – for 15 days; under 8 °C – for 30 days; under 4 °C – for 40 days.

Measurements

At the end of temperature treatment experiment, the fresh weight of the whole seedling was measured, the root of the seedling was removed right below the seed, the length and the fresh weight of the primary root was measured. The primary roots in most cases had not yet developed lateral roots, therefore lateral roots were not considered for the measurements. The primary root weight ratio (ratio of the root weight to the total plant weight, expressed in percentage) was calculated. In addition, percentage of germinated seeds, out of the total number of seeds used, was recorded. Seeds were considered as germinated when the primary root could be visible.

Data analyses

All statistical analyses were done using Excel (Microsoft Corporations, Redmond, Washington, USA). Obtained data were processed using Analyses of Variance (ANOVA). Differences were considered statistically significant when $p < 0.05$. Error bars for figures show the Least Significant Difference (LSD).

Data was transformed in the case of length of faba bean seedlings, to meet the requirements for homogeneity of variance. Data transformation was conducted as follows: each measured seedling length result was multiplied with a coefficient, which was obtained by dividing the population mean with the sample mean.

RESULTS

Primary root length

Under normal faba bean seed germination temperature treatment (20 °C), most of the cultivars had significantly longer primary roots ($p < 0.001$), when seeds were treated with a microorganism inoculum ('Rh', 'M', and 'Rh+M'), compared with control variant (Fig. 1). An exception was 'Fuego', where 'Rh' treatment had no significant root length

promoting effect, compared with control. Mycorrhiza preparation ('M') appears to have a stronger promoting effect on the early growth of primary roots under the temperature treatment of 20 °C. Only faba bean cultivar 'Bartek' had significantly ($p < 0.01$) longer primary roots under the combined rhizobia and mycorrhiza preparation treatment ('Rh+M'), compared to other treatments.

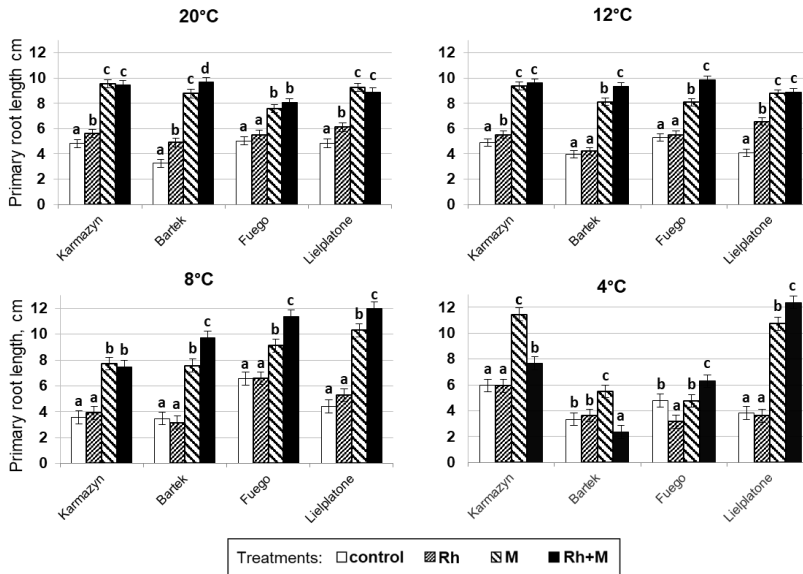


Figure 1. Length of faba bean seed primary roots depending on different microorganism inoculations under various temperature treatments. Different letters indicate significant differences between the different treatments within one cultivar at a certain temperature (LSD; $p < 0.05$).

When the germination temperature was decreased to 12 °C, only 'Karmazyn' and 'Lielplatone' seed inoculation with 'Rh' treatment resulted in significantly ($p < 0.05$) longer primary roots, compared with the control variant. The use of mycorrhiza fungi preparation – both alone or when added to rhizobia, significantly promoted primary root growth for all cultivars. Moreover, 'Bartek' and 'Fuego' seedlings had significantly longer primary roots ($p < 0.05$) under 'Rh+M' treatment, compared with single 'M' treatment.

At an even lower seed germination temperature (8 °C), none of the cultivars with 'Rh' treatment, had significantly longer primary roots, compared with control variant. The treatment 'M' and 'Rh+M', resulted in significantly longer primary roots for all bean cultivars. Furthermore, 'Bartek', 'Fuego' and 'Lielplatone' had significantly ($p < 0.001$) higher results of primary root growth under 'Rh+M' treatment, in comparison with 'M' preparation treatment alone.

When seedlings were exposed to a cold stress during germination (4 °C temperature treatment), primary root length strongly differed depending on the bean cultivar used. 'Karmazyn' seedlings had significantly longer primary roots compared with control and 'Rh' variant, when treated with 'Rh+M' ($p < 0.001$); however, the promoting effect was much larger when mycorrhiza was used alone ('M'). Like 'Karmazyn', also for 'Bartek' 'M' treatment achieved the longest primary roots ($p < 0.05$), compared to control, 'Rh'

and ‘Rh+M’ treatments. Primary roots for ‘Bartek’ under ‘Rh+M’ treatment resulted in significantly lower ($p < 0.05$) results compared to all the other treatments. ‘Fuego’ seeds treated with ‘Rh’ resulted in significantly ($p < 0.05$) lower results in comparison with other treatments, while ‘Rh+M’ variant had the longest primary roots ($p < 0.05$). For the faba bean cultivar ‘Lielplatone’ – ‘M’ and ‘Rh+M’ treatments were the most successful for promoting primary root length. In addition, primary root length under ‘Rh+M’ treatment significantly ($p < 0.05$) exceeded the results achieved with ‘M’ treatment.

Primary root weight ratio

The ratio of the primary root weight of the total plant weight was calculated (Fig. 2). Under the germination temperature of 20 °C primary root weight ratio for cultivars ‘Karmazyn’, ‘Bartek’ and ‘Lielplatone’ was significantly ($p < 0.05$) higher than control when treated with any of the bio-stimulants (‘Rh’, ‘M’ and ‘Rh+M’). For these three cultivars, single treatment with rhizobia (‘Rh’) had lower primary root weight ratio results than seed treatment with ‘M’ or ‘Rh+M’. For ‘Fuego’ primary root weight ratio results did not differ significantly between the seed treatment variants at 20 °C. Seed germination temperature reduction to 12 °C resulted in significantly higher primary root weight ratio for all the cultivars under seed treatment variants ‘M’ and ‘Rh+M’, compared with control and ‘Rh’.

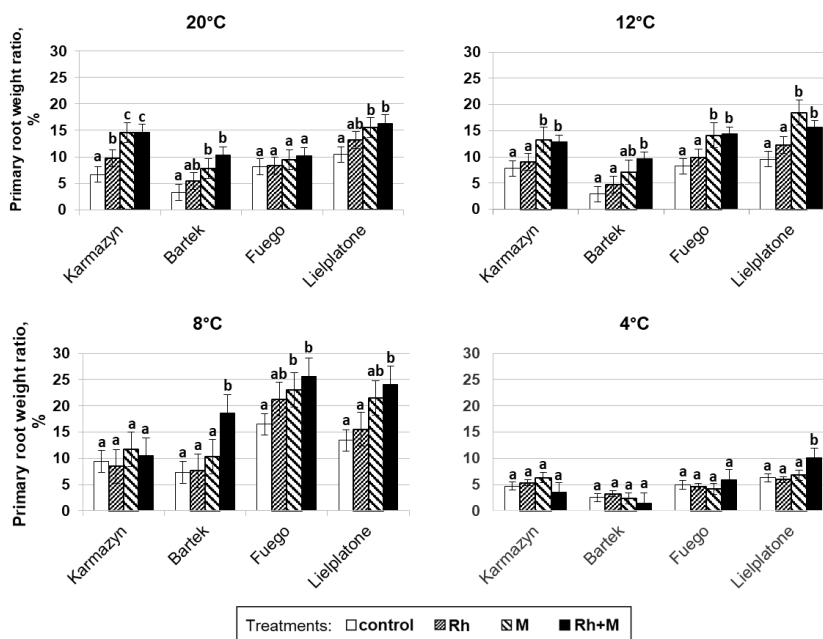


Figure 2. Primary root weight ratio in faba bean seedling depending on different microorganism inoculation under various temperature treatments. Different letters indicate significant differences between the different treatments within one cultivar at a certain temperature (LSD; $p < 0.05$).

When germination temperature was lowered to 8 °C, primary root weight ratios remained significantly higher compared to control and ‘Rh’ for cultivars ‘Bartek’ – variant ‘Rh+M’, ‘Fuego’ and ‘Lielplatone’ – variants ‘M’ and ‘Rh+M’. At 8 °C ‘Rh’

treatment has a significant promoting effect on the primary root growth only for cultivar ‘Fuego’. Unlike primary root length (Fig. 1), seed germination at 4 °C dramatically affected the primary root weight ratio. Almost no promoting effect of microorganisms can be observed under 4 °C treatment. ‘Lielplatone’ alone had significantly higher primary root weight ratio under ‘Rh+M’ treatment.

Percentage of germinated seeds

During the experiment it was observed that microorganism treatment has an important effect of on seed germination at temperatures ≤ 12 °C (data not shown). Percentage of germinated seeds mostly depended on bean cultivar. ‘Karmazyn’ had the highest number of germinated seeds (Fig. 3) under ‘M’ treatment; however, it was not significantly higher than control plants or variant ‘Rh+M’. The use of rhizobia slowed germination process significantly ($p < 0.05$) for cultivar ‘Karmazyn’. Broad bean cultivar ‘Bartek’ treated with ‘M’ had the highest percentage of germinated seeds, compared to any other treatment ($p < 0.05$). For ‘Fuego’ the highest number of germinated seeds was obtained when treated with the combined microorganism inoculum ‘Rh+M’, while single inoculation with ‘Rh’ and ‘M’ separately reached significantly higher ($p < 0.05$) percentage of germinated seeds compared to control. ‘Lielplatone’ seeds had the highest germination energy when treated with ‘Rh’ inoculum, although it did not significantly differ from treatments ‘M’ and ‘Rh+M’.

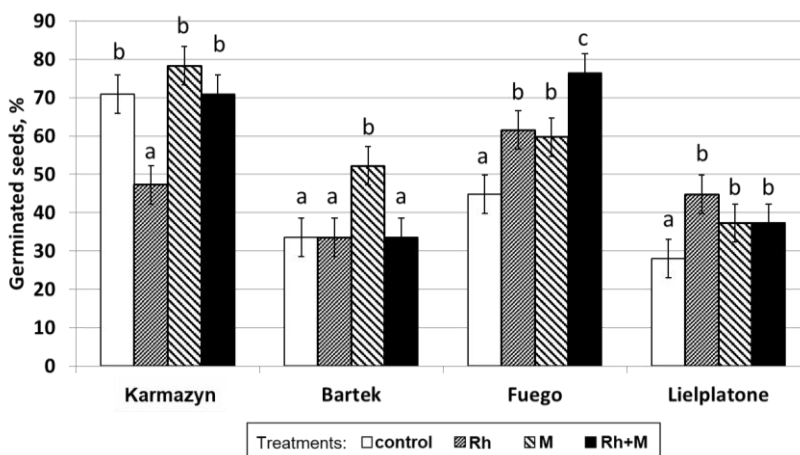


Figure 3. Percentage of germinated faba bean seeds depending on different microorganism inoculation. Different letters indicate significant differences between the different treatments within one cultivar (LSD; $p < 0.05$).

DISCUSSION

In this study the effect of different microorganisms at various temperatures (4, 8, 12 and 20 °C) was tested on the germination of seeds. Primary root length and primary root weight ratio were selected as indicators of seed germination activity. As it is stated by Fyson & Sprent (1982), root development indicates not only the plant growth potential, but also demonstrates the effect of microorganisms that the seedling is exposed

to, as delayed nodulation due to low RZT has been associated with slower plant development.

As expected, the growth promoting effect of rhizobia strain RV407 ('Rh') reduced with lower temperatures. Lower primary root parameters for seedlings initially treated with rhizobia could be explained as rhizobia consumes energy for early nodule development (Fyson & Sprent, 1982). Low root zone temperature has previously shown to cause delayed nodule formation – RZT of 4–5 °C resulted in up to 34-day delay in nodule formation (Воробьев, 1998). In addition, decrease in nodulation has been recorded when faba beans are exposed to 10 °C, compared with 15 and 20 °C treatments (Herdina & Silsbury, 1989). Although our experiment was not set-up as to monitor seedling further growth and nodulation, results obtained in this study suggest that the activity of rhizobia decreases below 8 °C, resulting in a potentially lower nitrogen fixation ability that has been previously shown to lead to reduced plant growth, reflected in a lower final yield (Prévost et al., 2003; Lira Junior et al., 2005; Dash & Gupta, 2011). From the results obtained in our study, it can be suggested that seed inoculation with only rhizobia ('Rh') is not efficient practice in the field when sown in early spring, when the RZT often does not exceed 4 °C. Although rhizobia are tolerant to 4 °C temperature (Drouin et al., 2000) and the bacterial activity is expected to increase with increasing temperature later in spring, if the rhizobia treated seeds are initially exposed to low RZT for a longer time, it might increase the bacterial lag phase, therefore delaying or even decreasing the final rhizobia cell number, leading to reduced nodulation (Fyson & Sprent, 1982; Beales, 2004).

Results obtained in this study indicate that adding mycorrhiza preparation to rhizobia inoculum can significantly enhance the early growth of primary roots, compared to single inoculation with only rhizobia. In many cases the results obtained for variants of the double inoculation were not significantly different from the ones treated with just mycorrhiza fungi (e.g. 'Karmazyn' at 8, 12 and 20 °C; 'Lielplatone' at 12 and 20 °C). Nevertheless, seed inoculation with only mycorrhiza is not recommended, as rhizobia treatment is crucial for nitrogen supply at later plant developmental stages. Root growth promoting effect caused by mycorrhiza fungi has been previously reported on maize plants, with higher root dry weight under both – optimal and low RZT (25, 15 and 5 °C; Zhu et al., 2010). The promoting effect of the microorganism treatments on primary root development, observed in this study, often depended on the *V. faba* cultivar used.

It was observed that a low seed germination temperature of 4 °C resulted in no consistent microorganism treatment effect. This is in line with previous studies, showing that not only rhizobia, but also root colonization with mycorrhiza fungi and corresponding shoot and root biomass is negatively affected by low RZT (Ruotsalainen & Kytöviita, 2004; Zhu et al., 2010). It could be argued that the experimental duration of two to six weeks (depending on the germination temperature) is not enough to develop a symbiosis between mycorrhiza fungi and bean seedlings. Nevertheless, data obtained in the present study showed a significant stimulating effect of single mycorrhiza inoculation and combined rhizobia and mycorrhiza inoculation on the development of primary roots.

The commercial preparation used in this study may contain mycorrhizal metabolites that could have been released from the previous symbiosis with the host plant during the mycorrhiza cultivation for this commercial product. It has been shown by Dash & Gupta (2011) that organic compounds, excreted by rhizosphere

microorganisms, can accelerate root growth; therefore, it could be possible that such organic compounds, left in the mycorrhiza preparation, could be directly used by the seedlings, stimulating primary root growth, as observed in the present experiment. As the commercial mycorrhiza fungi preparation used in this study is not sterile, another possibility could be that there are some other plant growth promoting rhizobacteria (PGPR) present in this preparation. However, the manufacturer does not provide the bacterial content of this mycorrhiza product, nor was it determined in this study. It has been previously shown that rhizosphere microorganisms, through various mechanisms, can effectively increase seed germination, including primary root development, leading to a better crop quality and quantity (Antoun et al., 1998; Dash & Gupta, 2011; Pérez-Montaña et al., 2014; Verbon & Liberman, 2016). This growth promoting effect is especially important when plants are exposed to abiotic stress, such as low root zone temperature (Grover et al., 2011; Souza et al., 2015). However, even if there are other PGPR present in the mycorrhiza preparation used in the present study, the significance of the seedling primary root growth promoting effect could not be attributed only to this possibility.

Combination of rhizobia and mycorrhiza fungi for seed inoculation has been suggested before. The synergic relationship between both microorganisms have been shown to have a plant growth promoting effect, including enhancing legume nodulation and providing mineral nutrition for the plant (Antoun et al., 1998; Dash & Gupta, 2011). An enhanced growth of soybeans has been observed due to the complementary interaction of rhizobia and mycorrhiza fungi, particularly in an environment with nitrogen and phosphorous deficiency (Wang et al., 2011). Soybean co-inoculation with rhizobia and mycorrhiza fungi preparation have showed an enhanced nitrogen fixation ability, compared with control plants and plants inoculated with only rhizobia (Mishra et al., 2011).

CONCLUSIONS

It can be concluded that seed germination significantly depends on bean cultivar and root zone temperature. *Vicia faba* var. *major* seeds require higher temperature compared to *Vicia faba* var. *minor*. For Latvian bean cultivar 'Lielplatone' the highest percentage of germinated seeds could be observed at 4 °C. Decrease in the percentage of germinated seeds was observed for *Vicia faba* var. *major* cultivars 'Bartek' and 'Karmazyn' because of single rhizobia treatment. The use of mycorrhiza preparation mitigated the effect of rhizobia. Inoculation of *Vicia faba* var. *minor* stimulated germination of seeds, and the most significant effect was obtained using of rhizobia. At temperatures higher or equal to 8 °C, stimulation of primary root growth was observed as a result of microorganism and plant interaction. In most cases the largest stimulating effect was obtained with combination of rhizobia and mycorrhiza fungi preparation. At 4 °C the stimulating effect persists only for *Vicia faba* var. *minor* cultivars, compared to the suppressive effect on *Vicia faba* var. *major*.

It can be concluded that seed inoculation with rhizobia should be supplemented with a mycorrhiza fungi preparation, especially when the sowing is done while the root zone temperature is still below the optimal. Double inoculation with both rhizobia and mycorrhiza fungi containing preparation is especially important for cultivars 'Bartek', 'Fuego' and 'Lielplatone'. In practice, as root zone temperature is crucial for seed

germination and development of effective symbiotic system, faba bean sowing is recommended when the root zone temperature reaches at least 8 °C.

ACKNOWLEDGEMENTS. This project is supported by EU 7th frame EUROLEGUME project (Enhancing of legumes growing in Europe through sustainable cropping for protein supply for food and feed).

REFERENCES

- Ahemad, M. & Kibret, M. 2014. Mechanisms and applications of plant growth promoting rhizobacteria: Current perspective. *Journal of King Saud University – Science* **26**, 1–20.
- Ahlawat, A., Jain, V. & Nainawatee, H.S. 1998. Effect of low temperature and rhizospheric application of naringenin on pea-*Rhizobium leguminosarum* biovar *viciae* symbiosis. *J. Plant Biochem. Biotechnol.* **7**, 35–38.
- Alexandre, A. & Oliveira, S. 2013. Response to temperature stress in rhizobia. *Crit. Rev. Microbiol.* **39**(3), 219–228.
- Antoun, H., Beauchamp, C.J., Goussard, N., Chabot, R. & Lalande, R. 1998. Potential of *Rhizobium* and *Bradyrhizobium* species as plant growth promoting rhizobacteria on non-legumes: Effect on radishes (*Raphanus sativus* L.). *Plant and Soil* **204**, 57–67.
- Balodis, R., Gaile, Z., Kreita, D. & Litke, L. 2016. Influence of different agrotechnical elements on yield of faba bean. In: *Proceedings of the Scientific and Practical Conference Harmonious Agriculture*. Latvia University of Agriculture, Jelgava, Latvia, pp. 8–12 (in Latvian, English abstr.).
- Beales, N. 2004. Adaptation of Microorganisms to Cold Temperatures, Weak Acid Preservatives, Low pH, and Osmotic Stress: A Review. *Compr. Rev. Food Sci. Food Saf.* **3**, 1–20.
- Dash, S. & Gupta, N. 2011. Microbial bioinoculants and their role in plant growth and development. *Int. J. Biotechnol. Mol. Biol. Res.* **2**(13), 232–251.
- Domisch, T., Finer, L., Lehto, T. & Smolander, A. 2002. Effect of soil temperature on nutrient allocation and mycorrhizas in Scots pine seedlings. *Plant and Soil* **239**, 173–185.
- Drouin, P., Prevost, D. & Antoun, H. 2000. Physiological adaptation to low temperatures of strains of *Rhizobium leguminosarum* bv. *viciae* associated with *Lathyrus* spp. *FEMS Microbiol. Ecol.* **32**, 111–120.
- Fyson, A. & Sprent, J.I. 1982. The Development of primary root nodules on *Vicia faba* L. grown at two temperatures. *Ann. Bot.* **50**, 681–692.
- Graham, P.H. 1992. Stress tolerance in *Rhizobium* and *Bradyrhizobium*, and nodulation under adverse soil conditions. *Can. J. Microbiol.* **38**, 475–484.
- Grover, M., Ali, Sk.Z., Sandhya, V., Rasul, A. & Venkateswarlu, B. 2011. Role of microorganisms in adaptation of agriculture crops to abiotic stresses. *World J. Microbiol. Biotechnol.* **27**, 1231–1240.
- El-Wakeil, N.E. & El-Sebai, T.N. 2007. Role of biofertilizer on faba bean growth, yield, and its effect on bean aphid and the associated predators. *Res. J. Agric. Biol. Sci.* **3**(6), 800–807.
- Herdina, J.A. & Silsbury, J.H. 1989. Nodulation and early growth of faba bean (*Vicia faba* L.) and pea (*Pisum sativum* L.) as affected by strain of *Rhizobium*, NO₃-supply, and growth temperature. *Aust. J. Agric. Res.* **40**, 991–1001.
- Kantar, F., Elkoca, E., Ogutcu, H. & Algur, O.F. 2003. Chickpea yields in relation to *Rhizobium* inoculation from wild chickpea at high altitudes. *J. Agron. Crop. Sci.* **189**(5), 291–297.
- Lira Junior, M.D.A., Lima, A.S.T., Arruda, J.R.F. & Smith, D.L. 2005. Effect of root temperature on nodule development of bean, lentil and pea. *Soil. Biol. Biochem.* **37**, 235–239.
- Lynch, D.H. & Smith, D.L. 1994. The effects of low root-zone temperature stress on two soybean (*Glycine max*) genotypes when combined with *Bradyrhizobium* strains of varying geographic origin. *Acta Physiol. Plant.* **90**, 105–113.

- Mishra, P.K., Bisht, S.C., Ruwari, P., Joshi, G.K., Singh, G., Bisht, J.K. & Bhatt, J.C. 2011. Bioassociative effect of cold tolerant *Pseudomonas spp.* and *Rhizobium leguminosarum*-PR1 on iron acquisition, nutrient uptake and growth of lentil (*Lens culinaris* L.). *Eur. J. Soil. Biol.* **47**, 35–43.
- Paulucci, N.S., Medeot, D.B., Dardanelli, M.S. & De Lema, M.G. 2011. Growth temperature and salinity impact fatty acid composition and degree of unsaturation in peanut-nodulating rhizobia. *Lipids* **46**, 435–441.
- Pawar, V., Pawar, P.R., Bhosale, A.M. & Chavan, S.V. 2014. Effect of Rhizobium on Seed Germination and Growth of Plants. *JAIR* **3**(2), 84–88.
- Pérez-Montaño, F., Alías-Villegas, C., Bellogín, R.A., del Cerro, P., Espuny, M.R., Jiménez-Guerrero, I., López-Baena, F.J., Ollero, F.J. & Cubo, T. 2014. Plant growth promotion in cereal and leguminous agricultural important plants: From microorganism capacities to crop production. *Microbiol. Res.* **169**, 325–336.
- Prévost, D., Drouin, P., Laberge, S., Bertrand, A., Cloutier, J. & Lévesque, G. 2003. Cold-adapted rhizobia for nitrogen fixation in temperate regions. *Can. J. Bot.* **81**, 1153–1161.
- Rowland, G.G. & Gusta, V. 1977. Effects of soaking, seed moisture content, temperature, and seed leakage on germination of faba bean (*Vicia faba*) and peas (*Pisum sativum*). *Can. J. Plant Sci.* **57**(2), 400–406.
- Ruotsalainen, A.L. & Kytöviita, M. 2004. Mycorrhiza does not alter low temperature impact on *Gnaphalium norvegicum*. *Oecologia* **140**, 226–233.
- Souza, R., De Ambrosini, A. & Passaglia, L.M.P. 2015. Plant growth-promoting bacteria as inoculants in agricultural soils. *Genet. Mol. Biol.* **38**(4), 401–419.
- Verbon, E.H. & Liberman, L.M. 2016. Beneficial microbes affect endogenous mechanisms controlling root development. *Trends Plant Sci.* **21**(3), 218–229.
- Voisin, A.S., Guéguen, J., Huyghe, C., Jeuffroy, M.H., Magrini, M.B., Meynard, J.M., Mougél, C., Pellerin, S. & Pelzer, E. 2014. Legumes for feed, food, biomaterials and bioenergy in Europe: a review. *Agron. Sustain. Dev.* **34**(2), 361–380.
- Wang, X., Pan, Q., Chen, F., Yan, X. & Liao, H. 2011. Effects of co-inoculation with arbuscular mycorrhizal fungi and rhizobia on soybean growth as related to root architecture and availability of N and P. *Mycorrhiza* **21**, 173–181.
- Zahran, H.H. 1999. Rhizobium-legume symbiosis and nitrogen fixation under severe conditions and in an arid climate. *Microbiol. Mol. Biol. Rev.* **63**(4), 968–989.
- Zhang, F., Lynch, D.H. & Smith, D.L. 1995. Impact of low root temperatures in soybean [*Glycine max.* (L.) Merr.] on nodulation and nitrogen fixation. *Environ. Exper. Bot.* **35**(3), 279–285.
- Zhang, F. & Smith, D.L. 1994. Effects of low root zone temperatures on the early stages of symbiosis establishment between soybean [*Glycine max* (L.) Merr.] and *Bradyrhizobium japonicum*. *J. Exp. Bot.* **45**(279), 1467–1473.
- Zhu, X.C., Song, F.B. & Xu, H.W. 2010. Arbuscular mycorrhizae improves low temperature stress in maize via alterations in host water status and photosynthesis. *Plant and Soil* **331**, 129–137.
- Воробьев, В.А. 1998. In: *Symbiotic nitrogen fixation and temperature*. (Eds И.Е. Илли, Г.П. Акимова) pp. 9–113 (in Russian: Симбиотическая азотфиксация и температура).
- State limited Liability Company ‘Latvian Environment, Geology and Meteorology Centre’ data base <https://meteo.lv/en/lapas/environment/climate-change/climate-of-latvia/climat-latvia?id=1471&nid=660>. Accessed 23.1.2018.

Intra–annual height growth of hybrid poplars in Latvia. Results from the year of establishment

S. Šēnhofa, M. Zeps, L. Ķēniņa*, U. Neimane, R. Kāpostiņš, A. Kārkliņa and
Ā. Jansons

Latvia State Forest Research Institute Silava, Rigas street 111, LV–2169 Salaspils, Latvia
*Correspondence: laura.kenina@silava.lv

Abstract. Fast growing hybrid poplars (*Populus* spp.) could be successfully used for bioenergy as well as wood production. Productivity of clones had been studied in Baltic States recently, however, little is known about the impact of weather conditions on poplar height growth, thus the potential effect of climate change. Therefore, the aim of this study was to characterize the intra–annual height growth of hybrid poplar clones in Latvia. Height increment of 12 hybrid poplar clones was measured on average with an 11–day interval in the first vegetation season in 2016. Annual shoot height was on average 81.0 ± 6.8 cm, significantly ($p < 0.001$) depending on the poplar clone. Use of long (0.5 m) instead of short (0.3 m) cuttings led to larger annual height increment during the year of establishment of the plantation. From June to September the mean growth intensity was 10 to 15 mm day⁻¹. The trend of height growth intensity, described by Gompertz model, indicated that the poplar clones with largest height had relatively fast increase of the growth intensity from June to July. Changes of growth intensity was linked both with the temperature and sum of precipitation. This tendency was not so pronounced for clones with largest height increment, emphasizing the importance of the phenotypic plasticity in selection of clones for plantations.

Key words: *Populus* spp., short–rotation forestry, cutting length, growth intensity.

INTRODUCTION

The importance of short–rotation forestry has been recognized lately in context of carbon sequestration both as a source for the fibre and solid–wood production as well as the fuelwood (Uri et al., 2011; Bronisz et al., 2016; Wang et al., 2016). Poplars (*Populus* spp.), mostly their hybrid clones, are promising tree species for intensive cultivation in boreal climate, considering their productivity, multiple use of the wood and relatively high resistance against biotic and abiotic stresses (Weih, 2004; Ball et al., 2005; Christersson, 2010; Tullus et al., 2013; Kutsokon et al., 2015).

The growth of poplars is determined by genetic properties of clones (Zhang et al., 2003; Mead, 2005), applied management strategies (DeBell et al., 1996; Mead, 2005; Bilodeau–Gauthiera et al., 2011; Wang et al., 2016), and climate (Olivar et al., 2009; Wang et al., 2016; Šticha et al., 2016). Genetics (species, as well as clones) has strong impact on growth traits and wood properties (Zhang et al., 2003), as well tolerance of trees against different stresses: drought, frost etc. (Mazzoleni & Dickmann, 1988; Ilstedt,

1996; Giovannelli et al., 2007; Chhin, 2010; Pollastrini et al., 2013; Lazdiņa et al., 2016), water–use strategy and efficiency (Schreiber et al., 2011). Therefore, effective selection of best genotypes for specific set of conditions (regions) can be carried out and its results applied in praxis promptly due to simple and cheap vegetative propagation (Mead, 2005; Tullus et al., 2013).

The impact of climatic factors such as temperature (Šēnhofa et al., 2016), length of vegetation period (Wang et al., 2016), frequency and severity of drought (Giovannelli et al., 2007; Olivar et al., 2009; Pollastrini et al., 2013) to growth rate of poplars have been studied extensively. However, under changing climate (Kirschbaum, 2000), the knowledge about the environmental stresses affecting poplar growth, is necessary for development of the sustainable short–rotation forestry (Kozłowski & Pallardy, 2002). Since that, the influence of temperature and precipitation might be modified to some extent by management decisions (Kutsokon et al., 2015) and selection of clones with proper adaptation to certain climate (DeBell et al., 1996; Chhin, 2010).

In different ecotypes the poplar growth has been determined by the photoperiod (Howe et al., 1995), although, temperature has been recognised as strong additional environmental factor, which modifies the sensitivity of the day–length signals at growth cessation and influence the duration of growth and bud formation (Rohde et al., 2011). Differences between the frost tolerance of poplar clones (Lazdiņa et al., 2016), as well as regeneration of trees after serious frost damages (Šēnhofa et al., 2017) have been studied also in Latvia. However, little is known about the intra–annual growth patterns and response to weather conditions. Numerous studies regarding effect of water availability on poplar productivity found that the precipitation has large effect of tree growth during the vegetation period (Leonelli et al., 2008; Jules et al., 2010), however, in Nordic countries it has not been recognised as a limiting factor (Messaoud & Chen, 2011). Temperature has been found as primary controlling factor of height growth intensity of a most widely used hybrid aspen (*Populus tremula* L. × *P. tremuloides* Michx.) in our region (Jansons et al., 2014). The impact of diurnal temperature and precipitation to variation of height growth intensity and, cumulatively, to annual height increment has not been widely discussed, however, it can be crucial for achieving growth superiority of poplars in expected changing climate in northern Europe. Therefore, the aim of this study was to characterize the intra–annual height growth of hybrid poplar clones in Latvia.

MATERIALS AND METHODS

Study area is located in central part of Latvia, near Vecumnieki (56°34' N, 24°31' E), on former agricultural land. In the spring of 2016 the plantation of poplars was established on flat area with deep drained fertile peat soil of pH 6.

Monoclonal row–plots in three replications were used; the distance between rows was 4 m, between the trees within a row 2 m. Unrooted 0.3 m and 0.5 m long (further 'short' and 'long', respectively) poplar cuttings of 12 clones were planted leaving 3–5 cm above ground (Table 1).

During the study, 20 ramets per clone and type of cutting were randomly selected (on average 6 per replication) for shoot height measurements. Nine measurements of shoot height with the interval of approximately 11 days (ranging from 5 to 18 days) were taken from the ground level in year of establishment. Eight periods of measurements

were defined: 17.06.–29.06., 30.06.–10.07., 11.07.–21.07., 22.07.–08.08., 09.08.–17.08., 18.08.–29.08., 30.08.–08.09., 09.09.–13.09.. About 50% of poplar shoots during the study period were browsed by cervids and damaged by snails; only undamaged trees were included in data analysis (Table 1).

Table 1. Description of the tested poplar clones

Clone	Number of ramets*	Length of cuttings, m	Species	Origin of cuttings**
OP 42	3	0.3	<i>P.maximowiczii</i> × <i>P.trichocarpa</i>	Germany
Max 1	6	0.3	<i>P.maximowiczii</i> × <i>P.nigra</i>	Germany
Max 3	7	0.3		
Matrix 24	6	0.3	<i>P.maximowiczii</i> × <i>P.trichocarpa</i>	Germany
Matrix 49	7	0.3		
Hybride 275	9	0.3	<i>P.maximowiczii</i> × <i>P.trichocarpa</i>	Germany
LV 1	3	0.3	Clones from section <i>Tacahamaca</i>	Sweden
LV 3	6	0.3		
LV 4	6	0.3		
Baldo	7	0.3	<i>P.deltoides</i> clones	Italy
	9	0.5		
Oudenberg	8	0.3	<i>P.deltoides</i> × <i>P.nigra</i>	Italy
	10	0.5		
Vesten	7	0.5	<i>P.deltoides</i> × <i>P.nigra</i>	Italy

* undamaged by cervids and snails; ** country from which the cuttings were obtained.

Mean growth intensity (mm day⁻¹) during measurement periods were calculated for individual trees. The mean annual height increment ± 95% confidence interval (CI) and mean growth intensity ± CI for each variant of planting material of poplar cuttings were calculated. At the end of the period of measurements all ‘short’ poplar clones were grouped depending on the length of annual height increment assessment: 1 – ‘short–max’ – Hybrid 275, Oudenberg 0.3 m; 2 – ‘short–average’ – Baldo 0.3 m, Max 1, Max 3, Matrix 24, Matrix 49; 3 – ‘short–min’ – OP 42, LV 1, LV 3, LV 4. Hourly data of weather parameters (i.e., temperature, precipitation) were obtained from the nearest weather station of Latvian Environmental, Geology and Meteorology Centre from the study site.

Analysis of variance (ANOVA) and the Tukey Honest Significant difference (HSD) test were used to assess the differences of height increment and growth intensity between cuttings of different length, as well as the differences between clones. The non-linear Gompertz model (Eq. 1) was fitted for individual trees to assess the intra-annual growth trend in growing season (Fekedulegn et al., 1999)

$$f(A) = \alpha \exp(-\beta \exp(-kA)) \quad (1)$$

where α – asymptote parameter; β – displacement parameter; k – growth intensity parameter; A – day since the start of the measurements.

The differences between obtained parameters (α , β , k) were compared using ANOVA to assess the clone effect. The Pearson correlation test was used to assess the relationship between height growth intensity from June till September and values of meteorological factors (i.e., including mean temperature and precipitation sum in the period). The differences in growth intensity and temperature between the measurement

periods were estimated using ANOVA; mean temperature \pm CI was calculated from temperatures of each day of a particular period. All statistical analyses were performed using R v.3.3.1 (R Core Team, 2016).

RESULTS AND DISCUSSION

Measurements had been started, when the length of annual shoot \pm CI had reached 4.0 ± 1.6 cm; it was significantly ($p < 0.05$) smaller for ‘short’ Baldo (1.6 cm) and OP 42 (1.8 cm). Contrary, ‘short’ Oudenberg as well as ‘long’ Vesten and Oudenberg had significantly ($p < 0.05$) larger shoot height before the measurements, 11.8, 12.1 and 14.2 cm, respectively. The mean height \pm CI of poplars at the end of the first growing season (June – September) was 81.0 ± 6.8 cm; it significantly differed ($p < 0.001$) between the poplar clones, ranging from 32 to 102 cm for ‘short’ cuttings and 73 to 132 cm for ‘long’ cuttings, respectively (Fig. 1).

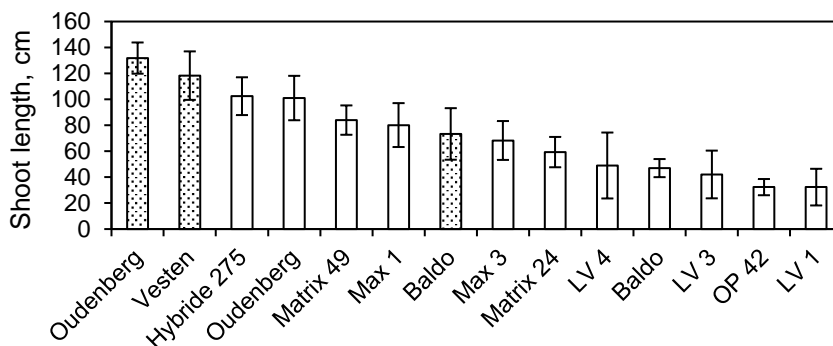


Figure 1. Height increment of poplar clones at the end of the first growing season \pm CI. Different fill patterns separate groups of different cuttings length: ‘short’, (0.3 m) – white columns; ‘long’, (0.5 m) – dotted columns.

At the end of September, mean height \pm CI of ‘short’ clones was 69.2 ± 6.9 cm. Shoot height of ‘short’ Hybride 275, Oudenberg and Matrix 49 were significantly higher than ‘short’ Baldo, LV 3, OP 42 and LV 1 clones. The significantly ($p < 0.05$) smaller height at the end of period of measurements was reached by clones LV 1 and OP 42 with 32 ± 14.1 cm and 32 ± 6.3 cm, respectively. Although clone OP 42 had poor growth, likely due to specific site conditions, it has been widely and successfully used in the south of Sweden, reaching the biomass of approximately $8 \text{ t dry mass ha}^{-1} \text{ yr}^{-1}$ (Christersson, 2008), suggesting that the limited number of replications requires additional studies.

The mean shoot height \pm CI of ‘long’ clones was 107.9 ± 13.4 cm. The ‘long’ Oudenberg and Vesten clones had significantly ($p < 0.05$) higher shoot height (131.8 cm and 118.3 cm, respectively) compared to ‘long’ Baldo (73.3 cm) at the end of September, likely due to the differences in the late–summer growth strategy (Devine et al., 2010).

For the clones with two different cutting lengths, Oudenberg and Baldo, shoot height was significantly ($p < 0.001$) influenced both by clone and length of the cuttings, while the effect of the interaction between these two factors was non–significant ($p = 0.74$; $R^2 = 0.75$). The ‘long’ cuttings of Oudenberg clone exceeded the shoot height

by 30% compared to ‘short’ cuttings, 132 ± 12.0 cm and 101 ± 17.1 cm, respectively. For Baldo, the ‘long’ cuttings exceeded the shoot height of ‘short’ cuttings by 50% (73 ± 20.0 cm and 47 ± 7.0 cm, respectively), suggesting that the ‘long’ cuttings resulted in largest height and biomass production (depending from the clone); it is in accordance to findings of other studies (Burgess et al., 1990; DeBell et al., 1996; Rossi, 1999; Camp et al., 2012). Such tendency can be explained by larger nutrient reserves for shoots of longer cuttings (Buhler et al., 1997; Marino & Gross, 1998). Moreover, the higher shoot height of ‘long’ cuttings may have occurred due to higher ability to reach the capillary flow of ground water compared to ‘short’ cuttings, considering the planting depth (Bloomberg, 1963; Vigl & Rewald, 2014). The mean growth intensity in all periods was 10 to 15 mm day⁻¹. Some of the clones (e.g., OP 42, LV 1, LV 3) did not show the height increment greater than 10 mm day⁻¹ in any period of measurements – contrary the ‘long’ Vesten, ‘long’ and ‘short’ Oudenberg, as well as ‘short’ Hybride 275 exceeded 15 mm day⁻¹ at least in two measuring periods. It suggests, that clones have different intra-annual growth trends (Devine et al., 2010).

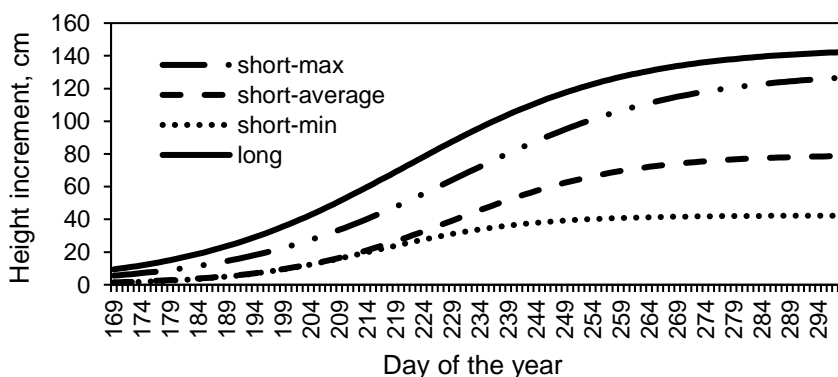


Figure 2. Gompertz model for groups of poplar clones. Clone groups of poplar: ‘short-max’ – Hybride 275, Oudenberg 0.3 m cuttings; ‘short-average’ – Baldo 0.3 m, Max 1, Max 3, Matrix 24, Matrix 49; ‘short-min’ – OP 42, LV 1, LV 3, LV 4; ‘long’ – Oudenberg 0.5 m, Vesten 0.5 m.

The non-linear Gompertz model was fitted to height growth intensity data for 4 clone groups of poplars after the mutual growth trend analysis: ‘short-min’, ‘short-average’, ‘short-max’, and ‘long’ (clone Baldo was excluded from this group due to significantly ($p < 0.05$) lower height compared to Oudenberg and Vesten) (Fig. 2). Model parameter α , showing the maximum value of the height increment, significantly ($p < 0.05$) differed between all ‘short-’ clone groups, although, parameter β , describing the initial phase of the growth, was similar. Significant ($p < 0.05$) differences between the slope (parameter k) of ‘short-min’ and ‘short-max’ groups indicated the sharper increase of height increment at the beginning of July for poplars with largest annual height increment at the end of the September. Obtained model parameters (α , β , k) revealed that the growth dynamics was similar between ‘long’ and ‘short-max’ poplar clones, showing that weather conditions (primarily temperature) play a significant role in their growth (Ilstedt, 1996; Šěnhofa et al., 2016). Generally, clones with largest height increment at the end of growing season showed the highest growth intensity in the beginning of growth and relatively fast increase during first part of the season; that partly

might be a result of genetically determined differences in leaf flushing (Jansons et al., 2014).

Link between growth intensity and meteorological parameters (i.e., temperature and precipitation) was observed (Fig. 3). In second period (30.06.–10.07.) the mean diurnal temperature decreased (from 19.3 °C to 17.6 °C) causing the growth intensity decrease by on average 2.2 mm day⁻¹ for all trees, although, the precipitation sum was 69 mm (Fig. 3). The maximum growth intensity was recorded when the precipitation reached the maximum (108 mm; 19.2 °C) at the end of July (22.07.–08.08.), increasing to an on average 12.7 mm day⁻¹. The growth intensity in fourth period varied greatly between the poplar clones, ranging from 4.6 mm day⁻¹ (LV 1) to 18.5 mm day⁻¹ ('long' Oudenberg). In the mid–August (09.08.–17.08.) temperature and precipitation felled to 14.9 °C and 60 mm, respectively, caused the growth intensity decrease to on an average of 10.2 mm day⁻¹. Although, the temperature increased in the next period (18.08.–29.08), the growth intensity remained approximately the same as in the previous period (10.3 mm day⁻¹). This suggests different late–summer growth strategy (Devine et al., 2010) for analysed poplar genotypes, confirming that weather conditions have a strong influence on growth and inwintering of poplars during the last month of growing season (Ilstedt, 1996). Further, the growth intensity decreased gradually with the decrease of temperature and precipitation as sum until the end of measuring.

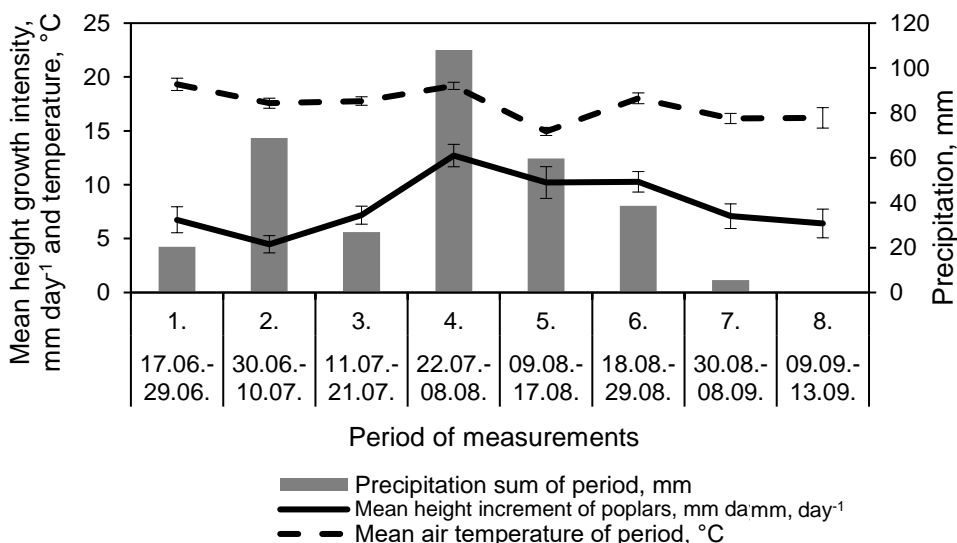


Figure 3. Mean height growth intensity (mm day⁻¹) of poplar ± CI in relation to meteorological parameters. The temperature for the period of measurements has been calculated as mean value of the recorded diurnal temperatures ± CI.

Growth intensity of the poplar clones had notable ($p > 0.05$) positive correlation with the precipitation sum, weaker – with the mean diurnal temperature, mean $r = 0.60$ and $r = 0.17$, respectively. Clones with longest annual height ('long' Vesten and 'long' Oudenberg) during the unusually cold period (09.08.–17.08.) continued their growth, when other poplar clones reduced it (Figs 1, 3). This suggested the robustness of fast-growing genotypes to weather conditions, as previously shown by Jansons et al. (2014).

Despite non-significant correlation, the temperature effect on poplar growth was evident by the notable differences of the height growth intensity between the periods with the prompt changes of mean diurnal temperature (Fig. 3), i.e.: between the first and second, the third and fourth, the fourth and fifth, as well as the sixth and seventh periods. It may indicate the short term acclimatization of poplars to environmental signals, showed by Rohde et al. (2011). However, at the first part of the growing season (i.e., between the second and third period) temperature was not deciding factor to ensure significant growth intensity increase (Fig. 3). It might be due to interaction with other environmental factors, like precipitation (Leonelli et al., 2008; Chhin, 2010). Also towards the end of the growing season (between the fifth and sixth period), sharp increase of temperature was not followed by notable rise of growth intensity, suggesting that other factors, e.g., photoperiod (Howe, 1995; Rohde et al., 2011; Soolanayakanahally et al., 2015) may have reduced the importance of temperature.

CONCLUSIONS

Mean annual shoot height of poplar clones was 81.0 ± 6.8 cm; it was significantly affected by genotype (clone). Slightly longer (0.5 vs. 0.3 m) cuttings (Baldo, Oudenberg) ensured notably (30–50%) larger annual shoot length. Intra-annual height curves, described by Gompertz model, indicated that the poplar clones with largest annual shoot height ('long' Vesten and 'long' Oudenberg) had relative sharp increase of the growth intensity from June to July. Link between growth intensity and temperature, precipitation was observed; it was weaker for the clones with largest annual height increment.

ACKNOWLEDGEMENTS. Research was carried out in accordance with the contract No. 1.2.1.1/16/A/009 between 'Forest Sector Competence Centre' Ltd. and the Central Finance and Contracting Agency, concluded on 13th of October, 2016, the study is conducted by the Latvian State Forest Research Institute 'Silava' with support from the European Regional Development Fund (ERDF) within the framework of the project 'Forest Sector Competence Centre'.

REFERENCES

- Ball, J., Carle, J. & Lungo, A.D. 2005. Contribution of poplars and willows to sustainable forestry and rural development. *Unasylva* **221**(56), 3–9.
- Bilodeau-Gauthiera, S., Pareb, D., Messiera, C. & Belangerc, N. 2011. Juvenile growth of hybrid poplars on acidic boreal soil determined by environmental effects of soil preparation, vegetation control, and fertilization. *For. Ecol. Manage* **261**, 620–629.
- Bloomberg, W.J. 1963. The significance of initial adventitious roots in poplar cuttings and the effect of certain factors on their development. *For. Chron.* **39**(3), 279–289.
- Bronisz, K., Strub, M., Cieszewski, C., Bijak, S., Bronisz, A., Tomusiak, R., Wojtan, R. & Zasada, M. 2016. Empirical equations for estimation aboveground biomass of *Betula pendula* growing on former farming in central Poland. *Silva Fenn.* **50**(4), id1559, doi:10.14214/sf.1559.
- Buhler, D.D., Netzer, A.D., Riemenschneider, D.E. & Hartzler, R.G. 1997. Weed management in short rotation poplar and herbaceous perennial crops grown for biofuel productions. *Biomass Bioenergy* **14**, 385–394.
- Burgess, D., Hendrickson, O.Q. & Roy, L. 1990. The importance of initial cutting size for improving the growth performance of *Salix alba* L. *Scand. J. For. Res.* **5**, 215–224.

- Camp, J.C., Rousseau, R.J. & Gardiner, E.S. 2012. Longer black willow cuttings result in better initial height and diameter growth in biomass plantations. In Butnor, J.R. (ed): *Proceedings of the 16th Biennial Southern Silvicultural Research Conference*. Southern Research Station, Asheville, NC, USA. pp. 43–46.
- Chhin, S. 2010. Influence of climate on the growth of hybrid poplar in Michigan. *Forests* **1**, 209–229.
- Christersson, L. 2010. Wood production potential in poplar plantations in Sweden. *Biomass Bioenergy* **34**(9), 1289–1299.
- Christersson, L. 2008. Poplar plantations for paper and energy in the south of Sweden. *Biomass Bioenergy* **32**(11), 997–1000.
- DeBell, D.S., Clendenen, G.W., Harrington, C.A. & Zasada, J.C. 1996. Tree growth and stand development in short-rotation *Populus* plantings: 7-year results for two clones at three spacings. *Biomass Bioenergy* **11**, 253–269.
- Devine, W.D., Harrington, C.A. & DeBell, V.B. 2010. Intra-annual growth and mortality of four *Populus* clones in pure and mixed plantings. *New For.* **39**, 287–299.
- Fekedulegn, D., Mac Siurtain, M.P. & Colbert, J.J. 1999. Parameter estimation of nonlinear growth models in forestry. *Silva Fenn.* **33**, 327–336.
- Giovannelli, A., Deslauriers, A., Fragnelli, G., Scaletti, L., Castro, G., Rossi, S. & Crivellaro, A. 2007. Evaluation of drought response of two poplar clones (*Populus* × *canadensis* Mönch ‘I-214’ and *P. deltoides* Marsh. ‘Dvina’) through high resolution analysis of stem growth. *J. Exp. Bot.* **58**, 2673–2683.
- Howe, G.T., Hackett, W.P., Furnier, G.R. & Klevorn, R.E. 1995. Photoperiodic responses of a northern and southern ecotype of black cottonwood. *Physiol. Plant.* **93**, 695–708.
- Ilstedt, B. 1996. Genetics and performance of Belgian poplar clones tested in Sweden. *For. Genet.* **3**(4), 183–195.
- Jansons, Ā., Zeps, M., Rieksts–Riekstiņš, J., Matisons, R. & Krišāns, O. 2014. Height increment of hybrid aspen *Populus tremuloides* × *P. tremula* as a function of weather conditions in central part of Latvia. *Silva Fenn.* **48**(5), id1124, doi: 10.14214/sf.1124.
- Jules, E.S., Carroll, A.L. & Kauffman, M.J. 2010. Relationship of climate and growth of quaking aspen (*Populus tremuloides*) in Yellowstone National Park. Final Report for RWO 81 Rocky Mountain Ungulates, Arcata, 26 pp.
http://digitalcommons.usu.edu/aspen_bib/7056/. Accessed: 13.09.2017.
- Kirschbaum, M.U.F. 2000. Forest growth and species distribution in a changing climate. *Tree Physiol.* **20**, 309–322.
- Kozłowski, T.T. & Pallardy, S.G. 2002. Acclimation and adaptive responses of woody plants to environmental stresses. *Bot. Rev.* **68**(2), 270–334.
- Kutsokon, N.K., Jose, S. & Holzmueller, E. 2015. A global analysis of temperature effects on *Populus* plantation production potential. *Am. J. Plant Sci.* **6**, 23–33.
- Lazdiņa, D., Šēnhofa, S., Zeps, M., Makovskis, K., Bebre, I. & Jansons, A. 2016. The early growth and fall frost damage of poplar clones in Latvia. *Agronomy Research* **14**(1), 109–122.
- Leonelli, G., Denneker, B., Bergeron, Y. 2008. Climate sensitivity of trembling aspen radial growth along a productivity gradient in northeastern British Columbia, Canada. *Can. J. For. Res.* **38**(5), 1211–1222.
- Marino, P.C. & Gross, K.L. 1998. Competitive effects of conspecific and herbaceous (weeds) plants on growth and branch architecture of *Populus* × *euramericana* cv. Eugenei. *Can. J. For. Res.* **28**, 359–367.
- Mazzoleni, S. & Dickmann, D.I. 1988. Differential physiological and morphological responses of two hybrid *Populus* clones to water stress. *Tree Physiol.* **4**(1), 61–70.
- Mead, D.J. 2005. Opportunities for improving plantation productivity. How much? How quickly? How realistic? *Biomass Bioenergy* **28**, 249–266.

- Messaoud, Y. & Chen, H.Y.H. 2011. The influence of recent climate change on tree height growth differs with species and special environment. *PLoS One* **6**(2), e14691, doi: 10.1371/journal.pone.0014691.
- Olivar, J., Duncker, P. & Spiecker, H. 2009. Impact of climatic variation on growth and wood density of young short rotation poplar trees. In Kaczka, R., Malik, I., Owczarek, P., Gärtner, H., Helle, G., Heinrich, I. (eds.): *Proceedings of the Dendrosymposium 2008. TRACE – Tree Rings in Archaeology, Climatology and Ecology*. Zakopane, Finland, Vol **7**, pp. 64–70.
- Pollastrini, M., Desotgiu, R., Camin, F., Ziller, L., Marzuoli, R., Gerosa, G. & Bussotti, F. 2013. Intra-annual pattern of photosynthesis, growth and stable isotope partitioning in a poplar clone subjected to ozone and water stress. *Water Air Soil Pollut.* **224**, 1761, doi:10.1007/s11270-013-1761-4.
- R Core Team 2016. R: A language and environment for statistical computing. R Foundation for Statistical Computing, Vienna, Austria. <https://www.R-project.org/>.
- Rohde, A., Bastien, C., Boerjan, W. & Thomas, S. 2011. Temperature signals contribute to the timing of photoperiodic growth cessation and bud set in poplar. *Tree Physiol.* **31**(5), 472–482.
- Rossi, P. 1999. Length of cuttings in establishment and production of short-rotation plantations of Salix ‘Aquatica’. *New For.* **18**, 161–177.
- Schreiber, S.G., Hacke, U.G., Hamann, A. & Thomas, B.R. 2011. Genetic variation of hydraulic and wood anatomical traits in hybrid poplar and trembling aspen. *New Phytol.* **190**, 150–160.
- Soolanayakanahally, R.Y., Guy, R.D., Street, N.R., Robinson, K.M., Silim, S.N., Albrechtsen, B.R. & Jansson, S. 2015. Comparative physiology of allopatric *Populus* species: geographic clines in photosynthesis, height growth, and carbon isotope discrimination in common gardens. *Front. Plant. Sci.* **5**, 528, doi: 10.3389/fpls.2015.00528.
- Šēnhofa, S., Neimane, U., Grava, A., Sisenis, L., Lazdina, D. & Jansons, A. 2017. Juvenile growth and frost damages of poplar clone OP42 in Latvia. *Agronomy Research* **15**, doi: doi.org/10.15159/AR.17.061.
- Šēnhofa, S., Zeps, M., Matisons, R., Smilga, J., Lazdiņa, D. & Jansons, Ā. 2016. Effect of climatic factors on tree-ring width of *Populus* hybrids in Latvia. *Silva Fenn.* **50**(1), id 1442, doi: doi.org/10.14214/sf.1442.
- Štícha, V., Macků, J. & Nuhlíček, O. 2016. Effect of permanent waterlogging on the growth of poplar clones MAX 4, MAX 5 (J-104, J-105) (*Populus maximowiczii* A. Henry × *P. nigra* Linnaeus) and evaluation of wood moisture content in different stem parts. *J. For. Sci.* **62**, 186–190.
- Tullus, H., Tullus, A. & Rytter, L. 2013. Short-rotation forestry for supplying biomass for energy production. In Kellomäki, S., Kilpeläinen, A., Alam, A. (eds.): *Forest bioenergy production*. Springer, New York. pp. 39–56.
- Uri, V., Löhmus, K., Mander, Ü., Ostonen, I., Aosaar, J., Maddison, M., Helmisaari, H.S. & Augustin, J. 2011. Long-term effects on the nitrogen budget of a short-rotation grey alder (*Alnus incana* (L.) Moench) forest on abandoned agricultural land. *Ecol. Eng.* **37**(6), 920–930.
- Vigl, F. & Rewald, B. 2014. Size matters? The diverging influence of cutting length on growth and allometry of two Salicaceae clones. *Biomass Bioenergy* **60**, 130–136.
- Wang, D., Fan, J., Jing, P., Cheng, Y. & Ruan, H. 2016. Analyzing the impact of climate and management factors on the productivity and soil carbon sequestration of poplar plantations. *Environ. Res.* **144**(B), 88–95.
- Weih, M. (2004). Intensive short rotation forestry in boreal climates: present and future perspectives. *Can. J. For. Res.* **34**(7), 1369–1378.
- Zhang, S.Y., Yu, Q., Chauret, G. & Koubaa, A. 2003. Selection for both growth and wood properties in hybrid poplar clones. *For. Sci.* **49**(6), 1–8.

Swelling Pressure and Form Stability of Cellular Wood Material

U. Spulle^{1,*}, E. Buksans^{1,2}, J. Iejavs² and R. Rozins¹

¹Latvia University of Life Sciences and Technologies, Forest faculty, Department of Wood Processing, Dobeles iela 41, LV-3001 Jelgava, Latvia

²Forest and Wood Products Research and Development Institute, Dobeles iela 41, LV-3001 Jelgava, Latvia

*Correspondence: uldis.spulle@llu.lv

Abstract. Cellular Wood Material (hereinafter CWM) middle layer of the Dendrolight® has been developed in the beginning of this century as a wood material for minimization of internal stresses, because of the material structure and reduced swelling and shrinking impact to products in end use application. Some research has been conducted on the physical – mechanical and physical – chemical properties of CWM, while dimensional stability has not been well researched. The goal of this research is to perform an assessment of the CWM shrinkage and swelling impact on dimensional characteristics of the CWM multilayer composite materials. CWM *swelling pressure* in length, width, and height of the material were determined and compared to the relevant indicators of pine solid wood. The *form stability* or the impact of combination of the CWM with some facing materials – wood particle board, medium density fibre board (hereinafter MDF), oriented strand board (hereinafter OSB), pine solid wood, gypsum plaster board used in wood products was investigated. The hypothesis that swelling pressure of CWM must be lower than that of pine solid wood was proved, it is 2.3 times lower in the radial direction and 3.9 times lower in tangential direction compared to pine solid wood. The CWM samples, manufactured for determining the form stability in wetting conditions deflected in the height direction by 4%, thus creating deflections also in the seams between separate lamellas of the CWM. Swelling pressure of the CWM is several times smaller than that of solid wood and can be further limited by creating complex wood and non-wood composite material panels using gluing technique.

Key words: dimensional stability, moisture uptake, wood, wood composites.

INTRODUCTION

Shrinkage and swelling create the biggest problems in manufacturing of wood construction and carpentry elements, since the wood materials used have a moisture content lower than 30% (Viteckopfs, 1944). Swelling pressure of wood has been studied (Tarkow & Turner, 1958; Perkitny & Helinska, 1963; Kollmann & Cote 1984; Mantanis et al., 1994).

Properties of earlywood and latewood have an impact on shrinkage and swelling. Latewood swells approximately twice as much as earlywood, because the density of earlywood is lower than that of latewood (Rowell, 1995; Rowell, 2012). According to a

research made in Russia, swelling pressure of 20×20×30 mm pine wood samples with moisture content of 12–15% in radial direction was between 0.82 and 1.1 MPa, while in tangential direction it was higher, 1.44–2.14 MPa (Wood Moisture Content, 2013).

In longitudinal direction, the maximal swelling and shrinking are the smallest, from 0.1 to 0.3%; in radial direction, may reach 5 to 7%, while in tangential direction 10 to 12%, therefore it may be 1.5 to 2.0 times greater than in radial direction (Bowyer, 2003).

When moisture content of wood composite material, such as plywood, changes by 1%, the length and width of plywood changes by approximately 0.15 mm per 1 meter, the relevant thickness changes from 0.3 to 0.4% (Handbook of Finnish Plywood, 2002). Other wood based materials like wood particle board, MDF and OSB are shrinking and swelling even more.

CWM is characterized as a dimensionally stable material. It is produced from integrated groove-profiled pinewood sawn materials (Fig. 1, type 1), glued together in four layers by placing each subsequent board perpendicularly on top of the previous one (Fig. 1, type 2), thus creating a cellular material block (Fig. 1, type 3). Subsequently, the cellular material block is being sawed into lamellas of the required thickness, (Fig. 1, type 4). The obtained cellular material lamella can easily be combined with different materials and can be used as an end-product in both carpentry production and construction products sector (Dendrolight Latvija, 2013).



Figure 1. CWM production steps – starting from left to right hand (Dendrolight Latvija 2013).

The inventor of CWM, Johann Berger (Berger, 2008), mentioned that material has a lower density, from 100 to 300 kg m⁻³, lower swelling in height direction, 2 to 4%, compared to other composite materials, and that changes are reversible. In a previously conducted research on CWM shrinkage and swelling indicators, it has been determined that swelling in width and length (hereinafter D g.p) directions of CWM (Fig. 2), is approximately 10 times lower than in height direction (hereinafter D) (New technological solutions..., 2012).

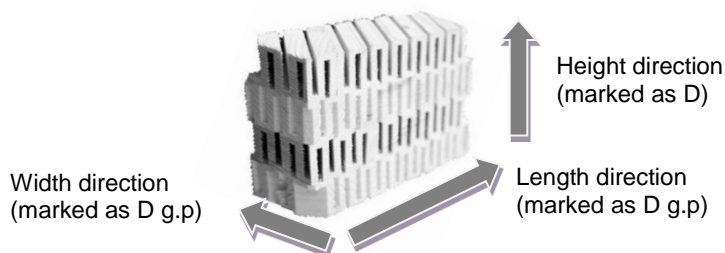


Figure 2. CWM directions.

The objectives of present research is to investigate swelling pressure of CWM in height direction and compare results with pine solid wood characteristics in tangential direction, as much as find out impact of CWM material to some wood based materials – plywood, wood particleboard, OSB, MDF and gypsum plasterboard and compare results with CWM panel with no added materials.

MATERIALS AND METHODS

In order to determine the CWM swelling pressure in height direction, 80 groove-profiled pinewood CWM specimens were produced (width × length × height: 35×35×25 mm). Lamellas without visual wood defects (equal width of annual rings and percentage of latewood) were chosen for the samples. Two lamellas were glued together, each other perpendicularly, with total height of sample 50 mm (Fig. 3.). Totally 40 CWM pinewood samples were prepared.

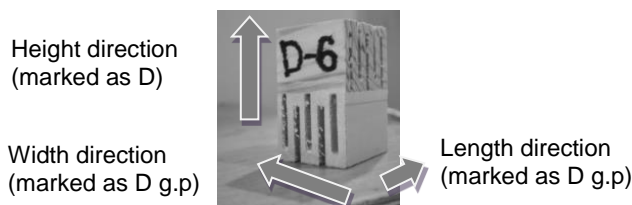


Figure 3. CWM swelling pressure determination sample.

After the samples had been produced, they were placed in a conditioning chamber with a constant temperature (shown in figures as t) 20 ± 2 °C and humidity (shown in figures as W_r) level $65 \pm 5\%$, in order to reach the equilibrium wood moisture content. The average moisture content of wood was 11.55 after the equilibrium moisture content was reached. Determination of moisture content was done accordance with standard EN 13183-1 (EN 13183-1, 2002) and density with standard ISO 3131 (ISO 3131, 1975) requirements. In order to determine the pine CWM swelling pressure, measuring equipment was constructed and it is shown in Fig. 4. The samples were inserted between lower support 2 and upper support 3 (Fig. 4). The swelling force was measured with load cell *K25* (Fig. 4) and data logger *ALMEMO* and data collecting software *WINCONTROL*.



Figure 4. Swelling pressure measurement equipment with CWM sample in height direction (marked as D): a – sample before immersion in water; b – sample in a time of testing; 1 – frame; 2 – lower support; 3 – upper support; 4 –screw; 5 – load cell.

In order to compare the swelling pressure between CWM height and length-width direction, one CWM specimen with dimensions 50×50×50 mm was prepared.

For comparison of the same swelling indicators with pine solid wood, 20 grain oriented pine wood specimens with dimensions 35×35×35 mm were prepared. Ten specimens were tested in radial and ten in tangential grain orientation direction. The description, marking, number and sizes are given in (Table 1).

Table 1. Samples description

Name	Marking	Number of samples	Dimensions: height, length, width; mm
CWM in height direction	D	40	35×35×50
Solid wood in radial direction	R	10	35×35×35
Solid wood in tangential direction	T	10	35×35×35
CWM in length and width direction	D g.p	1	50×50×50

The same measuring technics were used for determination of swelling force of all specimen variations.

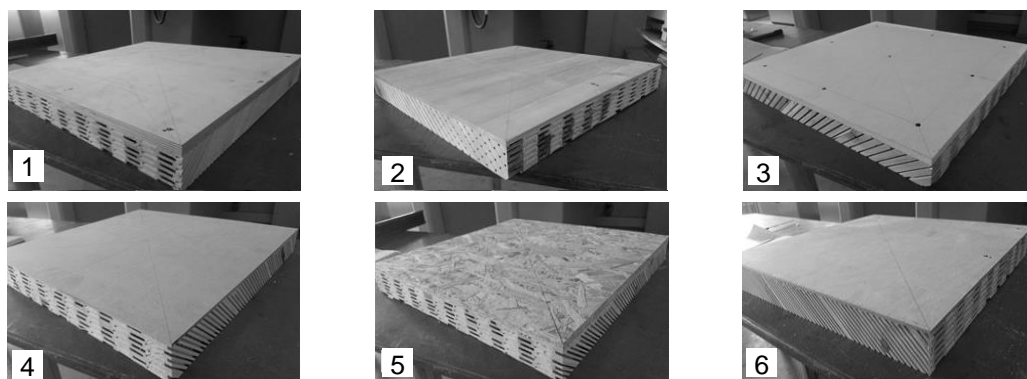


Figure 5. CWM combine samples of form stability: 1 – with plywood, 12 mm; 2 – with pine solid wood, 7 mm; 3 – with gypsum plasterboard, 12 mm; 4 – with MDF, 4 mm; 5 – with OSB, 12 mm; 6 – with plywood, 4.5 mm.

For determination of CWM composite panels form stability (deflection of flat surface) of the CWM in combination with other composite materials, CWM panel materials with length 600 mm, width 600 mm and thickness 52 mm were used. All the specimens were conditioned in constant climate to reach 10% moisture content before panels were glued together. Following composite materials were selected (Fig. 5): 12 mm thick birch plywood (Fig. 5, type 1), 7 mm thick pine solid wood (Fig. 5, type 2), 12 mm thick gypsum plasterboard (Fig. 5, type 3), 4 mm thick MDF (Fig. 5, type 4), 12 mm thick OSB (Fig. 5, type 5), 4.5 mm thick birch plywood (Fig. 5, type 6). Polyurethane glue *Kleiberit* 501, pressure 0.2 MPa and time under pressure 20 minutes were applied when gluing all the materials, except gypsum plasterboard. In order to stick together gypsum plasterboard with CWM panel (length 500 mm, width 500 mm and height 52 mm), the screws with diameter 3 mm and length 45 mm were used, placed within 5 cm from CWM panel edges, in the corners and lateral midpoints of the samples (Fig. 5). All the composite material panels were applied only from one side for better

understanding of CWM shrinkage-swelling effect on multilayer composite materials with CWM core. After applying cover materials samples were cut in square dimension with side length of 500 mm.

One sample was produced with no added composite material for determination of CWM panel form stability. For each group one sample was prepared. After the samples had been produced, they were placed in a conditioning chamber with a constant temperature 20 ± 2 °C and humidity level $65 \pm 5\%$, in order to reach the equilibrium wood moisture content. Average moisture content of samples were 11.5%.

After conditioning deflection of the samples were assessed in four surface directions, center lines of the sample (Fig. 6) (left hand), where a1 stands for CWM height direction, while a2 – length direction, and b1 and b2 – diagonal direction (Fig. 6) (right hand), and the deflections measuring performed at the center of sample.

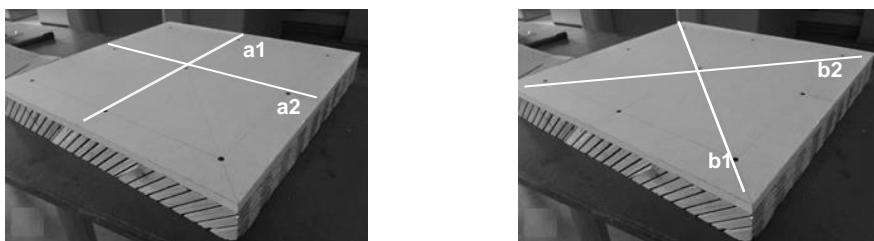


Figure 6. Measuring directions of deflection of samples: a1 – CWM height direction; a2 – CWM length direction; b1 and b2 – diagonal direction.

For assessment of sample deflection in the way of diagonal and center line, a calibrated metal band was used (Fig. 7,1.), placing it on the sample and determining the deflection incurred in the necessary direction (a1; a2; b1 and b2). A measuring probe with reading accuracy 0.5 mm were used for measuring the distance between metal band and sample in case it was there. (Fig. 7,1.).

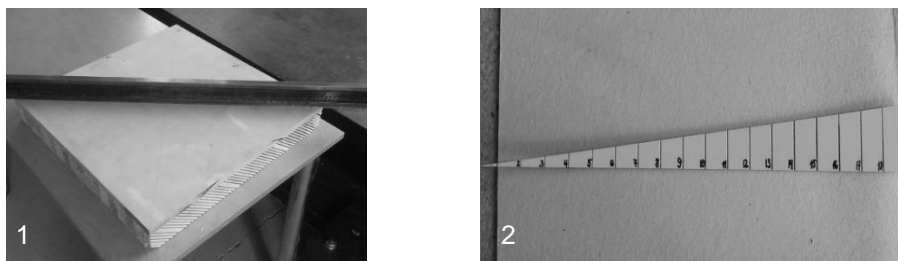


Figure 7. Equipment for measuring deflection of the samples: 1 – metal band; 2 – measuring probe.

Deflection was checked repeatedly after 24 hours and the measurement process was repeated every 48 hours. After 150 hours, sample deflection, the biggest one, were checked once again and samples were placed in a conditioning chamber with temperature 23 ± 2 °C and air humidity $25 \pm 5\%$ giving the target wood equilibrium moisture content 5.55. Sample deflection determination followed similar time interval pattern as described previously in this manuscript.

RESULTS AND DISCUSSION

At first the swelling pressure of pine solid wood was determined. A similar results achieved compared to previous research done which stated pine solid wood swelling pressure in radial direction between 0.82 to 1.10 MPa. The swelling pressure obtained in this research was on average 0.77 MPa (*standard deviation* (hereinafter s) 0.14 MPa, *coefficient of variation* (hereinafter ν) 17.9%). The discrepancy can be explained with structural characteristics of wood. The individual measurements showed that solid wood density has no significant impact on swelling pressure changes. The highest swelling pressure was in tangential direction. The swelling pressure indicators obtained as a result of the research, are 1.7 times higher in tangential than in the radial direction, demonstrating mean swelling pressure 1.3 MPa ($s = 0.12$ MPa, $\nu = 9.6\%$). Compared to the results of previous research stating that swelling pressure is between 1.44 and 2.14 MPa, as well as to radial swelling pressure, minimal difference was observed and can be explained with wood structural characteristics. There were no linear connection observed between tangential direction swelling pressure and solid wood density.

CWM swelling pressure in height direction (Fig. 3.) was between 0.178 and 0.554 MPa and on average 0.33 MPa ($s = 0.08$ MPa, $\nu = 23.7\%$). Relation between CWM density and swelling pressure shows weak correlation.

Fig. 8, depicts the pine solid wood in tangential direction (light grey curve) and radial direction (dark grey curve) demonstrating swelling force changes in time. When placing the sample in the measuring equipment, the force gradually increases until it reaches the peak and thereafter decreases very slowly. Average time required to reach peak swelling force for solid wood was about 10 hours in radial direction and 6 hours in tangential direction. CWM swelling force black curve (Fig. 8), shows that material reached peak swelling force considerably faster than solid wood thanks to its specific structure ensuring much faster water permeability inside the wood sample. Swelling force increases considerably at the beginning of the measuring, followed by a slower increase until it reaches the peak and a subsequent decrease. It occurs much faster than with pine solid wood (Fig. 8).

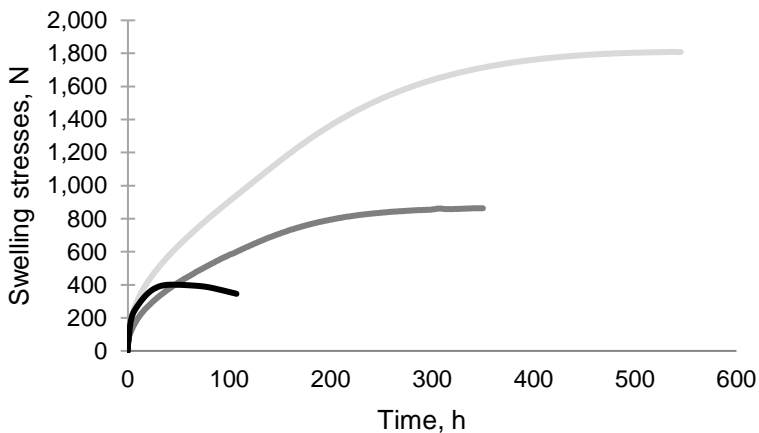


Figure 8. Solid wood in tangential direction (light grey curve), in radial direction (dark grey curve) and CWM in height (black curve) swelling force in a time scale.

When comparing the swelling pressure data obtained, it can be seen (Fig. 9), that CWM swelling pressure in the height direction is 11.5 times higher than in the length and width directions. The previous hypothesis that swelling pressure of CWM must be lower than that of solid wood was proved. It is 2.3 times lower in the radial direction and 3.9 times lower in tangential direction than in solid wood.

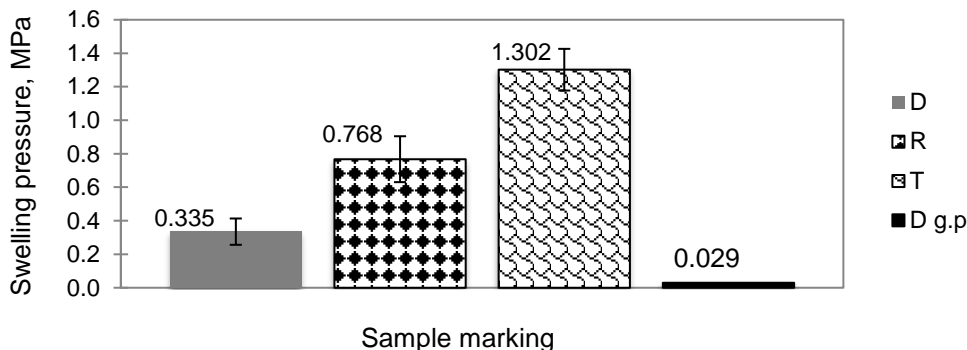


Figure 9. Swelling pressure of the CWM and pine solid wood: D – CWM in height direction; R – solid wood in radial direction; T – solid wood in tangential direction; D g.p – CWM in length and width direction.

Already after multilayer composite panels with CWM core sample preparation deformations occurred as a result of surrounding humidity and slightly glue induced humidity. Fig. 10, demonstrates that samples with solid wood and 12 mm plywood covered have identical indicators, CWM with 4.5 mm plywood covered shows a greater deflection, by 0.4% in height direction and 0.3% in direction of diagonals. Sample with gypsum plasterboard coating demonstrated good form stability after specimen preparation, while MDF gluing sample demonstrated a deflection in CWM longitudinal direction.

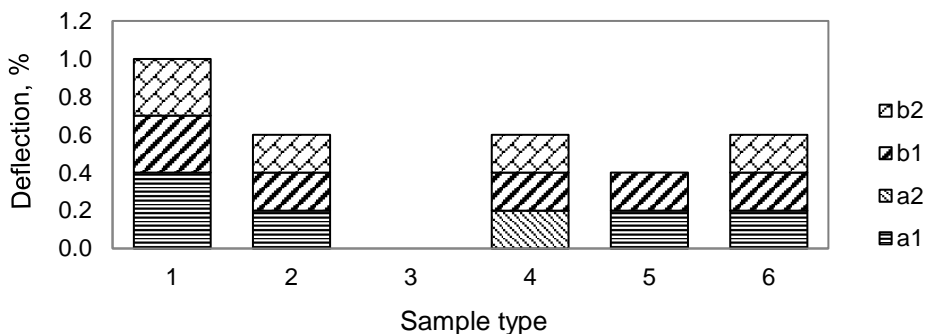


Figure 10. Form stability after preparing of samples: 1 – plywood (4.5 mm); 2 – solid wood (7 mm); 3 – gypsum plasterboard (12 mm); 4 – MDF (4 mm); 5 – OSB (12 mm); 6 – plywood (12 mm); a1 – height direction; a2 – length direction; b1, b2 – diagonal direction.

When environmental parameters change after spending 24 h in conditioning chamber (Fig. 11), in samples with solid wood, 12 mm and 4.5 mm plywood covered no deformation was observed, while the remaining samples showed a deflection in CWM

height and length direction. After conditioning, the moisture content of samples had increased up to 0.6% for 12 mm plywood covered samples and up to 1.9% for solid wood gluing CWM sample.

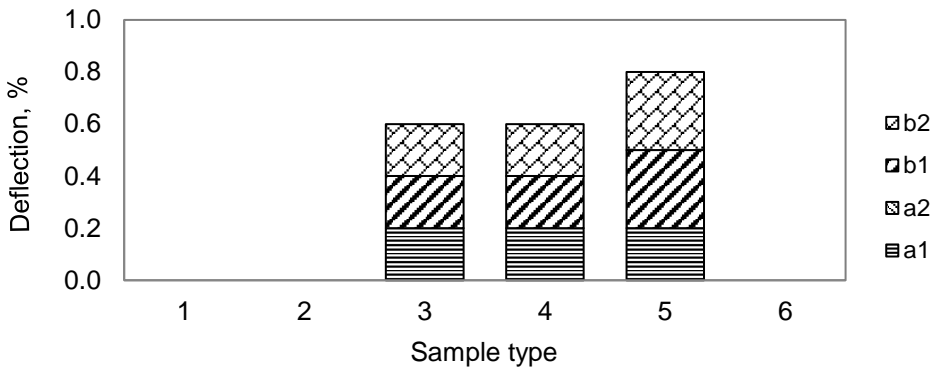


Figure 11. Form stability after 24 hours, $W_r = 65\%$, $t = 20\text{ }^\circ\text{C}$: 1 – plywood (4.5 mm); 2 – solid wood (7 mm); 3 – gypsum plasterboard (12 mm); 4 – MDF (4 mm); 5 – OSB (12 mm); 6 – plywood (12 mm); a1 – height direction, a2 – length direction, b1, b2 – diagonal direction.

After repeated measuring 48 h, all samples showed increased deflection (Fig. 12), and all the deflections were directed in composite material direction. When sample moisture content was increased by 0.9% to 2.2%, more distinct deflection was seen in OSB gluing sample with deflections in directions of both center lines and diagonals. In remaining samples, a distinct deflection was seen in height direction, between 0.2 and 0.3%.

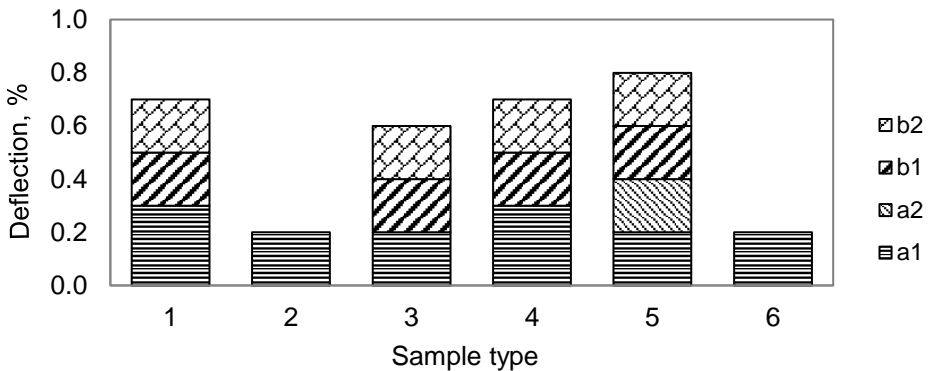


Figure 12. Form stability after 48 hours, $W_r = 65\%$, $t = 0\text{ }^\circ\text{C}$: 1 – plywood (4.5 mm); 2 – solid wood (7 mm); 3 – gypsum plasterboard (12 mm); 4 – MDF (4 mm); 5 – OSB (12 mm); 6 – plywood (12 mm); a1 – height direction; a2 – length direction; b1, b2 – diagonal direction.

After 150 hours of conditioning (Fig. 13), samples with MDF, OSB and 4.5 mm plywood covered demonstrated a distinct deflection, with moisture content increasing by 1.7 to 2.2%, peak form stability deflection in 0.6%. Sample with solid wood gluing demonstrated a deflection in all directions after conditioning, while sample gypsum

plasterboard coating retained the form stability deflection it had acquired at the beginning of conditioning.

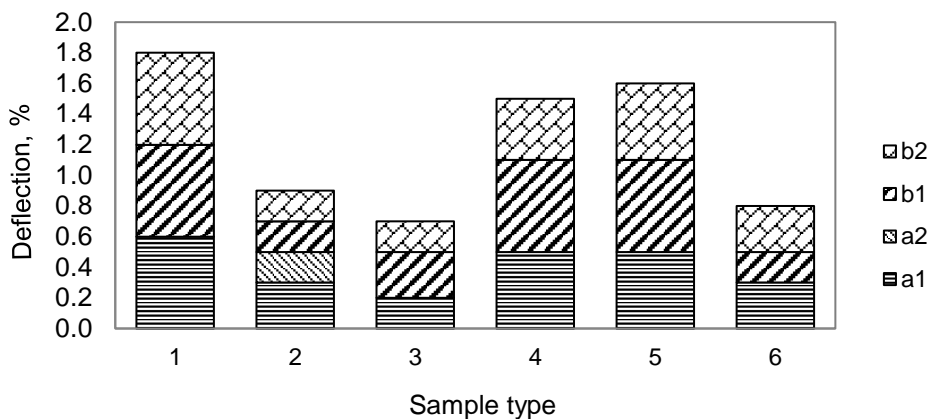


Figure 13. Form stability after 150 hours, $W_r = 65\%$, $t = 0^\circ\text{C}$: 1 – plywood (4.5 mm); 2 – solid wood (7 mm); 3 – gypsum plasterboard (12 mm); 4 – MDF (4 mm); 5 – OSB (12 mm); 6 – plywood (12 mm); a1 – height direction; a2 – length direction; b1, b2 – diagonal direction.

When changing the environmental conditions to drier one – W_r 25% and t 23 °C, a significant deflection was observed. When environmental humidity was reduced, the samples starts deflect in the opposite direction. Fig. 14, demonstrates that all samples, except MDF+CWM, change the direction of deflection. Solid wood gluing sample demonstrates the peak deflection 0.4% in height and directions of diagonals at level when moisture content reduced by 0.2%.

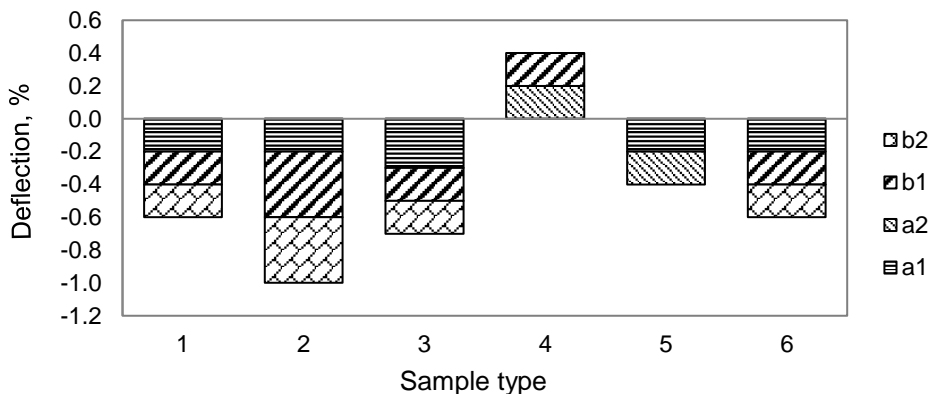


Figure 14. Form stability after 24 hours, $W_r = 25\%$, $t = 23^\circ\text{C}$: 1 – plywood (4.5 mm); 2 – solid wood (7 mm); 3 – gypsum plasterboard (12 mm); 4 – MDF (4 mm); 5 – OSB (12 mm); 6 – plywood (12 mm); a1 – height direction; a2 – length direction; b1, b2 – diagonal direction.

Keeping samples for 48 hours in the aforementioned conditions, their deflection on average increased twice (Fig. 15). Reducing moisture content in samples by 0.2 to 0.8%, the greatest deflection was observed in solid wood gluing sample with deflection of 0.7% in height direction and b1 diagonal 0.7%, b2 diagonal 0.8% in transversal direction.

MDF gluing sample was the only one demonstrating a deflection in CWM length direction, in opposite direction compared to deflection of other samples.

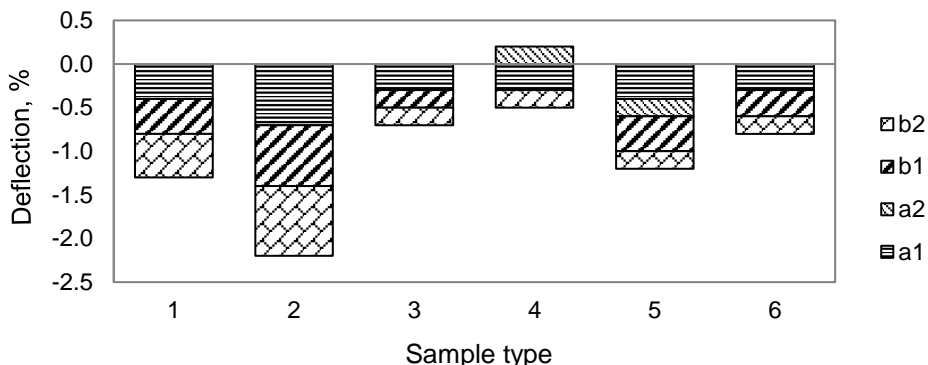


Figure 15. Form stability after 48 hours, $W_r = 25\%$, $t = 23\text{ }^\circ\text{C}$: 1 – plywood (4.5 mm); 2 – solid wood (7 mm); 3 – gypsum plasterboard (12 mm); 4 – MDF (4 mm); 5 – OSB (12 mm); 6 – plywood (12 mm); a1 – height direction; a2 – length direction; b1, b2 – diagonal direction.

When looking at (Fig. 16), we can see that deflections have on average increased twice. The greatest deflection for all samples occurred in CWM height direction and in directions of diagonals. Reducing the moisture content in samples from 2.1 to 3.3%, the deflection is between 0.2 to 1.3%.

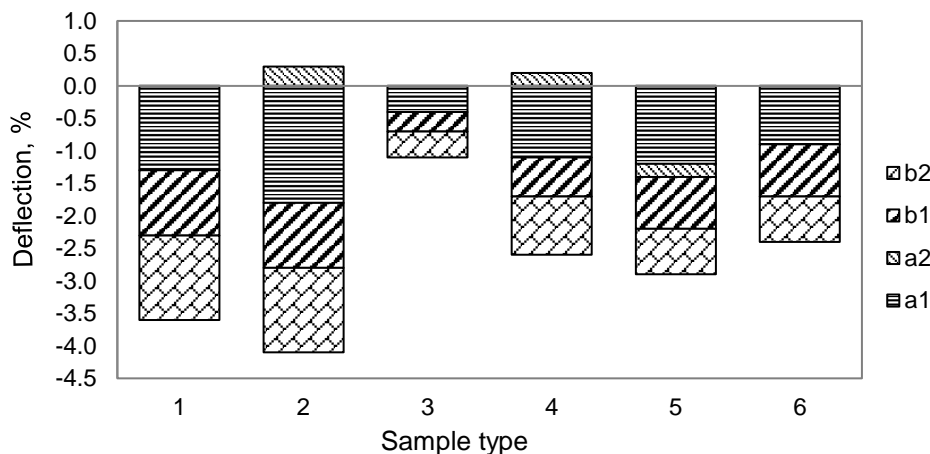


Figure 16. Form stability after 150 hours, $W_r = 25\%$, $t = 23\text{ }^\circ\text{C}$: 1 – plywood (4.5 mm); 2 – solid wood (7 mm); 3 – gypsum plasterboard (12 mm); 4 – MDF (4 mm); 5 – OSB (12 mm); 6 – plywood (12 mm); a1 – height direction; a2 – length direction; b1, b2 – diagonal direction.

In all CWM combinations with other materials influence on dimensional stability can be observed. The greatest deformation can be observed in CWM a1 or CWM height direction (Fig. 17), which can be explained with the largest differences between in swelling-shrinking properties between CWM and facing material.

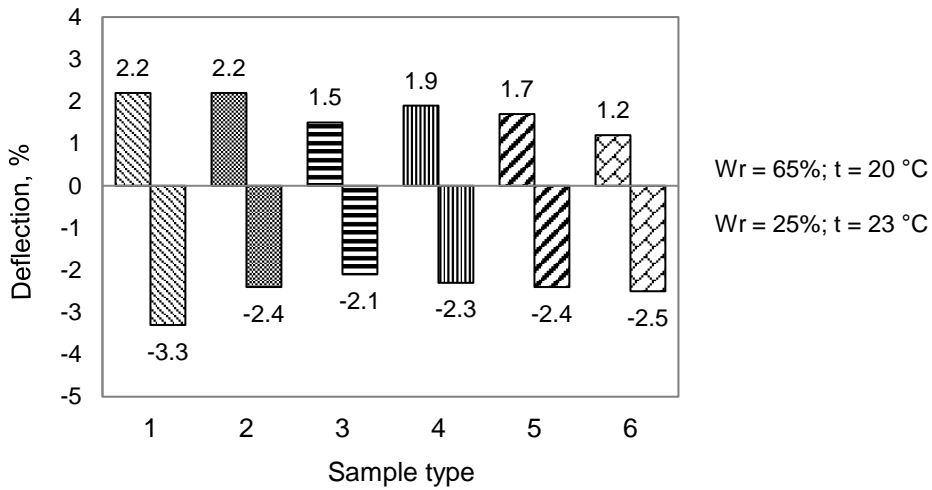


Figure 17. Influence of air condition to the samples moisture content: W_r – air relative humidity; t – air temperature.

Summarizing the results on changes in CWM moisture content (Fig. 17), the moisture content has increased by 1.2 to 2.2%. When samples were exposed 150 h in environment with relative humidity 65% and temperature 20 °C. When the samples were moved to an environment with relative humidity 25% and temperature 23 °C, the moisture content of samples sample decreased several times. The aforementioned changes in humidity are the reason for dimensional changes of samples. Fig. 18 demonstrates the peak deflection of a sample after keeping it in both environments.

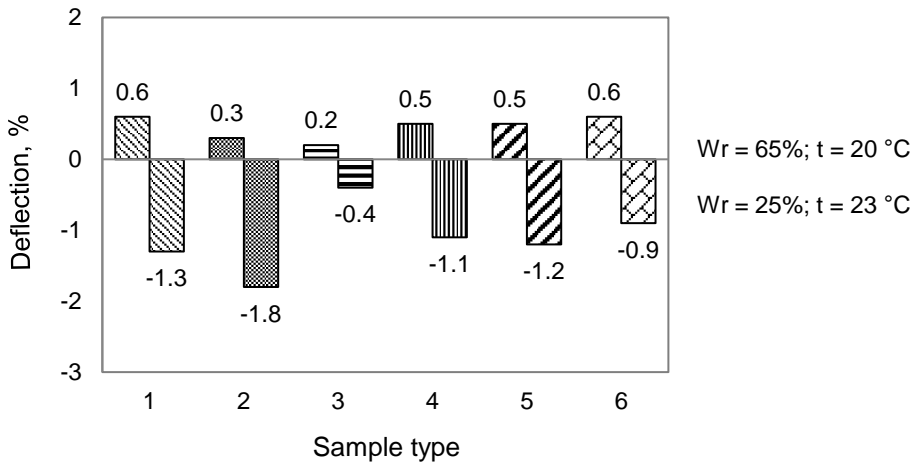


Figure 18. CWM maximal deflection at different environment conditions: W_r – air relative humidity; t – air temperature.

It was observed that the greatest deflection after keeping specimens in conditioning chamber can be observed in 4.5 mm plywood covered samples, which demonstrated a deflection in CWM height direction. When moved to a drier environment, the sample deflections change the direction radically to the opposite side demonstrating indicators almost twice as in height. In a drier environment, solid wood gluing samples show the greatest deflection – by 1.8% in CWM height direction.

When CWM sample without any facing materials was kept in a humid environment for 1h, it showed a deflection in material height direction by 2 cm or 4% (Fig. 19, 1). Upon changed humidity, sample demonstrated also deflection in lamella gluing seams (Fig. 19, 2.).

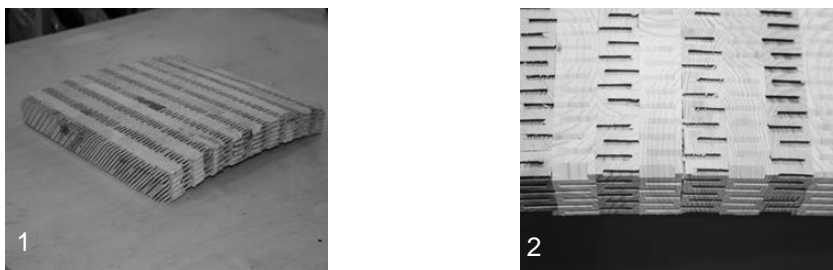


Figure 19. CWM deflection if asymmetric humidity applied to sample: 1 – global deflection; 2 – local deflection.

CONCLUSIONS

1. CWM swelling pressure in the length and width directions was 0.029 MPa, while in the height direction it was 0.335 MPa. CWM swelling pressure in the height direction is 11.5 times higher than in the length and width directions. Compared to pine solid wood, CWM swelling pressure in the height direction was more than 2.3 times lower in radial direction and more than 3.9 times in tangential direction.

2. Even small number of tested samples showed tendencies that CWM combination with different composite materials, such as plywood, MDF, OSB, gypsum plasterboard, solid wood, keeping them in an environment with different air relative humidity and temperature was observed that at heightened humidity, samples demonstrated a deflection in direction of the composite material gluing surface, while it turned in the opposite direction when moisture was reduced.

3. Dimensional changes were caused by different swelling-shrinking performance of CWM and facing materials. Symmetrical construction of multilayer wood based panel with CWM core layer should be produced to ensure panel flatness in products end use application.

4. When samples were kept in an environment with relative humidity 65% and temperature 20 °C, after 150 h the initial moisture content 11.5% has increased by 1.2 to 2.2%, and peak surface deflections is reached, 0.6%. When samples were kept in an environment with relative humidity 25% and temperature 23 °C, compared to initial moisture content decreased by 2.1 to 3.3% creating a peak surface deflections of 1.3%.

5. The existing relationship between CWM density and swelling was found as insignificant, since CWM consists of many lamellas of different density values.

6. The CWM without applying any composites form stability in the event of wetting had within 1h deformed in the height direction of lamella by 4%, damaging also the seams between lamella.

7. Since CWM swelling pressure is several times smaller than that of solid wood, it is much easier to create high dimensional stability multilayer composite materials using CWM core material than solid wood multilayer products.

REFERENCES

- Berger J. 2008. Dendrolight properties and performance. <http://www.dendrolightturkiye.com/data.pdf>. Accessed 19.4.2013.
- Bowyer Jim, L. 2003. *Forest products and wood science*. Wiley-Blackwell, 3 Edition, 484 p.
- Dendrolight Latvija. 2013. <http://dendrolight.lv/lv/>. Accessed 31.10.2017.
- EN 13183-1 Moisture content of a piece of sawn timber. Determination by oven dry method. 2002.
- Handbook of Finnish Plywood. 2002. <https://www.metsateollisuus.fi/uploads/2017/03/30041750/887.pdf>. Accessed 31.10.2017.
- New technological solutions for development of innovative wood materials and products with increased added value. 2012. State research program No. 2010.10-4/VPP-5 "Local resources (subsoil, forests, food and transportation) for sustainable use - new products and technologies (NatRes)" 3rd period overview, LUA, Jelgava. (in Latvian).
- ISO 3131 Wood — Determination of density for physical and mechanical tests. 1975.
- Kollmann, F. & Cote, W.A.Jr. 1984. *Principles of wood science and technology. I. Solid wood*. Springer-Verlag, Berlin, 592 pp.
- Mantanis, G.I., Young, R.A. & Rowell, M.R. 1994. Swelling of wood. *Wood Science and Technology* **28**(2), 119–134.
- Perkitny, T. & Helinska, L. 1963. Swelling pressure of wood in water and water-saturated air. *Holz Roh-Werkstoff* **21**(1), 19–22.
- Rowell, M.R. 1995. One way to keep wood from going this way and that., American record. <http://www.dolmetsch.com/rowel95d.pdf>. Accessed 14.12.2017.
- Rowell, M.R. 2012. Handbook of wood chemistry and wood composites. CRC press, 487 pp.
- Tarkow, H. & Turner, H.D. 1958. The swelling pressure of wood. *Forest Products Journal* **8**(7), 193–197.
- Vitckopfs, A. 1944. *Wood and Wood Processing*. Vaga, Riga, 395 pp. (in Latvian).
- Wood Moisture Content. 2013. <http://www.drevesinas.ru/woodstructura/humidity/6.html>, Accessed: 31.10.2017 (in Russian).

Energy valorisation of citrus peel waste by torrefaction treatment

B. Tamelová*, J. Malat'ák and J. Velebil

Czech University of Life Sciences Prague, Faculty of Engineering, Department of Technological Equipment of Buildings, Kamycka 129, CZ165 21 Prague, Czech Republic

*Correspondence: tamelova@tf.czu.cz

Abstract. The article deals with the issue of processing and utilization of citrus peel, which often ends unused with other biodegradable waste. The research is concerned with the energy potential of this raw material and its torrefaction conversion. The tested materials were orange peel (*Citrus sinensis* Osbeck cv 'Valencia', *Citrus sinensis* Osbeck cv 'Murcia') and grapefruit peel (*Citrus paradise* 'Ruby red'). Samples of dried materials underwent torrefaction treatment at 225 °C, 250 °C and 275 °C for 30 minutes. Samples before and after torrefaction were analysed for proximate and elemental composition and for calorific value. Consequently, stoichiometric combustion analyses were done. The torrefaction was performed in a LECO TGA 701 thermogravimetric analyzer under nitrogen atmosphere. The results of proximate and elemental analysis showed positive influence of torrefaction on the samples. The highest net calorific value for orange peel is 24.97 MJ kg⁻¹ at the temperature of 275 °C. The greatest differences in net calorific values are between 225 °C and 250 °C where the increase is almost 3 MJ kg⁻¹. Subsequently, the increase between the 250 °C and 275 °C torrefaction temperatures is 1 MJ kg⁻¹. Weight loss at respective torrefaction temperatures showed similar time-dependent curves for all samples. Stoichiometric combustion analysis shows slight differences between original samples, but great differences after torrefaction processing. Stoichiometric combustion parameters also change proportionately with increasing temperature of torrefaction. The resulting combustion balance figures show significantly lower need for mass of fuel in the case of the torrefied material for a given heat output thanks to the net calorific value being nearly doubled.

Key words: calorific value, heating value, elemental analysis, stoichiometry, heat output.

INTRODUCTION

Food processing industries, including fruit processing, generate significant amounts of waste, which have to be managed properly by recycling, incineration or landfilling (Aguilar et al., 2008). Citrus fruits crops are grown widely, producing over 120 million tons of oranges, lemons, grapefruits and mandarins worldwide (Ferreira-Leitao et al., 2010). They are harvested in many countries with tropical or subtropical climate, the principal producers being Brazil, China, Japan, Mexico, Pakistan, USA and countries of the Mediterranean region (Hernández-Montoya et al., 2009). In 2010 in Mexico alone, the orange production reached roughly 4 million tons, from which 40% (about 1.6 million tons of the total produced), are wet solid residues, corresponding approximately to 800,000 tons of dry residue (Lopez-Velazquez et al., 2013). Annually

in Italy, the juice and concentrated juice industries process 1.5 million tons of citrus fruit and 1 million tons of peel waste, 80% of which is produced in Sicily (Volpe et al., 2015). Citrus wastes, which are generated in juice production, are seen as a problematic but unavoidable waste (Lopez-Velazquez et al., 2013). Approximately, 50–60% of the processed fruit becomes citrus peel waste, which is composed of the peel, seeds and membrane residues left after juice extraction (Wilkins et al., 2007b). Until relatively recently, these waste products led to significant disposal problems, since there was no satisfactory means of disposal other than dumping on landfills. This led in some regions to the generation of large tracts of land contaminated with significant quantities of putrefying waste (Ángel Siles López et al., 2010). In general, the citrus fruit residues represent an abundant, inexpensive and readily available source of renewable biomass and their utilization is attracting increased interest worldwide. Orange peel is composed of cellulose, hemicellulose, lignin, pectin (galacturonic acid), chlorophyll pigments and other low-molecular weight compounds (e.g. limonene) (Pathak et al., 2017). Grapefruit peel contains several mono and disaccharides, the main ones being glucose, sucrose and fructose, as well as polysaccharides cellulose, hemicellulose and pectin (Ting & Deszyck, 1961; Wilkins et al., 2007a). Several authors recently studied pyrolysis and gasification of citrus peel wastes and their potential use as bio-fuel for electrical and thermal energy production (Aguiar et al., 2008; Miranda et al., 2009).

Pyrolysis is one of the most widely employed methods to convert biomass and organic residues into diverse products (Ranzi et al., 2008). Its application could diversify the energy supply in many situations, leading to a more secure and sustainable global energy supply chain (Lopez-Velazquez et al., 2013). Therefore, research on the pyrolysis process of various wastes is beneficial to better understanding of the pyrolytic processes and improving the products and their application as biofuels or raw materials for chemical industry (Mulligan et al., 2010). It has been studied largely on ligno-cellulosic plant biomass and wastes as a suitable sustainable way for production of conventional and new chemicals and fuels (Bridgwater & Peacocke, 2000; Kučerová et al., 2016). When biomass is employed for bioenergy, in some situations, pre-treatments of biomass are essential procedures for achieving higher efficiencies of fuel production or consumption. For example, after dewatering and drying, the calorific value of biomass is increased and the combustion efficiency of biomass is enhanced (Chen & Wu, 2009). Torrefaction is a type of pyrolytic treatment. In this process, raw biomass is heated in the temperature range of 200–300 °C under an inert or nitrogen atmosphere. Through torrefaction the properties of biomass can be improved to a certain extent (Chen & Kuo, 2011). The thermal treatment not only destructs the fibrous structure and tenacity of biomass, as well as increasing the calorific value, lowering oxygen to carbon ratio and moisture content. Generally, 80–95% of the energy and 70–90% of the dry mass of the biomass is retained in the torrefied product (Bates & Ghoniem, 2012). Also, after torrefaction the biomass has more hydrophobic characteristics and is more stable. This makes storage of torrefied biomass easier compared to non-torrefied biomass which will decompose in rate depending on storing conditions (Van der Stelt et al., 2011). Biomass properties can significantly influence both heat transfer and reaction rates during thermochemical treatment, the optimal operating conditions are highly variable (Zapata et al., 2009).

The aim of this paper was to evaluate fuel properties of the waste material from oranges and grapefruits before and after torrefaction. The contents of major elements as well as gross and net calorific value were determined. Stoichiometric parameters such as the theoretical amount of air for complete combustion and the amount of dry flue gas were determined and, also, the mass flow of the fuel depending on the desired heat output of the combustion device was determined.

MATERIALS AND METHODS

Sample preparation

Wastes from oranges and grapefruits were obtained from a company producing juices from fresh fruit and vegetable. There were two orange peel samples, orange peel 1 (*Citrus sinensis* Osbeck cv 'Valencia') and orange peel 2 (*Citrus sinensis* Osbeck cv but'Murcia'). The third sample was grapefruit peel (*Citrus paradise* 'Ruby red').

Prior to analysis, homogenous samples were prepared from the collected materials. Firstly, the materials were dried at room temperature for 7 days and after this period they were comminuted with RETSCH SM100 shear mill under the particle size of 1 mm.

Preparation of torrefied samples

Transformation of all samples by torrefaction process was performed in LECO TGA 701 thermogravimetric analyser under inert nitrogen atmosphere. For each of the samples, three measurements were made at three temperatures (225 °C, 250 °C and 275 °C) for 30 minutes. In each run, the samples were first dried at 105 °C to constant weight and then the furnace was filled with nitrogen and heated to target temperature with rate of 40 °C min⁻¹. During conversion of all samples, mass losses were monitored as time-dependent. Each sample was tested in triplicates for all conditions. The test sample size was 3 g each time. Analytical sample for each set of conditions was obtained after combining the three test samples and milling them to fine powder.

Moisture, ash, elemental composition and calorific value determinations

Investigated samples, namely orange peel 1 (OP 1), orange peel 2 (OP 2) and grape skins (GP), were analysed for moisture and ash contents, elemental composition, gross and net calorific value. Each parameter was tested at least in triplicate. Moisture and ash content were analysed in the LECO TGA 701 thermogravimetric analyser (TGA).

Determination of the elemental composition for the content of carbon (C), hydrogen (H) and nitrogen (N) was performed on a LECO CHN628+S analyzer by combustion method where the elements are measured in aliquote quantity of the flue gas. The carbon and hydrogen detection method is dispersed infrared absorption; nitrogen is detected using thermal conductivity cell. Oxygen was calculated as difference of the sum of ash and other elements from 100% on dry basis.

Gross calorific value was determined in isoperibol calorimeter LECO AC-600. The samples were pressed into pellets and then incinerated in a calorimetric bomb filled with oxygen to 3 MPa. The reference temperature was 28 °C. All measurements were repeated at least three times to obtain reliable results. Net calorific value was determined by calculation using elemental and proximate analyses. The calorimetric procedure and calculations were done according to ČSN ISO 1928:2010. Corrections for production of nitric and sulphuric acid were not determined.

Stoichiometric calculations

Combustion characteristics were calculated for all samples before and after torrefaction treatment. Stoichiometric calculations are recalculated to normal conditions (temperature $t = 0\text{ }^{\circ}\text{C}$ and pressure $p = 101.325\text{ kPa}$). In combustion calculation, the stoichiometric amount of oxygen O_{min} ($\text{m}^3\text{ kg}^{-1}$), the stoichiometric amount of dry air L ($\text{m}^3\text{ kg}^{-1}$), the stoichiometric amount of dry flue gas ($\text{m}^3\text{ kg}^{-1}$) and the theoretical amount of emission of CO_2 ($\text{m}^3\text{ kg}^{-1}$) have been determined for unit mass of fuel.

For each sample, the necessary mass flow rate of fuel to a combustion device is determined for required heat output. The efficiency of a generic combustion device was assumed to be 90% and the heat output was varied from 10 kW to 30 kW. The mass flow rate was calculated according to the equation:

$$\dot{m}_{pv} = \frac{P_k \cdot 100}{q_n \cdot \eta} \quad (1)$$

where \dot{m}_{pv} is the mass flow rate of fuel supplied into the combustion chamber (kg s^{-1}); P_k the heat output of the combustion device (W); q_n the net calorific value of the fuel (J kg^{-1}); η the efficiency of the combustion device (90%).

RESULTS AND DISCUSSION

In the biomass, the lowest ash content was measured in OP1, 3.42% wt. on dry basis. This is comparable with 2.94% wt. in orange peel in (Miranda et al., 2009), however, in (Stella Mary et al., 2016) the ash content in orange peel was $5.50 \pm 0.70\%$ on dry basis. The highest ash content was 4.41% wt. on dry basis in GP. Compared to wood these ash contents are ten times higher (Kučerová et al., 2016). The high ash content has a negative impact not only on the calorific value, but on the combustion process (Bradna et al., 2016). During torrefaction the ash content continually increases while the oxygen and, to a lower degree, hydrogen contents decrease. Table 1. shows the results of elemental analysis of orange and grapefruit peel samples before and after torrefaction at different temperatures. Although ash represents an incombustible portion of fuel, ash from biomass is a good source of various minerals and micronutrients to soil (Havrland et al., 2013; Pathak et al., 2017). The highest ash content was reached after torrefaction at 275 °C in OP 1 reaches 9.73%, OP 2 9.84% and Grapefruit peel 9.70%. Similar values were found by (Volpe et al., 2015), where the ash content in orange peel was 2.6 % wt. in original biomass and 8.7% wt. after slow pyrolysis at 650 °C.

When comparing the results of OP elemental analysis, Pathak et al. (2017), achieved very similar results, with the exception of higher proportion of oxygen (53.4% on dry basis). After torrefaction the oxygen content in both OP and GP samples decreased with rising treatment temperature, going to nearly 15% wt. at the temperature of 275 °C. Similar trend is true for hydrogen where the mass yield decreases with increasing torrefaction temperature to 35% at 275 °C.

As a consequence, the carbon content of OP and GP increases rapidly with increasing temperature, reaching a value of about 65% at a peak temperature of 275 °C. On the other hand, the nitrogen content of these samples remains almost constant. Similar results were determined in OP by Volpe et al. (2015), where the carbon content was 68% at 300 °C and in (Volpe et al., 2017), at temperature of 300 °C, the carbon content is 64.5%.

Table 1. Composition of orange peel (OP) and grapefruit peel (GP) before and after torrefaction treatment at varying temperatures and 0.5 h residence time (o.s. – original sample, d.b. – on dry basis, samples immediately after torrefaction are considered completely dry)

Sample	Water Content (% wt.)		Ash (% wt.)	Carbon (% wt.)	Hydrogen (% wt.)	Nitrogen (% wt.)	Oxygen (% wt.)	Gross Calorific Value (MJ kg ⁻¹)	Net Calorific Value (MJ kg ⁻¹)
	<i>W</i>	<i>A</i>							
OP 1, o.s.	69.52	1.04	14.38	1.81	0.31	12.91	5.57	3.47	
OP 1, d.b.		3.42	47.19	5.94	1.01	42.37	18.26	16.97	
OP 1 225 °C		6.54	57.60	5.09	1.58	29.10	21.91	20.80	
OP 1 250 °C		7.78	62.99	4.69	1.88	22.57	24.66	23.64	
OP 1 275 °C		9.73	67.05	4.46	2.04	16.64	25.60	24.63	
OP 2, o.s.	68.51	1.26	14.72	1.86	0.37	13.26	5.65	3.57	
OP 2, d.b.		4.01	46.74	5.90	1.18	42.11	17.95	16.66	
OP 2 225 °C		6.63	57.47	5.12	1.77	28.92	22.15	21.04	
OP 2 250 °C		8.36	63.52	4.69	2.12	21.22	24.90	23.88	
OP 2 275 °C		9.84	67.38	4.52	2.25	15.93	25.95	24.97	
GP, o.s.	69.99	1.32	14.26	1.80	0.36	12.25	5.48	3.38	
GP, d.b.		4.41	47.51	5.99	1.20	40.82	18.27	16.96	
GP 225 °C		6.67	57.96	5.10	1.76	28.43	22.19	21.07	
GP 250 °C		8.67	62.97	4.76	2.01	21.51	24.40	23.37	
GP 275 °C		9.70	66.75	4.57	2.18	16.72	25.64	24.64	

Gross calorific value increased after the torrefaction process in proportion with increasing temperature. The net calorific value of the samples after torrefaction rose even more. The greatest difference in the net calorific value is between 225 °C and 250 °C, where the increase is almost 3 MJ kg⁻¹. Subsequently, the increase between the 250 °C and 275 °C torrefaction temperatures is only 1 MJ kg⁻¹. Similar results have been published, for example, by Volpe et al. (2015).

The mass loss curves for individual samples at different temperatures are shown in Fig. 1.

The mass loss of the samples shows a decreasing mass yield in relation to time for all the samples examined. Mass losses of the OP 1 and 2 samples show similar time-dependent curves. These curves are slightly shifted from each other due to different elemental composition, especially in the moisture of individual samples and ash content. Similar results were determined in (Volpe et al., 2015 & Volpe et al., 2017), where the treatment temperatures were in the range of 200–650 °C. For grapefruit peel samples, the weight losses are lower by approximately 10% compared with orange peel samples.

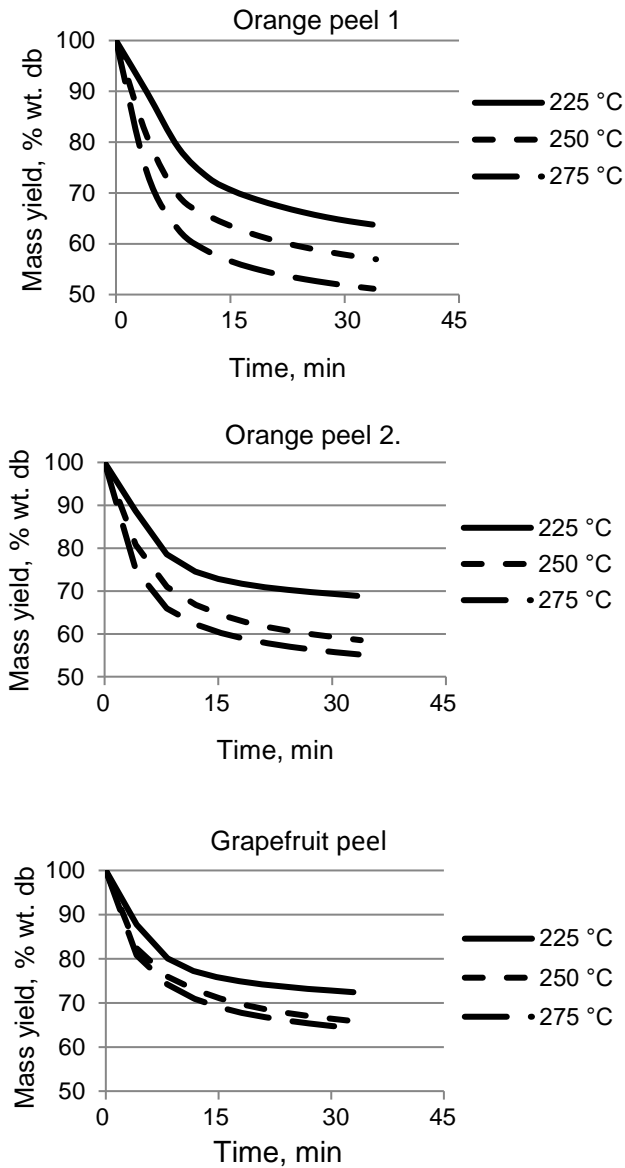


Figure 1. Mass loss curves of samples.

The results of stoichiometric analysis in Tables 2–4 show comparable values in the orange and grapefruit peels. However, in the torrefied samples the necessary volume of combustion air and subsequently created flue are increasing with each rise in torrefaction temperature. The resulting carbon dioxide emission concentrations also show that the properties of the processed samples change with temperature of torrefaction from the original biomass which has typically high concentration of CO₂ in flue gas (Malat'ák et al., 2017) and decrease to concentrations that correspond to the properties of coal (Vassilev et al., 2015). These stoichiometric parameters have a significant influence on

the total efficiency of combustion plants (Malat'ák & Bradna, 2017) and on emission concentrations. Similar results were obtained when evaluating the potential of waste biomass in (Brunerová et al., 2017).

Table 2. Stoichiometric amount of air and specific productions of flue gas components from combustion of orange peel 1

			OP 1 d.b.	OP 1 225 °C	OP 1 250 °C	OP 1 275 °C
L_{\min}	Stoichiometric volume of air for complete combustion	($\text{m}^3 \text{kg}^{-1}$)	4.35	5.49	6.08	6.58
V_{sspmin}	Stoichiometric volume of dry flue gas	($\text{m}^3 \text{kg}^{-1}$)	4.28	5.37	5.93	6.40
V_{CO_2}	Stoichiometric volume of CO_2	($\text{m}^3 \text{kg}^{-1}$)	0.88	1.07	1.17	1.25
$V_{\text{H}_2\text{O}}$	Stoichiometric volume of H_2O	($\text{m}^3 \text{kg}^{-1}$)	0.83	0.79	0.76	0.76
V_{N_2}	Stoichiometric volume of N_2	($\text{m}^3 \text{kg}^{-1}$)	3.40	4.30	4.76	5.57
CO_2max	Concentration of carbon dioxide in dry flue gas after stoichiometric combustion	(% vol.)	20.45	19.90	19.69	19.44

Table 3. Stoichiometric amount of air and specific productions of flue gas components from combustion of orange peel 2

			OP 2 d.b.	OP 2 225 °C	OP 2 250 °C	OP 2 275 °C
L_{\min}	Stoichiometric volume of air for complete combustion	($\text{m}^3 \text{kg}^{-1}$)	4.31	5.49	6.18	6.65
V_{sspmin}	Stoichiometric volume of dry flue gas	($\text{m}^3 \text{kg}^{-1}$)	4.28	5.37	6.02	6.46
V_{CO_2}	Stoichiometric volume of CO_2	($\text{m}^3 \text{kg}^{-1}$)	0.87	1.07	1.18	1.25
$V_{\text{H}_2\text{O}}$	Stoichiometric volume of H_2O	($\text{m}^3 \text{kg}^{-1}$)	0.83	0.79	0.77	0.77
V_{N_2}	Stoichiometric volume of N_2	($\text{m}^3 \text{kg}^{-1}$)	3.37	4.30	4.84	5.21
CO_2max	Concentration of carbon dioxide in dry flue gas after stoichiometric combustion	(% vol.)	20.45	19.90	19.58	19.35

Table 4. Stoichiometric amount of air and specific productions of flue gas components from combustion of grapefruit peel

			GP d.b.	GP 225 °C	GP 250 °C	GP 275 °C
L_{\min}	Stoichiometric volume of air for complete combustion	($\text{m}^3 \text{kg}^{-1}$)	4.44	5.55	6.13	6.58
V_{sspmin}	Stoichiometric volume of dry flue gas	($\text{m}^3 \text{kg}^{-1}$)	4.36	5.42	5.97	6.39
V_{CO_2}	Stoichiometric volume of CO_2	($\text{m}^3 \text{kg}^{-1}$)	0.88	1.08	1.17	1.24
$V_{\text{H}_2\text{O}}$	Stoichiometric volume of H_2O	($\text{m}^3 \text{kg}^{-1}$)	0.84	0.79	0.77	0.77
V_{N_2}	Stoichiometric volume of N_2	($\text{m}^3 \text{kg}^{-1}$)	3.48	4.35	4.80	5.15
CO_2max	Concentration of carbon dioxide in dry flue gas after stoichiometric combustion	(% vol.)	20.21	19.83	19.55	19.37

Table 5 shows the necessary mass flow rate of the fuel for a desired heat output. The heat output displayed from small household devices (20 kW) up to medium-sized combustion devices (300 kW). The mass flow rate of fuel decreases with the increasing torrefaction processing temperature. This decrease arises from increase in the net calorific value.

Table 5. The mass flow rate of fuel to the combustion device for given heat output

Sample	Heat output (kW)			
	20	50	100	300
OP 1, d.b.	4.71	11.79	23.58	70.74
OP 1 225 °C	3.84	9.61	19.23	57.69
OP 1 250 °C	3.38	8.46	16.92	50.76
OP 1 275 °C	3.24	8.12	16.24	48.72
OP 2, d.b.	4.80	12.00	24.00	72.02
OP 2 225 °C	3.80	9.50	19.01	57.05
OP 2 250 °C	3.35	8.37	16.75	50.25
OP 2 275 °C	3.20	8.01	16.02	48.07
GP, d.b.	4.71	11.79	23.58	70.74
GP 225 °C	3.80	9.50	19.01	57.04
GP 250 °C	3.42	8.56	17.12	51.36
GP 275 °C	3.24	8.11	16.23	48.69

CONCLUSIONS

Fuel parameters of orange and grapefruit peel before and after torrefaction treatment show considerable changes. Torrefaction is generally able to produce a superior fuel compared to original biomass, most notably by increasing the calorific value and decreasing oxygen content. In the studied materials and within the tested conditions, the highest net calorific value is reached in orange peel torrefied at 275 °C for 0.5 h. While increasing the torrefaction temperature, the increase in calorific value is greater at lower temperature ranges: 2.7 MJ kg⁻¹ between 225 °C and 250 °C versus 1.1 MJ kg⁻¹ between 250 °C and 275 °C as averages in all samples. In contrast to beneficial effects, torrefaction also has a detrimental effect in raising the ash content. Grapefruit peel, which had 4.41% wt. ash in dry state, reaches 9.7% wt. after torrefaction at 275 °C and 0.5 h residence time. Such a high ash content limits the use of torrefied fuel at least in some areas, e.g. in small home devices. The three citrus peel samples showed similar behaviour during torrefaction in weight loss and in the composition change. Therefore, it can be assumed that in practice most sources of citrus peel would be of similar value for torrefaction treatment. The results of the stoichiometric calculations show minor differences between the original materials but significant differences between them and the torrefied samples. In energy utilization of torrefied biomass this would mean significantly different combustion characteristics and possible need to adjust the combustion device. For example, the mass flow rate of fuel for a particular heat output decreases with its rising calorific value and therefore also depends on the treatment conditions. The theoretical calculations show considerable savings in the

weight of fuel in the case of torrefied materials due to the rising net calorific value. This would lead to decrease in cost associated with the transport and storage of fuel.

ACKNOWLEDGEMENTS. The article was financially supported by the Internal Grant Agency of the Czech University of Life Sciences Prague, Czech Republic, Grant No. 20173003.

REFERENCES

- Aguiar, L., Márquez-Montesinos, F., Gonzalo, A., Sánchez, J.L. & Arauzo, J. 2008. Influence of temperature and particle size on the fixed bed pyrolysis of orange peel residues. *Journal of Analytical and Applied Pyrolysis* **83**, 124–130.
- Ángel Siles López, J., Li, Q. & Thompson, I.P. 2010. Biorefinery of waste orange peel. *Critical Reviews in Biotechnology* **30**(1), 63–69.
- Bates, R.B. & Ghoniem, A.F. 2012. Biomass torrefaction: modeling of volatile and solid product evolution kinetics. *Bioresource Technology* **124**, 460–469.
- Bradna, J., Malaťák, J. & Hájek, D. 2016. The properties of wheat straw combustion and use of fly ash as a soil amendment. *Agronomy Research* **14**(4), 1257–1265.
- Bridgwater, A.V. & Peacocke, G.V.C. 2000. Fast pyrolysis processes for biomass. *Renewable and Sustainable Energy Reviews* **4**, 1–73.
- Brunerová, A., Malaťák, J., Müller, M., Valášek, P. & Roubík, H. 2017. Tropical waste biomass potential for solid biofuels production. *Agronomy Research* **15**(2), 359–368.
- Chen, W.H. & Wu, J.S. 2009. An evaluation on rice husk and pulverized coal blends using a drop tube furnace and a thermogravimetric analyzer for application to a blast furnace. *Energy* **34**, 1458–1466.
- Chen, Wei-Hsin & Kuo, Po-Chih. 2011. Torrefaction and co-torrefaction characterization of hemicellulose, cellulose and lignin as well as torrefaction of some basic constituents in biomass. *Energy* **36**, 803–811.
- Ferreira-Leitao, V., Fortes Gottschalk, L.M, Ferrara, M.A., Lima Nepomuceno, A., Correa Molinari, H.B. & Bon, E.P.S. 2010. Biomass residues in Brazil: availability and potential uses. *Waste and Biomass Valorization* **1**, 65–76.
- Havrland, B., Ivanova, T., Lapczynska-Kordon, B. & Kolarikova, M. 2013. Comparative analysis of bio-raw materials and biofuels. In: *12th International Scientific Conference on Engineering for Rural Development 2013*, Jelgava, 541–544 (in Latvia).
- Hernández-Montoya, V., Montes-Morán, M.A. & Elizalde-González, M.P. 2009. Study of the thermal degradation of citrus seeds. *Biomass and Bioenergy* **33**(9), 1295–1299.
- Kučerová, V., Lagaňa, R., Výbohová, E. & Hýrošová, T. 2016. The effect of chemical changes during heat treatment on the color and mechanical properties of fire wood. *Bioresources* **11**(4), 9079–9094.
- Lopez-Velazquez, M.A., Santes, V., Balmaseda, J. & Torres-Garcia, E. 2013. Pyrolysis of orange waste: A thermo-kinetic study. *Journal of Analytical and Applied Pyrolysis* **99**, 170–177.
- Miranda, R., Bustos-Martinez, D., Sosa Blanco, C., Gutiérrez Villarreal, M.H. & Rodriguez Cantú, M.E. 2009. Pyrolysis of sweet orange (*Citrus sinensis*) dry peel. *Journal of Analytical and Applied Pyrolysis* **86**, 245–251.
- Malaťák, J. & Bradna, J. 2017. Heating and emission properties of waste biomass in burner furnace. *Research in Agricultural Engineering* **63**(1), 16–22.
- Malaťák, J., Bradna, J. & Velebil, J. 2017. The dependence of CO_x and NO_x emission concentrations on the excess air coefficient during combustion of selected agricultural briquetted by-products. *Agronomy Research* **15**(S1), 1084–1093.

- Mulligan, C.J., Strezov, L. & Strezov, V. 2010. Thermal decomposition of wheat straw and mallee residue under pyrolysis conditions. *Energy and Fuels* **24**(1), 46–52.
- Ranzi, E., Cuoci, A., Faravelli, T., Frassoldati, A., Migliavacca, G., Pierucci, S. & Sommariva, S. 2008. Chemical kinetics of biomass pyrolysis. *Energy and Fuels* **22**, 4292–4300.
- Pathak, P.D., Mandavgane, S.A. & Kulkarni, B.D. 2017. Fruit peel waste: Characterization and its potential uses. *Current Science* **113**(3), 444–454.
- Stella Mary, G., Sugumaran, P., Niveditha, S., Ramalakshmi, B., Ravichandran, P. & Seshadri, S. 2016. Production, characterization and evaluation of biochar from pod (*Pisum sativum*), leaf (*Brassica oleracea*) and peel (*Citrus sinensis*) wastes. *International Journal of Recycling of Organic Waste in Agriculture* **5**(1), 43–53.
- Ting, S.V. & Deszyck, E.J. 1961. The carbohydrates in the peel of oranges and grapefruit. *Food Science* **26**, 146–152.
- Van der Stelt, M.J.C., Gerhauser, H., Kiel, J.H.A. & Ptasinski, K.J. 2011. Biomass upgrading by torrefaction for the production of biofuels: A review *Biomass and Bioenergy* **35**(9), 3748–3762.
- Vassilev, S.V., Vassileva, C.G. & Vassilev, V.S. 2015. Advantages and disadvantages of composition and properties of biomass in comparison with coal: An overview. *Fuel* **158**, 330–350.
- Volpe, M., Panno, D., Volpe, R. & Messineo, A. 2015. Upgrade of citrus waste as a biofuel via slow pyrolysis. *Journal of Analytical and Applied Pyrolysis* **115**, 66–76.
- Volpe, R., Menendez, J.M.B., Reina, T.R., Messineo, A. & Millan, M. 2017. Evolution of chars during slow pyrolysis of citrus waste. *Fuel Processing Technology* **158**, 255–263.
- Wilkins, M.R., Widmer, W.W., Grohmann, K. & Cameron, R.G. 2007a. Hydrolysis of grapefruit peel waste with cellulase and pectinase enzymes. *Bioresource Technology* **98**(8), 1596–1601.
- Wilkins, M.R., Suryawati, L., Maness, N.O. & Chrz, D. 2007b. Ethanol production by *Saccharomyces cerevisiae* and *Kluyveromyces marxianus* in the presence of orange-peel oil. *World Journal Microbiology Biotechnology* **23**(8), 1161–1168.
- Zapata, B., Balmaseda, J., Fregoso-Israel, E. & Torres-García, E. 2009. Thermo-kinetics study of orange peel in air. *Journal of Thermal Analysis and Calorimetry* **98**(1), 309–315.

Investigating the probable consequences of super absorbent polymer and mycorrhizal fungi to reduce detrimental effects of lead on wheat (*Triticum aestivum* L.)

H.R. Tohidi Moghadam¹, T. W. Donath², F. Ghooshchi¹ and M. Sohrabi^{2,*}

¹Department of Agronomy, Varamin-Pishva Branch, Islamic Azad University, Varamin, Iran

²Department of Landscape Ecology, Institute for Natural Resource Conservation, Kiel University, Olshausenstr. 75, DE24118 Kiel, Germany

*Correspondence: msohrabi@ecology.uni-kiel.de

Abstract. In many parts of the world, agricultural use of soils is restricted due to heavy metal contamination. Absorption of heavy metals, such as (Pb), in the tissue of plants increases the plant's metabolism and causes physiological disorders or even death. In order to study the potential of super absorbent polymers (SAP) and mycorrhiza fungi application to mitigate adverse effects of lead (Pb) on wheat, a greenhouse experiment was conducted. The experiment was setup as a completely randomized design, with two treatments arranged in a factorial scheme with three levels of lead (0, 100 and 200 mg per kg soil) and four levels of SAP and mycorrhiza fungi application (without SAP and mycorrhiza fungi application, SAP application alone, mycorrhiza fungi application alone, SAP and mycorrhiza fungi application combined). The results showed that Pb significantly affected all parameters measured of wheat. The Pb-contamination caused a significantly decreasing in plant height, total dry weight per plant and total chlorophyll contents. And also, the results indicated that the combined use of superabsorbent and mycorrhiza reduced the amount of superoxide dismutase enzyme. As well as, our results show that the application of super absorbent polymer and mycorrhizal fungi seems to be a promising path to reduce detrimental effects of heavy metal pollution of agricultural soils on plant performance.

Key words: Wheat, lead, super absorbent polymer, mycorrhizal fungi, enzymes superoxide dismutase.

INTRODUCTION

Heavy metal contamination of the environment did increase worldwide during the last years (Sheetal et al., 2016). The transfer and accumulation of heavy metals in soil-plant systems is influenced by multiple factors (Poschenrieder & Barceló, 2004; Wang et al., 2017). This is of primary concern in agricultural production due to adverse effects on crop growth and risk of crop and food chain contamination (Singh & Agrawal 2010). Consequently, attention on heavy metal induced effects increased during the last years. Removing of heavy metals from contaminated soils with traditional physical and chemical methods is inefficient and very costly (Benavides et al., 2005; Shrama & Dubey, 2005; Kinraide, 2007). Thus, efforts to develop effective and inexpensive

technologies to deal with heavy metal contamination of soils are increasing. In this context, the manipulation and use of mycorrhizal fungi was already identified as a potentially important tool to remediate copper-contaminated soils (Meier et al., 2015).

Lead (Pb) is a dangerous heavy metal pollutant in the environment, which influences the metabolic and physiological activity of living organisms. High doses of Pb likely result in metabolic disorders, growth inhibition and even death for most plant species (Shrama & Dubey, 2005). The rhizosphere is the few millimetres of soil surrounding a plant's roots that microorganisms have many biological activities there that are critically important to both plant health and soil carbon (C) transformation and stabilization (Pett-Ridge & K. Firestone 2017). The symbiosis between plants and mycorrhizal fungi is one of the most extensive bidirectional relations between plants and micro-organisms in the soil (Javaid, 2009). More than 80% of the higher plants have the ability to form arbuscular mycorrhizal associations (Garg et al., 2006). Arbuscular mycorrhizal (AM) fungi can facilitate the survival of their host plants growing on metal-contaminated land by improving nutrient acquisition, protecting them from the metal toxicity, absorbing metals, and also enhancing phytostabilization and phytoextraction (Jahromi et al., 2008; Javaid, 2009; Leung et al., 2013). These fungi reduce concentrations of heavy metals by binding these in the chitin cell wall (Hildebrandt et al., 2007) and the secretion of glomalin (Gonzalez-Chavez et al., 2004) Moreover, AM accumulate heavy metals in plant roots in non-toxic complexes (Joner & Leyval, 1997). On the other hand, the use of superabsorbent may improve physical and chemical soil properties (Kozlowskak & Badora, 2007; Bai et al., 2010) and thereby already reduces the risk of heavy metal uptake by plants. Therefore, in this study the physiological and biochemical effect of mycorrhizal fungi and super absorbent polymer on different parameters on wheat were examined. By doing this, we wanted to provide experimental evidence for the potential of mycorrhizal fungi and super absorbent polymers to reduce detrimental effects of lead on wheat performance (*Triticum aestivum L.*).

MATERIALS AND METHODS

The experiment was conducted in a greenhouse in Varamin in 2016. The study was designed as a two-factorial, completely randomized experiment. The first factor was lead concentration in the soil (Pb) ($k = 3$; 0, 100 and 200 mg per kg of soil) and the second factor were different combinations of super absorbent polymer and mycorrhizal fungi ($k = 4$; no super absorbent and no mycorrhiza = control, only super absorbent, only mycorrhiza, simultaneous application of super absorbent and mycorrhiza). The soil of the experimental site was a clay loam one, with a montmorillonite clay type, low in nitrogen (0.06–0.07%), low in organic matter (0.56–0.60), and alkaline in reaction with pH of 7.2 and $E_c = 0.66 \text{ dS m}^{-1}$. The soil texture was sandy loam, with 10% of neutralizing substances. Super absorbent polymer used in this study was a hydrophilic polymer (SUPERAB-A200) produced by the Rahab Resin Co. Ltd., under license of the Iran Polymer and Petrochemical Institute. It is a white granular powder with a 90% active ingredient, 75–1,000 μm particle size, and 0.60 g cm^{-3} bulk density, which swells to form a gel in water. All factor combinations were replicated three times. Soils were treated in a steam autoclave at a temperature of 121 °C and a pressure of 20 atmospheres for one hour to delete all spores and fungal propagules in the soil. Lead concentrations were selected according to the tentative map of soil pollution by heavy metals and the range

of lead concentration in contaminated soils of Iran (Instrument Manual Digesdahl Digestion Apparatus, 1999). The mycorrhizal inoculant fungi *Glomus intraradices* (producer of biotech company Turan, Semnan, Iran) was used for mycorrhizal inoculation. For this purpose, pots were filled with 100 g soil and in each pot 250 mycorrhizal propagules were added. Fifteen surface sterilized seeds of wheat (*Triticum aestivum* L c.v *SW*) were planted in the pots. In case of more than 5 emerged plants per pot excess seedlings were removed. Pots were regularly watered. During the growing season number of plants per pot was reduced to three. These plants were used to measure fitness traits during the growing season and at the end of the experiment. First, height of the plants was measured and averaged across three plants per pot. At the end of the experiment, biomass was assessed by drying these three plants for 48 hours at 70 °C in an oven. The chlorophyll content was measured with a spectrophotometer (Arnon, 1949). In order to evaluate the activity of superoxide dismutase Giannopolitis method was used (Ries, 1977). Therefore, 2.0 g of a sample were added in 3 mL of buffer containing 1.0 mM EDTA pH 7.8 with HEPES-KOH. The resulting product was centrifuged at around 15,000 rpm for 15 minutes at a temperature of 4 °C and the supernatant was used for measuring the activity of superoxide dismutase reaction mixture containing 50 mM KOH buffer at pH 8/7 with EDTA-HEPES 1.0 mM, 50 mM sodium carbonate at pH 2/10, L-methionine 12 mM, Nitro Blue Tetrazolium 75 mM, 1 mM and 200 mL extract the enzyme was riboflavin. The samples were exposed for 15 minutes, after which the absorption at a wavelength of 560 nm was measured using a spectrophotometer. A test tube containing the reaction mixture to a fermentation extract was used as a control. One unit of SOD activity was defined as the amount of enzyme that caused 50% inhibition of photochemical reduction of nitro blue tetrazolium. To determine the concentration of lead in the shoots and roots, 1 g of finely ground plant biomass was incinerated in an electric furnace at 550 °C for four. The ash obtained was mixed with 10 mL of two molar HCl. Subsequently, the concentration of the extracts was measured by atomic absorption AAS Vario 6. Finally, the experimental data were analyzed employing analysis of variance and the Duncan test using SAS software (SAS Institute, 2002).

RESULTS AND DISCUSSION

According to the analysis of variance, lead had a significant main effect on all measured traits (Table 1). The highest plant height was measured on plants not exposed to lead (Table 2 and Fig. 6). The lowest plant height was found at a lead concentration of 200 mg per kg soil. We also found that increased levels of lead decreased dry weight per plant (Fig. 2). Therefore, Pb contamination reduced both, growth and plant biomass. It was also observed that the highest biomass was reached when both superabsorbent plant and mycorrhizal were present (Table 2). SAP (Super absorbent polymer) leads to an increase of water and nutrient uptake, through increased cell division and growth (Neumann & George, 2005). Mycorrhiza can develop at the dorsal root tip, the original position of cell elongation and nutrient uptake. Ultimately, this will also increase the availability of water and nutrients and may enhance cell division and plant height (Neumann & George, 2005). Our results are also in accordance with results of other researchers who linked the decrease of plant performance by heavy metals to lower amounts of chlorophyll in leaves, which slows down photosynthesis (Gajewska &

Table 1. Analysis of variance on wheat attributes affected by lead stress condition, mycorrhiza fungi and super polymer absorbent

S.O.V	d.f	Plant height	Shoot dry weight	Total chlorophyll	Superoxide dismutase	Shoot Pb concentration	Root Pb concentration
Lead	2	171.18**	307.13**	0.944**	8425**	0.035**	10.10**
SAP and AMF	3	6.22**	35.65*	0.015**	3658.88**	0.003**	0.527**
Lead * SAP and AMF	6	2.19*	8.93**	0.003**	826.06**	0.0006ns	0.062**
Error	24	1.20	7.94	0.001	94.52	0.0002	0.030
C.V (%)		1.74	10.19	1.95	2.01	6.38	13.68

*,** and ns – significant at 0.05, 0.01 percentage and not significant; SAP = Super absorbent polymer; AMF = Arbuscular Mycorrhizal Fungi.

Table 2. Mean comparison of main effects of lead stress, mycorrhiza fungi and super polymer absorbent on some attributes of wheat

Treatment	Plant height, (cm)	Shoot dry weight, (g)	Total chlorophyll, (mg g ⁻¹ FW)	Superoxide Dismutase, (ΔA mg pro.min ⁻¹)	Shoot Pb concentration, (mg.g ⁻¹ DW)	Root Pb concentration, (mg.g ⁻¹ DW)
Lead concentration						
0	66.30a	33.33a	2.287a	194.46c	0.043c	0.391c
100	62.90b	25.89b	1.907b	533.87b	0.124b	1.233b
200	58.75c	23.67b	1.740c	716.62a	0.146a	2.225a
Mycorrhiza and Super absorbent						
Non-AMF and SAP	61.66c	25.22b	1.922c	507.10a	0.127a	1.288b
SAP	62.44bc	26.94ab	1.974b	484.66b	0.112ab	0.966c
AMF	62.83ab	28.57a	1.995ab	476.32b	0.097bc	1.555a
SAP and AM together	63.66a	29.80a	2.021a	458.53c	0.081c	1.322b

Treatment means followed by the same letter within each column are not significantly different ($P < 0.05$) according to Duncan's Multiple Range test; SAP = Super absorbent polymer; AMF = Arbuscular Mycorrhizal Fungi.

Skodowska, 2007; Ghasemi et al., 2009; Pakdaman et al., 2013). Accordingly, we found that the synthesis of chlorophyll of plants growing in soils contaminated with lead was reduced (Fig. 1). Heavy metals also increase decomposition of the chlorophyll pigment, thereby reducing the amount of chlorophyll in the tissue (Gajewska et al., 2006).

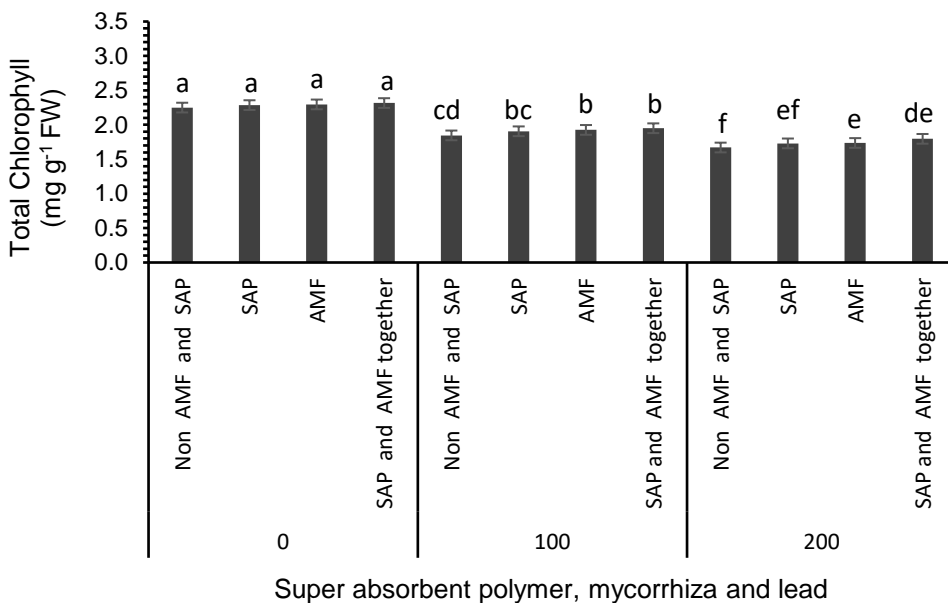


Figure 1. Interaction between lead stress (0, 100 and 200 mg kg⁻¹), AMF and SAP on Total Chlorophyll (mg g⁻¹FW). Treatment means followed by the same letter are not significantly different ($P < 0.05$) according to Duncan’s Multiple Range test; SAP = Super absorbent polymer; AMF = Arbuscular Mycorrhizal Fungi.

Other researchers have shown that the use of superabsorbent polymers can increase the chlorophyll content of sunflower plants under stress (Nazarli et al., 2010). In addition, mycorrhiza coexisting in plants can increase the speed and rate of photosynthesis and consequently biomass production. This is probably due to improved nutrient and water uptake through the host plant (Demir, 2004). Accordingly, Goussous & Mohammad (2009) report that the fungus *Glomus intraradices* affects the absorption of nutrients and increases growth of onions. In case of superoxide dismutase enzyme activity, our results showed a significant difference between treatments, i.e. the highest activity of superoxide dismutase was observed in the application of lead at a concentration of 200 mg per kg soil. And also the results indicated that the combined use of superabsorbent and mycorrhiza reduced the amount of superoxide dismutase enzyme from 764.88 to 672.93 ($\Delta A \text{ mg pro. min}^{-1}$) (Table 2 and Fig. 3). Superoxide dismutase is a key enzyme to protect cells against oxidative stress, since it accelerates the conversion of O_2^- to H_2O_2 and O_2 (Fukai & Ushio-Fukai, 2011). The highest activity of superoxide dismutase was found at a lead concentration of 200 milligrams per kilogram of soil. Plants exposed to heavy

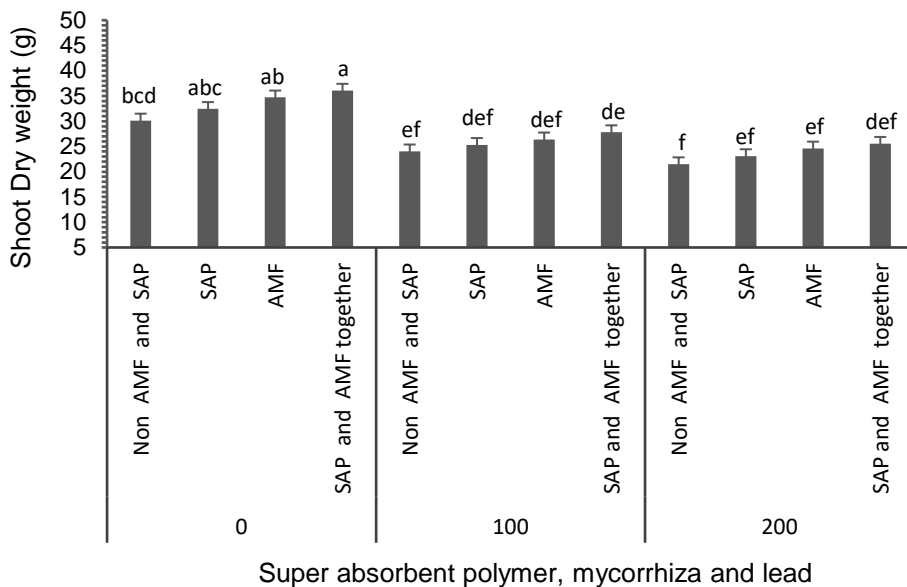


Figure 2. Interaction between lead stress (0, 100 and 200 mg kg⁻¹), AMF and SAP on Shoot Dry weight (g). Treatment means followed by the same letter are not significantly different ($P < 0.05$) according to Duncan's Multiple Range test; SAP = Super absorbent polymer; AMF = Arbuscular Mycorrhizal Fungi.

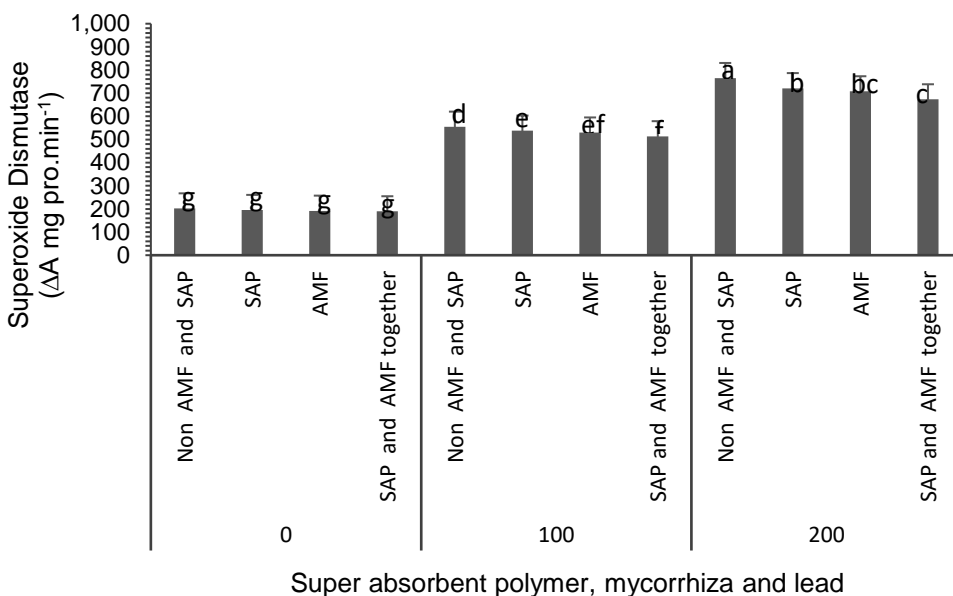


Figure 3. Interaction between lead stress (0, 100 and 200 mg kg⁻¹), AMF and SAP on Superoxide Dismutase (ΔA mg pro.min⁻¹). Treatment means followed by the same letter are not significantly different ($P < 0.05$) according to Duncan's Multiple Range test; SAP = Super absorbent polymer; AMF = Arbuscular Mycorrhizal Fungi.

metals often show specific enzyme activities and plant species exposed to heavy metals often respond differently (Dhir et al., 2009). Research by Parlak (2016) showed that increasing the concentration of nickel increased superoxide dismutase activity in wheat seedlings. Tohidi Moghadam (2017) also reported that SAP application could reduce harmful effects of arsenic by alleviating oxidative stress. Also in the present study, the use of super absorbent and mycorrhiza reduced the activity of superoxide dismutase in the leaves (Table 2 and Fig. 3). In addition, the results demonstrated that the highest lead content in shoots and roots was found at a lead concentration of 200 milligrams per kilogram of soil (Table 2, Figs 4 and 5). There the highest lead content was found in shoots of the control, i.e. no mycorrhiza and no super absorbent polymer (Fig. 5) and the highest lead content of roots is related to the level of mycorrhizal treatment (Table 2 and Fig. 4). Levels of lead in the shoots of wheat in the mycorrhiza treatment were lower. Comparing wheat without mycorrhiza addition with those plants in the mycorrhiza treatments prove a reduced transfer of lead from roots to shoots.

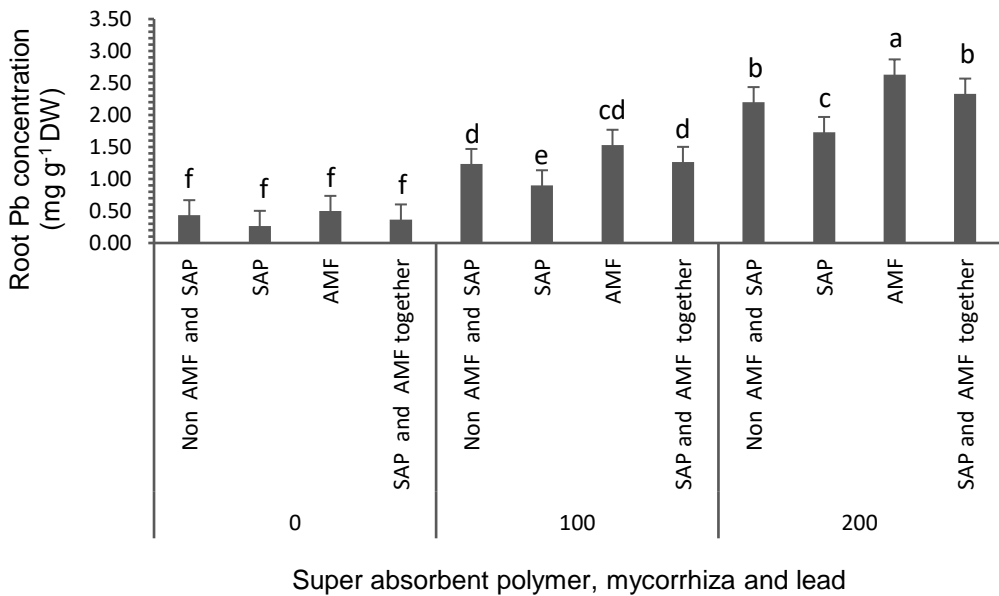


Figure 4. Interaction between lead stress (0, 100 and 200 mg kg⁻¹), AMF and SAP on Root Pb concentration (mg g⁻¹DW). Treatment means followed by the same letter are not significantly different ($P < 0.05$) according to Duncan’s Multiple Range test; SAP = Super absorbent polymer; AMF = Arbuscular Mycorrhizal Fungi.

In general, uptake of heavy metals by plants and the ability to accumulate these differs between species and will increase with increasing heavy metal pollution of the soils (Burken et al., 2011). This phenomenon is likely to be a physiological trait of the species. While some species can absorb high amounts of heavy metals from the environment without suffering serious injuries, others show a lower ability to absorb heavy metals and might experience poisoning and damage already at low heavy metal

levels (Gosh & Singh, 2005; Baycu et al., 2006). In this situation, superabsorbent polymers can improve soil physical and chemical properties (Bai et al., 2010). Super absorbent polymers stabilise heavy metals in the soil and consequently the absorption and accumulation of heavy metals in plants is reduced.

Interestingly, mycorrhizal fungi actively increase absorption of heavy metals through roots-mycorrhiza complex but at the same time maintain the active uptake of nutrients such as nitrogen and phosphorus. Reduced lead contents in the shoots of plants in the mycorrhiza treatments might be due to the deposition of heavy metals in the parenchyma cells of fungi in non-toxic form (Vivas et al., 2006; Gonzalez-Guerrero et al., 2008). Mycorrhizal fungi produce a non-soluble glycoprotein called glomalin that binds to toxic elements such as heavy metals and prevents their transfer into plants (Gonzalez-Chavez et al., 2004; Pyrzynska, 2007). Still, increasing levels of uptake will lead to increased lead contents in shoots and roots (Figs 4, 5). Under these circumstances, the use of super absorbent and mycorrhiza together simultaneously reduced the lead content of the shoot. Thus, there are two different mechanism that reduce heavy metal content in the plant: while mycorrhiza increases the amount of lead in the root-mycorrhiza system but hampers their uptake into the plant, super absorbent polymers prevent the uptake of heavy metals by immobilizing heavy metals.

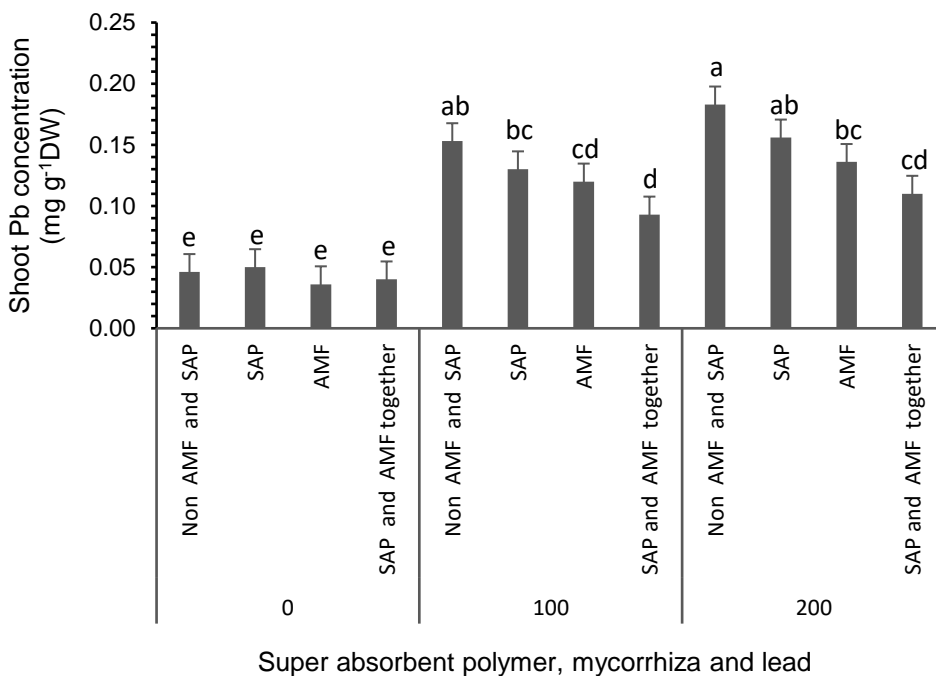


Figure 5. Interaction between lead stress (0, 100 and 200 mg kg⁻¹), AMF and SAP on Shoot Pb concentration (mg g⁻¹DW). Treatment means followed by the same letter are not significantly different ($P < 0.05$) according to Duncan's Multiple Range test; SAP = Super absorbent polymer; AMF = Arbuscular Mycorrhizal Fungi.

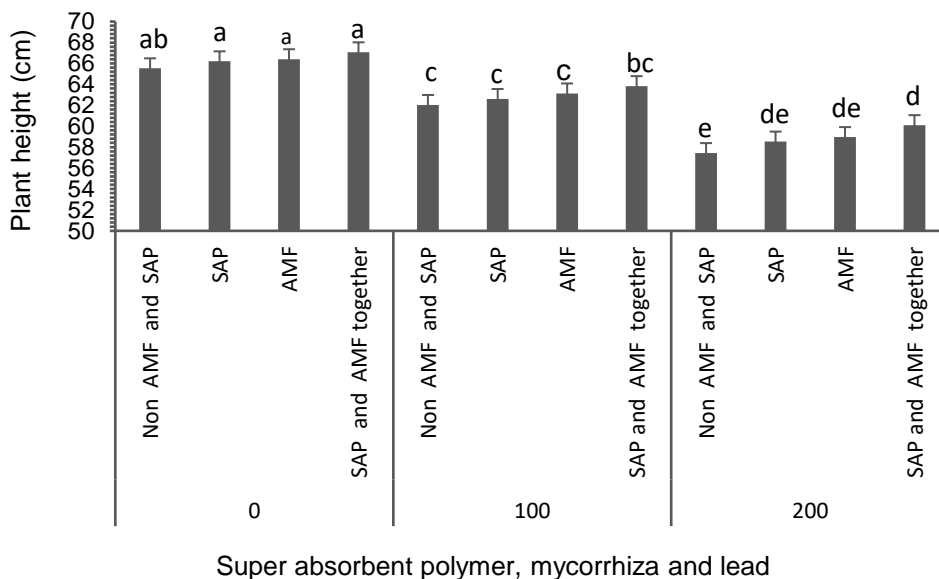


Figure 6. Interaction between lead stress (0, 100 and 200 mg kg⁻¹), AMF and SAP on Plant height (cm). Treatment means followed by the same letter are not significantly different ($P < 0.05$) according to Duncan's Multiple Range test; SAP = Super absorbent polymer; AMF = Arbuscular Mycorrhizal Fungi.

CONCLUSION

Our study showed that levels of lead in the shoots of wheat in the mycorrhiza treatment were lower. The current results compare to wheat without mycorrhiza, prove the reduced transfer of lead from roots to shoots. In contrast, the content of lead in the mycorrhizal roots is increased. As well as the results illustrated that the transfer of lead from the soil into the roots is higher than the transfer of lead from roots to the shoots. In addition, lead is immobilized in the soil by super absorbent polymers or stored in the plant root-mycorrhiza system. Both processes prevent transfer of lead into shoots and are effective in the phytoremediation of heavy metals. Therefore, the combined application of super absorbent polymer and mycorrhizal fungi may be a feasible measurement to re-integrate polluted soils with heavy metals into agricultural management.

REFERENCES

- Arnon, D.I. 1949. Copper enzymes in isolated chloroplasts, poly phenol oxidase in *Beta vulgaris*. *Plant Physiology* **24**, 1–150.
- Bai, W. 2010. Effects of super-absorbent polymers on the physical and chemical properties of soil following different wetting and drying cycles. *Soil Use and Management, Beijing* **26**(3), 253–260.
- Baycu, G., Ozden, H., Tolunay, D. & Gunebakan, S. 2006. Ecophysiological and seasonal variations in Cd, Pb, Zn, and Ni concentrations in the leaves of urban deciduous trees in Istanbul. *Environmental Pollution* **143**, 545–554.

- Benavides, M.P., Gallego, S.M. & Tomaro, M.L. 2005. Cadmium toxicity in plants. *Brazilian Journal of Plant Physiology* **17**, 21–34.
- Burken, J., Vroblesky, D. & Balouet, J.C. 2011. Phytoforensics, Thermochemistry and Phytoscreening: New Green Tools for Delineating Contaminants from Past and Present. *Environmental Science & Technology* **45**(15), 6218–6226.
- Demir, S. 2004. Influence of arbuscular mycorrhiza on some physiological growth parameters of pepper. *Turkish Journal of Biology* **28**, 85–90.
- Dhir, B., Sharmila, P., Saradhi, P.P. & Nasim, S.A. 2009. Physiological and antioxidant responses of Slavonia naans exposed to chromium-rich wastewater, Ecotox-icology and Environmental Safety **72**, 1790–1797.
- Fukai, T. & Ushio-Fukai, M. 2011. Superoxide Dismutases: Role in Redox Signaling, Vascular Function, and Diseases. *ANTIOXIDANTS & REDOX SIGNALING* **15**(6), 1583–1606.
- Gajewska, E., Słaba, M., Andrzejewska, R. & Skłodowska, M. 2006. Nickel-induced inhibition of wheat root growth is related to H₂O₂ production, but not to lipid peroxidation. *Plant Growth Regulation* **49**, 95–103.
- Gajewska, E. & Skodowska, M. 2007. Relations between tocopherol, chlorophyll and lipid peroxides contents in shoots of Ni-treated wheat. *Journal of Plant Physiology* **164**, 364–366.
- Garg, N., Geetanjali & Kaur., A. 2006. Arbuscular mycorrhiza: Nutritional aspects. *Archives of Agronomy and Soil Science* **52**, 593–606.
- Ghasemi, R., Ghaderian, S.M. & Krämer, U. 2009. Interference of nickel with copper and iron homeostasis contributes to metal toxicity symptoms in the nickel hyperaccumulator plant *Alyssum inflata*. *New Phycologist* **184**, 566–580.
- Giannopolitis, C. & Ries, S. 1977. Superoxide dismutase occurrence in higher plant. *Plant Physiology* **59**, 309–314.
- Gonzalez-Chavez, M., Carrillo-Gonzalez, R., Wright, S. & Nichols, K. 2004. The role of glomalin, a protein produced by arbuscular mycorrhizal fungi, in sequestering potentially toxic elements. *Environmental Pollution* **130**, 317–323.
- Gonzalez-Guerrero, M., Melville, L.H., Ferrol, N., Lott, J.N., Azcon-Aguilar, C. & Peterson, R.L. 2008. Ultra-structural localization of heavy metals in the extra radical mycelium and spores of the arbuscularmycorrhizal fungus *Glomus intraradices*. *Canadian Journal of Microbiology* **54**, 103–110.
- Gosh, M. & Singh, S.P. 2005. A review on phytoremediation of heavy metals and utilization of its hypo ducts. *Applied ecology and environmental research* **3**(1), 1–18.
- Goussous, S. & Mohammad, M. 2009. Comparative effect of two arbuscular mycorrhizae and N and P fertilizers on growth and nutrient uptake of onions. *International Journal of Agriculture and Biology* **11**, 463–467.
- Hildebrandt, U., Regvar, M. & Bothe, H. 2007. Arbuscular mycorrhiza and heavy metal tolerance. *Phytochemistry* **68**, 139–146.
- Instrument Manual Digesdahl Digestion Apparatus. 1999. Models 23130-20-21 (1989-91, 1995-97. Hach Company, all rights reserved. Printed in the USA.
- Jahromi, F., Aroca, R., Porcel, R. & Ruiz-Lozano, J.M. 2008. Influence of salinity on the in vitro development of *Glomus intraradices* and on the in vivo physiological and molecular responses of mycorrhizal lettuce plants. *Microbial Ecology* **55**, 45–53.
- Javaid, A. 2009. Arbuscular mycorrhizal mediated nutrition in plants. *Journal of Plant Nutrition* **32**, 1595–1618.
- Joner, E. & Leyval, C. 1997. Uptake of ¹⁰⁹Cd by roots and hyphae of a *Glomus mosseae*/*Trifolium subterraneum* mycorrhiza from soil amended with high and low concentrations of cadmium. *New Phytologist* **135**, 353–360.
- Kinraide, T.B. 2007. The controlling influence of cell-surface electrical potential on the uptake and toxicity of selenite (Seo₄-2). *Plant Physiology, Rockville* **117**(1), 64–71.

- Kozłowski, A. & Badora, A. 2007. Influence of chosen mineral sorbents on yields and concentration of cadmium and lead in cultivated mustard grown on sewage sludge. *Journal of Elementology, Lublin* **12**(1), 47–55.
- Leung, H.M., Wang, Z.W., Ye, Z.H., Yung, K.L., Peng, X.L. & Cheung, K.C. 2013. Interactions between arbuscular mycorrhizae and plants in phytoremediation of metal-contaminated soils: A review. *Pedosphere* **23**(5), 549–563.
- Meier, S., Cornejo, P., Cartes, P., Borie, F., Medina, J. & Azcón, R. 2015. Interactive effect between Cu-adapted arbuscular mycorrhizal fungi and biotreated agrowaste residue to improve the nutritional status of *Oenothera picensis* growing in Cu-polluted soils. *J. Plant Nutr. Soil Sci.* 126–135.
- Nazarli, H. 2010. The effect of water stress and polymer on water use efficiency, yield and several morphological traits of sunflower under greenhouse condition. *Notulae Scientia Biologicae, Urmia* **2**(1), 53–58.
- Neumann, E. & George, E. 2005. Does the presence of arbuscular mycorrhizal fungi influence growth and nutrient uptake of a wild-type tomato cultivar and a mycorrhiza-defective mutant, cultivated with roots sharing the same soil volume. *New Phytologist* **166**, 601–609.
- Pakdaman, N., Ghaderian, S.M., Ghasemi, R. & Asemaneh, T. 2013. Effects of calcium/magnesium quotients and nickel in the growth medium on growth and nickel accumulation in *Pistacia atlantica*. *Journal of Plant Nutrition* **36**, 1708–1718.
- Parlak, K.U. 2016. Effect of nickel on growth and biochemical characteristics of wheat (*Triticum aestivum* L.) seedlings. *NJAS – Wageningen Journal of Life Sciences* **76**, 1–5.
- Pett-Ridge, J & K. Firestone, M. 2017. Using stable isotopes to explore root-microbe-mineral interactions in soil. *Rhizosphere* **3**(2), 244–253.
- Poschenrieder, C. & Barcelo, J. 2004. *Water relations in heavy metal stressed plants*. In: Heavy Metal Stress in Plants (ed. Prasad, M.N.V.) Springer Berlin, pp. 207–229.
- Pyrzyska, K. 2007. *Selenium occurrence in environment*. In: Wierzbicka, M. (Eds.). Selenium as important element for health and fascinating element for researcher. Warszawa, Malamute, 25–30.
- SAS Institute Inc. 2002. The SAS System for Windows, Release 9.0. Statistical Analysis Systems Institute Cary NC USA.
- Sharma, P. & Dubey, R.S. 2005. Lead toxicity in plants. *Brazilian Journal of Plant Physiology* **17**(1), 35–52.
- Sheetal, K.R., Singh, S.D., Anand, A. & Prasad, S. 2016. Heavy metal accumulation and effects on growth, biomass and physiological processes in mustard *Indian Journal of Plant Physiology* **21**(2), 219–223.
- Singh, S. & Agrawal, M. 2010. Effects of municipal waste water irrigation on availability of heavy metals and morpho-physiological characteristics of *Beta vulgaris* L. *Journal of Environmental Biology* **31**, 727–736.
- Tohidi Moghadam, H. 2017. Super absorbent polymer mitigates deleterious effects of arsenic in wheat. *Rhizosphere* **3**, 40–43
- Vivas, A., Biro, B., Nemeth, T., Barea, J.M. & Azcon, R. 2006. Nickel-tolerant *Brevibacillus brevis* and arbuscular mycorrhizal fungus can reduce metal acquisition and nickel toxicity effects in plant growing in nickel supplemented soil. *Soil Biology and Biochemistry* **38**, 2694–2704.
- Wang, S.H., Wu, W., Liu, F., Liao, R. & Hu, Y. 2017. Accumulation of heavy metals in soil-crop systems: a review for wheat and corn. *Environmental Science and Pollution Research* DOI 10.1007/s11356-017-8909-5. REVIEW ARTICLE

Energy consumption of milking pump controlled by frequency convertor during milking cycle

P. Vaculik^{*}, M. Prikryl, J. Bradna and L. Libich

Czech University of Life Sciences Prague, Faculty of Engineering, Department of Technological Equipment of Buildings, Kamýcká 129, CZ165 21 Prague 6 – Suchbátka, Czech Republic

^{*}Correspondence: vaculik@tf.czu.cz

Abstract. The article deals with selected parameters affecting the energy consumption of a vacuum pump in a milking system during the whole milking cycle in variants with and without regulation by a frequency convertor. When put into practice, the latest research of creation, control and stabilization of vacuum in milking devices allows dairy farmers to obtain a vacuum system that ensures maximum stability of milking pressure, which is a basic requirement affecting the health of dairy cows. The choice of vacuum system prioritizes in particular high performance, maximum operational reliability, minimum maintenance, long service life, environmental friendliness and economy. The vacuum pump was a Roots vacuum pump with a rotary piston which is typical for this use. Use of a frequency convertor significantly affected the efficiency of this pump for control of vacuum pressure level and pump performance by varying the rotation frequency according to the actual airflow requirement. Using this control system, only as much vacuum pressure is produced as necessary. By measurement of an experimental setup, it was found that the average power requirement of a setup with a control valve was 3.8 kW compared to 1.7 kW in the case of the variant with frequency convertor. Measurements and calculations have shown that this system is capable of saving more than 50% of electric energy.

Key words: milking cycle, vacuum system, vacuum pump, frequency convertor, energy consumption.

INTRODUCTION

Milking is the process by which milk is obtained from the udders of dairy cow. Milking devices currently in use partly mimic the activity of a calf sucking. These devices harvest milk by exerting suction pressure on the udder of dairy cows. The teats and milk glands are, however, very sensitive to external influences, impurities and injuries. Therefore, milking machines must not adversely affect the health of milk gland (Walstra et al., 1999; Laurs & Priekulis, 2008).

Each milking device must be designed to conform to the characteristics of the dairy cows and be based on anatomical, physiological and hygienic requirements. Milking devices and machines are designed to be gentle to teats and udders, accommodate blood circulation during milking and prevent inflammation and infection of any part of mammary anatomy, allow adequate milk extraction from udder at the time of full

oxytocin effect, do not reduce quality of milk, have amiable influence to dairy cows (Doležal et al., 2015, Příkryl et al., 2016).

In order to meet the above mentioned requirements, each milking device must ensure compliance with several principles, such as keeping a stable vacuum, the quality of the milking machine and the quality of the pulsation.

All parts that come into contact with milk must be made of materials that are suitable food contact materials. Each milking device must be equipped with a cleaning and disinfecting system (Chládek et al., 2010). At present, demands for the amount of air supplied to the dairy piping are increasing, as well as the requirements for the performance and efficiency of the vacuum pumps. This is mainly due to increased milking capacity, higher milk yields of dairy cows and increasing the diameter of the milking pipeline (Gaworski & Leola, 2014; Doležal et al., 2015). Higher milk yields can be affected also by the conditions in stables (Šimon et al., 2017).

It is necessary to produce a sufficient supply of vacuum so that it does not fluctuate during milking process. When sanitizing and flushing of milking devices, the vacuum system needs to be powerful enough to create air plugs in the larger diameters of the milk pipeline when transporting the sanitizing solution, thereby ensuring that the piping is cleaned throughout the whole cross-section. At present, the so-called double-pressure system is used, where a lower level of vacuum is used during milking process and higher vacuum is used for sanitation, flushing and drying of the milk pipes for the purpose of more efficient cleaning of larger pipe diameters. All these necessary requirements greatly increases the demands placed on vacuum systems, their equipment, their ability to respond quickly to the immediate need of vacuum, the energy requirements and the associated economy of operation (Doležal et al., 2015).

With regard to the above requirements for a modern milking system, series of measurements was carried out with the following objectives:

1) To determine the energy requirements for creating the necessary air flow at a particular vacuum level with the use of a frequency convertor as a regulator and without the use of a convertor where the regulation of the vacuum is provided by a control valve;

2) Using wattmeter to verify the energy consumption of at least twenty milking processes with and without the use of a frequency convertor;

3) Statistically evaluate the differences in measured energy consumption between two variants of regulation of vacuum, firstly by a frequency convertor and secondly by a control valve and the degree to which the frequency convertor influences the overall efficiency of the vacuum pump motor.

MATERIAL AND METHODS

The measurement described in this article deals with selected parameters of the energy requirements of a milking machine pump complemented with a frequency convertor throughout the whole milking process.

Measurements were done on a parallel milking parlor with 2 rows by 8 milking positions. It is able to process 80 dairy cows per hour. The working vacuum pressure was 42 kPa. Measurements were carried out during all three phases of milking process which are:

1) The first milking phase – disinfection, flushing with lukewarm water and drying of the milking device before milking. The first phase (as measured on site) takes 27 minutes.

2) The second milking phase is milking. This involves the income of cows at the milking parlor standings, the treatment of udder before milking, stimulation, milking, teat treatment after milking and subsequent group leaving of the dairy cows.

3) The third milking phase – disinfection, flushing and drying of the milking device after milking. The third phase contains flushing of the milk system and the milking machines with lukewarm water, flushing with the alkaline solution and flushing with acidic solution. The phase is completed by drying the whole system. The third phase (as measured on site) takes 52 minutes.

Measurements were carried out during individual milking processes under the comparable conditions in the milking parlor to compare the two variants. In particular, this meant keeping the same number of dairy cows and the exact same milking practices performed by the same operator. The measurements were started at the moment of the automatic start of flushing before the milking process and continued until the vacuum pump stopped after flushing and disinfection after milking process.

Measurements were sampled at regular three-minute intervals firstly with regulation and secondly with the frequency convertor disconnected. In the latter case, the working vacuum pressure (42 kPa) was controlled by the control valve. Measured values were read from the frequency convertor display and from the measuring devices (voltmeter, 3 x amp meter and wattmeter) and recorded in tables and subsequently evaluated.

The diagram of the setup with frequency convertor is shown in Fig. 1. Using the frequency convertor, constant motor speed can be set manually. Both of these frequency convertor features were used for the measurement.

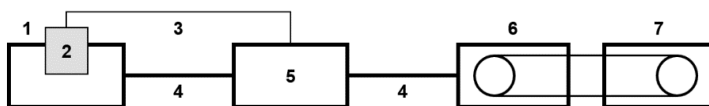


Figure 1. The diagram of the frequency convertor with the vacuum pump motor: 1 – vacuum pipeline; 2 – sensor; 3 – shielded data cable; 4 – power cord; 5 – frequency convertor; 6 – electric motor; 7 – vacuum pump.

In order to verify the measured values and to compare the energy consumptions, longer-term monitoring was carried out for both variants. In the above mentioned measurements, the energy consumption in the first ten days was measured on the existing setup with the frequency convertor and the next ten days it was the variant with the control valve only, which was set to the nominal vacuum pressure 42 kPa. Air suction through this valve was very noisy so the measurements could not take longer than ten days.

The data were used to compare the energy consumption of the two variants. The statistical difference between the measured energy consumptions in the variant when milking with or without the frequency convertor and the possible influence on the efficiency of the vacuum pump motor by using the frequency convertor during the milking cycle was evaluated at the end of the experiment. From the milking cycle, the data of the milking cycle itself (from 36 to 156 min.) were used for statistical evaluation. The descriptive statistic from the program Statistica was used as the first statistical evaluation. By descriptive statistics were calculated the most important statistical characteristics. It was necessary to perform statistical verification before we started the statistical processing of the measured values. In this case were used verification of the shape of the distribution and good compliance tests. These tests allow to confirm the assumption of random probability distributions and thus to use the statistical methods that are subject to this division.

This applies in particular to the normal distribution and tests based on it. In order to confirm the assumption of a normal distribution based on obliquity, a test of the normal distribution was carried out by the Statistica program.

RESULTS AND DISCUSSION

Determination of energy consumption of vacuum generation during the whole milking cycle

The measurements show the average power consumption is 3.8 kW with the control valve arrangement, compared to 1.7 kW for the variant with frequency convertor. Table 1 and 3 show the values measured over the whole milking cycle with frequency convertor and without frequency convertor, respectively. Table 2 and 4 show statistical evaluation of the values with and without frequency convertor, respectively.

Table 1. Average values measured over the whole milking cycle with frequency convertor

	A	B	C	D	E	F	G	A	B	C	D	E	F	G
	[min]	[rpm]	[Hz]	[kW]	[V]	[A]	[kPa]	[min]	[rpm]	[Hz]	[kW]	[V]	[A]	[kPa]
Start of the milking cycle								108	764	25.8	1.5	393	2.3	42.0
	0	0	0.0	0.0	393	0.0	0.4	111	867	29.3	2.3	390	5.8	42.4
	3	1,800	60.8	4.2	390	6.2	46.2	114	696	23.5	1.5	396	0.8	42.0
	6	0	0.0	0.0	393	0.0	0.3	117	752	25.4	1.6	396	1.8	42.0
	9	1,788	60.4	1.8	390	4.2	15.3	120	811	27.4	1.9	396	1.8	42.0
	12	0	0.0	0.0	393	0.0	0.3	123	699	23.6	1.3	393	1.8	42.0
	15	0	0.0	0.0	393	0.0	0.3	126	761	25.7	1.6	390	2.3	42.0
	18	0	0.0	0.0	393	0.0	0.3	129	1,264	42.7	3.3	396	6.7	41.9
	21	0	0.0	0.0	393	0.0	0.3	132	666	22.5	1.4	393	1.3	42.0
	24	1,791	60.5	3.1	393	5.2	23.2	135	820	27.7	1.6	390	2.8	42.0
	27	1,795	60.6	3.2	393	5.3	25.1	138	758	25.6	1.7	393	2.3	42.1
	30	0	0.0	0.0	393	0.0	0.3	141	1,380	46.6	3.6	396	6.3	42.0
	33	0	0.0	0.0	393	0.0	0.3	144	853	28.8	1.7	393	2.3	41.9
	36	1,255	42.4	2.1	390	4.8	42.1	147	675	22.8	1.5	393	1.8	42.0
	39	805	27.2	1.6	390	2.3	42.1	150	663	22.4	1.3	390	1.8	42.0
	42	737	24.9	1.5	390	0.8	42.0	153	666	22.5	1.5	393	1.3	41.9
	45	802	27.1	1.8	393	2.3	42.0	156	648	21.9	1.3	396	1.3	42.1

Table 1 (continued)

48	770	26.0	1.5	393	2.5	41.9	158	1,800	60.7	4.1	393	7.2	44.5
51	787	26.6	1.8	393	2.5	42.0	170	1,800	60.8	4.2	390	7.3	45.7
54	684	23.1	1.4	393	1.8	42.5	173	1,794	60.6	4.0	390	6.3	45.6
57	687	23.2	1.4	393	1.8	42.1	176	0	0.0	0.0	390	0.0	0.3
60	764	25.8	1.6	390	2.3	42.0	179	1,785	60.3	2.1	390	2.8	10.5
63	722	24.4	1.4	390	2.3	42.0	182	0	0.0	0.0	390	0.0	0.3
66	779	26.3	1.5	390	2.3	42.1	185	0	0.0	0.0	390	0.0	0.3
69	728	24.6	1.6	393	2.3	42.0	188	0	0.0	0.0	390	0.0	0.3
72	740	25.0	1.7	390	1.8	42.1	191	0	0.0	0.0	390	0.0	0.3
75	767	25.9	1.6	393	2.8	41.8	194	1,803	60.9	3.8	390	7.3	45.5
78	793	26.8	1.6	390	2.8	42.0	197	1,800	60.8	3.1	393	5.3	37.4
81	785	26.5	1.4	393	1.8	42.0	200	1,800	60.8	2.1	390	2.8	30.1
84	737	24.9	1.5	390	2.3	41.9	203	1,800	60.8	1.7	390	2.3	10.5
87	702	23.7	1.4	393	2.3	42.0	206	0	0.0	0.0	390	0.0	0.3
90	773	26.1	1.6	396	2.8	42.0	209	0	0.0	0.0	390	0.0	0.2
93	1,412	47.7	4.1	393	5.8	42.1	212	1,803	60.9	4.2	390	7.5	45.4
96	770	26.0	1.7	396	2.3	42.0	215	1,788	60.4	2.1	390	2.8	21.4
99	767	25.9	1.7	393	2.3	42.0	218	1,788	60.4	1.1	390	2.8	13.0
102	820	27.7	1.7	393	2.8	42.1	220	0	0.0	0.0	390	0.0	0.0
105	758	25.6	1.6	396	2.3	42.0	End of the milking cycle						

Note: A – Time of milking [min]; B – Frequency of motor rotation [rpm]; C – Frequency of output voltage [Hz]; D – Power [kW]; E – Voltage [V]; F – Current [A]; G – Vacuum [kPa].

Table 2. Statistical evaluation of the values measured throughout the milking cycle with frequency convertor

	Frequency of motor rotation [rpm]	Frequency of output voltage [Hz]	Power [kW]	Voltage [V]	Current [A]	Vacuum [kPa]
Average	806.9	27.3	1.7	392.7	2.6	42.0
Average error	28.5	0.96	0.09	0.3	0.2	0.01
Median	763.8	25.8	1.6	393.0	2.3	42.0
Modus	multiple	multiple	1.6	393.0	2.3	42.0
Standard deviation	182.2	6.2	0.6	2.2	1.4	0.1
Variation coefficient [%]	22.6	22.6	33.8	0.6	53.5	0.3
Scatter	33,206.7	37.9	0.35	4.86	1.87	0.01
Spikiness	5.4	5.4	8.6	-1.0	3.2	7.7
Skewness	2.5	2.5	2.9	0.2	1.9	2.2
Difference max-min	764.0	25.8	2.8	6.0	5.9	0.7
Minimum	648.0	21.9	1.3	390	0.8	41.8
Maximum	1,412.0	47.7	4.1	396	6.7	42.5
Total	33,086.6	1,117.6	71.4	16,101.0	104.6	1,723.1
Number	42.0	42.0	42.0	42.0	42.0	42.0
Confidence level (95%)	864.5	29.2	1.9	393.4	2.9	42.1

Table 3. Average values measured over the whole milking cycle without frequency convertor

	A	B	D	E	F	G		A	B	D	E	F	G	
	[min]	[rpm]	[kW]	[V]	[A]	[kPa]		[min]	[rpm]	[kW]	[V]	[A]	[kPa]	
Start of the milking cycle								108	1,800	3,8	393	7,5	42.0	
Flushing before milking	0	0	0.0	393	0.0	0.4		111	1,800	3.8	390	7.5	42.4	
	3	1,800	4.1	390	7.5	47.2		114	1,800	3.8	396	7.3	42.0	
	6	1,801	3.8	393	7.4	15.3		117	1,800	3.8	393	7.1	42.0	
	9	1,800	3.1	390	7.5	11.3		120	1799	3.8	396	7.5	42.0	
	12	0	0.0	393	0.0	0.3		123	1,800	3.8	393	7.5	42.5	
	15	0	0.0	393	0.0	0.3		126	1,800	3.8	390	7.3	42.0	
	18	0	0.0	393	0.0	0.3		129	1,800	3.8	396	7.2	41.9	
	21	1,799	3.9	392	7.2	0.3		132	1,800	3.8	393	7.5	42.0	
	24	0	0.0	393	0.0	25.6		135	1,800	3.8	390	7.3	42.0	
	27	1,800	2.8	393	7.5	11.6		138	1,800	3.8	393	7.6	42.1	
	30	0	0.0	393	0.0	0.3		141	1,800	3.8	396	7.5	42.0	
	33	0	0.0	393	0.0	0.3		144	1,800	3.8	393	7.5	41.9	
	Milking process	36	1,800	3.9	393	7.5	42.5		147	1,800	3.8	393	7.3	42.0
		39	1,800	3.9	390	7.5	42.1		150	1,800	3.8	390	7.5	42.0
42		1,800	3.9	390	7.3	42.0		153	1,800	3.8	391	7.6	42.0	
45		1,800	3.9	393	7.5	42.0		156	1,800	3.8	396	7.5	42.1	
48		1,800	3.8	393	7.4	41.9		158	1799	3.1	393	7.1	42.6	
51		1,800	3.8	393	7.3	42.2		170	1,800	4.2	390	7.5	45.7	
54		1,800	3.8	393	7.4	42.5		173	1,800	3.9	390	7.3	45.6	
57		1,800	3.8	393	7.3	42.1		176	0	0.0	390	0.0	0.3	
60		1799	3.8	389	7.5	42.0		179	1,800	2.8	390	7.3	10.8	
63		1,800	3.8	390	7.5	42.0		182	0	0.0	390	0.0	0.3	
66		1799	3.8	390	7.3	42.1		185	0	0.0	390	0.0	0.3	
69		1,800	3.8	393	7.1	42.1		188	0	0.0	390	0.0	0.3	
72		1,800	3.8	390	7.5	42.1		191	0	0.0	390	0.0	0.3	
75		1,800	3.8	393	7.5	41.8		194	1,800	4.1	390	7.2	45.5	
78	1,800	3.8	390	7.3	41.8		197	1,800	3.5	393	7.5	37.4		
Milking process	81	1,800	3.8	393	7.4	42.3		200	1,800	2.4	390	7.3	31.2	
	84	1,800	3.8	390	7.5	41.9		203	1,800	2.1	390	7.6	11.6	
	87	1799	3.8	393	7.5	42.0		206	0	0.0	390	0.0	0.3	
	90	1,800	3.8	396	7.3	42.0		209	0	0.0	390	0.0	0.2	
	93	1,800	3.8	393	7.5	42.1		212	1,800	4.2	396	7.3	45.4	
	96	1799	3.8	393	7.4	42.0		215	1799	3.2	390	7.5	23.8	
	99	1,800	3.8	393	7.3	42.0		218	1,800	1.1	390	7.2	15.7	
	102	1,800	3.8	393	7.4	42.1		220	0	0.0	390	0.0	0.3	
	105	1,800	3.8	396	7.3	42.0		End of the milking cycle						

Note: A – Time of milking [min]; B – Frequency of motor rotation [rpm]; D – Power [kW]; E – Voltage [V]; F – Current [A]; G – Vacuum [kPa].

Table 4. Statistical evaluation of the values measured throughout the milking cycle without frequency convertor

	Frequency of motor rotation [rpm]	Frequency of output voltage [Hz]	Power [kW]	Voltage [V]	Current [A]
Average	1,799.9	3.8	392.6	7.4	42.0
Average error	0.05	0.004	0.3	0.2	0.03
Median	1,800	3.8	393.0	7.5	42.0
Modus	1,800	3.8	393.0	7.5	42.0
Standard deviation	0.3	0.03	2.1	0.12	0.16
Variation coefficient [%]	0.02	0.8	0.5	1.6	0.4
Scatter	0.1	0.001	4.4	0.02	0.03
Spikiness	3.9	6.2	-0.76	-0.04	2.2
Skewness	-2.4	2.8	0.15	-0.7	1.5
Difference max-min	1	0.1	7	0.5	0.7
Minimum	1,799	3.8	389	7.1	41.8
Maximum	1,800	3.9	396	7.6	42.5
Total	73,795	156.2	1,095	303.7	1,724.5
Number	41	41	41	41	41
Confidence level (95 %)	1,800	3.8	393.2	7.4	42.1

Measurement of electric power consumption

Based on the monitoring of the consumption of electric energy in the process of vacuum generation the energy consumption of the variants was compared and percentage of electricity savings were determined in the variant with frequency convertor. Such evaluation of savings has been made for other parlor systems (Pittermann, 2008; Pavelka & Zdenek, 2010). Table 5 lists the measurement results along with other values from the milking parlor system database.

Table 5. Monitoring of electric energy consumption with and without frequency convertor

Measurement of electric energy consumption with frequency converter						Measurement of electric energy consumption without frequency converter					
No. of measurement	Start of milking process [-]	End of milking process [-]	Milking duration [h]	Number of tested dairy cows [pcs]	Energy consumption [kWh]	No. of measurement	Start of milking process [-]	End of milking process [-]	Milking duration [h]	Number of tested dairy cows [pcs]	Energy consumption [kWh]
1	15:10	17:23	2.22	173	6.7	21	15:10	17:23	2.22	172	12.6
2	03:54	6:27	2.55	174	7.0	22	03:54	6:27	2.55	173	12.8
3	15:09	17:25	2.27	173	6.8	23	15:09	17:25	2.27	172	12.6
4	03:49	6:12	2.38	172	6.9	24	03:49	6:12	2.38	171	12.7
5	15:14	17:36	2.37	172	6.9	25	15:06	17:25	2.32	170	12.7
6	03:52	6:12	2.33	172	6.8	26	03:43	6:16	2.55	172	12.8
7	15:12	17:35	2.38	172	6.9	27	15:10	17:27	2.28	169	12.7
8	03:49	6:12	2.38	173	6.9	28	03:47	6:17	2.50	171	12.8
9	15:13	17:39	2.43	174	7.0	29	15:11	17:20	2.15	171	12.6

Table 5 (continued)

10	03:40	6:16	2.60	175	7.1	30	03:46	6:01	2.25	172	12.7
11	15:15	17:28	2.22	173	6.8	31	15:15	17:32	2.28	172	12.7
12	03:42	6:12	2.50	173	7.1	32	03:49	6:14	2.42	173	12.8
13	15:13	17:27	2.23	172	6.8	33	15:03	17:25	2.37	173	12.8
14	03:49	6:10	2.35	171	6.9	34	03:45	6:04	2.32	172	12.8
15	15:10	17:24	2.23	173	6.7	35	15:13	17:27	2.23	172	12.7
16	03:44	6:03	2.32	172	6.8	36	03:49	6:10	2.35	172	12.8
17	15:17	17:26	2.15	172	6.8	37	15:15	17:28	2.22	171	12.7
18	03:41	6:11	2.50	172	7.1	38	03:40	6:16	2.60	171	12.9
19	15:06	17:27	2.35	172	6.9	39	15:13	17:39	2.43	172	12.8
20	03:39	6:03	2.40	172	7.0	40	03:54	6:17	2.38	172	12.7

Statistical evaluation of electricity consumption

Electric energy consumption is different when milking with or without the use of the frequency convertor, as confirmed by the results of the statistical evaluation of the consumption measurement for the individual measurements listed in Table 6.

In measured values and in calculations, it is evident that the use of the frequency convertor for the regulation of the vacuum was advantageous both in terms of energy savings, as well as in terms of noise in operation and the lifetime of the pump. Measurements and calculations have shown that this system saves more than 50% of the electricity. Also, the ecological safety of the vacuum system operation and the saving of oil, which is not necessary for the operation of an air pump, is not negligible (Přikryl et al., 2015, Přikryl et al., 2016).

Table 6. Statistical evaluation of energy consumption measurement with and without frequency convertor

	Statistical evaluation of energy consumption measurement with frequency inverter			Statistical evaluation of energy consumption measurement without frequency inverter		
	Milking duration [h]	Number of dairy cows [pcs]	Energy consumption [kWh]	Milking duration [h]	Number of dairy cows [pcs]	Energy consumption [kWh]
Average	2.35	172.60	6.89	2.35	171.70	12.74
Average error	0.03	0.21	0.03	0.03	0.22	0.02
Median	2.36	172.00	6.90	2.34	172.00	12.70
Modus	2.38	172.00	multiple	multiple	172.00	multiple
Standard deviation	0.12	0.94	0.12	0.12	0.99	0.08
Variation coefficient [%]	5.04	0.54	1.79	5.29	0.58	0.64
Scatter	0.01	0.88	0.02	0.02	0.98	0.01
Spikiness	-0.35	0.98	-0.73	-0.53	1.59	-0.41
Skewness	0.29	0.95	0.29	0.49	-1.01	-0.11
Difference max-min	0.45	4.00	0.40	0.45	4.00	0.30
Minimum	2.15	171.00	6.70	2.15	169.00	12.60
Maximum	2.60	175.00	7.10	2.60	173.00	12.90
Total	47.16	3,452.00	137.90	47.07	3,433.00	254.70
Number	20.00	20.00	20.00	20.00	20.00	20.00
Confidence level (95%)	2.41	173.00	6.95	2.41	172.10	12.77

The high quality of the milking process in modern milking systems, especially represented by milking robots and robotized milking parlors, is nowadays difficult to imagine without the use of frequency convertors (Ströbel et al., 2012; Příklad et al., 2015). Assessment of indoor environment quality in stables (Herbert et al., 2015) and the application of modern imaging (Libich et al., 2017) and monitoring methods (Hartová et al., 2017b) are going to improve livestock management. Other increase of milking process efficiency could be by better improvement of dairy cow movement and welfare monitoring (Hartová et al., 2017a).

CONCLUSION

The measurements and calculations clearly demonstrate the advantages of running vacuum systems with vacuum regulation by frequency convertors. This system can be recommended to all dairy farmers for creating, controlling and stabilizing vacuum. By measuring it was also found that although the maximum speed of the pump motor is 2,800 rpm, it is not necessary to set this rotation frequency in the basic adjustment of the frequency converter because the increase of the motor speed above 2,600 rpm does not increase pump performance. It is also important to ensure that the rotation speed of the pump does not fall below the minimum rotational speed set by the manufacturer to 1,000 rpm to ensure that the gears and bearings in the vacuum pump are thoroughly lubricated (spray lubrication). It is therefore necessary to set a minimum frequency of 28 Hz when adjusting the basic frequency drive (this is the recommendation for the service personnel who perform the installation and regular maintenance of the vacuum system).

ACKNOWLEDGEMENTS. Supported by the Internal Grant Agency of the Faculty of Engineering, Czech University of Life Sciences Prague, Czech Republic, Project No. 2015:31170/1312/3115.

REFERENCES

- Doležal, O., Staněk, S., Bečková, I., Černá, D. & Dolejš, J. 2015. Chov dojeného skotu: technologie, technika, management. (Breeding of milking cattle: technology, equipment, management) 1st Edition. Prague: Profi Press, s.r.o., 243 pp. ISBN 978-80-86726-70-0 (in Czech).
- Chládek, L., Příklad, M., Vaculík, P., Malašák, J. & Suchý, O. 2010. Possibilities of the verification of the efficiency of sanitation process in agricultural and food industry. *Conference Proceeding – 4th International Conference, TAE 2010: Trends in Agricultural Engineering, 7 September 2010 through 10 September 2010, Prague 2010, Czech Republic*, pages 236-240. ISBN 978-80-213-2088-8.
- Gaworski, M. & Leola, A. 2014. Effect of technical and biological potential on dairy production development. *Agronomy Research* **12**(1), 215–222. ISSN 1406-894X.
- Hartová, V., Hart, J. 2017a. Livestock monitoring system using bluetooth technology. *Agronomy Research* **15**(3), 707–712.
- Hartová, V. & Hart, J. 2017b. Modern methods of monitoring variables for racehorses. In *16th International Scientific Conference on Engineering for Rural Development 24.03.2017, Latvia*. Latvia: Latvia Univ Agriculture, Faculty Engineering, Inst Mechanics, 5 j cakstes blvd, Jelgava, lv-3001, Latvia, pp. 1018–1023.

- Herbut, P., Angrecka, S., Nawalany, G. & Adamczyk, K. 2015. Spatial and temporal distribution of temperature, relative humidity and air velocity in a parallel milking parlour during summer period. *Annals of Animal Science* **15**(2), 1 April 2015, pp. 517–526, DOI 10.1515/aoas-2015-0001, ISSN 1642–3402.
- Laurs, A. & Priekulis, J. 2008. Robotic milking of dairy cows. *Agronomy Research* **6**(special issue), 241–247. ISSN 1406-894X.
- Libich, L., Hruška, M., Vaculík, P. & Příkryl, M. 2017. The use of stereophotogrammetry to determine the size and spatial coordinates to generate a 3D model of an animal. *Research in Agricultural Engineering* **63**(2), 47–53. DOI 10.17221/65/2015-RAE. ISSN 1212-9151.
- Pavelka, J. & Zděnek, J. 2010. Elektrické pohony a jejich řízení. (Electric drives and their control) 1st Edition. Prague: Czech Technical University in Prague, 241 pp. ISBN 978-80-01-04642-5 (in Czech).
- Pittermann, M. 2008. Elektrické pohony: základy. (Electric drives: basics) 1st Edition. Pilsen: University of West Bohemia, 98 pp. ISBN 978-80-7043-729-2 (in Czech).
- Příkryl, M., Vaculík, P., Chládek, L., Libich, L. & Smetanová, P. 2016. The human factor's impact on the process of milking. *Agronomy Research* **14**(5), 1659–1670. ISSN 1406-894X.
- Příkryl, M., Vaculík, P., Smejtková, A., Hart, J. & Němec, P. 2015. Producing the vacuum in modern drawn milking systems. *Agronomy Research* **13**(1), 253–260. ISSN 1406-894X.
- Ströbel, U., Rose-Meierhöfer, S., Hoffmann, G., Ammon, C., Amon, T. & Brunsch, R. 2012. Vacuum application for individual quarters in modern milking systems. *Landtechnik* **67**(6), 405–408. ISSN 0023-8082.
- Šimon, J., Vegricht, J., Bradna, J. 2017. The effect of bedding amount on gas emissions from manure during storage. *Agronomy Research* **15**(5), 2126–2133. ISSN 1406-894X.
- Walstra, P., Geurts, T.J., Noomen, A., Boekel, A. & Jellema, A. 1999. Dairy technology: principles of milk properties and processes. New York: Marcel Dekker, 727 pp. ISBN 0-8247-0228-X.

INSTRUCTIONS TO AUTHORS

Papers must be in English (British spelling). English will be revised by a proofreader, but authors are strongly urged to have their manuscripts reviewed linguistically prior to submission. Contributions should be sent electronically. Papers are considered by referees before acceptance. The manuscript should follow the instructions below.

Structure: Title, Authors (initials & surname; an asterisk indicates the corresponding author), Authors' affiliation with postal address (each on a separate line) and e-mail of the corresponding author, Abstract (up to 250 words), Key words (not repeating words in the title), Introduction, Materials and methods, Results and discussion, Conclusions, Acknowledgements (optional), References.

Layout, page size and font

- Use preferably the latest version of **Microsoft Word**, doc., docx. format.
- Set page size to **B5 Envelope or ISO B5 (17.6 x 25 cm)**, all margins at 2 cm.
- Use single line spacing and justify the text. Do not use page numbering. Use indent 0.8 cm (do not use tab or spaces instead).
- Use font Times New Roman, point size for the title of article **14 (Bold)**, author's names 12, core text 11; Abstract, Key words, Acknowledgements, References, tables and figure captions 10.
- Use *italics* for Latin biological names, mathematical variables and statistical terms.
- Use single ('...') instead of double quotation marks ("...").

Tables

- All tables must be referred to in the text (Table 1; Tables 1, 3; Tables 2–3).
- Use font Times New Roman, regular, 10 pt. Insert tables by Word's 'Insert' menu.
- Do not use vertical lines as dividers; only horizontal lines (1/2 pt) are allowed. Primary column and row headings should start with an initial capital.

Figures

- All figures must be referred to in the text (Fig. 1; Fig. 1 A; Figs 1, 3; Figs 1–3). Use only black and white or greyscale for figures. Avoid 3D charts, background shading, gridlines and excessive symbols. Use font **Arial** within the figures. Make sure that thickness of the lines is greater than 0.3 pt.
- Do not put caption in the frame of the figure.
- The preferred graphic format is EPS; for half-tones please use TIFF. MS Office files are also acceptable. Please include these files in your submission.
- Check and double-check spelling in figures and graphs. Proof-readers may not be able to change mistakes in a different program.

References

- **Within the text**

In case of two authors, use '&', if more than two authors, provide first author 'et al.':

Smith & Jones (1996); (Smith & Jones, 1996);
Brown et al. (1997); (Brown et al., 1997)

When referring to more than one publication, arrange them by following keys: 1. year of publication (ascending), 2. alphabetical order for the same year of publication:
(Smith & Jones, 1996; Brown et al., 1997; Adams, 1998; Smith, 1998)

- **For whole books**

Name(s) and initials of the author(s). Year of publication. *Title of the book (in italics)*. Publisher, place of publication, number of pages.

Shiyatov, S.G. 1986. *Dendrochronology of the upper timberline in the Urals*. Nauka, Moscow, 350 pp. (in Russian).

- **For articles in a journal**

Name(s) and initials of the author(s). Year of publication. Title of the article. *Abbreviated journal title (in italic)* volume (in bold), page numbers.

Titles of papers published in languages other than English, German, French, Italian, Spanish, and Portuguese should be replaced by an English translation, with an explanatory note at the end, e.g., (in Russian, English abstr.).

Karube, I. & Tamiyra, M.Y. 1987. Biosensors for environmental control. *Pure Appl. Chem.* **59**, 545–554.

Frey, R. 1958. Zur Kenntnis der Diptera brachycera p.p. der Kapverdischen Inseln. *Commentat.Biol.* **18**(4), 1–61.

Danielyan, S.G. & Nabaldiyan, K.M. 1971. The causal agents of meloids in bees. *Veterinariya* **8**, 64–65 (in Russian).

- **For articles in collections:**

Name(s) and initials of the author(s). Year of publication. Title of the article. Name(s) and initials of the editor(s) (preceded by In:) *Title of the collection (in italics)*, publisher, place of publication, page numbers.

Yurtsev, B.A., Tolmachev, A.I. & Rebristaya, O.V. 1978. The floristic delimitation and subdivisions of the Arctic. In: Yurtsev, B. A. (ed.) *The Arctic Floristic Region*. Nauka, Leningrad, pp. 9–104 (in Russian).

- **For conference proceedings:**

Name(s) and initials of the author(s). Year of publication. Name(s) and initials of the editor(s) (preceded by In:) *Proceedings name (in italics)*, publisher, place of publishing, page numbers.

Ritchie, M.E. & Olf, H. 1999. Herbivore diversity and plant dynamics: compensatory and additive effects. In: Olf, H., Brown, V.K. & Drent R.H. (eds) *Herbivores between plants and predators. Proc. Int. Conf. The 38th Symposium of the British Ecological Society*, Blackwell Science, Oxford, UK, pp. 175–204.

Please note

- Use ‘.’ (not ‘,’) for decimal point: 0.6 ± 0.2; Use ‘,’ for thousands – 1,230.4;
- Use ‘-’ (not ‘-’) and without space: pp. 27–36, 1998–2000, 4–6 min, 3–5 kg
- With spaces: 5 h, 5 kg, 5 m, 5°C, C : D = 0.6 ± 0.2; $p < 0.001$
- Without space: 55°, 5% (not 55 °, 5 %)
- Use ‘kg ha⁻¹’ (not ‘kg/ha’);
- Use degree sign ‘°’ : 5 °C (not 5 ° C).